VNiVERSiDAD D SALAMANCA
CAMPUS DE EXCELENCIA INTERNACIONAL

Departamento de Fisiología Vegetal
Facultad de Biología
Universidad de Salamanca

CSIC
CONSEJO SUPERIOR DE INVESTIGACIONES CIENTÍFICAS

Instituto de Recursos Naturales y Agrobiología de Salamanca
Consejo Superior de Investigaciones Científicas
Departamento de Estrés Abiótico

Study of the wheat genotypic variability for the improvement of grain yield and quality and its dependence on leaf carbon-nitrogen metabolism under elevated CO_2 and high temperature

Tesis Doctoral · 2022
Emilio Luis Marcos Barbero

Departamento de Fisiología Vegetal
Facultad de Biología
Universidad de Salamanca

Instituto de Recursos Naturales y Agrobiología de Salamanca
Consejo Superior de Investigaciones Científicas
Departamento de Estrés Abiótico

Study of the wheat genotypic variability for the improvement of grain yield and quality and its dependence on leaf carbon-nitrogen metabolism under elevated CO_2 and high temperature

Tesis Doctoral presentada por **Emilio Luis Marcos Barbero** para optar al grado de Doctor con mención Internacional en Agrobiotecnología por la Universidad de Salamanca.

DIRECTORA, Dra. **Rosa María Morcuende Morcuende**. Investigadora Científica del Departamento de Estrés Abiótico. Instituto de Recursos Naturales y Agrobiología de Salamanca del CSIC.

Salamanca, enero de 2022

El presente trabajo ha sido financiado a través de los proyectos AGL2013-41363-R y AGL2016-79589-R concedidos por el Ministerio de Economía y Competitividad, así como los proyectos CSI083U16 otorgado por la Junta de Castilla y León (JCyL) y cofinanciado por el Fondo Europeo de Desarrollo Regional. Emilio Luis Marcos Barbero ha disfrutado de una ayuda para la contratación predoctoral de personal investigador financiada por la JCyL y el Fondo Social Europeo (E-37-2017-0066125), de un contrato "CLU-2019-05 – Unidad de Excelencia IRNASA-CSIC", financiado por la JCyL y la Unión Europea (FEDER "Europa impulsa nuestro crecimiento") y de una ayuda para la realización de una estancia en el centro INRA-Aquitainte de Burdeos (Francia), concedida por la *2nd Call for Transnational Access to European Plant Phenotyping Facilities EPPN2020 European Commission* (ID 178).

La **Dra. ROSA MARÍA MORCUENDE MORCUENDE**, Investigadora Científica de Organismos Públicos de Investigación, perteneciente al Consejo Superior de Investigaciones Científicas (CSIC),

CERTIFICA

Que la presente Tesis Doctoral titulada "*Study of the wheat genotypic variability for the improvement of grain yield and quality and its dependence on leaf carbon-nitrogen metabolism under elevated CO_2 and high temperature*", ha sido realizada por **D. EMILIO LUIS MARCOS BARBERO** en el Instituto de Recursos Naturales y Agrobiología de Salamanca (IRNASA-CSIC) y reúne originalidad y contenidos suficientes para que sea presentada ante el tribunal correspondiente y optar al grado de Doctor por la Universidad de Salamanca.

Y para que así conste, a efectos legales, firmo el presente certificado en Salamanca a 25 de enero de 2022.

MORCUENDE MORCUENDE ROSA MARIA - 04169531E

Firmado digitalmente por MORCUENDE MORCUENDE ROSA MARIA - 04169531E
Fecha: 2022.01.25 17:18:04 +01'00'

Fdo.: Dra. Rosa María Morcuende Morcuende

Acknowledgements

No siempre resulta fácil reconocer y agradecer el apoyo brindado por las personas que te rodean cuando te embarcas en una nueva aventura. Resulta aún más difícil cuando no conoces físicamente a esas personas y ellas no saben de tu existencia. Sin embargo, me gustaría que mis primeras palabras de agradecimiento fueran para Ainsworth, Bloom, Högy, Fangmeier, Shewry y para muchos otros grandes investigadores de los que he aprendido en estos años a través de sus trabajos y sin los cuales no podría haber realizado esta Tesis.

También me gustaría hacer una breve mención a los múltiples profesores que he tenido a lo largo de mi vida y que, con sus sabios consejos, me han conducido hasta aquí.

A Raquel Martínez Peña y a José Ramón Pardos Blas, por ser unos excelentes amigos y unos grandes compañeros de Tesis a distancia.

Me gustaría agradecer el cariño con el que todo el personal del IRNASA me acogió desde mi primer día. A las chicas de secretaría, a Miguel y a Juan Pablo (JuanPa) por esos momentos tan divertidos en el café, y a María José (Majo) por otros tantos similares durante la comida.

Un agradecimiento muy especial a mis compañeros “senior” del laboratorio. Al Prof. Dr. Rafael Martínez-Carrasco Tabuenca y a la Dra. Pilar Pérez Pérez por su apoyo y sus buenos consejos aun cuando el tiempo que coincidimos fue breve. Al Dr. Juan Bautista Arellano Martínez, por contagiarme parte de su infinita pasión por la Ciencia. A María Ángeles (Nines) Boyero San Blas y Ángel Luis Verdejo Centeno, por hacer tan amenas y entretenidas las mañanas de laboratorio. A los más recientes, Nara, Ouardia, Ismael y Ana, por su gran apoyo en las últimas fases de la elaboración de esta Tesis.

A mi Directora de Tesis, Rosa María Morcuende Morcuende, sin la cual ninguna de estas palabras existiría. Gracias por ser un ejemplo de constancia y de compromiso.

A Yasmina, a Edith y a mi madre, y en especial a mi padre. Ojalá hubiéramos llegado juntos al final de este camino.

A mis otros padres, Elena y Eloy, y a Ángeles, mi tercera hermana, por todo su afecto y apoyo.

A María, Manuel y el Dr. Leonardo, porque ellos también son familia.

A Elia,

Porque das vida a la mejor versión de mí.

Abbreviation

1-FEH	Fructan 1-exohydrolases.
1-FFT	Fructan:fructan 1-fructosyltransferase.
1-SST	Sucrose:sucrose 1-fructosyltransferase.
2-OG	2-oxoglutarate.
6-FEH	Fructan 6-exohydrolases.
6-SFT	Sucrose:fructan 6-fructosyltransferase.
8TH HTWSN	8th Heat-Tolerant Wheat Screening Nursery.
A	Photosynthetic CO_2 assimilation rate.
Aa	Amino acids.
AAPH	2,2′-azobis(2-methyl-propanimidamide) dihydrochloride.
ADH	Alcohol dehydrogenase.
ADP	Adenosine diphosphate.
ADP-glucose	Adenosine diphosphate glucose.
AGPase	ADP-glucose pyrophosphorylase.
AMT	Ammonium transporters.
ANOVA	Analysis of variance.
AOX	Alternative oxidase.
ARbcx	Maximum value of photosynthesis limited by Rubisco activity.
Asa	Ascorbic acid.
ATP	Adenosine triphosphate.
ATPase	ATP-synthase.
ATP-PFK	ATP-dependent phosphofructokinase.
Axs	Arabinoxylanes.
BPGA	1,3-bisphosphoglycerate.
BSA	Bovine serum albumin.
C	Carbon.
C%	Percentage of carbon.
C/N	Carbon-nitrogen ratio.
CA1P	Carboxyarabinitol 1-phosphate.
CAM	Crassulacean acid metabolism.
CB	Canonical biplot.
CCA	Canonical correlation analysis.
CFC	Chlorofluorocarbon.
Chl	Chlorophyll.
C_i	Leaf internal CO2 concentration.
CI	Confident intervals.
CIMMYT	Centro Internacional de Mejoramiento de Maíz y Trigo.
CLC	Chloride channel.
cm	Centimetres.
cm^2	Square centimetres.
CN	Correlation network.
CO_2	Carbon dioxide.
CoA	Coenzyme A.
Contr	Contribution.
Corr	Correlation.
Cos^2	Squared correlation.
CRbcx	CO_2 intercellular concentration at maximum photosynthesis limited by Rubisco activity.
Cyt b_6f	Cytochrome b_6f
DBEs	Starch-debranching enzymes.
DF	Dietary fibre.
df	Degrees of freedom.
DHAP	Dihydroxyacetone phosphate.
DIABLO	Multivariate dimension reduction discriminant analysis.
Dim	Dimension.
DTNB	6,6′-dinitro-3,3′-dithiodibenzoic acid.
DTT	Dithiothreitol.
DW	Dry weight.
E	Transpiration.
e^-	Electron.
F1,6bisP	Fructose 1,6-bisphosphate.
F6P	Fructose 6-phosphate.
$FADH_2$	Flavin adenine dinucleotide.
Fd	Ferredoxin.
Fd_{red}	Reduced ferredoxin.
FIES	Food insecurity experience scale.
Flav	Flavonoids.
FMN	Flavin mononucleotide.
FNR	Ferredoxin-$NADP^+$ reductase.
FRAP	Ferric ion reducing antioxidant power.
Fru	Fructose.
Fru1,6bisPase	Fructose-1,6-bisphosphatase.
Fruct	Fructans.
Fs_{ox}	Oxidated ferredoxin.
FTs	Fructosyltransferases.
FW	Fresh weight.
g	Grams.
G1P	Glucose 1-phosphate.
G3PDH	Glycerol-3-phosphate oxidase.
G3POX	Glycerol-3-phosphate dehydrogenase.
G6P	Glucose 6-phosphate.
G6PDH	Glucose-6-phosphate dehydrogenase.
GAP	Glyceraldehyde-3-phosphate.
GAPDH	Glyceraldehyde 3-phosphate dehydrogenase.
Gazul	Genotype 150.
GBSS	Granule-bound starch synthase.
GDC	Glycine decarboxylase.
GDH	Glutamate dehydrogenase.
GDW	Glucan-water dikinase.
GHG	Greenhouse gasses.
Gln	Glutamine.
Glu	Glutamate.
Gluc	Glucose.
glycerol-3-P	Glycerol-3-phosphate.
g_m	Mesophyll conductance.
GNE	Grain number per ear.
GOGAT	Glutamine 2-oxoglutarate amino transferase or glutamate synthase.
GR	Green revolution.
GS	Glutamine synthetase.
g_s	Stomatal conductance.
GSH	Glutathione.
GYE	Grain yield per ear.
H %	Water percentage.
H^+	Proton.
HATS	High-affinity transport systems.
HCPC	Hierarchical clustering on principal components.
HI	Harvest index.
HK	Hexokinase.
HMW	High-molecular weight glutenins.
ICDH	Cytosolic isocitrate dehydrogenase.
IDH	Isocitrate dehydrogenase.
IWIN	International wheat improvement network.
Jx	Maximum rate of electron transport.
K-W	Kruskal-wallis.
LATS	Low-affinity transport systems.
LDH	Lactate dehydrogenase.
LDMC	Leaf dry matter content.
LDMC	Dry matter content.
LHC	Light-harvesting complex.
LMA	Leaf dry mass per area.
LMA	Dry mass per area.
LMW	Low-molecular weight glutenins.
MANOVA	Multivariate analysis of variance.
Max	Maximum.
MDH	Malate dehydrogenase.
MFA	Multiple factorial analysis.
Min	Minimum.
MTT	3-(4,5-dimethylthiazol-2-yl)-2,5-diphenyl tetrazolium bromide.
N	Nitrogen.

Abbreviation

N%	Percentage of nitrogen.
N_2	Molecular nitrogen.
NADH	Nicotinamide adenine dinucleotide.
NADPH	Nicotinamide adenine dinucleotide phosphate.
NBI	Nitrogen balance index.
NH_3	Ammonia.
NH_4^+	Ammonium.
NiR	Nitrite reductase.
NNEDA	N-(1-naphthyll)-ethylenediamine.
NO_2^-	Nitrite.
NO_3^-	Nitrate.
NPF	Nitrate transporter 1/peptide transporter family.
NR	Nitrate reductase.
NUE	Nitrogen-use efficiency.
NupE	Nitrogen-uptake efficiency.
NUtE	Nitrogen-itilisation efficiency.
O_2	Oxygen.
OAA	Oxaloacetate.
ORAC	Oxygen radical absorbance capacity.
P680	Photosystem I.
P700	Photosystem II.
PAR	Photosynthetically active reaction.
Pc	Plastocyanin.
PCA	Principal component analysis.
PDH	Pyruvate dehydrogenase.
PDMC	Plant dry matter content.
PDMC	Dry matter content.
PEP	Phosphoenolpyruvate.
PEPCase	Phosphoenolpyruvate carboxylase.
PES	Phenazine ethosulfate.
PG	2-phosphoglycolate.
PGA	3-phosphoglycerate.
PGI	Phosphoglucose isomerase.
PGK	Phosphoglycerate kinase.
P_i	Inorganic phosphate.
PK	Pyruvate kinase.
PMA	Plant dry mass per area.
PMA	Dry mass per area.
PMS	Phenazine methosulfate.
PMSF	Phenylmethylsulfonyl fluoride.
PPI-PFK	PPI-dependent phosphofructokinase.
PQ	Plastoquinone.
PQ^-	Plastosemiquinone.
PQH_2	Plastohydroquinone.
PSI	Photosystem I.
PSII	Photosystem II.
Q1	First quartile.
Q3	Third quartile.
Rd	Day respiration.
ROS	Reactive oxygen species.
Ru5P	Ribulose 5-phosphate.
Rubisco	Ribulose 1,5-bisphosphate carboxylase/oxygenase.
RuBP	Ribulose 1,5-bisphosphate.
SBEs	Starch branching enzymes.
SLAC/SLAH	Slow anion channel-associated homologues.
SPP	Sucrose phosphate phosphatase.
SPS	Sucrose phosphate synthase.
SSs	Starch synthase soluble.
Suc	Sucrose.
SUS	Sucrose synthase.
SUT	Sucrose transporters.
T6P	Trehalose-6-phosphate.
TAC	Total antioxidant capacity.
TCA	Tricarboxylic acid cycle.
TP	Total protein.
TPhC	Total phenolic compounds content.
TPT	Triose phosphate transporter.
TPTZ	2,4,6-Tris(2-pyridyl)-s-triazine.
TPU	Maximum rate of triose phosphate use.
UDP	Uridine diphosphate.
UDP-glucose	Uridine diphosphate glucose.
UQ	Ubiquinone.
UQH2	Reduced ubiquinone.
UTP	Uridine triphosphate.
UV	Ultraviolet.
***Vcx*.**	Maximum carboxylation rate of Rubisco.
WUE	Water use efficiency.
Φ_{PSII}	Quantum yield of PSII electron transport.

Index

CHAPTER 1

Introduction

1.1. Agriculture and Domestication

1.1.1. Domestication, agriculture and its role in human society

1.1.1.1. Coevolution and domestication

Since the emergence of life on Earth, living beings have established complex relationships with other organisms and with the surrounding environment (Zunjarrao *et al.*, 2020). These associations sometimes involve two or more lineages of organisms in which changes in one of these evolutionary trajectories conditionate the other. This process, called *coevolution*, occurs between organisms belonging to the same or different kingdoms and shows a wide spectrum of interactions going from *mutualisms*, in which the specialisation benefits both species, to hostile relationships (Whitney and Glover, 2013). As sessile organisms, plants are subjected to numerous interactions with different organisms above- and below-ground, including animals, bacteria, fungi or viruses. Precisely, one of the first and more successful examples of coevolutionary systems described in literature implies the interaction stablished between plants and insects. Almost 298 million years ago, during the Permian period, *pollinivory*, the consumption of pollen by animals, took place firstly (Zunjarrao *et al.*, 2020). Not long after, during early and mid-Cretaceous, pollination driven by insect was already the main strategy of angiosperm reproduction (Hu *et al.*, 2008). Other examples of plant coevolution include the development of plant defence strategies against herbivore (i.e. resistance, tolerance, phenological escape and overcompensation), the recognition of chemical molecules in the mycorrhizal fungi and rhizobacteria symbiotic interactions, or the competitive genetic race established between the pathogenic-infection identification systems of plants and the ability of those pathogens to escape from that recognition (Occhipinti, 2013).

A very specific type of coevolution, with deep implications for the organisms involved in this relationship, is the so-called *domestication*. Meyer & Purugganan (2013) defined domestication as *a coevolutionary interaction that leads to the establishment of new domesticated species, the growth and reproduction of which are mostly controlled for the benefit of another species.* Domestication affects not only to plants but also to many different organisms and the mutualistic relationship established between the domesticated species and the domesticators leads to beneficial effects on both species. For the domesticators, domestication supposes meeting their needs, mainly but not exclusively, the nutritional requirements. At the same time, the domesticated species experiment an improvement in their fitness, leading to the raise in the size of their population and the geographical expansion of the individuals from their original area (Purugganan, 2019). A classic example of

domestication is the ability to grow fungi for food showed by three orders of insects: ants, termites and ambrosia beetles. The development of *fungiculture* has evolved independently at least nine times in the three orders about 40-60 million years ago (seven times in the case of beetles and once for ants and termites), involving multiple species of ants (approximately 200 species), termites (330 from more than 2,600 known termite species) and beetles (3,400 species). Together with the vast number of species implicated and the extraordinary length of the interactions, the fact that this ability is transmitted vertically across generations highlights the evolutive importance of domestication (Mueller and Gerardo, 2002; Mueller *et al.*, 2005).

1.1.1.2. Origin of agriculture

Humanity has also taken advantage of the benefits of these interactions. The domestication processes carried out by human beings are much more recent, but also high diverse. Nowadays, approximately 40 domesticated species of animal can be found distributed around the world, including dogs, cats, sheep, cows, goats, chicken or horses. Dogs (*Canis lupus* ssp. *familiaris*) were the first animals domesticated by humans, at around 17,000 years ago, while ancient domestication of cattle, goat or cats took place at about 10,000 years ago and others, such as sheep or horses, are even more recent (4,000–5,000 years ago) (Ahmad *et al.*, 2020). Similarly, plant domestication

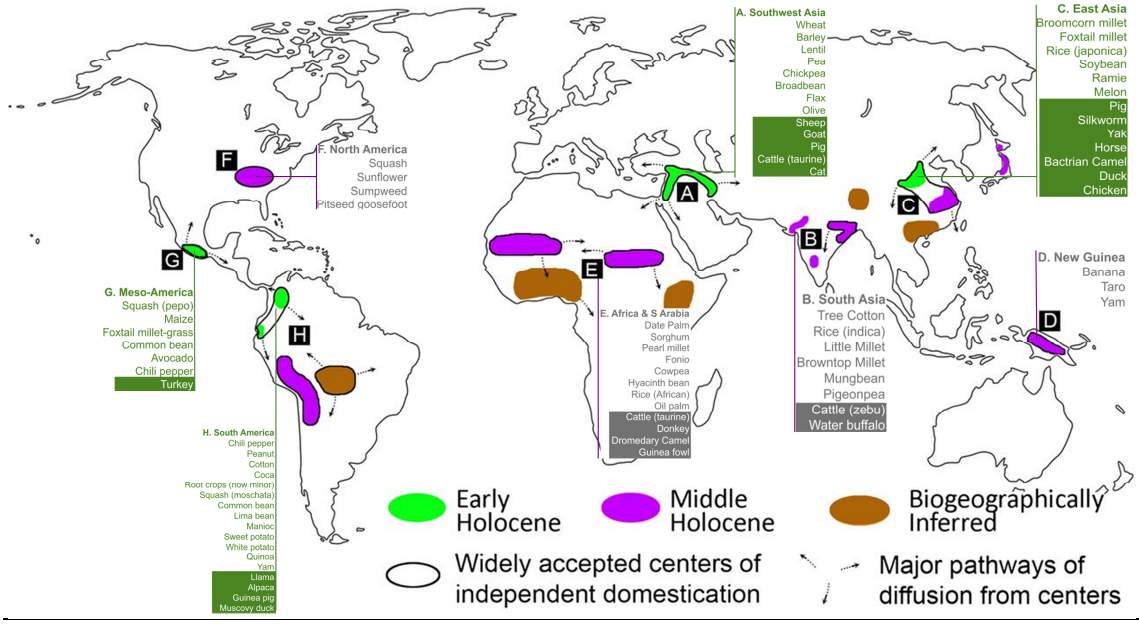

Figure 1.1. Centres of crop and animal domestication.

Black outlines represent independent centres of domestication. Arrows indicates diffusion of domesticates. Different colours are used to indicate the period of time taking place the domestication process. Further information can be found in Figure S1.1.

Retrieved and modified from (Larson *et al.*, 2014)

developed by human-gatherer societies began at approximately 12,000 years ago, as the main way to acquire nutrients and calories. Nevertheless, crop domestication has led to the existence of a profuse number of semi- and fully-domesticated plant species (1,000–2,500) from more than one hundred taxonomic families (Smýkal *et al.*, 2018; Purugganan, 2019). Archaeobotanical studies have revealed that the adoption of agriculture and animal domestication happened in different geographical points at different times (Figures 1.1 and S1.1). A region of the south-west of Asia enclosed by the Tigris and the Euphrates rivers, the *Fertil Crescent* area, witnessed the domestication of goats, sheep, pigs or cattle (Zeder, 2008), as well as eight crop species at 12,000 years ago. These crop species included: three cereals [diploid einkorn (*Triticum monococcum* ssp. *monococcum*) and tetraploid emmer (*Triticum turgidum* ssp. *dicoccum*) wheats and barley (*Hordeum vulgare*)], two pulses [lentil (*Lens culinaris*) and pea (*Pisum sativum*)], flax (*Linum usitatissimum*), bitter vetch (*Vicia ervilia*) and chickpea (*Cicer arietinum*) (Brown *et al.*, 2009). *Mesoamerica* (where maize was first cultivated), *South America* (source of potato, peanut and manioc) and the *Lower Yangtze River region of Asia* (where rice first appeared) were also major centres of crop domestication, all of them at approximately 10,000 years ago (Meyer and Purugganan, 2013).

1.1.1.3. Consequences of agriculture

Agriculture entailed profound changes for both domesticated plants and human societies. Crop domestication would have arisen as a dynamic process coming from hunter-gatherer leftovers during their seasonal migratory routes. Thus, the seeds and fruits discarded one year would sprout into crops in the following one. Over time, those plants with more desirable characteristics would be selected as food, becoming the dominant ones and promoting wild plants disappearance (Doebley *et al.*, 2006). As a consequence of human selection, domesticated plants would differ in several traits from their wild progenitors. This common set of characteristics is known as *domestication syndrome*, first coined by Hammer (1984), which in cereals includes: *increased grain retention* (non-shattering) and *grain size*, *loss of seed dispersal aids* and *dormancy*, *synchronous germination*, *compact growth size* and *improved culinary chemistry* (Brown *et al.*, 2009; Abbo *et al.*, 2014; Smýkal *et al.*, 2018; Purugganan, 2019). Dispersal seed reduction is usually associated with the loss of the abscission layer in the base of the spikelet, performing tough rachis. Evolution and fixation of non-shattering has been considered as a key trait for domestication because it links the survival and propagation of the crop plant to humans. However, these processes would have required a long period of time (of at least 2,000 years) due to a low selective pressure, whereas for other traits, such us the gain in grain size, they would have been quicker (Purugganan and Fuller, 2009). Notwithstanding, it is the combination

of all the domestication traits which determines a plant species as a possible eligible candidate for being grown because they simplify crop planting, cultivation and harvesting (Heslop-Harrison and Schwarzacher, 2012).

Adoption of agriculture also changed the relationship of humanity with the environment. It promoted a shift from hunter-gather societies to a selective hunting, herding, and settled agricultural model, diminishing dietary stress and leading to a raise in population (Berardy *et al.*, 2019). Indeed, food availability led to a raise in human population of nearly sixteen times over the existing one during the Mesolithic. This, eventually, resulted in the emergence of big urban centres, and as far as it was not necessary for everyone to be involved in food production, the specialisation of work also arose (Harper and Armelagos, 2013). Moreover, the increased carbohydrate intake associated with the emergence of agriculture boosted the calory intake and therefore provided more energy (Boukid *et al.*, 2018). Nevertheless, it is believed that the change in dietary intake also promoted negative consequences on human health. Archaeological studies of human skeleton have revealed evidence of porotic hyperostosis associated with iron deficiency anaemia, as well as a reduction in bone growth rates in children and height in adults possibly associated with nutritional deficiencies of iron, amino acids, vitamins A and B3 and proteins observed in maize, millet or wheat (Larsen, 2006). A raise in the frequency of dental caries has also been determined after domestication, possibly as a consequence of the production of acids from increased carbohydrate metabolization, while changes in microbiome towards a reduced gut flora diversity have also been described (Larsen, 2006; Harper and Armelagos, 2013). Furthermore, a higher interaction with agricultural-associated animals would have facilitated pathogenic transmission from domesticated animals to humans, increasing the number of zoonotic diseases such as malaria, AIDS or bubonic plague (Gross, 2013; Harper and Armelagos, 2013).

1.2. Wheat

1.2.1. Poaceae, Triticae and Wheat

1.2.1.1. Phylogeny of Poaceae family

Throughout history, more than 391,000 plant species have been identified in nature, but around 30,000 are edible plants of which only about 5,000 have ever been used as food (Figure 1.2). From them, less than 20 species are responsible of most of the food worldwide, with wheat (*Triticum aestivum*), rice (*Oryza sativa*), and maize (*Zea mays*) providing around a 60 % of the total food energy intake worldwide (Harper and Armelagos, 2013; Smýkal *et al.*, 2018; N'Danikou and Tchokponhoue, 2019). These three plant species belong to the large Poaceae family (or Gramineae family, usually named as grasses), constituted by almost 12,000 species of monocotyledonous flowering plants grouped into 740 genera and 12 subfamilies (Bánki *et al.*, 2021).

Traditionally, a functional classification of grasses has been employed based on the plant part under interest and the organism for which they would be used as food, distinguishing *cereals* and *forage grasses*. While cereals (including wheat, barley, rice, oats or maize, among others) have been selected as human and livestock food due to the high starch content present in their grains, the vegetative biomass of forage grasses (fescue, wheatgrass or goatgrass) is usually employed for feeding ruminant animals (Tetlow and Emes, 2017). The economic importance of cereals is indubitable, since over 700 million tonnes are annually harvested worldwide. Only in 2019, world cereal production exceeded 3,000 million tonnes (Figure S1.2), which supposed almost 114 million US$ in cereal exportations (FAO, 2021).

Phylogeny of Poaceae family and *Triticum* genus has been the central goal of multiple morphological, molecular, genetic and metabolomic studies (Löve, 1984; Davis *et al.*, 1985; Kimber and Feldman, 1987; Van Slagern MW, 1994; Inda *et al.*, 2008; Zaharieva *et al.*, 2010; Goncharov, 2011; Weide and Weide, 2015; Kellogg, 2015; Soreng *et al.*, 2015, 2017; Hodkinson, 2018), revealing a higher complexity for the organisation of species than this functional classification, sometimes

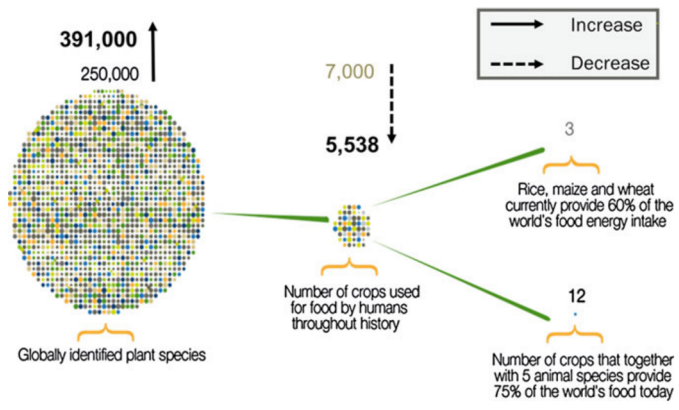

Figure 1.2. World's plant biodiversity and domestication.
Retrieved from (N'Danikou and Tchokponhoue, 2019).

hampered by the use of different taxonomic classifications. Indeed, the biological classification of many living beings is not exempt of controversy. Recently, a unified and hierarchical system called *Catalogue of Life* (*CoL*) was developed bringing together the consensus of more than 3,000 expert taxonomists about the biological classification of more than 1.6 million species (Ruggiero *et al.*, 2015), with public access through its website (https://www.catalogueoflife.org/). This system is supported by two similar projects, including *Species 2000* (https://sp2000.org/) and *ITIS* (*Integrated Taxonomic Information System*; https://www.itis.gov/), and all of them conform an integrated and stable classificatory "backbone" for the *Encyclopedia of Life* (*EOL*, http://eol.org) (Parr *et al.*, 2014).

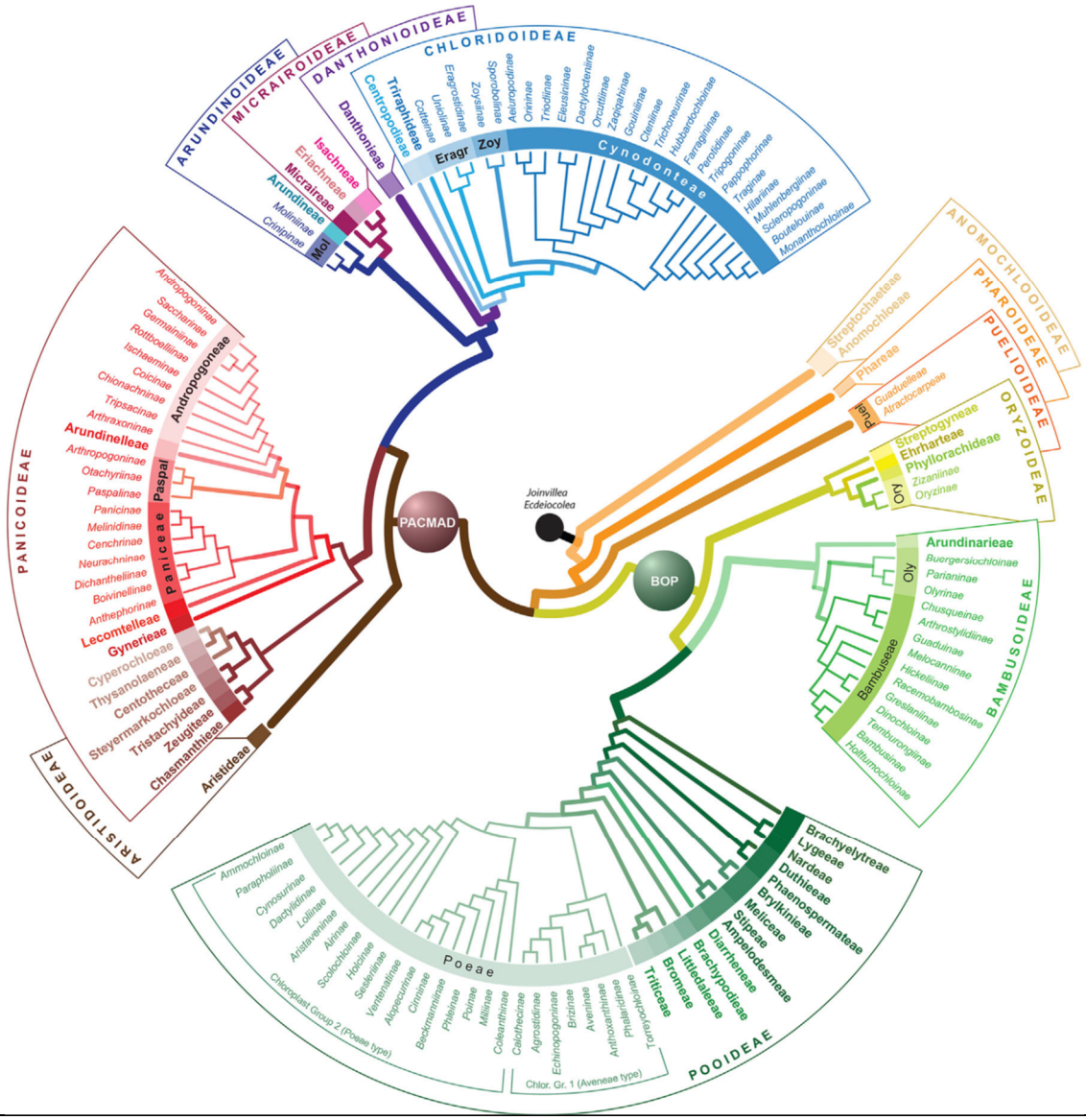

Figure 1.3. Poaceae (grasses) phylogenetic tree.

BOP: Bambusoideae, Oryzoideae, and Pooideae; *PACMAD*: Panicoideae, Aristidoideae, Chloridoideae, Micrairoideae, Arundinoideae, and Danthonioideae.

Thick, medium and thin branches represent subfamilies, tribes and genres, respectively.

Retrieved from (Soreng *et al.*, 2017)

In the following paragraphs, phylogeny of Poaceae species and the *Triticum* genus will be summarised according to literature, but in order to avoid discrepancies among studies due to the use of different taxonomical classifications (mostly associated with the publication date and the classification applied back then), nomenclature found in EoL is employed along the present document.

1.2.1.2. Phylogeny of Triticum genus

Poaceae family evolved at around 55–70 million years ago (Kellogg, 2001), diverging in three basal linages (Anomochlooideae, Pharoideae and Puelioideae) and two clades (BOP and PACMAD) containing the nine remaining subfamilies (BOP: **B**ambusoideae, **O**ryzoideae and **P**ooideae; PACMAD: **P**anicoideae, **A**ristidoideae, **C**hloridoideae, **A**rundinoideae, **M**icrairoideae and **D**anthonioideae; Figure 1.3) (Soreng *et al.*, 2017). From them, the Pooideae sub-family would have diverged around 21 million years ago (Inda *et al.*, 2008), leading to 16 different tribes including Triticeae, a group of 14 genuses including *Triticum* spp. (wheat), *Hordeum spp.* (barley) or *Secale* spp. (rye). *Triticum* spp. includes 13 different polyploid species (Table 1.1) of which only a few are involved in the evolution and domestication of bread and durum wheats, the major currently used forms of wheat (Figure 1.4). With a basic chromosome number of $x = 7$, diploid ($2n = 2x = 14$), tetraploid ($2n = 4x = 28$) and hexaploid ($2n = 6x = 42$) wheats can be found within this genus. As described previously, wheat domestication was placed in the Fertile Crescent area at about 12,000 years ago. First cultivated forms of wheat, the diploid *cultivated einkorn* wheat (*Triticum*

Table 1.1. Taxonomy of *Triticum* spp.

1. *Triticum aestivum* L. (**bread wheat**)
   a. *Triticum aestivum* ssp. *aestivum*
   b. *Triticum aestivum* ssp. *spelta* (L.) Thell. (**spelt wheat**)
2. *Triticum carthlicum* Nevski (**Persian wheat**)
3. *Triticum compactum* Host (**Club Wheat**)
4. *Triticum dicoccoides* (Asch. & Graebn.) Schweinf.
5. *Triticum macha* Dekapr. & Menabde
6. *Triticum monococcum* L. (**einkorn wheat**)
   a. *Triticum monococcum* ssp. *aegilopoides* (Link) Thell.
   b. *Triticum monococcum* ssp. *monococcum*
7. *Triticum soveticum* Zhebrak
8. *Triticum sphaerococcum* Percival
9. *Triticum timopheevii* (Zhuk.) Zhuk. (**Timopheev's wheat**)
10. *Triticum turanicum* Jakubz. (**Oriental wheat**)
11. *Triticum turgidum* L. (**rivet wheat**)
    a. *Triticum turgidum* ssp. *dicoccum* (Schrank ex Schübl.) Thell.
    b. *Triticum turgidum* ssp. *durum* (Desf.) Husn. (**durum wheat**)
    c. *Triticum turgidum* ssp. *polonicum* (L.) Thell.
    d. *Triticum turgidum* ssp. *turgidum*
12. *Triticum urartu* Thumanjan ex Gandilyan (**wheat**)
13. *Triticum zhukovskyi* Menabde & Erizin (**Zhukovsky's wheat**)

Names in bold represent common names of species. Classification retrieved from EoL (http://eol.org)

monococcum ssp. *monococcum*; A^mA^m) would have been domesticated from the wild subspecies *Triticum monococcum* ssp. *aegilopoides* (*wild einkorn*, also called *Triticum monococcum* ssp. *boeticum*; A^mA^m) and substituted by cultivated tetraploid and hexaploid wheats during the last 5,000 years (Tadesse *et al.*, 2016). Previously, around 500,000 years ago, hybridisation between diploids *Triticum urartu* (A^uA^u) and *Aegilops speltoides* ssp *speltoides* (BB) led to the emergence of tetraploid *wild emmer* (*Triticum dicoccoides*; A^uA^uBB). The following cultivation of wild emmer by hunter-gathers at about 10,000 years ago would have led to the advent of the *cultivated emmer* (*Triticum turgidum* spp. *dicoccum*; A^uA^uBB) and the later arise of *durum wheat* (*Triticum turgidum* ssp. *durum*; A^uA^uBB). A second event of hybridisation would have taken place between cultivated emmer and another diploid goat grass (*Aegilops tauschii* spp. *strangulata*; DD), giving rise to the first hexaploid

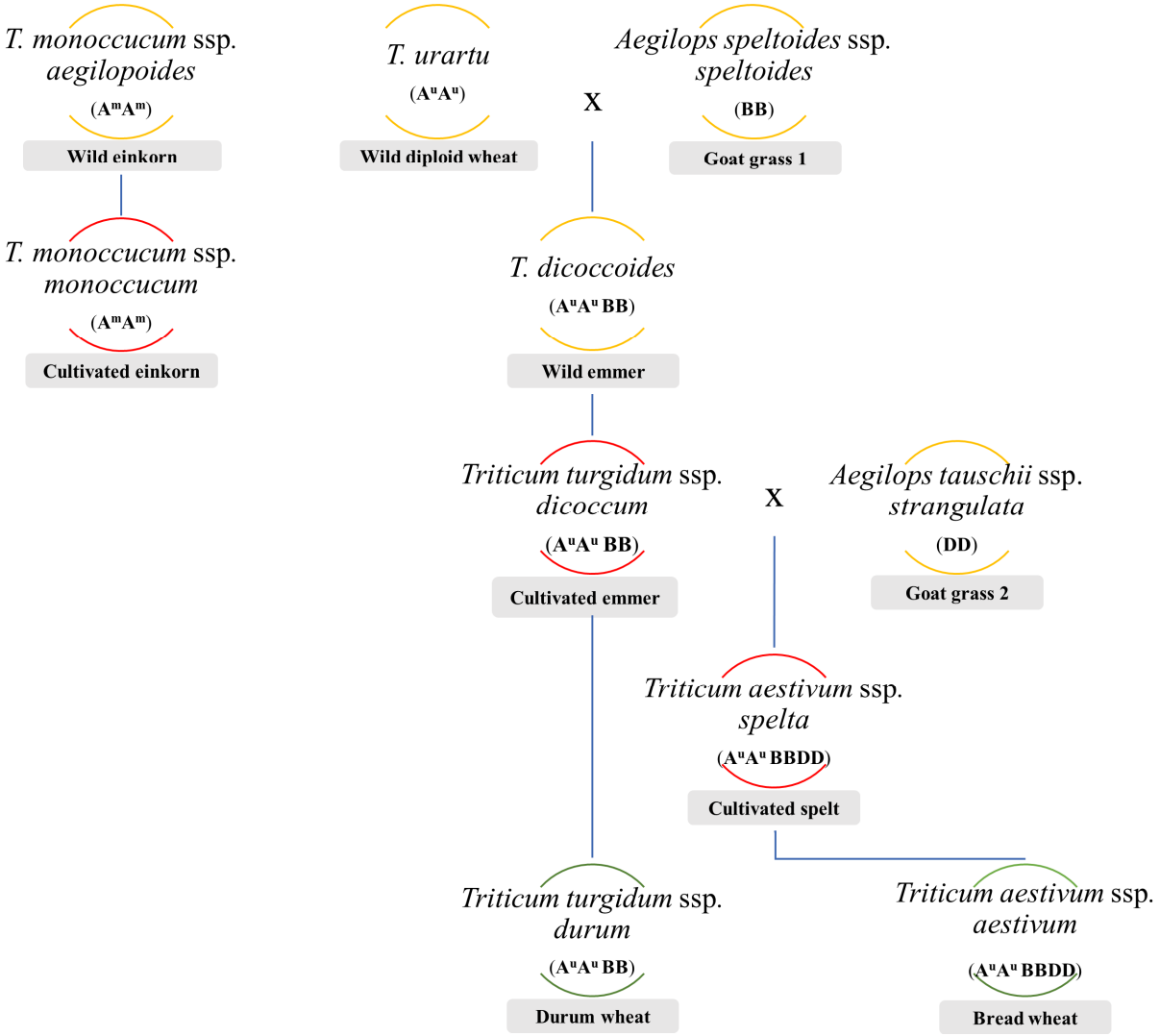

Figure 1.4. Phylogenetic tree of *Triticum* genus.

Proposed evolution tree of wheat. Different colours were employed to identify wild (yellow), cultivated (red) and currently more important (green) wheat species. Bold names inside rectangles represent common names. Present diagram represent the consensus based on (Peng *et al.*, 2011; Tadesse *et al.*, 2016; Arzani and Ashraf, 2017; Haas *et al.*, 2019).

wheat, the *cultivated spelt* (*Triticum aestivum* spp. *spelta*; A^uA^uBBDD), which is considered the most likely ancestor of *bread wheat* (*Triticum aestivum* spp. *aestivum*; A^uA^uBBDD) (Glémin and Bataillon, 2009; Peng *et al.*, 2011; Tadesse *et al.*, 2016; Haas *et al.*, 2019).

1.2.1.3. Domestication syndrome in Triticum genus

In this historical evolution of wheats, there has been two important events linked to domestication of these plants which have had a great impact in the feasibility of wheat cultivation: the *loss of shattering of the ear at maturity* and the *free-threshing ear appearance* (Peng *et al.*, 2011; Abbo *et al.*, 2014). While the first one would have arisen during domestication of wild emmer, leading to tough rachis and non-scattering ears of cultivated emmer at maturity, the low glume tenacity found in durum and bread wheats would have evolved from a natural mutation affecting both emmer and spelt at about 8,5000 years ago. Thus, selection of fragile rachis and free-threshing wheat varieties would have boost efficiency of harvesting.

1.2.2. Wheat anatomy

As an annual grass, bread wheat (also called *common wheat*) undergoes profound changes in morphology along the lifecycle (Anderson and Garlinge, 2000). Thus, the young and the matured wheat plants differ significantly in their structure.

1.2.2.1. Vegetative stage

At an early stage of development, wheat plants are composed by *the main stem* and the *roots*. The main stem (Figure 1.5, a) contains a few *leaves* fully developed or under expansion, the *shoot apex* (the terminal meristem) at the tip of the stem and the *crown* (Nelson and Moore, 2020). The shoot apex is a region of active cell division responsible for the production and initiation of the *leaf primordium* and *auxiliary buds* (which contains the apical meristem of the branches) in the *nodes* (the junction point between the leaf or the branches and the stem) (Taiz *et al.*, 2015). The crown is a structure condensing between 8 and 14 nodes separated by regions of the stem called *internodes* (Anderson and Garlinge, 2000). Two radicular systems can also be found in cereals: *seminal* and *nodal roots* (Figure 1.5, b). Seminal roots are developed from the primordia in the seed and acts as a primary radical system, allowing seed survival during the first steps of the germination. By contrast,

nodal roots (also called adventitious or crown roots) are developed from the crown at the base of the main stem and support the stem along the plant lifecycle (Hoad *et al.*, 2001).

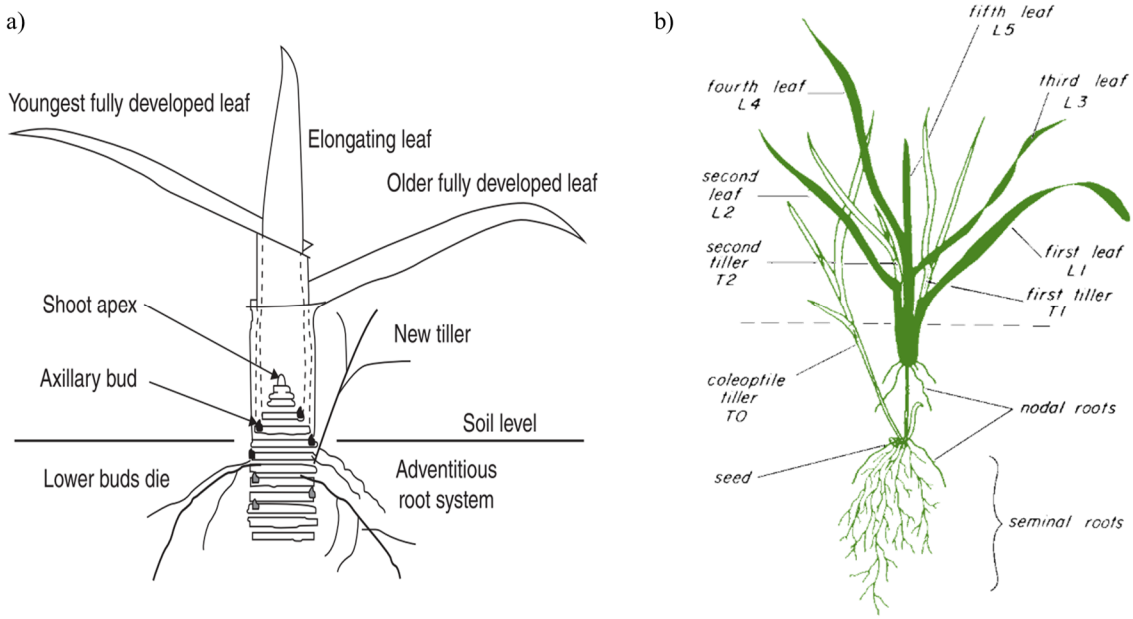

Figure 1.5. Anatomy of wheat plant at the vegetative stage.

Figure in a) shows the main stem and the shoot apex. Primary and secondary root systems, coleoptile, main stem and the first two primary tillers can be observed in figure b).

Retrieved and modified from (Johnson *et al.*, 2017; Nelson and Moore, 2020)

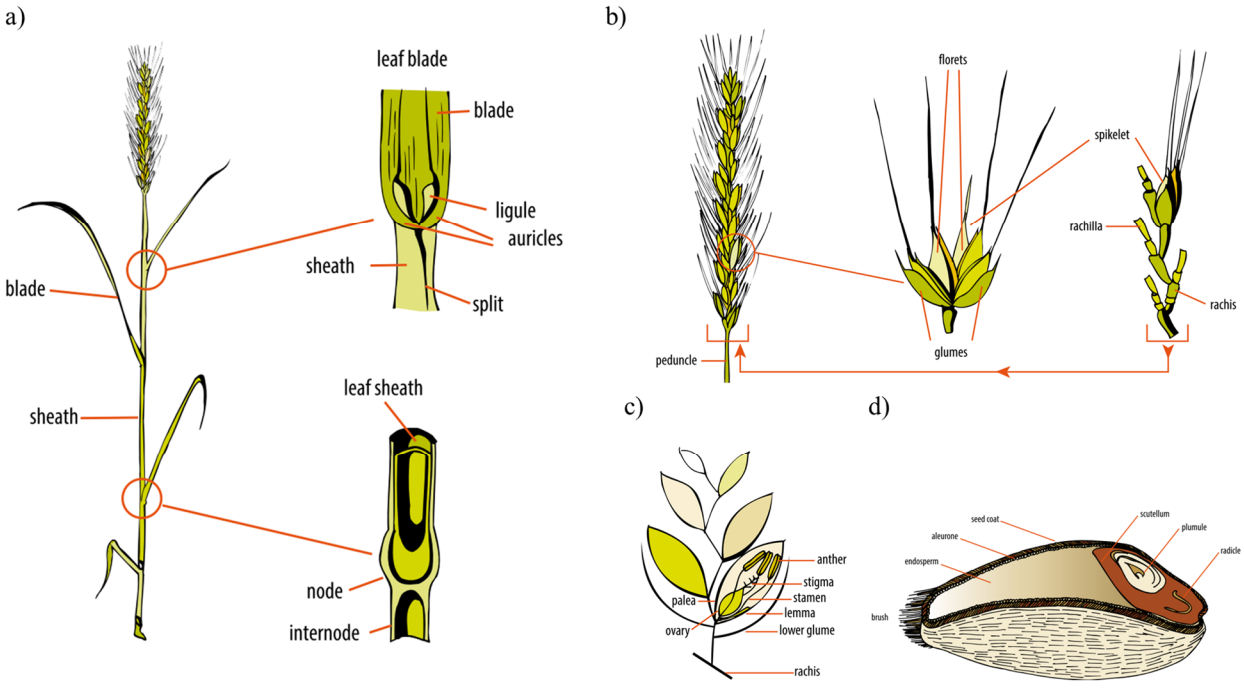

Figure 1.6. Anatomy of wheat tiller at the end of the reproductive stage.

Stem (a), ear (b), floret (c) and grain (d) structures.

Retrieved from (White, 2008)

1.2.2.2. Matured plant

The fully developed wheat plant includes nodal roots and several basal branches, called *tillers*, structurally identical to the main stem (Figure 1.6, a). Tillers are numbered in the plant according to the leaf order in the main stem from which they arise. Shoots are also designated as *primary tillers* when they are originated from leaves on the main stem, while *secondary tillers* are produced from primary tillers. Each tiller is constituted by a variable number of leaves, the stem (made up by the nodes and the elongated internodes) and the *ear*. Wheat leaves are long and narrow, they are disposed alternatively in the stem and they have two different parts: the *leaf blade*, the primary photosynthetic tissue of the plant, and the *basal sheath*, which surrounds the stem of the plant contributing to gain strength. In the point of the stem in which the blade and the sheath join together, lobule structures called *ligule* and *auricles* can also be found. The ear (also called spike; Figure 1.6, b) is the wheat inflorescence composed by a central rachis (a structure similar to the stem) and two rows of *spikelets*. A typical wheat ear has between 15 and 20 spikelets, each one showing ten individual flowers (called *florets*) contained in two chaffy bracts (lower and upper *glumes*). Every single floret (Figure 1.6, c) is enclosed by other two bracts (*lemma* and *palea*) and contains the reproductive organs (*carpel* and *stamens*). The *awns* are extensions of the tip of the lemma (Anderson and Garlinge, 2000; Brinton and Uauy, 2019).

1.2.2.3. Grain anatomy

The wheat *grain* is the typical fruit (unit of reproduction) of cereals, as well as the economic product. Three main constituents can be found in the grain (Figure 1.6, d): the *bran coat* (14 % of the seed) covering the grain; the *endosperm* (83 %), which acts as an storage of starch and proteins; and the *embryo* (*germ* or young plant; 3 %), divided into the *scutellum* (involved into the absorption of soluble sugars), the *plumule* (containing the leaf primordia and the shoot apex) and the *radicle* (a primary root system) (Anderson and Garlinge, 2000; White, 2008). The bran coat is formed by several layers with important attributes for the grain quality. These layers will be described more deeply in section *1.2.4.3. Distribution of nutrients in the wheat grain*.

1.2.3. Wheat development

Although bread wheat is a temperate cereal, some wheat seedlings need to experience temperatures close to 0 ºC for flowering (*anthesis*). This response under low temperatures is called *vernalisation* and the wheat varieties requiring cold for triggering anthesis are called *winter wheats* (S.R. Simmons *et al.*, 1985). Nevertheless, both winter and *spring wheats* (those varieties for which vernalisation is not necessary) show a similar growth development if they are exposed to optimal conditions (Figure 1.7). Even when crop lifecycle is a continuous process, there have been proposed several systems dividing wheat growth development into different stages in order to make easier the description of wheat phenology and the study of genetic and abiotic factor impacts. One of the most popular systems is the Zadoks' decimal code (Zadoks *et al.*, 1974) which classifies cereal phenology, from showing to ripening, in 10 different levels and 100 subcategories (Z00–Z100) based on observable phenotypic characteristics, such as leaf development (Table 1.2). Feekes (1941) and Haun (1973) scales, also employ similar codes but focusing on specific stages of crop development. Although practical, these approaches are essentially limited to the characteristics perceived in the plant, whereas they do not reflect the microscopical changes responsible for the macroscopic phenotypic. For that reason, Slafer *et al.* (2015) divided wheat lifecycle into three major growth stages: *vegetative*, *reproductive* and *grain filling growth stages*.

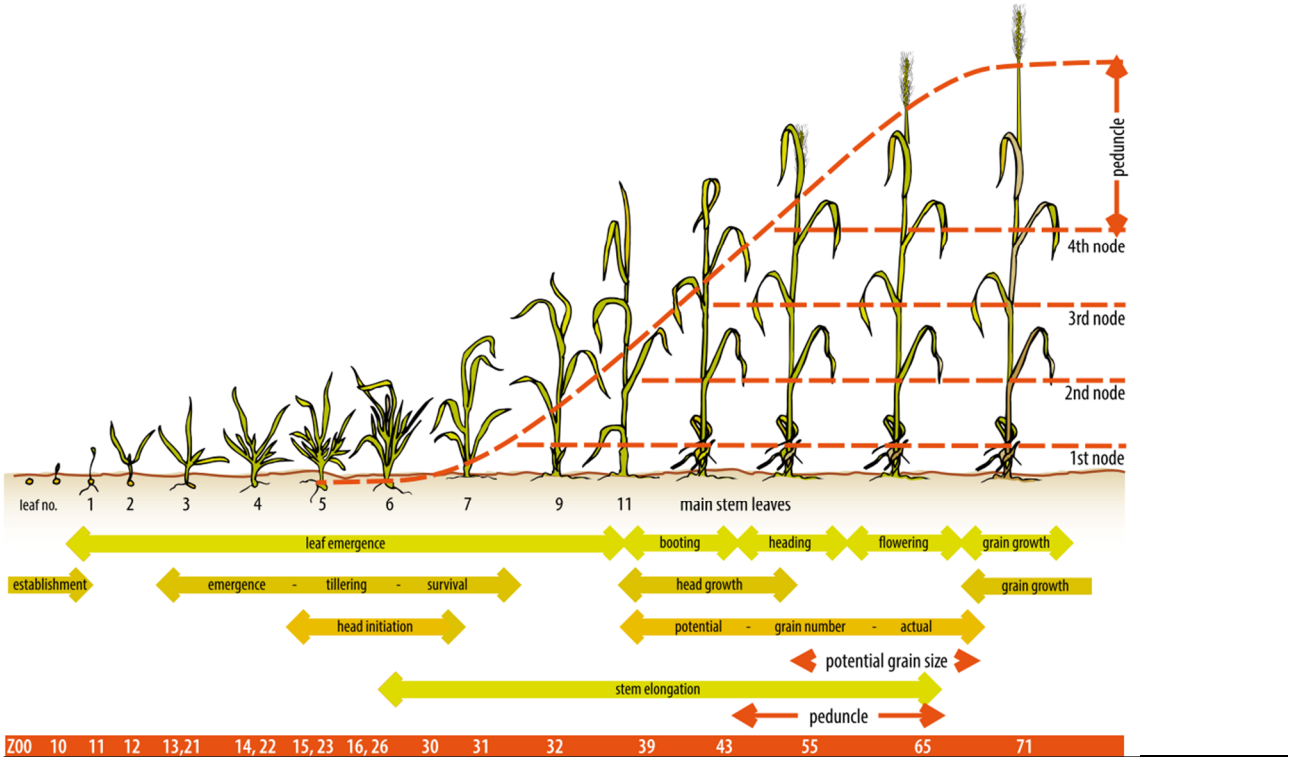

Figure 1.7. Wheat life cycle.

Retrieved from (White, 2008)

Table 1.2. Zadoks decimal code for growth stages.

GERMINATION	SEEDLING GROWTH	TILLERING	STEM ELONGATION	BOOTING	HEAD EMERGENCE	ANTHESIS (FLOWERING)	MILK DEVELOPMENT	DOUGH DEVELOPMENT	RIPENING
00 Dry seed.	**10** First leaf through coleoptile.	**20** Main shoot only.	**30** Stem starts to elongate, "head at 1 cm".	**41** Flag leaf sheath extending.	**50** 1st spikelet of head just visible.	**61** Beginning of anthesis.	**71** Seed watery ripe.	**83** Early dough.	**91** Seed hard (difficult to divide by thumbnail).
01 Start of imbibition.	**11** First leaf unfolded.	**21** Main shoot & 1 tiller.	**31** 1st node detectable.	**43** Boot just visibly swollen.	**53** 1/4 of head emerged.	**65** Anthesis 50 %.	**73** Early milk.	**85** Soft dough.	**92** Seed hard (can no longer be dented by thumbnail).
03 Imbibition complete.	**12** 2 leaves unfolded.	**22** Main shoot & 2 tillers.	**32** 2nd node detectable.	**45** Boot swollen.	**55** 1/2 of head emerged.	**69** Anthesis compete.	**75** Medium milk.	**87** Hard dough.	**93** Seed loosening in daytime.
05 Radicle emerged from seed.	**14** 4 leaves unfolded.	**24** Main shoot & 4 tillers.	**34** 4th node detectable.	**47** Flag leaf sheath opening.	**57** 3/4 of head emerged.		**77** Late milk.		**94** Overripe, straw dead & collapsing.
07 Coleoptile emerged.	**16** 6 leaves unfolded.	**26** Main shoot & 6 tillers.	**36** 6th node detectable.	**49** First awns Visible.	**59** Emergence of head complete.				**95** Seed dormant.
09 Leaf just at coleoptile tip.	**18** 8 leaves unfolded.	**28** Main shoot & 8 tillers.	**37** Flag leaf just visible.						**96** Viable seed giving 50 % germination.
			39 Flag leaf/collar just visible.						**97** Seed not dormant.
									98 Seed dormancy induced.

Numbers in bold represent subcategories of the decimal scale. Based on (Zadoks *et al.*, 1974; White, 2008)

The vegetative stage (Z00–14) starts after the grain is sown. During the first steps of germination, the radicle of the embryo emerges through the *coleorhiza* (a coat protecting the radicle in the embryo) which is shortly followed by the development of seminal roots from a group of cells present in the seed. This root system, comprised by three to six main roots, is soon replaced by nodal roots produced at the level of the first leaf node in the main stem of the plant (Z05). Frequently, the nodal system development is followed by the extension of the *coleoptile*, a sheath which protects seedlings during germination (Z10) (S.R. Simmons *et al.*, 1985; Anderson and Garlinge, 2000; Johnson *et al.*, 2017). Simultaneously, leaf primordia development initiates from the meristem apex, leading to single ridges at opposite sides of the meristem before their elongation and differentiation into leaves. The period of time between consecutive leaf primordium initiations is called *plastochron*, and it is constant along the growth of the plant (Slafer *et al.*, 2015; Nelson and Moore, 2020) at a rate of 4−5 days (S.R. Simmons *et al.*, 1985). After first leaf appearance (Z11), alternate new leaves begin to emerge until 8 or 9 leaves are usually produced (Z18−19) (S.R. Simmons *et al.*, 1985). *Tillering*, the production

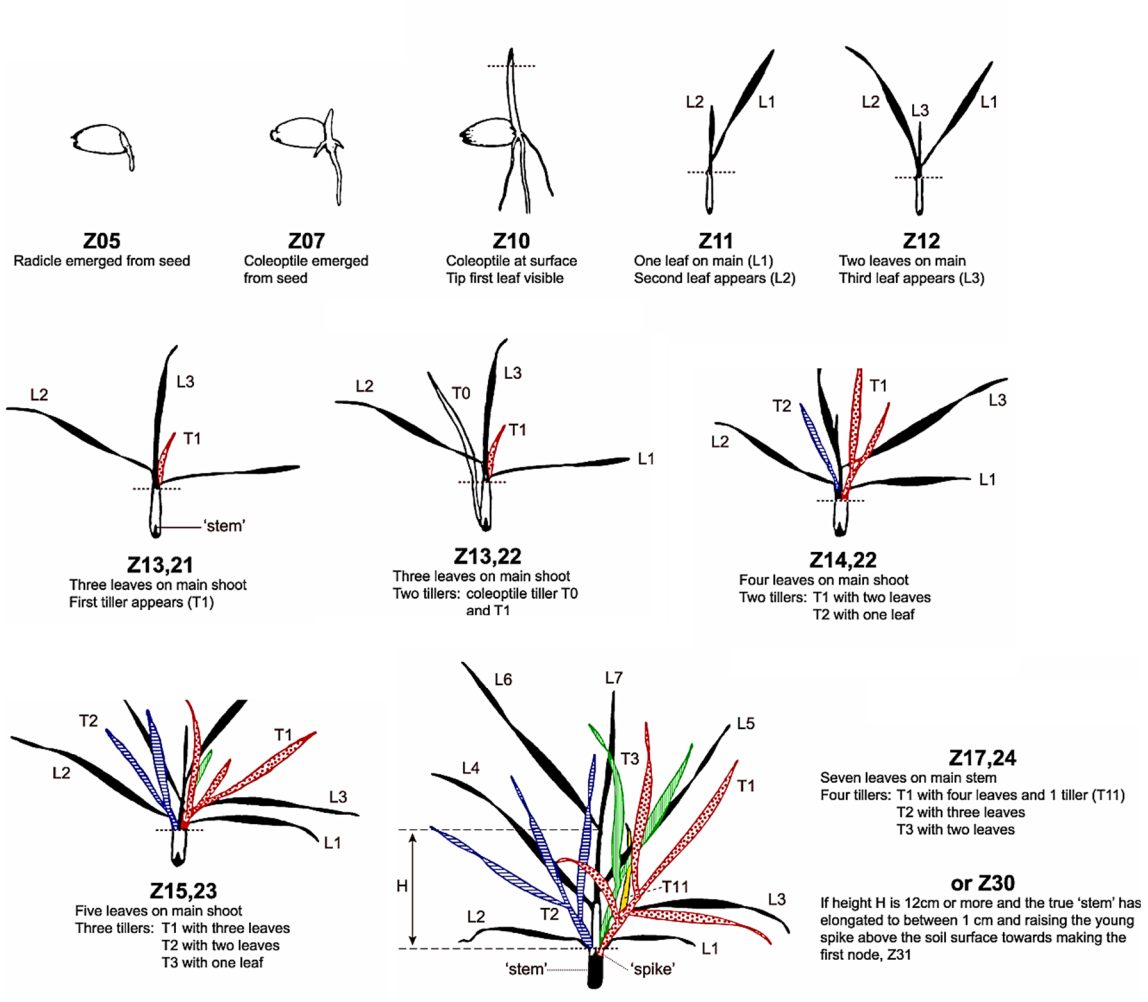

Figure 1.8. Wheat tillering at vegetative growth stage.

Retrieved from (Stapper, 2007)

of new branches, starts approximately at the moment in which the third leaf is also under expansion (Z13,21) from the tiller buds placed in the nodes below the leaves and they start to differentiate sequentially (Figure 1.8). Thus, the first new tiller grows between the first leaf and the main stem; the second tiller grows from the second leaf (Z14,22) while new leaves arise in the first stem; the third stem grows from the third leaf (Z15,23); and so on (Hall and Nleya, 2019). By the time that the second leaf of these new tillers is under expansion, nodal roots are developed at the basal level of each tiller, supporting the whole shoot and thus becoming them independent of the others (Hoad *et al.*, 2001).

In the reproductive stage, the wheat plant reaches its fully developmental structure through three main steps: the *formation of new tillers*, the *elongation of the stems* and the *development of ear*. The end of the vegetative phase starts with the transformation of the apical meristem into the *terminal spikelet* and its expansion (Figure 1.9). In this moment, the shoot apex of the main stem elongates and generates a double ridge instead of a single one (White, 2008). The destiny of lower ridge is to originate a new leaf, but this event never happens so the maximum number of leaves in the stem is determined. The upper ridge differentiates first into the spikelet primordia and then into the spikelets, leading to the development of floret organs (Hyles *et al.*, 2020; Slafer *et al.*, 2021). Thus, the maximum number of spikelets per ear is determined by the time comprised between the floral initiation and the formation of the terminal spikelet in the ear, together with the *spikelet plastochron* (the time between the initiation of one spikelet primordia and the following one). Floret development begins in the most proximal parts of the rachis even before the formation of the terminal spikelet has already finished, and it continuous until the emergence of the flag leaf (Z37) or the early booting (Z41), reaching around 6–12 floret primordia per spikelet (Slafer *et al.*, 2021). At this stage, the production of new roots ceases, but the growth of the existing ones still continues (Johnson *et al.*, 2017). Simultaneously to the beginning of the apical meristem transformation, the elongation of the stem take place from the nodes developed at the vegetative stage after a quick expansion and growth

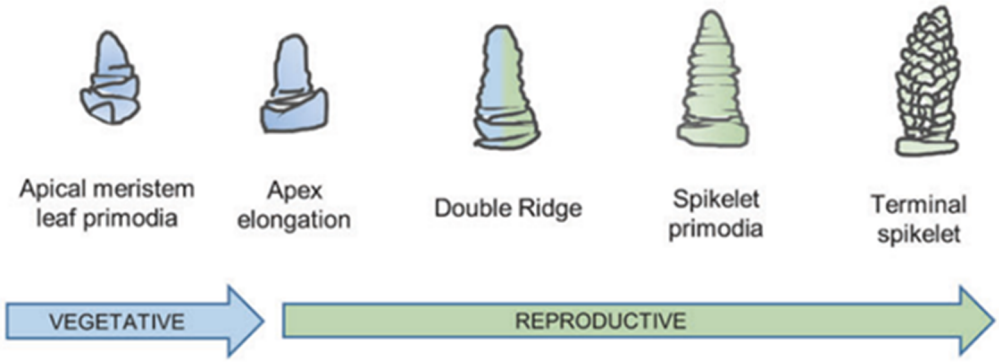

Figure 1.9. Apical morphological changes from vegetative to reproductive stages.

Retrieved from (Hyles *et al.*, 2020)

of the internodes. Stem elongation occurs concurrently with the spikelet differentiation and floret development, although it concludes after anthesis (Z60). It has been suggested that the competition in the use of assimilates for the expansion of the stem and the initiation of florets, which could explain the high rate of floret mortality just after their initiation (Slafer *et al.*, 2021). Pollination occurs prior to anthesis, with the fertilisation of the primary *ovule* of the carpel starting in the basal florets of the spikelets placed in the central portion of the ear, and then expanding along the rachis (McMaster,1997). Between 70 and 90 % of florets become in proper grains during this phase (Slafer *et al.*, 2015).

The ovule of flower plants presents two protective layers, called *integuments*, encasing the *embryo sac* (the female gametophyte). The latter also contains three *antipodal cells* (Figure 1.10, a) of unknown function, two *polar nuclei* and two *synergid cells* flanking an haploid *egg* cell, all of them surrounded by a mass of multinucleate cells (Campbell *et al.*, 2020). After wheat pollination (Figure 1.10, b), the diploid embryo is developed by the fusion of one pollen nucleus and the egg cell. Likewise, the fusion of a second pollen nucleus and the two polar nuclei leads to the formation of a triploid *endosperm nucleus*. This event, called *double fertilisation*, is accompanied by the transformation of the integuments into several layers of maternal tissue, such as the seed coat of the matured grain. Thereafter, the endosperm nuclei experiment an isotropic growth through multiple mitosis without cytokinesis, resulting in the formation of a multinucleate cell (*coenocyte*) with a large

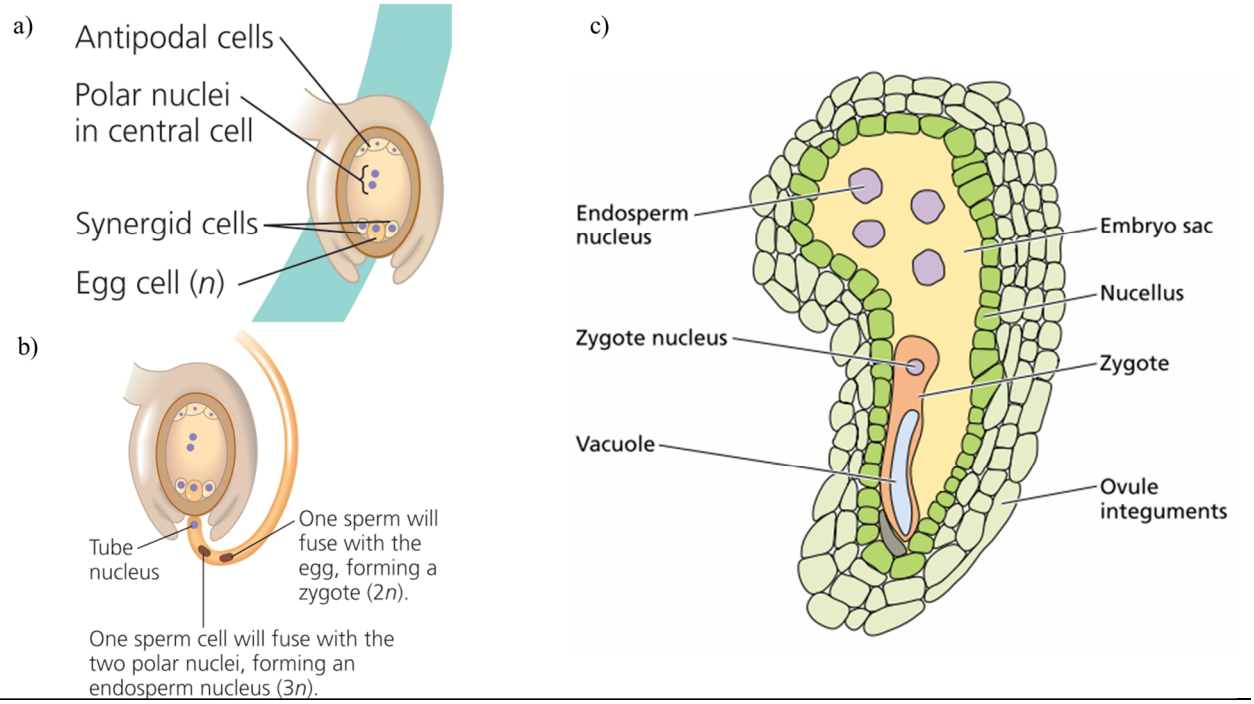

Figure 1.10. Ovule morphology and development after fertilisation.

a) Morphology of embryo sac (female gametophyte) in flower plants. b) Pollination process. c) Ovule of *Arabidopsis* 4 hours after double fertilisation.

Retrieved from (Taiz *et al.*, 2015; Campbell *et al.*, 2020)

vacuole (Figure 1.10, c). Six days after pollination, the endosperm begins to experiment an increase in its size due to several rounds of cell division and expansion, consistent with a progressive raise of *cytokines* and *trehalose-6-phosphate* (T6P) levels that reach their maximums 15 days after fertilisation. Simultaneously, endosperm cells undergo a differentiation process that gives rise of the *starchy endosperm* and *aleurone cells* found in the matured grain (Brinton and Uauy, 2019).

Grain filling stage starts after anthesis (Z70) when the basic structure of the grain has been fully established. It is usually divided in four stages attending on grain growth: *watery*, *milky*, *dough* and *hard stages*. The first stage (the *lag stage*; Z71) is characterised by a rapid increase in grain volume driven by the fast cell division and development experimented by the endosperm, together with an increase in water uptake, creating the strength of each grain. The second stage (Z73–77) involves the accumulation of starch, responsible of more than the 70 % of the total dry matter contained in the grain, and other complex carbohydrates such as *arabinoxylans*. Proteins, the major components of grain quality, are also accumulated in this phase although in a lower proportion whereas water content remained unchanged. Dough stage (80–89) is characterised by the loss of water content and the simultaneous decrease in the rate of grain growth. At the end of this stage, grain water content is still high (almost 40 %), but the grain becomes tough as far as it enters into a quiescent state. After reaching maturity, the grain water content decreases rapidly at the beginning but more slowly as the hard phase (Z90–99) progresses. This stage ends at harvesting (Slafer *et al.*, 2021).

1.2.4. Wheat production and grain quality

1.2.4.1. Wheat production and utilisation

Nowadays, bread wheat represents about 95 % of all wheat crops worldwide while most of the remaining 5 % belongs to durum wheat. The greatest success of bread wheat is based on its high adaptability to different ranges of temperate environments, mostly attributed to the widely plasticity of its hexaploid genome (Mastrangelo and Cattivelli, 2021). By contrast, the tetraploid durum wheat is adapted to more template temperatures and therefore it is usually cultivated in dry and semiarid climates, such as in the Mediterranean basin. Despite their higher tolerance against biotic and abiotic stresses (such as diseases and pests, droughts and extreme temperatures, soil salinity and nutrient shortage or pollution), einkorn, emmer and spelt wheats have been relegated to a secondary position due to their lower yields (Zaharieva *et al.*, 2010; Weide and Weide, 2015; Arzani and Ashraf, 2017). Thus, small populations of these *ancient wheats* have been set aside to some regions of Spain,

Turkery, the Balkans or India (Shewry, 2009). Worldwide, wheat was the crop with the second greatest production in the 2020/2021 marketing year (775.8 million metric tons; Figure 1.11, a) just behind maize (1,125 million metric tons). Wheat production has been constantly increasing since 592

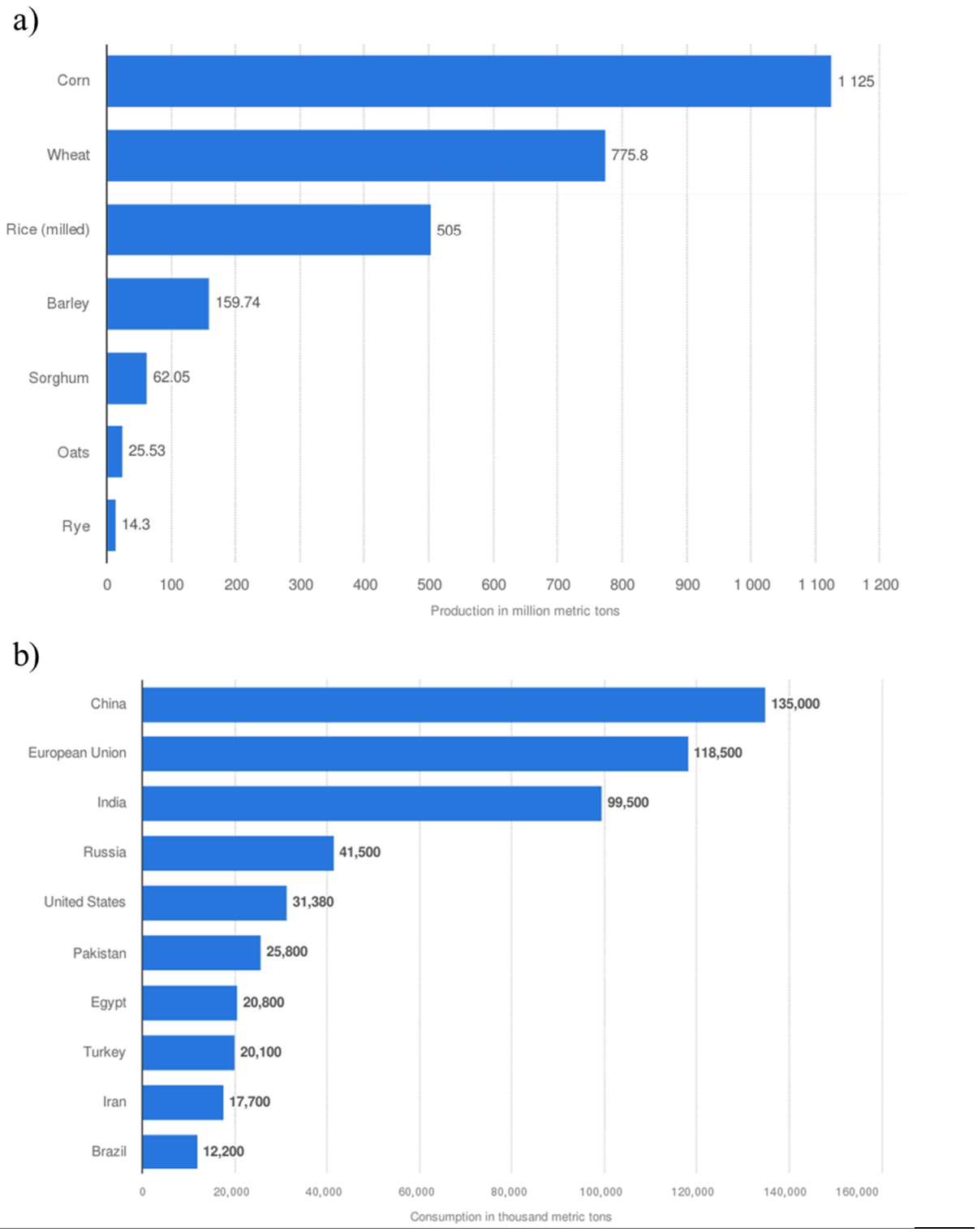

Figure 1.11. Global grain production in 2020/21.

a) Worldwide grain production by type; b) Wheat consumption by country. Only the first 10 countries with the highest wheat consumption are showed.

Retrieved from (Statista, 2019)

million tonnes in 1990/1991, but its utilisation is nowadays heterogeneously distributed among countries (Figure 1.11, b), with China, the European Union and India showing the highest consumptions over 99 thousand tonnes (Statista, 2019).

1.2.4.2. Nutritional constituents of wheat grain

The widely use of wheat as staple food is a consequence of the unique rheological properties showed by the flour of the grain after milling. Its use as a staple food provides almost 20 % of daily proteins and food calories (Arzani and Ashraf, 2017) and provides other valuable nutrients such as vitamins, minerals or bioactive phytochemicals (Wieser *et al.*, 2020) distributed along the different layers conforming the wheat grain bran. Although influenced by the growing conditions, species and genotypes, the chemical composition of the matured grain remains reasonably stable. Carbohydrates represent around 70 % of the total nutrient content found in the grain, but most of this proportion (58 %) belongs to the *starch* content while the remaining carbohydrates (13 %) are mainly *non-starch polysaccharides*. In a lower proportion, *proteins* represent almost the 11 % of the nutrients, followed by *lipids* and *minerals* (2 % each one) and, in a lesser extent, *vitamins* and *phytochemicals* (lower than 0.1 %) (Wieser *et al.*, 2020).

1.2.4.2.1. Carbohydrates

Carbohydrates, especially starch, represents the most abundant fraction of nutrients found in the grain of wheat, although a tendency towards lower starch contents have been found in ancient wheats (Arzani and Ashraf, 2017). Three different types of carbohydrates are usually distinguished according to their length: *mono-*, *oligo-* and *polysaccharides* (Nelson and Cox, 2013).

Mono– and oligosaccharides

Minor contents of *glucose* (Gluc) and *fructose* (Fru) are usually found in the wheat grain (<0.1 %; Figure 1.12, a). *Maltose* and *sucrose* (Suc), the disaccharides formed by two molecules of glucose or by one molecule of glucose and one of fructose (Figure 1.12, b), are also presented in the grain in low proportions (0.1–0.2 % and 0.5–1.6 %, respectively) whereas the most predominant oligosaccharides (0.8–1.9 %) are *fructans* (Wieser *et al.*, 2020). Fructans (Fruct) are complex oligosaccharides based on the molecule of Suc (Figure 1.12, c). The addition of one molecule of Fru to the existing one in Suc, through β(2-1) or β(2-6) bonds, results in the formation of long chains of carbohydrates classified according to the type of bond as *inulins* (β(2–1)), *levans* (β(2–6)), and *graminans* (mixed bonds). If the addition of the new Fru takes place in the C6 of the Gluc residue through a β(2–6) bond, a new molecule called *neoketose* is synthetised and acts as the base for the synthesis of neofructans. These are also classified as *neoinulins*, *neolevans*, and *agavins* (Tarkowski *et al.*, 2019). In cereals, the most

predominant fructans belongs to grasses, although neofructans have also been found in the grain (Cimini *et al.*, 2015).

In plants, Suc is the main soluble carbohydrate in the phloem and the primary form in which photoassimilates are transported through the plant, acting as the main source of energy and *carbon* (C) skeletons for the non-photosynthetic organs (Lemoine, 2000). On the other hand, fructans have been associated with the osmotic modulation, membrane stabilisation and antioxidant responses under plant stresses (Peshev *et al.*, 2013). Nevertheless, both carbohydrates have important functions in animal health. In humans, Suc is mostly hydrolysed into Gluc and Fru in the intestinal mucosa. Whereas Gluc triggers the typical insulinemic response, leading to its own uptake into the cells, Fru is metabolised in the liver through an insulin-independent pathway and the trioses formed are employed for the synthesis of triglycerides. Therefore, Suc can influence both the carbohydrate and lipid metabolisms. Fructans act as *prebiotics* regulating the gastrointestinal microbiota. Thus, fructans are involved in the modulation of blood glucose or pH of the colon, the reduction of the oxidative

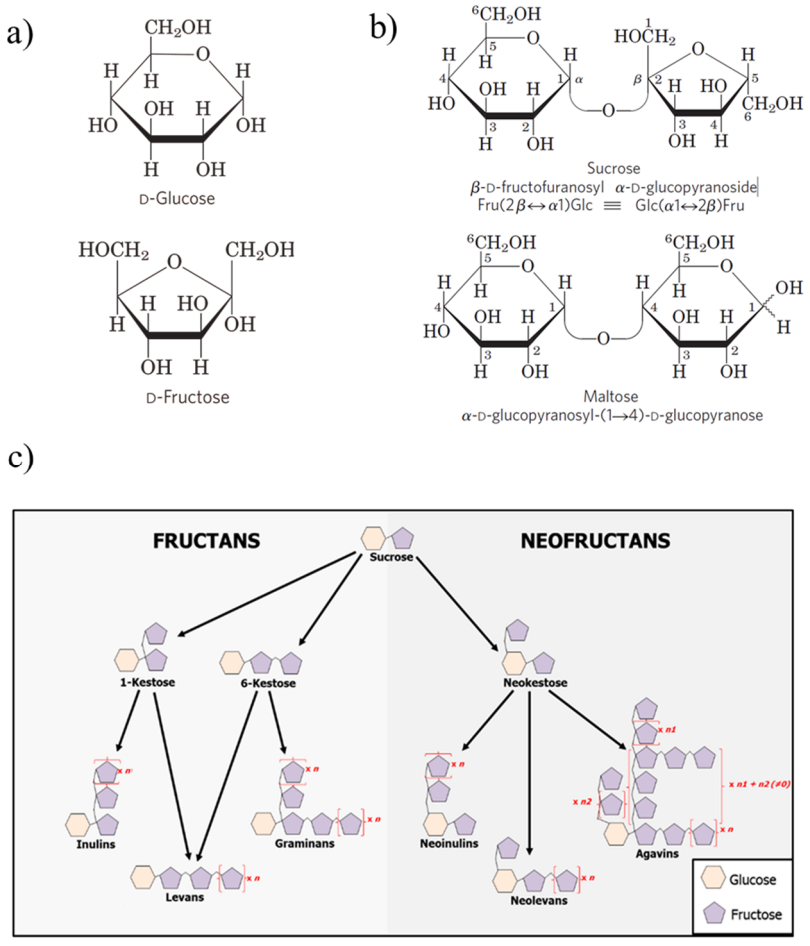

Figure 1.12. Major mono- and oligo-saccharides in the grain of wheat.

a) Structure of glucose and fructose; b) structure of sucrose and maltose; c) structural variants of fructans Retrieved from (Nelson and Cox, 2013; Svara *et al.*, 2020)

stress or the stimulation of the immune system among other functions (Franco-Robles and López, 2015).

Polysaccharides: Starch

Most of the polysaccharides found in the grain are found as water-insoluble, osmotically inert granules of starch presented in the starchy cells of the endosperm. The molecule of starch (Figure 1.13, a) is a polyglucan made up by two types of polymers found in different proportions in the grain: *amylose* (25 %) and *amylopectin* (75 %). Both polymers are chains of D-glucopyranose units, but while these units are linked by α-(1→4) glycosidic bonds forming a linear chain (Figure 1.13, b), the structure of amylopectin is branched due to its α-(1→6) bonds (Figure 1.13, c). In plants, starch has a physiological role acting as a short-term storage of C in several organs (such as leaves), but it can also have a long-term function as a source of energy for the following generation when it is stored in the grain (Tetlow and Emes, 2017). For human nutrition, wheat starch represents the major source of energy (around 11.4 kJ/g of whole grain flour) released during the gastrointestinal digestion by the action of *amylase enzymes.* The resistant starch, around a 3 % of the whole grain flour, represents a proportion of starch inaccessible to amylases in the upper gastrointestinal tract and the small intestine. Therefore, it is fermented by the microbiota of the colon, promoting a normal function of the large intestine. They are also involved in other health benefits, such as improved insulin sensitivity, lower levels of fatty acids in the body or reduced oxidative stress (Wieser *et al.*, 2020).

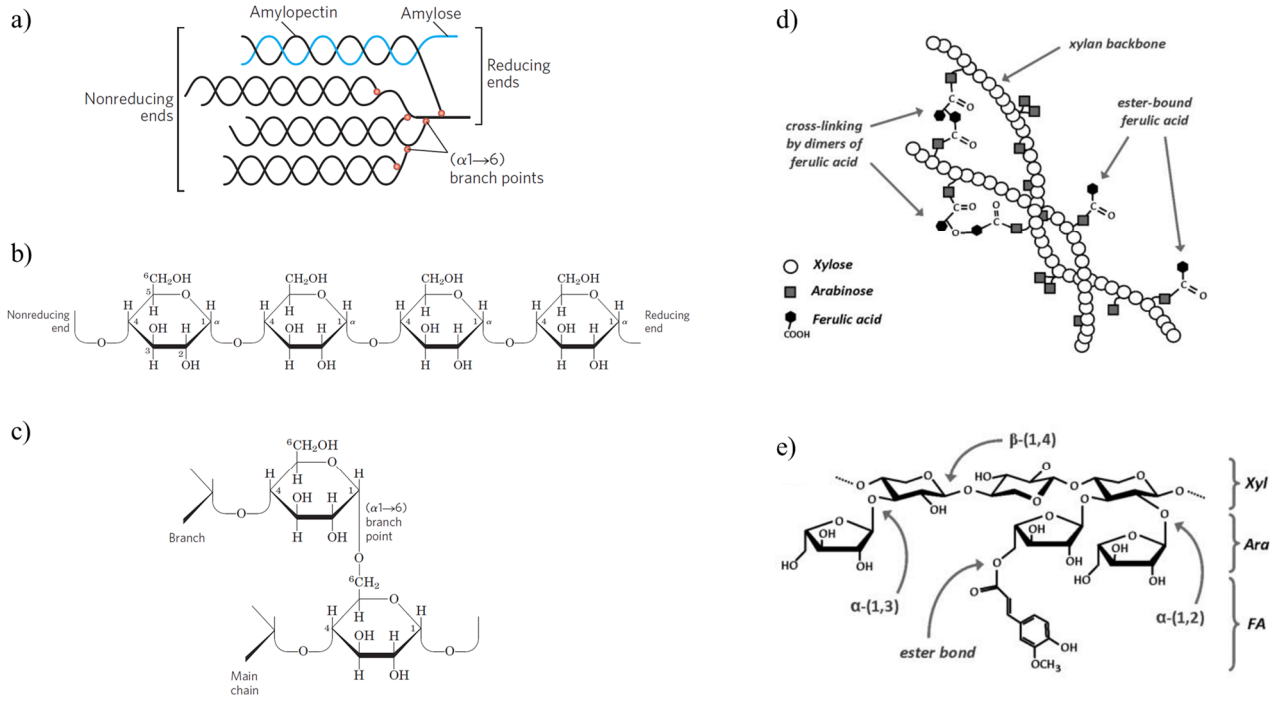

Figure 1.13. Structure of major polysaccharides in the wheat grain.

Ara: arabinose; *FA*: feluric acid; *Xyl*: xylan.

a) basic structure of starch; b) segment of amylose; c) a branch of amylopectin; d) general structure of arabinoxylanes; e) chemical structure of arabinoxylanes

Retrieved from (Brouns *et al.*, 2012; Nelson and Cox, 2013)

Dietary fibre

Dietary fibre (DF) refers to a compound complex containing fructans and *cell wall polysaccharides* (including non-starch polysaccharides and *lignin*) which escape of the hydrolytic digestion in the upper part of the gastrointestinal tract (Onipe *et al.*, 2015; Shewry and Hey, 2015).

Among the non-starch polysaccharides, the *arabinoxylanes* (AXs) represents the major component in the grain (5.5–7.4 %), followed by *cellulose* (1.7–3.0 %), *β-glucans* (0.5–1.0 %) and other polysaccharides of minor proportions (*glucomannan*, *callose*, *xyloglucan*, and *pectins*) (Wieser *et al.*, 2020). AXs are composed by α-(1,3) and/or α-(1,2) chains of *α-L-arabinofuranose* (*arabinose*) units with esterified ferulic acid residues, all of them linked to long backbones of *β-(1,4) xylan* molecules (Figure 1.13, d and e). AXs show a high diversity of structures due to their high degree of branching, the distribution of arabinose chains and their polymerisation, which also influence their physical properties (Brouns *et al.*, 2012). β-glucans present glucose residues linked by (1→3) and (1→4) bonds with low solubility (Shewry and Hey, 2015).

Evidence about beneficial wheat fibres are widespread in literature, but largely unexplored. Although sometimes it remains unclear, the mechanism of action proposed for these fibres includes the stimulation of beneficial colonic bacteria growth through the manipulation of the content and the composition of non-digestible carbohydrates in the diet (prebiotic) (Shewry and Hey, 2015). A rich diet in AXs has been associated with a reduction in the risk of developing diabetes type II, linked to lower postprandial glycaemic response and the modulation of intestinal microbiota. It has also been associated with antioxidative properties from *in vitro* experiments (de Sousa *et al.*, 2021). Similarly, β-glucans can play a role in the regulation of the immune response against tumors and inflammatory processes (Shewry and Hey, 2015).

1.2.4.2.2. Proteins

The wheat grain protein fraction is the most important nutritional component of the grain as far as its content and composition determines the bread-making qualities of wheat (Wieser *et al.*, 2020). The wheat protein content generally represents between 9 % and 18 % of the whole grain, but modern wheats seem to have lower contents than ancient species. Bread wheat used for cakes and biscuits contains between 7 % and 11 % of proteins whereas wheat flour employed for bread requires a 12 % or higher proportion. Durum wheat also provides more proteins and amino acids than most of the cereals but it is still lower than ancient wheats such as einkorn, whose protein content is ranged between 15.5–22.8 % (Arzani and Ashraf, 2017; de Sousa *et al.*, 2021). Interestingly, spring wheats

also shows lower protein concentrations than winter wheats, highlighting that proteins also differs among varieties of the same specie (Zörb *et al.*, 2018).

Both the content and the composition of proteins depend on genetic and environmental factors. More than 100 different proteins have been identified in the whole protein fraction found in the grain of wheat and are classified according to their functions as storage, metabolic, protective and miscellaneous proteins (Wieser *et al.*, 2020). However, the most popular classification of grain proteins is based on the work performed by Osborne (1907) based on their different solubilities in several solvents. Thus, bread wheat proteins are currently grouped in *gluten* and *non-gluten* proteins (Figure 1.14). The gluten fraction includes a group of structural and evolutionary related proteins highly rich in proline, defined as *prolamins*, which represents around 85 % of the total protein content of the wheat grain endosperm (Ma *et al.*, 2019). Once upon mixed with water, the prolamins produce an insoluble viscoelastic aggregate known as *gluten*, which is mostly responsible for the rheological properties and structure of dough (Mastrangelo and Cattivelli, 2021). According to their molecular weight, gluten proteins can be divided into monomeric *gliadins* and polymeric *glutenins*. Gliadins are monomeric proteins of 28–55 kDa of weight and soluble at diluted alcohols (70 %). Based on their mobility in a electrophoretic gel at low pH, gliadins are split up into the cysteine and methionine high-rich *α-*, *β-*, *γ- gliadins*, and *ω-gliadins*, which do not have cysteine residues (de Sousa *et al.*, 2021). Glutenins, which are partially soluble in acids and bases, show long chains of polypeptides of variable length linked by intermolecular disulphide bridges (Thierry and Larbi, 2018). They can be classified as *low-molecular weight glutenins* (LMW; 30–45 kDa) and *high-molecular-weight* (HMW; 70–90 kDa) (de Sousa *et al.*, 2021). Non-gluten proteins include water-soluble *albumins* and soluble

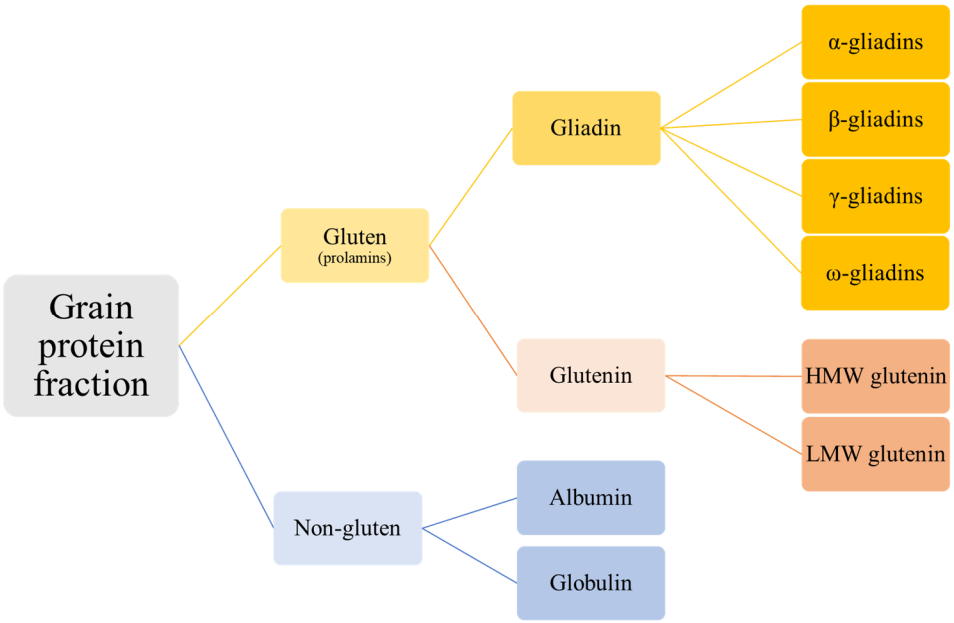

Figure 1.14. Wheat grain protein fraction.

Retrieved from (Brouns *et al.*, 2012)

globulins to neutral-saline solutions. They are associated with structural and metabolic functions and can form polymers through the formation of disulphide bonds. Metabolic proteins include different types of hydrolases (amylases, peptidases, lipases), oxidoreductases or transferases among other enzymes (Wieser *et al.*, 2020).

Individually, gliadins and glutenins are essential during the bread formation process. Gliadins are responsible for the viscosity and extensibility properties of the dough while hydrated glutenins provides strength and elasticity. However, it is the combined effect of both prolamins which allows the formation of the gluten network and its ratio determines its essential quality and end use (de Sousa *et al.*, 2021). The nutritional value of wheat grain proteins is defined by the contents of the essential amino acids *isoleucine*, *leucine*, *lysine*, *methionine/cysteine*, *phenylalanine/tyrosine*, *threonine* and *valine*, together with *arginine* and *histidine* (Wieser *et al.*, 2020). Although consumption of wheat-based food is highly recommended due to its excellent nutritional profile, some immune-mediated adverse reactions have been described. These hypersensitivities, usually referred as wheat-related disorders, includes *celiac disease*, *gluten ataxia*, *dermatitis herpetiformis*, *non-celiac gluten sensitivity* or *irritable Bowel syndrome* (Wieser *et al.*, 2020). Although the causes in some of these diseases are not completely known, it has been confirmed that α-and ω-gliadins are responsible of celiac disease and wheat intolerance (Ma *et al.*, 2019).

1.2.4.2.3. Minor constituents

Minor nutritional components of grain weight (2 % or lower) include *non-polar* and *polar lipids*, such as triacylglycerols or free fatty acids, *E* and *B vitamins* (especially B_1, B_2, B_3, B_6 and B_9), K, P, Mg, Ca, Zn, Mn and Fe *minerals* and *phytochemicals*. The latter are defined as non-nutritive active biomolecules with beneficial effects in human health, promoting well-being and preventing illnesses (Wieser *et al.*, 2020).

Terpenoids and *phenolic compounds* are the major phytochemical components of the wheat grain. Terpenoids are biomolecules derived from the five-carbon molecule *isoprene*. Wheat grain includes three major terpenoids:

- *Sterols*: They are *steroid alcohols* divided into:
  - *4- desmethyl sterols*: It is the most abundant sterol in plant tissue.
  - *Stanols*: A saturated form of sterols. It is presented in cereals.
- *Tocols*: A chromanol ring containing a phytol side chain in C16. Includes:
  - *Tocopherols*: The phytol chain is saturated.
  - *Tocotrienols*: Containing three double bonds at C3, C7 and C11.

- *Carotenoids*: They are derived from long chains of polyenes containing 35–40 carbon atoms with two major forms:
    - *Xanthophylls*: They contain oxygen atoms and include *lutein* and *zeaxanthin.*
    - *Carotenes*: They are unoxygenated carotenes. Include *α*- and *β-carotenes*.

Phenolic compound structure includes an aromatic ring with at least one hydroxyl group. It conforms the largest and the most complex and diverse group of secondary metabolites found in the grain of cereals.

- *Phenolic acids*: This is the greatest group of phenolic compounds. They are derived from cinnamic or benzoic acids and they can be found as free compounds, soluble conjugates linked to low molecular weight compounds or bound to cell wall polysaccharides. The most abundant phenolic acid in wheat is *ferulic acid.*
- *Flavonoids*: They are based on a 15-C ring structure.
- *Lignans*: Polyphenols derived from phenylalanine.

Multiple positive effects have been associated with phytochemicals in human health, including antioxidant properties or improved vascular functions, although further investigations seem to be necessary to verify these functions (Shewry and Hey, 2015). Much more attention has been recently paid to phenolic compounds due to their antioxidant properties, preventing or delaying the oxidative stress (Žilić, 2016; Leváková and Lacko-Bartošová, 2017), but other health benefits, such as intestinal microflora modulation, have also been attributed to phenolic compounds (Hernández *et al.*, 2011).

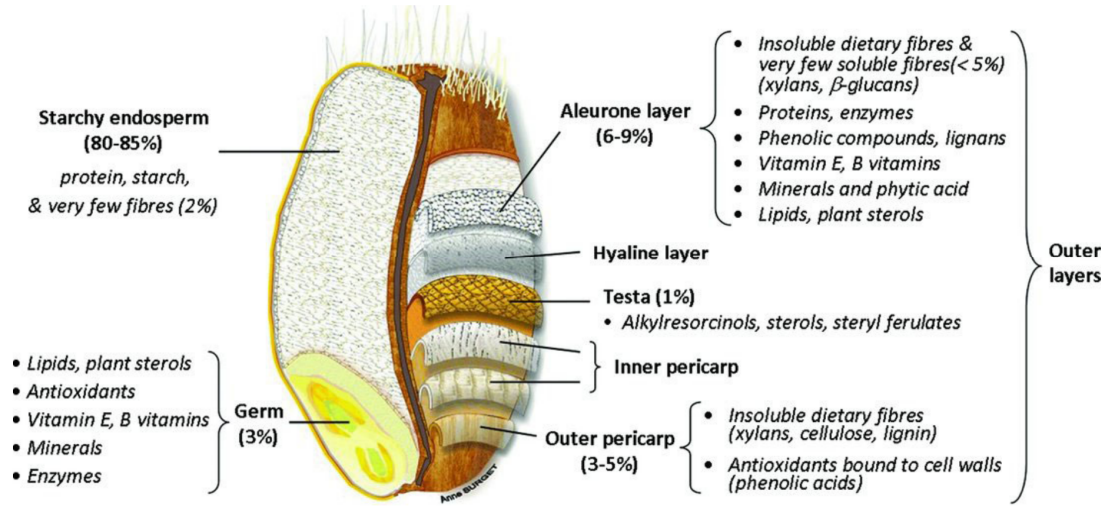

Figure 1.15. Nutritional wheat grain structure.

Modified from (Onipe *et al.*, 2015)

1.2.4.3. Distribution of nutrients in the wheat grain

All these nutritional components can be found distributed along the different layers conforming the grain of the wheat. These layers are characterised by different structures and compositions which are the result of their varietal functions during grain development (Figure 1.15). The endosperm retains most of the starch and proteins found in the grain, as well as a few fibres (around 2 %), while the remaining nutrients (vitamins, minerals phytochemicals and the majority of the fibres) are concentrated in the embryo (usually called germ when it is referred for its nutritional value) and the bran (Brouns *et al.*, 2012). Indeed, the greatest percentages of proteins are usually found in the grain germ (34 %) (Wieser *et al.*, 2020).

From the inside to the outside, the grain bran is composed by the *aleurone* layer, the *nucellar epidermis* (*hyaline layer*), the *testa* and the inner and outer layers of the *pericarp*. The aleurone layer is formed by a single layer of living cells representing almost a 50 % of the grain bran. Botanically, it conforms the outer layer of the endosperm but because it remains attached to the hyaline layer at grinding, it is usually considered as the insider layer of bran. More than 40 % of the mass contained in this layer is found in the very thick non-lignified cell walls displayed by the aleurone cells, which mostly contains AXs (65 %) and β-glucans (29 %), although proteins, minerals and B vitamins can also be found. While the hyaline layer is very rich in poorly cross-linked AXs, the testa contains predominantly lignin and the pericarp has insoluble dietary fibres (lignin, cellulose and xylans) and ferulic acid (Brouns *et al.*, 2012).

1.2.5. Yield components.

At the same time that the grain emerged as the most economic value part of the wheat plant, yield has become the major target of breeders. Grain yield results from the ensemble of two main components: the *average grain weight* and the *number of grains* per square metre (Figure 1.16). The latter one is also driven by both, the *number of grains per ear* (the product of *grains per spikelet* and the *spikelets per ear*) and the *number of ears* per square metre (brought by the *ears per plant* and the number of *plants per square metre*) (Slafer, 2007; Johnson *et al.*, 2017). This approximation has allowed the study and description of major determinants of grain, providing opportunities for the improvement of productivity. Theoretically, it also suggests that variations in wheat yield can be accomplished by the improvement or the reduction of any one of this components, but experimental studies have shown that modifications of yield determinants lead to a compensation by the remainders

with almost no modification on productivity (Anderson and Garlinge, 2000). These results highlight the complexity behind yield and bring out the need of a dynamic perspective of yield, now understood as the integration of multiple interactions between growth and development, the influence of genotypic diversity and the effect of the environmental factors (Slafer *et al.*, 2021). Studies performed for understanding the intricate wheat productivity have revealed important clues about the regulation of yield determinants. Some of them are summarised hereunder.

1.2.5.1. Determination of grain weight

The final grain weight is determined by many factors. Genetic and environmental variations influence grain development, altering the grain weight within genotypes, among plants of the same cultivar, along the ears of the same plant or even across an ear. Here, major determinants of grain weight have been grouped into *factors directly influencing grain development* and *sink-source limitation*s.

1.2.5.1.1. Factors influencing grain development

Differences in the growth of the grain have been associated with *limitations imposed during the own grain development* and *by maternal structures*.

Most of the research focused on the determination of grain weight potential have pointed at the watery phase of the grain filling as the critical stage for grain size achievement. This is consistent with the rapid grain development observed in this stage (or phase) due to the high rate of cell division experimented by the endosperm cells, suggesting that the weight of the grain could be conditioned

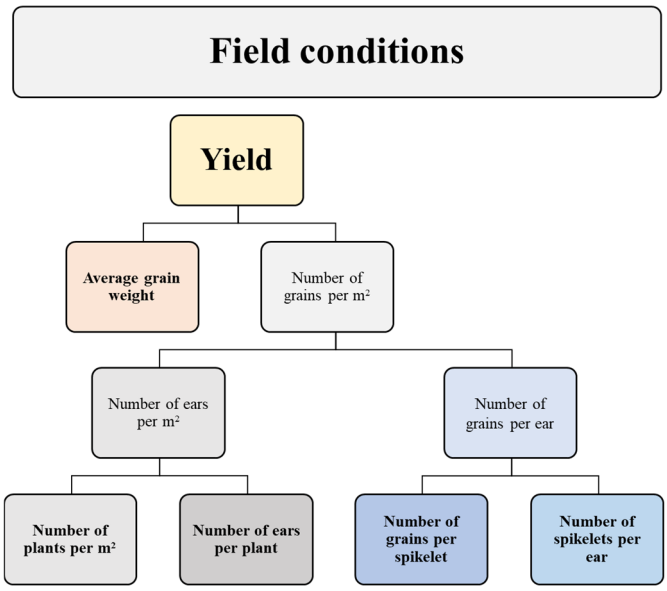

Figure 1.16. Yield and yield components.

Modified from (Slafer *et al.*, 2021)

by the number of these cells (Slafer, 2007). Indeed, it has been found that the expression of the genes *GW2* and *OsSPL16* can regulate grain size through limiting or promoting grain cell proliferation in wheat, respectively, which reinforce the theory of grain weight modulation due to cell number (Brinton and Uauy, 2019). However, the association found between the grain weight potential and a group of *expansins* and *XTH* genes involved in cell wall loosening and cell expansion indicates that cell size could also influence final grain weight (Slafer *et al.*, 2021). In this line, it has been characterised the genetic influence of several grain weight subcomponents (length and width), together with several genes with demonstrated roles in the metabolism of starch, such as the activity of the enzymes *ADP-glucose pyrophosphorylase* or *sucrose synthase 2* (Brinton and Uauy, 2019). These latest findings suggest that grain weight potential could finally be regulated by the accumulation of carbohydrates in the increasingly numerous starchy cells of the endosperm.

There is also evidence of grain growth limitations caused by non-grain tissues. The study carried out by Calderini *et al.* (2001) evaluating the effect of high temperature at pre- and post-anthesis on several genotypes showed a reduction in grain weight due to increases in temperature at the period comprised between booting and anthesis, indicating that not only the post-anthesis period but also pre-anthesis is important for the setting of grain size. Nevertheless, this study also found a strong relationship between the weight of the grain and the size of the carpels at anthesis. Since carpel growth happens a few days before anthesis, these findings suggest that grain expansion could be limited by the size of the carpels inside the florets (Calderini *et al.*, 2001; Slafer, 2007). Indeed, the inhibition in grain growth as a consequence of the physical pressure applied by the glume, lemma and palea bracts of florets indicates that the own floret volume could also be constraining grain size development, as suggested by Brinton and Uauy (2019).

1.2.5.1.2. Sink–source limitation

Grain weight potential is determined by events happening at pre- and post-anthesis. However, the transition of this potential into all the grains of the plant (the sink) depends on the supply of nutrients along the grain-filling stage (the source) from both, the own assimilation at this growth phase or the water-soluble carbohydrates accumulated until anthesis (Fischer, 2011). Investigations performed by different researchers exploring the impacts of source-sink manipulations during grain filling on grain weight potential under multiple conditions (including different treatments, environmental factors or genetic backgrounds) have found little or non-significant variation in the weight of the grain at maturity. This indicates that sink limitation could dominate over source availability of assimilates during grain filling, affecting to the capacity of the grain for growing. All together, these results

pointing to unlikely competition among grains for assimilates after the watery stage of grain filling (Slafer, 2007).

1.2.5.2. Grain number and its influence over grain weight

Grain number is also an intricated parameter and its variation is usually associated with changes in wheat productivity. The origin of the complexity is based on the high number of components of the grain number and the compensatory relationships established among them, causing no variations in grain yield even with modification in one of these determinants. Grain number usually presents a negative association with grain weight and the most common explanation includes the competition of resources for grain formation and growth. However, this perspective does only take into account the translocation of assimilates, without considering if a real compensation relationships is happening (Slafer *et al.*, 2021).

Additionally, as it has been described above, the grain weight seems to be sink-limited since modifications in the availability of assimilates after anthesis did not alter the size of the grain. Fischer (1985) synthesised previous works exploring the effect of artificial shading and temperature on the grain number per square metre in wheat crops at different weather conditions, sowing dates and locations. One of the most important conclusions of this work was that both grain yield and number were especially sensitive to radiation and temperature during the 30 days before anthesis, indicating that grain number is source limited and the final number of grains is achieved by the accumulation and allocation of assimilates during this critical period of time (Slafer, 2007). In this regard, the grain number has also been linked with the dry weight of the ear accumulated at flowering and the partitioning up to florets (Fischer, 2011). In bread wheat, the pollination event happens before anthesis when floret primordia are completely developed, and most of the matured florets became into grains because plants of this species are *cleistogamous*. Thus, final grain number is determined by the rate of floret survival, which is dependent on nutrient availability.

These results point to that the number of grains would be conditioned by the dry weight in the ear through the translocation of assimilates to developed florets, influencing their survival ratio and their transformation into fully grains (Slafer *et al.*, 2021). In line with this observation, the increased number of grains observed in semi-dwarf plants is consistent with the fact that stem elongation occurs at the same time that floret setting, indicating that a shorter elongation could improve found translocation to the developing florets and promote their survival (Trethowan *et al.*, 2007). Nevertheless, this proposition does not explain the negative relationship between grain number and grain weight. To achieve that explanation, it should be taken into account that the terminal primordia

grow and develop at different rates, so spikelets and ears are initiated and developed at different times. It could even happen that anthesis takes place at different days along a single ear. Indeed, spikelet development starts at the middle of the ear towards the top or the bottom, while floret development goes from the bottom of the spikelet and later ascend (Brinton and Uauy, 2019). Therefore, the negative relationship would not necessarily involve competition amongst growing grains. Instead, it could implicate other non-competitive causes, such as an increase in the number of grains in the distal positions of the ear which would lead to a higher number of grains, but with smaller size (Slafer *et al.*, 2021).

In summary, the number of grains set and the grain weight potential is achieved in a short, but critical, period of time comprised between 3 weeks before flowering and 7 days after anthesis. This period is the most important since major changes in yield are influenced by variations in floret development and setting, size and number of cells in the grain and translocation of assimilates to the ear during this period of time.

1.2.6. Green revolution.

1.2.6.1. Historical overview

From 1960 to 2000, the global production of the three major cereal crops (wheat, rice and maize) increased almost three times (Figure S1.3) (FAO, 2021). This historic breakthrough in yield potential was the results of the *Green Revolution* (GR), a set of political strategies and agricultural improvements based on the development and quickly spread of modern cereal crop varieties, known as *high yielding varieties* (Chhetri and Chaudhary, 2011). The development of these varieties took place at the *International Rice Research Institute* (IRRI) of Philippines and at the *International Maize and Wheat Improvement Centre* (CIMMYT) in Mexico, and involved six major genetic strategies to achieve greater crop productivity and yield adaptability (Khush, 2001), including:

- Selection of varieties with improved yield potential.
- Enhancement of crop adaptability to multiple environments.
- Reduction in growth duration.
- Resistance to diseases and insects (biotic stress).
- Tolerance to abiotic stress.
- Grain quality improvements.

The unequal improvements in wheat production among countries (Figure 1.17) reflects the variations in the adoption of GR techniques among the countries through the time. Even though, two different stages of GR are globally differentiated. The *early GR* comprised the first steps of GR between 1960s and 1970s and it was based on the development and quick adoption of a productive "plant type" with better yield potentials, in conjugation with the improvement of some farming techniques such as the expansion of irrigation and the use of agrochemicals. The *late GR* (1981–2000) differed in several important aspects including reduction in prices and the expansion of modern

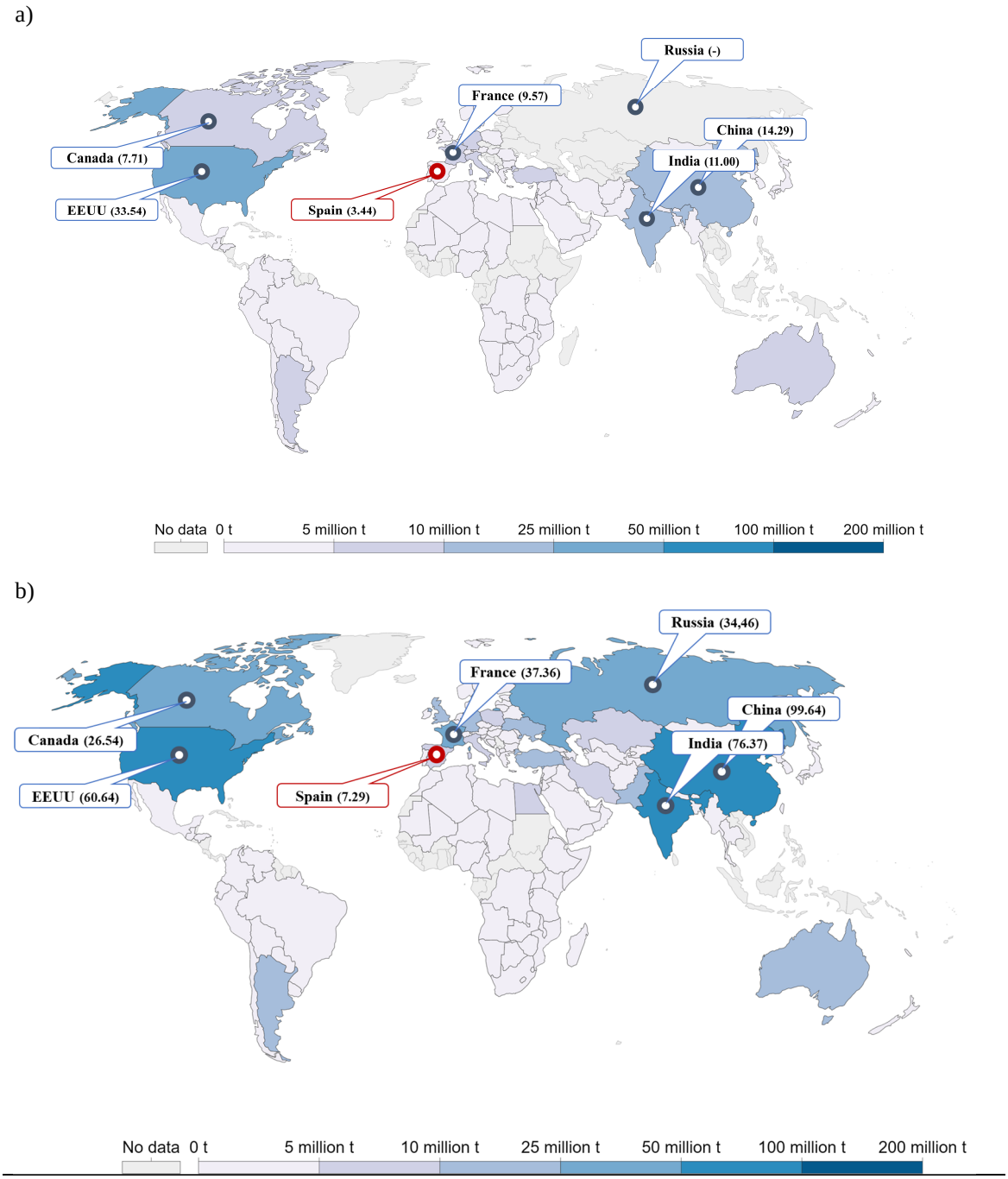

Figure 1.17. Changes in wheat global production per country between 1961 and 2000.

a) 1961; b) 2000. Data from the six countries with the highest production in 2018 are added. Spain is marked in red. Data from Russia in 1961 was not available.

Retrieved from (*Wheat production, 2018*, 2020)

varieties with resistances to biotic and abiotic stresses, although the negative ecological consequences of fertilisers and pesticides began to be noticed (Davies, 2003; Evenson and Gollin, 2003; Pingali, 2012).

1.2.6.2. Crop modifications

To improve yield potential, a series of plant architectural and photoperiod modifications were performed in wheat and rice. Thus, short stature cultivars, called *dwarfing varieties* or *semi-dwarf plants*, were developed though the introduction of the dwarfing genes *Rht1* and *Rht2*. Reductions in plant height led to improvements in lodging tolerance, harvest index and partitioning of photoassimilates from the stem in growth to florets in development, increasing fertile distal florets and, therefore, the number of grains per area (Trethowan *et al.*, 2007). This is in concordance with several studies focused on wheat improvement during GR, which have found that the improvement in yield was mostly accompanied by an increase in the number of grains per area without modification of the grain weight (Austin *et al.*, 1989; Slafer and Andrade, 1991; Donmez *et al.*, 2001; Shearman *et al.*, 2005; Sanchez-Garcia *et al.*, 2013; Philipp *et al.*, 2018). In line with the reduction in plant height, other desirable traits such as higher tillering and darker-green erected leaves have been reported (Khush, 2001).

Another important improvement was the insensitivity to photoperiod through the selection of insensitivity dominant alleles found in Ppd_1, Ppd_2, and Ppd_3 genes, allowing its adaptation to multiple places and its growth at any season. Other changes in wheat physiology have also been described, including improvements in the *nitrogen use efficiency* (NUE), water scarcity tolerance or disease resistance (Khush, 2001; Davies, 2003; Evenson and Gollin, 2003; Chhetri and Chaudhary, 2011), but the effect of GR on nutritional quality has not been further explored. Some studies have showed that the emphasised productivity in high-energy staple food during the GR resulted in more caloric edibles on market (Gómez *et al.*, 2013), together with a decrease in the quality of the grain (Fan *et al.*, 2008). In contrast, it has also been pointed out that the grain protein content hardly varied during GR (Trethowan *et al.*, 2007) while the micronutrient content of the grain diminished (Guarda *et al.*, 2004; Garvin *et al.*, 2006; Murphy *et al.*, 2008; Pingali, 2012).

1.1.6.3. Genetic erosion

It has been suggested that the detrimental impacts of GR could have reduced wheat genetic diversity around a 75 %, limiting opportunities for the development of new varieties (Khush, 2001;

Davies, 2003; Trethowan *et al.*, 2007; Chhetri and Chaudhary, 2011). However, the study of the work performed by Reif *et al.* (2005) evaluating the influence of domestication and breeding in wheat genetic variation showed that the narrow genetic diversity found between 1950 and 1989 was latter enhanced, suggesting that breeders noticing this loss of diversity took measures to avoid it, mainly through the introgression of novel material. This findings has been recently reinforced by the research of Sthapit *et al.* (2020), providing evidence that there were not variations in the genetic diversity of soft white spring and winter wheats from 1930 to 2019. Thus, the implications of domestication and GR on wheat genetic diversity remains unclear and more studies evaluating the current wheat genetic diversity are therefore required.

1.3. C-N Metabolism

1.3.1. Photosynthesis

1.3.1.1. General features

Solar radiation is the primary source of energy for living beings on Earth and *photosynthesis* is the only known biological process that can harvest this energy (Taiz *et al.*, 2015). Photosynthesis comprises a series of processes which allows organisms to stored solar energy into the biochemical bonds of molecules such as carbohydrates. According to the way of energy and C skeletons acquisition, organisms are classified as *autotrophs*, when they are able to produce their organic molecules from inorganic raw material and CO_2; or *heterotrophs*, if they obtain their energy and organic molecules from living beings. Plants are considered as *photoautotrophs* because carry out photosynthesis. However, photosynthesis is not limited to plants. It can occur in other organisms such as algae or some protist and prokaryotes (Campbell *et al.*, 2020).

In plants, photosynthesis is driven in a lens-shaped subcellular organelle with 5 µm of diameter and 2.5 µm of width called *chloroplast* (Staehelin, 2003). Each green part of the plants contains chloroplast, but leaves have the highest density found in the *mesophyll*, the internal tissue of the leaf (Figure 1.18, a) (Campbell *et al.*, 2020). The structure of a typical chloroplast (Figure 1.18, b) includes a double-membrane envelope which separates the chloroplast from the cytosol and modulates the translocation of metabolites and proteins between the organelle and the cell. It contains a third system of membranes with an internal lumen, called *thylakoids*, and suspended in an enzyme-rich dense fluid known as the *stroma*. This thylakoidal membrane system can form singly or stack *sacs*, the latter called *grana*, and contains all the necessary components of photosynthetic light harvesting (including *chlorophyll*), *electron* (e^-) *transport*, and *adenosine triphosphate* (ATP) synthesis (Staehelin, 2003).

Chlorophyll (Chl) is a tetrapyrrole ring pigment containing magnesium and linked to a long side chain which can absorb red and blue light and transmit it into green (Figure 1.19, a). In plants, pigments content in the chloroplast includes two different types of chlorophylls (Chl *a* and *b*) and the accessory pigment *carotenoids* (*b-carotene*). Their different structures allow them to vary in the range of wavelength absorption, but all of them are coincident with the maximum solar output in the visible spectrum range (Figure 1.19, b y c). Once chlorophyll is excited due to the capture of photons, it becomes very unstable and quickly releases some of its energy as heat or fluorescence, although it can also transfer part of this energy between adjacent molecules of chlorophyll by resonance (Taiz *et al.*, 2015). During the *oxygenic photosynthesis*, the energy absorbed by the chlorophylls and the

accessory pigments is employed for the hydrolysis of water (hydrolysis), releasing *oxygen* (O_2) as waste gas and electrons that are employed for the reduction and fixation of *carbon dioxide* (CO_2) into organic molecules (Peretó, 2011; Fleischman, 2012). The initial hydrolytic reaction can be summarised as:

Hydrolysis: $2H_2O \rightarrow O_2 + 4H^+ + 4e^-$

and thus, the general equations describing the chemical reactions of photosynthesis is:

Photosynthesis: $6CO_2 + 12H_2O + \text{light energy} \rightarrow C_6H_{12}O_6 + 6O_2 + 6H_2O.$

These equations are a simplistic summary of the complex photosynthetic process which, in turn, encompasses two main processes known as *the light reactions* and *the Calvin cycle*, both of them with several steps. The light reactions involve the transformation of the light energy into chemical energy (ATP) and reducing power (*nicotinamide adenine dinucleotide phosphate*; NADPH) by reactions taking place in the thylakoidal membrane of the chloroplast. These high-energy molecules will be subsequently employed for the assimilation of CO_2 and the synthesis of carbohydrates and other organic molecules at the Calvin cycle, by the enzymes located in the stroma (Taiz *et al.*, 2015).

1.3.1.2. Light reactions

The light reaction process includes the harvesting of the light by the chloroplast pigments and its transformation into an electro-chemical potential through the thylakoidal membrane which is used for the synthesis of ATP and NADPH. The Z-scheme (Figure 1.20, a) describes the absorption of solar energy, the e^- and *proton* (H^+) movements through the membrane and the redox reactions associated with the first step of the photosynthesis.

1.3.1.2.1. Energy capture

The functional units for photosynthesis are the *photosystems*, which are pigment-protein complexes located within the thylakoidal membrane. They act as *reaction centres* driving the electro-transfer reactions mediated by light that results in the separation of charges across the membrane. Depending on the final electron acceptor, two major classes of reaction centres can be distinguished in plants:

- Type 1 reaction centre (*photosystem I*, PSI or P700): Uses Fe_4S_4 clusters as electron acceptors. Its maximum of energy absorbance is found in the far-red light at 700 nm.
- Type 2 reaction centre (*photosystem II*, PSII or P680): Employs pheophytin/ quinones, with its maximum of absorbance found at 680 nm.

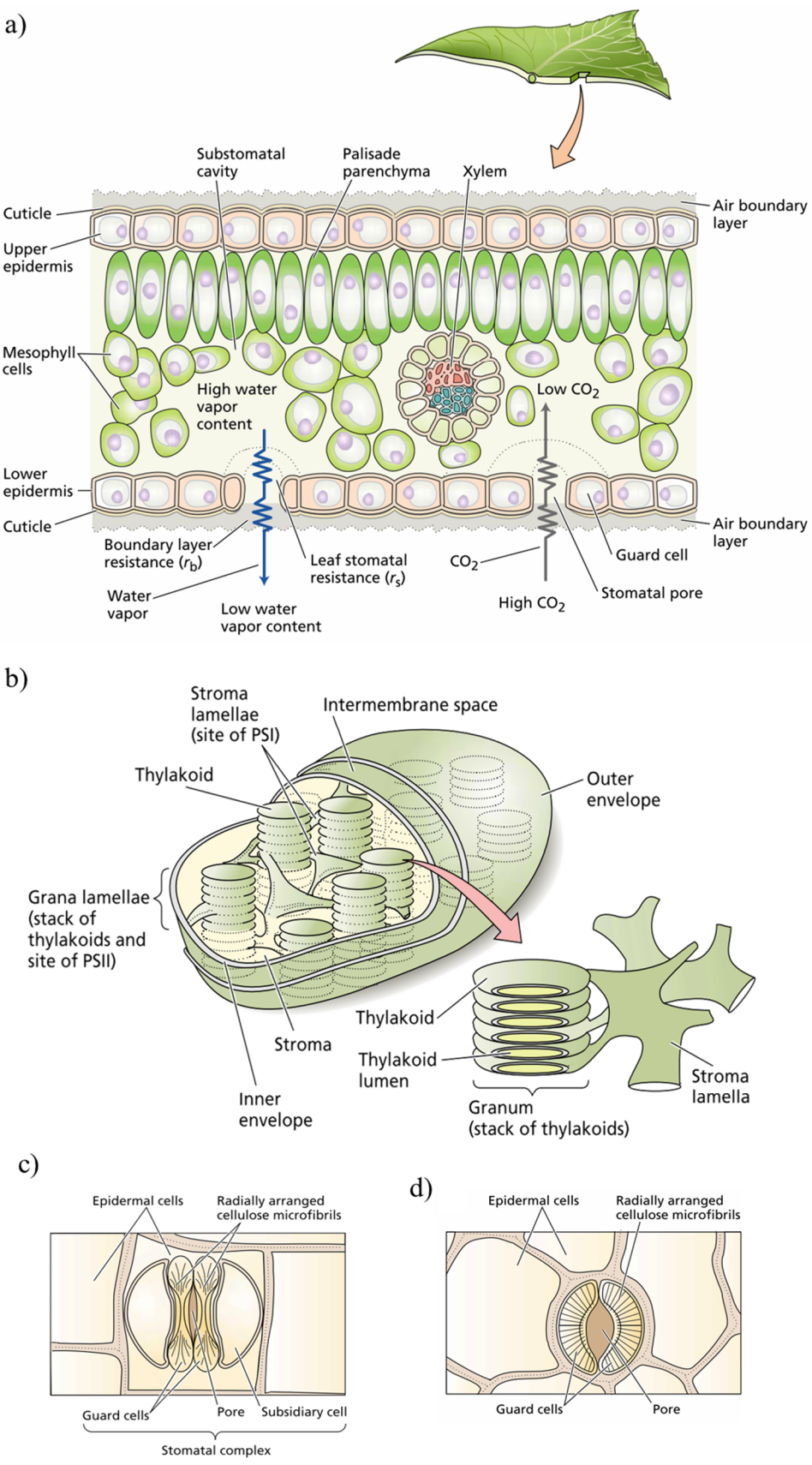

Figure 1.18. Leaf, chloroplast and stomata structures.

a) Leaf mesophyll; b) chloroplast and thylakoid system; c) grass-like stoma; d) kidney-shaped stoma.
Retrieved from (Taiz *et al.*, 2015).

Each photosystem accounts with its own *antenna or light-harvesting complex* (LHC) formed by several chlorophylls (*a* and *b*) and carotenoids bound to proteins. The function of these antenna complexes is to collect the energy contained in the solar radiation and to transfer it until the reaction centres. It is believed that the transmission of the energy occurs by resonance among the multiple chlorophyll molecules. Together with chlorophylls *a* and *b*, some of the most abundant proteins of the antenna complexes are usually associated with the photosystems I or II. Therefore, they are called as LHC I and LHC II (Fleischman, 2012; Leegood, 2013; Taiz *et al.*, 2015).

Concurrently with the photosystems, there are other protein complexes participating in the transportation of e^- and H^+ and the synthesis of ATP:

- *Plastoquinone* (PQ): A small lipophilic electron carrier placed within the thylakoidal membrane. It carries out the transference of e^- from PSII to the cytochrome b_6f and the translocation of H^+ from the stroma to the lumen.
- *Cytochrome* b_6f (Cyt b_6f): A multisubunit protein of several prosthetic groups which acts as a plastoquinol–plastocyanin oxidoreductase. It allows the transference of e^- from PQ to Pc.
- *Plastocyanin* (Pc): A small, water-soluble electron carrier protein with Cu in its active site, cycling between its reduction and oxidation states (Cu^{2+} and Cu^{+}). It is placed in the thylakoidal lumen space and transfers e^- from Cyt b_6f to PSI.

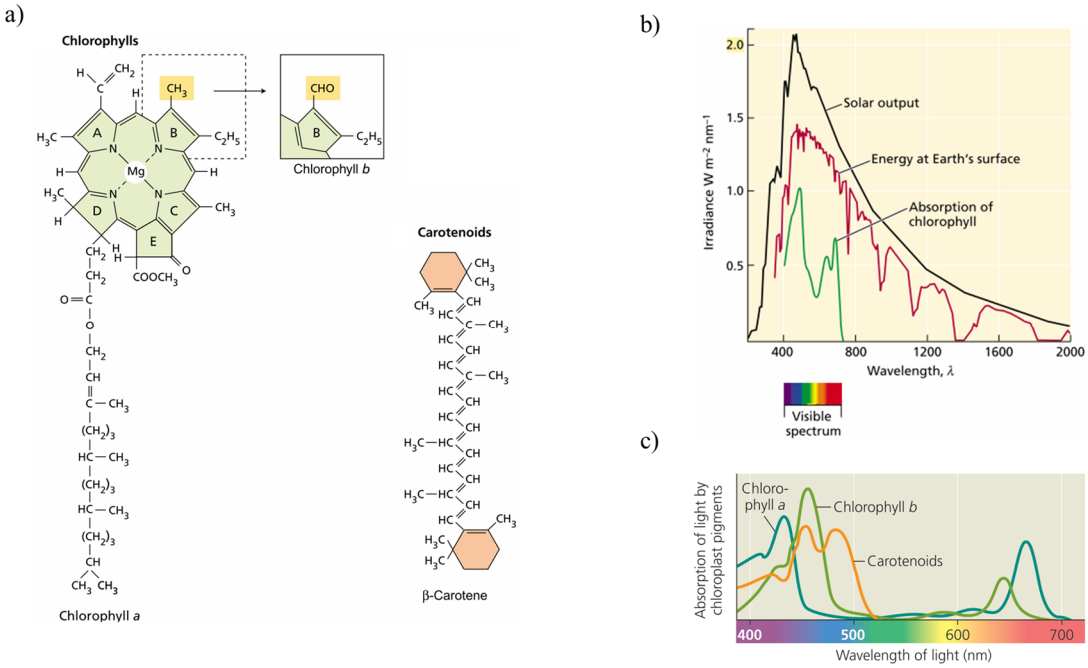

Figure 1.19. Chlorophyll structure and light absorption.

a) Basic structure of chlorophylls *a* and *b* and *β*-carotene; b) relationship between solar spectrum and absorption spectrum chlorophyll; c) absorption spectrum of chloroplast pigments.

Retrieved from (Taiz *et al.*, 2015; Campbell *et al.*, 2020).

- *Ferredoxin* (Fd): A small, water-soluble electron carrier protein with an iron-sulphur cluster in its active site, cycling between its reduction and oxidation states (Fe^{2+} and Fe^{3+}). It is placed in the chloroplast stroma.
- *Ferredoxin-NADP$^+$ reductase* (FNR): The FNR complex is a membrane-associated flavoprotein which can be found soluble in the stroma or bounded to the thylakoidal membrane. It mediates the reduction of $NADP^+$ to NADPH in the stroma (Johnson, 2016).
- (ATPase): The ATP synthetase is a large enzymatic complex composed by two functional subunits:
    - F_0: Is a transmembrane proton pore formed by multiple membrane proteins which allows the flux of H^+ from the lumen to the stroma.
    - F_1: Is a peripheral protein complex in which the synthesis of ATP takes place powered by the proton-motive force. It has 3 β subunits for: *adenosine diphosphate* (ADP) + *inorganic phosphate* (P_i) binding, ATP synthesis and ATP release (Nelson and Cox, 2013).

1.3.1.2.2. Photophosphorylation

During photophosphorylation, the hydrolysis of water releases O_2 and electrons which are employed in a series of oxide-reductant processes leading to the synthesis of NADPH and ATP associated with the movement of protons between the stroma and the lumen. This process is known as the *non-cycling photophosphorylation* and involves the action of both photosystems. However, under high-energy demanding conditions, a cyclic flux of electrons allows to raise the number of protons pumped through the thylakoidal membrane, increasing the number of ATP molecules synthesised without synthesis of NADPH. This is known as the *cyclic photophosphorylation* in which only PSI participate.

Non–cyclic photophosphorylation

Figure 1.20 (b) summarises the non-cyclic photophosphorylation. The process starts with the harvesting of photons by LHC II and its transference to PSII, triggering the hydrolysis of water and the subsequent release of 2 e^- and a molecule of oxygen (Lopez and Barclay, 2017). PQ is later reduced to *plastohydroquinone* (PQH_2) by the 2 e^- retrieved from the electron acceptor pheophytin of PSII, together with two H^+ taken from the stroma. The two e^- are then transferred to Cyt b_6f in a process leading to the oxidation of PQH_2 into PQ and the expelling of two H^+ into the lumen. This is a critical step since it contributes to alkalinise the stroma while increasing the concentration of H^+ in the lumen (Taiz *et al.*, 2015; Johnson, 2016). The *Mitchell's chemiosmotic hypothesis* suggests that

the differences in the proton concentration across the membrane and associated electrical potential create an electrochemical potential gradient that is used for the synthesis of ATP.(Fleischman, 2012).

One of the electrons in Cyt b_6f is transferred to Pc, which reduces P700 of PSI. The other electron reduces another PQ bounded to Cyt b6f into a *plastosemiquinone* (PQ^-). Parallelly, the Fe_4S_4 clusters of PSII is also excited by another photon replacing the lost electron in Cyt b6f. The two electrons are transferred to FNR through Fd and used to generate NADPH in the stroma. Moreover, the energy stored in the proton gradient is dissipated by the migration of protons from the lumen to the stroma through the F_0 subunit of the ATPase, causing the rotation of the subunit F_1. This rotational movement triggers a series of conformational changes of the β subunits leading with the synthesis and release of ATP (Leegood, 2013; Taiz *et al.*, 2015).

a)

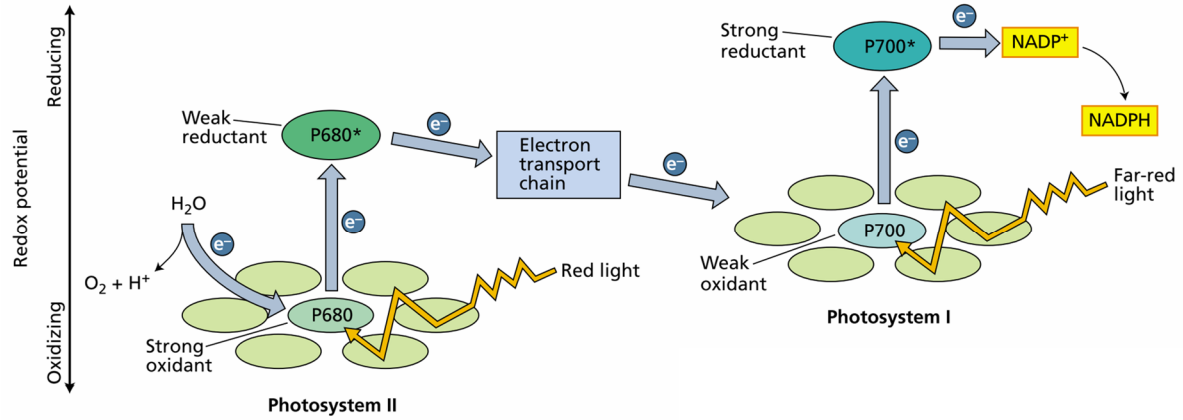

b)

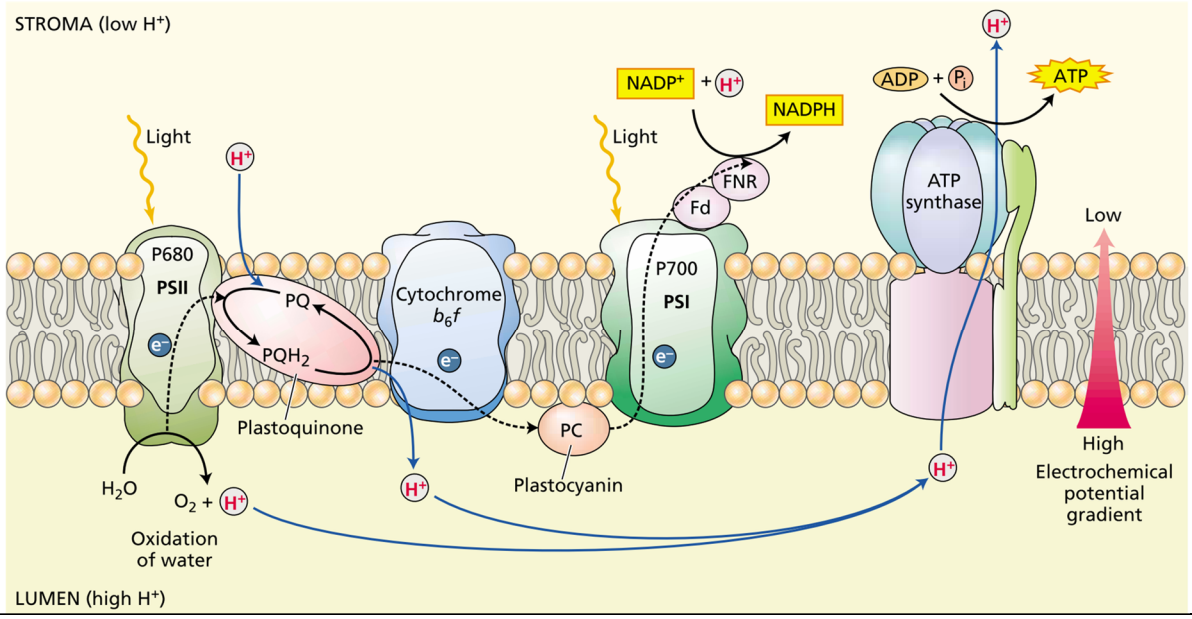

Figure 1.20. Schematic representation of light reactions in the photosynthesis.

a) Z-scheme of photosynthesis; b) electron and proton transference in the thylakoidal membrane during the non-cyclic photophosphorylation. Retrieved from (Taiz *et al.*, 2015).

Cyclic photophosphorylation

An alternative electron transport pathway involves the recycling of e^- from Fd to PQ without production of NADPH. Occasionally, photoexcited electrons from PSI are transferred from Fd to Cyt b_6f and returns to PSI through Pc, generating ATP (Johnson, 2016). This process would involve the reduction of the PQ^- performed during the non-cycling process into a PQH_2 picking up other 2 H^+ from the stroma. Its following oxidation would contribute for the increasing of the H^+ concentration in the lumen and the synthesis of ATP without NADPH generation. Thus, the ratio NADPH/ATP can be controlled to meet metabolic need (Johnson, 2016).

1.3.1.3. Calvin cycle

The second step in photosynthesis involves the use of the photochemical energy stored in the molecules of ATP and NADPH in the assimilation of carbon dioxide (CO_2) into organic molecules for different biosynthetic pathways inside and outside of the chloroplast (Stitt *et al.*, 2010). The Calvin cycle (also called *Benson-Calvin cycle* or *reductive pentose phosphate cycle*) take place in the stroma of the chloroplast and leads to the synthesis of two molecules of a three-carbon sugar phosphate called *glyceraldehyde-3-phosphate* (GAP), later employed for the synthesis of carbohydrates such as sucrose or starch (Figure 1.21). The whole process is driven by the action of several enzymes

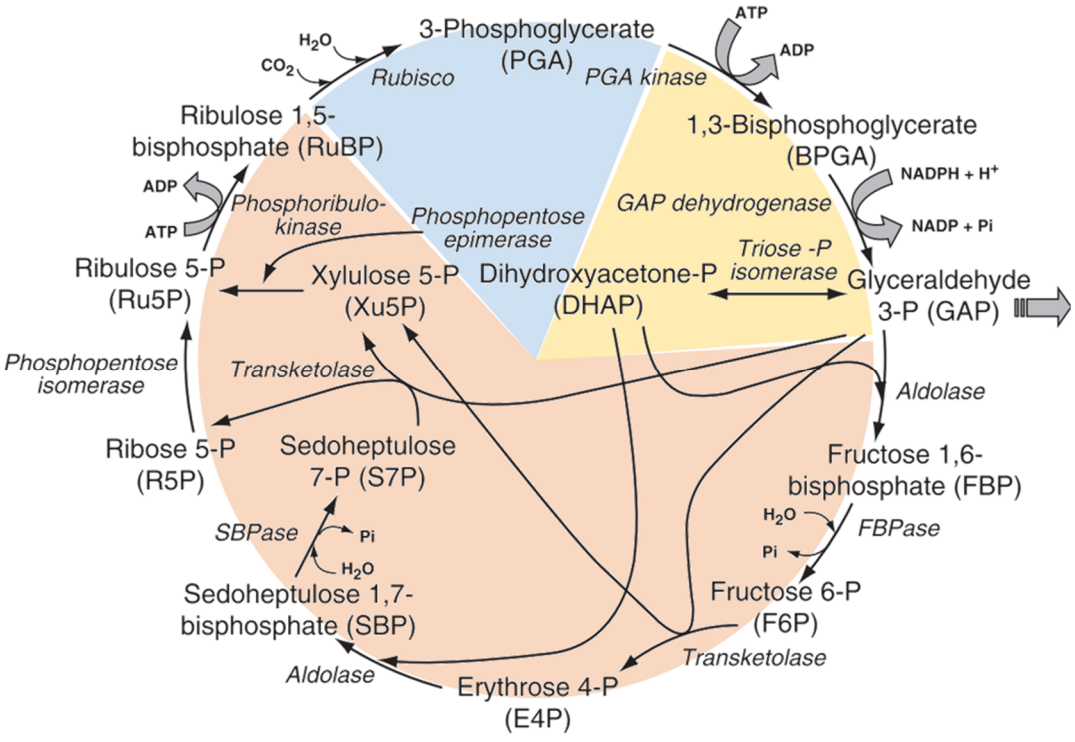

Figure 1.21. The Calvin cycle.

Three phases are distinguished: carbon fixation (blue), reduction (yellow) and regeneration of RuBP (orange)
Modified from (Raghavendra, 2003).

including *Ribulose 1,5-bisphosphate carboxylase/oxygenase* (Rubisco), the most abundant protein on Earth and the key enzyme in the fixation of CO_2. The Calvin cycle involves three main phases: *carboxylation, reduction* and *regeneration of the CO_2 acceptor*

1.3.1.3.1. Carbon fixation

The atmospheric CO_2 enters the leaf mesophyll through opened stomatal pores by exchange with water vapour (Figure 1.18, c and d). The incorporation of CO_2 to the five-carbon molecule *ribulose 1,5-bisphosphate* (RuBP) leads to the formation of 2 molecules of *3-phosphoglycerate* (PGA), a reaction catalysed by the Rubisco (Raghavendra, 2003). This process occurs three times in each complete cycle, and thereby six molecules of PGA are generated. The slow catalytic rate and the low substrate affinity of Rubisco require the production of high levels of the enzyme, reaching up 50% of the soluble protein in C_3 plants (Raghavendra, 2003; Fleischman, 2012).

1.3.1.3.2. Reduction

After the CO_2 fixation, each one of the molecules of PGA are first phosphorylated using the ATP synthetised during the photophosphorylation by the enzyme *phosphoglycerate kinase* (PGK). The resulting molecule, *1,3-bisphosphoglycerate* (BPGA) is subsequently reduced by NADPH to GAP through the reaction catalysed by the *glyceraldehyde 3-phosphate dehydrogenase* (GAPDH). The GAP can be converted into *dihydroxyacetone phosphate* (DHAP) mediated by the *triose phosphate isomerase*.

For every three molecules of CO_2 combined with RuBP, six molecules of GAP are synthetised but only one molecule is used in the synthesis of final products, sucrose and starch, while the remaining five are used for the regeneration of RuBP in the last phase of the cycle. The molecule of GAP can be either converted to starch in the chloroplast or exported from the chloroplast to be used in the synthesis of sucrose in the cytosol and other important organic compounds through different metabolic pathways (Stitt et al., 2010). Certain amino acids and lipids are also synthesised in the chloroplast from the C fixed in photosynthesis (Fleischman, 2012; Johnson, 2016).

1.3.1.3.3. Regeneration of RuBP

The continued fixation of CO_2 by Rubisco requires the regeneration of the CO_2 acceptor RuBP in order to avoid the depletion of the Calvin cycle metabolites. During this phase, 3 molecules of *ribulose 5-phosphate* (Ru5P) are synthetised from 5 molecules of trioses phosphate (GAP and DHAP) by a complex series of reactions and rearrangements catalysed by *transketolases* and *aldolases*. The process also requires energy consumption in the form of ATP as well as the use of two molecules of H_2O, which is accompanied by the release of other two molecules of P_i. The final step, the

phosphorylation of 3 molecules of Ru5P in RuBP, is catalysed by the *phosphoribulokinase* mediated by ATP (Fleischman, 2012; Taiz *et al.*, 2015).

In order to synthetise one molecule of hexose, two rounds of Calvin cycle are needed with the fixation of 6 molecules of CO_2 and the use of 18 and 12 molecules of ATP and NADPH, respectively (Taiz *et al.*, 2015). The net stoichiometry of the Calvin cycle is:

$$6\ CO_2 + 11\ H_2O + 12\ NADPH + 18\ ATP \rightarrow \text{Fructose-6-phosphate} + 12\ NADP+ + 6\ H^+ + 18\ ADP + 17\ P_i$$

1.3.1.3.4. Regulation of the Calvin cycle

Regulation of photosynthesis involves long- and short-term modifications of the enzymes driving the process. Long-term modifications implicate changes in nuclear and chloroplast gene expression and protein synthesis regulating the concentration of the enzymes. The short-term regulation is driven by two major mechanisms:

- The structural modification of the enzyme through the transformation of covalent bonds. This includes the reduction and oxidation of the disulphide bonds found in several enzymes of the Calvin cycle (such as the GAPDH) via the ferredoxin–thioredoxin system or the carbamylation of Rubisco.
- Modification of non-covalent interactions. This includes the binding of metabolites or variations in the cellular milieu (e.g., modifications in the pH) (Raghavendra, 2003; Taiz *et al.*, 2015).

1.3.1.3.5. Rubisco

The ribulose 1,5-bisphosphate carboxylase/oxygenase is a complex soluble protein placed in the stroma of the chloroplast. It contains eight large subunits and eight small subunits with masses of 58 and 18 KDA, respectively (Andersson and Backlund, 2008). The large subunits contain the catalytic centres whereas the smallest seems to act stabilising the Rubisco complex (Raghavendra, 2003). The catalytic activity of Rubisco is regulated by a mechanism that includes the reversible carbamylation of an ε-amino group of the Lys201 residue, located in the active centre of the protein, and the subsequent stabilisation of the carbamate by the union of Mg^{2+} fully activates Rubisco, allowing the binding of RuBP and its carboxylation (Raghavendra, 2003; Taiz *et al.*, 2015).

In the active state, the protonation of RuBP creates an enediolate intermediate that, in combination with the CO_2 substrate molecule, forms an unstable 6C intermediate that is quickly hydrolysed to two molecules of PGA (Johnson, 2016). However, the union of sugar phosphates, such as RuBP or *carboxyarabinitol 1-phosphate* (CA1P), inactivates Rubisco. Indeed, CA1P is accumulated in leaves and bound to Rubisco at night.

The Rubisco also requires the action of the enzyme *Rubisco activase* to be active. This protein facilitates the ATP dependent elimination of CA1P or RuBP strongly bound to the enzyme, inducing a conformational change that promotes the carbamylation and subsequent catalysis of Rubisco (Jensen, 2000; Raghavendra, 2003; Taiz *et al.*, 2015). Wheat do not have CA1P, but the daytime inhibitor pentadiulose-1,5- bisphosphate (PDBP) has been identified in this specie (Parry *et al.*, 2008).

1.3.1.4. Alternative photosynthetic mechanisms

1.3.1.4.1. Photorespiration

Rubisco carries on a dual role as a carboxylase as well as oxygenase. As mentioned above, the enzyme catalyses the carboxylation of RuBP, the first step of the Calvin-Benson cycle. It can also catalyse the oxygenation of RuBP to produce a molecule of PGA and another of *2-phosphoglycolate* (PG) in the photorespiration (Suzuki and Makino, 2013).

$$RuBP + O_2 \rightarrow PGA + PG$$

While the PGA continues in the Calvin cycle, PG is metabolised in the glycolate pathway with the net loss of CO_2, ATP and NADPH. Thus, biological function of photorespiration remains unknown and sometimes it is considered as a wasteful process or an evolutionary baggage (Raghavendra, 2003; Lopez and Barclay, 2017; Campbell *et al.*, 2020).

1.3.1.4.2. C_3, C_4 and CAM plants

The above-described mechanism of C fixation is the most common photosynthetic process in plants. Since PGA is the first compound synthetised in the Calvin cycle, this process usually receives the name of *C_3 photosynthesis*. Nevertheless, alternative modes of C fixation and CO_2 concentration have been developed in order to avoid photorespiration and to optimise the Calvin cycle in hot, arid climates (Leegood, 2013; Johnson, 2016).

In *C_4 plants*, the high levels of the enzyme *phosphoenolpyruvate carboxylase* (PEPCase) in mesophyll cells fix CO_2 into *oxaloacetate* (OAA). This 4C carboxylic acid is reduced to *malate* and transported to the *bundle sheath cells*, where it is decarboxylated to pyruvate releasing NADPH and CO_2 (Leegood, 2013; Johnson, 2016).

The *crassulacean acid metabolism* (CAM) is mostly typical of plants growing in hot brightly-dry environments where stomata must be closed for a large part of the day in order to avoid dryness. As a consequence, CO_2 concentration in the leaf remains very low. To counteract this deficiency, CO_2 is accumulated during the night as malate via PEPCase and stored in the vacuoles of the mesophyll

cells. With the sunrise, stomata become closed and malic acid breaks down releasing CO_2 that is used by the Rubisco in the Calvin cycle. Relatively higher levels of CO_2 are found in CAM than in C_3 plants, so photorespiration is usually lower (Johnson, 2016; Lopez and Barclay, 2017)

1.3.2. Metabolism of carbohydrates

1.3.2.1. General features

Although the Calvin cycle can occur at day or night, it is conditioned by the synthesis of ATP and NADPH produced in the light-dependent reactions conforming photophosphorylation. Thus, nutrient availability of plants could be exposed to large variations along the day. To buffer these fluctuations, photoassimilates are mostly stored as metabolic pools that are employed according to the physiological necessities of the plant. The two major metabolic pools for the products of the Calvin cycle are the *trioses phosphate* (GAP and DAHP) and *hexoses phosphate* [*glucose 1-P* (G1P), *glucose 6-P* (G6P), *fructose 6-P* (F6P), and *adenosine diphosphate glucose* (ADP-glucose)] (Chibbar *et al.*, 2015).

Under conditions of elevated photosynthetic activity, the pool of trioses phosphate produced by the mesophyll cells of leaves can be retained in the chloroplast for the regeneration of RuBP or temporally stored as granules of starch. However, trioses can also be transported to the cytosol via *triose phosphate transporter* (TPT) placed in the inner membrane of the chloroplast (Figure 1.22, a), which acts as an antiporter exchanging trioses for P_i (Hofius and Börnke, 2007). The cytosolic pool of trioses phosphate is used as a source of energy through glycolysis, as well as a precursor for the synthesis of proteins, lipids, and organic acids. However, trioses can also be translocated to other organs as Suc after their transformation in the cytosol (Yahia *et al.*, 2019). The balance between storage and translocation is tightly regulated and coordinated by the rate of C fixation through a variety of regulatory mechanisms responding to changes in light (Nelson and Cox, 2013).

In leaves, hexose phosphate pools are found in both the chloroplast and the cytosol, but due to the lack of hexose phosphate carriers in chloroplasts, the translocation of hexoses between the cytosol and the chloroplast is driven as trioses through TPT. Indeed, the hexose phosphate pool is kept in balance due to the reverse transformation of G1P in G6P and G6P in F6P due to the activity of the enzymes *phosphoglucomutase and glucose 6-phosphate isomerase*, respectively (Yahia *et al.*, 2019).

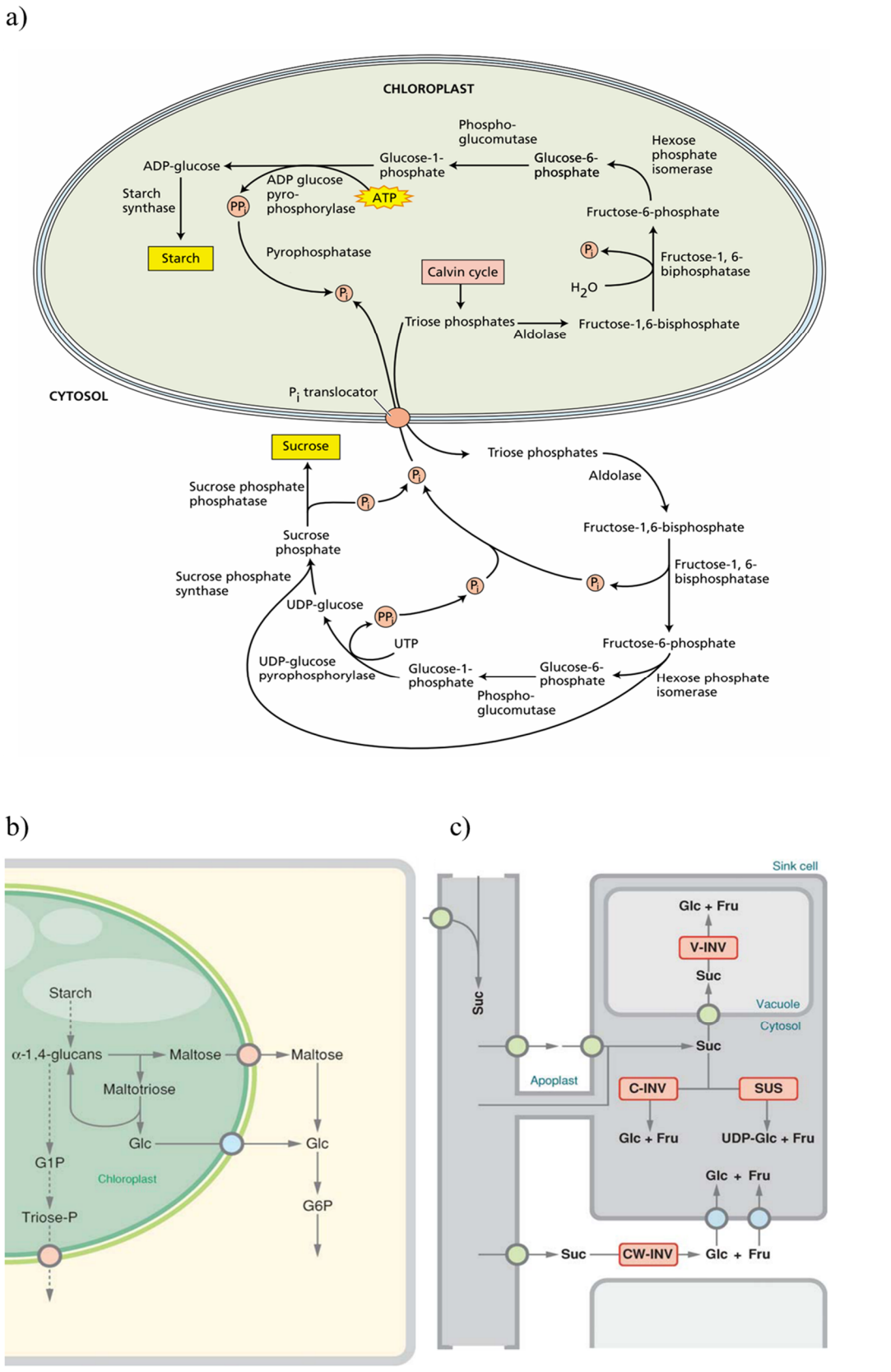

Figure 1.22. Metabolism of starch and sucrose.

C-INV: cytosolic invertase; *CW-INV*: cell wall invertase; *G1P*: glucose 1-phosphate; *G6P*: glucose 6-phosphate; *Glc*: glucose; *SUS*: sucrose synthase; *V-INV*: vacuolar invertase.

a) Synthesis of starch and sucrose; b) Starch degradation; c) translocation and degradation of sucrose into sink cells.

Retrieved from (Rolland *et al.*, 2006; Taiz *et al.*, 2015).

However, it is necessary the previous condensation of trioses GAP and DHAP into *fructose 1,6-bisphosphate* (F1,6bisP) and its dephosphorylation into F6P in two reactions catalysed by the enzymes *fructose-1,6,bisphosphate aldolase* and f*ructose-1,6-bisphosphatase* (Taiz *et al.*, 2015). In non-photosynthetic organs, by contrast, amyloplasts have a modified TPT which can exchange G6P and G1P with the cytoplasm (Chibbar *et al.*, 2015; Yahia *et al.*, 2019).

1.3.2.2. Synthesis of carbohydrates

1.3.2.2.1. Synthesis of starch

The excess of photoassimilates synthetised during the day is transiently stored as starch in leaves or as a long-term C storage in the amyloplast of non-photosynthetic organs, such as in seeds or roots (Nelson and Cox, 2013). The key enzyme regulating the synthesis of starch is the *ADP-glucose pyrophosphorylase* (AGPase), which mediates the phosphorylation of G1P in *ADP-glucose* and is modulated by the levels of GAP and P_i (Avigad and Dey, 1997). The biochemical processes involved in the synthesis of transitory and long-term starches are complex, but it is believed that a basic mechanism is shared (Figure 1.22, a). These processes include the production of ADP-glucose and its availability, the priming of starch granulates, the initiation and elongation of the chain and the introduction of the branches (Chibbar *et al.*, 2015). After ADP-glucose has been generated, starch is synthesised by the action of two forms of *starch synthase, starch synthase soluble* (SS_S) and *granule-bound starch synthase* (GBSS), together with the *starch branching enzymes* (SBEs). Three different isoforms of SSs have been identified involving the production of linear chains with different degrees of polymerisation: SSsI (6–12 DP), SSsII (higher than 24) and SSsIII (13–24(Yahia *et al.*, 2019). The presence of a starch granule core, known as *hilum*, indicates the existence of a priming mechanism for the synthesis of the starch. Although it is not well understood, it is believed that priming mechanisms of starch glucan polymerisation involves the action of SSsI, GBSS and SBE in the extension and branching of maltodextrins to form a molecule with a backbone of amylopectin. The primary glucan polymer would be synthesised by cycling steps of extension and branching catalysed by SSsI and SBE, whereas *starch-debranching enzymes* (DBEs) would also participate trimming the ends of pre-amylopectin molecules to produce the final amylopectin chain (Chibbar *et al.*, 2015). Moreover, the polymerisation of amylose is performed by GBSS enzymes transferring glucosyl units from ADP-glucose to the existing glucan chain, increasing its length. However, it still remains unclear if amylose is synthesised as a product of the amylopectin debranching or if both molecules are simultaneously formed (Yahia *et al.*, 2019).

1.3.2.2.2. Synthesis of sucrose

The synthesis of Suc in leaves and other photosynthetic tissues comes from the pool of hexoses phosphate placed in the cytosol (Figure 1.22, a). The first step includes the synthesis of the nucleotide sugar *uridine diphosphate glucose (*UDP-glucose) from *uridine triphosphate* (UTP) and G1P in a reaction catalysed by the enzyme *UDP-glucose pyrophosphorylase,* with the release of PPi (Yahia *et al.*, 2019). The following combination of UDP-glucose and F6P by *sucrose phosphate synthase* (SPS) leads to the synthesis of *sucrose phosphate*, which is dephosphorylated by the enzyme *sucrose phosphate phosphatase* (SPP) to form Suc (Stein and Granot, 2019). This last step is highly exergonic, making the overall process of Suc synthesis almost irreversible (Yahia *et al.*, 2019).

1.3.2.2.3. Synthesis of fructans

As described in the section of the nutritional constituents of the wheat grain (*section 1.2.4.2*), fructans are complex oligosaccharides constituted by β(2-1) or β(2-6) chains of fructose linked to a molecule of Suc. Depending on the position of the chain, three types of Fruct could be identified: inulins (β(2–1)), levans (β(2–6)), and graminans (mixed bonds; Figure 1.12, c).

The synthesis of Fruct take place in the vacuole from sucrose in several reactions catalysed by the enzymes known as *fructosyltransferases* (FTs) (Chibbar *et al.*, 2015). In wheat, three different types of FTs have been identified , including the *sucrose:sucrose 1-fructosyltransferase* (1-SST), *fructan:fructan 1-fructosyltransferase* (1-FFT) and *sucrose:fructan 6-fructosyltransferase* (6-SFT) (Cimini *et al.*, 2015), whose combined action allows the synthesis of graminan type fructans. The first steps in the synthesis of fructans involves the synthesis of the molecules 1-kestose (inulin type) or 6-kestose (levan type) by the action of the enzymes 1-SST and 6-SFT, which catalyse the transference of a single unit of Fru provided by one molecule of Suc to another molecule of Suc. These saccharides, 1-kestose and 6-kestose, act as the primary substrate for the synthesis of the remaining fructans, by the elongation of their backbones due to the activity of 1-FFT and 6-SFT (Chibbar *et al.*, 2015).

In wheat and other cereals, fructans accumulate not only in leaves but also in other organs, including stem, roots, grain, depending on the developmental stage and the growing conditions (Morcuende et al., 2004; Morcuende et al., 2005; Vicente et al., 2016). The Fruct synthesis is dependent on the accumulation of Suc, and it has been demonstrated that there is a threshold concentration of Suc for the production of Fruct (Chibbar *et al.*, 2015). The accumulation of Fruct is induced by illumination (Morcuende *et al.*, 2004a), drought (Méndez *et al.*, 2011), low temperatures (Pérez *et al.*, 2001), CO_2 enrichment (Vicente *et al.*, 2015b, 2016, 2019) and N deficiency (Vicente *et al.*, 2016) due to an increase in the activity of the FTs (Morcuende et al., 2004). However, nitrate

and phosphate decrease the Fruct content, whereas nitrate is a negative sign6al for the expression of the 6-SFT (Morcuende *et al.*, 2004a) phosphate decrease the SPS activity and the level of Suc, the substrate for Fruct synthesis (Morcuende *et al.*, 2005).

1.3.2.3. Degradation of carbohydrates

1.3.2.3.1. Starch breakdown

Degradation of starch is qualitatively similar in photosynthetic and non-photosynthetic organs as far as similar enzymatic reactions are developed. However, it differs in the dynamic of the fluxes and regulation between tissues. For example, starch degradative enzymes are very low or remains inactive in amyloplast of seeds and they are only activated after germination. By contrast, starch breakdown occurs concurrently in balance with starch biosynthesis in photosynthetic organs (Avigad and Dey, 1997).

In leaves, starch degradation happens mostly in the chloroplast of leaf cells at night (Figure 1.22, b), acting as a source of glucose (Rolland *et al.*, 2006). Similarly, its breakdown to simple sugars in fruits contributes to the generation of energy and the establishment of flavours and aromas (Yahia *et al.*, 2019). The degradation of starch in cereal grains involves three main steps: *the reduction of the starch granule into soluble maltodextrins*; *debranching and breakdown of maltodextrins into glucose and G1P*; and *the transport and storage of these products from the organ to the hexose phosphate pool of the plant cells* (Chibbar *et al.*, 2015). Previous to the starch degradation, the phosphorylation of a small proportion of glucosyl residues by the action of the enzyme *glucan-water dikinase* seems to be necessary, leading to the release of soluble glucans (Hofius and Börnke, 2007). The hydrolysis of the starch granule is driven by the enzymes *α-* and *β-amylases*, which catalyses the breakdown of the α(1,4) bonds found in amylose and amylopectin. While α-amylase randomly hydrolyses α(1,4) linkages of amylose, leading to the production of 10 glucose-unit glucans known as *maltodextrins*, β-amylase catalyses the removal of the maltose molecules slowly hydrolysed from maltodextrins (Yahia *et al.*, 2019). These maltose molecules are completely broken into G1P by the enzymes *starch phosphorylases*, which are widespread along the plant but mostly missing in the germinating cereal grain, although the action of *maltases* can also catalyse the transformation of starch to glucose. Furthermore, α(1,6) glucan bonds of amylopectin are hydrolysed by starch DBEs, proportioning additional end groups that allows the action of amylases and phosphorylases (Chibbar *et al.*, 2015).

Transportation of both, maltose and glucose, from plastids to the cytosol is carried out by specific transporters, whereas maltose is the major metabolite translocated from chloroplast to the cytosol in

leaves (Hofius and Börnke, 2007). It is also believed that G1P is transported by a similar mechanism, not discovered yet (Yahia *et al.*, 2019).

1.3.2.3.2. Sucrose translocation and degradation

As the primary product of photosynthesis, Suc is the main carbohydrate transported from source organs to non-photosynthetic sink tissues through the phloem. In those organs, Suc is the raw material in many metabolic processes, including energy production or the synthesis of other carbohydrates, lipids or amino acids (Stein and Granot, 2019). Transportation of Suc from the mesophyll cells of leaves into the phloem of the sieve cells can occur by two major pathways: the *symplastic* pathway involves the transportation between cells through intercellular cytoplasmatic channels called *plasmodesmata*; or by the *apoplastic* pathway, in which water and nutrients are transported through the space between the plasmatic membrane and the cell wall (the *apoplast*). In this process, plasma membrane *sucrose transporters* (SUT) are thought to perform an important role acting as sucrose/H^+ symporters that mediates the active transport of Suc to the phloem (Hofius and Börnke, 2007). In wheat, three SUT genes (*TaSUT1A, 1B* and *1D*) have been isolated from grains of bread wheat (Aoki *et al.*, 2002)

Sucrose unloading mostly follows a symplastic route through the plasmodesmata that connects the phloem with the parenchymatic cells of the sink organ (Figure 1.22, c). Nevertheless, the apoplastic pathway has also been suggested as a possible alternative, including the release of Suc in the boundary between the sieve cells and the parenchyma cells or at the boundaries between different types of parenchyma cells. Similarly, different hypothesis about the uptake of sucrose have been explored, distinguishing three different routes: the first one would involve SUT symporter; in the second one, a cell-wall *invertase* transforms Suc into Gluc and Fru that are first release in the apoplast and then transferred into the sink cells by hexose transporters; or into a vesicle through endocytosis (Hofius and Börnke, 2007). Once inside the sink cells, Suc is cleaved by a cytosolic invertase or through the enzyme *sucrose synthase* (SUS). Similarly, to the cell-wall invertase, the cytosolic invertase hydrolyses Suc into Gluc and Fru, whereas SUS catalyses the reversible breakdown of Suc into UDP-glucose and Suc with the use of *uridine diphosphate* (UDP). Suc can also be transported to the vacuole where it is stored as Suc or as fructans, after their transformation by FTs (Stein and Granot, 2019)

It is important to highlight that the routes supporting the synthesis and degradation of starch and sucrose and their interchange of C skeletons differ in photosynthetic and non-photosynthetic organs (Avigad and Dey, 1997). In photosynthetic organs, hexoses produced in the cytosol as a consequence of Suc or in the chloroplast due to starch degradation need to be firstly transformed into trioses in order to be exchanged trough TPT. But in non-photosynthetic organs, starch is mostly synthetised

from products of Suc degradation, including G6P and G1P, which are transported into the amyloplast from the cytosol and employed in the synthesis of ADP-glucose (Chibbar *et al.*, 2015). Similarly, depolymerisation of starch leads to the release of maltose, glucose or G1P, which are directly transported into the cytosol and reincorporated for Suc synthesis (Avigad and Dey, 1997).

1.3.2.3.3. Fructan degradation

Fructan cleavage is performed by the hydrolytic activity of the enzymes *fructan 1-exohydrolases* (1-FEH) or *fructan 6-exohydrolases* (6-FEH), breaking the terminal β(2,1)- or β(2,6)- end groups in fructans (Chibbar *et al.*, 2015). In wheat, together with 1-FEH and 6-FEH, 6&1-FEH has also been identified (Cimini *et al.*, 2015).

1.3.3. Cell respiration

1.3.3.1. General features

In the photosynthetic processes, plants employ solar energy and water to reduce CO_2 into complex high-rich C compounds, such as starch, sucrose or fructans. However, more than 70 % of the total CO_2 fixed along the photosynthesis is released back into the atmosphere through *cell respiration* process. During aerobic respiration, carbohydrates are oxidated and their products are employed for generating useable energy and C-intermediates needed in the synthesis of several precursors (Atkin *et al.*, 2000). As sessile organisms, plants generally acclimate to environmental changes through modifications in their metabolism and physiology. In this sense, the respiratory pathways play a key role in the capacity of the plants to face these stresses due to the overproduction or removal of metabolites synthetised (O'Leary and Plaxton, 2016).

The net balance of respiration in plants can be obtained from the oxidation of a single molecule of sucrose and 12 molecules of O_2, following this reaction:

$$C_{12}H_{22}O_{11} + 12\ O_2 \rightarrow 12\ CO_2 + 11\ H_2O$$

This is the reversal reaction of the photosynthesis and describes the complete oxidation of sucrose to CO_2 and the reduction of O_2 to water (Taiz *et al.*, 2015).

Cell respiration coordinates several biochemical reactions taking place in plastids, cytosol and *mitochondria* (Figure 1.23), and involves three major metabolic pathways: *glycolysis,* the

tricarboxylic acid cycle (TCA) and *oxidative phosphorylation* (or *mitochondrial electron transport chain*).

1.3.3.2. Glycolysis

Glycolysis is a catabolic pathway in which carbohydrates are partially oxidised, leading to the formation of ATP, NADPH, *pyruvate* and malate, as well as the production of substrates for anabolism (Taiz *et al.*, 2015). It is driven in all living organisms; however, deeper differences in structural and bioenergetic characteristics have been found between plant and non-plant cells. In plants (Figure 1.24), glycolysis takes place in the cytosol or inside plastids. Both, sucrose and starch acts as primary substrates of the pathway, but the immediate products of their degradations (pentoses or trioses) can also be employed (Plaxton, 1996). Depending on the organelle, different functions have been attributed to glycolysis. Non-green plastids and chlorophylls under light absence uses

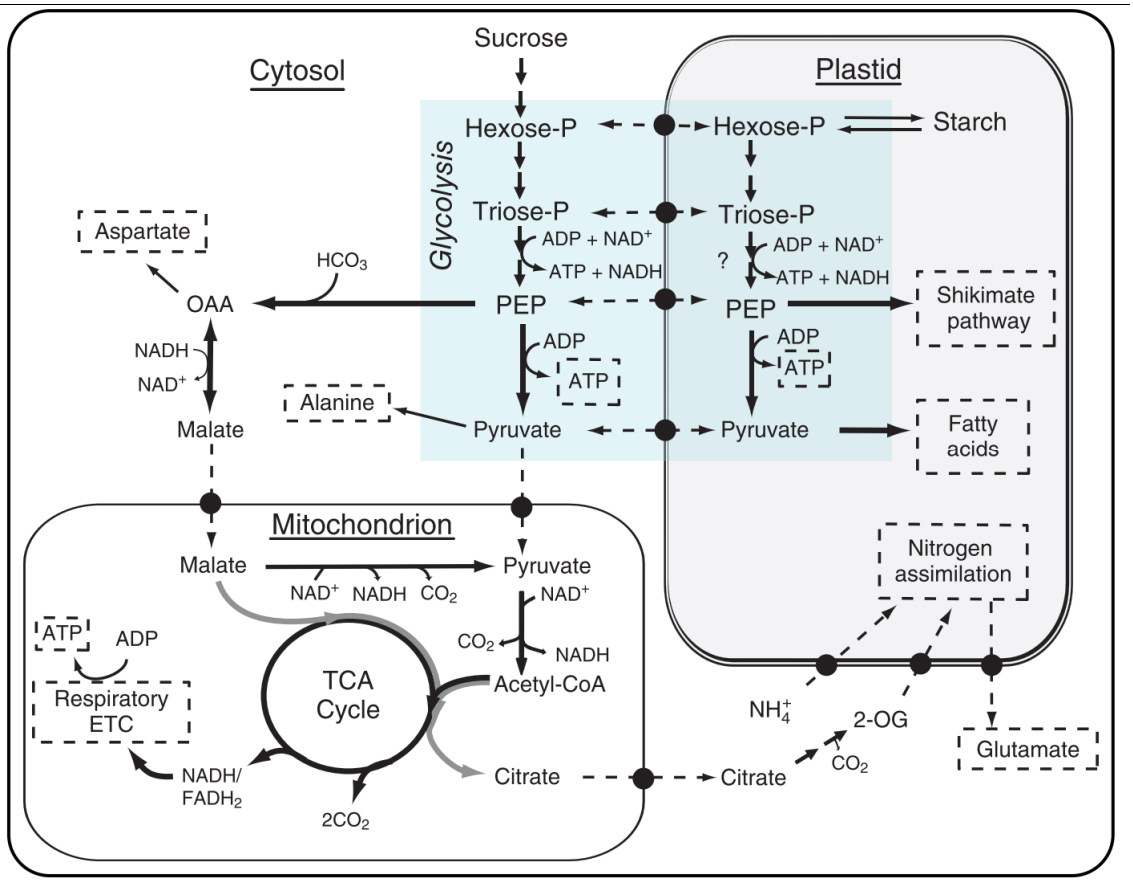

Figure 1.23. Respiratory pathways of carbon metabolism in plants.

Dashed lines indicate metabolite transport processes. Dashed boxes show major metabolic demands of C flux through the respiratory pathways.

Retrieved from (O'Leary and Plaxton, 2016).

glycolysis to participate in the breakdown of starch and the production of C-skeletons, ATP or reducing power employed in other biosynthetic pathways (fatty acids or Shikimate pathway). By

contrast, the main function of cytosolic glycolysis is to provide energy and pyruvate (O'Leary and Plaxton, 2016).

Three main steps can be distinguished in the cytosolic glycolysis in plants. Firstly, sucrose is metabolised by the action of invertases and SUS enzymes, leading to the release of G6P and F6P hexoses (as described earlier). In a second step, the enzymes *PPI-dependent phosphofructokinase* (PPI-PFK) and *ATP-dependent phosphofructokinase* (ATP-PFK) catalyse the phosphorylation of F6P to F1,6bisP. Because of PFKs are dependent on PPI and ATP concentrations and it is believed that these enzymes have regulatory properties and contribute to modulate the glycolysis under different conditions (O'Leary and Plaxton, 2016). The third step, the energy-conserving phase, begins with the cleavage of F1,6bisP into GAP and DHAP, closely followed by the conversion of trioses phosphate into *phosphoenolpyruvate* (PEP) through the serial enzymatic reactions catalysed by GAPDH, PGK, *phosphoglycerate mutase* and enolase, leading to the synthesis of *nicotinamide adenine dinucleotide* (NADH) and ATP (Taiz *et al.*, 2015). PEP can be converted either to pyruvate or OAA via *pyruvate kinase* (PK) or PEPCase. Under high NADH conditions, OAA is reduced to malate by the enzyme *malate dehydrogenase* (Atkin *et al.*, 2000), although it can also be converted into *aspartate* (Sweetlove *et al.*, 2010). While PK is inhibited by elevated concentrations of ATP, PEPCase seems to be modulated by malate, aspartate and glutamate concentrations, suggesting a tightly regulation of these enzymes (Atkin *et al.*, 2000).

Under aerobic conditions, pyruvate, malate, aspartate and OAA are transported to the mitochondria to be used as substrates in the TCA cycle (Sweetlove *et al.*, 2010). In addition, *glycine* produced in the peroxisome as the final product of photorespiration is also transferred to the mitochondria for its oxidation (Atkin *et al.*, 2000). However, in absence of oxygen, TCA and oxidative phosphorylation cannot be carried out due to a limitation in NAD^+ that also hampers the activity of GAPDH. To overcome this problem and met the energy requirement of the plant, the *fermentative metabolism* of pyruvate is employed in plant and non-plant organisms. In *alcoholic fermentation*, pyruvate is firstly decarboxylated by *pyruvate decarboxylate*. The *acetaldehyde* produced is subsequently reduced into *ethanol* in a reversible reaction catalysed by the *alcohol dehydrogenase*, in which NAD^+ is produced. In an alternative pathway, pyruvate can also be reduced to *lactate* via *lactate dehydrogenase*, producing NAD^+. The net glycolytic reaction release only 4 molecules of ATP for each molecule of sucrose converted to pyruvate, but due to the fact that most of the energy found in sucrose remains stored in lactate and ethanol molecules, it makes that the efficiency of the anaerobic fermentation was very low, at about 4 % (Taiz *et al.*, 2015).

Although the modulation of the PK and PEPCase plays an important role in glycolysis regulation, a fine control is mostly exerted by the enzymes catalysing the synthesis of hexoses phosphate from Suc and starch, as well as the conversion of hexoses phosphate to trioses phosphate by PFKs. Other mechanisms of regulation, such as variations in pH or reversible covalent modifications, seem to be implicated in the fine control of glycolysis (Plaxton, 1996).

1.3.3.3. Tricarboxylic acid cycle

TCA cycle (also called *Krebs cycle*) takes place in the mitochondrion, an organelle with some similarities to the chloroplast. It is enclosed by a double-membrane system in which the *outer membrane* surrounds an invaginated *inner membrane*, and the region between them is known as the *intermembrane space*. Inside the inner membrane, there is an aqueous phase called mitochondrial *matrix*, where TCA reactions carried out (Taiz *et al.*, 2015). Nevertheless, other oxidative reactions are developed in the mitochondrial matrix. The glycine accumulated as a consequence of photorespiration has been proposed as the first mitochondrial substrate oxidised in leaf cells. The conversion of glycine is catalysed by the enzyme *glycine decarboxylase* (GDC), releasing *serine* and CO_2. GDC consumes NAD^+ and therefore competes for the cofactor with the dehydrogenase enzymes of the cycle, limiting the activity of TCA (Atkin *et al.*, 2000).

Under low levels of energy, the cyclic flux of TCA is the major pathway for energy-yielding in cells. It provides most of the reduced coenzymes employed during the oxidative phosphorylation for the production of ATP. However, when cellular ATP requirements are met (thus is, under high energy conditions) TCA operates as two disconnected cycling and non-cycling (*anaplerotic*) pathways, providing intermediates for the synthetic and degradative pathways of several biomolecules, especially the synthesis of amino acids (O'Leary and Plaxton, 2016).

The typical cycling activity of TCA (Figure 1.25, a) begins once pyruvate is transported inside the mitochondrion and it is decarboxylated into *acetyl-CoA* via the activity of the enzyme complex *pyruvate dehydrogenase* (PDH). This reaction requires the participation of *coenzyme A* (CoA) and release NADH and CO_2. The action of the enzyme *citrate synthase* condenses one molecule of acetyl-CoA with another of OAA to give the tricarboxylic acid *citrate*. After isomerised to *isocitrate* by an *aconitase*, this molecule experiments two consecutive decarboxylation reactions mediated by the *isocitrate dehydrogenase* (IDH) and *2-oxoglutarate dehydrogenase*, leading firstly to the formation of *2-oxoglutarate* (2-OG) and then to *succinyl-CoA*. Furthermore, in each one of these reactions, a molecule of NADH is released, but CoA is also used by the 2-oxoglutarate dehydrogenase. In the following step, this molecule of CoA is again released to the cytoplasm and one molecule of ATP is

produced during the transformation of succinyl-CoA to *succinate*, mediated by the *succinyl-CoA synthetase*.

The final steps of the cycle involve the transformation of succinate to OAA through the conversion in *fumarate* and *malate*, respectively. These reactions are driven by the enzymes *succinate dehydrogenase*, *fumarase* and *malate dehydrogenase*, releasing the reduced forms of *flavin adenine*

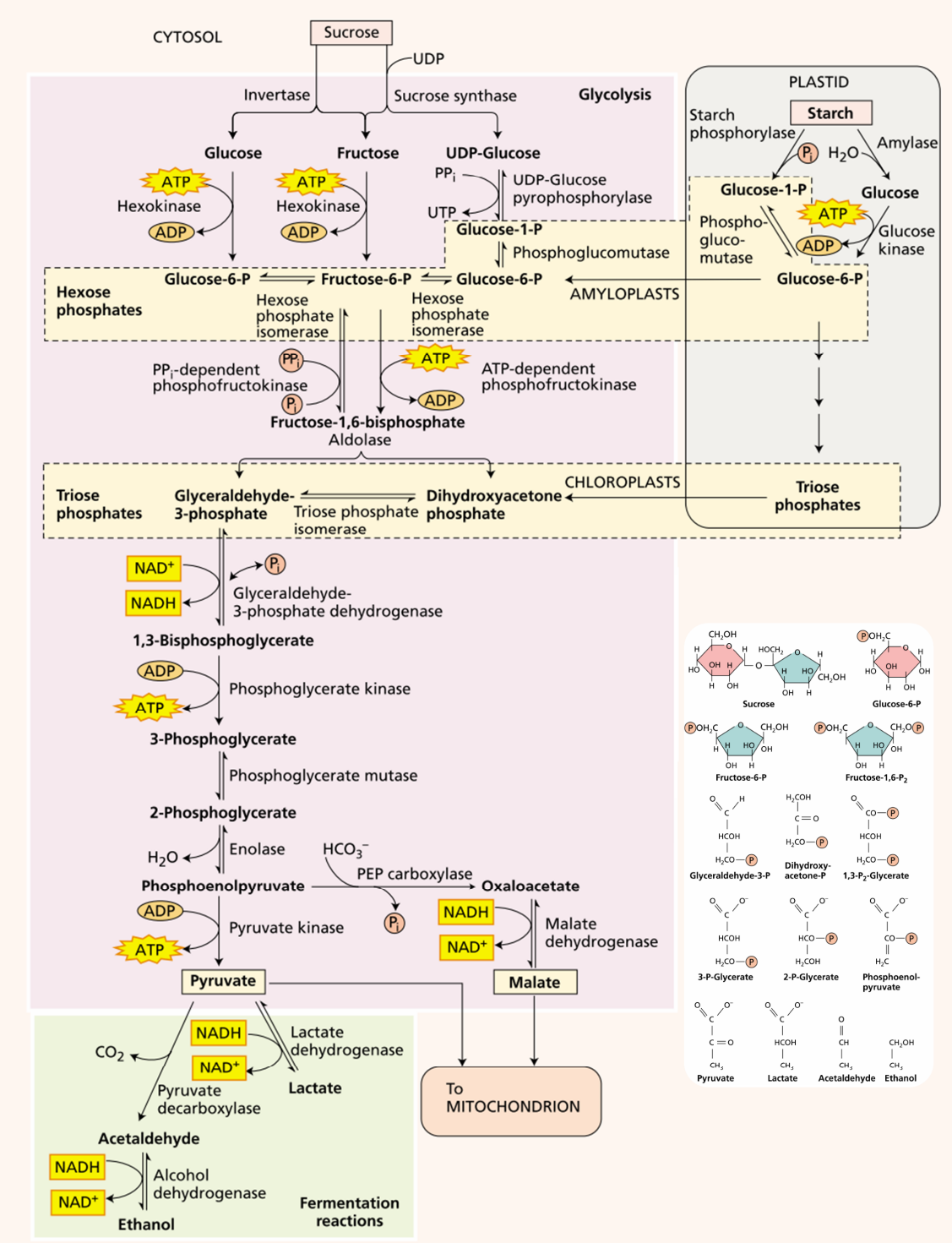

Figure 1.24. Reactions of plant glycolysis and fermentation.

Modified from (Taiz *et al.*, 2015).

dinucleotide ($FADH_2$) and NADH (Taiz *et al.*, 2015). For each molecule of acetyl-CoA entering in the TCA cycle, 3 molecules of NADH, and 1 molecule of $FADH_2$ and ATP are produced, whereas 2 molecules of CO_2 are released (Bender, 2003).

Several models of non-cycling TCA fluxes have been proposed in plants (Steuer *et al.*, 2007), including the conversion of malate into citrate and its later exportation to the cytosol to participate in the synthesis of N (represented as grey arrows in Figure 1.23). After being transported into the mitochondrion, malate can be oxidised by the *malic* enzyme to form pyruvate, CO_2 and NADH or it can replace the TCA intermediates used in biosynthesis (Taiz *et al.*, 2015). The presence of this enzyme has been confirmed only in plants and supposes an alternatively pathway to ATP-limited PK (O'Leary and Plaxton, 2016). Indeed, the metabolic fate of pyruvate is highly conditioned by the availability of acetyl-CoA and the need of OAA to maintain the activity of the TCA cycle. While PDH is inhibited by acetyl-CoA and NADH, PEPCase requires acetyl-CoA for driving its activities (Bender, 2003). Thus, in abundance of acetyl-CoA and NADH, pyruvate is derived through PEPCase to malate and used for the replenishment of the intermediates consumed in the TCA during N-assimilation. In this regard, PEPCase plays a key role regulating the anaplerotic pathway of TCA (O'Leary and Plaxton, 2016).

1.3.3.4. Oxidative phosphorylation

Each molecule of Suc oxidised in aerobic glycolysis and cyclic TCA leads to the formation of four molecules of NADH in the cytosol and 16 in the mitochondrial matrix, as well as four molecules of $FADH_2$. During the oxidative phosphorylation, electrons flow from NADH and $FADH_2$ to O_2 through a chain of electron carriers immersed in the inner membrane of the mitochondrion (Figure 1.25, b). The flux of electrons through the membrane is accompanied by the transport of H^+ from the matrix to the intermembrane space, creating an electrochemical gradient similar to the one found in the chloroplast during photophosphorylation. Dissipation of the proton gradient is also accomplished to an ATPase which drives the synthesis of ATP from ADP (Jones *et al.*, 2013).

The translocation of protons from the matrix to the intermembrane space requires energy that is provided by the oxidation of NADH following this reaction:

$$2\ NADH + 2\ H^+ + O_2 \rightarrow 2\ NAD^+ + 2\ H_2O$$

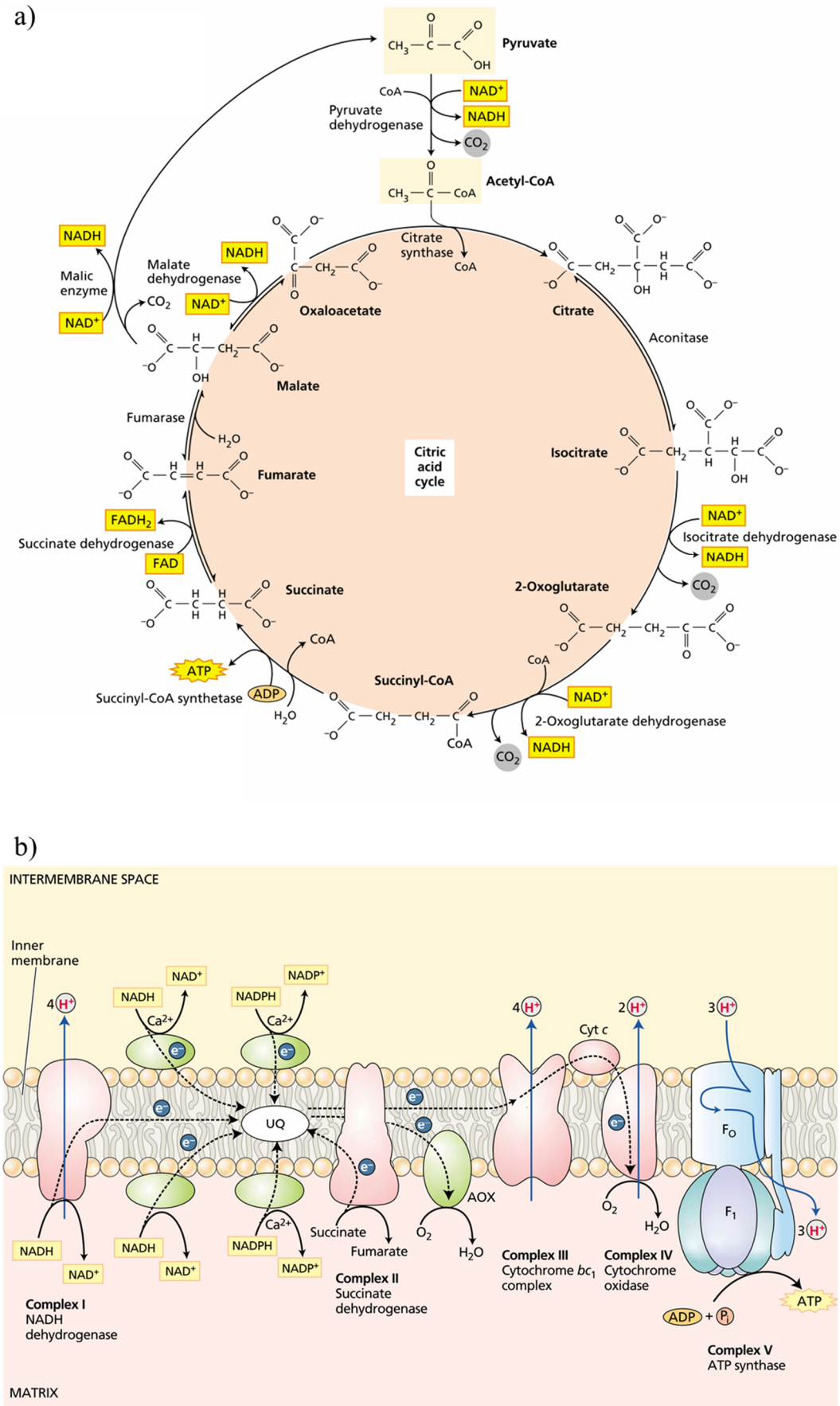

Figure 1.25. Tricarboxylic acid cycle (a) and oxidative phosphorylation (b).

Modified from (Taiz *et al.*, 2015).

The different components of the mitochondrial electron transport chain are organised in supramolecular protein complexes constituted by many protein subunits and different redox cofactors. These includes:

- *Complex I* (*NADH dehydrogenase*): A large complex of 40 subunits containing the NADH dehydrogenase. It also contains *flavin mononucleotide* (FMN), multiple *iron-sulphur clusters* and bound ubiquinone (Roehm, 2001).
- *NAD(P)H dehydrogenases*: They are four flavoproteins placed in the intermembrane space and in the matrix surface of the mitochondrial inner membrane (O'Leary and Plaxton, 2016).
- *Ubiquinone* (UQ): It is a small electron-proton carrier soluble in lipids. It is placed within the inner mitochondrial membrane and it can diffuse through the hydrophobic core of the membrane (Taiz *et al.*, 2015).
- *Complex II* (*succinate dehydrogenase*): The UQ pool also receives electrons from the activity of the enzyme succinate dehydrogenase. Although this enzyme participates in the TCA cycle, it is place inside the inner mitochondrial membrane and therefore acts as the second complex of the chain. It also contains FAD and iron-sulphur clusters (Roehm, 2001).
- *Alternative oxidase* (AOX): It is a homodimer protein bound noncovalently or covalently to the inner membrane (O'Leary and Plaxton, 2016). It has antioxidant and thermogenic properties controlling the formation of *reactive oxygen species* (ROS) and increasing loss of energy as heat (Jones *et al.*, 2013).
- *Complex III* (*cytochrome bc1 complex*): It is a protein complex containing two b-type cytochromes (b_{565} and b_{560}), a membrane-bound *cytochrome* c_1 and an iron-sulphur centre.
- *Cytochrome C*: It is a small mobile protein linked to the outer surface of the inner membrane which acts transferring electrons from Complex III to Complex IV.
- *Complex IV* (*cytochrome c oxidase*): It is the terminal oxidase of the chain, constituted by two copper centres (Cu_A and Cu_B) and two cytochromes (*a* and a_3).
- *Complex V (ATPase)*: This is a protein complex similar to the ATPase of the photophosphorylation, with a F_0 transmembrane complex which acts as a channel for H^+ translocation and a F_1 protein complex containing the catalytic site for the ATP synthesis (Taiz *et al.*, 2015).

The electrons released by NADH are transferred to the pool of UQ via the Complex I while H^+ are translocated from the matrix to the intermembrane space (Roehm, 2001). For each NADH oxidised,

4 protons are pumped from the mitochondrial matrix (Jones *et al.*, 2013). Together with the Complex I, plants also have 4 additional dehydrogenases located in the mitochondrial inner membrane which can oxidise both NADH and NADPH. They act as a bypass of the Complex I, releasing e^- to the UQ pool, but they do not catalyse any transference of H^+ through the membrane. Therefore, this alternative appears to contribute to the maintenance of the cellular redox poise without ATP synthesis (Møller, 2001; O'Leary and Plaxton, 2016). Furthermore, the UQ pool is also fed by the e^- released during the succinate transformation to fumarate catalysed by the complex II. Each reduced UQ (UQH_2) diffuses through the membrane and transfers 2 e^- to the Complex III, triggering the translocation of other 4 H^+ to the intermembrane space by a mechanisms called *Q cycle* (Roehm, 2001; Jones *et al.*, 2013).

During the Q cycle, UQ is reduced by 2 e^- taken from Complex I or II, which is accompanied by the uptake of 2 H^+ from the mitochondrial matrix. When UQH_2 is bound to the *P centre* (the UQ-binding site of Complex III), oxidised UQ transfers an e^- to the Fe-S centre and the other to the cytochrome b_{566}. This reaction also triggers the transference of 2 H^+ from the matrix to the intermembrane space. While the e^- contained in the Fe-S centre is transferred to the cytochrome C through the cytochrome c_1 of the Complex III, the e^- contained into the cytochrome b_{566} is first transferred to the cytochrome b_{560} and then to an oxidated UQ bounded to another UQ-binding site (the *N centre*) of the complex III. In a second turn of the redox cycle, another UQ transfers a couple of e^- to the Cytochrome C (promoting the transference of two new H^+) and to the semi-reduced UQ. The completely reduced UQH_2 uptakes two H^+ from the matrix. The net balance of the Q cycle is of 4 H^+ transferred from the matrix to the intermembrane space for each pair of e^- transferred to the Cytochrome C (Jones *et al.*, 2013).

In this point, a second bypass of the electron transport chain can also be found in plants since some ubiquinone transfer e^- to AOX. The alternative oxidase diverts electrons from the standard route of the electron transport chain to catalyse the reduction of O_2 to H_2O in a highly exergonic reaction. AOX reduces the synthesis of ATP because there is not proton-pumping activity associated to the reaction and the energy produced is released as heat. Nonetheless, alternative functions in the tolerance of the plant under several stresses (including low temperature, phosphate starvation, pathogen attack or osmotic stress) have also been attributed to AOX (O'Leary and Plaxton, 2016).

In the final steps of the oxidative phosphorylation, Complex IV receives the pair of e^- from Cytochrome C. They are yielded in the Cu_A centre and conducted through to the cytochrome *a*, the centre Cu_b and the cytochrome a_3 to a molecule of O_2. As the terminal oxidase, Complex IV brings about the reduction of O_2 to H_2O employing 4 e^- (Roehm, 2001), accompanied by the transference of

H^+ for each e^- transferred to the oxygen. The attached ATPase dissipates the electrochemical gradient allowing the entrance of protons from the intermembrane space to the matrix through F_0. This transference is coupled to the synthesis of ATP, in a ratio of one molecule of ATP for each 3 H^+ translocated.

The complete oxidation of a single molecule of Suc leads to the formation of approximately 60 molecules of ATP, approximately 720 kcal mol^{-1}, which represents about the 52 % of the standard free energy available (Taiz *et al.*, 2015).

1.3.4. Nitrogen assimilation

1.3.4.1. Nitrogen sources and uptake

1.3.4.1.1. Nitrogen availability

N*itrogen* (N) is an essential nutrient for plant growth and biomass production and a primary component of nucleotides, amino acids, proteins, many cofactors and secondary metabolites (Scheible *et al.*, 2004). N is quantitatively the nutrient required in largest amounts by plants and its demand greater than that of any other mineral nutrient. Therefore, it is often the limiting growth nutrient (Nunes-Nesi *et al.*, 2010). N assimilation is tightly linked to C metabolism because photosynthesis provides C skeletons and reducing power for assimilating inorganic N into organic N compounds as amino acids. Plants acquire inorganic N from the soil as *nitrate* (NO_3^-) and *ammonium* (NH_4^+), but root import of amino acids and other organic N compounds also plays a role in some soils, environments and plant species (Bloom, 2015b). NUE can be defined as the ability of a system to transform N inputs into outputs, but for crops it can also be described as the maximum economic yield (of grain and straw) produced by the plants per unit of N applied, absorbed or utilised. Thus, NUE is determined by the ability of the plant to recover N from the soil (*N-uptake efficiency*; NupE) and the utilisation of the N retrieved to produce grain yield (*N-utilisation efficiency*; NUtE). Although a deep interaction between N acquisition and utilisation has been described, there is not a clear consensus about the relative importance of each one of these components (Kaur *et al.*, 2017).

In soils, a vast majority of N (98 %) is found as organic matter, which is unavailable for plants. The fixation of *molecular nitrogen* (N_2) into *ammonia* (NH_3) and the transformation of organic N to inorganic matter requires the participation of soil microorganisms (Taiz *et al.*, 2015; Castro-Rodríguez *et al.*, 2017). The most predominant form of inorganic N in agricultural soils is NO_3^-, being

the most important source of N available for crops (Nacry *et al.*, 2013; Bhattacharya, 2019). Due to the low affinity of NO_3^- to form surface complexes with soil minerals, NO_3^- can be easily leached and diffused to areas of depletion. Thus, NO_3^- availability in the soil is spatially and temporally variable and dependent on several factors, including the microbial activity or the type of the soil (Dechorgnat *et al.*, 2011). In addition, legumes can fix atmospheric N_2 through a symbiotic association with bacteria in root nodules.

1.3.4.1.2. Nitrogen uptake transporters

N uptake is mostly determined by the difference in the influx and efflux of NO_3^- and NH_4^+ in the root cells, but to date, most of the N transporters identified are unidirectional transporters (either influx or efflux). Under non-stress conditions, factors affecting NO_3^- and NH_4^+ influx are the main determinants of the net N uptake, suggesting that influx carriers exert the main control in the acquisition of N (Nacry *et al.*, 2013). In roots, two major systems ensure the optimal N uptake at low (< 100 µM) and high concentrations (> 100 µM) of NO_3^- and NH_4^+. The *high-affinity transport systems* (HATS) are saturable systems which operates under low concentrations of NO_3^- or NH_4^+, while *low-affinity transport systems (*LATS) acts under higher concentrations. The dual kinetic of both systems ensure the optimal inorganic N acquisition in plants (Castro-Rodríguez *et al.*, 2017).

Nitrate transporters

Most of the NO_3^- transporters identified in plants belongs to five protein families known as NRT1, NRT2, CLC, ALMT and SLAC1, but only *nitrate transporters* NRT1 and NRT2 are involved in NO_3^- uptake in roots. NRT1 and NRT2 transporters have either high or low affinity for nitrate, supporting the idea that different carriers drive HATS and LATS activity (Nacry *et al.*, 2013). Characterisation of NRT1 and NRT2.1 (TaNRT2.1) transporters in wheat roots have been reported (Yin *et al.*, 2007; Guo *et al.*, 2014).

Under low-nitrate conditions, NRT2.4 and NRT2.5 are highly expressed in the epidermis of root, but it is NRT2.1 which performs the greatest contribution to NO_3^- transportation while NRT2.2 barely takes part of this activity (Krapp, 2015). It has been estimated that NRT2.1 is responsible of more than 70 % of HATS activity, although it could require the collaboration of a second protein (NAR2). Indeed, this protein is physically associated to NRT2.1 at the plasma membrane, suggesting that the NO_3^- transporter is a tetramer with two subunits conformed by NRT2.1 and NAR2.1 (Dechorgnat *et al.*, 2011).

Low-affinity NO_3^- transporters includes 9 different NRT proteins in *Arabidopsis thaliana*, although only two (NRT1.1 and NRT1.2) are involved in nitrate transportation in roots (Nacry *et al.*, 2013). The expression of *NRT1.1* gene takes place in the apical part of the root and is nitrate-induced.

The NRT1.1 protein plays a key role for the acquisition and sensing of NO_3^-, it promotes the expression of nitrate-related genes and, thus, it is involved in developmental signalling pathways such as root growth or seed germination (Dechorgnat *et al.*, 2011; Castro-Rodríguez *et al.*, 2017). Moreover, its transport activity depends on the phosphorylated state of the T101 residue. Therefore, phosphorylated NRT1.1 displays a high affinity for NO_3^- whereas the non-phosphorylated state of NRT1.1 leads to a low-affinity transporter activity (Nacry *et al.*, 2013). NRT1.2 is also expressed in the epidermis, but it only has LATS activity (Kaur *et al.*, 2017)

Ammonium transporters

Uptake of NH_4^+ in roots is mediated by *ammonium transporters* (AMT), homo- or heterodimers constituting a central pore through which NH_4^+ is firstly acquired (Castro-Rodríguez *et al.*, 2017). The family of AMTs involves six AMT-type transporters (AMT1.1−AMT1.5 and AMT2.1) in *Arabidopsis thaliana* (Nacry *et al.*, 2013), while at least 23 AMT members (TaAMTs) have been found in bread wheat (Li *et al.*, 2017). AMT1.1, AMT1.2, AMT1.3 and AMT1.5 shows AHTS capacity, but around 30 % of NH_4^+ HATS capacity is displayed by the activity of AMT1.1 and AMT1.3, which are placed in the plasma membrane of cortical and epidermal cells of the roots. Similarly, AMT2.1 is also found in the endodermal and cortical cells of the root while AMT1.4 genes are not expressed in the radical system. AMT2.1 acts as a low-affinity transporter of the NH_4^+ uptake, the ammonium retrieval from the apoplast and its translocation to vasculature (Nacry *et al.*, 2013). After NH_4^+ acquisition, the subsequent assimilation into amino acids in the root cells is carried out by the action of the enzymes *glutamate synthetase* (GS) and *glutamine oxoglutarate aminotransferase* (GOGAT) (Castro-Rodríguez *et al.*, 2017).

1.3.4.2. Nitrate and ammonium assimilation

Once nitrate has been acquired, NO_3^- can be directly metabolised in the cell roots, stored in the vacuole or transferred to the aerial plant part through the xylem. This last alternative depends on the transpiration stream and the interactions between xylem and phloem (Figure 1.26, a), influenced by the families of transporters and channels NRT1, NRT2, NPF (*nitrate transporter 1/peptide transporter family*), CLC (*chloride channel*), SLAC/SLAH (*slow anion channel-associated homologues*) and the proteins NAXT (Dechorgnat *et al.*, 2011; Krapp, 2015). The assimilation of nitrate in organic N compounds involves several steps, NO_3^- is firstly reduced to *nitrite* (NO_2^-) and then to NH_4^+, which is subsequently incorporated into amino acids, as the amide nitrogen form of glutamine (Figure 1.26, b), in a series of reactions consuming 12 ATPs (Taiz *et al.*, 2015). However, NO_3^- reduction steps are spatially separated in the cells of roots and leaves. Nitrate reduction takes

place in the cytosol and is catalysed by the enzyme *nitrate reductase* (NR) (Masclaux-Daubresse *et al.*, 2010), as describes the following stoichiometric reaction:

$$NO_3^- + NAD(P)H + H^+ + 2\ e^- \rightarrow NO_2^- + NAD(P)^+ + H_2O \text{ (Taiz } et\ al.\text{, 2015)}$$

The reducing power required (NAD(P)H) for the reaction can be derived from three main sources: photosynthesis (in leaves) via DHAP:PGA or OAA-malate; glycolysis, through the oxidation of GAP to BPGA); and/or TCA (during the malate oxidation to OAA) (Atkin *et al.*, 2000). Nitrite is subsequently translocated from the cytosol to the plastids, where it is reduced to ammonium by the action of the enzyme *nitrite reductase* (NiR) following this reaction:

$$NO_2^- + 6\ Fd_{red} + 8\ H^+ + 6\ e^- \rightarrow NH_4^+ + 6\ Fd_{ox} + 2\ H_2O$$

where Fd corresponds to the reduced (Fd_{red}) or oxidated (Fs_{ox}) states of ferredoxin molecules derived from the photosynthetic electron transport in the chloroplast (Taiz *et al.*, 2015).

The ammonium produced through the reduction of nitrate, the photorespiration and/or the amino acid recycling is assimilated by the GS/GOGAT cycle. GS fixes NH_4^+ into a molecule of *glutamate* (Glu) to produce a molecule of *glutamine* (Gln), which subsequently reacts with 2-OG to form two molecules of Glu (Figure 1.26, c). Two different forms of GOGAT have been described with different distribution in the plant. While the ferredoxin-dependent Fd-GOGAT is mostly placed in the chloroplast, NADH-GOGAT using NADH as electron donor is located in plastids of non-photosynthetic organs. Likewise, two isoforms of GS have been identified in mesophyll cells of the

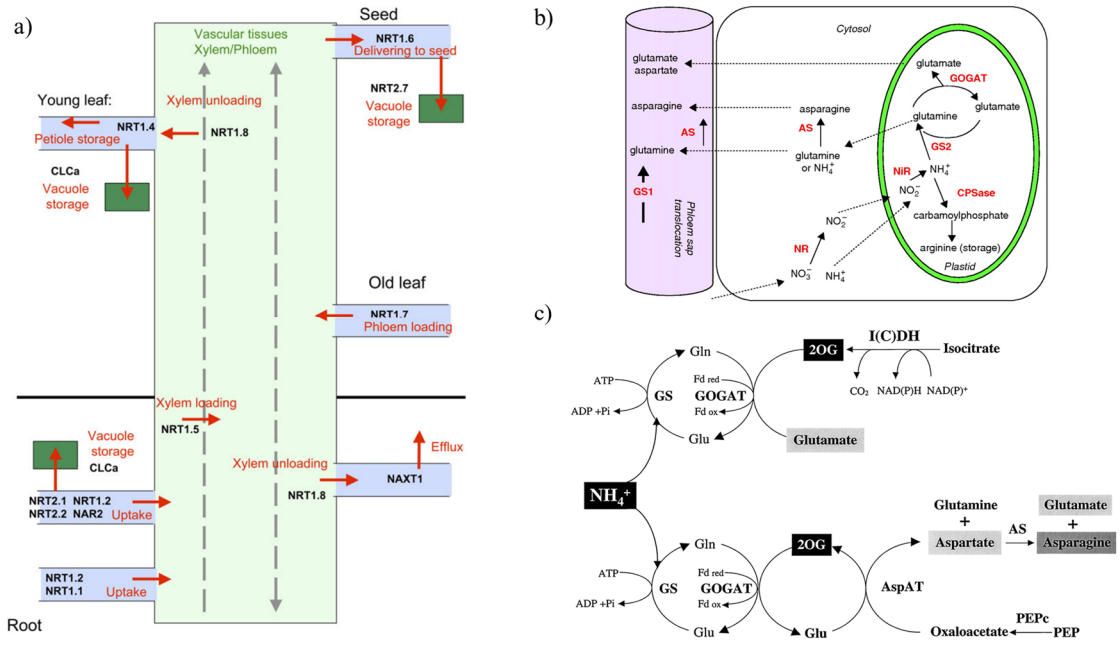

Figure 1.26. Nitrogen transportation and assimilation.

a) Schematic representation of nitrate pathways within the *Arabidopsis thaliana*; b) nitrate assimilation in leaves; c) GS/GOGAT cycle. Retrieved from (Lancien *et al.*, 2000; Masclaux-Daubresse *et al.*, 2010; Dechorgnat *et al.*, 2011).

leaves (GS2) or in non-green tissues such as seed or roots (GS1), but since the expression of GS1 is induced during senescence, it is possible that this isoform will be involved in N remobilisation (Masclaux-Daubresse *et al.*, 2010).

Together with the GS/GOGAT cycle, other enzymes participate in the ammonium assimilation:

- IDH: This enzyme catalyses the decarboxylation of isocitrate to 2-OG (Figure 1.26, c). Two isoforms, NAD- and NADP-dependent IDH, have been described, and although IDH is only located in the mitochondria, several IDH isoenzymes are placed in the cytosol (ICDH1), mitochondria, plastids or peroxisomes. Due to the fact that GOGAT is placed in plastids, two hypotheses about the origin of 2-OG have been suggested:
    1. 2-OG required for GOGAT activity could be originated in TCA reactions of mitochondria, leaving it and migrating to the plastids.
    2. Involves ICDH1. In this hypothesis, citrate transported from mitochondria to the cytosol would be used to produce isocitrate by the action of a cytosolic aconitase. The subsequent reaction catalysed by ICDH1 would allow to produce 2-OG which would be imported to the plastid (Figure 1.23).
- GDH: Catalyses the reversible assimilation of ammonium and 2-OG into Glu, following this reaction:

  $$\text{2-Oxoglutarate} + NH_4^+ + \text{NAD(P)H} \leftrightarrow \text{glutamate} + H_2O + \text{NAD(P)}^+$$

  Two types of GDH, NAD(H) – and NADP(H)-dependent GDH, have been found as mitochondrial or chloroplastic forms, respectively.
- *Aspartate aminotransferase*: It mediates the production of 2-OG and aspartate from Glu and OAA. This enzyme is found in plastids, cytosol, mitochondria and peroxisomes (Lancien *et al.*, 2000).
- Cytosolic *asparagine synthetase*: Catalyses the transference of an amide group of Gln to aspartate, producing asparagine and glutamate (Masclaux-Daubresse *et al.*, 2010):

  $$\text{Glutamine} + \text{aspartate} + \text{ATP} \rightarrow \text{asparagine} + \text{glutamate} + \text{AMP} + PP_i$$
- *Carbamoylphosphate synthase*: It performs the synthesis of the citrulline and arginine precursor *carbamoylphosphate* (Lancien *et al.*, 2000).

The synthesis of other amino acids, such as lysine, methionine, threonine or isoleucine are derived forms of aspartate through several branched pathways, while aromatic amino acids such as tryptophan, phenylalanine or tyrosine are produced from *chorismate*, the final product in the shikimate pathway (Misran and Jaafar, 2019).

Finally, it is important to highlight that the limiting step in the N assimilation pathway is the reduction of NO_3^- catalysed by the NR. The enzyme is highly regulated by NO_3^-, carbohydrates and downstream metabolites of N assimilation at transcriptional level (Scheible *et al.*, 1997b; Morcuende *et al.*, 1998; Stitt, 2002), and a complex post-transcriptional and post-translational regulation adjust its activity to the N status of the plant (Scheible *et al.*, 2004). Moreover, dependent on the plant species and the environmental conditions, the acquired inorganic N is reduced to amino acids in roots or photosynthetically active leaves (Rentsch *et al.*, 2007).

1.3.4.3. Nitrogen remobilisation

Nitrogen uptake mostly happens at the vegetative stage of the crop, therefore N supplied early during the season stimulates vegetative growth. By contrast, N application late in the season improves the grain nitrogen concentration at maturity (Bhattacharya, 2019). In line with this observation, N remobilisation from photosynthetic proteins contained in leaves provides a main source of N during senescence, which is employed to feed new organs, such as seeds, with N compounds. Indeed, studies employing ^{15}N long-term labelling have proposed that contribution of leaf N remobilisation to wheat, rice and maize grain N concentration varies around 50−90 %, although it is also influenced by the environmental factors and favoured in N-limiting conditions (Masclaux-Daubresse *et al.*, 2010).

As mentioned above, Rubisco is the most abundant protein in plants, greatly exceeding the requirements for the photosynthetic activity. Due to its abundance, it has been proposed that Rubisco constitutes a main N storage in the plant. The hydrolysis of Rubisco begins early in senescence, but the enzymes catalysing this process are still unknown. Among the several mechanisms hypothesised, the action of vacuolar enzymes, the catalysis of cysteine proteases and the participation of the ubiquitin-proteasome proteolytic system have been proposed. In wheat, the maintained levels of *20S proteasome* supports the latest proteolytic pathway (Barneix, 2007).

During the grain filling stage, N uptake is repressed in roots due to the high levels of amino acids and the general good N status of the plant. As a consequence, the levels of *cytokinin* remain elevated, proteins are not degraded and, therefore, amino acids in the phloem keep stable (Barneix, 2007). By contrast, during senescence, amino acids produced after proteolysis are stored in the central vacuole of the mesophyll cells before they are released into the phloem. In cereals, glutamine is the main form of N-compound transportation, and therefore concentrations of this amino acid increase during senescence in the phloem (Masclaux-Daubresse *et al.*, 2010).

1.3.5. Carbon–Nitrogen Balance

Along the present review of the C-N metabolism, a close interaction between both metabolisms has been shown. In fact, photosynthesis is first driven by the photon-yield carried out by the light-harvesting complexes found in the chloroplast and the photophosphorylation reactions involve a series of protein carriers or long enzymatic complexes such as plastocyanin or the ATPase. The subsequent reactions in the Calvin cycle would not be performed without the catalytic activity of Rubisco, the most abundant protein in plants and the main source of N during senescence. Both, the synthesis and cleavage of complex carbohydrates require the participation of several enzymes, as well as the ATP produced or generated in the mitochondria. Furthermore, many reactions including the aspartate synthesis from oxaloacetate, the deviation of the tricarboxylic acid citrate to the plastids for the nitrogen assimilation or the synthesis of amino acids (Figure 1.27), reflect the interconnection of both metabolisms. Since regulation of both metabolic pathways has been shown a critical point for plant growth and development (Kaur *et al.*, 2017), the investigation of central C-N metabolism is crucial to improve crop productivity and quality, including wheat, in response to the environmental conditions.

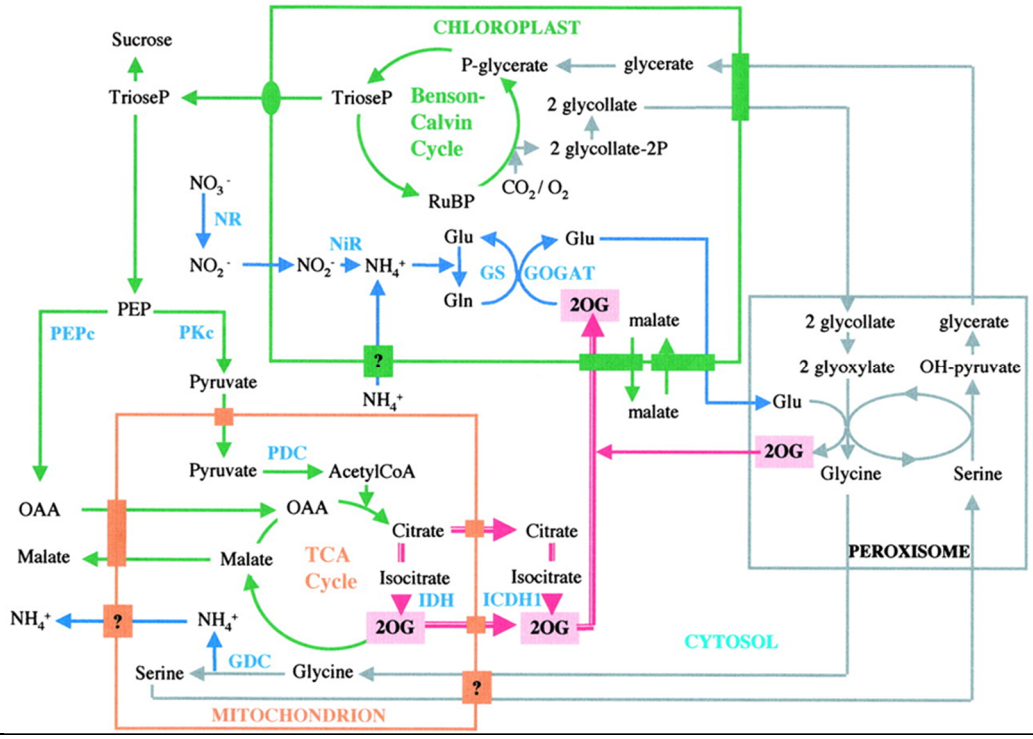

Figure 1.27. A simplified scheme of C and N flow between organelles.

Retrieved from (Lancien *et al.*, 2000).

1.4. Future agriculture challenges

1.4.1. Challenges of agriculture

1.4.1.1. Meeting the growing population food demand

World population has changed along the time (Figure 1.28). In 1800, the number of human beings on Earth reached one billion for the first time, after centuries of very slow increase. 150 years later, global population increased to 2.5 billion people (Bongaarts, 2009), while in 1994 and 2007 attained about 5.7 and 6.7, respectively (United Nations, 2019). Currently, the world population has exceed 7.9 billion people (United Nations, 2021; Worldometers, 2021), and although the global growth rate has decreased from 2.09 % in 1968 to 1.05 % in 2020, it is expected to continue rising until reach around 10 billion people in 2050 and between 9.4 and 12.7 billion in 2100 (United Nations, 2019). This rapid change in demography responds to a transition from a high birth and death rate to a lower ratio. A transient period is critical to explain the increase in population since the raise in the growth ratio is driven by a temporary decoupling between deaths and births, with deaths declining before births, prior to stabilisation. This transition is usually accompanied by the transformation of an agricultural society into an industrial one (Bongaarts, 2009).

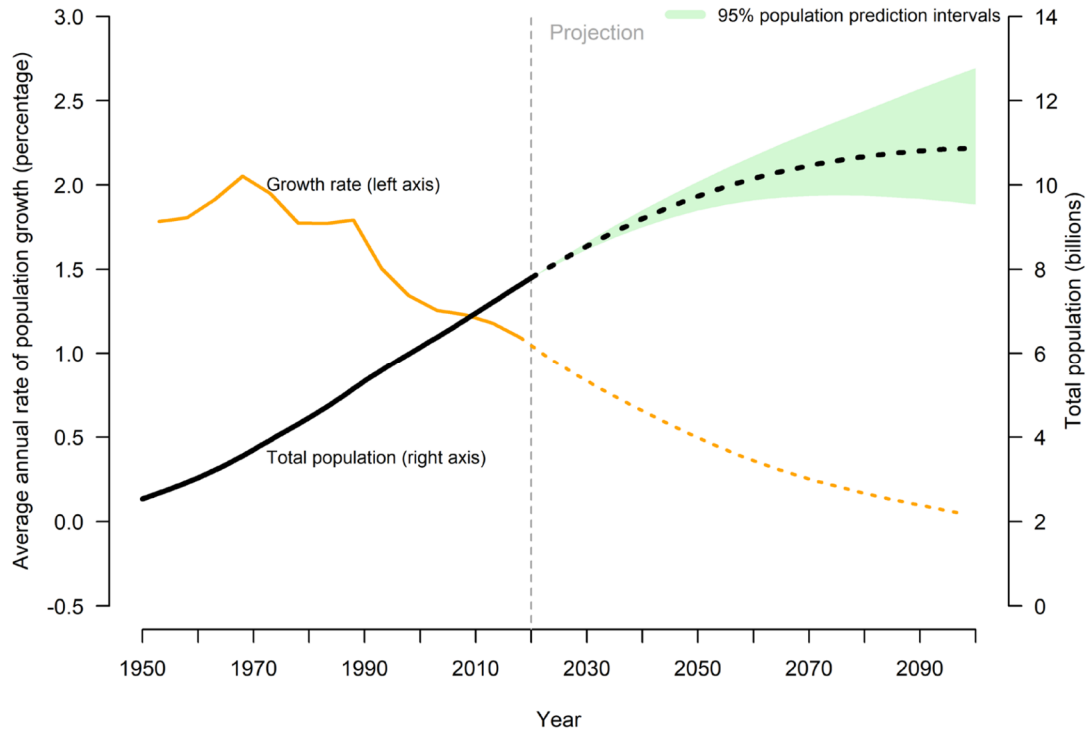

Figure 1.28. Human population size and growth rate worldwide from 1950 to 2020.

Retrieved from (United Nations, 2019).

The food demand is driven by the increase in world population. To meet the growing population demand by 2050, food production needs to increase at least a 50 % more than in 2012. Crop productivity increased significantly worldwide during the Green Revolution due to the increase in the cultivated land and the improvement in agronomic practices, including the use of agrochemical N fertilisers, herbicides and pesticides. As a consequence of the Green Revolution, the cultivation of traditional landraces was progressively replaced by the introduction of improved, more productive and genetically uniform semi-dwarf cultivars. This has led to an enormous decrease in biodiversity (Khush, 2001). At the same time, that demand for food is increasing, production is gradually being limited by the loss in the area of arable land to urban sprawl, land degradation (erosion and salinisation), non-food uses of crops (bioenergy production as biofuels) and climate change (Parry and Hawkesford, 2010). In fact, the reported global annual increases in productivity of main staple crops, such as maize, rice or wheat, are close to 1 % during the last decades, whereas wheat yield gain was higher than 3 % in the period comprised between 1965 and 1974 (FAO, 2014). To meet the growing food demand is highly improbable that the cultivated area can increase and, in turn, the increment of N fertiliser input does not seem to be the most appropriate option for the agricultural sustainability because of its harmful environmental impacts, such as degradation of soil, water contamination, greenhouse gas emissions, etc. This implies that genetic improvement will have to be much more effective increasing crop yield than in the past and the development of stress-resilient plants will be required to ensure food security in the coming decades.

1.4.1.2. Nutrient dietary assessment

A different but related challenge is to feed population with sufficient nutrients to ensure health. In 2018, the *State of Food Security and Nutrition in the World* report (FAO *et al.*, 2018) used for the first time the *Food Insecurity Experience Scale* (FIES) in order to measure and classify the severity

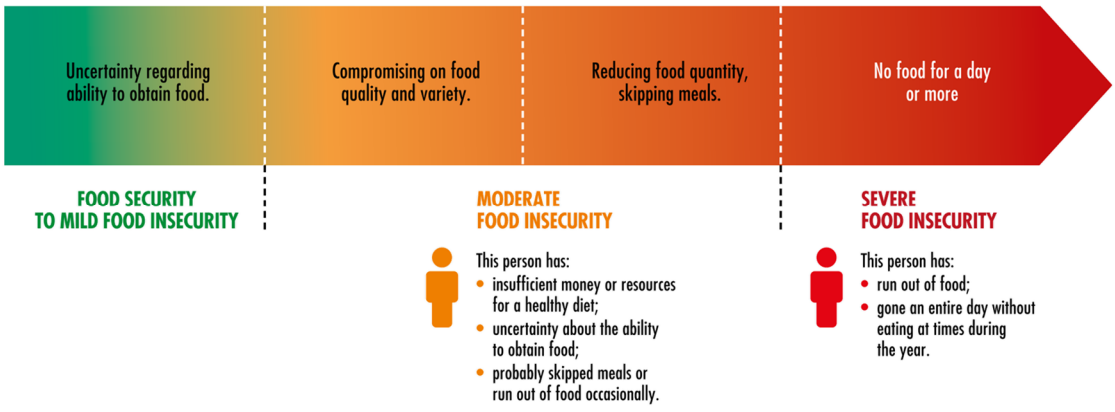

Figure 1.29. FIES scale of food security.

Retrieved from (FAO *et al.*, 2018).

of food scarcity (Figure 1.29). In this scale, individuals are distributed in three major classes defined by two main thresholds: *food secure*, when the access to food is guaranteed; *moderately food insecure* if there is a compromise in the quality (first) and quantity (later) of food; and *severely food insecure* in absence of food for a day. Moderate food insecurity is driven by a consistent lack of access to food, diminishing the dietary quality and disrupting the normal patterns of eating, which negatively impacts on health and well-being. By contrast, people experiencing severe food insecurity have food deprivation and, in the most extremely cases, they gone for days without eating (FAO *et al.*, 2019). Thus, this scale reflects that severe scarcity in food resources is the last step in a large chain of events in which that lack of nutrients and the access to healthier food is firstly compromised.

Malnutrition is defined as a condition of deficiency, excess, or imbalance in a wide range of nutrients which leads to a series of adverse effects on body function, composition and clinical outcome (Saunders *et al.*, 2019). Malnutrition comprises two major disorders:

- *Overweight, obesity and diet-related diseases*: Overweight describes a condition of fat overaccumulation with the potential of putting health in jeopardy. Obesity implies a higher storage of fat than overweight.
- *Undernutrition*: It is a diet-related condition originated due to the insufficient food intake to satisfy energy and nutrient demand. It includes:
    - *Stunting*: Childhood stunting implies an impairment in growth and development, leading to a lower height according to the age.
    - *Wasting*: Childhood wasting refers to a low weight for height
    - *Underweight*: A form of undernutrition characterised by a low body weight for the age.
    - *Micronutrient deficiencies*: Insufficient intake or absorption of minerals or vitamins (Initiatives, 2021).

Malnutrition is a universal issue holding back development of human society by bringing about more ill health and economical losses than any other cause. Since the lack of nutrients and the sporadic food deprivation happen before than extreme periods of starvation, malnutrition disorders are highly frequent worldwide but further less noticed, and therefore are known as *hidden hunger* (Gödecke *et al.*, 2018). The large decrease in the prevalence of undernourishment experienced in the world since 2005 has already come to a halt, increasing from 8.4 % in 2019 to the average expected 9.9 % for 2020 (Figure 1.30). Although this increase is partially associated with the COVID-19 pandemic, the fact is that more than 650 million people suffered from hunger in 2019 and the expected projections for 2020 increase this number to a range between 720 and 811 million people (FAO *et al.*, 2021). It

has also been estimated that almost 149 million of children under 5 years of age suffered for stunning, 45 million for wasting and 38.9 million are overweight, while obesity and overweight affects to 2.2 billion adults (Initiatives, 2021). In line with this, crop biofortification to improve the nutritional value of staple foods has showed effectivity supplying micronutrients to population, as well as positive results in the socio-economic and environmental aspects (Olson *et al.*, 2021). Nevertheless, a global trend towards lower grain quality in highly yielding agronomical conditions and modern cultivars has been reported since breeders are mainly selecting for grain yield but not grain quality (Fan *et al.*, 2008). Thus, the possible genetic erosion and the reduction in grain micronutrient content found in varieties introduced during the Green Revolution (Guarda *et al.*, 2004; Garvin *et al.*, 2006; Murphy *et al.*, 2008; Pingali, 2012) may lead to a serious threat to human nutrition and health. Food availability largely relies on economic development, which is important in dealing with hidden and chronic hunger and poverty in developing and underdeveloped countries (Gödecke *et al.*, 2018; Razzaq *et al.*, 2021). Efforts to increase agricultural productivity in a sustainable manner might not be enough to reduce malnutrition and hunger as there are many factors affecting global food security, including climate change, which may adversely affect crop productivity and quality.

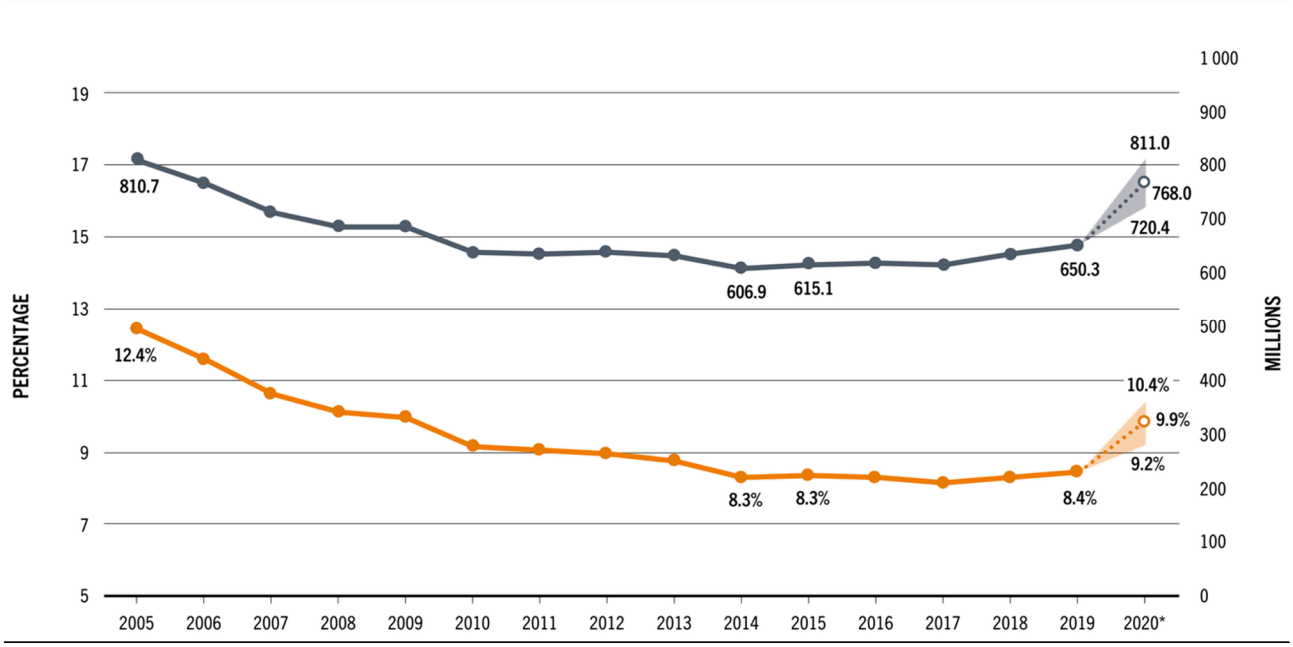

Figure 1.30. Undernourished people in the world from 2005 to 2019.

Number of undernourished people is showed in grey (millions, right axis). Prevalence is showed in orange (percentage, left axis). Projected values for 2020 are illustrated by dotted lines. Shaded areas show lower and upper bounds of the estimated ranges.

Retrieved from (FAO *et al.*, 2021).

1.4.2. Climate change

1.4.2.1. Historical perspective of the climate change

The climate on Earth is not changeless. For the last 540 million years, the global climate has been oscillating from a "warm-greenhouse" to a "cold-icehouse" state (Anagnostou *et al.*, 2016). These shifts can take thousands or hundreds of millions of years to happen and, in some cases, they are associated with biotic crises or events of massive extinction (Link, 2009). The last transition between the warm and the cold global states happened between 65 and 34 million years ago and supposed the glaciation of the Antarctica. In the last 3.8 billion of years, the temperature on Earth has remained relatively constant within an optimum range for life development, with atmospheric CO_2 playing a fundamental role in in the maintenance of the habitable conditions (Link, 2009; Anagnostou *et al.*, 2016; Mills *et al.*, 2019).

Global warming refers to the increase in the average temperature on the surface of Earth as a consequence of the raise in the concentration of *greenhouse gases* (GHGs), including CO_2 but also other gases such as *water vapour*, *ozone*, *methane*, *nitrous oxide* and *chlorofluorocarbon* (CFCs). The special property which allows GHGs to increase surface temperature comes from their ability to absorb and reradiate solar energy. While CO_2 and methane absorb energy in the infrared light spectrum, ozone does it with ultraviolet waves. Since almost half of the total solar energy belongs to infrared radiation (Al-Ghussain, 2019), CO_2 and methane seem to have a fundamental role modulating the temperature. For the last 800,000 years, oscillations in global temperature fit with the variations in atmospheric CO_2 concentration ($r^2 = 0.82$; Figure 1.31, a), including the end of glacial periods coinciding with the raise in CO_2 concentration (Lüthi *et al.*, 2008). This relationship has gained great prominence in recent centuries because of the tendency towards lowest temperatures observed in the last 2,000 years have been turned back since 1850 (Figure 1.31, b), coinciding with the anthropogenic release of about 2,390 $GtCO_2$ after *Industrial Revolution* (IPCC, 2021b). Although alternative hypothesis for the simultaneous increases in atmospheric CO_2 concentration and surface temperature have been explored, such us variations in solar radiation, the eccentricity, obliquity and precession of the Earth (*Milankovitch cycle*) or volcanic eruptions, the impact of these natural events seems to be low in comparison with the effect of GHGs associated with human activity (Al-Ghussain, 2019). Indeed, the *Climate Change* report of 2018 from the *Intergovernmental Panel on Climate Change* (IPCC, 2018) pointed at the human activities as the main cause of the increase in temperatures from the last two centuries. Their latest report (IPCC, 2021b) not only showed that variations in the Earth's surface temperature cannot been explained without anthropogenic activities (Figure 1.31, c), but also provided evidence that there is a near-linear relationship between the cumulative human-CO_2

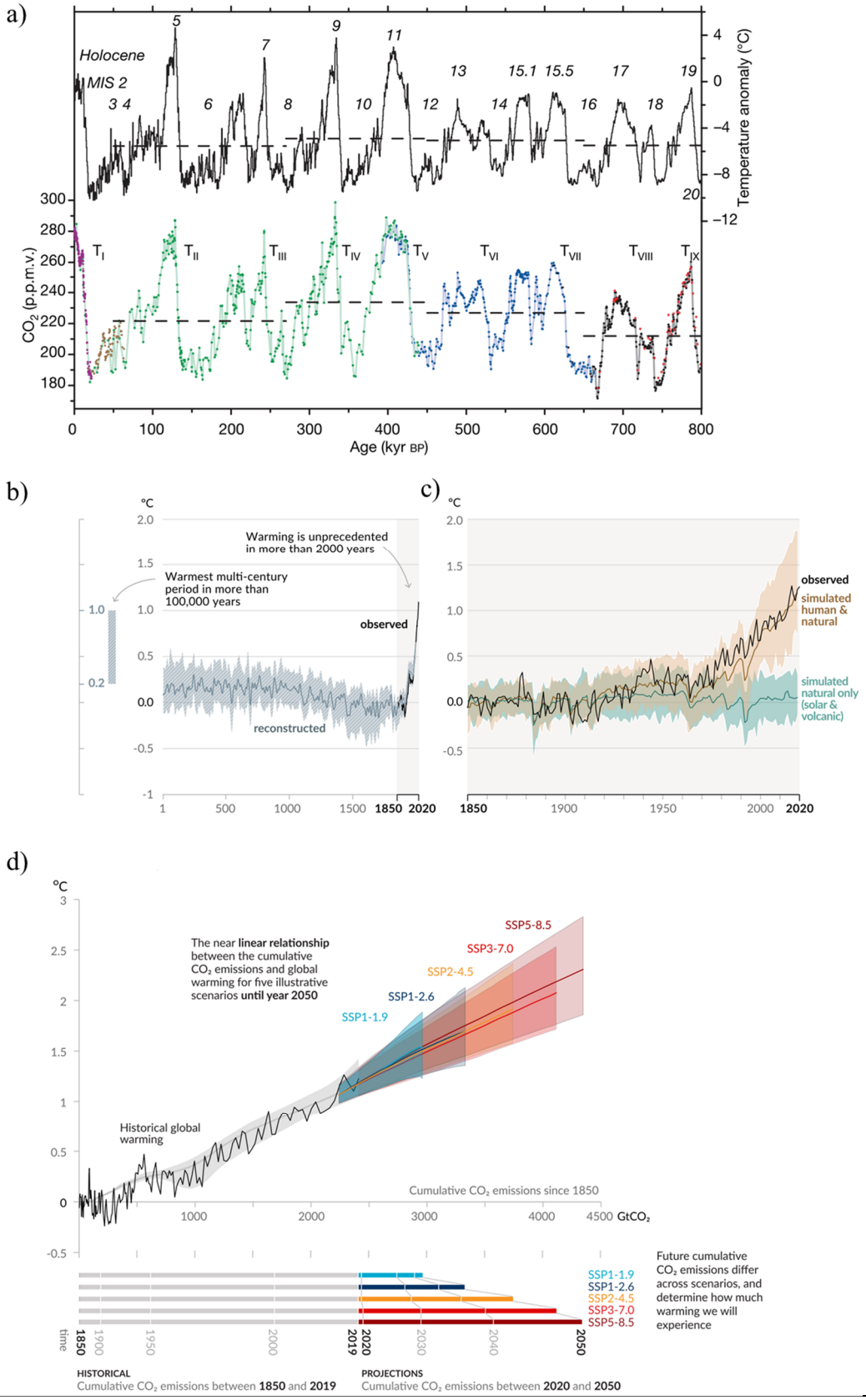

Figure 1.31. Tendences in global CO_2 and temperature.

a) Compilation of CO_2 and temperature anomalies over the last 800,000 years. Glacial terminations are indicated using Roman numerals in subscript. Marine Isotope Stages (MIS) are given in italic Arabic numerals; b) changes in global surface temperature in the last two millennia; c) changes in global surface temperature in the last 170 years; d) near-linear relationship between cumulative CO_2 and surface temperature. More details in the articles.

Retrieved from (Lüthi *et al.*, 2008; IPCC, 2021b).

emissions and global warming (Figure 1.31, d). For each 1,000 $GtCO_2$ of cumulative CO_2, the global surface temperature increases about 0.27 ºC and 0.63 ºC, with the best estimation of 0.45 ºC (IPCC, 2021b). At the beginning of 2022, the global atmospheric CO_2 concentration exceeded 416 ppm (NOAA-ESRL, 2022), but it is expected to continue raising along the century varying among different scenarios: SSP1-1.9, SSP1-2.6, SSP2-4.5, SSP3-7.0, and SSP5-8.5. In the worst of the scenarios, but also the most consistent with the current emissions, the atmospheric CO_2 concentration is expected to raise until 550 and nearly 940 ppm by 2050 and 2100, respectively (Smith and Myers, 2018). This would lead to future raise in temperature ranging between 0.5 ºC and 1.5 ºC from present to 2050 (Figure 1.31, d) and almost 4 ºC by the end of the century (IPCC, 2021b).

These changes in climate have already led to a raise in the frequency of more extreme climatic events. For the last century, the incidence of floods has increased substantially while the number of drought events grew at both (northern and southern) hemispheres, as well as the prevalence of heat waves (Al-Ghussain, 2019). These extreme events directly affect to human health, mostly causing cardiovascular and respiratory disorders. However, the climate change can also impact on health through the reduction in the quality and the availability of food and water. For example, a reduction in maize and wheat productivity has been observed from 1980 to 2008 associated with the effects of global warming (Ciardini *et al.*, 2016). In line with these observations, growing concern about the rising emissions of greenhouse gases to the atmosphere, in special CO_2, and their contribution to the increase of Earth´s surface temperature has prompted social sensitivity, policy discussions and international negotiations. Major concerns are also raised about the effects of global climate change on agriculture. This climate variability will directly or indirectly affect crop development and grain yield and quality, including wheat, which could substantially undermine future global security. Thus, global climate change is one of the main challenges that agriculture will have to face in the following decades.

1.4.2.2. Impact of climate change on crop productivity

1.4.2.2.1. Effects of elevated atmospheric CO_2 concentration on plant development

Plant growth and biomass accumulation are driven by the photosynthetic carbon assimilation and the inorganic nutrient assimilation of which N is quantitatively the most important. As a key substrate for photosynthesis, the primary effect of raising CO_2 in crops, including wheat, is a direct stimulation of the *photosynthetic carbon assimilation rate* (*A*), which may thereby enhance plant growth and consequently increase grain yield (Long *et al.*, 2004, 2006a). At the current atmospheric CO_2 concentration, Rubisco is not saturated and, thus, a higher substrate concentration promotes

carboxylation while the competitive oxygenation reaction of Rubisco is inhibited (Ainsworth and Long, 2004; Ainsworth *et al.*, 2004), decreasing photorespiration. A second effect of elevated CO_2 is a decrease in *stomatal conductance* (g_s) because of the closure of stomata leading to an improvement in the plant *water use efficiency* (*WUE*) (Ainsworth and Rogers, 2007; Wang and Liu, 2021). Therefore, elevated CO_2 can positively impact wheat production by stimulating photosynthesis rates (Pérez *et al.*, 2005; Long *et al.*, 2006a; Aranjuelo *et al.*, 2011; Vicente *et al.*, 2015a). In fact, increases in photosynthesis and/or biomass induced by elevated CO_2 have been reported in many studies carried out in field free air CO_2 enrichment (FACE) (Ainsworth and Long, 2004; Leakey *et al.*, 2009; Rezaei *et al.*, 2018), field temperature gradient chambers (Martínez-Carrasco *et al.*, 2005; Pérez *et al.*, 2005; Aranjuelo *et al.*, 2011; Vicente *et al.*, 2011) and controlled environment growth chambers (Vicente *et al.*, 2016, 2017), but the increase is less than expectation (Ainsworth and Long, 2004; Leakey *et al.*, 2009; Rezaei *et al.*, 2018). This could be partly attributed to a decreased stomata conductance under elevated CO_2 (Bernacchi *et al.*, 2007; Zhao *et al.*, 2021), while a limitation in N availability is another factor constraining the increase in productivity (Zhao *et al.*, 2021).

Long-term exposition to elevated CO_2 leads to a down-regulation of photosynthetic capacity (Long *et al.*, 2004; Martínez-Carrasco *et al.*, 2005; Gutiérrez *et al.*, 2009a), accompanied by a reduction in Rubisco activity and protein amount, and enhanced leaf carbohydrate content and lower plant N concentration (Bloom *et al.*, 2002; Long *et al.*, 2004; Pérez *et al.*, 2005; Aranjuelo *et al.*, 2011; Tausz-Posch *et al.*, 2020). Different factors have been proposed to explain this phenomenon of *photosynthetic acclimation to elevated CO_2*, including the repression of genes encoding for both small and large Rubisco (*rbcS* and *rbcL*) subunits by the accumulation of non-structural carbohydrates in leaves (Nie *et al.*, 1995; Moore *et al.*, 1999; Rolland *et al.*, 2006), accelerated leaf senescence (Zhu *et al.*, 2009), a limitation by N availability (Stitt and Krapp, 1999) and insufficient sink capacity (Long *et al.*, 2004; Aranjuelo *et al.*, 2011). In line with this latter explanation, it has been proposed that genetic or environmental factors limiting the development of sink strength make plants susceptible to a higher photosynthetic acclimation, and lessen the stimulation of photosynthesis by elevated CO_2 (Long *et al.*, 2004; Ainsworth and Rogers, 2007). So, the source-sink relationship has been suggested as playing an important role in the regulation of plant growth and yield response to elevated CO_2 concentrations (Ainsworth *et al.*, 2004; Tausz-Posch *et al.*, 2013b). Moreover, a higher growth and yield response to elevated CO_2 has been found in some older wheat cultivars when compared to modern ones, a finding which seems to be associated with the capacity of the older cultivars to produce further tillers functioning as vegetative sinks for the allocation of excess carbohydrates (Ziska *et al.*, 2004; Ziska, 2008). In accordance with the promotion of axillary meristems and subsequent increase in the number of tillers observed in wheat grown under elevated

CO_2 (Christ and Körner, 1995; Gray and Brady, 2016). Increased tillering is not the only sink of relevance for wheat crops to deal with excess carbohydrates. The translocation of carbohydrates into grains during the reproductive growth stages is entailed in determining grain yield, and the sink strength of the maturing ears and grains becomes crucial (Aranjuelo et al., 2011; Schynder, 1993; Yang and Zhang, 2006).

Additionally, a reduction in leaf N content is fairly common in plants grown under elevated CO_2, as reported in previous enclosure or field studies (Stitt and Krapp, 1999; Pérez *et al.*, 2005; Leakey *et al.*, 2009; Bloom *et al.*, 2014; Vicente *et al.*, 2015b, 2019; Tausz-Posch *et al.*, 2020), suggesting that the photosynthetic acclimation is associated with the plant N status (Bloom *et al.*, 2010). Indeed, the down-regulation of photosynthesis is more exacerbated in plants with a low N supply than in well-fertilized ones (Stitt and Krapp, 1999; Vicente *et al.*, 2015a, 2016). Nevertheless, no acclimation to elevated CO_2 is found in wheat grown hydroponically with a low nitrate supply in association with enhanced root N assimilation that could partly compensate for slower shoot N assimilation (Vicente *et al.*, 2017). Similarly, leaf transcriptional response reveals that acclimation of photosynthesis to elevated CO_2 leads to a loss of N compounds owing to the repression of genes involved in photosynthesis and N assimilation, which is exacerbated in N deficient plants (Vicente *et al.*, 2015a). Thus, the extent to which C and N assimilation can be reduced depends upon the N supply (Vicente *et al.*, 2015a, 2016) and N source, being more pronounced with nitrate than ammonium (Carlisle *et al.*, 2012). This alteration of the plant C-N balance reflects the tight coordination between C and N metabolism for maintaining plant growth and development under changing climate conditions (Stitt and Krapp, 1999; Morcuende *et al.*, 2011; Vicente *et al.*, 2018). The mechanism proposed to explain the decline in N content induced by elevated CO_2 enrichment, include N dilution by accumulation of non-structural carbohydrates (Stitt and Krapp, 1999; Gifford *et al.*, 2000), N limitation associated with faster growth and development (Bernacchi *et al.*, 2007), reallocation of N away from leaves (Nakano *et al.*, 1997), restricted N uptake owing to decreased transpiration (del Pozo *et al.*, 2007; Taub and Wang, 2008), and the limitation of N assimilation into proteins (Bloom *et al.*, 2002, 2010; Vicente *et al.*, 2016). The latter is partly associated with the inhibition of photorespiration and the dependence of N assimilation on photorespiration (Bloom et al., 2015). It has also been shown recently that the impairment of primary metabolism triggered by elevated CO_2 is accompanied by an induction of secondary metabolism as a mechanism to divert excess C from central metabolism (Vicente *et al.*, 2019).

The alteration of the C-N balance outlined above can result in changes in the plant chemical composition, and a decrease in the grain protein concentration has been frequently found in wheat

grown under elevated CO_2 (Högy and Fangmeier, 2008; Wieser *et al.*, 2008; Högy *et al.*, 2009b; Erbs *et al.*, 2010; Fernando *et al.*, 2012; Högy *et al.*, 2013; Fernando *et al.*, 2014; Nuttall *et al.*, 2017). Similarly, CO_2 enrichment may also lead to a reduced mineral concentrations in the grain of wheat (Högy *et al.*, 2009b; Erbs *et al.*, 2010; Fernando *et al.*, 2012; Högy *et al.*, 2013; Fernando *et al.*, 2014; Broberg *et al.*, 2017; Nakandalage and Seneweera, 2018), barley (Erbs *et al.*, 2010) and legumes (Myers *et al.*, 2014) . In this latter plant species, a lack of effect of elevated CO_2 on grain protein concentration has been observed as compared to other species, which may reflect the ability of leguminous crops to divert excess C for N fixation (Ainsworth *et al.*, 2004; Bourgault *et al.*, 2017; Ainsworth and Long, 2021). These results reveal that the impoverishment in grain protein and mineral nutrients might compromise the grain nutritional quality with serious consequences for human health, in special in countries where the main protein source comes from C_3 grains.

1.4.2.2.2. Effects of high temperature on plant development

As a temperate crop, wheat is adapted to temperatures below 30 ºC, but the optimum growth temperature varies depending on the developmental stage. Thus, optimal temperatures for wheat growth varies among 16 ± 2.3 ºC, 23 ± 1.75 ºC, and 26 ± 1.53 ºC for the ear emergence, anthesis and grain filling growth stages, respectively.(Khan *et al.*, 2021). Rising temperatures above the functional or developmental optimum may lead to alterations in plant growth, development and physiological processes with important consequences in wheat productivity (Cossani and Reynolds, 2012; Djanaguiraman *et al.*, 2020), particularly during the reproductive stage which is more sensitive to high temperatures than the vegetative phase (Farooq *et al.*, 2011). For instance, it has been reported annual wheat global yield shortfalls of 19 million tonnes from 1981 to 2002, which supposed global losses of 2.6 billion dollars per year (Lobell and Field, 2007). Likewise, Asseng *et al.* (2015) estimated a 6 % decrease in global wheat production for each degree Celsius of further increase in Earth´s mean surface temperature. Elevated temperatures affect grain yield through the acceleration of crop development and shortened of the life cycle (Barnabás *et al.*, 2008), which lead to a reduction in the uptake duration and the translocation of assimilates (Khan *et al.*, 2021). Increases of temperature during the pre-anthesis spikelet differentiation and floral setting can reduce the number of grains per ear, lowering the total grain number, while increases in floret abortion and pollen sterility have also been observed at anthesis. However, the double-ridge formation stage seems to be the most sensitive period of development to elevated temperatures since the ear is under formation, leading to a reduced number of spikelets per ear and grains per spikelet (Farooq *et al.*, 2011; Prasad and Djanaguiraman, 2014; García *et al.*, 2015). Exposure to high temperatures at the grain filling stage can also reduce the grain filling rate and duration, and therefore the final grain weight by altering the ability of the grain to grow (Slafer, 2007).

Other factors associated with changes in plant development and physiology may also influence yield in response to temperature (Salvucci and Crafts-Brandner, 2004; Barnabás *et al.*, 2008; Hatfield *et al.*, 2011; Bergkamp *et al.*, 2018; Macabuhay *et al.*, 2018). Among the physiological processes, photosynthesis is one of the most sensitive to high temperatures with inhibition occurring at temperatures only slightly higher than those for optimal growth. The temperature optimum for photosynthesis varies between species (Sage *et al.*, 2008), with species adapted to hot environments having a higher temperature optimum compared to those adapted to more moderate or cold environments (Gray and Brady, 2016). While the rate of Rubisco carboxylation increases with temperature, the solubility of CO_2 relative to O_2 and the specificity of the enzyme for CO_2 decrease, leading to an enhancement in photorespiration (Salvucci and Crafts-Brandner, 2004) The increasing flux through photorespiration, together with the increased rates of dark respiration, reduces the potential increase in CO_2 fixation at warmer temperatures (Berry and Bjorkman, 1980; Kobza and Edwards, 1987). The photosystem II is considered one of the most heat-labile components of the photosynthetic apparatus (Berry and Bjorkman, 1980), while Rubisco itself is heat-stable up to 50 ºC (Salvucci and Crafts-Brandner, 2004). Despite the ability of Rubisco carboxylation to increase up to high temperatures, limitations of photosynthesis at moderate-high temperatures can be associated with reduced function of Rubisco activase, which removes inhibitory molecules from the catalytic site of Rubisco (see section *1.3.1.3.5. Rubisco*) or reduced regeneration of RuBP through Calvin cycle (Sage *et al.*, 2008). In previous studies of the group with durum wheat grown in field gradient temperature chambers, the photosynthesis was not inhibited by prolonged exposure to moderate-warm temperatures because a higher stomatal conductance improves photosynthesis, favours leaf cooling and compensates for the decline in Rubisco activity and protein, while enhancing C translocation to ear for growth adjustment to higher temperature (Vicente *et al.*, 2015a, 2019). In addition, a general decline of transcripts for genes encoding for proteins involved in photosynthesis, respiration and C metabolism (Vicente *et al.*, 2015b, 2019), as well as those associated with secondary metabolism, pointing to a shift away from C-rich secondary metabolites as a mechanism to adjust C requirements for growth at warming temperatures (Vicente *et al.*, 2019).

Aside from the effects outlined above, exposure to high temperatures affects grain development owing to a limitation in the supply of assimilates, duration of grain filling rate, and starch biosynthesis and deposition (Nuttall *et al.*, 2017; Wang and Liu, 2021). The effects seem to depend on the intensity, duration and frequency of heat stress, as well as the genetic variability (Nuttall *et al.*, 2017) and may have important consequences on grain nutritional quality. A higher leaf transpiration rate has been found in wheat plants growing at high temperatures which can lead to improved micronutrient concentrations in the grain (Nakandalage and Seneweera, 2018) but a shorter duration of starch

deposition on the grain translates into smaller grains (Nuttall *et al.*, 2017). The deposition of proteins in the grain is also reduced, but the decrease is more marked in starch than protein (Wang and Liu, 2021). As a consequence, the protein concentration is enhanced in the grain, but the composition is altered as a result of the increase in the concentration of gliadins and the decrease in albumins and globulins (Khan *et al.*, 2021).

High temperatures can also promote the production and accumulation of ROS, such as hydrogen peroxide and hydroxyl or superoxide radicals (Farooq *et al.*, 2011), which may alter the cellular redox homeostasis and impair biological processes (Foyer and Noctor, 2016). ROS are also recognized as signalling molecules playing a key role in the regulation of plant responses to developmental and environmental factors (Baxter *et al.*, 2014; You and Chan, 2015). A complex enzymatic and non-enzymatic antioxidative system is involved in the protection against oxidative damage triggered by ROS (Foyer and Noctor, 2016). ROS scavenging enzymes include *catalase*, *peroxidase* and *superoxide dismutase*, which catalyse the transformation of O^{-2} to H_2O_2 and this one into H_2O, as well as the enzyme *glutathione reductase*, which drives the reduction of the tripeptide, c-L-glutamyl-L-cysteinyl-glycine, known as *glutathione* (GSH) (Khan *et al.*, 2021). Through a series of thiol-disulphide interactions, GSH is continuously oxidized by H_2O_2 to a *disulphide form of glutathione* (GSSG) and then recycled by the glutathione reductase with the participation of the *sulfhydryl protein* (Forman *et al.*, 2009; Noctor *et al.*, 2012). The non-enzymatic antioxidant defence system consists of low molecular mass compounds, such as ascorbate, glutathione, carotenoids, flavonoids and tocopherols etc. (You and Chan, 2015). In maize, exposure to high temperature has been associated with an impairment in the activity of the antioxidant enzymes, whereas wheat genotypes with acquired thermotolerance were correlated with higher catalase and superoxide dismutase activities, as well as with improved contents of non-enzymatic antioxidants such as ascorbate (Barnabás *et al.*, 2008; Farooq *et al.*, 2011).

The prediction of the potential impact of global warming on crop production is complex because CO_2 enrichment could lead to enhanced biomass and yield, and when combined with higher temperatures, it could attenuate the detrimental effects induced by temperature on crop yield (Zinta *et al.*, 2014; AbdElgawad *et al.*, 2015; Cai *et al.*, 2016; Fitzgerald *et al.*, 2016; Pan *et al.*, 2018; Vicente *et al.*, 2019; Ainsworth and Long, 2021; Wang and Liu, 2021). Thus, these findings suggest that plant responses to combined environmental conditions cannot be inferred from the response to a single factor and more attention should be paid to crop performance evaluation under concurrence of elevated CO_2 and high temperature to ensure food security.

1.4.3. Exploration of wheat variability

1.4.3.1. Genetic diversity. Defining concepts?

Diversity is the most fundamental foundation of biological world. There are not two identical organisms on Earth. Therefore, each one represents a single successful opportunity of living as well as a unique way of relationship with the environment. The description of the *biological diversity* has a venerable history, coming from ancient cave paintings to the accounting of the natural variability of species carried out by explorers and naturalists in the early 19th century. However, the concept of biological diversity is relatively recent in the scientific literature, firstly mentioned in 1950s (Magurran, 2005), as an extraordinarily wide concept. Diversity is broadly described as *any variation in the nucleotides, genes, chromosomes, or genomes of a species at a level of individual, population, species, or region for a given time* (Fu, 2015). It can also be defined as *the variety and abundance of organisms at a given place and time* (Magurran, 2005). Bhandari *et al.* (2017) described genetic diversity as the *degree of differentiation between or within species* and *variation* as the *difference in one or few traits of the organism*. These three examples reflect the inconsistence surrounding the concept of genetic diversity, as well as the multiple levels (species, variety and genetic) that involves (Khoury *et al.*, 2022). In studies of ecology, the term diversity can also be found associated with the role of functional groups in the adaptative capacity of ecosystems (Elmqvist *et al.*, 2003).

Bhandari *et al.* (2017) also distinguished between *genetic variability* and *genetic diversity*. While the former would reflect the variation in the sequences of ADN or ARN in the genetic pool of a species or population, the latest is a broad term accounting the total variability among different genotypes with respect to the total genetic make-up of genotypes within and between species. Genetic variability is expressed as alternate forms of the phenotype and thus, it could only be expected to occur but not to be accounted. By contrast, genetic diversity could be measured quantifying those different genes existing in a gene pool.

Diversity is defined by three components: *richness*, *evenness* and *disparity*. Richness is the most important characteristic and represents the absolute number of species, varieties or alleles found in a population. In ecological terms, richness leads to an enhancement in the functionality of the community and to stabilises the community under disturbances (*resilience*). Almost as important as the richness is the evenness, since represent the equitability of a community's species abundance distribution. It is the number of individuals representing each species in the community. Thus, although a community can have a high richness with an elevated number of species, if most of the individuals of that community belongs to a few species, the evenness would be low, reflecting a low diversity. Moreover, disparity measures the differences in phenotype among species in a population,

independently of the number of species found in the community (Purvis and Hector, 2000; Daly *et al.*, 2018).

1.4.3.2. Crop breeding and erosion

Another concept intimately associated with the genetic diversity is the genetic erosion. It is described as the loss of genetic diversity, usually intensified by human activities and its quantification depends on the method employed for measuring the genetic diversity. At the population genetic level, genetic erosion is calculated as the reduction in the frequency of alleles, while at higher levels (species, landscape or ecosystem, farmscape and national agricultural production) still have the population genetic diversity as an implicit foundation (Rogers and McGuire, 2015). The early conceptualisation of genetic erosion involved crop management and it was focused on the disappearance of landraces due to the replacement with modern varieties. The application of new systematic approaches in traditional agricultural systems have led to a deeper understanding of genetic erosion, revealing patterns of loss, maintenance or improvement of diversity (Khoury *et al.*, 2022).

The genetic diversity is the primary resource providing opportunities to breeders for the development of new cultivars with desirable traits (Bhandari *et al.*, 2017). However, the effect of breeding on genetic diversity seems to be not well understood yet. Indeed, several studies have reported losses of genetic diversity in crops (Hammer *et al.*, 1996; Rasmusson and Phillips, 1997; Hammer and Laghetti, 2005; Cowling, 2007; Fu and Somers, 2009; Dyer *et al.*, 2014), improvements (Almanza-Pinzón *et al.*, 2003; Thudi *et al.*, 2016), simultaneous losses and improvements (Reif *et al.*, 2005), or no effects (Huang *et al.*, 2007) of breeding on genetic diversity. Furthermore, many reviews or meta-analysis pointed a high variability in the results (Fu, 2006, 2015; Rauf *et al.*, 2010; van de Wouw *et al.*, 2010b, 2010a; Khoury *et al.*, 2022). In a meta-analysis performed by van de Wouw *et al.* (2010a) using 44 published articles, a short depletion in genetic diversity was found, corresponding with a reduction of 6 % occurred before 1960. Similarly, a recent revision performed by Khoury *et al.* (2022) of 105 articles focused on the study of the genetic diversity of modern crops released between 1984 and 2021 showed that most of the publications analysed the changes in genetic diversity in two periods comprised between 1900−1970 and 1990−2000. From them, more than two-thirds of the publications found supporting evidence for a decline in diversity over time as a result of plant breeding. Fu (2006) identified genetic reductions, increases and maintenances of genetic diversity in 23 studies performed between 2000 and 2005, together with genetical shifts and allelic reduction at individual chromosomal segments. For wheat, Rauf *et al. (*2010) found reductions in genetic diversity

at different parts of the world and variations along the time, reporting increases after 1990s. Similar spatiotemporal trends were also present for other crops such as rice. In this line, Fu (2015) indicated that the lack of consensus could be the reflect of the wide definition of genetic diversity and the consequent variety of measurement methods. Likewise, van de Wouw *et al.* (2010b) also suggested that the genetic erosion could happen twice during the breeding process (Figure 1.32). A first event of genetic erosion could happen just after substitution of the landraces by modern cultivars as a consequence of an intense selection of a small founder population. A latter, but more intense, erosion could arise as a consequence of dissemination of the crop, leading to an impairment of the breeding progress.

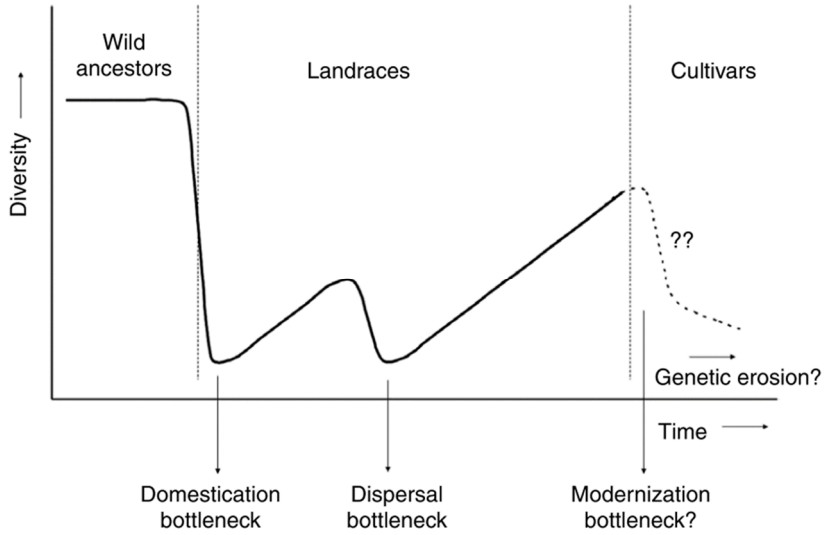

Figure 1.32. Model of crop-diversity trend from wild ancestors to modern cultivars.

Retrieved from (van de Wouw *et al.*, 2010b).

Independently if there are loses or gains in crop genetic diversity as a consequence of breeding, these results show the necessity of further investigations about the current state of the genetic diversity in modern crops.

1.4.3.3. Exploitation of genetic diversity

In a previous section of this chapter (*1.2.1.1. Phylogeny of Poaceae family*), it was mentioned that from the more than 30,000 edible plants, only three species (wheat, rice and maize) support more than 60 % of global food requirements (Harper and Armelagos, 2013; Smýkal *et al.*, 2018; N'Danikou and Tchokponhoue, 2019). This fact, by itself, should be enough to think about the vulnerability of crop systems and the importance of diversifying food sources. Nevertheless, agriculture will have to

face greater challenges in the coming decades (Khush, 1999), including: the improvement of productivity in nutritional quality and quantity to meet the food demand of a growing population (Bongaarts, 2009; Gödecke *et al.*, 2018; Initiatives, 2021); limitations in the use of land, water, pesticides and fertilisers, as well as the adoption of GHG-reducing techniques in order to perform a more resilient and sustainable agricultural system (Pimentel, 1996; Cole *et al.*, 1997; Wilson and Lovell, 2016); the fast increase in atmospheric CO_2 and the global warming (Cole *et al.*, 1997; Korres *et al.*, 2016), the extreme climatic events, such as droughts, floods, heat-waves or storms (IPCC, 2018, 2021a); and the biotic factors associated with climate change, such as pests or spread of pathogens (Newton *et al.*, 2011).

In this context, improvements in crop yield and grain quality, tolerance to biotic stress and resistance to abiotic factors will be required to perform a more resilient and robust agriculture in a sustainable manner (Khush, 2001; Chhetri and Chaudhary, 2011). The genetic diversity, as the main source of crop improvement, can provide opportunities for developing new and improved cultivars with these desirable characteristics (Bhandari *et al.*, 2017). To date, the exploitation of genetic variations in wheat responses to future warmer and CO_2-enriched environmental conditions might be a promising approach for the selection of widely adapted climate resilient wheat genotypes with improved quality to ensure food security in the face of a growing worldwide population. It can also may provide new insights into adaptation strategies to cope with the impact of climate change on global wheat production and consequent grain nutritional quality,

CHAPTER 2

Objectives

2.1. Objectives of the Thesis

Wheat is one of the most important crops worldwide and is extensively cultivated in the Mediterranean region, one of the most vulnerable to climate change. The predicted increase in atmospheric CO_2 concentrations will be accompanied by a rise in the temperature of the earth's surface. Both environmental factors regulate the physiological and phenological processes of plants, so they will have a potential impact on crop productivity and grain quality and should be evaluated together. Thus, improving yield and its sustainability at a time of unprecedented climatic variability is becoming more and more urgent to meet the demand for food from the increasing world population. To tackle these limitations, improved crop varieties will be required to ensure food security and the exploration of natural variation in wheat responses to future climatic conditions can be a suitable approach, using the CIMMYT heat tolerant wheat screening nursery (8TH HTWSN).

The working hypothesis is based on the investigation of natural variation for tolerance to combined elevated CO_2 and high temperature in a large number of wheat genotypes, with variability in their response to warmer temperatures, will allow the identification of those with contrasting productivity. These genotypes will constitute a powerful tool for the characterisation of changes in physiological parameters and the metabolic and antioxidant status that confer adaptation to the conditions anticipated by global climate change.

With this purpose, the **main objective of this Doctoral Thesis** was to investigate the adaptation mechanisms of growth and production of wheat to combined elevated CO_2 and high temperature, studying the relationship of biomass with the metabolites and enzyme activities of primary carbon and nitrogen metabolism, and the antioxidant status of the CIMMYT collection, as well as their repercussion on grain nutritional quality.

To achieve this overall objective, the following **specific objectives** were proposed:

1) To assess the natural existing variation in wheat yield performance in response to combined elevated CO_2 and high temperature.

   To reach this objective, a wide set of 60 bread wheat genotypes were grown in controlled environment chambers to gain full control of climatic parameters. This study included 59 genotypes of the CIMMYT collection previously selected for high performance under warmer temperatures, together with the Gazul genotype with high adaptability to the Mediterranean climate of the Salamanca region (Spain).

2) To investigate the variation in yield performance and grain nutritional quality traits across different bread wheat genotypes with contrasting productivity grown under combined elevated CO_2 and high temperature.

   With this purpose, we used 10 genotypes out of the 60 wheat genotypes that were previously screened for yield performance under the same environmental conditions.

3) To characterize the physiological and biochemical mechanisms involved in the variation in yield among 10 bread wheat genotypes previously shown to differ in yield and grain nutritional quality under combined elevated CO_2 and high temperature.

   With this aim, the genotypic variability on a range of leaf physiological parameters, antioxidant status, metabolites and enzyme activities of primary metabolism, as well as their associations with grain yield and quality traits was assessed.

This research activity was in line with the Societal Challenges, in particular Challenge 2: **Safety, food quality; productive and sustainable agricultural activity**

CHAPTER 3

Materials and methods

3.1. Experimental design

3.1.1. Plant material

3.1.1.1. Brief description of the plant species

The plant species used in this study is bread wheat or common wheat (*Triticum aestivum* ssp. *aestivum*). Wheat is a polyploid complex in which is possible to find wild and cultivated species with three different ploidy levels: diploid, tetraploid and hexaploid. Although different species of wheat have been used throughout history, two specific species are used today: durum wheat (*Triticum turgidum* ssp. *durum*, tetraploid) and bread wheat (*T. aestivum* ssp. *aestivum*, hexaploid). Bread wheat is one of the most widely distributed crops across the world and represents roughly 90 % to 95 % of the total wheat production, being an essential crop for human dietary (for more details, see section *1.2. Wheat*). Its use as a staple food provides almost 20 % of daily proteins and food calories (Arzani and Ashraf, 2017), together with minerals, lipids, vitamins and phytochemicals (Wieser *et al.*, 2020). Wheat production represents a quarter of total cereal production with 775.8 million tons produced in the 2020/2021 marketing year (Figure 1.11, a) (Statista, 2019). Bread wheat was selected for this experimental work due to the socio-economic and nutritional importance of this crop at a global and regional level.

3.1.1.2. Plant material

After a series of rust epidemic attacks that destroyed between the 60 % and the 75 % of the wheat harvest in the early 1950s, the US Department of Agriculture requested for international cooperation in order to test 1000 lines selected from the wheat world collection. The collaborative effort led to the development of the first international multilocation testing of experimental germplasm and the origin of the first international spring wheat yield nursery in 1960. Soon after and as a consequence of the successful results obtained, the *International Centre for the Improvement of Maize and Wheat* (Centro Internacional de Mejoramiento de Maíz y Trigo; CIMMYT) developed the *International Spring Wheat Yield Nursery* in 1964. Today, CIMMYT is the core of one of the largest international testing networks in the world, the *International Wheat Improvement Network* (IWIN), which accounts with participants in more than 100 countries worldwide. While CIMMYT distributes spring bread wheat, durum wheat and triticale nurseries from Mexico, winter wheats are provided by the *TURKEY/CIMMYT/ICARDA International Winter Wheat Improvement Program* (*Nurseries*, 2021).

In the experiments carried out in the present work, the plant material used belongs to a spring bread wheat population from the *8th Heat-Tolerant Wheat Screening Nursery* (8TH HTWSN) collection of the IWIN (Figure 3.1), distributed by CIMMYT. The 121 cultivars conforming this collection were previously selected for high performance in warmer temperatures (Gourdji *et al.*, 2013). From them, 59 genotypes were chosen to represent the germplasm of the 8TH HTWSN collection to carry out the first of the experiments planned in this research work (Table 3.1). Data from several studies performed with this collection can be found on the following web page: http://orderseed.cimmyt.org/iwin/iwin-results-1.php?c=2013&o=BW; adjusting the parameters: *Nurseries distributed from*: Spring Bread Wheat, CIMMYT Mexico; *Select cycle*: 2013; *Select Nursery*: 8TH HEAT TOLERANT WHEAT SN.

In addition, the spring wheat genotype *Gazul* (*Triticum aestivum* ssp. *aestivum* cv. Gazul), widely used in Spain due to its high adaptability to the Mediterranean climate, was also used in this study. Gazul is characterised for being a short-cycle spring wheat, awned, with a medium-high height. It is usually employed as a control variety among the high-yielding lines and those with an average

Bread Wheat Nurseries - Spring Wheat	
ASWSN	Acid-Soils Wheat Screening Nursery
EBWYT	Elite Bread Wheat Yield Trial
ESWYT	Elite Spring Wheat Yield Trial - grain color = WHITE • ESWYT-CHN (special edition for China) • ESWYT-LGY
HLAYT	High Latitude Adaptation Yield Trial
HLWSN	High Latitude Wheat Screening Nursery
HRWSN	High Rainfall Wheat Screening Nursery - grain color = RED
HRWYT	High-Rainfall Wheat Yield Trial - grain color = RED • HRWYT-CHN (special edition for China) • HRWYT-LGY
HTWSN	Heat Tolerance Wheat Screening Nursery
HTWYT	High Temperature Wheat Yield Trial • HTWYT-CHN (special edition for China)
IBWSN	International Bread Wheat Screening Nursery (for irrigated conditions) - grain color = WHITE • IBSWN-CH (special edition for China)
ISWSN	International Spring Wheat Screening Nursery
SATYN	Stress Adaptive Trait Yield Nursery
SAWSN	Semi-Arid Wheat Screening Nursery(for low rainfall conditions) - grain color = WHITE
SAWYT	Semi-Arid Wheat Yield Trial
WAWSN	Warmer Areas Wheat Screening Nursery

Bread Wheat Nurseries - Facultative and Winter Wheat	
FAWWON-IR	Facultative and Winter Wheat Observation Nursery for Irrigated Environments
FAWWON-SA	Facultative and Winter Wheat Observation Nursery for Semi-Arid Environments
IWWYT-IR	International Winter Wheat Yield Trial for Irrigated Environments
IWWYT-SA	International Winter Wheat Yield Trial for Irrigated Environments
WWSRRN	Winter Wheat Stem Rust Resistance Nursery
Durum Wheat Nurseries	
EDUYT	Elite Durum Yield Trial, unreplicated
IDSN	International Durum Screening Nursery
IDYN	International Durum Yield Nursery
Triticale Nurseries	
FWTCL	Facultative and Winter Triticale
ITYN	International Triticale Yield Nursery
ITSN	International Triticale Screening Nursery

Special and Project - Specific Nurseries	
CSISAHT	CSISA Heat Trial (CSISA = Cereal Systems Initiative for South Asia)
CSISASB	CSISA Spot Blotch (CSISA = Cereal Systems Initiative for South Asia)
FHBSN	Fusarium Head Blight Screening Nursery (earlier Scab Resistance Screening Nursery - SRSN)
GAWYT	Global Adaptation Wheat Yield Trial
HPYT	Harvest Plus Yield Trial
HPSAN	Harvest Plus South Asia Nursery
IAT	International Adaptation Trial
ISEPTON	International Septoria Observation Nursery (earlier Septoria Monitoring Nursery – SMN)
KBSN	Karnal Bunt Screening Nursery
SMN	Septoria Monitoring Nursery (now International Septoria Observation Nursery – ISEPTON)
SRSN	Scab Resistance Screening Nursery (now Fusarium Head Blight Screening Nursery)
STEMRRSN	Stem Rust Resistance Screening Nursery
WYCYT	Wheat Yield Consortium Yield Trial

Figure 3.1. List of IWINI nurseries for wheat.

Retrieved from (http://wheatatlas.org/nurseries/iwin).

Table 3.1. Catalogue of the 60 bread wheat genotypes (*Triticum aestivum* ssp. *aestivum*).

Genotype	Cultivar	Pedigree	Accesion	Reception year	Top Name
4	**SUPER 152**	PFAU/SERI.1B//AMADINA/3/WAXWING	BW 43354	2009	CGSS-02-Y-00153S-099M-099Y-099M-46Y-0B
5	**BAJ #1**	WAXWING/4/SONOITA F 81/TRAP #1/3/KAUZ*2/TRAP//KAUZ	BW 42811	2009	CGSS01Y00134S-099Y-099M-099M-13Y-0B
6	**REEDLING #1**	-	-	-	CMSS06Y00605T-099TOPM-099Y-099ZTM-099Y-099M-11WGY-0B
8		KACHU/KIRITATI	BW 49924	2012	CMSS07Y00127S-0B-099Y-099M-099NJ-099NJ-6WGY-0B
9		KACHU #1//WEEBILL1*2/KUKUNA	BW 49925	2013	CMSS07Y00129S-0B-099Y-099M-099NJ-099NJ-14WGY-0B
10		KIRITATI/WEEBILL1//FRANCOLIN #1	BW 49926	2012	CMSS07Y00174S-0B-099Y-099M-099Y-5M-0WGY
11		SUPER 152/BAJ #1	BW 49927	2012	CMSS07Y00195S-0B-099Y-099M-099Y-16M-0WGY
13		BAJ #1/3/KIRITATI//ATTILA*2/PASTOR	BW 49930	2012	CMSS07Y00288S-0B-099Y-099M-099Y-17M-0WGY
15		SUPER 152/AKURI//SUPER 152	BW 49936	2012	CMSS07Y00965T-099TOPM-099Y-099M-099Y-23M-0WGY
16		BECARD/FRANCOLIN	BW 49948	2012	CMSS07B00235S-099M-099Y-099M-25WGY-0B
18		BECARD//ND643/2*WEEBILL1	BW 49950	2012	CMSS07B00377S-099M-099NJ-099NJ-23WGY-0B
19		FRET2*2/BRAMBLING//BECARD/3/WEEBILL1*2/BRAMBLING	BW 49952	2013	CMSS07B00560T-099TOPY-099M-099Y-099M-19WGY-0B
21		KACHU/BECARD//WEEBILL1*2/BRAMBLING	BW 49954	2012	CMSS07B00580T-099TOPY-099M-099Y-099M-10WGY-0B
22		KAUZ/PASTOR//PBW343/3/KIRITATI/4/FRANCOLIN	BW 49955	2012	CMSS07B00585T-099TOPY-099M-099Y-099M-11WGY-0B
23		SUPER 152*2/TECUE #1	BW 49956	2012	CMSS07B00614T-099TOPY-099M-099Y-099M-49WGY-0B
25		WEEBILL1*2/4/SONOITA F 81/TRAP #1/3/KAUZ*2/TRAP//KAUZ/5/BAJ #1	BW 49388	2012	CMSS06B00162S-0Y-099ZTM-099Y-099M-7WGY-0B
26		NACOZARI F 76/TH.ACUTUM//3*PAVON F76/3/MIRLO/BUCKBUCK/4/2*PASTOR/5/T.DICOCCON PI94624/AE.SQUARROSA (409)//BACANORA T 88/6/WEEBILL4//BABAX.1B.1B*2/PARULA/3/PASTOR	BW 50018	2013	CMSS06B01043T-099TOPY-099Y-39M-0Y-2B-0Y
29		CHIBIA//PARULA II/CM65531/3/SUPER KAUZ/BAVIACORA M 92/4/MUNAL #1	BW 50026	2013	CMSS07Y00066S-0B-099Y-099M-099Y-43M-0WGY
31		FRET2/TUKURU//FRET2/3/MUNAL #1	BW 50028	2012	CMSS07Y00093S-0B-099Y-099M-099NJ-099NJ-9WGY-0B
33		KACHU #1//WEEBILL1*2/KUKUNA	BW 50036	2013	CMSS07Y00129S-0B-099Y-099M-099NJ-099NJ-12WGY-0B
35		KACHU//KIRITATI/WEEBILL1	BW 50038	2013	CMSS07Y00130S-0B-099Y-099M-099NJ-099NJ-8WGY-0B
41		SUPER 152/BAJ #1	BW 50048	2013	CMSS07Y00195S-0B-099Y-099M-099Y-5M-0WGY
42		SUPER 152/BAJ #1	BW 50049	2012	CMSS07Y00195S-0B-099Y-099M-099Y-25M-0WGY
43		SUPER 152//WEEBILL1*2/BRAMBLING	BW 50050	2012	CMSS07Y00196S-0B-099Y-099M-099Y-6M-0WGY
46		BAJ #1/3/KIRITATI//ATTILA*2/PASTOR	BW 50059	2012	CMSS07Y00288S-0B-099Y-099M-099Y-3M-0WGY
48		WHEATEAR*2/3/FRET2/WEEBILL1//TACUPETO F2001	BW 50085	2012	CMSS07Y00794T-099TOPM-099Y-099M-099Y-3M-0WGY
53		SUPER 152*2/MUU	BW 50107	2012	CMSS07Y00964T-099TOPM-099Y-099M-099Y-8M-0WGY
58		WEEBILL1*2/BRAMBLING//JUCHI F2000/3/WEEBILL1*2/BRAMBLING	BW 50117	2013	CMSS07Y01044T-099TOPM-099Y-099M-099Y-6M-0WGY
59		WEEBILL1/KUKUNA//TACUPETO F2001*2/6/PAVON F 76//CARIANCA 422/ANAHUAC F 75/5/BOBWHITE/CROW//BUCKBUCK/PAVON F 76/3/YECORA F 70/4/TRAP #1	BW 50119	2012	CMSS07Y01070T-099TOPM-099Y-099M-099Y-20M-0WGY
61		TOBARITO M 97/PASTOR*2//AKURI	BW 50122	2013	CMSS07Y01094T-099TOPM-099Y-099M-099NJ-099NJ-17WGY-0B
63		INQALAB 91*2/KUKUNA*2//HUIRIVIS #1	BW 50126	2012	CMSS07Y01115T-099TOPM-099Y-099M-099Y-9M-0WGY
65		SUPER 152/VILLA JUAREZ F2009	BW 50150	2013	CMSS07B00144S-099M-099Y-099M-5WGY-0B
69		BECARD/FRANCOLIN	BW 50181	2012	CMSS07B00235S-099M-099Y-099M-8WGY-0B
70		BECARD/CHYAKHURA	BW 50184	2013	CMSS07B00236S-099M-099Y-099M-13WGY-0B

Table 3.1 Catalogue of the 60 bread wheat genotypes (*Triticum aestivum* ssp. *aestivum*) (continuation).

Genotype	Cultivar	Pedigree	Accesion	Reception year	Top Name
71		WEEBILL1*2/KUKUNA/4/WHEATEAR/KUKUNA/3/C80.1/3*BATAVIA//2*WEEBILL1	BW 50185	2012	CMSS07B00240S-099M-099Y-099M-12WGY-0B
73		WEEBILL1/KUKUNA//TACUPETO F2001/4/WHEATEAR/KUKUNA/3/C80.1/ 3*BATAVIA//2*WEEBILL1	BW 50191	2012	CMSS07B00245S-099M-099Y-099M-10WGY-0B
74		WEEBILL1/KUKUNA//TACUPETO F2001/3/QUAIU #2	BW 50193	2012	CMSS07B00246S-099M-099Y-099M-5WGY-0B
76		WHEATEAR/KUKUNA/3/C80.1/3*BATAVIA//2*WEEBILL1/4/QUAIU	BW 50196	2012	CMSS07B00264S-099M-099NJ-099NJ-2WGY-0B
77		WHEATEAR/KUKUNA/3/C80.1/3*BATAVIA//2*WEEBILL1/4/QUAIU	BW 50197	2012	CMSS07B00264S-099M-099NJ-099NJ-7WGY-0B
79		SUPER 152/CHYAKHURA #1	BW 50208	2013	CMSS07B00339S-099M-099Y-099M-11WGY-0B
81		PBW 65/2*PASTOR/3/KIRITATI//PBW 65/2*SERI.1B/4/DANPHE #1	BW 50215	2012	CMSS07B00513T-099TOPY-099M-099Y-099M-12WGY-0B
83		CIANO T 79//PF70354/MUSALA/3/PASTOR/4/BAVIACORA M 92/5/KIRITATI// ATTILA*2/PASTOR/6/CHYAKHURA	BW 50229	2013	CMSS07B00550T-099TOPY-099M-099Y-099M-6WGY-0B
87		KACHU/BECARD//WEEBILL1*2/BRAMBLING	BW 50238	2013	CMSS07B00580T-099TOPY-099M-099NJ-099NJ-32WGY-0B
88		KACHU/BECARD//WEEBILL1*2/BRAMBLING	BW 50239	2013	CMSS07B00580T-099TOPY-099M-099NJ-099NJ-34WGY-0B
92		SUPER 152*2/TECUE #1	BW 50248	2013	CMSS07B00614T-099TOPY-099M-099Y-099M-16WGY-0B
93		WEEBILL1*2/KUKUNA//KIRITATI/3/WEEBILL1*2/KUKUNA	BW 50263	2013	CMSS07B00682T-099TOPY-099M-099Y-099M-22WGY-0B
94		WEEBILL1*2/KURUKU*2//SUPER 152	BW 50264	2013	CMSS07B00685T-099TOPY-099M-099Y-099M-17WGY-0B
95		FRET2/KUKUNA//FRET2/3/HEILO/4/BLOUK #1	BW 50266	2013	CMSS07B00715T-099TOPY-099M-099Y-099M-7WGY-0B
97		ND643/2*WEEBILL1//ATTILA*2/PBW 65/3/MUNAL	BW 50270	2012	CMSS07B00807T-099TOPY-099M-099NJ-099NJ-1WGY-0B
99		ND643//2*ATTILA*2/PASTOR/3/WEEBILL1*2/KURUKU/4/WEEBILL1*2/BRAMBLING	BW 50276	2012	CMSS07B00833T-099TOPY-099M-099NJ-099NJ-3WGY-0B
105		REH/HARE//2*BACANORA T 88/3/CROC_1/AE.SQUARROSA (213)//PAPAGO M 86/ 4/HUITES F 95/5/T.DICOCCON PI94624/AE.SQUARROSA (409)//BACANORA T 88/ 6/REH/HARE//2*BACANORA T 88/3/CROC_1/AE.SQUARROSA (213)//PAPAGO M 86/4/HUITES F 95/7/MUTUS	BW 49979	2013	CMSS07Y01305T-099Y-43M-0Y-2B-0Y
107		BLOUK #1//TACUPETO F2001*2/KIRITATI	BW 50284	2013	CMSS07Y00036S-0B-099Y-099M-099NJ-099NJ-1RGY-0B
110		QUAIU #3//TACUPETO F2001*2/KIRITATI	BW 50287	2013	CMSS07Y00040S-0B-099Y-099M-099NJ-099NJ-5RGY-0B
113		FRANCOLIN #1/2*BLOUK #1	BW 50296	2013	CMSS07Y00670T-099TOPM-099Y-099M-099Y-11M-0RGY
114		PFAU/WEAVER*2//TUKURU/3/BLOUK #1/4/QUAIU	BW 50298	2013	CMSS07Y00695T-099TOPM-099Y-099M-099Y-11M-0RGY
115		VOROBEY/FISCAL//KACHU/3/WEEBILL1*2/BRAMBLING	BW 50299	2013	CMSS07Y00706T-099TOPM-099Y-099M-099Y-11M-0RGY
117		WEEBILL1*2/BRAMBLING/5/WEEBILL1*2/4/SONOITA F 81/TRAP #1/3/KAUZ*2/ TRAP//KAUZ/6/WEEBILL1*2/BRAMBLING	BW 50303	2013	CMSS07Y00815T-099TOPM-099Y-099M-099Y-9M-0RGY
118		BLOUK #1/MUNAL	BW 50308	2013	CMSS07B00024S-099M-099Y-099M-21RGY-0B
119		BECARD/3/PASTOR//MUNIA/ALTAR 84	BW 50313	2013	CMSS07B00468S-099M-099Y-099M-18RGY-0B
150	**GAZUL**		20351	1992	

Pedigree, accession code and top name of genotypes belonging to the 8th Heat Tolerance Wheat Screening Nursery (8TH HTWSN) collection of the International Maize and Wheat Improvement Centre (CIMMYT) are provided.

production. It also stands out for its good grain quality, being a benchmark among strength wheats due to its high protein content (Agencia Estatal Boletín Oficial del Estado, 2010), which confers excellent bread-making quality (Royo and Briceño-Felix, 2011). Other important feature is its high resistance to diseases such as powdery mildew and brown and yellow rusts, but medium resistance to *Septoria lycopersici* funguses (data provided by GENVCE–Group for the Evaluation of New Cereal Varieties and Limagrain Iberica; Figure S3.1). Furthermore, Gazul has been previously characterised by our research group in field temperature gradient chambers studies (Gutiérrez *et al.*, 2009b, 2009a). A numerical code was assigned to each of the genotypes used in the present work (Table 3.1), being the number 150 associated with the Gazul genotype. The plant material used in each of the two experiments planned in this study is described as follows:

- *1st experiment*: 59 spring wheat genotypes from the 8TH HTWSN collection of CIMMYT + Gazul (genotype 150).
- *2nd experiment*: 10 genotypes with contrasting productivity selected from the 60 genotypes were used in the first experiment, 9 from the 8TH HTWSN collection of CIMMYT and Gazul. These genotypes were: 8, 23, 41, 43, 61, 74, 76, 94, 95 and 150.

3.1.2. Growth conditions

3.1.2.1. Climate chambers

Both experiments were conducted under the same growth conditions. Plant cultivation was carried out using two *controlled environment growth chambers* (Phytotron Service, IRNASA-CSIC) with dimensions 3.6 m long x 4.8 m wide x 2.4 m high and biological isolation from the outside (Figure 3.2). Growth chambers provide to researchers the advantage to gain enough control over environmental conditions to determine the effects of specific biotic or abiotic factors on plant development (Porter *et al.*, 2015). Each chamber is provided with two tables in which the environmental factors temperature, light intensity and photoperiod are individually regulated, as well as the concentration of CO_2 and the humidity of the air inside each room. Three narrow corridors inside the chambers allow the manipulation of the plants over the tables.

To rise CO_2 level in the air, pure CO_2 was injected and the atmospheric CO_2 concentration was continuously recorded inside the chambers with a *GM20 gas sensor* with double beam infrared NDIR technology (Vaisala) connected to an *OK412 PID controller* (Osaka Solutions). These controllers regulated the opening time of some solenoid valvules for the injection of pure CO_2 stored in cylinders

at the height of the fans to allow the correct homogenisation of the CO_2 injected into the air inside the chambers. Every 10 minutes, the environmental data were recorded by a computer with a system that collected information from the air temperature and humidity *high-precision HMD40Y sensor* (Vaisala) and the GM20 gas sensor.

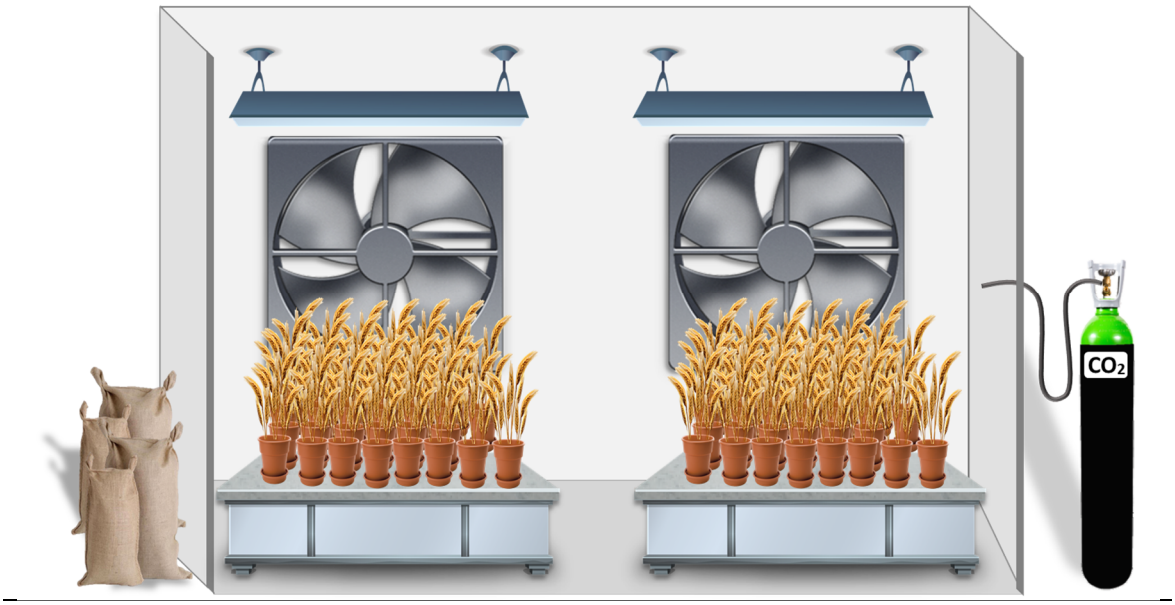

Figure 3.2. Schematic representation of a growth chamber.

3.1.2.2. Growth environmental conditions

In both experiments, wheat plants were cultivated at a *high atmospheric CO_2 concentration* of 700 µmol mol^{-1}, a *photoperiod* of 8 h of darkness (0:00−8:00) and 16 h of light (8:00−24:00) with a *light intensity* (PAR; photosynthetically active reaction) of 400 µmol m^{-2} s^{-1} at the top of the canopy, provided by a combination of blue- plus red-peak fluorescent lamps, and relative *air humidity* of 40 %/60 % day/night (Vicente *et al.*, 2015a, 2016). The temperature inside the chambers was increased 4 ºC above current temperatures simulating the daily and seasonal oscillations of typical temperatures in natural environments of the Salamanca region (Spain), based on the average temperatures collected over 10 years at *Muñovela* IRNASA-CSIC's experimental farm (40º 95´N, 5º 5´W, 800 m a.s.l.) (Vicente *et al.*, 2015b). For daily temperature fluctuations, four different sections were established corresponding to the night, and the initial, central and final parts of the photoperiod (morning, afternoon and evening, respectively) as described by (Marcos-Barbero *et al.*, 2021a). Moreover, these temperatures (Figure 3.3) were also increased by three levels to reproduce the seasonal oscillations throughout wheat development (Figure 1.7), corresponding to vegetative, ear emergence and grain filling growth stages (Marcos-Barbero *et al.*, 2021a, 2021b). Thus, the daily and seasonal oscillations of temperatures simulated throughout wheat development were:

- *1st vegetative*: 8 ºC, 14 ºC, 21 ºC and 16 ºC for night, morning, afternoon and evening.
- *2nd ear emergence*: 11 ºC, 18 ºC, 26 ºC and 20 ºC for night, morning, afternoon and evening.
- *3th grain filling*: 17 ºC, 26 ºC, 34 ºC and 28 ºC for night, morning, afternoon and evening.

In addition, in both experiments, seeds of each wheat genotype were sown in 5L plastic pots filled with 1.2 Kg of a mixture of peat and perlite (4:1) *substrate*. At the time of sowing, fertilizer consisting of 4 g of KNO_3 and 4 g of KH_2PO_4 was applied to each pot, the peat providing enough amount of other nutrients (Córdoba *et al.*, 2015; Marcos-Barbero *et al.*, 2021a, 2021b).

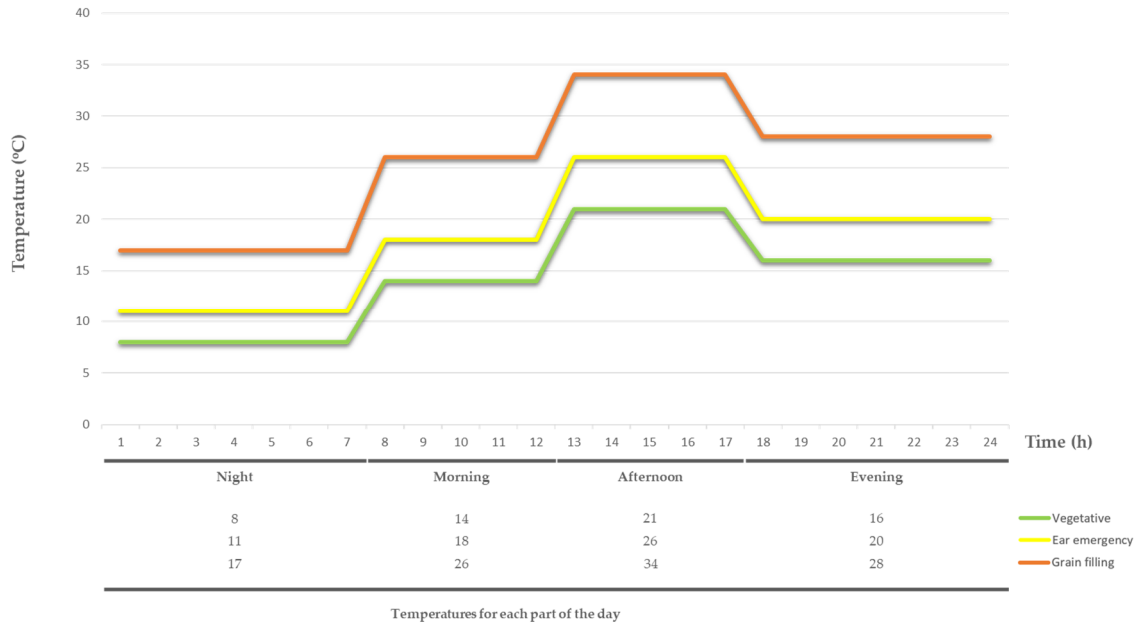

Figure 3.3. Schematic representation of the daily and seasonal oscillations of temperatures simulated throughout wheat development.

3.1.2.3. Experimental procedure

Briefly, the first experiment was carried out with 60 bread wheat genotypes to evaluate the natural variation in wheat yield performance in response to combined elevated CO_2 and high temperature. It was conducted in a completely randomized design, with four replicates/pot per each of the studied genotypes. Pots were randomly distributed among the 4 tables of the growth chambers at a rate of one pot per genotype in each of the tables (Figure 3.4). The environmental conditions established in the growth chambers were maintained throughout wheat development from sowing to crop maturity as described previously (see *section 3.1.2.2. Growth environmental conditions*). Initially, seven seeds of each genotype were sown in pots filled with the substrate previously mentioned. Five seedlings per pot remained by thinning one week after emergence. Once germinated, 1,200 plants were grown in 240 pots at a rate of 4 pots per genotype (4 x 60 = 240) and 5 plants per pot (5 x 240 = 1,200). At

physiological maturity, the aboveground plant parts were harvested from each pot for the estimation of wheat grain yield and its related traits.

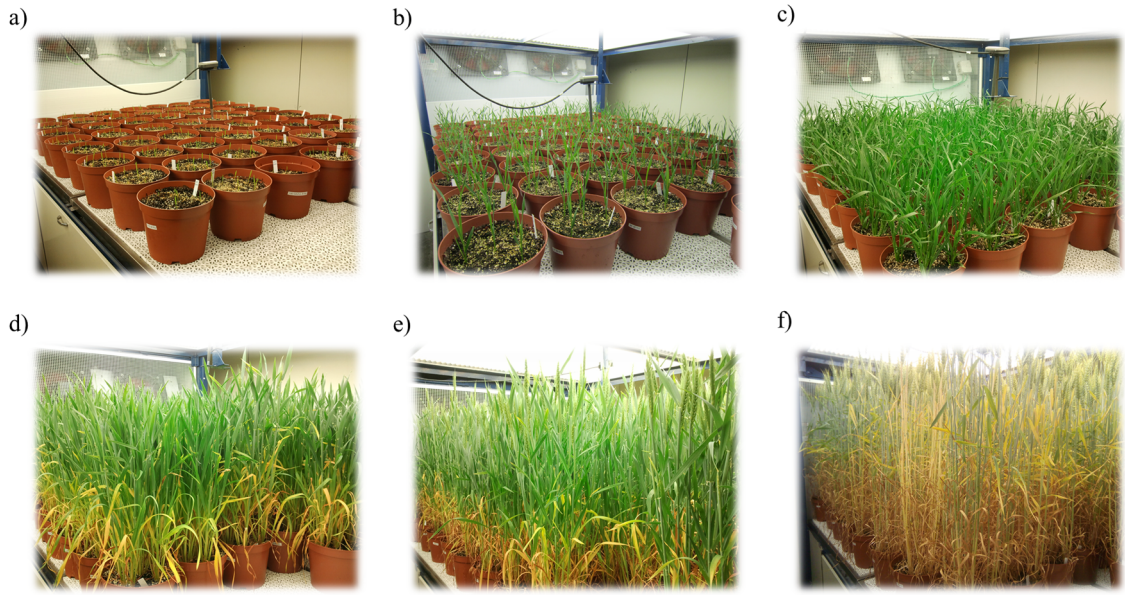

Figure 3.4. Composition of images that show the evolution in crop development of the first experiment involving 60 wheat genotypes grown under elevated CO_2 and high temperature.

a) Germination; b) early vegetative stage; c) late vegetative stage; d) ear emergence stage; e) anthesis; f) grain filling stage.

The second experiment (Figure 3.5) was conducted with 10 genotypes of bread wheat out of the 60 genotypes that were previously screened for yield performance under combined elevated CO_2 and high temperature (Marcos-Barbero *et al.*, 2021b). They were used to evaluate the variation in grain yield and nutritional quality and its dependence on the regulation of the leaf primary carbon-nitrogen metabolism under the same environmental conditions used in the first experiment. Seeds of each genotype were also sown in pots, with a density of five plants per pot after emergence, and they were placed in the controlled environment chambers. At variance with the first experiment, physiological and biochemical measurements were carried out on the flag leaves of the main stem of wheat plants at ear emergence growth stage (Zadoks stage 59) when 50 % of the plants per each of the studied genotypes had fully emerged ears. With this objective, forty days after the seeds were sown, when several tillers have already emerged in each plant, the main stem and the next two older tillers (i.e., the three oldest tillers) of each plant were labelled with different coloured thread of plastic (selected tillers) to aid measurements and sampling. Photosynthesis and foliar pigments were measured and, in parallel, flag leaf plant material was also harvested for different biochemical analyses. The experiment was a completely randomized design with five replicates (pot) per each of the studied genotypes and growth stages. Plant material was not only harvested at maturity growth stage, but also at ear emergence for both biochemical and growth analyses. Therefore, a total of 750 plants were

grown in 150 pots, at a rate of 5 pots per genotype (5 x 10 = 50) and 5 plants per pot (5 x 50 = 250) in each of the 3 samplings (3 x 250 = 750).

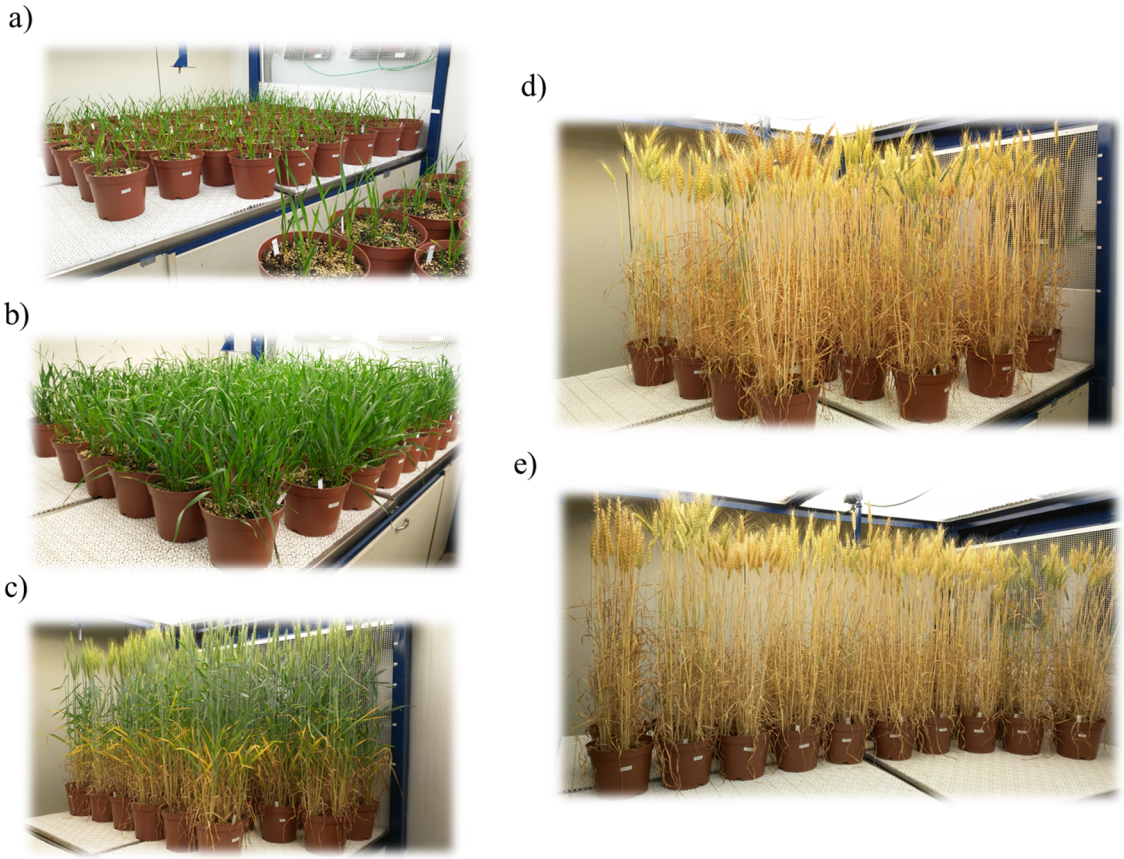

Figure 3.5. Composition of images that show the evolution in crop development of the second experiment involving 10 wheat genotypes grown under elevated CO_2 and high temperature.

a) Early vegetative stage; b late vegetative stage; c) ear emergence stage; d) grain filling stage; e) maturity stage.

In addition, both experiments extended from sowing to crop maturity. Water was supplied during crop development three times per week to maintain pot field capacity, and they were rotated inside the chamber twice a week in order to avoid edge effect. Temperature increases reproducing the seasonal oscillations were established when at least 50 % of the plants reached the development stage of ear emergence and anthesis, respectively (Figure 3.3).

3.1.3. Sampling and evaluation of phenological traits

3.1.3.1. Evaluation of plant phenology

The phenology of the bread wheat genotypes was evaluated through periodic observation three times a week in each one of the experiments carried out in the present study. Other traits were also determined, including the number of days from sowing to ear emergence (days until heading) was recorded when 50 % of the plants per each of the studied genotypes had fully emerged ears, days from sowing to anthesis were estimated when 50 % of ears showed extruded anthers along the head and the days from anthesis to maturity were also evaluated as we have previously described (Marcos-Barbero *et al.*, 2021b).

3.1.3.2. Sampling of plant material at different growth stages

3.1.3.2.1. Plant material collection

Samples were harvested with two main goals:

- *Plant growth analysis*: samples were collected for the estimation of the biomass and grain yield components at physiological maturity of the crop (Zadoks stage 91) in both experiments, as well as for the determination of the grain nutritional quality related traits in the second experiment. Moreover, plant material for plant growth analysis was also collected at ear emergence (Zadoks stage 59) in the second experiment.
- *Analysis of plant metabolism*: leaf plant material was also harvested to carry out different biochemical analyses mainly associated with the primary carbon and nitrogen metabolism and antioxidants at ear emergence in the second experiment as detailed below.

3.1.3.2.2. Parameters measured at crop maturity

At maturity, plant height was measured through the estimation of the length from the base of the stem to the ear tip, excluding awns, of the main stem of the plant and expressed in centimetres (cm). For yield parameter determinations, the aerial plant parts (*aboveground*) were collected and the ears were separated from the *stalk* [stems (leaves, nodes and internodes) and leaves]. Grains and *chaff* components (ear components; bracts and rachis) were separated from the ears by manual threshing. A more detailed description of the matured wheat plant anatomy can be found in section *1.2.2.2. Matured plant*. The separated parts of the plants at maturity are described below:

- *Aboveground* (aerial part) = stalk + ears.
- *Stalk* = stems + leaves.
- *Stems* = nodes + internodes.

- *Ears* = chaff + grain.
- *Chaff* (ear components) = glume, lemma and palea bracts + rachis.

From these fractions, there were determined:

- The *total number* of tillers, ears, and grains per plant.
- The *dry weight* (DW) of each fraction was obtained, expressed in grams (g), after drying in a *Digitronic* (JP Selecta) *oven* at 60 ºC for 48 hours. A *Mettler P1210 triple beam balance* was used to determine the weight of the heaviest fractions while a *XT 220A* (Precisa) *precision scale* was employed for the lightest ones.
- The following parameters were also determined:
    - *Harvest index* (HI): DW grain / DW aboveground part.
    - *Number of grains per ear* (GNE): number of grains per plant / number of ears per plant.
    - *Weight of grains per ear* (GYE; grain yield per ear): DW of grains per plant / number of ears per plant.

3.1.3.2.3. Parameters measured at ear emergence

Growth samples

As outlined above, samples were collected for the estimation of plant growth (green area and biomass) at ear emergence. The aboveground part was divided into the *selected tillers* and the *remaining tillers* of the plant. In the formers, once the flag leaves of the selected tillers were detached, they were divided into the last stem internodes, ears, rest of leaves and rest of stems. The remaining tillers were also divided into leaves, stems and ears. The different separated fractions of the plant at ear emergence were as follows:

- *Aboveground* (aerial part) = selected tillers + remaining tillers.
- *Selected tillers* = flag leaves + last stem internodes + ears + rest of leaves + rest of stems.
- *Remaining tillers*: leaves + stems + ears.

Thus, there were estimated:

- The *total number* of tillers per plant.
- The *green area* of the aboveground fractions was determined, expressed as square centimetres (cm^2), using an electronic planimeter Li-3050A (Li-Cor). The projected area of both faces of the ear was considered for the estimation of the area of this plant organ.

Because of the stem approximately has a cylinder shape, the area of the stem was calculated as the projected area multiplied by π.

- The *fresh weight* (FW) and DW of each of the fractions was obtained and expressed in g. DW was recorded after drying in an oven at 60 ºC for 48 hours.
- The *water content* (humidity content or humidity percentage; H %) of each fraction of the plant was calculated as: ((FW – DW) / DW) × 100 and expressed as a %.
- The following parameters were also determined:
    - *Dry biomass content*: DW / FW. It was distinguished between:
        - *Leaf dry matter content* (LDMC): the dry biomass of the flag leaf.
        - *Plant dry matter content* (PDMC): the dry biomass of the aboveground part of the plant.
    - *Dry biomass per area*: DW / area (g/cm^2). It was distinguished between:
        - *Leaf dry mass per area* (LMA): the dry biomass per unit area of the flag leaf.
        - *Plant dry mass per area* (PMA): the dry biomass per unit area of the aboveground part of the plant.

Samples for analysis of plant metabolism

In the second experiment, foliar samples were also taken for different biochemical analyses mainly related to primary C-N metabolism and antioxidants at ear emergence as mentioned above. Sample harvesting for biochemical measurements was carried out in parallel to the growth analysis of the different wheat genotypes included in the study. At the time of maximum photosynthesis, four hours after the beginning of the photoperiod, for each of the five replicates flag leaves of the selected tillers (the three oldest tillers) of two plants per genotype were sampled and pooled, under the same growth conditions and immediately frozen by immersion in liquid N, and then transferred to a labelled aluminium envelope. The samples were kept in liquid N until their storage in freezers at -80°C for a later use.

3.2. Physiological and biochemical determinations

3.2.1. In vivo analysis of the flag leaf at ear emergence

3.2.1.1. Photosynthesis

Measurements of photosynthetic gas exchange and chlorophyll fluorescence were performed in the central segment of the flag leaf on the main stem of the plant (Figure 3.6, a). Five replicates per genotype were analysed in the second experiment using an *open-path infra-red gas analyser* (IRGA-CIRAS-3; PP Systems) with an integrated leaf chamber fluorometer. Photosynthetic CO_2 assimilation rate (*A*), stomatal conductance (g_s), *intercellular* CO_2 *concentration* (C_i), *transpiration* (*E*) and *day respiration* (R_d) were recorded in a 1.7 cm^2 window leaf chamber connected to the CIRAS-3 equipment (Figure 3.6, b). Parameters measured at 700 µmol mol^{-1} are shown in this study. The measurements were performed in the period of time comprised between the 2 h and the 6 h after the beginning of the photoperiod at an air flow rate of 300 mL min^{-1}, a light intensity of 1,500 µmol m^{-2}

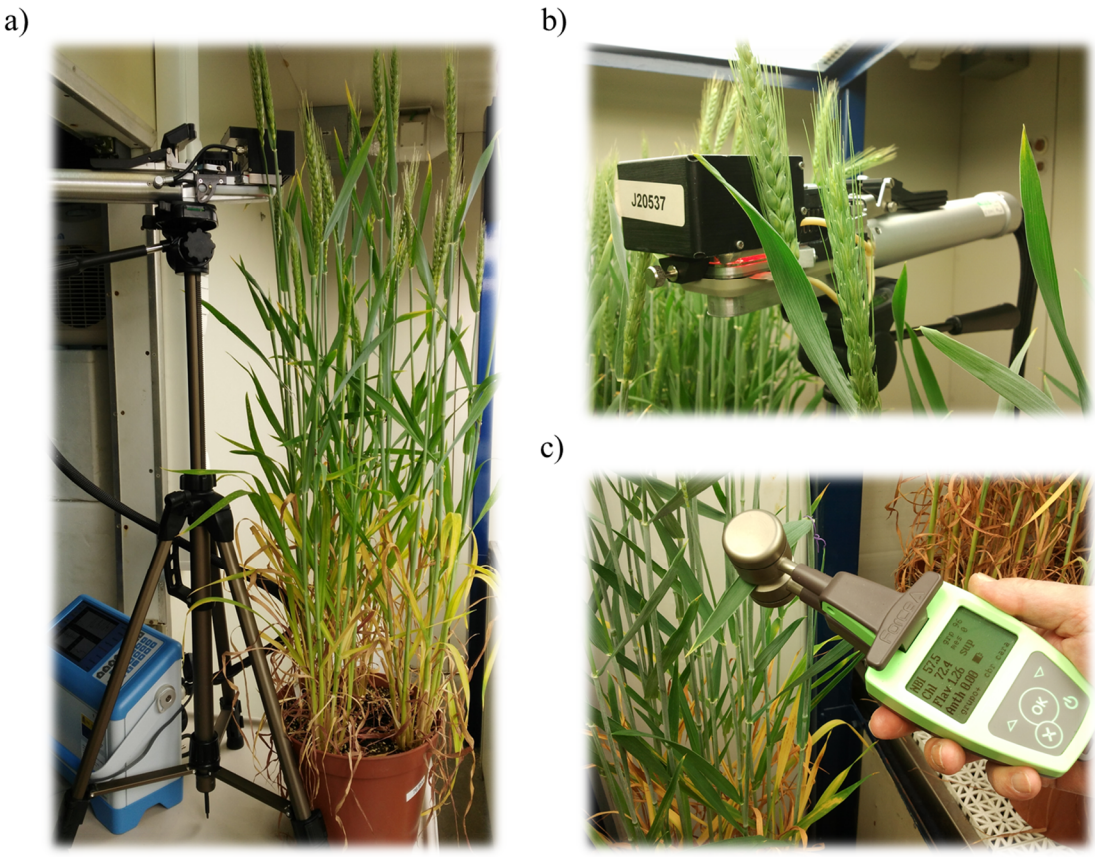

Figure 3.6. Measurement of photosynthesis and chlorophyll in the flag leaves of wheat plants using a CIRAS3 and Dualex, respectively.

a) Complete IRGA (CIRAS-3) equipment; b) a closer view of the PLC3 leaf cuvette; c) Dualex® (Force A SCIENTIFIC).

s^{-1} with a 1.6 ± 0.23 kPa vapour pressure deficit, while the temperature was kept at 25 °C using the Peltier system. The gas exchange-CO_2 response curves were recorded by decreasing CO_2 concentration in five steps, from 390 to 60 µmol mol^{-1} (about 10 min), followed by an increase from 390 to 1,800 µmol mol^{-1} (about10 min) in six steps (Córdoba *et al.*, 2016).

The response of *A* to the increases in CO_2 concentration provides valuable information about the biochemical processes driven photosynthesis in plants. It is usually expressed in terms of the ratio between *A* and C_i, defining a curve known as *curve A/Ci* (Figure 3.7). The model of Farquhar *et al.* (1980), later modified by Sharkey *et al.* (2007), is used to calculate the biochemical parameters driving the CO_2 uptake. This model predicts *A* as the function of three different processes: the activity of the rubisco, the regeneration of RuBP and the metabolism of the trioses phosphate.

At low C_i, there is not enough CO_2 to be used by the rubisco, so a minimum increase in C_i leads to the increase in CO_2 assimilation. This part of the curves is known as *rubisco-limited* and, in the response of *A* to the concentration of CO_2 can be described as:

$$A = Vx\left[\frac{C_c - \Gamma^*}{C_c + K_c(1+O/K_o)}\right] - R_d \qquad \text{(Equation 1)}$$

where *Vcmax*, here referred as *Vcx*, is the *maximum carboxylation rate of rubisco*; *Cc* and *O* are the *CO_2 and O_2 partial pressures* in the chloroplast; K_C and K_O are the *Michaelis constant of rubisco for CO_2 and O_2*; Γ^* is the CO_2 photocompensation point due to photorespiration and R_d is the *day respiration*. Because of this part of the curve is limited by the availability of CO_2, the relationship between *A* and C_i is at its steepest (Haworth *et al.*, 2018). Thus, the equation leads to a linear regression, allowing the estimation of *Vx* as the slope while - *Rd* as the intercept (Sharkey *et al.*, 2007).

At increased levels of C_i, *A* is no longer limited by the availability of CO_2. Instead, it is *limited by the maximum rate of electron transport* (*Jmax* here referred as *Jx*) required for the regeneration of RuBP and *A* is defined as:

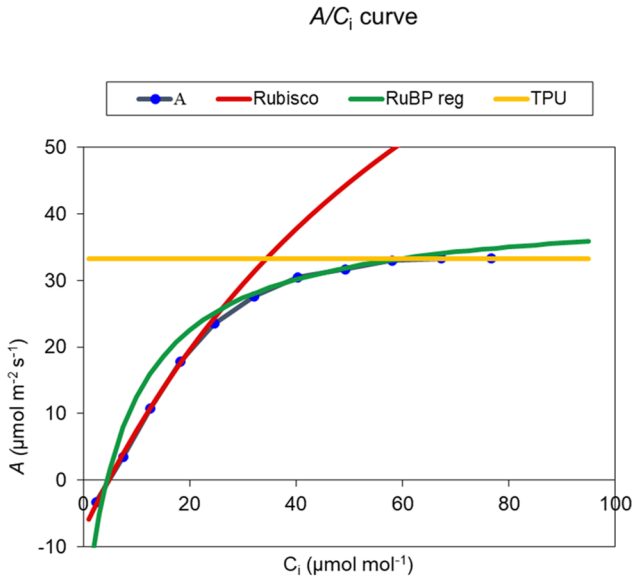

Figure 3.7. A/C_i curve.

Each colour represents the photosynthetic CO_2 assimilation (blue) or the three limiting factors (rubisco in red, regeneration of RuBP in green and TPU in yellow).

Retrieved from (Sharkey *et al.*, 2007).

$$A = Jx \frac{C_c - I^*}{4C_c + 8I^*} - R_d \quad \text{(Equation 2)}$$

This equation assumes that four electrons are required per carboxylation or oxygenation, although there are several uncertainties about the relation between electrons transported and ATP molecules synthetised, oscillating from 4 to 10.5 (Sharkey *et al.*, 2007).

At very high levels of CO_2, it is possible to find evidence on limitations of the phosphate availability required for the RuBP regeneration. Thus, it is said that this part of the curve is *phosphate-limited* due to the high concentrations of trioses phosphate and, therefore, is characterised by the parameter *maximum rate of triose phosphate utilisation* (TPU). When *A* is limited by TPU, the equation describing the photosynthetic carbon assimilation rate is:

$$A = 3TPU - R_d \quad \text{(Equation 3)}$$

To asses a more accurately approach of the biochemistry of the photosynthesis, the curve A/C_i was recalculated as de relationship between *A* and the concentration of CO_2 within the chloroplast. To calculate Cc, the following formula was employed:

$$C_c = C_i - (A/g_m) \quad \text{(Equation 4)}$$

Thus, the g_m (mesophyll conductance) was calculated through the substitution of the new expression of C_c (Equation 4) in the previous equations (Equations 1 and 2). Taking into account these considerations, the template provided by the LeafWeb utility (https://www.leafweb.org/) was fitted and sent (Gu *et al.*, 2010). The photosynthetic parameters obtained included *Vcx*, *Jx*, *Rd*, *TPU*, *CRbcx* (CO_2 intercellular concentration at maximum photosynthesis limited by Rubisco activity) and *ARbcx* (maximum value of photosynthesis limited by Rubisco activity). The water use efficiency (WUE) was calculated as the photosynthetic CO_2 assimilation rate divided by the transpiration rate at growth CO_2 concentration. The *quantum yield of PSII electron transport* (Φ_{PSII}) was also recorded with the integrated fluorometer.

3.2.1.2. Chlorophylls, flavonoids and NBI determination

The determination of the content of *chlorophyll* (Chl) and *flavonoid* (Flav), and the *nitrogen balance index* (NBI) were carried out on the same five replicates flag leaves as those used in for photosynthesis measurements using a *Dualex® (Force A SCIENTIFIC) optical leafclip meter* (Figure 3.6, c). Dualex performs non-destructive measurements of the chlorophyll and flavonoid contents taking advantage of the property of flavonoids as natural *ultraviolet* (UV) filters. Two wavelengths at 375 nm (UV) and 650 nm (infrared) are emitted by the equipment and both are absorbed by

chlorophyll, but only the UV wavelength is absorbed by the flavonoids (Cerovic *et al.*, 2002; Goulas *et al.*, 2004). Thus, the difference in the fluorescence of the chlorophyll measured in the infrared and the UV is proportional to the flavonoid amount existing in the leaf epidermis.

Dualex also takes advantage of the chlorophyll transmittance ratio of two light waves at different lengths: the red (720 nm) absorbed by the chlorophyll and the near infrared (over 800 nm) used as reference (Goulas *et al.*, 2004). Thus, the chlorophyll content is estimated as the difference between the transmittance of chlorophyll in the infrared and in the red, divided by the transmittance in the red.

$$\text{Chlorophyll content} = \frac{\text{Infrared trans. - Red trans.}}{\text{Red trans.}}$$

Both, the chlorophyll and the flavonoid contents are expressed as *Dualex® units*. The NBI was determined as the ratio between chlorophylls and flavonoids.

3.2.2. Physiological and biochemical determinations

3.2.2.1. Extraction and determination of carbohydrates.

3.2.2.1.1. Carbohydrate extraction

Carbohydrate extraction was performed on 75 mg aliquots of leaf frozen material after manual maceration with liquid nitrogen using a pestle and a mortar and later storage in 1.5 mL safe-lock plastic containers (Eppendorf™). The carbohydrate extraction was carried out with ethanol/water according to the method described by Morcuende *et al.* (2004). This protocol was also used for carbohydrate extraction in wheat grain at maturity. The procedure contemplates the homogenisation of the plant material with 700 µL of 80 % ethanol buffered with 10 mM N-(2-hydroxyethyl)-piperazine-N'-(2-ethane-sulfonic acid) (*HEPES*), adjusted with KOH to pH 7.5. After incubation for 30 min at 60 ºC, the samples were centrifuged at 13,2000 rpm for 10 min using a *5415R centrifuge* (Eppendorf) and the supernatant was transferred to a 5 mL flask that was kept cold and in the dark. This step was repeated two more times and the extraction supernatants were combined with the previous extract. Next, three new extractions with water and incubation at 80 ºC were carried out to extract the high molecular weight fructans. The supernatants were combined with the previous ones and brought to the final volume with 40 % ethanol. The supernatant was stored in a freezer at -20 °C for subsequent analysis of glucose, fructose, sucrose, and fructans when they were required, in addition to total amino acids. Similarly, the precipitate generated during the extraction was kept at -20 °C until it was used for starch quantification. Previous to the analysis, the ethanol has to be

removed at 70 ºC using a *vacuum dryer Lyoalfa 60* (Telstar) coupled to a *Savant Spead Var SPD 121P centrifuge* (Thermo Scientific). Subsequently, samples are brough to the same volume that they had with deionised water and centrifuged at 13,2000 rpm for 2 min.

3.2.2.1.2. Determination of glucose and fructose

The measurement of free glucose, fructose, sucrose and fructans in the sample extracted with ethanol and water was performed by a series of oxidation-reduction reactions (Jones *et al.*, 1977; Stitt *et al.*, 1989) monitored in a *plate spectrophotometer Synergy 2 Multi-Mode Microplate Reader* (BioTek). For this, the commercial Test D-glucose Boehringer Mannheim/R-biopharm kit (Roche) was used.

In a first step, an aliquot of the sample was transferred to a 96-well plate and mixed with 100 µL of a buffer (Boheringer buffer) containing 3 mM NADP, 10 mM ATP, Mg_2SO_4 and 86 mM TEA at pH 7.6. After adding ultrapure water until a volume of 200 µL, the plate was centrifuged at 2,000 g for 10 s in a Sorvall ST16R plate centrifuge (Thermo Scientific). The plate was placed in the spectrophotometer Synergy 2 and the initial absorbance was measured for 5 min, and then an aliquot of the mixture of enzymes *G6PDH* and *hexokinase* (HK) was added. The latter enzyme catalysed the phosphorylation of Gluc and Fru to G6P and F6P, respectively (reaction 1), while G6PDH catalysed the oxidation of G6P to 6-phosphogluconate in a reaction that releases NADPH (reaction 2). The reduction of NADP to NADPH can be measured at 340 nm, using a wavelength of 400 nm as a reference. The increase in absorbance associated with the formation of NADPH in these reactions was equivalent to the amount of free Gluc in the sample. In a subsequent step, the addition of the enzyme *phosphoglucose isomerase* (PGI) transformed F6P into G6P, which was in turn converted into 6-phosphogluconate (reaction 3). The increase in absorbance in this step was associated with the content of free Fru in the sample. The content of both carbohydrates was expressed in µmol g FW^{-1}. The sequence of enzymatic reactions is shown below:

HK:	$Glu + Fru + 2\ ATP \rightarrow G6P + F6P + 2\ ADP$	(Reaction 1)
G6PDH:	$2\ G6P + 2\ NADP^{+} \rightarrow 2$ 6-Phosphogluconate $+ 2\ NADPH$	(Reaction 2)
PGI:	$F6P \rightarrow G6P$	(Reaction 3)

3.2.2.1.3. Determination of sucrose and fructans

The measurement of Suc was carried out after the hydrolysis of the disaccharide into Gluc and Fru (Reaction 4) by the action of the enzyme sucrase (McCleary *et al.*, 2000), and its subsequent determination by the previous procedure. To do this, a new aliquot of the ethanolic-aqueous extract of the leaf samples was transferred to a 96-well plate and 4 µL of 100 mM sodium maleate buffer at

pH 6.5 was added, together with 8 U of sucrase (Megazyme) and ultrapure water up to a volume of 54 µL. The plate was covered with an aluminum adhesive foil to prevent the evaporation of the extracts during the incubation at room temperature for 30 min. Afterwards, the content of Gluc and Fru was determined and the values of free Gluc and free Fru were subtracted to obtain only those corresponding to Suc. The final result of Suc was expressed as the content of Gluc in µmol g FW^{-1}, since this and Fru are equimolecular in Suc.

Similarly, the determination of Fruct was carried out by analysing the Gluc and Fru generated after hydrolysis with fructanases (Fructanase Mixture Purified-Liquid, Megazyme), and their assessment at 340 nm following the procedure previously described. First, an aliquot of the ethanolic-aqueous extract of the leaf samples was mixed with 2 µL of 100 mM sodium acetate buffer at pH 4.5, 2 U of fructanases and ultrapure water was added to a volume of 54 µL. The samples were incubated in the covered plate for 30 min and then measured at 340 nm.

The content of Fruct was expressed as the content of Gluc plus Fru as µmol hexoses g FW^{-1} after subtracting the free Gluc and Fru contents and those associated with sucrose.

3.2.2.1.3. Determination of starch

The insoluble residue obtained after the ethanol-water extraction was employed for the determination of starch as described by (Hendriks *et al.*, 2003). To do this, the pellet was resuspended in 900 µL of 100 mM NaOH and incubated for 30 min at 95 °C. After neutralisation of the solubilized pellet with 180 µl of 0.5 M HCl, an aliquot of 120 µL of that extract was mixed with 180 µL of 50 mM sodium acetate at pH 7.9 containing 0.7 U of α-amylase and 0.5 U of amyloglucosidase (Roche). After incubation for 16 h at 37 ºC, starch was hydrolysed into Gluc and the supernatant obtained after centrifugation at 13,200 rpm for 2 min was used for Gluc determination by the habitual protocol.

3.2.2.2. Soluble protein determination

The estimation of the soluble proteins in frozen leaf plant material from the second experiment was performed using the insoluble residue obtained in the ethanol-water extraction according to Hendriks *et al.* (2003). The pellet was solubilised with 900 µL of 100 mM NaOH and incubated at 95 ºC for 30 min. After cooling at room temperature, the samples were centrifuge at 13,200 rpm for 5 min and used for the determination of proteins by the method of Bradford (1976). Thus, an aliquot of the supernatant was mixed with water to a volume of 54 µL and then 3,240 mL of Bradford reagent diluted 1:5 (Bio-Rad Protein Assay, Bio-Rad) was added. After incubation for 5 min at room temperature, the protein content was measured at 595 nm in the *8452A Diode Array*

spectrophotometer (Hewell-Packard) using polystyrene cuvettes. A standard curve with bovine serum albumin (BSA) at a concentration of 1 mg mL^{-1} was prepared and the soluble protein content was expressed as mg g FW^{-1}. Five replicates per genotype were evaluated.

3.2.2.3. Amino acid determination

The determination of total amino acids was carried out using the colorimetric *method of ninhydrin* (McCaldin, 1960; Hare, 1977; Lennard, 2005) in the five replicates of the flag leaf samples harvested in the second experiment. This method is based on the reaction of the 2,2-dihidroxi-1,2-dioxohidrindeno (ninhydrin) reagent, which is colourless, with α-amino acids to give a dark purple product known as *Ruhemann's purple* (Figure 3.8). An aliquot of the ethanolic extract was homogenised in 500 µL of *ninhydrin reagent* and water was added up to a volume of 1 mL Previously, the ninhydrin reagent was prepared by mixing two solutions:

- *Solution I*: 1 mL of glacial acetic acid, 50 mg of cadmium acetate and 5 mL of water.
- *Solution II*: 0.5 g ninhydrin diluted in 50 mL of acetone.

Thus, the ninhydrin reagent was freshly prepared by the combination of 6 mL of the solution I and 50 mL of solution II. After incubating the samples for 10 min at 70 ºC, they were allowed to cool at room temperature and their absorbances were measured at 570 nm in an *8452A Diode Array spectrophotometer* (Hewell-Packard) using optical glass cuvettes. A standard curve was made with L-glutamine (G3126 Reagent Plus, Sigma-Aldrich) in a range of 10−200 µM and the results expressed as µmol g FW^{-1}.

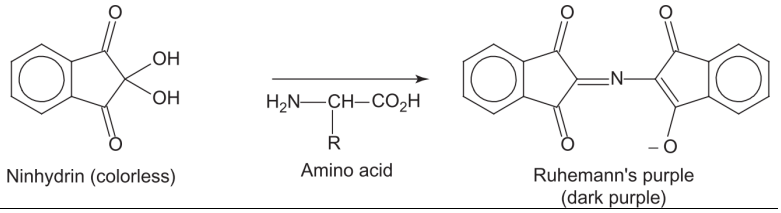

Figure 3.8. Ninhydrin reaction.

Retrieved from (Lennard, 2005).

3.2.2.4. Nitrate determination

The determination of NO_3^- in the leaf samples was performed following the method described by Cawse (1967). An aliquot of approximately 50 mg of ground dry plant material was homogenised with 1 mL of ultrapure water, and the mixture was autoclaved at 120 ºC for 1 hour. They were

centrifuged at 13,200 rpm for 10 min, collecting the supernatant. After clarifying with activated charcoal for 10 min, it was centrifuged under the same conditions. The supernatant was incubated with 0.6 % sulfamic acid and 4 % $HClO_3$ for 30 min to remove NO_2^- and the interferences produced by organic matter, respectively. The absorbance was measured at 210 nm in a *visible 8453 ultraviolet spectrophotometer* (Hewell-Packard) using quartz cuvettes. A standard curve with KNO_3 in a range of 10−200 µM was used for the determination of nitrate content expressed as µmol g FW^{-1}. Five replicates per genotype were evaluated.

3.2.2.5. C-N determination

The determination of the total C and N of the leaf samples was carried out following a method first described by Jean-Baptiste Dumas in 1831. This method has been proposed as an alternative of the Kjeldahl procedure for the determination of N in agricultural samples (Ebeling, 1968). It involves the pyrolysis of the sample and the analysis of the gases released in the subsequent combustion through a universal detector [an *elemental analyser for determination of total Carbon and Nitrogen LECO* oven (CHN 628)]. For this purpose, aliquots of about 80 mg of ground dry powder material were loaded into small tin capsules. The results were expressed as the percentage by mass of the C and N content, whereas their ratio (C/N) was subsequently calculated. Five replicates per genotype were evaluated.

3.2.2.6. Determination of total antioxidant capacity and low-molecular weight antioxidants

3.2.2.6.1. ORAC determination

The *oxygen radical absorbance capacity* (ORAC) assay was carried out following the protocol described by Gillespie *et al.* (2007). An amount of 5 mg of fine powder grinded from the flag leaf of the five replicates of each wheat genotypes was weighed and mixed with 1.0 mL of 50 % (v/v) acetone. The mixture was sonicated in an ultrasonic bath for 30 min at 8 ºC and then centrifuged at 5,000 *g*. The clarified supernatant was collected and kept on ice at 4 ºC until the ORAC measurement was initiated in the *FLUOstart® Omega microplate reader* (BMG Labtech, Germany). Previously, samples were transferred to *Brand® 96-well plates with black flat bottom* wells for the assay. The wavelength selection for the fluorescence excitation and emission of fluorescein and the designed scripts to inject the solutions containing *2,2'-azobis(2-methyl-propanimidamide) dihydrochloride* (AAPH) and fluorescein were described in detail in the study performed by Mellado-Ortega *et al.* (2017). Several dilutions of the clarified supernatants were performed to ensure that the calculated

areas under the curve of the fluorescein fluorescence emission intensity of the samples were within the range used for the trolox standard curve. Five replicates per genotype were evaluated. The results were expressed as µmol of trolox equivalent g FW^{-1}.

3.2.2.6.2. FRAP determination

The *ferric ion reducing antioxidant power* (FRAP) method was followed as described in the study by Benzie and Strain (1996). The FRAP reagent was prepared by mixing 300 mM sodium acetate buffer pH 3.6, 10 mM 2,4,6-Tris(2-pyridyl)-s-triazine (TPTZ) in 40 mM HCl, and 20.35 mM $FeCl_3$ at a ratio of 10:1:1 (v:v:v). An amount of 5 mg from each flag leaf sample was extracted in 1.0 mL of 50 % (v/v) acetone as described for the ORAC assay. Eight µL of the clarified supernatants, 8 µL of PBS, and 200 µL of the FRAP reagent were added to each well of *Nunc® 96-well plates with clear flat bottom* and incubated at room temperature for 30 min. A number of four technical replicates were measured per each flag leaf sample or ground wheat grain. The absorbance was measured at 593 nm in the microplate reader. The results were expressed as µmol Trolox equivalent g FW^{-1}. Five replicates per genotype were evaluated.

3.2.2.6.3. TPhC determination

When *total phenolic compounds content* (TPhC) was measured in flag leaves, the clarified supernatants of the extractions performed for the FRAP assay were also used to quantify TPhC according to the *Folin-Ciocalteu method* (Ainsworth and Gillespie, 2007). A volume of 100 µL of the clarified supernatants were mixed with 500 µL of the Folin-Ciocalteu reagent (Scharlab Chemie SA). After 5 min, a volume of 400 µL of 0.7 M Na_2CO_3 was added. The reaction mixture was kept at room temperature for 60 min. After incubation, aliquots of 300 µL from each sample were loaded in the microplate wells and the absorbance recorded at 765 in the microplate reader. A number of four technical replicates were measured per each flag leaf sample. Gallic acid was used as a reference standard, and the results were expressed as µmol gallic acid equivalent g FW^{-1} of flag leaves. Five replicates per genotype were evaluated.

3.2.2.6.4. GSH determination

Total content of *glutathione* (GSH) was determined in flag leaf of the five biological replicates by an enzymatic recycling procedure in which GSH was sequentially oxidized with 6,6′-dinitro-3,3′-dithiodibenzoic acid (DTNB) and reduced with NADPH in the presence of glutathione reductase (Griffith, 1980). The DTNB reduction rate was followed at 412 nm. A weighed amount of about 40−45 mg of fine powder of the flag leaf samples were mixed with 0.8 mL of 3 % (w/v) HCl, 1 mM Na_2EDTA in microfuge tubes containing approximately 100 mg of 0.75−1.0 mm glass grinding beads. The sample mixtures were vigorously shaken in a *Mini-Beadbeater-16 homogenizer* for 1 min.

The homogenized plant material was centrifuged for 5 min at 16,000 *g* at 4 ºC and the clarified supernatants were collected. A volume of 30 µL of the supernatants was pre-mixed in a microfuge tube in the following order with an equal volume of the extraction buffer, 105 µL of 1 M sodium succinate, 0.5 M NaOH and 105 µL of 250 mM Tris-HCl, 6.3 mM EDTA, 0.32 mM NADPH pH 7 to neutralize the acidic character of the extraction buffer. The neutralized reaction mixture was transferred into the microplate wells containing 3 µL of a stock solution of 100 U/mL glutathione reductase. The 412 nm absorbance reading started immediately after the addition of 30 µL of 6 mM DTNB in the wells. A number of three technical replicates were measured per each flag leaf sample. The GSH content was then evaluated by comparing the results with a standard curve with GSH (Griffith, 1980). The results were expressed as µmol g FW^{-1}. Five replicates per genotype were evaluated.

3.2.2.6.5. Asa determination

The *ascorbic acid* (Asa) extraction from flag leaf samples followed the same procedure as the one described for GSH. A volume of 30 µL of the clarified supernatants was mixed with an equal volume of the extraction buffer, 180 µL of H_2O and 60 µL of 1 M sodium succinate, 0.5 M NaOH. The volume mixing was repeated twice per biological replicate. In a first step, the absorbance values at 265 nm were recorded without further additions. In a second step, the absorbance values at 265 nm were newly recorded after the addition of 3 µL of 300 mM *dithiothreitol* (DTT) in one of the duplicated wells per biological replicate and 3 µL of 100 U/mL of ascorbate oxidase in the other duplicated well. Before the absorbance reading started, the reaction mixtures were kept inside the microplate reader for 3 min to ensure complete redox reactions. The total content of Asa was determined as the 265 nm absorbance difference between wells containing DTT and oxidized ascorbate. A number of three technical replicates were measured per each flag leaf sample. An extinction coefficient of 13,250 $M^{-1}cm^{-1}$ at 265 nm for Asa was determined in the reaction mixture at pH 5.18. The results were expressed as µmol g FW^{-1}. Five replicates per genotype were evaluated.

3.2.2.7. Determination of enzyme activities

3.2.2.7.1. General features

The analysis of the activity of the C and N metabolism enzymes *ADP-glucose pyrophosphorylase* (AGPase), *cytosolic fructose-1,6-bisphosphatase* (Fru1,6bisPase), *glucose-6-phosphate dehydrogenase* (G6PDH), *glutamate dehydrogenase* (GDH), *glutamine synthetase* (GS), *NADP-dependent isocitrate dehydrogenase* (IDH), *phosphoenolpyruvate carboxylase* (PEPCase) and *pyruvate kinase* (PK) was performed through *continuous* (direct) or *discontinuous* (cycling) *assays*

following the high-throughput methods previously optimised in Arabidopsis (Gibon *et al.*, 2004) and subsequently described by Bénard and Gibon (2016). The procedure involves three steps: the *extraction of soluble enzymes*, the *optimisation of the enzyme assay* using a biological or chemical

standard and the *measure of the enzyme activity* in the samples. The analyses of the enzyme activities were performed using the *HiTMe Platform* (High Throughput Metabolic phenotyping platform; Figure 3.9) at the Bordeaux Metabolome facility in the French National Institute for Agricultural Research (INRA, France) within the framework of the OPTENZWHEAT project financed by the EPPN2020 Program, European Commission. A collaborative project between Yves Gibon's group and IRNASA-CSIC.

3.2.2.7.2. Extraction of soluble enzymes

For the extraction of the soluble enzymes aliquots of 20 mg of frozen leaf powder were transferred to 1.10 mL cryogenic plastic tubes (micronics) placed in roborack-96 wells and immersed in liquid

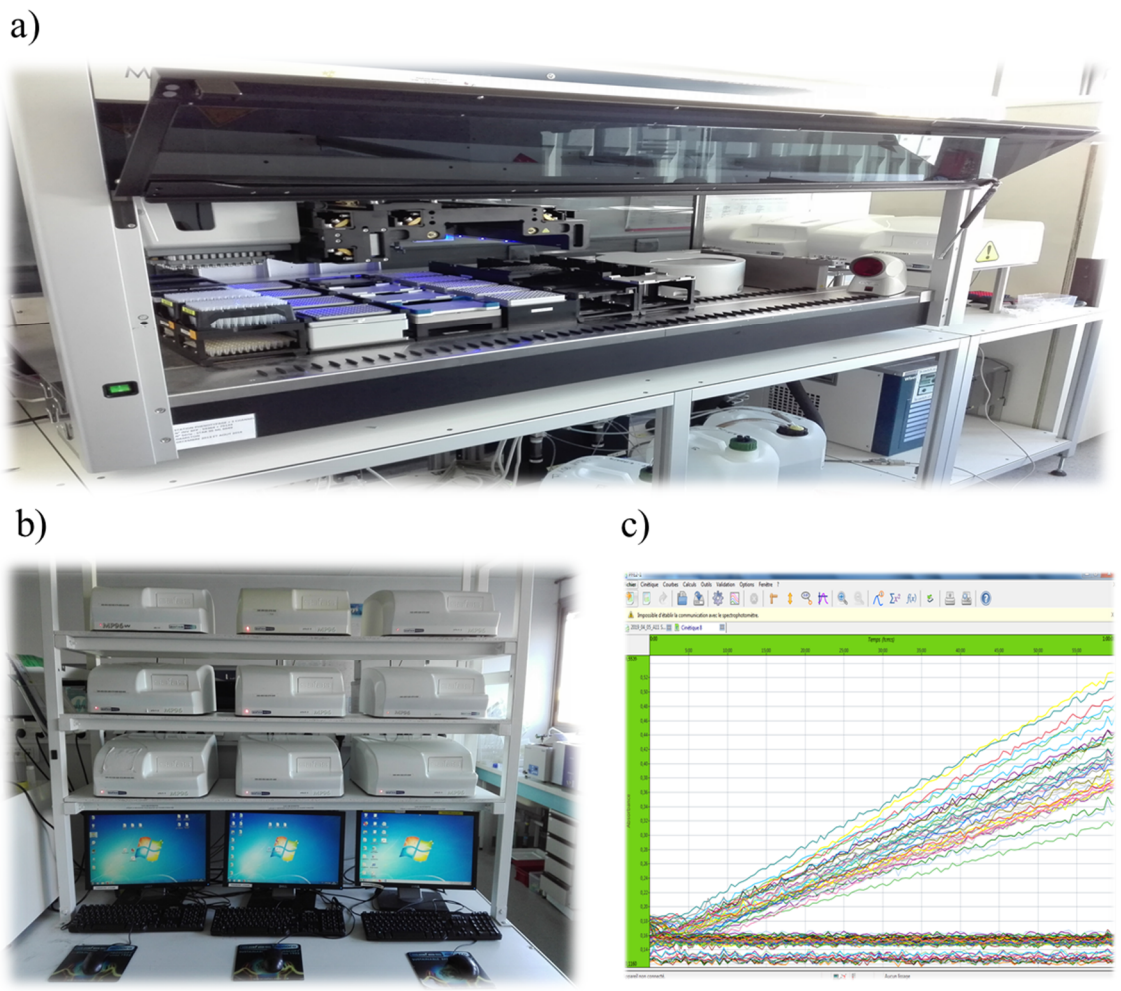

Figure 3.9. HiTME facilities.

a) Hamilton robotic pipetting station; b) MP96 SAFAS-Monaco plate readers; c) software SAFAS SP 2000.

nitrogen. Afterwards, the leaf plant material was vigorously mixed with 500 µl of extraction buffer containing 20 % (v/v) glycerol, 0.25 % (w/v) bovine serum albumin, 1 % Triton X-100 (v/v), 50 mM Hepes-KOH pH 7.5, 10 mM $MgCl_2$, 1 mM EDTA, 1 mM EGTA, 1 mM aminocaproic acid, 1 mM benzamidine, 20 µM leupeptin, 0.5 mM dithiothreitol, 1 mM phenylmethylsulfonyl fluoride (PMSF) as described by Gibon *et al.* (2004). The samples were then cold centrifuged at 4 ºC and 4,000 rpm for 7 min. A fraction of supernatants was transferred to a V-bottomed 96-well plate with the robotic arm of a *Hamilton robotic pipetting station* (STAR 96 ML 6649; Figure 3.9, a) and kept on ice to be used for the optimisation of enzyme activities assays, while another fraction was transferred to a 96-well plate and quickly frozen by placing the plate on a thin layer of liquid nitrogen.

3.2.2.7.3. Optimisation of enzyme activity assays

The robot-based procedure for the optimisation of enzyme assays includes the comparison of a biological (tomato leaf) or a chemical standard with the biological material representative for the wheat plant material under study (a mixture of leaf material from the different wheat genotypes) with the aim of finding the optimal dilution in which the enzyme assay can be carry out. The optimisation of the enzyme assays involved different steps:

1. A *dilution series of the extract* to find the optimal dilution: Three technical replicates (extracted in parallel) of the *representative material under study*, together with six *blanks* (extraction buffer alone) and six technical replicates of a *biological or a chemical standard* in which the measured activity is well known and validated, were placed in a 96-well plate as described in Figure 3.10, a. All the material was diluted by mixing 200 µL of the extracts with other 200 µL of the buffer extraction 5 times, leading to 1, 2, 4, 8, 16, and 32-fold dilutions using an automated program on the robot.
2. *Mixture and transference of the extract and the standards*: Diluted extracts were randomised in the first half of the 96-well plate with the help of the robotic arm by redistributing the micronics as showed in Figure 3.10, b. Then, 40 µL of each sample were transferred to the upper part of a V-bottomed 96-well plate and 20 µL to the lower part Figure 3.10, c.
3. *Performance of the assay*: Continuous or discontinuous assays were performed after the transference of 5 µL and 2 µL aliquots to a 96-well plate, respectively (see the following section). The activity was calculated by the comparison of the signals between the complete assay buffer (V_{Sat}) and when the substrate was omitted (V_0) and the change in the absorbance was recorded using *MP96 SAFAS-Monaco plate readers* (Figure 3.9, b) at the corresponding measurement wavelength.

4. *Estimation of the optimal dilution*: Once the assay was finished, the calculation of the activity was performed with the *software SAFAS SP 2000* (Figure 3.9, c) of the plate reader to define the time interval at which all rates were constant and calculate the rate for each well by using the function of linear regression. Additionally, the recovery of the standards and the error, expressed as the coefficient of variation [the ratio of the standard deviation (SD) to the mean; CV in %], was calculated and the optimal dilution of the extract was selected for the plant material under study.

3.2.2.7.4. Determination of enzyme activities in the flag leaf of wheat

Once the enzyme activity assays were successfully validated and the optimal dilution selected, the robot-platform was used to perform high-throughput enzyme assays in leaf material from the five replicates per genotype of the second experiment. Thus, the extraction of the soluble proteins was carried out as described above using three randomly distributed technical replicates of each sample and six blanks on micronics placed on roborack-96 wells.

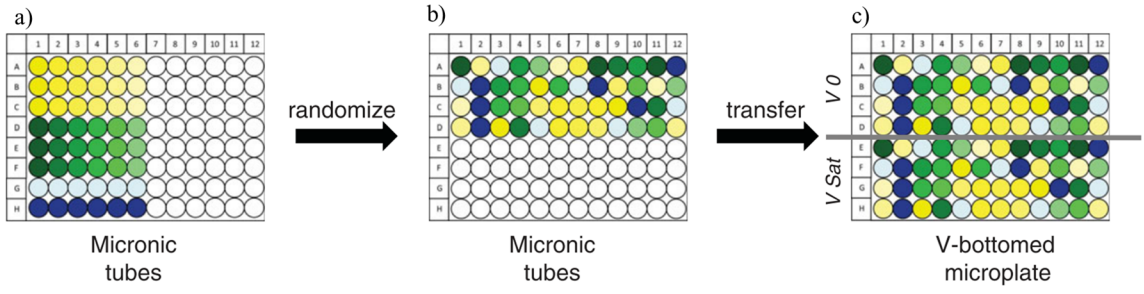

Figure 3.10. Pipetting scheme for microplate-based assay optimisation.

a) Preparation of the enzymatic extracts (lines A-C, in yellow, 6 dilutions), mixes (lines D-E, in green, 6 dilutions of the extract mixed 1:1 with one concentration of the standard); blanks (line G, light blue, extraction buffer) and standards (line H, dark blue); b) randomisation of the samples in the upper half by redistributing the tubes; c) transference of the sample into a new microplate used for measurements.

Retrieved from (Bénard and Gibon, 2016).

Each enzyme required different reagents, but most of them shared a common procedure. In the continuous methods, the evolution of the reaction is directly measured and monitored through the quantification of a substrate or a product of the enzyme with enough sensitivity for being recorded, directly or via a coupling reaction. By contrast, discontinuous assays are employed when the reactions cannot be recorded directly or when the activity of the enzyme is too low for being detected. Then, this type of reaction is run for one or more given durations, stopped through the incubation with 0.5M HCL or NAOH and followed by the quantification of a direct or indirect product of the reaction, leading to measurements in the pmol range and providing much higher sensitivity compared to direct assays. Three different discontinuous assay procedures can be distinguished: *G3POX* cycling method (Figure 3.11 a and b), when glycerol-3-phosphate (glycerol-3-P) and dihydroxyacetone-phosphate are measured by a glycerol-3-P dehydrogenase/glycerol-3-P oxidase cycle (G3POX/G3PDH); *G6PDH* cycling method (Figure 3.11 c and d), when $NADP^+$ and NADPH are determined by a glucose-6-P dehydrogenase/phenazine methosulfate cycle (G6PDH/PMS) with the reduction of 3-(4,5-dimethylthiazol-2-yl)-2,5-diphenyl tetrazolium bromide (MTT); and *ADH* cycling method (Figure 3.11 e and f), when NAD^+ and NADH are quantified by an alcohol dehydrogenase/phenazine ethosulfate cycle (ADH/PES) with the reduction of MTT (Gibon, 2004; Bénard and Gibon, 2016).

In the present study, the activity of GS, PEPCase and G6PDH was measured by direct assays at 340 nm and 25 ºC through in the presence of PK and lactate dehydrogenase (LDH), malate dehydrogenase (MDH) or G6P, respectively. AGPase and PK were measured through discontinuous assays leading to the formation of glycerol-3-phosphate (glycerol-3-P). The reaction was stopped with 20 µl of 0.5 M HCl, and after neutralisation with 20 µl of 0.5 M NaOH, glycerol-3-P was measured in the presence of glycerol-3-P oxidase and glycerol-3-P dehydrogenase, 1 M NADH, 1.5 mM $MgCl_2$ and100 mM Tricine/KOH pH 8, in a final volume of 100 µl. The absorbance was read at 340 nm until the rates were stabilized. The activity of the enzymes Fru1,6bisPase and IDH was determined at 570 nm via assays based on NADP-cycling in the presence of glucose-6-P

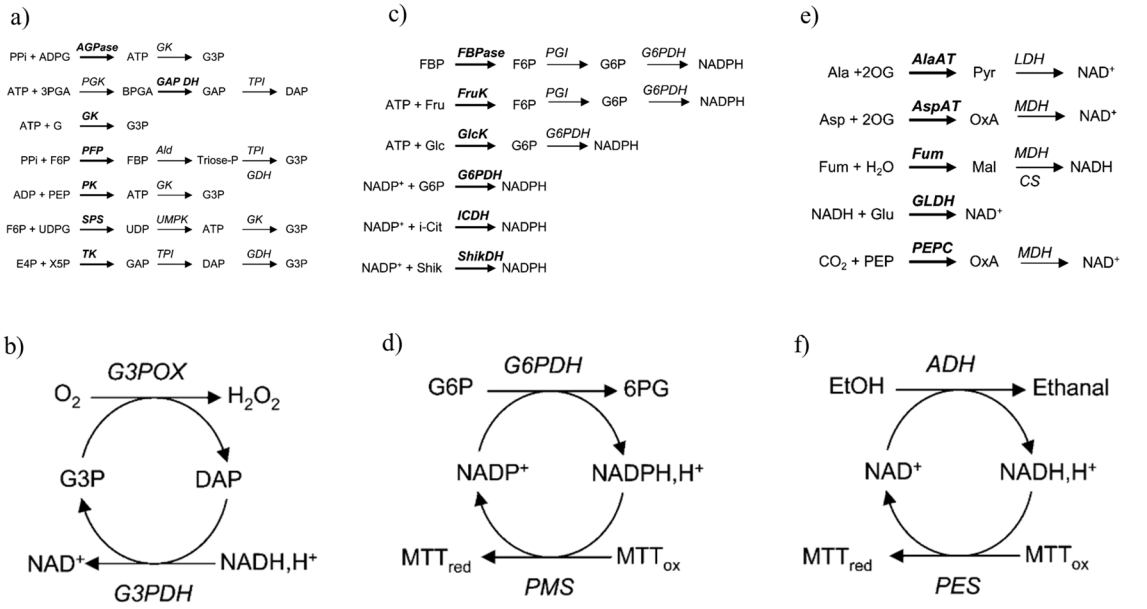

Figure 3.11. Principles of discontinuous assays.

*(*a) and (b) Determinations based on the glycerol-3P-cycling assay; (c) and (d) Determinations based on the NADP-cycling assay; (e) and (f) Determinations based on the NAD-cycling assay; (a), (c), and (e) represent the stopped step leading to glycerol-3P or dihydroxyacetone-P, NADPH, or NAD(H), respectively, directly or via coupled reactions. The enzyme measured is in bold. For clarity, products that are not measured have been omitted as well as the cosubstrates required for the coupling reactions; (B), (D), and (f) represent the principles of the cycling reactions for the determination of glycerol-3P or dihydroxyacetone-P, NADP(H), or NAD(H), respectively.

AGPase: glucose-1-phosphate adenyltransferase; *Ald*: aldolase; *AlaAT*: Ala aminotransferase; *AspAT*: Asp aminotransferase; *CS*: citrate synthase; *FBPase*: fructose-1,6-bisphosphatase; *FruK*: fructokinase; *Fum*: fumarase; *G3PDH*: glycerol-3P dehydrogenase; *G3POX*: glycerol-3P oxidase; *G6PDH*: glucose-6P dehydrogenase; *GlcK*: glucokinase; *GA PDH*: glyceraldehyde-3P dehydrogenase; *GK*: glycerokinase; *GLDH*: glutamate dehydrogenase; *ICDH*: isocitrate dehydrogenase; *LDH*: lactate dehydrogenase; *MDH*: malate dehydrogenase; *PEPC*: phosphoenolpyruvate carboxylase; *PFP*: pyrophosphate-dependent phosphofructokinase; *PGI*: phosphoglucose isomerase; *PGK*: phosphoglycerate kinase; *PK*: pyruvate; kinase; ShikDH: shikimate dehydrogenase; SPS: sucrose-phosphate synthase; TPI: triose-P isomerase; UMPK: UMP kinase. Abbreviations for chemicals are as follows: 2OG: 2-oxoglutarate; 3PGA: 3-phosphoglycerate; 6PG: 6-phosphogluconate; ADPG: adenine-diphosphoglucose; BPGA: bisphosphoglycerate; DAP: dihydroxyacetone-P; F6P: fructose-6P; FBP: fructose-1,6-bisP; Fum: fumarate; G: glycerol; G3P: glycerol-3P; GAP: glyceraldehyde-3P; i-Cit: isocitrate; Mal: malate; MTT: methylthiazolyldiphenyl-tetrazolium bromide; OxA: oxaloacetate; PEP: phosphoenol pyruvate; Pyr: pyruvate; Shik: shikimate.

Retrieved from (Gibon *et al*., 2004).

dehydrogenase and phenazine methosulfate. The reaction was stopped with 20 µl of 0.5 M NAOH, and after neutralisation with 20 µl of 0.5 M HCl, $NADP^+$ was measured in the presence G6PDH, 250 mM G6P, 10 mM MTT, 4 mM PES, 1 M Tricine/KOH and 200mM EDTA, in a final volume of 110

µl. The absorbance was read at 340 nm until the rates were stabilized. Similarly, the estimation of the activity of GDH also involved the PADH/PES cycling method, but with HCl, instead of NaOH, as the agent for stopping the reaction. Absorbance was also estimated at 570 nm.

The activity of the enzymes was expressed as nmol g FW^{-1} min^{-1}. A further detailed protocol of each enzyme can be found in Tables S3.1 – S3.8 of the section *Supplementary material*.

3.2.2.8. Nitrate reductase activity determination

Frozen leaf plant material was ground in a mortar with liquid nitrogen and aliquots of 120 mg were used for the *in vitro* maximal *nitrate reductase* (NR) activity assay following the protocol that measures nitrite formation (Scheible *et al.*, 1997a; Morcuende *et al.*, 2004b). The leaf plant material was vigorously homogenised with four volumes (w/v) of ice-cold extraction buffer containing 100 mM HEPES-KOH pH 7.5, 10 % (v/v) glycerol, 1 mM EDTA, 5 mM magnesium acetate pH 7.5, 0.1 % Triton x-100, 1 % (w/v) BSA, 5 µM Na_2MoO_4, 1 % (w/v) PVPP, 5 mM DTT, 10 µM FAD, 0.5 mM PMSF and 10 µM leupeptin.

The NR activity was assessed through the incubation, at 30 ºC of 165 µL of the homogenised extract with 775 µL of the *assay buffer* (100 mM HEPES-KOH pH 7.5, 5 mM KNO_3, 5 mM EDTA pH 7.5, 10 µM leupeptin, 10 µM FAD, 5 mM DTT, 5 µM Na_2MoO_4 and 0.25 mM NADH). At different time intervals (every 2 min for a total of 6 min), 300 µL aliquots were removed from the assay mixture and the reaction was stopped by adding 25 µl of 0.6 M Zn acetate together with 75 µl of 0.25 mM PMS. Samples were homogenized and kept in the dark for 15 min before adding 300 µl of 1 % (w/v) sulphanilamide in 3 N HCl and 300 µl of 0.02 % (w/v) NNEDA in water. After mixing, they were kept at room temperature for 20 min. The samples were centrifuged at maximum speed for 5 min and the absorbance of the generated azo-dye in the supernatant was measured in a *8452A Diode Array spectrophotometer* (Hewell-Packard) with glass cuvettes at 540 nm. Controls at time zero were also prepared in the presence or absence of 10 nmol nitrite under identical conditions for all extracts by adding 25 µl of 0.6 M Zn acetate before the extract. The difference in absorbance between the time zero controls with and without added nitrite was set as equivalent to 10 nmol nitrite in order to calculate the activity. It was checked the linearity of the reaction with time, as well as for proportionality of the activity to the amount of extract used in the assay. The results of the five biological replicates per genotype were expressed as µmol NO_2^- g FW^{-1} h^{-1}.

3.2.3. C-N compounds, total antioxidant capacity, phenolic compounds and mineral nutrients in the grain at maturity

3.2.3.1. Determination of starch

Wheat grains were ground into whole meal flour using a *mill* (IKA Micro Fine Mill Grinder Culatti MFC, Germany). To quantify the grain starch content, an aliquot of 30 mg of the ground grain material was successively extracted with ethanol/water and the starch was determined in the insoluble residue from the extraction following the same procedure described above for the leaf. The concentration of starch was expressed as mg g^{-1}. Five replicates per genotype were used for these measurements.

3.2.3.2. N and protein determination

Estimation of the total N in the matured grain samples was performed using the *Kjeldahl method* (Miller and Horneck, 1997). This method is based on the transformation of N bounded in the plant tissue into NH_4^+ using sulfuric acid, some catalysts and salts. Several catalysts can be used, including Hg, Cu, Se, Cr and Ti. The produced NH_4^+ can be subsequently measured by multiple methods.

One hundred mg of dried and ground grain material was digested in glass test tubes (Pyrex®) with 300 mg of a mixture containing Se, $CuSO_4$ $5H_2O$ y K_2SO_4 and 4 mL of H_2SO_4. Both, Se and $CuSO_4$ $5H_2O$ were employed as catalysers whereas K_2SO_4 was applied in order to increase the melting point of the H_2SO_4. The whole mixture was incubated at 150 ºC, 250 ºC and 350 ºC during 1 h for each temperature and then cooled until 25 ºC. The samples were diluted to 50 mL with deionised water and stored at 4 ºC until they were used for N measurement using the Ammonia Rapid Kit (Megazime, Ireland). The estimation of the NH_4^+ was performed through the spectrophotometric measurement, at 340 nm, of the $NADP^+$ released in the conversion of NH_4^+ and 2-OG to L-glutamate in a reaction catalysed by the enzyme GDH (Figure 3.12). To do this, the pH of the samples was adjusted to 3-4 using 1 M triethanolamine buffer (TEA; pH 7.2) and 5 M KOH. After centrifugation at 13,200 rpm for 3 min, the reaction was measured using a *UV-Visible 8453 spectrophotometer* (Hewlett - Packard). The *total protein* (TP) concentration in the wheat grain was calculated by multiplying the N concentration by a conversion factor of 5.7 (Högy *et al.*, 2009a; Marcos-Barbero *et al.*, 2021a). The concentration of TP was expressed as mg g^{-1}. Five replicates per genotype were evaluated.

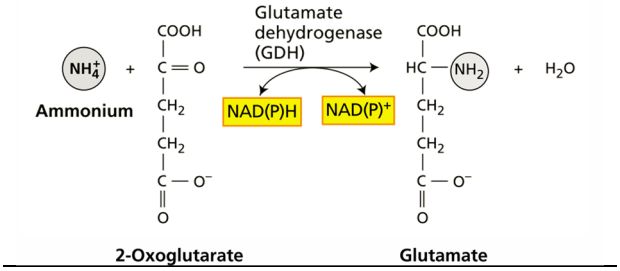

Figure 3.12. GDH reaction.

Retrieved from (Taiz *et al.*, 2015).

3.2.3.3. Determination of total antioxidant capacity and phenolic compounds

3.2.3.3.1. TAC measurement

The estimation of the *total antioxidant capacity* (TAC) in the grain was performed in five replicates using the FRAP method previously described for the leaf but with a larger amount of material, about 170 mg for the wheat ground grain (Benzie and Strain, 1996).

3.2.3.3.2. TPhC measurement

The determination of the total phenolic compounds was made using the Folin-Ciocolteau colorimetric method (Ainsworth and Gillespie, 2007) described above. When TPhC was measured in ground wheat grain, the weighed amount was adjusted to ensure that the absorbance values were within the range of the linear standard curve. Before loading the aliquots of 300 µL from the grain samples into the wells, they were centrifuged at 16,000 g to avoid cloudiness in the solutions. TPhC was expressed as µmol equivalent of Trolox g^{-1}. Five replicates per genotype were evaluated.

3.2.3.4. Determination of grain mineral nutrients

Approximately 500 mg of dry grain powder were weight and stored in 1.5 mL plastic containers for the measurements of mineral nutrients. The aliquot of plant material was transferred to a digestion tube and mixed with 8 mL of 60 % HNO_3 and 2 mL of 30 % hydrogen peroxide. Samples were heated to 200 °C in a *ETHOPS UP* (Milestone) *microwave digestion system* at controlled pressure. Soon after the digested solution was cooled, it was diluted to 25 mL with deionised water. The quantification of the macro and micronutrients in the grain (S, P, B, K, Ca, Cu, Fe, Mg, Na and Zn) was carried out by inductively coupled plasma optical emission spectrometry with an *ICP-OES Varian 720-ES* (Agilent). Subsequently, the grain content of each mineral was calculated and expressed as µg g^{-1}.

3.3 Statistical analysis

3.3.1. Experimental design and statistical analysis

The experimental design applied to both experiments corresponded to a randomised complete block model where each one of the chambers is a block and every table inside the chamber is a subplot.

The statistical analysis chosen to evaluate the two experiments conducted in this study was performed following the approach described by DePoy & Gitlin (2016). Thus, three different categories of analysis were employed: *descriptive*, *inferential* and *associational statistics*. All of them were conducted using the R environment (R Core Team, 2021) and the software *R Studio*. In the first study corresponding to the first one of the experiments, four replicates for each one of the 60 wheat genotypes were employed in the statistical analyses. For the studies carried out in the second of the experiments, five replicates for each of the ten genotypes studied were used.

3.3.1.1. Descriptive statistics

The descriptive methods allow to reduce large sets of observations into more compact and interpretable forms in order to summarise the data derived from the samples. To do this, the large sets of data were resumed employing an *estimator of the central tendency* and *dispersion* of the data per genotype, together with estimators of the whole population including: central tendency and dispersion, minimum and maximum values, Q1 and Q3 quartiles, skewness and kurtosis. Descriptive analysis of the data was performed employing the package *psych* (Revelle, 2020) from the R environment.

3.3.1.2. Inferential statistics

The aim of the inferential statistics is to draw conclusions about the parameters of the population based on the findings of the sample and to examine groups differences within the samples. Thus, the comparison of the traits under study between the population of 59 wheat genotypes from CIMMYT and Gazul was performed in the first study using *one-sample tests* Table 3.2. Comparisons among genotypes or clusters (comparisons of multiple groups) performed in the three studies were carried out through a *one-way analysis of variance* (ANOVA). Because of ANOVA requires several assumptions, it was developed a hierarchical outline showing the appropriate ANOVA test to perform

ANOVA without or with one or several violations of these assumptions Table 3.3. The chosen test was indicated in each ANOVA table, together with the number of replicates employed. The evaluation of the *normality*, *homoscedasticity* and *absence of extreme outliers* assumptions was tested using the *Shaphiro* and *Levene tests* for the formers, and the function identify_outliers for the latter, included in the packages *desctools* and *rstatix* (Signorell and mult. al., 2020; Kassambara, 2021). After the validation of all the assumptions required, a *multiple analysis of variance* (MANOVA) was also performed among the traits under studied in the first study using the function *manova* of the package *stats* (Team R Development Core, 2018).

Histograms were performed using the package *ggstatsplot* (Patil, 2021) while boxplots for ANOVA were created with the package *ggplot2* (Wickham, 2016).

3.3.1.3. Associational statistics

The associational statistics refers to a set of statistical procedures designed to find relationships among multiple variables, contained in one or more datasets, which allows the investigator to make predictions about future performance of these characteristics (DePoy and Gitlin, 2016). Here, the associational statistics employed can be classified in two groups according to the number of datasets using.

Table 3.2. Hierarchical outline for the selection of one-sample tests.

Assumptions			**One-group comparison**	
			Normal distribution	**Independence of normal distribution**
			Absence of extreme outliers	Absence of extreme outliers
Type of analysis			**T test (I)**	**Wilcoxon test (II)**
R function			*t_test* (Kassambara, 2021)	*wilcox_test* (Kassambara, 2021)
Central tendency estimator			*Mean*	*Median*
Effect size	Indices		$\mathbf{d_{Cohen}}$	**r**
	R function		*cohens_d* (Kassambara, 2021)	*wilcox_effsize* (Kassambara, 2021)
	Interpretation	No effect	$d < 0.20$	$r < 0.10$
		Small	$0.20 \leq d < 0.50$	$0.10 \leq r < 0.30$
		Medium	$0.50 \leq d < 0.80$	$0.30 \leq r < 0.50$
		Large	$d \geq 0.80$	$r \geq 0.50$

3.3.1.3.1. One dataset

The multivariate analyses performed included:

- Analyses of *spearman correlations* among parameters using the package *psych* (Revelle, 2020). They were represented through *correlograms* using the package *corrplot* (Wei and Simko, 2021), or with Correlation Networks (CN) developed with the software *Cytoscape* (Shannon, 2003).
- *Analysis of principal components* (PCA) of variables and the hierarchically clustering of genotypes based on PCA (*hierarchical clustering on principal components*; HCPC) from the R packages *FactoMineR and factoextra* (Lê *et al.*, 2008)
- *Canonical Biplot* from the package *MultBiplotR* (Vicente-Villardon, 2019) for the characterisation of the genotypes based on the traits analysed.
- The technique m*ultiple factorial analysis* (MFA) was also employed for the evaluation of quantitative and factor variables in the population using the R packages *FactoMineR and factoextra* (Lê *et al.*, 2008)

3.3.1.3.2. Multiple dataset

The associations among parameters from different datasheets were measured through a multivariate dimension reduction discriminant analysis (DIABLO) from the package *mixOmics* (Rohart *et al.*, 2017) as described in (González *et al.*, 2012; Singh *et al.*, 2019).

Table 3.3. Hierarchical outline for the selection of test in multiple group comparison (ANOVA) of independent measures.

		Normal distribution							**Independence of normal distribution**	
		Homogeneity of variances		**Heterogeneity of variances**					**Homogeneity of variances**	**Heterogeneity of variances**
Assumptions		Balanced groups	Unbalanced groups	Un/balanced groups					Un/balanced groups	Un/balanced groups
		Absence of extreme outliers	Absence of extreme outliers	Absence of extreme outliers		Dealing with extreme outliers			Dealing with extreme outliers	Dealing with extreme outliers
Type of analysis		**ANOVA (I)**	**ANOVA (II)**	**ANOVA with heteroscedasticity correction (III)**		**Robust ANOVA for trimmed means (IV)**			**Kruskal-Wallis (K-W) test (V)**	**Robust ANOVA for medians (VI)**
Number of factors		1, 2 or 3	1, 2 or 3	1	1, 2 or 3	1	2	3	1	1	2
R function		*anova_test* (Kassambara, 2021)	*anova_test* (Kassambara, 2021)	*welch_anova_test* **(IIIa)** (Kassambara, 2021)	*anova_test* **(IIIb)** (Kassambara, 2021)	*t1way* (Mair *et al.*, 2016)	*T2way* (Mair *et al.*, 2016)	*T3way* (Mair *et al.*, 2016)	*Kruskal_test* (Kassambara, 2021)	*med1way* (Mair *et al.*, 2016)	*Med2way* (Mair *et al.*, 2016)
Post-hoc test		**Tukey**	**Pairwise T test**	**Tamahane test**	**Pairwise T test**	**Lincon test**	**Pairwise two-sample permutation tests**		**Wilcox**	**Pairwise permutation tests for medians**	
R function		*TukeyHSD* (Team R Development Core, 2018)	*pairwise.t.test* (Team R Development Core, 2018)	*tamhaneT2Test* (Pohlert, 2020)	*pairwise.t.test* (Team R Development Core, 2018)	*Lincon* (Mair *et al.*, 2016)	*pairwisePermutationMatrix* (Mangiafico, 2020)		*pairwise.wilcox.test* (Kassambara, 2021)	*pairwiseMedianMatrix* (Mangiafico, 2020)	
Central tendency estimator		*Mean*	*Mean*	*Mean*		*Trimmed mean (20 %)*	*Trimmed mean (20 %)*		*Median*	*Median*	
	Indices	**η^2**	**η^2**	**η^2**		**ξ**	**η^2**		**ω^2**	**ω^2**	
	R function	*Included in anova_test* (Kassambara, 2021)	*Included in anova_test* (Kassambara, 2021)	*eta.F* (Buchanan *et al.*, 2019)		*Included in t1way* (Mair *et al.*, 2016)	*eta.F* (Buchanan *et al.*, 2019)		*omega.F* (Buchanan *et al.*, 2019)	*omega.F* (Buchanan *et al.*, 2019)	
Effect size	Interpretation: No effect	$\eta^2 < 0.01$	$\eta^2 < 0.01$	$\eta^2 < 0.01$		$\xi < 0.10$	$\eta^2 < 0.01$		$\omega^2 < 0.01$	$\omega^2 < 0.01$	
	Small	$0.01 \leq \eta^2 > 0.06$	$0.01 \leq \eta^2 > 0.06$	$0.01 \leq \eta^2 > 0.06$		$0.10 \leq \xi < 0.30$	$0.01 \leq \eta^2 > 0.06$		$0.01 \leq \omega^2 > 0.06$	$0.01 \leq \omega^2 > 0.06$	
	Medium	$0.06 \leq \eta^2 > 0.14$	$0.06 \leq \eta^2 > 0.14$	$0.06 \leq \eta^2 > 0.14$		$0.30 \leq \xi < 0.50$	$0.06 \leq \eta^2 > 0.14$		$0.06 \leq \omega^2 > 0.14$	$0.06 \leq \omega^2 > 0.14$	
	Large	$\eta^2 \geq 0.14$	$\eta^2 \geq 0.14$	$\eta^2 \geq 0.14$		$\xi \geq 0.50$	$\eta^2 \geq 0.14$		$\omega^2 \geq 0.14$	$\omega^2 \geq 0.14$	

Note*: *pairwise.t.test* (Team R Development Core, 2018) performs pairwise comparisons with or without assumption of equal variances. "fdr" method was used in *pairwise.t.test* for controlling the false discovery rate.
Since *T2way* and *T3way* does not provide measurements for the size of the effect or degrees of freedom (*df*), **η^2** was performed using df retrieved from *anova_test* in combination with the function *eta.F* in concordance with the calculation for ANOVA with heteroscedasticity correction.

Other references employed to perform this table:
Selection of tests: (García-Pérez, 2005; Kassambara, 2019; Mair and Wilcox, 2020; Mair *et al.*, 2021)
Effect size: (Ellis, 2010; Kotrlik *et al.*, 2011; Sullivan and Feinn, 2012; Brydges, 2019; Ben-Shachar *et al.*, 2020; Mair *et al.*, 2021)

CHAPTER 4

First study:

Screening for higher grain yield and biomass among sixty bread wheat genotypes grown under elevated CO_2 and high-temperature conditions

4.1. Results of the first study

4.1.1. Wheat Production and Grain Yield Components

Table 4.1 summarizes a list of descriptive statistics for wheat production and grain yield components in response to the combined elevated atmospheric CO_2 and high temperatures across a population of 60 wheat genotypes, cultivated in climate chambers. Among genotypes, grain yield ranged from 4.63 to 10.70 g per plant, although 50 % of the genotypes produced between 6.96 and 8.43 g per plant. The mean grain yield was 7.66 ± 1.12 g per plant, with genotypes 150, 74, 23, 8, and 76 as the lowest yielding genotypes, and 43, 94, 95, 61 and 41 as the highest yielding genotypes. The aboveground, stalk and chaff biomasses also ranged between 13.13−25.50, 5.99−12.21 and 1.54−4.42 g per plant, respectively, with 19.16 ± 2.51, 8.78 ± 1.20 and 2.72 ± 0.55 g per plant on average for the whole population. The mean plant height was 86.82 ± 4.88 cm per plant, ranging from 76.35 to 105.30 cm per plant. GNE and grain number per plant varied from 19.4 and 116.39 grains to 54.02 and 315.33 grains, respectively, with an average of 34.99 ± 5.63 grains per ear and 197.01 ± 36.05 grains per plant. The number of ears per plant ranged between 3.20 and 8.20, with a mean value of 5.67 ± 0.84 ears per plant. Grain weight and GYE varied from 29.73 to 48.93 mg per grain and from 0.89 to 1.96 g per ear respectively, with 5.67 ± 3.68 mg per grain and 1.36 ± 0.19 g per ear on average. The mean HI was 0.40 ± 0.03, ranging from 0.26 to 0.46. Skewness and kurtosis of variables in the population were generally located around zero, suggesting symmetry and tail weight similar to that of normal distribution. However, the skewness and kurtosis of HI accounted for -0.77 and 2.68, indicating a non-normal distribution with moderate left-skewed asymmetry. Statistically significant differences among genotypes were found for the studied traits (Table 4.1, S4.1).

Table 4.1. Wheat production (aboveground, stalk and chaff biomasses and plant height) and grain yield components (grain yield, grain number, ear number, grain weight, grain yield per ear, grain number per ear and harvest index) in the response of 60 wheat genotypes grown under elevated CO_2 and high temperature at maturity.

Genotype	Grain yield (g plant^{-1})		Aboveground (g plant^{-1})		Stalk (g plant^{-1})		Chaff (g plant^{-1})		Height (cm plant^{-1})		Grain number (No. plant^{-1})		Ear number (No. plant^{-1})		Grain weight (mg grain^{-1})		GYE (g ear^{-1})		GNE (No. ear^{-1})		HI	
	Mean	SD	Mean	SD	Mean	SD	Mean	SD	Mean	SD	Mean	SD	Mean	SD	Mean	SD	Mean	SD	Mean	SD	Mean	SD
150	5.45	± 1.05	14.38	± 1.64	6.82	± 0.44	2.12	± 0.35	80.36	± 0.77	156.10	± 32.80	4.10	± 0.48	34.97	± 0.81	1.32	± 0.10	37.79	± 3.34	0.38	± 0.03
74	6.18	± 0.68	16.29	± 1.82	8.23	± 1.26	1.88	± 0.30	89.71	± 1.21	151.79	± 19.87	5.65	± 0.30	40.95	± 3.61	1.10	± 0.12	26.98	± 4.23	0.38	± 0.04
23	6.42	± 0.53	15.17	± 1.31	6.83	± 0.48	1.91	± 0.35	79.86	± 0.19	159.37	± 12.57	4.45	± 0.57	40.27	± 0.42	1.45	± 0.08	36.02	± 2.24	0.42	± 0.01
8	6.46	± 1.22	17.14	± 3.79	7.88	± 1.72	2.80	± 0.86	81.49	± 3.04	161.55	± 32.03	5.30	± 1.16	40.04	± 1.60	1.22	± 0.06	30.58	± 1.55	0.38	± 0.01
76	6.50	± 0.77	17.12	± 1.72	8.46	± 0.86	2.16	± 0.26	87.15	± 2.16	160.50	± 24.84	5.40	± 0.63	40.63	± 1.60	1.20	± 0.07	29.70	± 2.47	0.38	± 0.02
15	6.53	± 0.85	16.11	± 2.41	7.18	± 1.27	2.39	± 0.39	77.14	± 1.38	158.58	± 22.88	5.55	± 0.53	41.28	± 1.08	1.18	± 0.09	28.51	± 2.19	0.41	± 0.02
73	6.59	± 0.94	18.81	± 1.49	9.59	± 0.63	2.63	± 0.23	91.38	± 0.59	158.99	± 15.40	4.95	± 0.10	41.34	± 2.39	1.33	± 0.18	32.14	± 3.25	0.35	± 0.03
21	6.62	± 0.59	16.35	± 1.07	7.78	± 0.28	1.94	± 0.27	88.73	± 1.92	163.79	± 8.89	5.00	± 0.52	40.44	± 2.71	1.34	± 0.19	32.94	± 2.81	0.40	± 0.01
9	6.64	± 0.73	17.19	± 1.80	8.18	± 0.66	2.38	± 0.44	88.13	± 3.34	148.69	± 18.14	4.95	± 0.55	44.71	± 1.92	1.34	± 0.05	30.04	± 1.74	0.39	± 0.01
118	6.67	± 0.23	17.19	± 1.40	8.00	± 0.95	2.53	± 0.43	84.70	± 4.05	176.82	± 4.29	6.80	± 0.49	37.75	± 1.48	0.99	± 0.08	26.07	± 1.32	0.39	± 0.03
81	6.75	± 1.03	17.15	± 2.14	8.01	± 1.27	2.39	± 0.07	94.69	± 2.02	164.49	± 28.73	5.00	± 1.40	41.20	± 2.23	1.40	± 0.26	33.88	± 5.17	0.39	± 0.02
77	6.86	± 0.96	17.42	± 1.88	8.49	± 0.63	2.07	± 0.34	91.03	± 4.86	168.32	± 19.71	5.25	± 0.64	40.66	± 1.95	1.31	± 0.19	32.32	± 4.74	0.39	± 0.02
115	6.92	± 0.94	18.23	± 1.64	8.64	± 0.84	2.67	± 0.25	87.08	± 2.59	160.01	± 25.82	5.55	± 0.44	43.49	± 2.81	1.25	± 0.10	28.80	± 3.72	0.38	± 0.03
87	6.96	± 1.43	18.14	± 3.64	8.62	± 1.82	2.55	± 0.48	87.36	± 1.30	184.34	± 43.52	4.90	± 0.48	38.03	± 2.24	1.44	± 0.35	38.03	± 9.69	0.38	± 0.01
29	7.04	± 0.77	17.26	± 1.00	7.89	± 0.21	2.33	± 0.07	82.15	± 2.20	184.91	± 16.88	4.75	± 0.34	38.03	± 1.02	1.48	± 0.08	38.90	± 1.70	0.41	± 0.02
46	7.06	± 0.32	18.39	± 0.84	8.23	± 0.57	3.11	± 0.27	88.99	± 3.74	147.54	± 7.81	5.45	± 0.10	47.84	± 1.22	1.30	± 0.07	27.09	± 1.81	0.38	± 0.02
119	7.09	± 0.90	18.33	± 1.63	8.84	± 0.86	2.40	± 0.23	92.60	± 1.93	170.30	± 5.50	5.10	± 0.35	41.63	± 5.21	1.39	± 0.15	33.50	± 2.44	0.39	± 0.02
6	7.20	± 0.75	16.94	± 1.73	7.51	± 0.75	2.23	± 0.33	79.49	± 1.19	194.79	± 17.84	4.35	± 0.34	36.91	± 0.71	1.65	± 0.08	44.78	± 2.35	0.42	± 0.01
110	7.25	± 0.81	18.25	± 1.07	8.77	± 0.43	2.24	± 0.06	85.64	± 3.54	202.72	± 19.43	5.75	± 0.38	35.73	± 1.16	1.26	± 0.07	35.21	± 1.56	0.40	± 0.02
71	7.29	± 0.65	18.70	± 0.87	9.02	± 0.57	2.39	± 0.34	93.69	± 1.18	169.53	± 12.76	4.85	± 0.34	42.97	± 1.26	1.50	± 0.10	35.03	± 2.76	0.39	± 0.03
16	7.34	± 0.32	17.69	± 0.36	7.94	± 0.12	2.40	± 0.20	83.21	± 3.08	181.28	± 9.93	6.35	± 0.38	40.54	± 1.26	1.16	± 0.08	28.58	± 1.32	0.42	± 0.01
22	7.44	± 0.79	18.10	± 1.96	8.10	± 1.11	2.56	± 0.26	85.10	± 0.27	199.14	± 21.75	6.15	± 0.60	37.39	± 0.74	1.21	± 0.07	32.38	± 1.56	0.41	± 0.02
13	7.49	± 1.01	18.87	± 2.29	8.43	± 1.13	2.95	± 0.32	89.96	± 0.86	166.74	± 23.43	5.45	± 0.68	45.03	± 3.37	1.38	± 0.15	30.67	± 3.44	0.40	± 0.02
92	7.50	± 0.68	18.40	± 1.24	8.47	± 0.43	2.43	± 0.27	83.39	± 1.90	199.36	± 17.06	5.60	± 0.37	37.61	± 0.98	1.34	± 0.11	35.69	± 3.41	0.41	± 0.01
117	7.53	± 0.35	18.56	± 1.17	8.42	± 0.58	2.60	± 0.34	89.48	± 0.78	173.98	± 5.18	5.65	± 0.19	43.31	± 1.77	1.33	± 0.07	30.80	± 0.52	0.41	± 0.01
79	7.56	± 0.91	19.75	± 2.48	9.12	± 1.34	3.06	± 0.31	84.79	± 2.56	181.24	± 19.11	5.95	± 0.41	41.69	± 1.43	1.27	± 0.14	30.47	± 2.52	0.38	± 0.02
33	7.60	± 1.35	21.98	± 0.67	10.76	± 0.66	3.61	± 0.47	85.28	± 4.74	168.38	± 37.34	5.65	± 0.41	45.58	± 3.37	1.36	± 0.30	30.02	± 7.23	0.35	± 0.06
69	7.66	± 1.50	17.81	± 2.54	7.63	± 0.89	2.51	± 0.45	79.86	± 2.44	193.14	± 28.90	6.35	± 0.85	39.48	± 1.79	1.21	± 0.20	30.62	± 4.64	0.43	± 0.03
31	7.71	± 1.26	18.71	± 2.69	8.27	± 1.09	2.73	± 0.36	87.35	± 3.87	177.91	± 29.82	6.50	± 1.16	43.38	± 2.12	1.20	± 0.17	27.52	± 3.13	0.41	± 0.01
19	7.73	± 0.66	19.04	± 1.21	8.74	± 0.58	2.57	± 0.10	87.91	± 3.11	193.25	± 3.79	5.10	± 0.38	40.03	± 3.77	1.52	± 0.11	38.04	± 2.65	0.41	± 0.01
114	7.75	± 0.32	20.64	± 1.03	10.42	± 0.53	2.46	± 0.37	100.68	± 3.35	214.96	± 15.27	5.65	± 0.34	36.11	± 1.47	1.37	± 0.04	38.03	± 0.75	0.38	± 0.01
97	7.79	± 0.35	19.89	± 1.06	9.42	± 0.50	2.68	± 0.35	88.10	± 3.37	213.71	± 8.05	6.55	± 0.19	36.49	± 2.51	1.19	± 0.06	32.67	± 2.01	0.39	± 0.01
113	7.79	± 0.87	20.01	± 2.47	9.91	± 1.27	2.31	± 0.39	90.13	± 4.00	237.19	± 44.64	6.40	± 1.02	33.16	± 2.30	1.22	± 0.06	36.96	± 1.32	0.39	± 0.01
25	7.81	± 0.47	18.72	± 1.04	8.22	± 0.64	2.69	± 0.16	83.50	± 4.10	197.07	± 12.53	5.60	± 0.28	39.63	± 0.68	1.40	± 0.10	35.23	± 2.36	0.42	± 0.02

Genotype	Grain yield (g plant^{-1})		Aboveground (g plant^{-1})		Stalk (g plant^{-1})		Chaff (g plant^{-1})		Height (cm plant^{-1})		Grain number (No. plant^{-1})		Ear number (No. plant^{-1})		Grain weight (mg grain^{-1})		GYE (g ear^{-1})		GNE (No. ear^{-1})		HI	
	Mean	SD	Mean	SD	Mean	SD	Mean	SD	Mean	SD	Mean	SD	Mean	SD	Mean	SD	Mean	SD	Mean	SD	Mean	SD
18	7.83	± 1.28	19.61	± 2.49	8.82	± 1.01	2.97	± 0.61	87.00	± 2.85	202.67	± 31.10	5.75	± 0.98	38.62	± 2.16	1.37	± 0.13	35.37	± 2.38	0.40	± 0.04
70	7.84	± 1.17	19.75	± 3.23	8.98	± 1.72	2.93	± 0.73	93.44	± 3.93	220.48	± 43.49	5.85	± 1.23	35.89	± 3.65	1.37	± 0.24	37.98	± 4.14	0.40	± 0.04
63	7.89	± 0.82	20.21	± 1.54	9.23	± 0.77	3.09	± 0.31	85.29	± 2.36	215.34	± 14.60	6.00	± 0.43	36.59	± 1.61	1.32	± 0.10	35.96	± 2.46	0.39	± 0.03
105	7.91	± 0.89	18.50	± 1.33	8.21	± 0.60	2.38	± 0.12	82.40	± 2.10	207.79	± 28.23	4.40	± 0.00	38.17	± 1.69	1.80	± 0.20	47.22	± 6.42	0.43	± 0.02
88	8.00	± 0.78	20.27	± 1.31	9.21	± 0.79	3.05	± 0.23	87.35	± 2.97	200.75	± 19.37	5.25	± 0.34	39.88	± 1.76	1.53	± 0.22	38.35	± 4.41	0.39	± 0.02
93	8.01	± 1.51	20.01	± 3.21	9.01	± 1.47	2.99	± 0.53	88.54	± 1.84	192.90	± 23.42	5.70	± 0.60	41.28	± 3.34	1.40	± 0.17	33.84	± 1.97	0.40	± 0.03
35	8.02	± 1.11	21.93	± 2.59	10.30	± 1.39	3.61	± 0.59	87.33	± 1.71	195.70	± 8.82	4.90	± 0.62	40.91	± 4.55	1.63	± 0.02	40.28	± 3.92	0.37	± 0.03
4	8.06	± 0.63	18.18	± 0.90	7.45	± 0.38	2.67	± 0.05	85.81	± 1.84	219.29	± 9.45	6.25	± 0.19	36.71	± 1.34	1.29	± 0.08	35.09	± 1.15	0.44	± 0.02
26	8.12	± 0.44	20.35	± 1.49	9.58	± 0.91	2.65	± 0.24	87.34	± 1.58	204.17	± 6.84	6.05	± 0.41	39.77	± 0.95	1.34	± 0.03	33.81	± 1.15	0.40	± 0.01
48	8.15	± 0.43	20.28	± 1.18	9.34	± 0.76	2.79	± 0.28	90.09	± 4.08	185.85	± 20.06	6.35	± 0.47	44.08	± 2.62	1.29	± 0.10	29.31	± 2.95	0.40	± 0.01
99	8.19	± 0.63	20.80	± 1.14	9.62	± 0.23	3.00	± 0.52	88.19	± 1.78	238.56	± 11.01	5.50	± 0.26	34.34	± 2.81	1.49	± 0.10	43.39	± 1.40	0.39	± 0.02
53	8.19	± 0.72	20.25	± 1.45	8.78	± 0.76	3.27	± 0.33	82.55	± 1.55	221.46	± 14.92	6.40	± 0.33	36.96	± 0.85	1.28	± 0.12	34.65	± 2.60	0.40	± 0.02
59	8.24	± 1.32	20.47	± 2.57	9.20	± 1.02	3.03	± 0.33	86.99	± 0.61	192.70	± 29.26	5.95	± 0.70	42.73	± 1.07	1.38	± 0.10	32.33	± 1.78	0.40	± 0.01
83	8.28	± 0.56	21.10	± 2.28	9.70	± 1.19	3.12	± 0.58	85.04	± 7.27	216.33	± 16.38	5.70	± 0.84	38.31	± 0.37	1.47	± 0.23	38.52	± 6.17	0.39	± 0.02
10	8.31	± 0.98	19.66	± 2.19	8.43	± 0.97	2.92	± 0.33	82.31	± 2.65	226.90	± 26.78	5.40	± 0.78	36.71	± 2.78	1.55	± 0.15	42.14	± 1.38	0.42	± 0.02
65	8.35	± 0.89	20.65	± 2.87	9.13	± 1.67	3.17	± 0.54	91.61	± 5.93	217.74	± 8.02	6.30	± 0.62	38.29	± 2.87	1.33	± 0.16	34.81	± 3.61	0.41	± 0.03
42	8.51	± 0.65	21.34	± 1.32	9.34	± 0.87	3.49	± 0.22	88.88	± 0.71	250.79	± 12.25	6.80	± 0.52	33.91	± 1.12	1.25	± 0.09	36.96	± 1.86	0.40	± 0.02
107	8.56	± 1.37	20.33	± 3.43	9.10	± 1.42	2.68	± 0.74	84.05	± 2.79	249.29	± 47.63	5.75	± 0.50	34.48	± 1.63	1.49	± 0.16	43.14	± 5.03	0.42	± 0.01
11	8.65	± 0.21	20.15	± 0.90	8.78	± 0.72	2.72	± 0.21	86.24	± 2.95	232.13	± 13.49	6.30	± 0.62	37.33	± 1.50	1.38	± 0.11	36.96	± 1.64	0.43	± 0.02
58	8.70	± 0.81	21.47	± 2.01	9.85	± 0.82	2.92	± 0.56	86.29	± 1.27	247.08	± 13.25	5.90	± 0.50	35.16	± 1.55	1.48	± 0.08	41.99	± 2.19	0.41	± 0.02
5	8.76	± 1.17	22.09	± 2.40	9.88	± 0.86	3.46	± 0.40	84.75	± 1.54	238.93	± 21.61	6.80	± 0.59	36.60	± 3.13	1.28	± 0.09	35.13	± 0.78	0.40	± 0.01
43	8.97	± 0.99	20.86	± 1.66	8.64	± 0.77	3.26	± 0.13	89.44	± 1.97	232.37	± 31.09	5.65	± 0.25	38.77	± 3.25	1.58	± 0.12	41.12	± 5.22	0.43	± 0.02
94	8.99	± 0.68	21.36	± 1.95	9.59	± 1.18	2.79	± 0.28	94.06	± 3.87	226.96	± 24.88	6.00	± 0.59	39.71	± 1.44	1.50	± 0.12	37.88	± 3.00	0.42	± 0.02
95	9.00	± 0.66	21.73	± 2.01	9.59	± 1.04	3.14	± 0.44	85.65	± 3.43	231.89	± 18.72	6.15	± 1.00	38.84	± 1.48	1.48	± 0.15	38.15	± 3.88	0.41	± 0.01
61	9.03	± 0.71	22.21	± 1.52	10.27	± 1.23	2.92	± 0.72	85.68	± 1.24	259.49	± 13.43	5.90	± 0.62	34.75	± 1.25	1.53	± 0.09	44.23	± 3.49	0.41	± 0.01
41	9.68	± 0.85	23.25	± 1.59	9.80	± 0.73	3.78	± 0.22	82.73	± 3.39	252.73	± 27.81	7.25	± 0.44	38.38	± 1.53	1.33	± 0.05	34.82	± 2.47	0.42	± 0.01
Average	7.66	± 1.12	19.16	± 2.51	8.78	± 1.20	2.72	± 0.55	86.82	± 4.88	197.01	± 36.05	5.67	± 0.84	39.26	± 3.68	1.36	± 0.19	34.99	± 5.63	0.40	± 0.03
Min	4.63		13.13		5.99		1.54		76.35		116.39		3.20		29.73		0.89		19.40		0.26	
Max	10.70		25.50		12.21		4.42		105.30		315.33		8.20		48.93		1.96		54.02		0.46	
Q1	6.96		17.58		7.95		2.36		83.80		171.31		5.00		36.87		1.24		31.23		0.39	
Q3	8.43		21.03		9.65		3.04		89.75		221.81		6.20		41.23		1.48		38.22		0.42	
Skewness	-0.02		0.02		0.14		0.37		0.41		0.27		0.09		0.36		0.29		0.32		-0.77	
Kurtosis	-0.25		-0.23		-0.28		-0.08		0.51		-0.10		-0.06		-0.10		0.27		0.27		2.68	
***p*-value**	**4.08×10^{-11}**		**8.82×10^{-12}**		**6.67×10^{-10}**		**8.18×10^{-17}**		**6.38×10^{-30}**		**2.85×10^{-25}**		**1.37×10^{-16}**		**2.85×10^{-28}**		**4.72×10^{-14}**		**2.32×10^{-28}**		**5.22×10^{-6}**	

GNE: grain number ear^{-1}; *GYE*: grain yield ear^{-1}; *HI*: harvest index; *Max*: Maximum; *Min*: Minimum; *Q1* and *Q3*: first and third quartile.

Values represent measures of central tendency (*Mean*: mean) and dispersion (*SD*: standard deviation) of four replicates (n=4) for each genotype. Within columns, all genotypes and replicates (N=240) were employed for the calculation of *Average*, *Min*, *Max*, *Q1*, *Q3*, *Skewness* and *Kurtosis*. The calculation of statistical significances (p-value) for each trait is based on MANOVA. Values in bold represent significance ($p < 0.05$). Genotypes are ranked according to decreasing values of grain yield.

Traits

Minimum Maximum

4.1.2. Comparison between the CIMMYT Population and Gazul

The mean responses of the genotype 150 (Gazul) for wheat production and grain yield traits were compared with a population of 59 selected wheat genotypes belonging to the CIMMYT 8TH HTWSN collection (Figure 4.1). The one-sample test for the comparison of the mean responses showed significant differences between Gazul and the CIMMYT population for all the traits under study. Gazul exhibited lower aboveground, chaff and stalk biomasses, grain yield, grain and ear numbers per plant, and lower GYE and HI, but a greater GNE than the CIMMYT population. The effect size was considered as large for almost all the variables, with the exception of the effect size for GYE and GNE, which were considered as small and medium-size, respectively.

4.1.3. Correlation Network and Coefficient Matrix

To study the relationship among the traits under study in the population of the 60 wheat genotypes, both a correlation matrix and a correlation network were performed (Figure 4.2; Figure S4.1). Positive correlations were found among the aboveground, stalk, chaff, grain yield, grain number and ear number traits, with very high correlations of aboveground biomass to stalk biomass (0.90), grain yield (0.88), chaff biomass (0.77) and grain number (0.76), as well as between grain yield and grain number (0.85). GYE and GNE were also positively correlated with each other (0.78), and both were correlated, to a lesser extent (0.11−0.61), with aboveground, stalk and chaff biomasses, grain yield and grain number traits. Furthermore, they were also negatively correlated with ear numbers (-0.44 and -0.29, respectively). Grain weight showed no correlation with chaff biomass and very low negative correlation with HI, stalk and aboveground biomasses, grain yield and ear number (ranged from -0.02 to -0.16), but it was negatively correlated with GNE (-0.54) and grain number per plant (-0.58). HI showed positive correlations with grain yield, GYE, grain number and GNE, but negative correlations with plant height and stalk and chaff biomasses, all of them lower than |0.45|. Plant height was in turn positively correlated with grain weight and with stalk and aboveground biomasses (0.28−0.15).

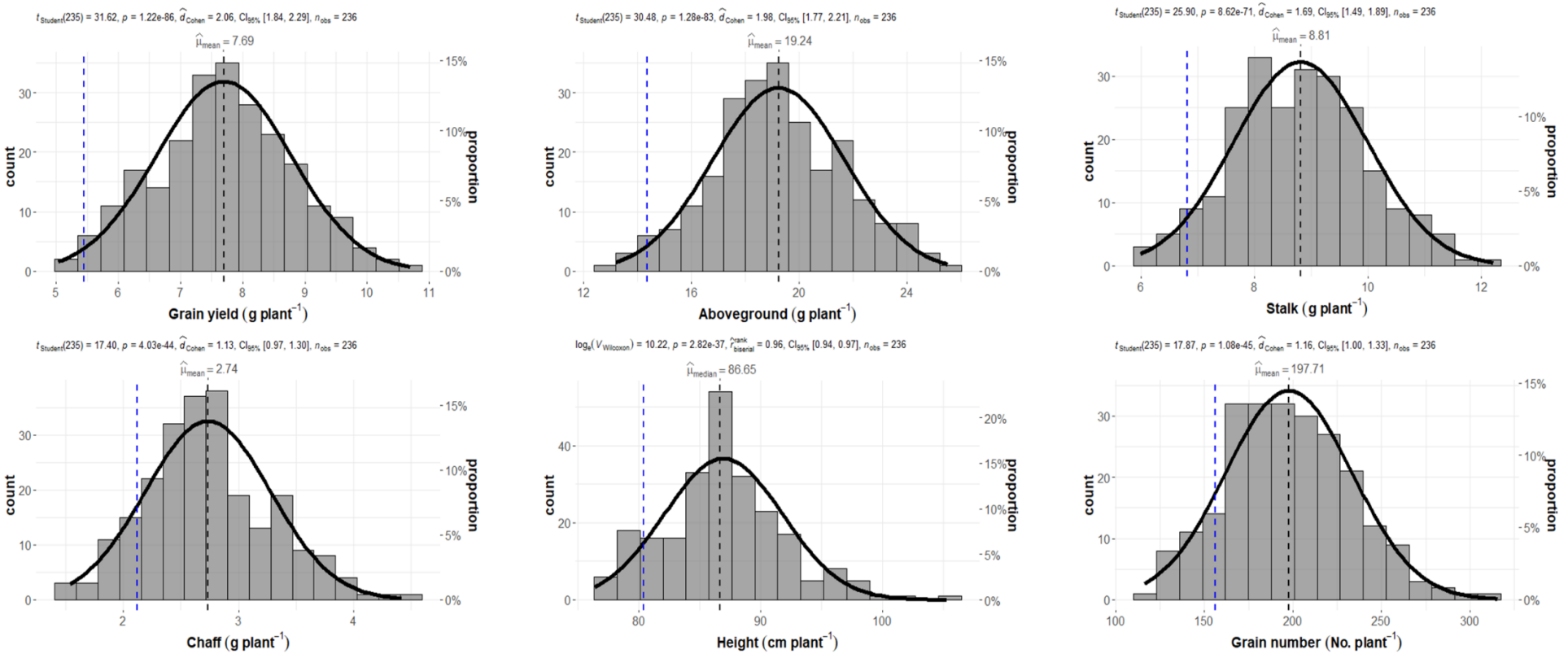

Figure 4.1. Histograms with one-sample test of wheat production and grain yield components in the response of 59 wheat genotypes from CIMMYT grown under elevated CO_2 and high temperature at maturity.

Each plot shows distribution of frequencies with super-imposed normal curve for the selected trait among a population of 59 wheat genotypes belonging to CIMMYT and their four replicates (n_{obs}=236). For each trait, one-sample test was performed for the comparison between CIMMYT population and average Gazul genotype. Black dotted line represents the mean or median of population according to the test employed (Student's t-test ([I]) or Wilcoxon test ([II])). Statistics ($t_{student}$ and $V_{Wilcoxon}$), *p*-value (*p*) and size of the effect (d_{Cohen} and $r_{Wilcoxon}$) with confident intervals (CI) for one-sample test are added. Blue dotted line represents the mean value for the four replicates (n=4) of genotype 150 (Gazul). Differences were considered statistically significant at $p < 0.05$.

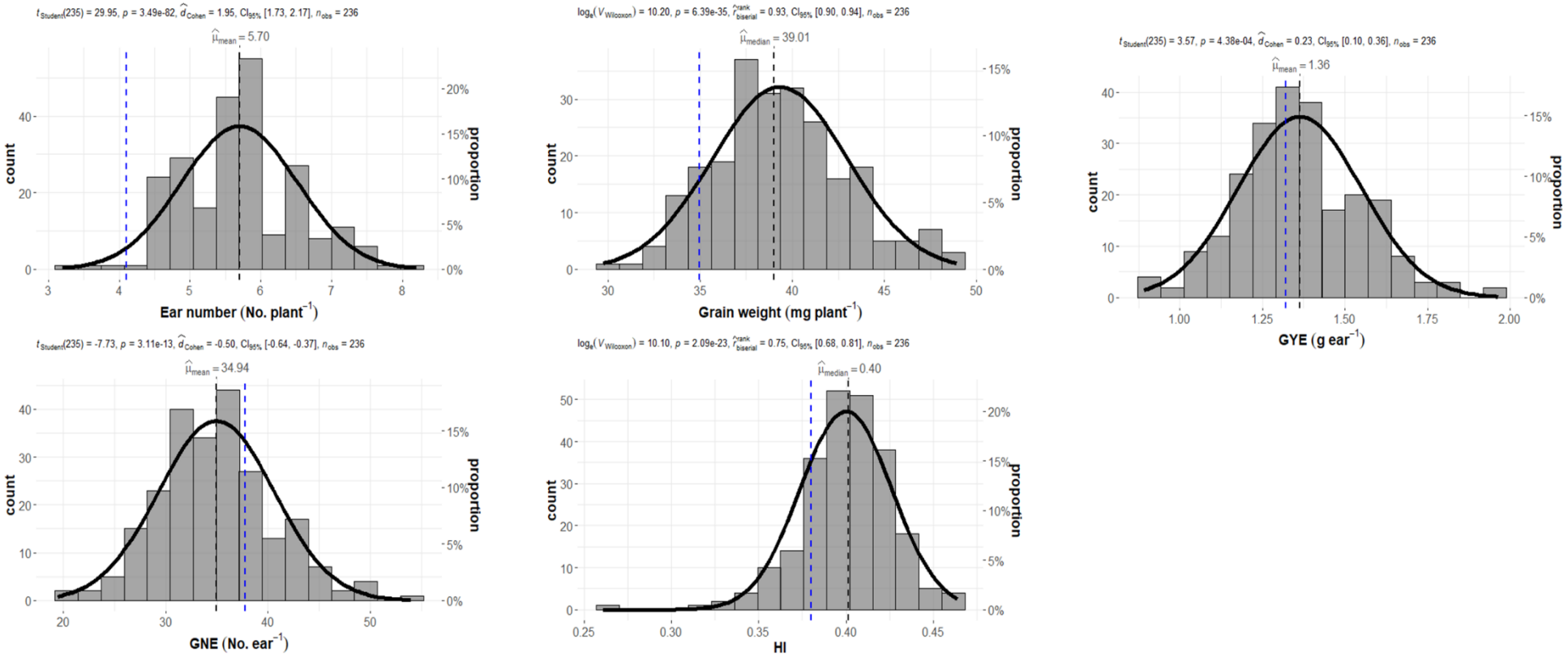

Figure 4.1. Histograms with one-sample test of wheat production and grain yield components in the response of 59 wheat genotypes from CIMMYT grown under elevated CO_2 and high temperature at maturity (continuation).

GNE: grain number ear^{-1}; *GYE*: grain yield ear^{-1}; *HI*: harvest index.

Each plot shows distribution of frequencies with super-imposed normal curve for the selected trait among a population of 59 wheat genotypes belonging to CIMMYT and their four replicates (n_{obs}=236). For each trait, one-sample test was performed for the comparison between CIMMYT population and average Gazul genotype. Black dotted line represents the mean or median of population according to the test employed (Student's t-test ([I]) or Wilcoxon test ([II])). Statistics ($t_{student}$ and $V_{Wilcoxon}$), *p*-value (*p*) and size of the effect (d_{Cohen} and $r_{Wilcoxon}$) with confident intervals (CI) for one-sample test are added. Blue dotted line represents the mean value for the four replicates (n=4) of genotype 150 (Gazul). Differences were considered statistically significant at $p < 0.05$.

4.1.4. Principal Component and Hierarchical Clustering Analyses

The natural variation in plant biomass and grain yield within the 60 wheat genotypes was further investigated using principal component analysis. Graphs of variables and individuals from PCA are shown in Figure 4.3, a and b. Almost all the variables under study were positively correlated with the first dimension of the PCA (Table 4.2). Grain yield, grain number and aboveground biomass per plant were the most commonly contributing eigenvectors (18.85, 18.07 and 18.01, respectively) and correlated variables (0.95, 0.93 and 0.93) with the first dimension of the PCA. The stalk and chaff biomasses, GNE and ear number were also highly correlated variables, with correlation values ranging between 0.74 and 0.52, followed by GYE, HI and plant height. The grain weight was the only variable that was negatively correlated with the first dimension of the PCA (-0.49). Weaker positive correlations were found for the second dimension of the PCA, while the number of negatively correlated variables increased, together with their intensity. GNE, GYE and HI were the most contributing variables (21.58, 14.96 and 14.24) and the highest negatively correlated ones with this second dimension (-0.73, -0.61 and -0.59). Grain number per plant was also negatively correlated with the second dimension (-0.21), although it barely contributed to this dimension (1.81). Ear number, grain weight and stalk biomass were the most positively correlated variables (0.53−0.46), followed by the height of the plant and the chaff and aboveground biomasses. The grain yield barely correlated with this second dimension (0.02).

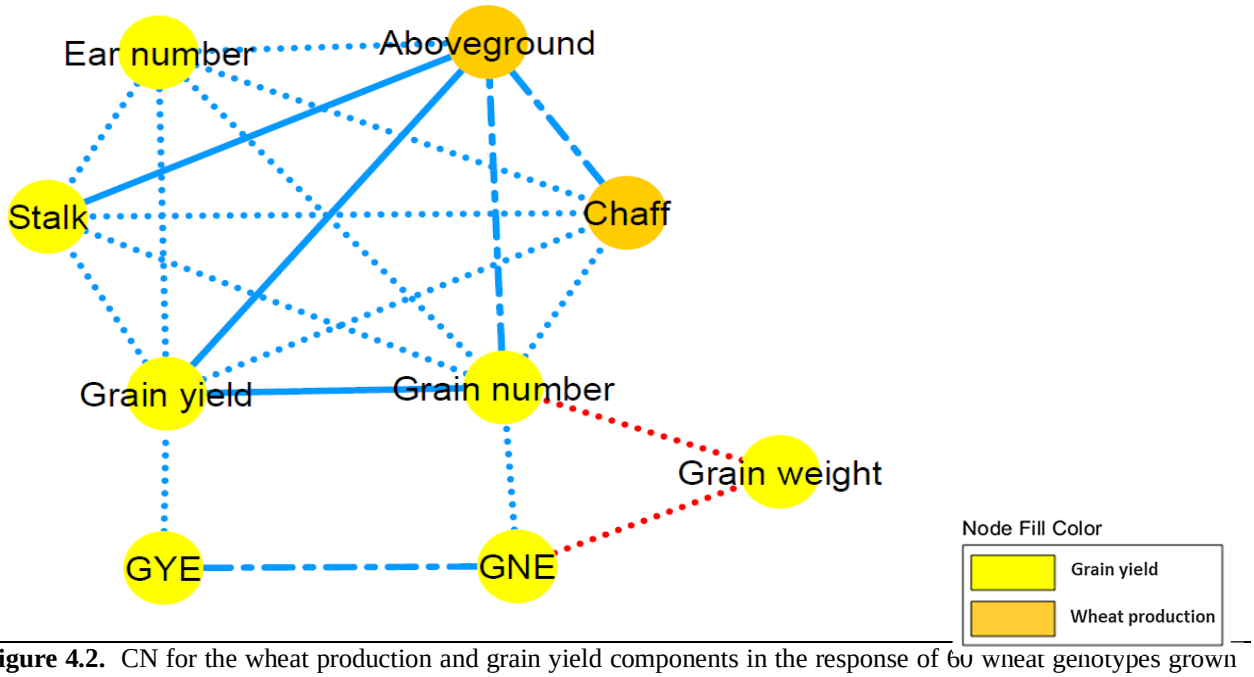

Figure 4.2. CN for the wheat production and grain yield components in the response of 60 wheat genotypes grown under elevated CO_2 and high temperature at maturity.

GNE: grain number ear^{-1}; *GYE*: grain yield ear^{-1}.

The different traits (nodes) were classified by colours according to their grain yield or wheat production nature (see legend). Edges stand for a Spearman's correlation $r_s \geq |0.45|$, split up as dot ($|0.65| > r_s \geq |0.45|$), dash and dot ($|0.85| > r_s \geq |0.65|$) or solid ($|1| > r_s \geq |0.85|$) line types. Blue edges indicate a positive correlation, whereas red lines implicate negative correlation.

HCPC for the 60 wheat genotypes was performed, based on the PCA results. Cutting of the tree defined three major clusters (clusters 1, 2 and 3; Figure 4.3c). Grouped by clusters, the distribution of the genotypes in the PCA is shown in Figure 4.3d, whereas Figure 4.4 shows boxplots of wheat production and grain yield components with a one-way ANOVA for clusters. Cluster 3 included the 28 genotypes most related to grain yield, aboveground biomass and grain number, whereas the 27 genotypes from cluster 2 were mainly associated with grain weight. Cluster 1 was composed of 5 genotypes, including genotype 150. The one-way ANOVA found statistically significant differences for wheat production and grain yield components when the three clusters were compared (Figure 4.4, Table S4.2). Cluster 3 showed significantly higher grain yield and grain number per plant than clusters 2 and 1, whereas no differences between the latter two were found. Aboveground, stalk and chaff biomasses were also significantly greater for cluster 3 than for clusters 2 and 1, as well as for cluster 2 than for cluster 1. Cluster 2 showed higher grain weight than clusters 1 or 3 but lower HI, with non-significant differences between clusters 1 and 3 for any variable. Furthermore, cluster 2 also had lower GYE and GNE than clusters 1 and 3, whereas cluster 1 had the highest. Finally, cluster 1 showed the lowest ear number and plant height, with no differences between clusters 2 and 3. All the traits under study exhibited a large effect ranging between 0.18−0.57, except for HI, which showed a middle-sized effect (0.06).

Table 4.2. Correlations and contributions between the original variables with the first two dimensions of the PCA.

Dim. 1				Dim. 2			
Continuous variables	**Corr.**	**Cos^2**	**Contr.**	**Continuous variables**	**Corr.**	**Cos^2**	**Contr.**
Grain yield	0.95	0.91	18.85	**Ear number**	0.53	0.28	11.39
Grain number	0.93	0.87	18.07	**Grain weight**	0.48	0.23	9.44
Aboveground	0.93	0.87	18.01	**Stalk**	0.46	0.21	8.69
Stalk	0.74	0.55	11.33	**Height**	0.44	0.19	7.80
Chaff	0.72	0.52	10.88	**Chaff**	0.39	0.15	6.09
GNE	0.59	0.35	7.18	**Aboveground**	0.31	0.10	4.00
Ear number	0.52	0.27	5.52	**Grain yield**	0.02	0.00	0.02
GYE	0.40	0.16	3.39	**Grain number**	-0.21	0.04	1.81
HI	0.27	0.07	1.48	**HI**	-0.59	0.35	14.24
Height	0.13	0.02	0.33	**GYE**	-0.61	0.37	14.96
Grain weight	-0.49	0.24	4.96	**GNE**	-0.73	0.53	21.58

Dim.: dimension; *Contr.*: contribution; *Corr.:* correlation*; GNE*: grain number ear^{-1}; *GYE*: grain yield ear^{-1}; *HI*: harvest index;

Corr. indicates the correlation between each variable and the dimension. The squared correlation (*Cos^2*) values between the variables and the dimensions are used to estimate the quality of the representation. *Cont.* expresses the contributions, in percentage, of each variable in accounting for the variability in the dimension.

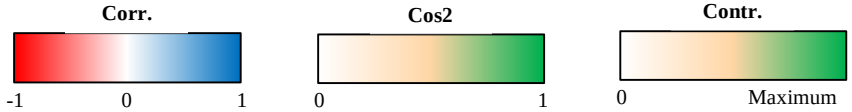

4.1.5. Days from Sowing to Ear Emergence, Anthesis and Maturity

Growth duration varied among genotypes. Days from sowing until plants reached ear emergence, anthesis and maturity growth stages ranged between 57−68, 60−69 and 92−102 days after sowing, respectively (Table S4.3). Negative correlations were found of the average number of days until plants reached these growth stages to wheat production and grain yield components, although all of

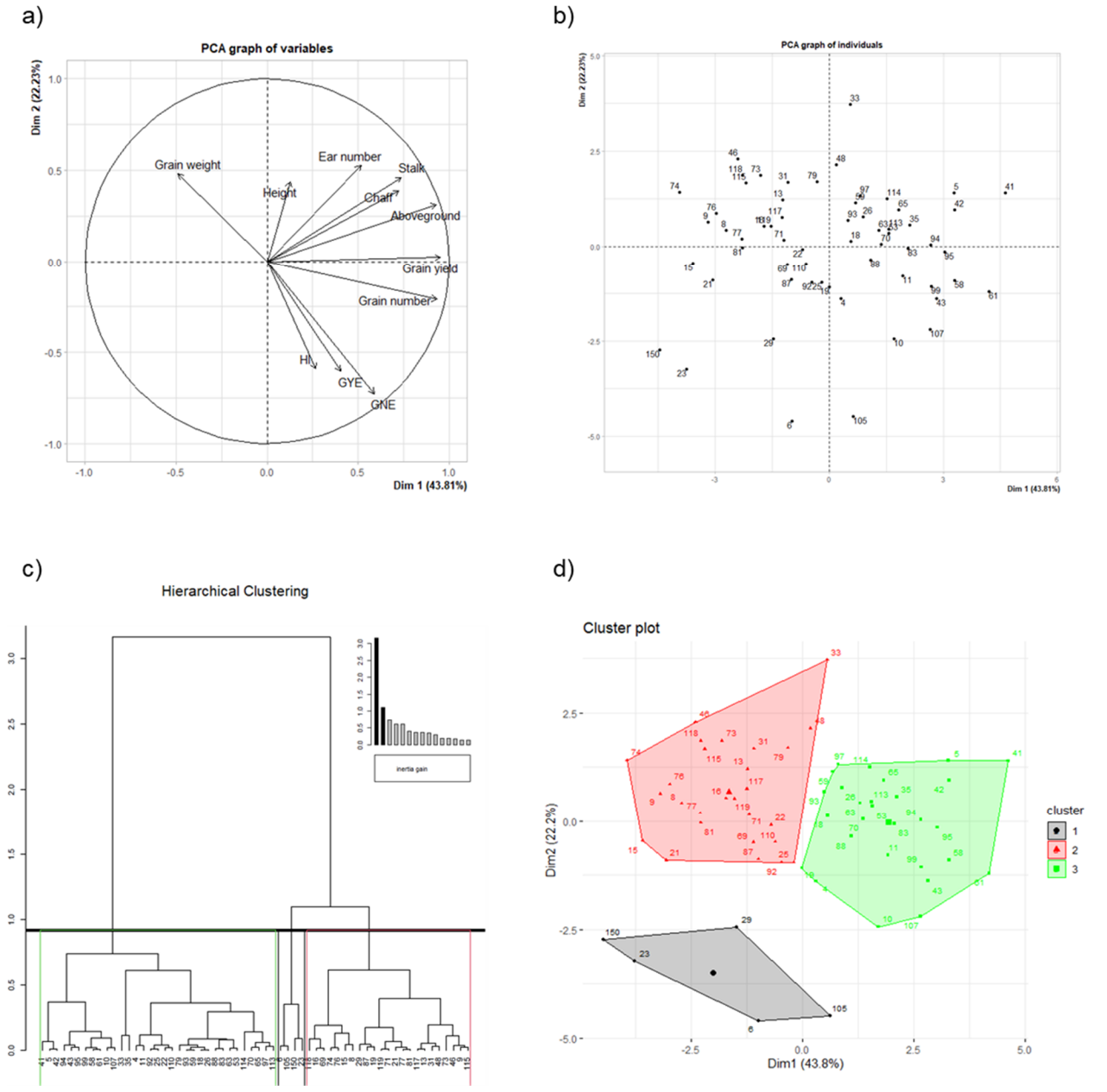

Figure 4.3. HCPC in the response of 60 wheat genotypes grown under elevated CO_2 and high-temperature conditions at maturity.

GNE: grain number ear^{-1}; *GYE*: grain yield ear^{-1}; *HI*: harvest index.

(a) The variables plot represents the correlation of traits with the PCA axes. (b) The individuals plot exhibits the position of genotypes in the PCA. (c) Hierarchical clustering of genotypes based on their distribution on the PCA. (d) Cluster plot of genotypes distributed in the PCA. PCA and hierarchical clustering were performed using individuals as the mean of the four replicates (n = 4) for each genotype

them were under |0.45| (Table S4.4). Weak positive correlations were found among growth durations and GYE, GNE, HI and plant height.

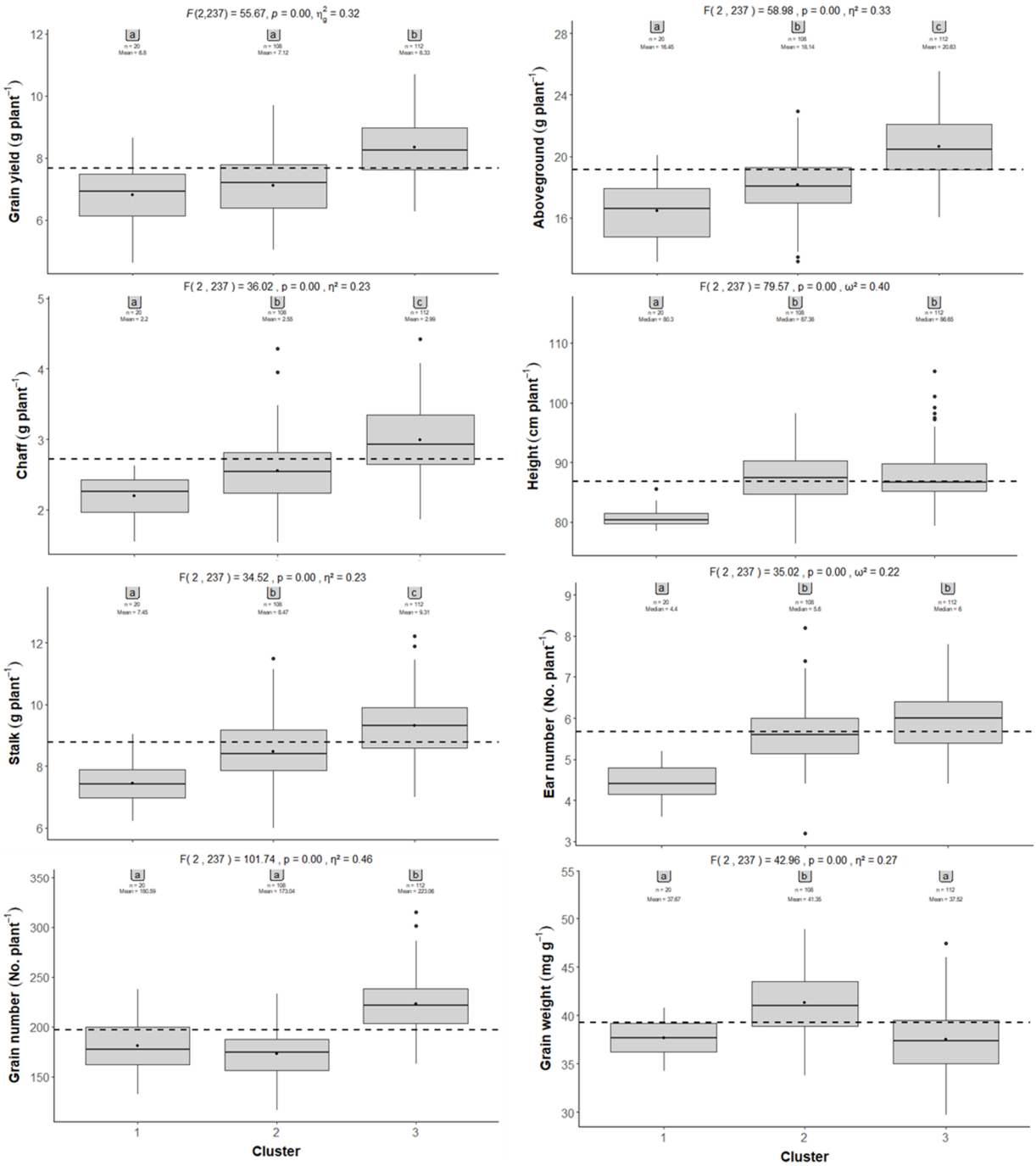

Figure 4.4. Wheat production and grain yield components in the response of the three defined clusters from the 60 wheat genotypes grown under elevated CO_2 and high temperature at maturity.

Black dots represent the mean of the replicates per cluster (Cluster 1, n = 20; Cluster 2, n = 108; Cluster 3, n = 112). The black dotted line represents the mean for all the genotypes and replicates (N = 240). Statistics (F and X^2), degrees of freedom, p-value (p) and size of the effect (η^2 and ω^2) for one-way ANOVA were added. Among columns, numbers followed by the same letter are not significantly different at $p < 0.05$ for post-hoc tests.

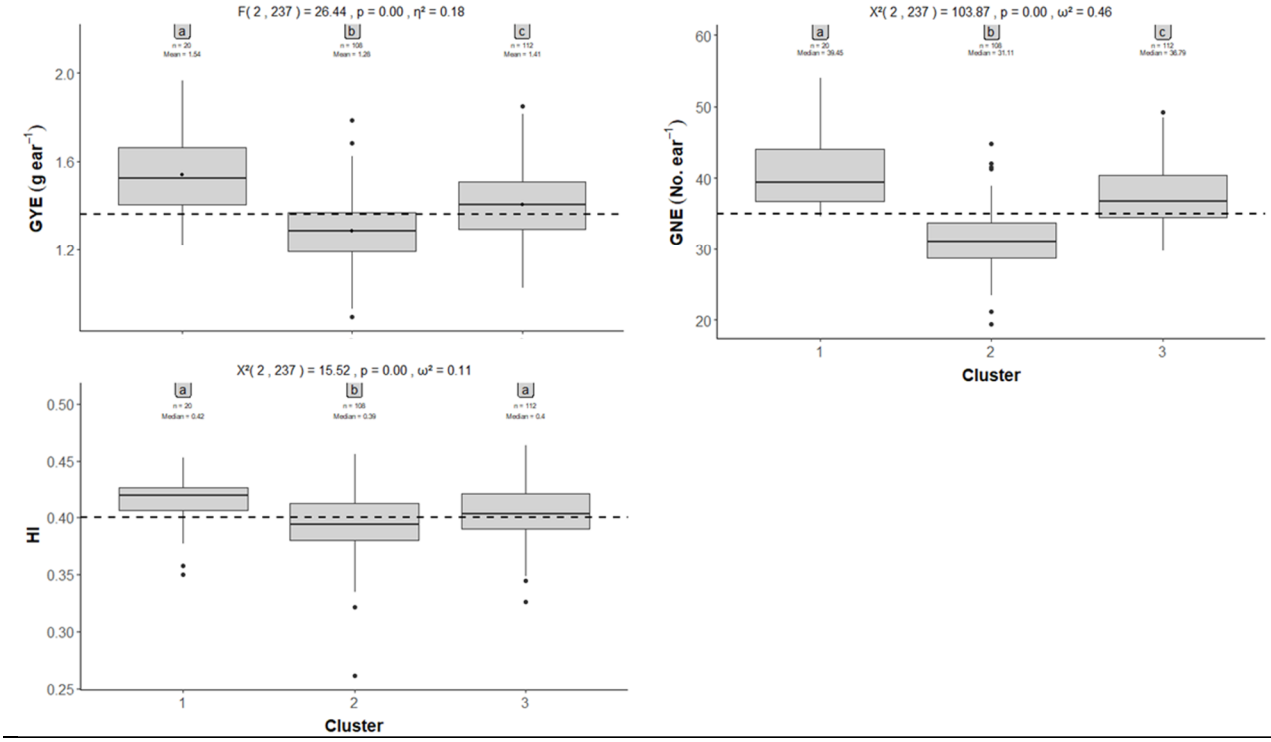

Figure 4.4. Wheat production and grain yield components in the response of the three defined clusters from the 60 wheat genotypes grown under elevated CO_2 and high temperature at maturity (continuation).

GNE: grain number ear^{-1}; *GYE*: grain yield ear^{-1}; *HI*: harvest index.

Black dots represent the mean of the replicates per cluster (Cluster 1, n = 20; Cluster 2, n = 108; Cluster 3, n = 112). The black dotted line represents the mean for all the genotypes and replicates (N = 240). Statistics (F and X^2), degrees of freedom, p-value (p) and size of the effect (η^2 and ω^2) for one-way ANOVA were added. Among columns, numbers followed by the same letter are not significantly different at $p < 0.05$ for post-hoc tests.

4.2. Discussion

4.2.1. Genotypic diversity in wheat grain yield and related traits

Climate change will inevitably affect crop development and productivity, increasing uncertainty regarding food production. In recent years, more attention has been paid to the risks of concomitant increases in atmospheric CO_2 concentrations and temperature for plant performance, and both factors should be assessed together to build up a realistic picture of how global warming will impact the productivity of food crops. In this context, the potential to exploit genetic variation becomes an essential strategy for the selection of crops with better adaptation to future climate conditions. So far, the effects of elevated CO_2 when combined with increasing temperatures on wheat yield have rarely been investigated under field conditions or enclosure facilities, and most of those studies have used either a single genotype or a very limited number of cultivars (Sánchez De La Puente *et al.*, 2000; Cai *et al.*, 2016; Fitzgerald *et al.*, 2016; Högy *et al.*, 2019; Sabella *et al.*, 2020; Ainsworth and Long, 2021; Marcos-Barbero *et al.*, 2021a). Here, the genotypic variation in grain yield is investigated across a set of 60 bread wheat genotypes, using controlled environmental chambers as an approach to perform a more accurate simulation of predicted daily and seasonal variations of temperature during the wheat-growing cycle in the region of Salamanca (Spain) by the end of the century. Among the 60 wheat genotypes under study (Table 4.1), there were several genotypes for which the range of values in biomass production and yield-related traits were more than double the average values achieved by the lowest-ranking genotypes, showing evidence for variability in the performance of the 60 genotypes under combined elevated CO_2 and high-temperature conditions. This implies that the selection of genotypes achieving greater productivity in a future climate scenario is feasible, as is in accordance with previous works by the authors regarding bread wheat (Marcos-Barbero *et al.*, 2021a), and of others regarding durum wheat (Sabella *et al.*, 2020). It is worth noting that the CIMMYT genotypes exhibited higher biomass and grain yield when compared to Gazul (Figure 4.1), a result that can be interpreted as the former having better adaptability to the environment. In spite of the higher grain number per ear observed in Gazul, this was insufficient to compensate for the reduction in ear number per plant and grain weight, thus resulting in lower grain yield and biomass. Taken together, these findings suggest that the CIMMYT genotypes performed better than the Gazul genotype under combined elevated CO_2 and high-temperature conditions, and also provide evidence for the success of breeding programs conducted under warmer temperature environments.

Likewise, we observed a strong positive correlation of grain yield with aboveground biomass and grain number (Figure 4.2; Figure S4.1), as well as a highly positive correlation of grain yield with ear

number and stalk and chaff biomasses; all of them, in turn, correlated with each other. These results suggest that increased grain yield was attained by a higher grain number due to a larger number of ears, but not from an increase in grain weight, as is in agreement with previous studies in wheat grown under elevated CO_2 (Högy *et al.*, 2009b; Tausz-Posch *et al.*, 2012; Wang *et al.*, 2013; Erice *et al.*, 2019). Data from the chamber experiments (Wang *et al.*, 2013) also reported increased grain numbers per ear, but not the FACE experiments (Högy *et al.*, 2010). As is consistent with our finding, the grain number per square meter was the most important yield component, accounting for the effects of elevated CO_2 and temperature in wheat and rice (Cai *et al.*, 2016). Altogether, these findings suggest that tillering capacity, and hence the increased number of fertile tillers, is an important factor in yield response to elevated CO_2 (Ziska, 2008; Tausz-Posch *et al.*, 2015), especially under higher temperatures and dryland conditions (Fitzgerald *et al.*, 2016; Sabella *et al.*, 2020). In a study comprising 20 wheat genotypes grown in glasshouses and controlled environment chambers, it was also found that CO_2 enrichment stimulated tillering, regardless of the cultivars (Bourgault *et al.*, 2013). For nine durum wheat varieties grown hydroponically, Sabella et al. (2020) observed a higher yield for the old cultivar, Cappelli, when compared to modern cultivars under elevated CO_2 and high temperatures, and this was associated with a larger number of ears per plant rather than to changes within the ears. These data resemble previous studies showing a greater response to elevated CO_2 by older wheat varieties than the more recently released ones, because of the higher plasticity of the former in tiller production (Ziska, 2008; Tausz *et al.*, 2013). Evaluating plant developmental responses to CO_2 enrichment has underlined the importance of sink strength at the whole plant level, both as a mechanism to increase plant growth and to avoid photosynthetic acclimation (Ainsworth *et al.*, 2004). Enhanced leaf carbohydrate content caused by higher photosynthesis rates under CO_2 enrichment might be efficiently used for the development of further sinks, such as new tillers, to distribute the photoassimilates (Makino and Tadahiko, 1999). Consequently, this ability to develop new tillers when an extra carbon source is made available is in accordance with the previous suggestion that ensuring adequate sink strength is essential for maximizing the response to elevated CO_2.

Furthermore, we observed that grain weight was negatively correlated with grain number per plant and per ear (Figure 4.2; Figure S4.1), indicative of the change in size distribution toward smaller grains, as previously shown in wheat plants grown under elevated CO_2 (Högy *et al.*, 2009b). This finding is in contrast to the slight shifts toward a larger grain size, as reported by Högy et al. (2013), and the increase in grain size found in three wheat cultivars by Panozzo et al. (2014), although most previous results from FACE experiments showed slight changes in grain weight or that it simply remained unchanged (Högy *et al.*, 2010; Tausz-Posch *et al.*, 2012). Such contradictory results in

wheat grain weight could be associated with the co-influence of other factors related to differences in growing conditions (Högy and Fangmeier, 2008; Högy *et al.*, 2009b), such as water availability (Fernando *et al.*, 2014; Erice *et al.*, 2019). Increased temperature adversely impacts grain development, owing to several limitations in assimilate supply, the length of the grain-filling period, and the starch biosynthesis and deposition rates, together leading to smaller grains (Farooq *et al.*, 2011; Nuttall *et al.*, 2017). Wheat is most sensitive to abrupt heat stress around flowering, and becomes more tolerant to higher temperatures during the grain-filling stage (Tashiro and Wardlaw, 1990). In line with this observation, Wollenweber *et al.* (2003) found distinct effects on grain weight according to the timing of heat application. Weichert et al. (2017) reported the adverse impact of a post-anthesis heatwave on wheat grain yield, being responsible for reduced grain size in the last term. In addition, it is worthy of highlighting that central spikelets and proximal florets flower earlier and receive priority in the deposition of assimilates, and thus tend to have a larger grain size when compared to distal spikelets and florets (González *et al.*, 2005; Nuttall *et al.*, 2017). Higher temperatures may induce upper and lower spikelets and distal florets to abort or develop constitutively smaller grains; this may, therefore, bring together a greater heterogeneity in the crop grain size and a shift in the distribution toward smaller grain size (Nuttall *et al.*, 2017). Even genetic differences among cultivars may contribute to the inconsistent results on wheat grain under elevated CO_2 (Tausz-Posch *et al.*, 2015). Among wheat genotypes, a negative relationship between grains per square meter and grain weight has frequently been observed (Foulkes *et al.*, 2011). In fact, with the advent of the semidwarf cultivars, there was a trend toward a decrease in grain weight, accompanied by more grains in the distal positions in spikelets having a lower potential grain weight (Waddington *et al.*, 1986). These observations may explain the negative relationship between grain weight and yield components, including the grain number per plant and per ear, as observed in our study, which is not related to competition among grains for assimilates but to the increasing contribution of grains of low potential weight that are, thereby, smaller (Miralles and Slafer, 1995; Acreche and Slafer, 2006).

4.2.2. Wheat population clustering and high-yielding strategies

From the hierarchical clustering analysis (Figure 4.3c), we inferred that the wheat genotypes were grouped into three clusters with similar variation sources in each of them (Figure 4.3d), although differences in biomass and yield-related traits among clusters were identified in line with the PCA analysis (Figure 4.3, a and b). These findings suggest that there were contrasting yield strategies among the wheat genotypes under the studied environmental conditions. Despite the larger number of grains per ear exhibited by genotypes of cluster 1, and the improved grain weight of those of cluster 2, the highest yielding genotypes were found within cluster 3, in association with the highest aboveground, stalk and chaff biomasses, grain number, and ears per plant (Figure 4.4). This suggests that genotypes that can preferentially increase these yield-related traits will lead to better yield response under combined elevated CO_2 and high temperature. In line with this observation, most of the previous studies worldwide have shown that grain yield progress in wheat was mostly correlated with grain number per square meter rather than grain weight (Sayre *et al.*, 1997; Shearman *et al.*, 2005; Xiao *et al.*, 2012). Similarly, in Spain, the bread wheat genetic improvement on yield from 1930 to 2000 was also achieved by an increase in grain number, while grain weight was unchanged (Sanchez-Garcia *et al.*, 2013). In fact, the introduction of semidwarf cultivars throughout the 1960s increased grains per square meter by increasing assimilate allocation to the ear during the pre-flowering period, allowing more floret primordia to become fertile florets (Miralles *et al.*, 1998). Therefore, past genetic gains in bread wheat yield have been widely linked to an increase in harvest index and a decline in plant height (Canevara *et al.*, 1994). Overall, improved semidwarf high-yielding bread wheat varieties from Mexico and European countries, mostly France and Italy, have played a major role in yield improvements in Spain (Royo and Briceño-Felix, 2011), where the scarcity of rain is frequent in spring when temperatures rise rapidly. Thus, the incorporation of drought tolerance has always been one of the main goals of Spanish wheat-breeding programs, because drought and high temperature are the prevalent stresses during the reproductive stages constraining wheat production in Spain (Araus *et al.*, 2008). During the 1990s, the private seed sector successfully introduced and marketed 74 bread wheat varieties, including Gazul, which is currently cultivated in Spain (Royo and Briceño-Felix, 2011). Tillering is regulated genotypically, but it is also influenced by the environment (Dreccer *et al.*, 2013). In this context, tillering reduction has been proposed as a suitable feature under terminal drought stress because it decreases soil water use before anthesis (Duggan *et al.*, 2005). Improved tiller economy could enhance the partitioning of assimilates to the ear, leading to increased grain yield per ear, mainly resulting from higher grain number per ear, but decreased grain per square meter (Duggan *et al.*, 2005; Reynolds *et al.*, 2009). In accordance with these findings, cluster 1 grouped the lowest-yielding genotypes, driven by a decreased number of

productive tillers with improved ear fertility but decreased grain yield. The fact that genotype 150 (Gazul) was closely related to four CIMMYT genotypes highlights the important contribution of CIMMYT germplasm in the release of Spanish varieties during the last century (Royo and Briceño-Felix, 2011; Sanchez-Garcia *et al.*, 2013), as reported by the seed company (Limagrain Iberica SA) involved in the marketing of improved bread varieties. It is interesting, however, that the genotypes grouped into cluster 2 seem to sustain grain yield production by higher grain weight, to compensate for reduced grain numbers per ear. Therefore, these intermediate yielding genotypes, when compared with the lowest and highest yielding genotypes, had different attributes with heavier grains rather than higher grain numbers per square meter. In agreement with these results, it has been found that the grain yield progress of CIMMYT advanced lines from 1977 to 2008 was driven by higher grain weight, rather than more grains per square meter (Lopes *et al.*, 2012). Other earlier studies have also reported that grain weight has contributed to yield progress (Morgounov *et al.*, 2010; Zheng *et al.*, 2011).

Breeding programs have focused on developing germplasm adapted to different crop-producing geographic regions and, in Mediterranean areas, the earliness of heading has been recognized as an adaptive trait of modern cultivars aiming to escape drought/heat terminal stress (Reynolds *et al.*, 2009; del Pozo *et al.*, 2014). Indeed, Lopes et al. (2012) reported that, in warmer environments, the reduction in days until heading displayed in high-yielding spring wheat advanced lines allowed an escape from drought/heat episodes at the most sensitive stage of grain setting. In our study, there were differences among genotypes in the number of days from sowing to ear emergence, which could partly explain the better performance under the studied conditions of the early-heading genotypes when compared to the late-heading ones (Table S4.3). Nevertheless, genotype 150 (Gazul) performed poorly under combined elevated CO_2 and high temperature, although it was one of the earliest-heading genotypes. Hence, other features should be considered, because phenology does not appear to be the only cause of variability in grain yield (Table S4.4). It must be highlighted that one of the highest yielding genotypes in our study (genotype 5) has also exhibited good and stable performance under warm temperatures in previous studies (Mondal *et al.*, 2020).

CHAPTER 5

Second study:

Genotypic variability on grain yield and grain nutritional quality characteristics of wheat grown under elevated CO_2 and high temperature

5.1. Results of the second study

5.1.1. Wheat production and grain yield

In the present study, the highest aboveground biomass and grain yield were found for genotypes 41, 43, and 61, followed by genotype 95, with mean values for the productivity of 10.27, 10.83, 9.98, and 9.48 g per plant (Table 5.1), respectively. Furthermore, genotypes 41, 43, and 61 also exhibited the greatest grain number, ear number, HI, chaff biomass and, together with genotype 94, the highest GNE. In addition to genotype 150, genotype 8 had the lowest aboveground biomass, grain yield and HI, as well as the lowest stalk weight along with genotype 23 and the smallest grain number per ear and per plant together with genotypes 74 and 76. The lowest ear number was found for genotypes 23, 94, 95, and 150. Genotype 95, in addition to genotypes 23, 74, and 76, also had the greatest grain weight, and, together with genotype 43, the highest GYE. Genotypes 41, 61, 94, and 150 exhibited the lowest grain weight, whereas genotypes 8, 41, and 76 had the shortest GYE.

5.1.2. Wheat grain nutritional quality

Variation for most of the nutritional quality traits analysed was found across the studied genotypes. Thus, the grain starch concentration did not change among genotypes (Table 5.2). The TP concentration was higher in the grain of genotypes 8, 23, and 150, and lower for genotypes 43 and 95. In turn, the maximum TAC and TPhC concentration in the grain were found for genotypes 23, 41, 43, and 95, with the minimum TAC for genotypes 8 and 150 and the TPhC concentration for genotypes 74 and 150. A similar pattern of changes was found for the B, Cu, Fe, Mg, and Zn concentrations (Table 5.3), although some of these changes were not statistically significant. Genotypes 8 and 23 exhibited the greatest values (as well as genotype 150 for the B and Zn concentrations) and genotypes 43 and 76 (together with genotypes 61 and 150 for Fe and Mg) the lowest. In contrast, genotype 41 exhibited the highest concentrations of Ca, K, P, and S, alone or together with genotypes 95 (for Ca and S) or 61 (K), while the lowest concentrations were found in the grain of genotype 150, along with genotype 8 for the Ca concentration and genotypes 8 and 23 for the K concentration. Table S5.1 summarises the results of the statistical analyses for the wheat production, grain yield and nutritional quality traits by ANOVA.

Table 5.1. Wheat production (aboveground, stalk and chaff biomasses) and grain yield components (grain yield, grain number, ear number, grain weight, grain yield per ear, grain number per ear and harvest index) in the response of ten wheat genotypes grown under elevated CO_2 and high temperature at maturity.

Genotype	Aboveground (g plant^{-1})			Stalk (g plant^{-1})			Chaff (g plant^{-1})			Grain yield (g plant^{-1})			Grain number (No. plant^{-1})		
	Mean	SD		Mean	SD		Mean	SD		Mean	SD		Mean	SD	
8	19.78	±1.77	**b**	8.39	±0.52	**ab**	3.26	±0.33	**ab**	8.13	±1.27	**ac**	207.89	±35.01	**a**
23	20.61	±2.52	**ab**	8.18	±0.70	**ab**	3.14	±0.68	**ab**	9.30	±1.25	**abc**	229.82	±34.95	**a**
41	23.12	±1.24	**ab**	8.93	±0.56	**ab**	3.92	±0.35	**ab**	10.27	±0.95	**ab**	308.75	±63.99	**a**
43	24.41	±2.75	**ab**	9.40	±1.59	**ab**	4.18	±0.39	**a**	10.83	±1.08	**b**	281.74	±22.12	**a**
61	24.90	±2.08	**a**	10.44	±1.16	**a**	4.47	±0.65	**ab**	9.98	±0.73	**abc**	287.37	±41.80	**a**
74	20.78	±2.97	**ab**	9.30	±1.81	**ab**	2.77	±0.48	**b**	8.71	±1.54	**abc**	202.84	±39.23	**a**
76	21.42	±2.85	**ab**	9.64	±1.19	**ab**	3.51	±0.69	**ab**	8.27	±1.26	**ac**	205.46	±37.47	**a**
94	20.53	±2.11	**ab**	8.45	±1.49	**ab**	3.53	±0.38	**ab**	8.56	±0.59	**ac**	240.53	±29.85	**a**
95	22.25	±2.25	**ab**	9.18	±1.05	**ab**	3.60	±0.39	**ab**	9.48	±1.02	**abc**	230.08	±23.11	**a**
150	19.46	±2.52	**b**	7.71	±1.32	**b**	3.79	±0.80	**ab**	7.96	±0.59	**c**	220.05	±22.42	**a**
Average	21.73	± 2.80		8.96	± 1.34		3.62	± 0.68		9.15	± 1.35		241.45	± 49.30	
***p*-value**	**5.22x10^{-2}**			**4.41x10^{-2}**			**8.00x10^{-2}**			**7.06x10^{-4}**			**7.00x10^{-2}**		

Genotype	Ear number (No. plant^{-1})			Grain weight (mg grain^{-1})			GYE (g ear^{-1})			GNE (No. ear^{-1})			HI		
	Mean	SD		Mean	SD		Mean	SD		Mean	SD		Mean	SD	
8	6.15	±0.65	**a**	39.33	±3.79	**ab**	1.32	±0.11	**b**	33.63	±2.4	**c**	0.41	±0.03	**ab**
23	5.90	±1.07	**a**	40.58	±1.58	**ab**	1.59	±0.12	**abc**	39.14	±1.47	**abc**	0.45	±0.01	**a**
41	7.60	±1.27	**a**	34.03	±4.73	**ab**	1.37	±0.13	**ab**	40.43	±2.86	**ab**	0.44	±0.02	**ab**
43	6.35	±0.42	**a**	38.58	±4.35	**ab**	1.71	±0.16	**c**	44.59	±5.31	**a**	0.44	±0.03	**ab**
61	7.05	±0.74	**a**	35.16	±4.11	**ab**	1.42	±0.10	**abc**	40.70	±3.38	**a**	0.40	±0.03	**ab**
74	6.00	±0.85	**a**	43.09	±1.63	**a**	1.45	±0.14	**abc**	33.78	±3.83	**bc**	0.42	±0.05	**ab**
76	6.20	±1.46	**a**	40.49	±2.70	**ab**	1.37	±0.21	**ab**	33.65	±3.44	**c**	0.39	±0.02	**b**
94	5.90	±0.76	**a**	35.88	±3.53	**ab**	1.47	±0.18	**abc**	40.92	±3.70	**a**	0.42	±0.04	**ab**
95	5.85	±0.52	**a**	41.21	±1.96	**ab**	1.62	±0.05	**ac**	39.30	±0.87	**abc**	0.43	±0.01	**ab**
150	5.65	±0.72	**a**	36.30	±2.38	**b**	1.42	±0.15	**abc**	39.07	±1.84	**abc**	0.41	±0.03	**ab**
Average	6.27	± 1.00		38.46	± 4.11		1.47	± 0.18		38.52	± 4.55		0.42	± 0.03	
***p*-value**	1.76x10^{-1}			**4.00x10^{-2}**			**1.14x10^{-2}**			**7.37x10^{-6}**			**8.64x10^{-4}**		

GNE: grain number ear^{-1}; *GYE*: grain yield ear^{-1}; HI: harvest index.

Values represent measures of central tendency (*Mean*: mean) and dispersion (*SD*: standard deviation) of five replicates (n=5) for each genotype or all genotypes and replicates (*Average*; N=50). The calculation of statistical significances (*p-value*) for each trait is based on one-way ANOVA applying corrections for ANOVA assumptions. Values in bold represent significance ($p < 0.05$). Within columns, numbers followed by the same letter indicate non-statistically significant differences at $p < 0.05$ as determined by post-hoc tests.

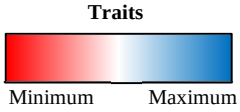

Table 5.2. Grain non-mineral nutrients (starch and total protein concentrations, total antioxidant capacity and total phenolic compound concentration) in the response of ten wheat genotypes grown under elevated CO_2 and high temperature at maturity.

Genotype	Starch (µmol (g grain)$^{-1}$)			TP (mg (g grain)$^{-1}$)			TAC (µmol eq Trolox (g grain)$^{-1}$)			TPhC (µmol eq Galic Ac. (g grain)$^{-1}$)		
	Mean	SD		Mean	SD		Mean	SD		Mean	SD	
8	3589.29	± 213.82	**a**	94.93	± 13.43	**ab**	1.19	± 0.21	**ab**	6.23	± 0.61	**ab**
23	3272.55	± 197.88	**a**	86.23	± 2.66	**a**	1.35	± 0.12	**a**	6.51	± 0.41	**a**
41	3356.48	± 123.52	**a**	80.09	± 11.35	**ab**	1.40	± 0.20	**a**	6.25	± 0.62	**a**
43	3661.72	± 330.58	**a**	77.72	± 8.43	**ab**	1.35	± 0.15	**a**	6.26	± 0.25	**a**
61	3515.85	± 170.01	**a**	83.11	± 12.12	**ab**	1.25	± 0.18	**ab**	6.03	± 0.49	**ab**
74	3507.61	± 89.15	**a**	83.00	± 6.00	**ab**	1.26	± 0.17	**ab**	5.27	± 0.33	**b**
76	3310.92	± 108.57	**a**	81.47	± 7.35	**ab**	1.30	± 0.11	**a**	6.03	± 0.55	**ab**
94	3448.82	± 263.92	**a**	85.86	± 17.54	**ab**	1.39	± 0.18	**a**	6.10	± 0.40	**ab**
95	3690.14	± 330.48	**a**	74.79	± 3.79	**b**	1.43	± 0.09	**a**	6.29	± 0.53	**a**
150	3446.49	± 233.64	**a**	90.63	± 7.29	**ab**	0.97	± 0.10	**b**	5.82	± 0.15	**ab**
Average	3479.99	± 241.88		83.78	± 10.68		1.29	± 0.19		6.08	± 0.53	
***p*-value**	$6.02x10^{-2}$			**$1.30x10^{-2}$**			**$1.49x10^{-2}$**			**$1.33x10^{-2}$**		

TAC: total antioxidant capacity; TP: total protein; TPhC: total phenolic compounds.

Values represent measures of central tendency (Mean: mean) and dispersion (SD: standard deviation) of five replicates (n=5) for each genotype or all genotypes and replicates (Average; N=50). The calculation of statistical significances (p-value) for each trait is based on one-way ANOVA applying corrections for ANOVA assumptions. Values in bold represent significance ($p < 0.05$). Within columns, numbers followed by the same letter indicate non-statistically significant differences at $p < 0.05$ as determined by post-hoc tests.

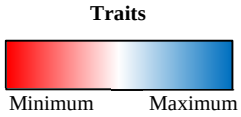

Table 5.3. Grain mineral nutrient (B, Ca, Cu, Fe, K, Mg, Na, P, S and Zn) concentrations in the response of ten wheat genotypes grown under elevated CO_2 and high temperature at maturity.

Genotype	B (µg (g grain)$^{-1}$)			Ca (µg (g grain)$^{-1}$)			Cu (µg (g grain)$^{-1}$)			Fe (µg (g grain)$^{-1}$)			K (µg (g grain)$^{-1}$)		
	Mean	SD		Mean	SD		Mean	SD		Mean	SD		Mean	SD	
8	2.14	±0.53	**a**	280.37	±23.24	**c**	6.92	±0.42	**a**	22.76	±2.95	**a**	3436.69	±203.07	**a**
23	1.67	±0.42	**a**	317.57	±33.71	**abc**	6.43	±0.83	**abc**	21.77	±2.12	**a**	3410.14	±98.87	**a**
41	1.56	±0.62	**a**	388.19	±32.76	**d**	6.56	±0.55	**ab**	21.21	±1.69	**a**	4097.08	±152.49	**b**
43	1.19	±0.33	**a**	330.20	±8.44	**abcd**	5.66	±0.38	**bc**	17.98	±2.28	**a**	3644.07	±240.32	**ac**
61	1.98	±0.34	**a**	347.96	±18.93	**abd**	6.36	±0.90	**abc**	19.57	±2.21	**a**	3921.67	±188.12	**bc**
74	1.53	±0.65	**a**	309.98	±37.66	**abc**	6.50	±0.61	**abc**	24.18	±8.14	**a**	3487.24	±190.11	**a**
76	1.27	±0.24	**a**	339.24	±48.76	**abcd**	5.30	±0.47	**c**	19.34	±1.11	**a**	3681.37	±167.47	**ac**
94	1.33	±0.35	**a**	357.77	±31.20	**abd**	6.35	±0.57	**abc**	21.36	±2.17	**a**	3393.57	±148.70	**a**
95	1.33	±0.24	**a**	364.81	±14.56	**bd**	5.90	±0.49	**abc**	19.37	±1.99	**a**	3716.26	±131.68	**ac**
150	1.70	±1.01	**a**	302.97	±17.26	**ac**	6.21	±0.20	**abc**	20.92	±1.97	**a**	3484.80	±163.20	**a**
Average	1.57	±0.56		333.91	±40.58		6.22	±0.69		20.85	±3.43		3627.29	±273.80	
***p*-value**	**$4.90x10^{-2}$**			**$2.11x10^{-5}$**			**$3.47x10^{-2}$**			$1.52x10^{-1}$			**$2.01x10^{-7}$**		

Genotype	Mg (µg (g grain)$^{-1}$)			Na (µg (g grain)$^{-1}$)			P (µg (g grain)$^{-1}$)			S (µg (g grain)$^{-1}$)			Zn (µg (g grain)$^{-1}$)		
	Mean	SD		Mean	SD		Mean	SD		Mean	SD		Mean	SD	
8	1314.49	±48.84	**a**	14.37	±5.99	**a**	5488.15	±212.79	**ab**	33.97	±31.37	**a**	35.47	±3.04	**a**
23	1322.06	±82.92	**a**	12.42	±5.82	**a**	5359.80	±160.00	**ab**	41.83	±15.25	**a**	37.67	±2.28	**a**
41	1276.31	±63.32	**ab**	14.38	±9.53	**a**	5603.18	±143.59	**a**	101.52	±33.43	**b**	35.00	±3.44	**a**
43	1194.65	±69.17	**ab**	3.74	±1.56	**a**	5309.50	±235.44	**ab**	76.01	±26.39	**ab**	31.38	±3.55	**a**
61	1152.71	±17.78	**b**	13.22	±9.19	**a**	5447.82	±97.35	**ab**	77.37	±19.35	**ab**	34.06	±3.73	**a**
74	1303.19	±79.88	**ab**	7.44	±1.09	**a**	5388.58	±353.24	**ab**	74.24	±21.05	**ab**	38.67	±5.72	**a**
76	1176.51	±96.62	**ab**	18.06	±12.50	**a**	5312.23	±141.24	**ab**	76.60	±13.21	**ab**	32.68	±2.70	**a**
94	1295.18	±69.67	**ab**	12.44	±5.27	**a**	5284.17	±256.79	**ab**	66.56	±9.92	**ab**	37.79	±5.32	**a**
95	1232.46	±69.16	**ab**	9.94	±6.24	**a**	5424.47	±195.71	**ab**	90.37	±15.18	**b**	33.51	±2.27	**a**
150	1172.26	±110.51	**ab**	6.38	±1.90	**a**	5045.06	±305.33	**b**	64.56	±15.59	**ab**	37.31	±2.76	**a**
Average	1243.98	±92.35		11.24	±7.48		5366.30	±246.71		70.30	±27.42		35.35	±4.06	
***p*-value**	**$1.39x10^{-2}$**			**$6.00x10^{-2}$**			**$4.24x10^{-2}$**			**$4.29x10^{-4}$**			**$3.82x10^{-2}$**		

Values represent measures of central tendency (Mean: mean) and dispersion (SD: standard deviation) of five replicates (n=5) for each genotype or all genotypes and replicates (Average; N=50). The calculation of statistical significances (p-value) for each trait is based on one-way ANOVA applying corrections for ANOVA assumptions. Values in bold represent significance ($p < 0.05$). Within columns, numbers followed by the same letter indicate non-statistically significant differences at $p < 0.05$ as determined by post-hoc tests.

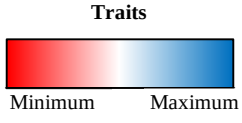

5.1.3. Genotypic characterisation

The CB (Figure 5.1) shows the maximum differences among genotypes and the traits responsible for this discrimination, while the correlations between the traits studied and the canonical axes are described in Table 5.4. The first two dimensions of the CB collected a cumulative variance of 53.18 % (Table S5.2), with the first dimension positively associated with wheat production (aboveground, chaff, and stalk biomasses) and most of the grain yield components (grain yield, grain and ear numbers, GNE, GYE, and HI), as well as with K, Ca, and S concentrations, but negatively correlated with TP, grain weight, and grain Zn, Fe, Mg, Cu, and B concentrations. By contrast, the grain number per ear and per plant, chaff weight and TP, B, and Cu concentrations were the major traits positively correlated with the second dimension of the CB, while TAC, grain weight, and Ca, Mg, S, and Na concentrations were negatively associated. As a result, genotypes 41, 43, 61, and 95 were associated with improved grain yield, aboveground biomass and K concentration. However, in comparison with

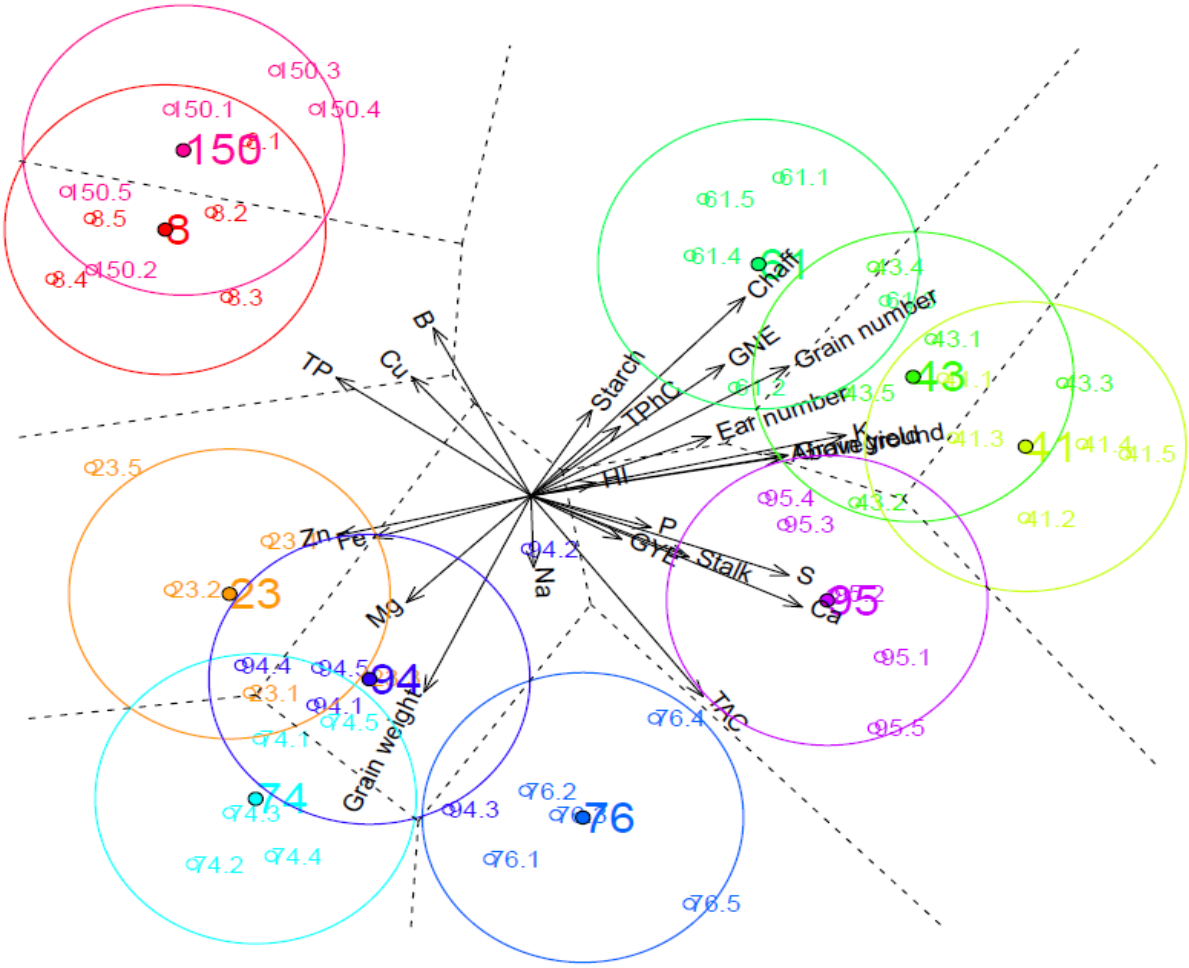

Figure 5.1. CB for the wheat production, grain yield, non-mineral and mineral quality components in the response of ten wheat genotypes grown under elevated CO_2 and high temperature at maturity.

GNE: grain number ear^{-1}; *GYE*: grain yield ear^{-1}; *HI*: harvest index; *TAC*: total antioxidant capacity; *TP*: total protein; *TPhC*: total phenolic compounds.

Individuals are represented by empty dots, labelled based on their genotype and numbered as one of the five replicates (n=5) for each group. Filled points represent projections of the averages of the genotypes on the biplot with confidence circles based on Bonferroni's post-hoc tests. Dotted lines indicate the boundaries of the regions for each group on the Voronoi diagram.

genotype 95, genotypes 41, 43, and 61 were also associated with higher chaff dry weights, ear number and grain number per ear and per plant. In concordance with data reported from ANOVA (Table 5.3), both genotypes 41 and 95 were also associated with improved S and Ca concentrations, whereas genotypes 61 and 95 had the greatest GYE and TAC. Furthermore, genotypes 8, 23, 74, and 150 were related to improved Fe and Zn concentrations in the grain. While genotypes 8 and 150 were characterized by improved grain TP, B, and Cu concentrations and low TAC, genotypes 23 and 74 were associated with higher grain weight and Mg concentration.

Table 5.4. Correlations of wheat production, grain yield, non-mineral and mineral quality components in the response of ten wheat genotypes grown under elevated CO_2 and high temperature at maturity with the first two dimensions of the CB.

Dim.1			Dim.2		
Traits	**Corr.**	**Cos²**	**Traits**	**Corr.**	**Cos²**
K	0.72	0.52	**Chaff**	0.41	0.17
Ca	0.62	0.39	**B**	0.35	0.12
Grain number	0.59	0.35	**GNE**	0.27	0.07
S	0.59	0.35	**Grain number**	0.27	0.07
Grain yield	0.59	0.35	**Cu**	0.25	0.06
Aboveground	0.58	0.34	**TP**	0.25	0.06
Chaff	0.49	0.24	**Starch**	0.18	0.03
GNE	0.44	0.20	**TPhC**	0.14	0.02
Ear number	0.41	0.17	**K**	0.13	0.02
TAC	0.40	0.16	**Ear number**	0.12	0.02
Stalk	0.36	0.13	**Grain yield**	0.08	0.01
P	0.28	0.08	**Aboveground**	0.08	0.01
GYE	0.21	0.04	**HI**	0.03	0.00
TPhC	0.21	0.04	**P**	-0.07	0.00
HI	0.15	0.02	**Zn**	-0.08	0.01
Starch	0.14	0.02	**Fe**	-0.09	0.01
Na	0.01	0.00	**GYE**	-0.09	0.01
B	-0.23	0.05	**Stalk**	-0.13	0.02
Grain weight	-0.25	0.06	**Na**	-0.15	0.02
Cu	-0.28	0.08	**S**	-0.17	0.03
Mg	-0.29	0.08	**Mg**	-0.22	0.05
Fe	-0.36	0.13	**Ca**	-0.23	0.05
Zn	-0.44	0.20	**Grain weight**	-0.41	0.17
TP	-0.45	0.20	**TAC**	-0.42	0.17

Corr.: correlation; *Dim.*: Dimension; *GNE*: grain number ear^{-1}; *GYE*: grain yield ear^{-1}; *HI*: harvest index; *TAC*: total antioxidant capacity; *TP*: total protein; *TPhC*: Total phenolic compounds.

Corr. indicates the correlation between the variable and the dimension. The squared correlation (*Cos*^{2}) values between the variables and the dimensions are used to estimate the quality of the representation.

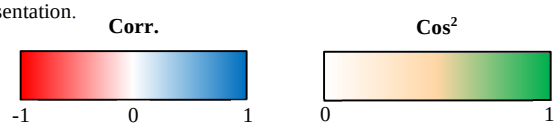

5.1.4. Wheat production, grain yield, and nutritional quality traits

MFA was performed to study the existing relationships among vegetative biomass, grain yield components, and non-mineral and mineral nutrients in grain. The variables studied were split up into four groups: *Wheat production*, *Yield components*, *Non-mineral nutrients*, and *Mineral nutrients*. A factor group *Genotype* was also employed in order to analyse the impact of genotypic variation. Figure 5.2, (a) shows the correlations of the factor group *Genotype* and the four variable groups with the first two dimensions of the MFA. In turn, Table 5.5 shows numerically both, the correlation and the contribution of the groups and the traits to the dimensions.

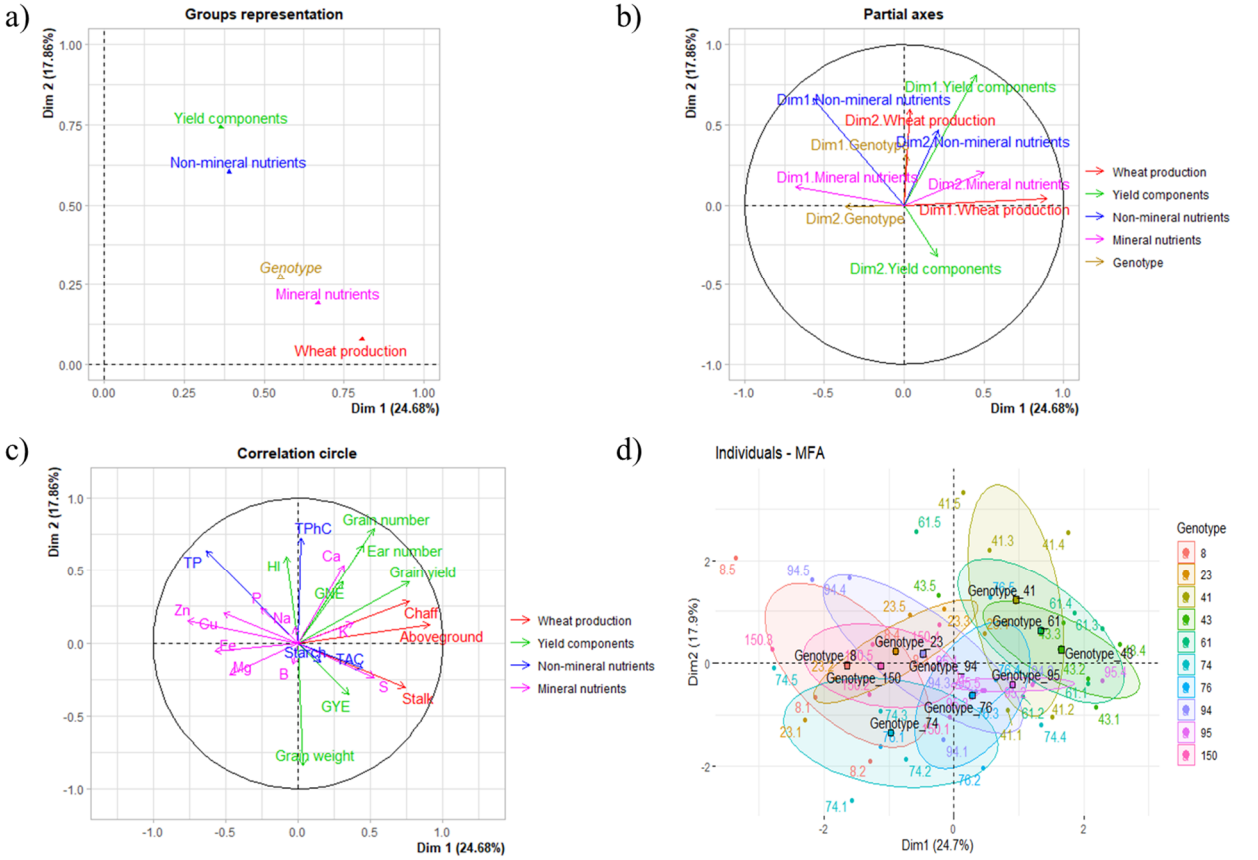

Figure 5.2. Multiple factorial analysis for the wheat production, grain yield, non-mineral and mineral quality components in the response of ten wheat genotypes grown under elevated CO_2 and high temperature at maturity.

Dim.: Dimension; *GNE*: grain number ear^{-1}; *GYE*: grain yield ear^{-1}; *HI*: harvest index; *TAC*: total antioxidant capacity; *TP*: total protein; *TPhC*: Total phenolic compounds.

Genotype is the group based on a categorical variable specifying the genotypic identity of each sample. The vegetative biomass, grain yield and nutritional quality traits were split up into four groups: *Wheat production* (aboveground, stalk and chaff biomasses), *Yield components* (grain yield, grain number, ear number, grain weight, grain yield ear^{-1}, grain number ear^{-1} and harvest index), *Non-mineral nutrients* (starch, total protein, total phenolic compound concentrations and total antioxidant capacity) and *Mineral nutrients* (B, Ca, Cu, Fe, K, Mg, Na, P, S and Zn mineral concentrations).

(a) The *group representation plot* illustrates the correlation between the variable groups and the supplementary group with axes; (b) The *partial axes plot* shows the relationship between the main axes of the MFA and the first two dimensions of each group. (c) The *correlation circle plot* represents the correlation of traits with the MFA axes. (d) The *individual plot* exhibits the position of individuals in the MFA by genotype variation. *Triangles* indicate the relative position of each group with the axes. *Dots* represent individuals. *Squares* represent group mean points for categorical variables. Ellipses around each genotype (d) were added.

The first two dimensions of the MFA collected a cumulative variance of 42.54 %, with the variable group *Wheat production* as the main contributing group and the more correlated with the first dimension of the MFA (36.17, 0.81; Table 5.5), followed by the *Mineral nutrients* (29.99, 0.67), *Non-mineral nutrients* (17.49, 0.39) and *Yield components* (16.35, 0.37) groups. In contrast, the *Yield*

Table 6.5. Correlations and contributions between the variable groups, the supplementary group and the continuous variables with the first two dimensions of the MFA.

Dim. 1				Dim. 2			
Variable groups	**Corr.**	**Cos²**	**Contr.**	**Variable groups**	**Corr.**	**Cos²**	**Contr.**
Wheat production	0.81	0.63	36.17	Yield components	0.74	0.40	46.01
Mineral nutrients	0.67	0.22	29.99	Non-mineral nutrients	0.60	0.20	37.41
Non-mineral nutrients	0.39	0.08	17.49	Mineral nutrients	0.19	0.02	11.80
Yield components	0.37	0.10	16.35	Wheat production	0.08	0.01	4.79
Supplementary group				**Supplementary group**			
Genotype	0.55	0.03		Genotype	0.27	0.01	
Continuous variables				**Continuous variables**			
Aboveground	0.91	0.83	15.26	Grain number	0.79	0.62	10.91
Chaff	0.77	0.59	10.83	TPhC	0.72	0.52	20.05
Grain yield	0.77	0.59	7.43	Ear number	0.68	0.46	8.01
Stalk	0.74	0.55	10.07	TP	0.64	0.41	15.55
Grain number	0.53	0.28	3.49	HI	0.60	0.36	6.26
S	0.53	0.28	4.15	Ca	0.54	0.29	5.97
Ear number	0.45	0.20	2.59	GNE	0.42	0.18	3.15
TAC	0.45	0.20	5.57	Grain yield	0.42	0.18	3.11
K	0.38	0.15	2.20	Chaff	0.28	0.08	2.04
GYE	0.35	0.12	1.54	P	0.24	0.06	1.19
Ca	0.32	0.10	1.53	Cu	0.21	0.04	0.89
GNE	0.31	0.10	1.21	Zn	0.15	0.02	0.49
Starch	0.16	0.02	0.67	K	0.14	0.02	0.40
Grain weight	0.04	0.00	0.02	Aboveground	0.13	0.02	0.42
TPhC	0.02	0.00	0.01	Na	0.11	0.01	0.25
Na	-0.02	0.00	0.01	Fe	-0.05	0.00	0.06
B	-0.03	0.00	0.01	Starch	-0.13	0.02	0.65
HI	-0.08	0.01	0.08	B	-0.15	0.02	0.45
P	-0.26	0.07	1.00	TAC	-0.17	0.03	1.17
Mg	-0.48	0.23	3.41	Mg	-0.22	0.05	0.97
Cu	-0.52	0.27	4.01	S	-0.24	0.06	1.16
Fe	-0.57	0.33	4.92	Stalk	-0.30	0.09	2.33
TP	-0.64	0.41	11.25	GYE	-0.35	0.13	2.20
Zn	-0.76	0.58	8.75	Grain weight	-0.84	0.71	12.37

Dim.: dimension; *Contr.*: contribution; *Corr.*: correlation; *GNE*: grain number ear^{-1}; *GYE*: grain yield ear^{-1}; *HI*: harvest index; *TAC*: total antioxidant capacity; *TP*: total protein; *TPhC*: Total phenolic compounds.

Genotype is the group based on a categorical variable specifying the genotypic identity of each sample. The vegetative biomass, grain yield and nutritional quality traits were split up into four groups: *Wheat production* (aboveground, stalk and chaff biomasses), Y*ield components* (grain yield, grain number, ear number, grain weight, grain yield ear^{-1}, grain number ear^{-1} and harvest index), *Non-mineral nutrients* (starch, total protein, total phenolic compound concentrations and total antioxidant capacity) and *Mineral nutrients* (B, Ca, Cu, Fe, K, Mg, Na, P, S and Zn mineral concentrations).

Corr. indicates the correlation between the variable and the dimension. The values for the squared correlation (*Cos²*) between the variables and the dimensions are used to estimate the quality of the representation. *Contr.* expresses the contributions, in percentage, of each variable in accounting for the variability in the dimension.

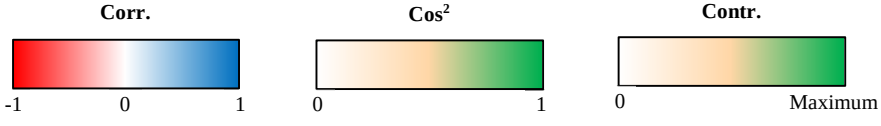

components group contributed better to the second dimension (46.01, 0.74; Table 5.5) than the *Non-mineral nutrients* (37.41, 0.60), *Mineral nutrients* (11.80, 0.19), and *Wheat production* (4.79, 0.08). Furthermore, the traits that better contributed to the first dimension were the aboveground biomass, the TP, and the chaff and stalk weights (15.26, 11.25, 10.83, and 10.07; Table 5.5), while TPhC, TP, grain weight and grain number were the most contributing variables for the second dimension of the MFA (20.05, 15.55, 12.37, and 10.91, respectively). The plots for the partial axes (Figure 5.2, b) and the correlation circle (Figure 5.2, c) showed an opposite distribution for the first dimensions of groups *Mineral nutrients* and *Wheat production*, together with the second dimension of the *Mineral nutrients*. Similarly, the first dimension of the *Non-mineral nutrients* and the *Yield components* showed an opposite association with the first axis of the MFA but a similar correlation with the second dimension of the plot. Thus, TP and B, Cu, Fe, Mg, Na, P, and Zn mineral concentrations in the grain were associated with genotypes 8, 23, 74, and 150 in the individuals MFA plot (Figure 5.2d), whereas the aboveground, chaff, and stalk biomasses, grain yield, grain and ear number, GNE, and Ca, K, and S concentrations in the grain were mostly associated with genotypes 41, 43, 61, and 95. Moreover, the aboveground, stalk and chaff biomasses were the most positively correlated with the first dimension of the MFA (0.91, 0.77, and 0.74, respectively; Table 5.5) together with grain yield (0.77). The grain number (0.53), ear number (0.45), GYE (0.35), and GNE (0.31) were also positively correlated with the first axis of the plot, together with S (0.53), K (0.38), Ca (0.32), and TAC (0.45). In contrast, the TP, Zn, Fe, Cu, Mg, and P concentrations were negatively correlated with the first dimension of the MFA in a range from -0.76 to -0.26. These negative correlations of plant production and grain yield components to TP and mineral concentrations, as well as of grain weight and grain dry weight per ear to grain and ear numbers for the second dimension, were later confirmed by the CN and the correlogram shown in Figure 5.3 and Figure S5.1.

The correlation network showed positive correlations among aboveground biomass, stalk and chaff weights, grain yield, and grain and ear numbers (Figure 5.3). It must be highlighted the strong correlations of aboveground biomass with grain yield (0.86; Figure S5.1) and stalk weight (0.81), as well as between grain yield and grain number (0.84) and between grain number and ear number (0.75). It is also worth mentioning the negative correlations found between grain weight and the remaining grain yield components, with the highest correlation found between grain weight and grain number (-0.56), while the only positive correlation was found with GYE (0.51). Among the non-mineral nutrient traits, only a remarkable negative correlation between TP and TAC (-0.55), but a positive correlation with TPhC (0.30), must be highlighted. Overall, the B, Cu, Fe, K, Mg, Na, P, and Zn mineral concentrations in grain were positively correlated among them, whereas Ca and S concentrations were negatively correlated with them (excepting K). These mineral concentrations

were also negatively correlated with wheat production and grain yield components. Highly negative correlations were found of the aboveground, stalk, and chaff biomasses to the concentrations in grain of Cu, Fe, Mg, and Zn (in a range between -0.28 and -0.60), as well as of Na and P, but with lower correlations (-0.13 to -0.26). Likewise, negative correlations of these mineral concentrations to grain yield components were also observed, with the highest negative correlations specially found between Cu, Fe, Mg, and Zn with grain yield, grain number, ear number, and GYE (-0.14 to -0.49).

Nevertheless, Ca, K, and S concentrations showed positive correlations with plant biomass and most of the grain yield components. Both TAC and TPhC were also positively correlated with wheat production and grain yield components, although no consistent correlations with the mineral

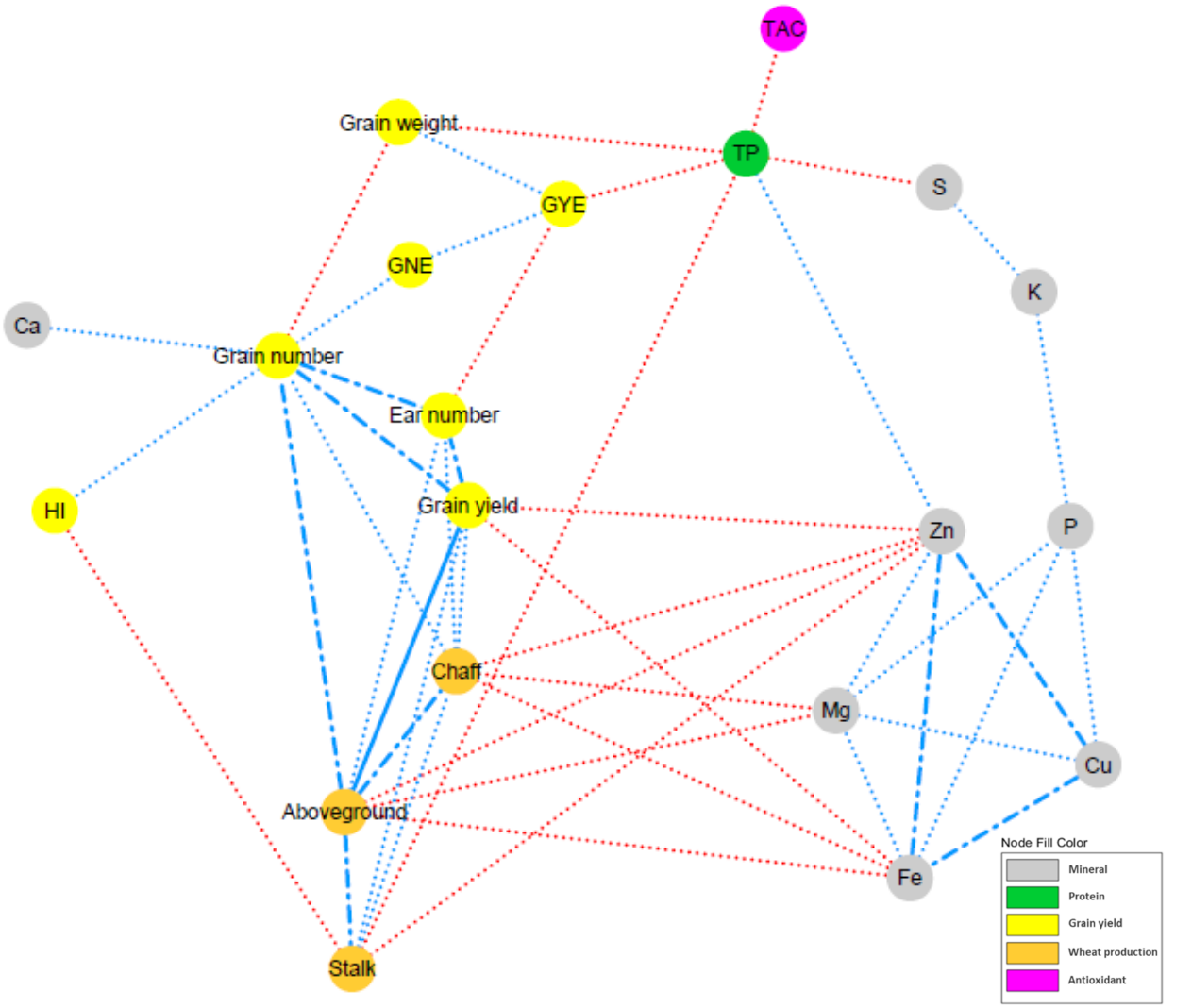

Figure 6.3. CN for the wheat production, grain yield and nutritional quality traits in the response of ten wheat genotypes grown under elevated CO_2 and high temperature.

GNE: grain number ear^{-1}; *GYE*: grain yield ear^{-1}; *HI*: harvest index; *TAC*: total antioxidant capacity; *TP*: total protein; *TPhC*: Total phenolic compounds.

The different traits (nodes) were classified by colours according to their wheat production, grain yield, non-mineral or mineral nutritional quality nature (see legend). Edges stand for a Spearman's correlation $r_s \geq |0.45|$, split up as dot ($|0.65| > r_s \geq |0.45|$), dash and dot ($|0.85| > r_s \geq |0.65|$) or solid ($|1| > r_s \geq |0.85|$) line types. Blue edges indicate positive correlation whereas red edges implicate negative correlation.

concentrations were found. The TP was highly negatively correlated with stalk weight (-0.62), GYE (-0.59), S concentration (-0.56), and grain weight (-0.51), and less correlated with the aboveground biomass (-0.39), K concentration (-0.35), chaff weight (-0.26), and yield (-0.15). However, it was positively correlated with grain and ear numbers (0.14 and 0.26, respectively), HI (0.42) and Cu (0.32), Fe (0.25), and Zn (0.46) concentration. There was not a clear tendency for correlations between grain weight and the nutritional quality traits. Besides the negative correlation described above with the TP, the matrix showed the highest negative correlation between grain weight and TPhC (-0.41) concentrations in grain, while the correlations with the mineral concentrations ranged between -0.33 and 0.32.

5.1.5. Grain nutrient content

Table S5.3 shows the results of ANOVA for the grain nutrient contents expressed as mass of these nutrients per grain (e.g., grain starch content) or per plant (e.g., grain starch yield or grain B uptake). The average values per genotype and the multiple comparison are presented in Tables S5.4 and S5.5. Graphical comparisons between content per grain and per plant is showed in Figures S5.2 and S5.3. Genotype 41 showed the lowest grain starch and TP content and, together with genotypes 61 and 150, TPhC. Genotypes 95 and 74 had a higher starch content than genotype 41, while genotypes 74 and 23 also showed a higher TP content than genotypes 41, 43, and 61. Genotype 23 exhibited higher TPhC content than genotypes 41, 61, and 150. Likewise, genotypes 23 and 95 also showed higher TAC in the grain than genotype 150. Among genotypes, a similar pattern of changes for grain starch, TP, TPhC, and TAC yields was found, genotypes 41, 43, 61, and 95 showing the greatest values and 8, 74, 76, and 150 the lowest. Genotype 43, as compared to 76, showed the largest starch, TPhC and TAC yields and both genotypes 43 and 61 exhibited higher grain starch yield than 150. TPhC yield was higher in genotype 43 than 76 and, along with genotype 41, higher than genotypes 74 and 150. The TAC yield was higher in genotypes 23, 41, 43, 61, and 95 than 150 and it was also higher in genotypes 41 and 43 than genotype 8.

Regarding the grain mineral contents, a different pattern of changes among genotypes was also found. The grain B, K, and S content remained unchanged. The grain Cu, Fe, Mg, P, and Zn contents were higher for genotypes 8, 23, and 74 than 41, 43, and 61, but only higher than 150 for the grain Mg and P contents. In line with this pattern of changes, the grain Na content was higher for genotype 74 than 43, and the Ca content higher for genotypes 76 and 95 than genotypes 8 and 150. By contrast,

greater Ca, Cu, K, Mg, P, S, and Zn uptakes were found for genotypes 41, 43, 61, and 95 than genotypes 8, 74, 76, and 150, exhibiting the same trend observed for the non-mineral nutrient yields. However, the grain B, Fe, and Na uptake did not change among genotypes.

5.2. Discussion

Increases in atmospheric CO_2 and temperature are likely to modify plant growth and nutrient demand, with the consequent impact on crop productivity and quality.

5.2.1. Grain yield and related traits

The few experiments conducted to investigate the interactive effects of elevated CO_2 and high temperature reported that the stimulation of crop performance and yield by CO_2 enrichment was counteracted by increasing temperature (Cai *et al.*, 2016; Högy *et al.*, 2019; Zhang *et al.*, 2019a). Therefore, the exploration of genotypic variability might be a promising approach for the selection of improved crop varieties to ensure food security and the improvement of our knowledge on plant production and adaptation to future climatic conditions. Only a limited range of crop germplasm is possible in the rather small size of free air CO_2 enrichment (FACE) plots (Ainsworth and Long, 2021). In contrast, a set of 64 wheat varieties grown in the field in ambient CO_2 was examined relative to growth traits and photosynthetic capacity (Driever *et al.*, 2014). Following a screening with 60 wheat lines, here we have compared 10 genotypes for biomass, yield, and nutritional quality under elevated CO_2 and high temperature, thus providing for significant genetic variation. We found significant differences in the aboveground biomass and grain yield across the 10 wheat genotypes as well as in other yield related traits, although the grain and ear numbers did not differ statistically among genotypes. These results confirm the importance of the evaluation of the genotypic variability on yield performance under a changing climate. Even though grain yield was poorly correlated with grain weight, we observed that grain yield was positively correlated with aboveground biomass and grain and ear numbers and all of them were correlated with each other. These findings suggest that grain yield production was sustained by increased grain number due to a higher number of productive tillers rather than heavier grains. Our data resemble previous work where the increased grain yield by elevated CO_2 was closely associated with higher grain number per unit ground area due to a higher number of tillers (Fangmeier *et al.*, 1999; Högy *et al.*, 2009b). While grain number per ear was also increased in another study, both grain number per unit ground area and grain number per ear contributed to the increase in grain yield due to the fact that ear number was not affected by elevated CO_2 (Högy *et al.*, 2010). In the present work, the most productive genotypes (41, 43, and 61) exhibited higher grain and ear numbers than the less productive ones (8 and 150), as well as a higher grain number per ear as shown by genotype 43. In this regard, it is important to highlight that increases in

grain yield due to the implementation of the Green Revolution have been driven mostly by grain number per unit area and ear rather than grain weight (Hawkesford *et al.*, 2013). In the case of bread wheat in Spain, genetic improvement of yield from 1930 to 2000 was accounted by an increase in grain number while grain weight remained unchanged (Sanchez-Garcia *et al.*, 2013). Similarly, grain yield progress was correlated with grain number per square meter, but not with other yield components in the spring wheat breeding program at CIMMYT (Sayre *et al.*, 1997). The positive relationship between harvest index and grain number and, to a lesser extent, grain yield is in agreement with most studies of yield progress in cereals (Sayre *et al.*, 1997; Royo *et al.*, 2008), in line with the fact that grain yield is usually related to the grain number per square meter (Slafer, 2003), as the most important yield component.

In spite of the yield stimulation induced by elevated CO_2, higher temperatures accelerate crop phenological development, resulting in a shortened grain filling period and impaired grain yield through a reduction of grain number per ear, ear number and grain weight (Hatfield *et al.*, 2011; Weichert *et al.*, 2017; Zhang *et al.*, 2019b). In spring wheat grown under field conditions, Lizana and Calderini (2013) applied moderately high temperatures at different growth stages and found varying relationships between reduction in grain yield and grain weight depending on the timing of temperature stress. A negative effect of a post-anthesis heatwave on wheat grain yield associated with decreased grain size was also reported by Weichert et al. (2017). In our study, the negative correlation found between grain number and grain weight could indicate that there is competition between growing grains for limited assimilates. Although that is the most common interpretation, Acreche and Slafer (2006) proved that grain weight was concomitantly reduced when grain number increased by increasing the proportion of grains that are constitutively smaller in the canopy independently of any competition among grains. Regardless of the origin of the negative relationship, grain size is more heritable and, therefore, less plastic than grain number (Sadras and Slafer, 2012). In general, genotypes with higher grain yield exhibited a trend towards lower grain weight.

5.2.2. Grain nutritional quality traits

Mineral nutrients play important roles in the biochemical and physiological functions of biological systems. While higher plants obtain their minerals primarily from the soil, animal and humans depend mostly on higher plants to supply them with minerals (Chatzav *et al.*, 2010). Humans require nutrients in adequate amount for proper development and healthy lives. In our study, there were considerable variations in grain protein and mineral nutrient concentrations among wheat genotypes. These results

resemble previous findings in two wheat genotypes grown in the field in temperature gradient chambers (Sánchez De La Puente *et al.*, 2000), and they are in good agreement with the well-documented large variation observed in various kinds of wheat and their related species in previous studies under multiple environmental conditions (Oury *et al.*, 2006; Murphy *et al.*, 2008; Chatzav *et al.*, 2010; Pandey *et al.*, 2016). Variation for both Fe and Zn concentrations did not reach statistical significance, which contrasts with the high variability reported in wild emmer wheat (Gomez-Becerra *et al.*, 2010), although lower levels of variability for these elements have also been found in old and modern French bread wheats (Oury *et al.*, 2006).

The amount of minerals in the grain depends on different processes including uptake by the root system, translocation and redistribution within the plant tissues, remobilisation to the grain, and accumulation in the developing grain (Chatzav *et al.*, 2010). In the present study, several significant relationships have been identified between grain mineral nutrients, which may indicate the existence of one or more common genetic or physiological mechanisms related to the processes previously mentioned. Thus, we found a strong positive correlation between Fe and Zn, as well as an association of Zn and TP concentration of wheat grains consistent with some previous studies performed on bread wheat (Pandey *et al.*, 2016). These relationships presumably might be linked to QTLs controlling grain Fe, Zn, and TP concentrations as found in emmer wheat, double haploid populations, and diploid wheat (Uauy *et al.*, 2006; Morgounov *et al.*, 2007) and in a recombinant inbred line population derived from a cross between durum wheat and wild emmer (Peleg *et al.*, 2009), although QTL information in bread wheat is limited (Shi *et al.*, 2008). Distelfeld et al. (2007) suggested that the *Gpc-B1* locus encoding a transcription factor of the NAC family (*NAM-B1*) induces accelerated senescence and contributes to the remobilisation of protein, Fe and Zn from leaves to grain, and consequently greater grain concentrations. Uauy et al. (2006) discovered that delayed senescence could simultaneously decrease N, Fe, and Zn content in wheat plants, indicating that the remobilisation of Fe and Zn is linked to the remobilisation of N. Likewise, co-localisation of QTLs for Zn and Fe concentrations has been reported in rice (Stangoulis *et al.*, 2007). Not only Fe and Zn showed high correlation with each other, but also Cu was highly correlated with them in the current study, in accordance with the results obtained in the work conducted by Pandey et al. (2016) on Indian and Turkish bread wheat genotypes. This can be related to a major QTL on chromosome 5 controlling high Fe, Zn, Cu, and Mn content in *Triticum monococcum* genotypes (Ozkan *et al.*, 2007). There was also a relatively high correlation among Mg and micronutrients such as Zn, Fe, and Cu, suggesting physiological coupling of the accumulation processes of minerals in wheat grain. QTLs analysis for cationic mineral concentrations in seeds of *Arabidopsis thaliana* (Vreugdenhil *et al.*, 2004) revealed no co-localisation of QTLs for Mg, Zn, and Fe. However, in their study the correlations between the

three minerals were very low compared to the correlations we observed in bread wheat, as reported previously (Oury *et al.*, 2006), which may indicate that the accumulation of grain constituents is different in crop species like wheat. Another important relationship was found between P and Mg concentrations, in agreement with other published works with wheat (Morgounov *et al.*, 2007; Pandey *et al.*, 2016). Similarly, positive correlations were found between P and Cu, Fe, K, and, to a lesser extent, with Zn, which were possibly related to the known effect of phytic acid for binding Mg and other cations in grains (Oury *et al.*, 2006; Murphy *et al.*, 2008; Shi *et al.*, 2008; Gomez-Becerra *et al.*, 2010).

Interestingly, we observed a negative correlation between S and grain TP concentration, possibly reflecting a loss of S-containing amino acids. Despite the similarity between nitrate and sulphate assimilatory pathways (Hesse *et al.*, 2004), their regulation in response to the availability of the respective nutrient ions and the environment is different (Bielecka *et al.*, 2015). The observed association is relevant because metabolic proteins (albumin, globulin), which account for 15–20 % of the total wheat grain protein, are rich in S-containing amino acids (i.e., cysteine and methionine), as well as in lysin (Molino *et al.*, 1988; Högy and Fangmeier, 2008). Hence, it is tempting to speculate that a preferential decline of metabolic proteins is likely to make the wheat grain quality poorer with regard to nutritional value, irrespective of any further change in gluten storage proteins responsible for grain processing quality. In our previous work of the group (Vicente *et al.*, 2019), where it was investigated the transcriptional response induced by elevated CO_2 combined with a high temperature in the flag leaf of durum wheat grown in field chambers at ear emergence, the transcript levels for a gene involved in glucosinolate degradation were increased. This result suggests that plants may catabolize glucosinolates to use the released sulphur to assist primary metabolism, such as protein synthesis in the leaf, allowing a readjustment to adverse conditions. Such a finding adds further support to the previous suggestion in the current study with bread wheat grown under similar conditions in growth chambers. Several studies have reported that protein concentration and composition in mature wheat grain are strongly affected by nitrogen and sulphur supply (Ercoli *et al.*, 2011; Dai *et al.*, 2015). Therefore, further research is needed to assess the grain amino acids and protein composition and the coordination of nitrogen and sulphur metabolism through the development of wheat genotypes under the studied environmental conditions.

Wheat grains are not only a source of proteins and minerals, but also of carbohydrates, vitamins, fibers, and bioactive compounds that are important for human health due to their antioxidant activity (Shewry, 2009). With regard to the starch concentration, as the main C pool in grains, we did not find differences among the bread wheat genotypes studied, whereas variation in TPhC concentration and

TAC was observed, as it was reported in a previous study with six wheat genotypes grown at four different locations (Mpofu *et al.*, 2006). Large genotypic variability in the TPhC has also been observed in earlier reports in wheat (Li *et al.*, 2008; Fernandez-Orozco *et al.*, 2010; Bencze *et al.*, 2020), although variation related to environmental conditions seems to be larger than genotypic differences (Fernandez-Orozco *et al.*, 2010). In comparison between high yielding and low yielding genotypes, genotypes 41 and 43 had the highest concentration of TPhC, whereas genotype 150 had the lowest, suggesting that it may be possible to select genotypes enriched in bioactive compounds with benefits to the health of consumers.

5.2.3. Grain yield and quality trade-off

Although much work has been done to assess the effects of elevated CO_2 or temperature on wheat regarding yield and quality, comparatively little attention has been paid to the relevance of the plant biomass, grain yield, and grain nutritional quality traits relationships when both factors are applied simultaneously to explore the genotypic variability.

In the current experiment, the maximum variability explained by the genotypic variation was highly associated with the *Wheat production* components (i.e., aboveground, stalk, and chaff biomasses) and the *Mineral nutrients* in the grain (B, Ca, Cu, Fe, K, Mg, Na, P, S, and Zn; Figures 5.2a, Table 5.5), providing evidence of plant biomass relevance for the nutritional quality of the grain. Nevertheless, the first dimension of both variable groups showed opposite correlations for the first dimension of the MFA (Figure 2b), suggesting a trade-off between plant biomass and mineral composition in the grain. Among the *Yield components* and the *Non-mineral nutrients* traits, a lesser contribution, but still with a similar opposite relationship, was found with TP and grain yield as the most related traits. Thus, the genotypes with higher biomass production (41, 43, 61, and 95) showed the highest grain yield, grain and ear numbers and grain Ca, K and S concentrations, but the lowest concentrations in the grain for TP, Cu, Fe, Mg, and Zn. These findings suggest that increased wheat biomass and yield can be counteracted by the altered chemical composition of the grain, leading to reduced quality (Högy and Fangmeier, 2008). In line with this, several studies have reported a decline of macro and microelements under elevated CO_2 (Sánchez De La Puente *et al.*, 2000; Högy and Fangmeier, 2008; Fernando *et al.*, 2012; Myers *et al.*, 2014), with differences depending on genotypes, exposure system, and rooting volume. Likewise, the opposite relationship between grain yield and grain TP concentration resembles previous findings in wheat grown under elevated CO_2 since CO_2 yield stimulation has been linked to decreased grain protein concentration (Högy and

Fangmeier, 2008; Taub and Wang, 2008; Myers *et al.*, 2014; Tausz-Posch *et al.*, 2020). Explanations for the decline in protein concentration include N dilution by increased concentrations of non-structural carbohydrates, restricted N uptake due to decreased transpiration, and N assimilation inhibition or even other unclear mechanisms (Taub and Wang, 2008; Bloom *et al.*, 2014; Vicente *et al.*, 2016, 2019; Tausz-Posch *et al.*, 2020). Although little information about the effects of CO_2 on macro and microelements in wheat grains is known (Högy and Fangmeier, 2008), a dilution of grain components as a consequence of CO_2-stimulated carbohydrate production has also been proposed (Myers *et al.*, 2014). In agreement with our results, other studies have often found negative associations between grain yield and grain protein concentration, indicating that the dilution of N compounds in grain of genotypes was a consequence of the breeding process (Calderini *et al.*, 1995). Similarly, evidence for a negative relationship between grain yield and grain mineral nutrient concentrations is well documented, pointing to modern wheat cultivars with greater yield capacity having lower grain mineral concentrations than the old varieties with lower yield [8,49,69].

In our study, the most productive genotypes (41, 43, 61, and 95) exhibited an increasing trend in grain Cu, Mg, P, and Zn uptakes that were accompanied by lower concentrations of those minerals, while the least productive ones showed the opposite trend. Although these results might be consistent with a possible dilution effect due to higher biomass, the high yielding genotypes also showed a higher grain starch yield, while the starch concentration remained unchanged. Therefore, these findings seem inconsistent with the mineral dilution by an accumulation of carbohydrates operating alone, which cannot explain this trade-off between minerals and biomass to any large extent. Interestingly, Myers et al. (2014), using a meta-analysis approach, suggested that dilution cannot be the only reason for the decrease in grain mineral concentrations under CO_2 enrichment because the extent of the decline in concentration varies between different nutrients. In line with this proposal, we have observed a similar trend to a more marked increase of grain Ca, Cu, K, Mg, P, and S uptakes in the most productive genotypes, which was accompanied by higher concentrations of Ca, K, and S but lower concentrations of Cu, P, or Mg. The general negative correlations of the Cu, Fe, Mg, Na, P, and Zn concentrations with the aboveground, stalk, and chaff biomasses, grain yield, and grain and ear numbers suggest that other mechanisms more complex than dilution could also be involved, such as nutrient uptake, distribution or translocation to the grain.

Similarly, the decrease in grain TP concentration in the high yielding genotypes (41, 43, and 61) was accompanied by lower grain TP content but higher grain TP yield. These results suggest that although these genotypes were able to take up more N and they had higher grain TP yield (Pleijel and Uddling, 2012; Asif *et al.*, 2017), the increase in biomass accumulation could be larger than the

increase in N acquisition (Pleijel and Högy, 2015). Thus, the decrease in grain protein concentration can be partially attributed to dilution effect due to increased grain yield (Taub and Wang, 2008; Wieser *et al.*, 2008). In this sense, it is worth nothing that apart from the associations described above, the MFA (Table 5.5) showed that for the second dimension the TP concentration was positively correlated with HI and grain and ear numbers, and all of them negatively correlated with grain weight. Our results indicate that the TP concentration is mainly and negatively associated with improved plant biomass and grain yield, whereas an amelioration in the decline of grain TP concentration might be associated with greater grain yield based on higher grain and ear numbers rather than heavier grains. Therefore, the selection of wheat varieties with greater grain and ear numbers could be used as a strategy for the improvement of grain yield and offset any loss of grain TP concentration, contributing to the maintenance of the wheat grain nutritional quality in the future climatic scenario. Hence, the dilution hypothesis cannot be fully supported since the yield of TP and minerals are enhanced in the highest yielding genotypes under combined elevated CO_2 and temperature, but possibly to a lesser extent than grain yield. Other features could be considered, such as their ability to store and distribute minerals in the vegetative tissues or to scavenge them from the soil prior to redistribution to the grain. All these processes may be likely altered by elevated CO_2 and high temperature applied simultaneously, making it difficult to draw any further conclusions.

Finally, our study provides information on the nutritional profile of the genotypes and shows that the two least productive genotypes (8 and 150) exhibited higher grain TP concentration than the three highest productive ones (41, 43, and 61). This suggests that improved grain protein nutritional quality can be achieved at the cost of lower yield, which is accompanied by lower grain mineral nutrient concentrations and total antioxidant capacity, particularly in genotype 150 (Gazul). Several genotypes contained high concentrations of certain minerals as well as phenolic compounds. Thus, genotype 41 can be selected as that combining superior grain yield with comparably high nutritional quality characteristics because it is a high yielding genotype with slightly lower total grain protein concentration, which is compensated by the enrichment of most of the mineral nutrients and bioactive compounds as well as a higher total antioxidant capacity, both with beneficial effects on human health.

CHAPTER 6

Third study:

Differential regulation of leaf primary carbon and nitrogen metabolism among bread wheat genotypes grown under elevated CO_2 ad high temperature. Implications in grain yield and nutritional quality.

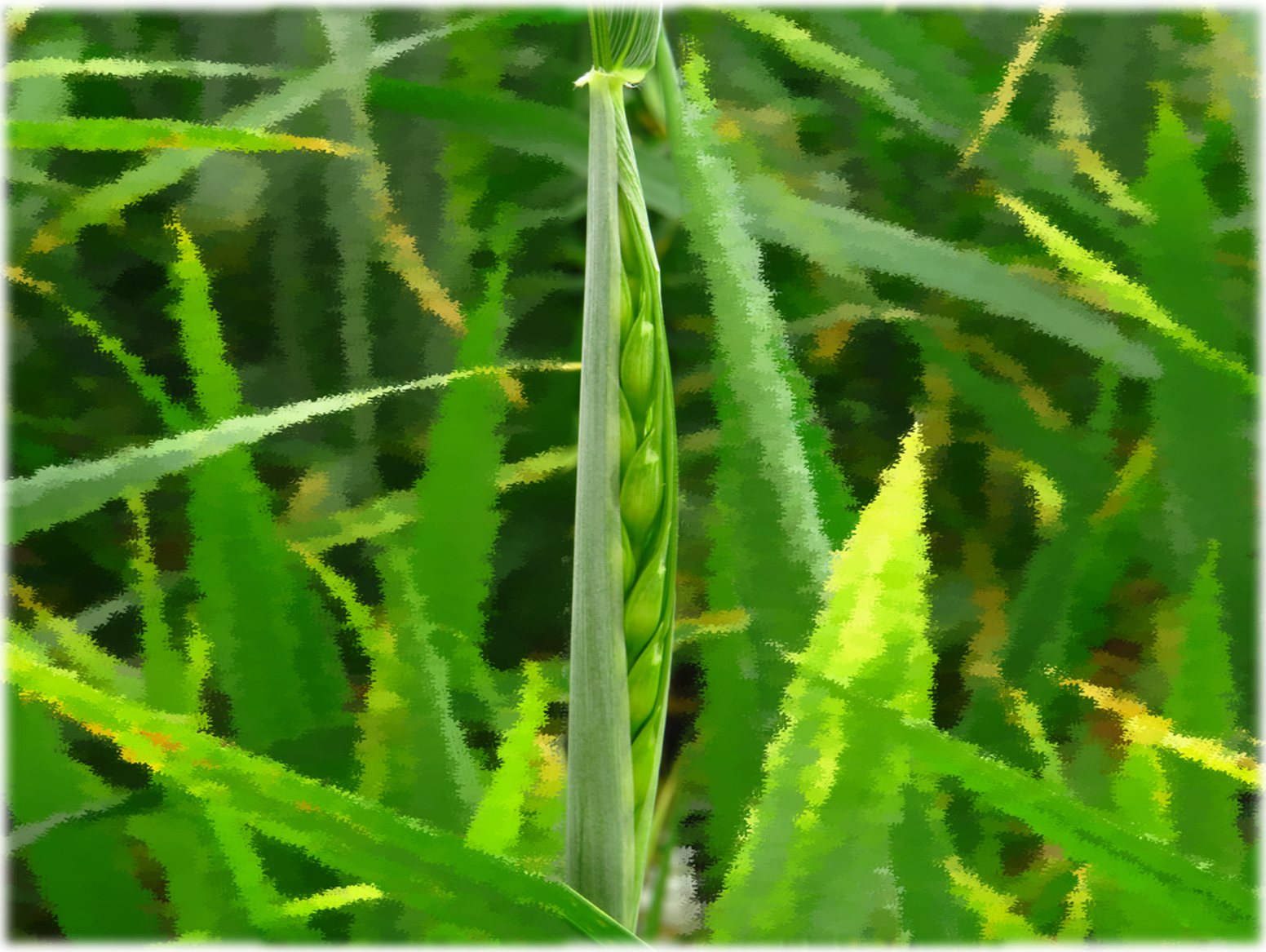

6.1. Results of the third study

6.1.1. Multiple factorial analysis of physiological and biochemical traits in the flag leaves of wheat genotypes at ear emergence

In the present study, a multiple factorial analysis (MFA) was carried out to study the existing relationships among the physiological and biochemical traits evaluated in the flag leaves of ten wheat genotypes grown under combined elevated atmospheric CO_2 concentration and temperature at ear emergence. The studied traits were split up into nine groups, including *Biomass, Morphology, C and N metabolites, Enzyme activities, Chlorophyll spectral indices, Photosynthesis, Antioxidants and C-N %* (Figure 6.1, legend). A factor *Genotype* was also included in order to estimate the impact of genotypic variation. The maximum variability in the data was attributed to the groups *N-metabolites, C-N %* and *Biomass* followed by the *Enzyme activities* group (Figure 6.1, a), showing correlations between 0.67 and 0.61 with the first dimension of the plot (Table 6.1). Regarding the second dimension of the MFA, the factor *Genotype* and the *C-metabolite* group of variables were found as the major sources of variation, with correlations of 0.84 and 0.53, respectively. Furthermore, strong differences were detected among the traits contained into the *Biomass, Antioxidants, Photosynthesis* and *C-N %* groups, with the first and second dimensions of these groups oppositely correlated for the first dimension of the MFA in the partial axes plot (Figure 6.1, b). The analysis of traits also showed that the nitrogen and water percentages (N and H %), together with the Aa content were the variables more positively correlated with the first dimension of the MFA (Table 6.1; 0.84, 0.78 and 0.76, respectively), followed by the NBI (0.66), the activities of the enzymes PEPCase, IDH, G6PDH, GS, PK, AGPase, NR and Fru1,6bisPase (0.65−0.45), and the leaf FW, DW and area (0.64, 0.52 and 0.60). In contrast, the C/N ratio and the starch content negatively correlated with the first dimension (-0.85 and -0.81, respectively), and so did the LDMC (-0.78), Fruct, Flav, Asa and nitrate contents (from -0.65 to -0.44), GDH activity (-0.54) and ORAC capacity (-0.49). The second dimension of the MFA was positively associated with the leaf DW, FW and area (0.76, 0.68 and 0.71), FRAP and ORAC antioxidant capacities (0.63 and 0.44), TPhC (0.56), g_s, *ARbcx, A* and *CRbcx* photosynthetic traits (0.57−0.26) and C/N ratio (0.24), but negatively correlated with Gluc and Fru content (-0.74), C and N % (-0.52 and -0.26) and NBI (-0.37).

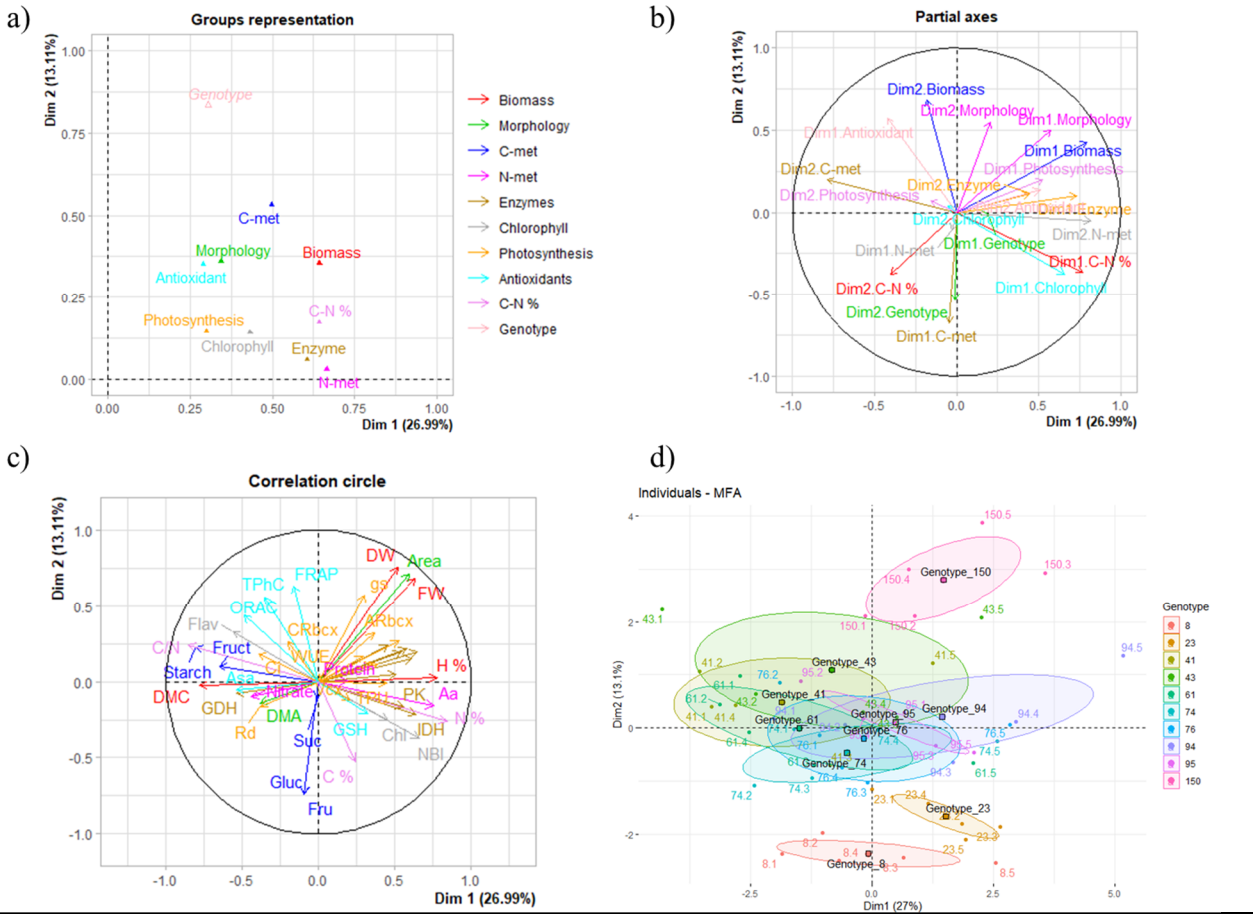

Figure 6.1. MFA for the flag leaf biomass, morphology, C-N metabolite concentrations, percentages and enzyme activities, antioxidant concentrations and photosynthetic, fluorescent and chlorophyllic traits in the response of ten wheat genotypes grown under elevated CO_2 and high temperature at ear emergence.

A: photosynthetic CO_2 assimilation rate ; *Aa*: amino acids; *AGPase*: ADP-glucose pyrophosphorylase; *ARbcx*: maximum value of photosynthesis limited by Rubisco activity; *Asa*: ascorbic acid; *Chl*: chlorophyll; C_i: intercellular CO_2 concentration; *C/N*: carbon-nitrogen ratio; *C %*: carbon percentage; *CRbcx*: intercellular CO_2 concentration at maximum photosynthesis limited by Rubisco activity; *DW*: dry weight; *E*: transpiration; *Flav*: flavonoids; *FRAP*: ferric ion reducing antioxidant power; *Fru*: fructose; *Fru1,6bisPase*: cytosolic fructose-1,6-bisphosphatase; *Fruct*: fructans; *FW*: fresh weight; *G6PDH*: glucose-6-phosphate dehydrogenase; *GDH*: glutamate dehydrogenase; *Gluc*: glucose; *GS*: glutamine synthetase; g_s: stomatal conductance; *GSH*: glutathione; *H %*: water percentage; *IDH*: NADP-dependent isocitrate dehydrogenase; *Jx*: maximum rate of electron transport; *LDMC*: leaf dry matter content; *LMA*: leaf dry mass per area; *NBI*: nitrogen balance index; *N %*: nitrogen percentage; *NR*: nitrate reductase; *ORAC*: oxygen radical absorbance capacity; *PEPCase*: phosphoenolpyruvate carboxylase; Φ_{PSII}: quantum yield of PSII electron transport; *PK*: pyruvate kinase; *Rd*: day respiration; *Suc*: sucrose; *TPhC*: total phenolic compounds; *TPU*: maximum rate of triose phosphate use; *Vcx*: maximum carboxylation rate of Rubisco; *WUE*: water-use efficiency.

Genotype is the group based on a categorical variable specifying the genotypic identity of each sample. The biomass, morphology, C and N metabolite contents and percentages, enzyme activities, antioxidants, chlorophyll spectral indices and photosynthesis related traits were split up into nine groups: *Biomass* (FW, DW, LDMC and H %), *Morphology* (Area and LMA), *C-met* (Gluc, Fru, Suc, Fruct and Starch), *N-met* (Protein, Nitrate and Aa), *Enzymes* (AGPase, Fru1,6bisPase, G6PDH, GDH, GS, IDH, PEPCase and PK), *Chlorophyll* (Chl, Flav and NBI), *Photosynthesis* (*Vcx*, *Jx*, *Rd*, *TPU*, *CRbcx*, *ARbcx*, C_i , g_s, *A*, *E*, *WUE* and Φ_{PSII}), *Antioxidants* (GSH, Asa, FRAP, TPhC and ORAC) and *C-N %* (C %, N % and C/N). (a) The *group representation plot* illustrates the correlation between the variable groups and the supplementary group with axes; (b) The *partial axes plot* shows the relationship between the main axes of the MFA and the first two dimensions of each group. (c) The *correlation circle plot* represents the correlation of traits with the MFA axes. (d) The *individual plot* exhibits the position of individuals in the MFA by genotype variation. *Triangles* indicate the relative position of each group with the axes. *Dots* represent individuals. *Squares* represent group centroids for categorical variables. *Ellipses* around each genotype (d) were added.

Table 6.1. Correlations and contributions between the variable groups, the supplementary group and the continuous variables with the first two dimensions of the MFA.

Dim.1				Dim.2			
Variable groups	**Corr.**	**Cos²**	**Contr.**	**Variable groups**	**Corr.**	**Cos²**	**Contr.**
N-met	0.67	0.21	15.06	C-met	0.53	0.17	24.77
Biomass	0.64	0.37	14.55	Morphology	0.36	0.12	16.81
C-N %	0.64	0.38	14.53	Biomass	0.35	0.11	16.50
Enzyme	0.61	0.31	13.71	Antioxidants	0.35	0.10	16.39
C-met	0.50	0.15	11.27	C-N %	0.17	0.03	8.05
Chlorophyll	0.43	0.17	9.77	Photosynthesis	0.15	0.01	6.77
Morphology	0.34	0.10	7.77	Chlorophyll	0.14	0.02	6.59
Photosynthesis	0.30	0.06	6.78	Enzyme	0.06	0.00	2.77
Antioxidants	0.29	0.07	6.57	N-met	0.03	0.00	1.37
Supplementary group				**Supplementary group**			
Genotype	0.31	0.01		Genotype	0.84	0.08	
Continuous variables				**Continuous variables**			
N %	0.84	0.71	6.90	DW	0.76	0.57	9.09
H %	0.78	0.61	4.67	Area	0.71	0.51	16.16
Aa	0.76	0.57	10.75	FW	0.68	0.47	7.39
NBI	0.66	0.44	4.45	FRAP	0.63	0.40	6.87
PEPcase	0.65	0.42	2.00	g_s	0.57	0.33	3.17
IDH	0.64	0.41	1.94	TPhC	0.56	0.31	5.40
FW	0.64	0.40	3.11	ORAC	0.44	0.19	3.28
G6PDH	0.61	0.37	1.77	Flav	0.33	0.11	2.28
Area	0.60	0.36	5.49	*ARbcx*	0.32	0.10	0.98
GS	0.58	0.33	1.58	*A*	0.27	0.07	0.69
PK	0.56	0.31	1.47	*CRbcx*	0.26	0.07	0.65
AGPase	0.54	0.29	1.39	C/N	0.24	0.06	1.17
A	0.53	0.28	1.30	Fru1,6bisP	0.24	0.06	0.54
DW	0.52	0.27	2.10	Starch	0.23	0.05	1.10
NR	0.51	0.26	1.21	GS	0.22	0.05	0.45
Fru1,6bisP	0.45	0.21	0.97	PEPcase	0.20	0.04	0.38
Chl	0.45	0.21	2.10	AGPase	0.20	0.04	0.37
TPU	0.45	0.20	0.94	C_i	0.18	0.03	0.32
E	0.39	0.15	0.70	Φ_{PSII}	0.17	0.03	0.27
ARbcx	0.36	0.13	0.62	G6PDH	0.16	0.02	0.23
Jx	0.36	0.13	0.59	*Jx*	0.12	0.01	0.13
GSH	0.32	0.10	0.86	*E*	0.12	0.01	0.13
g_s	0.31	0.09	0.44	Fruct	0.10	0.01	0.22
Φ_{PSII}	0.29	0.09	0.41	*WUE*	0.05	0.00	0.02
C %	0.24	0.06	0.56	NR	0.05	0.00	0.02
Vcx	0.21	0.04	0.20	H %	0.02	0.00	0.01
Protein	0.19	0.04	0.69	Protein	0.00	0.00	0.00
WUE	0.01	0.00	0.00	*TPU*	-0.01	0.00	0.00
Suc	-0.01	0.00	0.00	LDMC	-0.02	0.00	0.01
Fru	-0.09	0.01	0.09	Asa	-0.06	0.00	0.06

Table 6.1. Correlations and contributions between the variable groups, the supplementary group and the continuous variables with the first two dimensions of the MFA (continuation).

Dim.1				Dim.2			
Continuous variables	**Corr.**	**Cos²**	**Contr.**	**Continuous variables**	**Corr.**	**Cos²**	**Contr.**
Gluc	-0.10	0.01	0.10	GDH	-0.08	0.01	0.06
FRAP	-0.16	0.03	0.22	Nitrate	-0.10	0.01	0.37
CRbcx	-0.20	0.04	0.18	Suc	-0.11	0.01	0.27
TPhC	-0.35	0.12	1.03	*Vcx*	-0.12	0.02	0.15
Rd	-0.38	0.15	0.68	LMA	-0.14	0.02	0.64
LMA	-0.38	0.15	2.27	Aa	-0.16	0.03	1.00
C_i	-0.39	0.16	0.72	*Rd*	-0.16	0.03	0.25
Nitrate	-0.44	0.19	3.62	PK	-0.17	0.03	0.27
ORAC	-0.49	0.24	2.01	GSH	-0.21	0.05	0.78
Asa	-0.54	0.29	2.44	IDH	-0.22	0.05	0.46
GDH	-0.54	0.29	1.38	Chl	-0.25	0.07	1.36
Flav	-0.56	0.32	3.22	N %	-0.26	0.07	1.37
Fruct	-0.65	0.42	4.38	NBI	-0.37	0.14	2.95
LDMC	-0.78	0.61	4.67	C %	-0.53	0.28	5.51
Starch	-0.81	0.65	6.71	Gluc	-0.74	0.54	11.58
C/N	-0.85	0.73	7.07	Fru	-0.74	0.55	11.59

A: photosynthetic CO_2 assimilation rate ; *Aa*: amino acids; *AGPase*: ADP-glucose pyrophosphorylase; *ARbcx*: maximum value of photosynthesis limited by Rubisco activity; *Asa*: ascorbic acid; *Chl*: chlorophyll; C_i: intercellular CO_2 concentration; *C/N*: carbon-nitrogen ratio; *Contr*: contribution; *Corr*: correlation; *C %*: carbon percentage; *CRbcx*: intercelular CO_2 concentration at maximum photosynthesis limited by Rubisco activity; *Dim.*: dimension; *DW*: dry weight; *E*: transpiration; *Flav*: flavonoids; *FRAP*: ferric ion reducing antioxidant power; *Fru*: fructose; *Fru1,6bisPase*: cytosolic fructose-1,6-bisphosphatase; *Fruct*: fructans; *FW*: fresh weight; *G6PDH*: glucose-6-phosphate dehydrogenase; *GDH*: glutamate dehydrogenase; *Gluc*: glucose; *GS*: glutamine synthetase; g_s: stomatal conductance; *GSH*: glutathione; *H %*: water percentage; *IDH*: NADP-dependent isocitrate dehydrogenase; *Jx*: maximum rate of electron transport; *LDMC*: leaf dry matter content; *LMA*: leaf dry mass per area; *NBI*: nitrogen balance index; *N %*: nitrogen percentage; *NR*: nitrate reductase; *ORAC*: oxygen radical absorbance capacity; *PEPCase*: phosphoenolpyruvate carboxylase; Φ_{PSII}: quantum yield of PSII electron transport; *PK*: pyruvate kinase; *Rd*: day respiration; *Suc*: sucrose; *TPhC*: total phenolic compounds; *TPU*: maximum rate of triose phosphate use; *Vcx*: maximum carboxylation rate of Rubisco; *WUE*: water-use efficiency.

Genotype is the group based on a categorical variable specifying the genotypic identity of each sample. The biomass, morphology, C and N metabolite contents and percentages, enzyme activities, antioxidants, chlorophyll spectral indices and photosynthesis related traits were split up into nine groups: *Biomass* (FW, DW, LDMC and H %), *Morphology* (Area and LMA), *C-met* (Gluc, Fru, Suc, Fruct and Starch), *N-met* (Protein, Nitrate and Aa), *Enzymes* (AGPase, Fru1,6bisPase, G6PDH, GDH, GS, IDH, PEPCase and PK), *Chlorophyll* (Chl, Flav and NBI), *Photosynthesis* (*Vcx*, *Jx*, *Rd*, *TPU*, *CRbcx*, *ARbcx*, C_i , g_s, *A*, *E*, *WUE* and Φ_{PSII}), *Antioxidants* (GSH, Asa, FRAP, TPhC and ORAC) and *C-N %* (C %, N % and C/N). *Corr*. indicates the correlation between the variable and the dimension. The values for the squared correlation (Cos^2) between the variables and the dimensions are used to estimate the quality of the representation. *Contr*. expresses the contributions, in percentage, of each variable in accounting for the variability in the dimension.

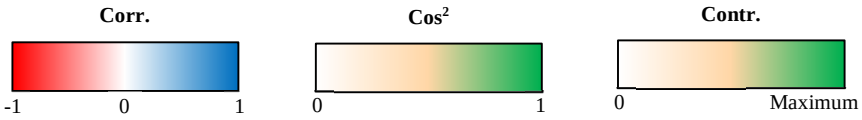

6.1.2. Genotypic variability in leaf C-N metabolism, biomass and morphology related traits

The MFA revealed differences among genotypes. The correlation circle and individual plots (Figure 6.1, c and d) revealed a high degree of association of genotypes 41, 43 and 61 with the starch, Fruct, nitrate and Asa contents, LDMC, C/N ratio and GDH activity, but low correlations with the content of Aa and GSH, the C, N and H percentages (C, N and H %) and the activity of Fru1,6bisPase, G6PDH, GS, IDH, PEPCase and PK. These results were also observed in data reported from ANOVA (Tables 6.2, 6.3 and 6.4; and Table S6.1), although in some of the traits no significant differences were found among genotypes. The opposite results were found for genotypes 8, 23 and 150, which had the lowest content of starch, Fruct and Asa, LDMC, and C/N ratio, as well as a higher content of Aa and GSH, N and H % and activity of the enzymes IDH and PK. Together with genotypes 94 and 95, genotypes 8, 23 and 150, also exhibited the highest Fru1,6bisPase, G6PDH, GS and PEPCase activities. Furthermore, genotypes 8, 23 and 94 had the lowest TPhC and total antioxidant capacities (FRAP and ORAC), while genotype 150 showed the highest. Genotype 8 also exhibited the highest content of Gluc, Fru and Suc, whereas genotypes 41, 43 and 150 showed the lowest Gluc and Fru content, and genotypes 41, 61 and 23 the lowest Suc content. Moreover, genotype 150 showed the

Table 6.2. Flag leaf biomass (FW, DW, LDMC and H %) and morphology related traits (Area and LMA) in the response of ten wheat genotypes grown under elevated CO_2 and high temperature at ear emergence.

Genotype	FW (mg leaf^{-1})			DW (mg leaf^{-1})			LDMC			H %			Area (cm^2 leaf^{-1})			LDMA (mg leaf DW cm^{-2})		
	Me	MAD		Me	MAD		Trim	MAD		Me	MAD		Me	MAD		Trim	MAD	
8	592.25	± 107.45	**a**	167.75	± 9.16	**a**	0.28	± 0.02	**a**	71.68	± 2.12	**a**	26.09	± 6.81	**a**	6.62	± 0.64	**a**
23	783.60	± 28.76	**a**	210.05	± 19.38	**a**	0.27	± 0.01	**a**	73.07	± 0.89	**a**	32.48	± 2.48	**a**	6.60	± 0.59	**a**
41	703.75	± 177.36	**a**	211.75	± 24.13	**ab**	0.29	± 0.03	**a**	70.68	± 2.52	**a**	27.52	± 4.23	**ab**	7.29	± 0.51	**a**
43	793.12	± 255.19	**a**	258.25	± 99.56	**abc**	0.28	± 0.03	**a**	71.26	± 2.90	**a**	35.23	± 10.50	**abc**	6.28	± 0.49	**a**
61	826.00	± 161.97	**a**	256.75	± 35.95	**ab**	0.30	± 0.02	**a**	69.95	± 1.54	**a**	33.94	± 7.43	**ab**	7.56	± 0.21	**a**
74	711.85	± 160.79	**a**	198.00	± 44.11	**ab**	0.29	± 0.01	**a**	71.02	± 1.17	**a**	35.48	± 2.21	**ab**	6.21	± 0.09	**a**
76	679.68	± 42.92	**a**	209.25	± 5.71	**ab**	0.30	± 0.00	**a**	69.89	± 0.34	**a**	34.07	± 8.31	**ab**	6.61	± 0.48	**a**
94	812.60	± 52.63	**a**	250.75	± 20.87	**bc**	0.29	± 0.02	**a**	69.70	± 2.22	**a**	38.81	± 4.03	**bc**	6.25	± 0.31	**a**
95	900.35	± 106.30	**a**	251.75	± 21.98	**ab**	0.28	± 0.01	**a**	72.04	± 0.89	**a**	37.16	± 3.26	**ab**	6.60	± 0.18	**a**
150	1228.62	± 116.75	**a**	366.92	± 65.12	**c**	0.27	± 0.02	**a**	72.78	± 2.48	**a**	56.16	± 8.10	**c**	6.28	± 0.60	**a**
Average	788.68	± 209.82		227.56	± 48.02		0.28	± 0.02		71.39	± 2.21		34.32	± 8.35		6.65	± 0.78	
***p*-value**	**1.32x10^{-2}**			**4.49x10^{-3}**			**6.23x10^{-3}**			3.06x10^{-1}			**3.03x10^{-3}**			**1.14x10^{-3}**		

DW: dry weight; *FW*: fresh weight; *H %*: water percentage; *LDMC*: leaf dry matter content; *LMA*: leaf dry mass per area.

Values represent measures of central tendency (*Me*: median; *Trim*: 20% trimmed mean) and dispersion (*MAD*: median absolute deviation) of five replicates (n=5) for each genotype or all genotypes and replicates (*Average*; N=50). The calculation of statistical significances (p-value) for each trait is based on one-way ANOVA applying corrections for ANOVA assumptions. Values in bold represent significance ($p < 0.05$). Within columns, numbers followed by the same letter indicate non-statistically significant differences at $p < 0.05$ as determined by post-hoc tests.

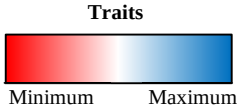

largest FW, DW and leaf area, while genotypes 8, 23 and 41 had the smallest. Not a clear pattern of changes among genotypes was found for LMA, protein content or AGPase and NR activities.

Table 6.3. Flag leaf C-N metabolite contents (Gluc, Fru, Suc, Fruct, Starch, Protein, Nitrate, and Aa) and percentages (C %, N % and C/N) in the response of ten wheat genotypes grown under elevated CO_2 and high temperature at ear emergence.

Genotype	Gluc (µmol g FW^{-1})			Fru (µmol g FW^{-1})			Suc (µmol g FW^{-1})			Fruct (µmol g FW^{-1})			Starch (µmol g FW^{-1})			Protein (µmol g FW^{-1})		
	Trim	MAD		Trim	MAD		Trim	MAD		Trim	MAD		Trim	MAD		Me	MAD	
8	13.29	± 4.03	**ab**	11.05	± 0.25	**a**	94.74	± 23.80	**ab**	43.81	± 6.59	**ab**	17.86	± 12.33	**a**	29.30	± 0.72	**a**
23	7.44	± 0.81	**ab**	5.76	± 0.57	**b**	55.10	± 4.46	**a**	17.08	± 1.65	**a**	22.69	± 0.04	**a**	31.22	± 3.94	**a**
41	3.00	± 0.20	**a**	2.14	± 0.82	**ab**	59.93	± 3.09	**ab**	63.77	± 0.51	**b**	70.33	± 49.37	**a**	26.39	± 3.03	**a**
43	3.45	± 1.22	**ab**	2.99	± 0.87	**ab**	75.21	± 24.36	**ab**	50.10	± 41.30	**ab**	55.01	± 23.64	**a**	29.62	± 0.51	**a**
61	4.94	± 0.09	**b**	4.21	± 0.88	**ab**	60.51	± 4.44	**ab**	52.05	± 4.57	**ab**	78.64	± 39.52	**a**	26.54	± 3.78	**a**
74	6.28	± 2.73	**ab**	5.30	± 3.03	**ab**	75.68	± 3.92	**b**	49.94	± 7.07	**ab**	37.31	± 36.71	**a**	30.18	± 1.71	**a**
76	6.05	± 0.99	**ab**	4.57	± 1.89	**ab**	77.47	± 2.07	**ab**	67.19	± 33.49	**ab**	41.94	± 28.80	**a**	28.07	± 2.61	**a**
94	3.64	± 0.64	**ab**	4.42	± 3.11	**ab**	88.20	± 0.75	**ab**	50.68	± 18.81	**ab**	29.18	± 29.07	**a**	29.41	± 0.58	**a**
95	5.28	± 1.82	**ab**	3.58	± 2.33	**ab**	80.18	± 8.08	**ab**	46.76	± 8.30	**ab**	31.16	± 24.35	**a**	27.02	± 2.74	**a**
150	2.05	± 0.24	**a**	2.17	± 0.60	**ab**	71.99	± 9.18	**ab**	31.43	± 9.45	**ab**	15.58	± 10.58	**a**	27.73	± 2.93	**a**
Average	4.99	± 2.57		4.21	± 2.41		73.54	± 18.04		45.84	± 24.40		35.43	± 25.08		29.24	± 2.80	
***p*-value**	**1.35x10^{-6}**			**1.90x10^{-7}**			**1.88x10^{-6}**			**1.67x10^{-8}**			3.47x10^{-1}			2.02x10^{-1}		

Genotype	Nitrate (µmol g FW^{-1})			Aa (µmol g FW^{-1})			C %			N %			C/N		
	Trim	MAD		Mean	SD		Mean	SD		Trim	MAD		Trim	MAD	
8	109.43	± 1.06	**ab**	20.65	± 7.76	**a**	46.73	± 0.60	**ab**	3.14	± 0.50	**a**	14.98	± 2.13	**a**
23	112.23	± 12.12	**ab**	19.43	± 4.59	**a**	46.68	± 0.51	**ab**	3.54	± 0.22	**a**	13.24	± 0.64	**a**
41	111.61	± 17.55	**ab**	13.56	± 5.71	**a**	46.07	± 0.52	**a**	2.67	± 0.51	**a**	17.73	± 4.09	**a**
43	123.73	± 6.38	**ab**	15.22	± 3.78	**a**	46.25	± 0.52	**ab**	2.98	± 0.25	**a**	15.58	± 1.01	**a**
61	130.92	± 5.66	**a**	18.71	± 10.77	**a**	46.34	± 0.19	**ab**	2.55	± 0.27	**a**	18.17	± 1.75	**a**
74	120.84	± 11.00	**ab**	18.67	± 9.11	**a**	46.92	± 0.39	**b**	3.03	± 0.42	**a**	15.58	± 1.91	**a**
76	107.54	± 3.38	**ab**	19.89	± 10.28	**a**	46.99	± 0.13	**b**	3.21	± 0.59	**a**	14.74	± 2.33	**a**
94	96.49	± 3.46	**b**	19.69	± 10.16	**a**	46.28	± 0.26	**ab**	3.03	± 0.59	**a**	15.46	± 2.86	**a**
95	98.62	± 6.83	**ab**	16.94	± 7.38	**a**	46.59	± 0.24	**ab**	2.95	± 0.24	**a**	15.81	± 1.29	**a**
150	110.68	± 0.47	**ab**	18.45	± 5.96	**a**	46.29	± 0.23	**ab**	3.23	± 0.10	**a**	14.38	± 0.18	**a**
Average	111.73	± 13.96		18.12	± 7.46		46.51	± 0.46		3.06	± 0.51		15.38	± 2.49	
***p*-value**	**3.06x10^{-4}**			9.27x10^{-1}			**5.46x10^{-3}**			1.56x10^{-1}			1.13x10^{-1}		

Aa: amino acids; *C/N*: carbon-nitrogen ratio; *C %*: carbon percentage; *Fru*: fructose; *Fruct*: fructans; *Gluc*: glucose; *N %*: nitrogen percentage; *Suc*: sucrose.

Values represent measures of central tendency (*Me*: median; *Mean*: mean; *Trim*: 20% trimmed mean) and dispersion (*MAD*: median absolute deviation; *SD*: standard deviation) of five replicates (n=5) for each genotype or all genotypes and replicates (*Average*; N=50). The calculation of statistical significances (p-value) for each trait is based on one-way ANOVA applying corrections for ANOVA assumptions. Values in bold represent significance ($p < 0.05$). Within columns, numbers followed by the same letter indicate non-statistically significant differences at $p < 0.05$ as determined by post-hoc tests.

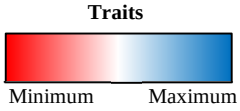

Table 6.4. Flag leaf enzyme activities (AGPase, Fru1,6bisPase, G6PDH, GS, IDH, PEPCase and PK) and antioxidants (GSH, Asa, FRAP, TPhC and ORAC) in the response of ten wheat genotypes grown under elevated CO_2 and high temperature at ear emergence.

Genotype	AGPase (nmol g FW^{-1} min^{-1})		Fru1,6bisPase (nmol g FW^{-1} min^{-1})		G6PDH (nmol g FW^{-1} min^{-1})		GDH (nmol g FW^{-1} min^{-1})		GS (nmol g FW^{-1} min^{-1})		IDH (nmol g FW^{-1} min^{-1})		PEPCase (nmol g FW^{-1} min^{-1})	
	Me	MAD	Trim	MAD	Trim	MAD	Trim	MAD	Trim	MAD	Trim	MAD	Trim	MAD
8	113.04	± 28.79 **a**	683.04	± 144.98 **a**	1164.94	± 459.22 **a**	104.90	± 69.10 **a**	4003.21	± 1735.66 **a**	525.74	± 134.23 **a**	668.13	± 36.55 **a**
23	190.10	± 16.75 **a**	748.05	± 92.03 **a**	1058.79	± 135.45 **a**	87.72	± 40.37 **a**	4559.85	± 1484.05 **a**	526.21	± 57.85 **a**	488.30	± 52.89 **a**
41	149.44	± 80.67 **a**	616.25	± 346.10 **a**	784.45	± 140.81 **a**	143.51	± 25.67 **a**	2427.89	± 281.05 **a**	293.66	± 39.47 **a**	387.16	± 78.77 **a**
43	234.68	± 99.02 **a**	757.05	± 111.27 **a**	837.31	± 171.76 **a**	90.62	± 23.40 **a**	4005.81	± 195.73 **a**	376.18	± 5.11 **a**	486.21	± 52.08 **a**
61	168.35	± 18.49 **a**	605.48	± 239.66 **a**	668.78	± 246.07 **a**	123.64	± 23.25 **a**	1970.66	± 636.21 **a**	301.50	± 51.13 **a**	389.48	± 70.61 **a**
74	219.60	± 63.58 **a**	597.51	± 343.64 **a**	782.21	± 104.19 **a**	97.54	± 26.33 **a**	3682.31	± 912.25 **a**	442.91	± 113.08 **a**	533.75	± 185.15 **a**
76	218.20	± 62.35 **a**	850.15	± 127.20 **a**	882.79	± 53.38 **a**	75.31	± 12.20 **a**	4371.76	± 1216.75 **a**	407.69	± 156.98 **a**	543.98	± 52.06 **a**
94	234.36	± 66.87 **a**	1171.30	± 345.21 **a**	1394.62	± 921.87 **a**	82.07	± 15.35 **a**	6460.49	± 1352.10 **a**	445.30	± 124.16 **a**	641.94	± 247.94 **a**
95	139.10	± 71.88 **a**	991.02	± 167.43 **a**	1164.47	± 713.47 **a**	71.68	± 7.51 **a**	4975.46	± 2960.37 **a**	455.68	± 175.20 **a**	620.75	± 266.99 **a**
150	169.85	± 40.32 **a**	996.43	± 268.35 **a**	1383.61	± 868.91 **a**	69.28	± 9.69 **a**	6002.81	± 2200.78 **a**	477.69	± 176.68 **a**	936.35	± 129.64 **a**
Average	188.31	± 68.50	786.05	± 291.10	962.47	± 302.46	94.73	± 34.29	4105.78	± 1621.02	418.03	± 137.30	543.37	± 181.96
***p*-value**	5.67x10^{-2}		1.49x10^{-1}		2.32x10^{-1}		8.08x10^{-2}		7.53x10^{-2}		**1.97x10^{-2}**		**9.45x10^{-3}**	

Genotype	PK (nmol g FW^{-1} min^{-1})		NR (µmol g FW^{-1} min^{-1})		GSH (µmol g FW^{-1} min^{-1})		Asa (µmol g FW^{-1} min^{-1})		FRAP (µmol eq trolox g FW)$^{-1}$		TPhC (µmol eq galic ac. g FW^{-1})		ORAC (µmol eq trolox g FW^{-1})	
	Mean	SD	Me	MAD	Trim	MAD	Trim	MAD	Trim	MAD	Trim	MAD	Trim	MAD
8	1885.26	± 442.54 **b**	1.25	± 0.50 **a**	0.82	± 0.05 **a**	3.36	± 0.22 **a**	59.67	± 9.89 **ab**	64.22	± 1.13 **a**	247.76	± 8.63 **a**
23	1697.41	± 240.93 **ab**	2.80	± 1.12 **a**	0.69	± 0.08 **a**	3.97	± 0.25 **a**	58.67	± 5.68 **ab**	60.83	± 4.05 **a**	231.35	± 7.91 **a**
41	1134.55	± 236.12 **a**	1.92	± 1.03 **a**	0.59	± 0.10 **a**	4.18	± 0.35 **a**	64.06	± 3.68 **ab**	66.38	± 2.36 **a**	245.01	± 26.60 **a**
43	1450.19	± 189.20 **ab**	2.46	± 0.81 **a**	0.60	± 0.11 **a**	3.66	± 0.88 **a**	75.04	± 13.01 **ab**	70.60	± 4.05 **a**	289.05	± 31.99 **a**
61	1147.07	± 217.18 **a**	2.08	± 0.71 **a**	0.62	± 0.03 **a**	3.85	± 0.23 **a**	61.56	± 14.63 **ab**	63.29	± 2.53 **a**	274.42	± 12.94 **a**
74	1525.05	± 328.56 **ab**	1.66	± 0.58 **a**	0.66	± 0.14 **a**	4.26	± 0.31 **a**	72.46	± 3.06 **a**	72.01	± 5.49 **a**	298.91	± 82.67 **a**
76	1452.66	± 370.60 **ab**	2.84	± 0.81 **a**	0.51	± 0.08 **a**	3.73	± 0.26 **a**	69.89	± 3.32 **ab**	68.24	± 3.95 **a**	287.60	± 62.90 **a**
94	1588.01	± 316.83 **ab**	2.85	± 0.60 **a**	0.67	± 0.10 **a**	3.59	± 0.73 **a**	56.12	± 2.41 **b**	57.65	± 4.83 **a**	219.23	± 28.03 **a**
95	1575.89	± 502.33 **ab**	1.99	± 0.22 **a**	0.58	± 0.14 **a**	3.27	± 0.22 **a**	65.16	± 4.91 **ab**	64.81	± 5.19 **a**	246.30	± 35.22 **a**
150	1735.04	± 309.77 **ab**	1.87	± 0.12 **a**	0.70	± 0.06 **a**	3.28	± 0.32 **a**	87.92	± 11.48 **ab**	80.47	± 6.15 **a**	314.75	± 28.39 **a**
Average	1519.11	± 375.96	2.21	± 0.89	0.65	± 0.14	3.70	± 0.72	66.17	± 10.57	66.17	± 5.13	263.46	± 44.39
***p*-value**	**1.69x10^{-2}**		2.80x10^{-1}		**1.66x10-^{2}**		**4.24x10^{-2}**		**1.15x10^{-3}**		1.92x10^{-1}		**6.32x10^{-3}**	

AGPase: ADP-glucose pyrophosphorylase; *Asa*: ascorbic acid; *FRAP*: ferric ion reducing antioxidant power; *Fru1,6bisPase*: cytosolic fructose-1,6-bisphosphatase; *G6PDH*: glucose-6-phosphate dehydrogenase; *GDH*: glutamate dehydrogenase; *GS*: glutamine synthetase; *GSH*: glutathione; *IDH*: NADP-dependent isocitrate dehydrogenase; *NR*: nitrate reductase; *ORAC*: oxygen radical absorbance capacity; *PEPCase*: phosphoenolpyruvate carboxylase; *PK*: pyruvate kinase; *TPhC*: total phenolic compounds.

Values represent measures of central tendency (*Me*: median; *Mean*: mean; *Trim*: 20% trimmed mean) and dispersion (*MAD*: median absolute deviation; *SD*: standard deviation) of five replicates (n=5) for each genotype or all genotypes and replicates (*Average*; N=50). The calculation of statistical significances (p-value) for each trait is based on one-way ANOVA applying corrections for ANOVA assumptions. Values in bold represent significance ($p < 0.05$). Within columns, numbers followed by the same letter indicate non-statistically significant differences at $p < 0.05$ as determined by post-hoc tests.

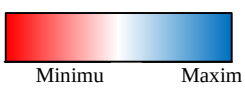

Table 6.5. Flag leaf photosynthetic (*Vcx*, *Jx*, *Rd*, *TPU*, *CRbcx*, *ARbcx*, C_i, g_s, *A*, *E*, *WUE* and Φ_{PSII}) and chlorophyll spectral indices (Chl, Flav and NBI) traits in the response of ten wheat genotypes grown under elevated CO_2 and high temperature at ear emergence.

Genotype	*Vcx* (µmol CO_2 m^{-2} s^{-1})				*Jx* (µmol e^- m^{-2} s^{-1})				*Rd* (µmol CO_2 m^{-2} s^{-1})				*TPU* (µmol trioses m^{-2} s^{-1})				*CRbcx* (µmol CO_2 mol^{-1})			
	Me	±	MAD		Trim	±	MAD		Me	±	MAD		Trim	±	MAD		Trim	±	MAD	
8	153.46	±	37.40	**a**	180.25	±	59.13	**a**	3.86	±	2.04	**a**	12.49	±	0.70	**a**	245.80	±	93.51	**a**
23	144.30	±	21.84	**a**	199.91	±	54.59	**a**	2.28	±	2.73	**a**	14.48	±	3.51	**a**	251.22	±	59.07	**a**
41	135.93	±	15.87	**a**	184.02	±	64.67	**a**	2.17	±	1.39	**a**	12.51	±	1.96	**a**	186.34	±	44.41	**a**
43	117.82	±	60.39	**a**	173.57	±	49.54	**a**	2.22	±	0.52	**a**	12.98	±	1.92	**a**	295.63	±	122.24	**a**
61	117.12	±	47.72	**a**	185.54	±	35.27	**a**	2.01	±	1.10	**a**	11.95	±	3.85	**a**	309.28	±	53.22	**a**
74	145.14	±	3.11	**a**	170.39	±	44.52	**a**	3.44	±	1.42	**a**	12.53	±	5.84	**a**	231.02	±	91.75	**a**
76	89.97	±	20.31	**a**	165.55	±	30.44	**a**	2.37	±	0.43	**a**	10.28	±	5.12	**a**	320.17	±	49.08	**a**
94	121.59	±	46.48	**a**	190.51	±	52.41	**a**	2.01	±	0.23	**a**	13.54	±	2.56	**a**	266.63	±	27.17	**a**
95	123.59	±	39.99	**a**	184.42	±	19.84	**a**	2.00	±	0.81	**a**	13.51	±	2.14	**a**	266.27	±	89.51	**a**
150	114.84	±	3.75	**a**	193.87	±	10.08	**a**	1.99	±	1.29	**a**	13.50	±	1.16	**a**	286.08	±	26.20	**a**
Average	122.59	±	38.08		188.89	±	54.00		2.31	±	0.08		12.82	±	2.78		265.05	±	66.72	
***p*-value**	$8.53x10^{-1}$				$8.29x10^{-1}$				$2.72x10^{-1}$				$8.59x10^{-1}$				$3.92x10^{-1}$			

Genotype	*ARbcx* (µmol CO_2 m^{-2} s^{-1})				C_i (µmol CO_2 mol^{-1})				g_s (mmol H_2O m^{-2} s^{-1})				*A* (µmol CO_2 m^{-2} s^{-1})				*E* (mmol H_2O m^{-2} s^{-1})			
	Mean	±	SD		Mean	±	SD		Trim	±	MAD		Trim	±	MAD		Trim	±	MAD	
8	16.93	±	5.64	**a**	461.40	±	22.55	**a**	232.83	±	24.46	**a**	27.42	±	3.11	**a**	4.38	±	1.79	**a**
23	24.75	±	12.48	**a**	456.10	±	75.62	**a**	276.67	±	118.61	**a**	34.82	±	15.94	**a**	4.50	±	3.06	**a**
41	17.32	±	11.85	**a**	505.60	±	45.61	**a**	325.00	±	14.83	**a**	27.75	±	9.64	**a**	5.02	±	0.90	**a**
43	24.98	±	7.4	**a**	482.60	±	56.38	**a**	343.83	±	32.62	**a**	35.77	±	9.19	**a**	5.92	±	2.56	**a**
61	25.13	±	10.92	**a**	478.20	±	31.85	**a**	302.67	±	25.20	**a**	34.83	±	1.56	**a**	4.70	±	0.71	**a**
74	19.79	±	13.24	**a**	522.20	±	56.61	**a**	320.17	±	48.93	**a**	29.18	±	11.79	**a**	4.54	±	0.84	**a**
76	23.38	±	4.73	**a**	492.00	±	39.91	**a**	319.67	±	71.91	**a**	31.92	±	4.37	**a**	5.06	±	1.64	**a**
94	26.74	±	4.45	**a**	483.60	±	61.72	**a**	327.00	±	40.03	**a**	35.92	±	12.68	**a**	5.18	±	2.23	**a**
95	22.88	±	7.82	**a**	490.50	±	39.72	**a**	320.33	±	23.72	**a**	35.53	±	4.89	**a**	4.80	±	1.80	**a**
150	30.57	±	2.63	**a**	460.50	±	28.42	**a**	362.17	±	70.42	**a**	40.73	±	5.49	**a**	6.32	±	2.12	**a**
Average	23.25	±	8.99		483.27	±	48.13		316.75	±	48.93		33.23	±	11.23		5.17	±	1.50	
***p*-value**	$3.58x10^{-1}$				$5.16x10^{-1}$				**$3.64x10^{-2}$**				$4.51x10^{-1}$				$9.89x10^{-1}$			

Genotype	*WUE* (µmol CO_2 (mmol H_2O)$^{-1}$)				Φ_{PSII}				Chl (Dualex units)				Flav (Dualex units)				NBI			
	Trim	±	MAD		Trim	±	MAD		Me	±	MAD		Trim	±	MAD		Trim	±	MAD	
8	7.03	±	2.30	**a**	0.20	±	0.01	**a**	58.49	±	3.48	**a**	1.46	±	0.12	**ab**	40.51	±	6.46	**ab**
23	7.10	±	0.99	**a**	0.24	±	0.07	**a**	64.55	±	2.16	**a**	1.23	±	0.04	**a**	51.92	±	1.52	**a**
41	6.02	±	0.79	**a**	0.26	±	0.09	**a**	49.04	±	3.56	**b**	1.36	±	0.04	**ab**	36.19	±	3.44	**ab**
43	6.68	±	0.75	**a**	0.24	±	0.03	**a**	54.55	±	1.56	**a**	1.44	±	0.11	**ab**	39.39	±	5.03	**ab**
61	6.97	±	1.98	**a**	0.25	±	0.01	**a**	55.69	±	1.16	**ab**	1.44	±	0.08	**ab**	38.96	±	2.79	**b**
74	6.34	±	1.83	**a**	0.22	±	0.04	**a**	56.20	±	3.85	**a**	1.42	±	0.10	**ab**	40.31	±	4.01	**ab**
76	6.52	±	1.79	**a**	0.22	±	0.01	**a**	58.78	±	4.62	**a**	1.40	±	0.02	**ab**	41.66	±	2.25	**ab**
94	6.40	±	2.04	**a**	0.25	±	0.09	**a**	59.50	±	5.19	**a**	1.28	±	0.11	**ab**	48.83	±	2.87	**ab**
95	6.71	±	2.34	**a**	0.25	±	0.02	**a**	59.96	±	3.26	**a**	1.40	±	0.05	**ab**	43.38	±	2.76	**ab**
150	6.87	±	0.42	**a**	0.27	±	0.05	**a**	61.28	±	0.41	**a**	1.53	±	0.03	**b**	39.87	±	1.77	**b**
Average	6.60	±	1.61		0.24	±	0.04		58.87	±	4.60		1.40	±	0.14		42.14	±	5.17	
***p*-value**	$9.58x10^{-1}$				**$3.52x10^{-2}$**				**$1.51x10^{-3}$**				**$2.72x10^{-3}$**				**$1.11x10^{-4}$**			

A: photosynthetic CO_2 assimilation rate; *ARbcx*: maximum value of photosynthesis limited by Rubisco activity; *Chl*: chlorophyll; C_i: intercellular CO_2 concentration; *CRbcx*: intercellular CO_2 concentration at maximum photosynthesis limited by Rubisco activity; *E*: transpiration; *Flav*: flavonoids; g_s: stomatal conductance; *Jx*: maximum rate of electron transport; *NBI*: nitrogen balance index; Φ_{PSII}: quantum yield of PSII electron transport; *Rd*: day respiration; *TPU*: maximum rate of triose phosphate use; *Vcx*: maximum carboxylation rate of Rubisco; *WUE*: water-use efficiency.

Values represent measures of central tendency (*Me*: median; *Mean*: mean; *Trim*: 20% trimmed mean) and dispersion (*MAD*: median absolute deviation; *SD*: standard deviation) of five replicates (n=5) for each genotype or all genotypes and replicates (*Average*; N=50). The calculation of statistical significances (p-value) for each trait is based on one-way ANOVA applying corrections for ANOVA assumptions. Values in bold represent significance ($p < 0.05$). Within columns, numbers followed by the same letter indicate non-statistically significant differences at $p < 0.05$ as determined by post-hoc tests.

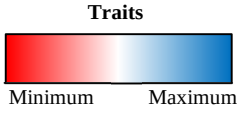

6.1.3. Genotypic variability in photosynthetic traits and spectral indices

The pattern of changes among genotypes reported for the photosynthetic traits, as well as the spectral parameters estimated using the Dualex portable sensor differed from those previously described for the C-N metabolism traits. Genotype 150 had the highest values for *A*, *E*, g_s, Φ_{PSII}, *ARbcx* and *CRbcx*, but one of the lowest for C_i and *Rd*, although no statistical significance was found (Table 6.5). The lowest values were showed by genotype 8 for Φ_{PSII}, genotypes 8 and 23 for g_s and genotypes 8, 23 and 74 for *E*. Similarly, genotypes 8, 41 and 74 exhibited the shortest *A* and *ARbcx* and while genotype 74 had the highest C_i, genotypes 8 and 23 also showed the lowest. Genotype 23 was associated with the greatest *Vcx*, *Jx*, *TPU* and *WUE*, and genotype 76 with the lowest. Genotype 8 also exhibited an upward trend to the highest *Vcx* and *WUE*, along with genotypes 23, 41 and 74 for *Vcx*, although the last two showed the lowest *WUE*. Furthermore, genotype 23 had the highest chlorophyll and NBI indices, whereas genotypes 41, 43 and 61 showed the lowest values for those traits. The highest level of Flav was found for genotype 150, and the lowest for genotypes 23 and 94.

6.1.4. Correlation network of physiological and biochemical traits

A correlation network of the traits studied in this work was built and clearly illustrated three major groups of variables, the greatest one showing the separation of two major clusters (Figure 6.2). A first cluster comprised the activities of enzymes involved in glycolysis, oxidative pentose phosphate and TCA cycles and N assimilation pathway (NR, IDH, PEPCase, G6PDH, Fru1,6bisPase, GS and PK), N and H %, content of Aa, and NBI and chlorophyll indices, which showed positive correlations among them ranging between 0.45 and 0.86 (Figure S6.1). The second one was composed by two subsets of variables, including a) the content of starch and Fruct, LDMC and C/N ratio (r_s = 0.57−0.75), and b) the content of Flav, nitrate and phenolic compounds, along with FRAP and ORAC (r_s = 0.47−0.85), whereas both the content of Flav and the C/N ratio also showed a positive correlation (0.46). In general, these two major clusters were negatively associated, including the obviously strong negative correlation between N and H % to C/N ratio and LDMC, respectively (r_s = -1). There were also highly negative correlations of the content of starch to Aa (-0.80), N % (-0.72), PEPCase (-0.70) and IDH (-0.69), as well as of the C/N ratio to the H % and Aa content (-0.75 and -0.68), LDMC with

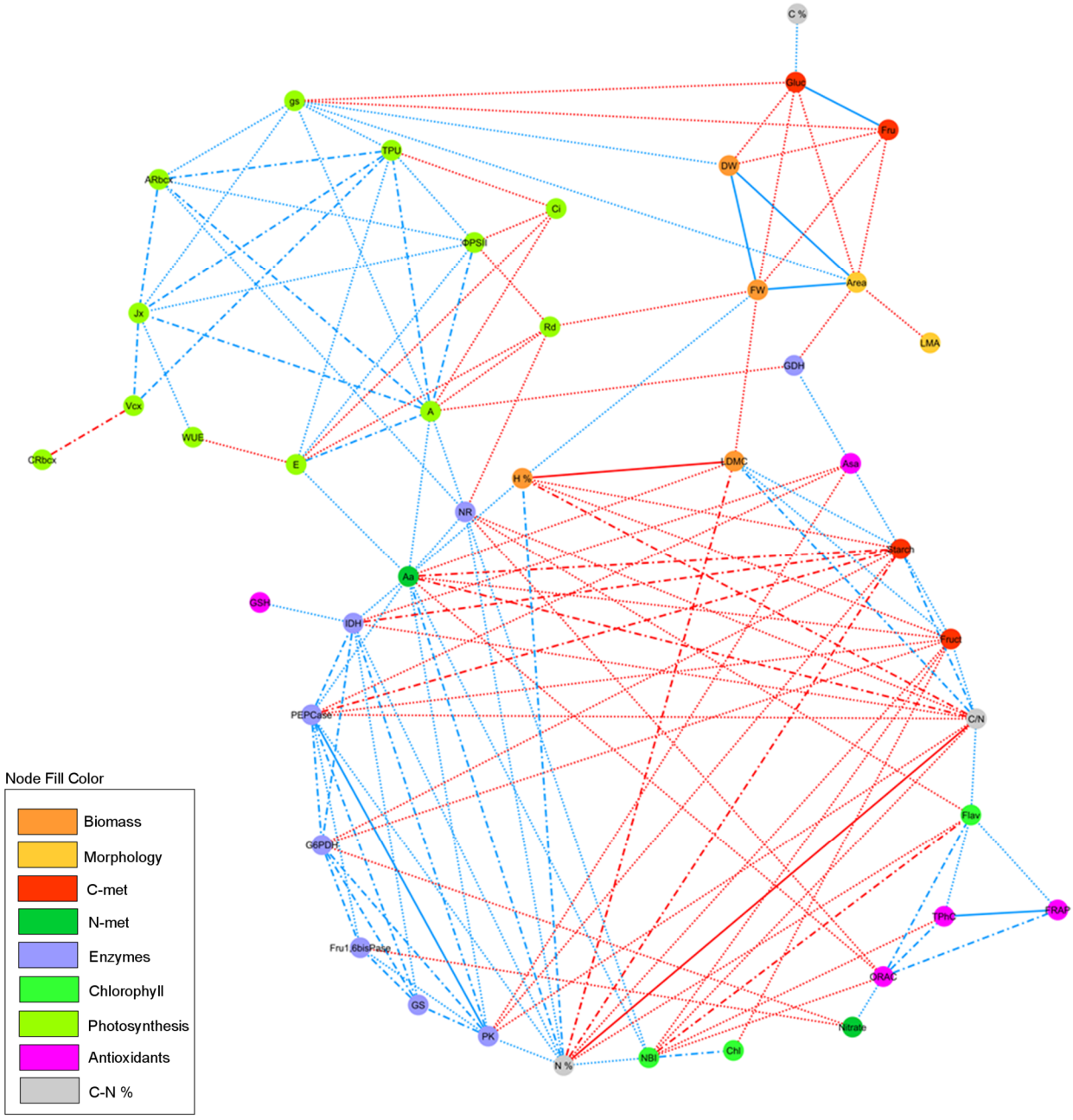

Figure 6.2. CN for the flag leaf for the biomass, morphology, C and N metabolites, enzyme activities, chlorophyll spectral indices, antioxidants and C-N percentages related traits in the response of ten wheat genotypes grown under elevated CO_2 and high temperature at ear emergence.

A: photosynthetic CO_2 assimilation rate ; *Aa*: amino acids; *AGPase*: ADP-glucose pyrophosphorylase; *ARbcx*: maximum value of photosynthesis limited by Rubisco activity; *Asa*: ascorbic acid; *Chl*: chlorophyll; C_i: intercellular CO_2 concentration; *C/N*: carbon-nitrogen ratio; *C %*: carbon percentage; *CRbcx*: intercellular CO_2 concentration at maximum photosynthesis limited by Rubisco activity; *DW*: dry weight; *E*: transpiration; *Flav*: flavonoids; *FRAP*: ferric ion reducing antioxidant power; *Fru*: fructose; *Fru1,6bisPase*: cytosolic fructose-1,6-bisphosphatase; *Fruct*: fructans; *FW*: fresh weight; *G6PDH*: glucose-6-phosphate dehydrogenase; *GDH*: glutamate dehydrogenase; *Gluc*: glucose; *GS*: glutamine synthetase; g_s: stomatal conductance; *GSH*: glutathione; *H %*: water percentage; *IDH*: NADP-dependent isocitrate dehydrogenase; *Jx*: maximum rate of electron transport; *LDMC*: leaf dry matter content; *LMA*: leaf dry mass per area; *NBI*: nitrogen balance index; *N %*: nitrogen percentage; *NR*: nitrate reductase; *ORAC*: oxygen radical absorbance capacity; *PEPCase*: phosphoenolpyruvate carboxylase; Φ_{PSII}: quantum yield of PSII electron transport; *PK*: pyruvate kinase; *Rd*: day respiration; *Suc*: sucrose; *TPhC*: total phenolic compounds; *TPU*: maximum rate of triose phosphate use; *Vcx*: maximum carboxylation rate of Rubisco; *WUE*: water-use efficiency.

The different traits (*nodes*) were classified by colours as described by the legend. *Edges* stand for a Spearman's correlation $r_s \geq |0.45|$, split up as dot ($|0.65| > r_s \geq |0.45|$), dash and dot ($|0.85| > r_s \geq |0.65|$) or solid ($|1| > r_s \geq |0.85|$) line types. *Blue edges* indicate positive correlation whereas *red lines* implicate negative correlation.

N % (-0.74) and NBI with Flav content (-0.79). In addition, positive correlations were recorded among photosynthetic traits, the photosynthetic rate (*A*) was highly correlated with *ARbcx* (0.82), *TPU* (0.82), *Jx* (0.74), Φ_{PSII} (0.73) and, to a lesser extent, with *E* (0.65). *TPU* showed a positive correlation with *ARbcx* (0.67), *Jx* (0.67) and *Vcx* (0.67), while *Jx* was positively correlated with *ARbcx* and *Vcx* (0.70). Negative correlations were also observed between *Vcx* and *CRbcx* (-0.66), WUE and *E* (-0.50). Likewise, C_i was negatively correlated with Φ_{PSII} (-0.62), *A* (-0.60), *E* (-0.57) and *TPU* (-0.46), and *Rd* with *E* (-0.62), Φ_{PSII} (-0.53) and *A* (-0.47). Leaf dry and FWs and area were strongly correlated with each other (r_s = 0.96−0.89), but weakly negatively correlated with Gluc and Fru (-0.25 to -0.41), which in turn showed a strong positive correlation between them (0.88). It was also observed a slight positive correlation of g_s to leaf dry and FWs and area (0.42−0.48), but slight negative correlations of g_s to Gluc and Fru (-0.50 and -0.49, respectively).

6.1.5. Plant growth parameters at ear emergence

Total biomass and green area related traits estimated at ear emergence are shown in Table S6.2. In spite of the fact that there were not so many significant changes in the parameters among genotypes, we observed that genotypes 8, 23 and 94 showed the lowest FW and DW per plant, whereas genotype 61 exhibited the highest FW per plant. Tiller number was significantly lower for genotypes 8, 23, 43 and 150 than genotypes 41 and 61, while a similar pattern of changes was found for the plant area. Moreover, genotype 150 exhibited an upward trend to the highest H %, followed by genotypes 23, 41 and 94, whereas genotypes 8 and 61 tended to have the lowest.

6.1.6. Multivariate dimension reduction discriminant analysis at two growth stages

The relation of the flag leaf and the whole plant parameters at ear emergence to plant biomass, grain yield and related traits and grain nutritional quality parameters at maturity growth stage was also explored. For this purpose, a Data Integration Analysis for Biomarker discovery using Latent cOmponents (DIABLO) method was employed using three datasets collected from a) the *flag leaf at ear emergence* (LEEm), b) the *whole plant at ear emergence* (PEEm) and c) the *whole plant at maturity* (PMa). The PMa and LEEm data sets correlated at 0.81, while lower correlations of PMa and LEEm with PEEm (0.53 and 0.58, respectively) were found (Figure S6.2, a). Projections of samples from each dataset into separately or combined plots are shown in Figures S6.2, b and c.

Plant and leaf N % at ear emergence were the most positively correlated variables (0.93 and 0.83, respectively) with the first dimension of the DIABLO plot (Figure 6.3, a; Table S6.3), followed by TP and Zn concentrations in the mature grain (0.80 and 0.72), plant and leaf H % at ear emergence (0.78 and 0.76) and foliar Aa (0.73). Enzyme activities in the flag leaf (PEPCase, IDH, G6PDH, PK, GS, AGPase, Fru1,6bisPase and NR) were also positively correlated with the first dimension of DIABLO (0.69−0.48), as well as the photosynthetic traits (*A*, *Jx*, *ARbcx*, *E*, g_s, Φ_{PSII} and *Vcx*; 0.54 – 0.24), leaf FW, DW and area (0.63−0.52), NBI and chlorophyll indices (0.64 and 0.45) and grain Cu, Fe and Mg concentrations at maturity (0.46, 0.42 and 0.36, respectively). Plant biomass at maturity (stalk, aboveground and chaff) and at ear emergence [plant dry weight (plant DW), plant dry matter content (PDMC) and plant mass per area (PMA)], together with the leaf C/N ratio, the starch and Fruct contents and LDMC were the main traits negatively correlated with the first dimension of DIABLO (-0.87 to -0.64). Grain yield (-0.51), leaf antioxidants (Asa, GDH, ORAC and TAC; -0.55 to -0.41) and grain S and K concentrations (-0.63 and -0.44) were also negatively correlated with that dimension. The second dimension was positively associated with plant area (0.94), plant FW (0.92), tiller number (0.89) and plant DW (0.64) at ear emergence, as well as with most of grain yield components including grain and ear numbers (0.94 and 0.76), grain yield (0.65) or HI, GNE and chaff DW (0.57−0.49). Grain Ca (0.72) and phenolic compounds (0.53), leaf NR activity (0.52) and photosynthetic traits (g_s, Φ_{PSII} and *A*; 0.46−0.41) at ear emergence were also positively correlated with the second dimension. Together with the grain weight at maturity (-0.80), leaf Fru, Gluc and Suc contents (-0.75 to -0.51), *Rd* (-0.57), chlorophyll (-0.46), PK and IDH activities (-0.48 and -0.36) and protein content (-0.34) were the most negatively associated traits with the second dimension of DIABLO.

6.1.7. Relevant associations between flag leaf and plant traits at different growth stages

The hierarchically-clustered heatmap of associations based on the DIABLO analysis revealed three major clusters for paired correlations among variables of different datasets (Figure 6.4). The first cluster contained grain quality components and HI, plant area and N and H % at ear emergence. These traits were positively correlated with the leaf photosynthetic traits, enzyme activities, C, N and H %, biomass, area, Aa, Chl and NBI, together with the plant N and H % at ear emergence, showing

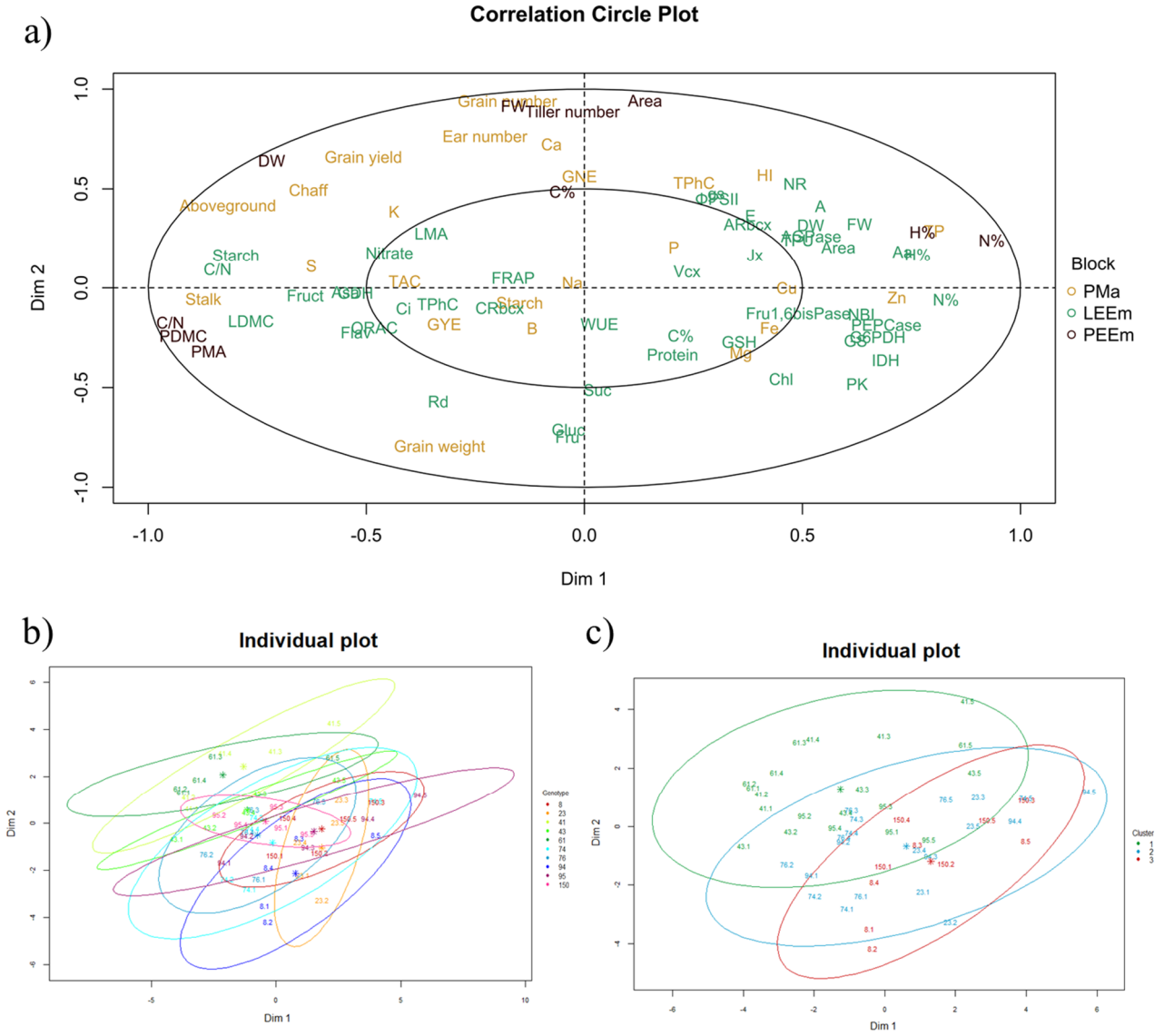

Figure 6.3. DIABLO analysis of three datasets from flag leaf and plant traits measured at ear emergence growth stage and grain yield and quality components at maturity in the response of ten wheat genotypes grown under elevated CO_2 and high temperature.

A: photosynthetic CO_2 assimilation rate ; *Aa*: amino acids; *AGPase*: ADP-glucose pyrophosphorylase; *ARbcx*: maximum value of photosynthesis limited by Rubisco activity; *Asa*: ascorbic acid; *Chl*: chlorophyll; C_i: intercellular CO_2 concentration; *C/N*: carbon-nitrogen ratio; *C %*: carbon percentage; *CRbcx*: intercellular CO_2 concentration at maximum photosynthesis limited by Rubisco activity; *DW*: dry weight; *E*: transpiration; *Flav*: flavonoids; *FRAP*: ferric ion reducing antioxidant power; *Fru*: fructose; *Fru1,6bisPase*: cytosolic fructose-1,6-bisphosphatase; *Fruct*: fructans; *FW*: fresh weight; *G6PDH*: glucose-6-phosphate dehydrogenase; *GDH*: glutamate dehydrogenase; *Gluc*: glucose; *GNE:* grain number ear^{-1}*;* *GS*: glutamine synthetase; g_s: stomatal conductance; *GSH*: glutathione; *GYE*: grain yield ear^{-1}: *H %*: water percentage; *IDH*: NADP-dependent isocitrate dehydrogenase; *Jx*: maximum rate of electron transport; *LDMC*: leaf dry matter content; *LMA*: leaf dry mass per area; *NBI*: nitrogen balance index; *N%*: nitrogen percentage; *NR*: nitrate reductase; *ORAC*: oxygen radical absorbance capacity; *PDMC*: plant dry matter content; *PEPCase*: phosphoenolpyruvate carboxylase; Φ_{PSII}: quantum yield of PSII electron transport; *PK*: pyruvate kinase; *PMA*: plant mass per area; *Rd*: day respiration; *Suc*: sucrose; *TAC*: total antioxidant capacity; *TP*: total protein; *TPhC*: total phenolic compounds; *TPU*: maximum rate of triose phosphate use; *Vcx*: maximum carboxylation rate of Rubisco; *WUE*: water-use efficiency.

Three datasets containing values of plant grain yield-quality components at maturity (*PMa*) and leaf and plant traits at ear emergence growth stage (*LEEm* and *PEEm*) were employed to perform DIABLO analysis. (a) The *correlation circle plot* represents the projections of the variables comprised in the datasets onto the common plane defined by DIABLO analysis. Correlation circumferences with radius 1 and 0.5 were plotted. The *individual plots* exhibit the position of individuals in the DIABLO plot by genotype (b) or yield-quality relationship performance at maturity growth stage (c). *Ellipses* around each genotype (b) or cluster (c) and were plotted. *Asterisks* indicate group centroids for categorical variables.

correlations reaching a value of 0.82. This first cluster was mostly negatively associated with the foliar starch content and the leaf and plant dry matter contents, the leaf and plant mass per area and C/N ratios, especially for the grain TP and plant N and H % (-0.57 to -0.81). Lower negative correlations were also found with leaf content of nitrate, Gluc, Fru, Suc and Fruct, antioxidants, C_i and *CRbcx* parameters and LMA. Whereas HI and grain phenolic compounds positively correlated with plant FW, DW and area, tiller number and C % at ear emergence (reaching a value of 0.59), very low positive correlations or even negative associations were found for the remaining grain quality traits, indicating a possible subdivision of variables in this cluster.

The second cluster was composed by plant biomass at both developmental growth stages, plant C/N ratio at ear emergence and grain starch, K, Na, S and B content and TAC. This group of traits was negatively associated with plant N and H % at ear emergence, as well as with most of leaf characteristics including the photosynthetic traits, enzyme activities, leaf FW, DW and area, protein and Aa contents and C, N and H %. By contrast, this cluster also had positive correlations with the remaining plant traits measured at ear emergence and the leaf starch, Fruct and nitrate content, antioxidants, *CRbcx* and C_i parameters. Positive correlations (0.44−0.84) were found for leaf starch, C/N ratio and LDMC with plant C/N ratio, PMA and PDMC, as well as all of them with aboveground and stalk biomass. Negative correlations of grain weight with plant FW, DW and area, tiller number and C % (-0.26 to -0.80) were also recorded.

The third cluster included tiller number, C % and plant FW at ear emergence, grain and ear numbers, GNE, and grain Ca concentration at maturity. This cluster showed a trend similar to that of the second one, showing positive correlations with plant biomass, area, tiller number and C % at ear emergence (0.27−0.89), and negative correlations with leaf enzyme activities, C and N %, Chl, NBI or proteins. Nevertheless, slightly weak positive correlations were found with the photosynthetic parameters, leaf FW, DW and area, and Aa, plant C % and leaf and plant H %. This cluster also showed negative correlations with the content of Gluc, Fru and Suc (-0.25 to -0.70), and low positive correlations with leaf starch, nitrate, C/N ratio and LMA. Furthermore, negative associations with leaf antioxidants, C_i and *CRbcx* parameters, plant C/N ratio and leaf and plant dry matter content and leaf and dry mass per area were found.

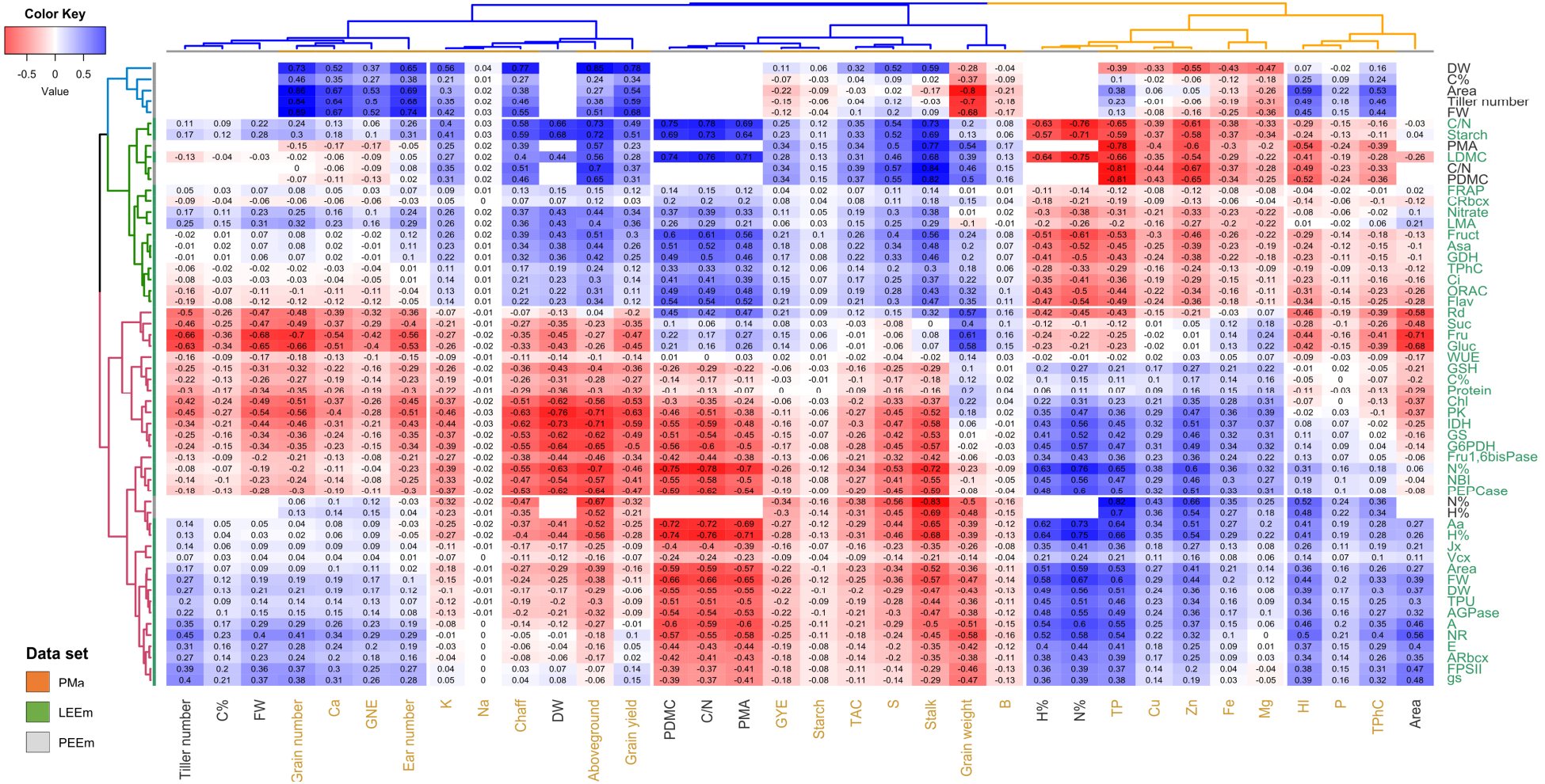

Figure 6.4. Hierarchically–clustered heatmap of associations based on DIABLO analysis of three datasets from flag leaf and plant traits measured at ear emergence growth stage and grain yield and quality components at maturity in the response of ten wheat genotypes grown under elevated CO_2 and high temperature.

Three datasets containing values of plant grain yield-quality components at maturity (*PMa*) and leaf and plant traits at ear emergence growth stage (*LEEm* and *PEEm*) were employed to perform DIABLO analysis. Different colours were employed to identify traits belonging to each dataset (PMa: orange; LEEm: green; PEEm: black). Only correlations among datasets are showed.

6.2. Discussion

Most of the studies on crop responses to climate change have investigated individual effects of either rising atmospheric CO_2 concentration or high temperature on plant productivity and development, although these environmental changes occur concurrently. So, they should be considered together because plant performance in realistic combined environmental conditions cannot be predicted from the sum of responses to single factors (Valladares and Pearcy, 1997; Vicente *et al.*, 2015b), demonstrating the plasticity of plant adaptation to complex environmental cues (Vicente *et al.*, 2019) In addition, the photosynthesis and primary C-N metabolism, which strongly influence grain yield and quality, have rarely been investigated under combined environmental factors in a wide set of genotypes. In this context, ten genotypes with contrasting productivity were used to explore the genotypic variability on a range of leaf physiological parameters, antioxidant status, metabolites and enzyme activities of primary metabolism, as well as their associations with grain yield and quality traits under concomitant increases in atmospheric CO_2 concentrations and temperature according to climate change projections by the end of this century.

6.2.1. Genotypic variability in the photosynthetic response is driven by changes in leaf morphology and antioxidant capacity under elevated CO_2 and high temperature

In this study, we observed that the flag leaf area and dry weight of Gazul (genotype 150), the least productive genotype, increased significantly compared to those of the CIMMYT genotypes at ear emergence, but the fresh weight and water percentage did not increase significantly (Table 6.2). These changes in the leaf morphology of Gazul were accompanied by a downward trend in leaf dry mass per area, indicating thinner leaves. This finding is consistent with our previous study with the same wheat genotype grown in the field in temperature-gradient chambers at anthesis (Gutiérrez *et al.*, 2009b), highlighting that there was consistency in its response to the combined environmental cues at earlier growth stages. Although genotype 43 had an LMA similar to that of Gazul, the other two high-yielding genotypes, 41 and 61 (Marcos-Barbero *et al.*, 2021a), exhibited substantially higher LMA and lower water percentage than Gazul, which indicates thicker leaves. Genotype 8 had a slightly higher LMA and lower water percentage than Gazul, a result that can be interpreted as the loss of thickness found in the low-yielding genotypes (8 and Gazul) was associated with an increase

in tissue water. Taken together, these results illustrate the plasticity of leaf morphology among wheat genotypes to adapt to elevated CO_2 and high temperature, which may have physiological implications. Brestic *et al.* (2018) proved that differences in photosynthetic traits on field grown modern and old wheat varieties compared to wild wheat relative species were linked to changes in leaf anatomy and morphology.

A decline in LMA has been recognized to be favourable for photosynthesis (Roderick *et al.*, 1999) because the light interception is enhanced (Evans and Poorter, 2001). Therefore, the lower LMA found in Gazul might reflect an adaptive advantage (Gutiérrez *et al.*, 2009b). In spite of the fact that there were no significant changes in the photosynthetic parameters among genotypes, a trend towards increased photosynthetic rates was observed in Gazul compared to the CIMMYT genotypes in association with reduced intercellular CO_2 concentration and increased stomatal conductance and transpiration (Table 6.5). One of the most consistent responses of plants to CO_2 enrichment is a reduction in g_s (Long *et al.*, 2004; Ainsworth and Rogers, 2007), which would partly explain the down-regulation of photosynthetic carboxylation capacity frequently found under elevated CO_2 (Xu *et al.*, 2016). In contrast, our results reflect that a higher stomatal conductance enhances photosynthesis in Gazul by increasing CO_2 diffusion into the chloroplast, while simultaneously, it can favour leaf cooling through high transpiration rates (Vicente *et al.*, 2015b) (Cramer *et al.*, 2009) and contribute to the regulation and maintenance of optimal leaf temperature for photosynthesis (Lawson and Blatt, 2014) and, thereby, diminishing photorespiration (Salvucci and Crafts-Brandner, 2004; Long *et al.*, 2006b). A previous work evaluating the flag leaf anatomy in relation to photosynthetic rates in *Triticum* and *Aegilops* species showed that plant species with thinner leaves, lower LMA and chlorophyll per unit area exhibited higher photosynthetic rates than those with thicker and dense leaves (Kaminski *et al.*, 1990).

Further analysis of the A/C_i responses revealed that most of the photosynthetic parameters, particularly the maximum rate of electron transport (J_x) for RuBP regeneration, showed an increasing trend similar to the CO_2 assimilation rate in Gazul compared to the other genotypes (Table 6.5). In the case of the maximum carboxylation rate of Rubisco (V_{cx}), a surrogate for *in vivo* activity of Rubisco, a shift to lower values was observed in Gazul, which is consistent with a downward acclimation to elevated CO_2 (Martínez-Carrasco *et al.*, 2005; Pérez *et al.*, 2005; Gutiérrez *et al.*, 2009a; Aranjuelo *et al.*, 2011; Seneweera *et al.*, 2011; Tausz *et al.*, 2013). It has been proposed that crops can decrease Rubisco activity at elevated CO_2 to a greater extent than the capacity for regeneration of RuBP (Ainsworth and Rogers, 2007). The fact that the maximum electron transport rate slightly increased suggests that even a possible decline in V_{cx} may not affect the photosynthetic

assimilation rates (Zhu *et al.*, 2010). This result is in accordance with the strong positive correlation found between J_x and A in our study (Figure 6.2). A decline of Rubisco activity and protein has often been observed in wheat grown under CO_2 enrichment in the field or controlled environment chambers (Pérez *et al.*, 2005; Aranjuelo *et al.*, 2011; Vicente *et al.*, 2015a, 2016, 2019), but Pérez *et al.* (2011) reported that the negative effects of elevated CO_2 and high temperature on V_{cx} were counteracted by combined increases of CO_2 and temperature. Likewise, we observed that the quantum yield of PSII electron transport (Φ_{PSII}) was also higher in Gazul compared to the CIMMYT genotypes (Table 6.5), indicative of a positive effect on photochemical efficiency, as shown earlier in wheat grown under combined increases in atmospheric CO_2 concentration and temperature in field temperature-gradient chambers (Gutiérrez *et al.*, 2009a). It has recently been reported that elevated CO_2 can attenuate the effect of high temperatures on photosynthesis by increasing the capacity for regeneration of RuBP and decreasing photochemical damage in wheat grown in a glasshouse (Chavan *et al.*, 2019). Although increases in photochemical activity under elevated CO_2 have frequently been found in different plant species (Habash *et al.*, 1995; Hymus *et al.*, 2001; Yang and Zhang, 2006), no changes (McKee *et al.*, 1995) or decreases (Scarascia-mugnozza *et al.*, 1996; Aranjuelo *et al.*, 2008) have also been reported possibly due to the impact of fluctuating environmental conditions.

Changes in photochemical processes can result in excessive excitation energy in photosystem II and lead to a homeostatic imbalance of plant metabolism and also to promote the formation of ROS, causing oxidative stress (Mittler *et al.*, 2012; Munné-Bosch *et al.*, 2012; Baxter *et al.*, 2014). In this sense, it is worth noting that the total antioxidant capacity was slightly enhanced in Gazul when compared to that of the CIMMYT genotypes, as well as the content of total phenolic compounds (Table 6.4). A surrogate estimation of leaf chlorophyll, flavonoids and NBI using the spectral sensor Dualex (Table 6.5) showed a tendency of flavonoids to increase in Gazul. These results are in agreement with the observation that total phenolic compounds were positively correlated with flavonoids and total antioxidant capacity and all of them, in turn, were correlated with each other (Figure 6.2), highlighting the antioxidant role of both flavonoids and polyphenols and their potential contribution to plant protection against lipid peroxidation and the maintenance of thylakoid membrane stability (Foyer and Noctor, 2005). In addition, they can also play a role in light attenuation avoiding indirectly ROS formation in chloroplasts (Zheng *et al.*, 2021). These metabolites can also be accumulated as a consequence of the enhanced C-fixation after exposure to elevated CO_2 (Ainsworth *et al.*, 2006; Ghasemzadeh *et al.*, 2010; Zinta *et al.*, 2014; Vicente *et al.*, 2019), acting as a reservoir of C in plants.

The ascorbate-glutathione cycle is considered an important pathway to scavenge ROS and reduce oxidative damage, so increased antioxidative defence compounds have been associated with improved stress tolerance (Foyer and Noctor, 2011). The total glutathione and ascorbate content did not show a clear pattern of changes among genotypes in our study. We observed a slight increase in glutathione accompanied by a slight decrease in ascorbate in Gazul as compared to the high-yielding genotypes, suggesting lower levels of photo-oxidative stress (Aranjuelo *et al.*, 2008). In a FACE study with two wheat cultivars, (Tausz-Posch *et al.*, 2013a) reported that, under the more stressful growing conditions used in their study, elevated CO_2 increased the photosynthetic rates, while the photochemical processes were not affected and the ascorbic acid was reduced. By contrast, elevated CO_2 contributed to mitigate the negative effects of combined heat wave and drought in Arabidopsis by improving ROS detoxification as a result of increased antioxidant capacity, polyphenols and ascorbate levels, and antioxidant activities (Zinta *et al.*, 2014). In line with these observations, it is worthy highlighting that ascorbate synthesis has been related to carbohydrate metabolism (Smirnoff *et al.*, 2001), and its decline may be triggered by a lower accumulation of carbohydrates in such genotype (Table 6.3), in accordance with the positive correlation found between ascorbate and starch in our study (Figure 6.2). Our findings indicate that, although the attenuation of oxidative stress by elevated CO_2 in Gazul might be the result of reduced photorespiration, the increased antioxidant capacity and accumulation of flavonoids may contribute to the maintenance of redox homeostasis and counteract the adverse effect of ROS production.

6.2.2. Enhanced transpiration leads to improved leaf N status and photoassimilate translocation in association with a lower accumulation of starch and fructans in the least productive genotype

Nitrogen supply and sink capacity are also involved in the response of photosynthesis to elevated CO_2 through their influence on photosynthetic acclimation (Ruiz-Vera *et al.*, 2017; Tausz-Posch *et al.*, 2020; Ainsworth and Long, 2021). It is known that the main driving force for nitrate movement in the soil is transpiration (Cramer *et al.*, 2009; Matimati *et al.*, 2014) and the reduction in leaf N content often found in plants exposed to elevated CO_2 has been attributable to decreases in transpiration due to stomatal closure (Conroy and Hocking, 1993; del Pozo *et al.*, 2007; Taub and Wang, 2008; Feng *et al.*, 2015; Jauregui *et al.*, 2016) among other mechanisms (Taub and Wang, 2008; Bloom *et al.*, 2014; Tausz-Posch *et al.*, 2020). Moreover, transpiration is the main process that

controls water distribution within the plant (Kramer and Boyer, 1995). In our study, increased transpiration in Gazul could improve N uptake by enhancing mass flow to the vicinity of roots, which in turn could contribute to an improvement in leaf N status. This result supports the better leaf N status found in this genotype, as well as the lower leaf C/N ratio, compared to the high-yielding genotypes (Table 6.3). A strong positive correlation was observed between leaf N and water percentages, while both of them were negatively correlated with the C/N ratio (Figure 6.2), more strongly the former than the latter, providing evidence that improved N and water status lead to lower leaf C accumulation. In agreement with this suggestion, the starch and fructan contents were negatively correlated with the water and N percentages, but positively with the C/N ratio, whereas the NR activity and amino acid content were negatively correlated with the C/N ratio (Figure 6.2). These results point to the fact that enhanced C-fixation rates induced by elevated CO_2 lead to an increase in the C/N ratio owing to the accumulation of storage carbohydrates and the reduction of the conversion of nitrate into amino acids and subsequent protein synthesis, as a strategy for the adaptation of the metabolic status to the plant development under a changing environment as a consequence of the close interaction between C and N metabolism (Stitt and Krapp, 1999; Bloom *et al.*, 2010; Vicente *et al.*, 2018). Both fructans and starch contents were positively correlated not only with the C/N ratio, but also with the leaf dry matter content and all of them with each other (Figure 6.2), highlighting the role of starch and fructans as major reserve carbohydrates in leaves of wheat and other cereals (Vicente *et al.*, 2015b; Córdoba *et al.*, 2017), as well as other organs (Morcuende *et al.*, 2004a), and their increases together with C-rich structural compounds may account for the rise in dry matter content of flag leaves found in this study.

Interestingly, the greater accumulation of starch and, to a lesser extent, fructans in the flag leaves of the three high-yielding genotypes differs from the lower accumulation of those carbohydrates found in Gazul (Table 6.3) and it might be indicative of a sink limitation (Ainsworth *et al.*, 2004). This fact suggests that an insufficient demand for carbohydrates from developing sinks may contribute to a C sink-source imbalance (White *et al.*, 2016), which may lead to the repression of genes involved in photosynthesis and a down-regulation of photosynthetic capacity (Ainsworth *et al.*, 2004; Aranjuelo *et al.*, 2011; Vicente *et al.*, 2015b, 2016). In this regard, we observed a significant increase in the dry matter of the last stem internode (ranging from 1.39 to 0.84 g) and, to a lesser extent, of the ear (1.78−1.22 g) in Gazul compared to the CIMMYT genotypes. The stronger sink capacity of these organs could help to promote the distribution of photoassimilates from the flag leaves and avoid carbohydrate build-up under CO_2 enrichment. That improved leaf C balance in Gazul may have also allowed to maintain N status, and consequently maximized photosynthetic capacity as outlined above. These data resemble a recent work with two barley genotypes that showed

improved photosynthetic acclimation responses to elevated CO_2 in the genotype with higher C/N compounds storage capacity in the peduncles (Torralbo *et al.*, 2019). Thus, it seems likely that the flag leaf of Gazul exhibits improved nutrient and water status, which allow a more efficient translocation of carbohydrates and amino acids to growing organs.

6.2.3. A higher accumulation of reserve carbohydrates in high-yielding genotypes brings together a decline in C flux to organic acid synthesis and further N assimilation

Plant biomass and grain yield enhancement in genotypes 41, 43 and 63 (Marcos-Barbero *et al.*, 2021a) was accompanied by an increase in carbohydrate content in the leaves, mainly starch, as indicated above (Table 6.3). A higher foliar accumulation of carbohydrates caused by enhanced photosynthetic rates at elevated CO_2 has often been observed in different plant species (Pérez *et al.*, 2005; Vicente *et al.*, 2015b, 2016; Zinta *et al.*, 2018; Torralbo *et al.*, 2019; Gámez *et al.*, 2020; Padhan *et al.*, 2020). This accumulation has been found to be more exacerbated at low than high N supply in durum wheat (Vicente *et al.*, 2015b, 2016) and tobacco (Geiger *et al.*, 1999) due to an impaired C and N metabolism. We also observed a downward trend in the content of amino acids and percentage of N in the flag leaves, as well as a higher C/N ratio (Table 6.3), suggesting a reduction in the leaf N status (Bloom *et al.*, 2002; Pérez *et al.*, 2005; Aranjuelo *et al.*, 2011; Vicente *et al.*, 2015b). All this is consistent with the negative correlation found between fructans and leaf chlorophyll and between starch and fructan contents with amino acids (Figure 6.2), as we have previously reported in durum wheat (Vicente *et al.*, 2018). These findings reflect that high-yielding genotypes are more prone to N deficiency under the studied environmental conditions. Impaired leaf N assimilation could be related to the leaf C sink-source imbalance (Ainsworth *et al.*, 2004; White *et al.*, 2016).

In this regard, there was no noticeable pattern of changes in the NR activity between high- and low-yielding genotypes, possibly a decreasing trend in the latter (Table 6.4), although previous studies with different plant species, including wheat, have reported either increases (Geiger *et al.*, 1998), decreases (Bloom *et al.*, 2002; Morcuende *et al.*, 2011; Vicente *et al.*, 2015b, 2019) or unchanged activities under elevated CO_2 (Vicente *et al.*, 2016; Torralbo *et al.*, 2019). Despite this fact, NR activity was positively correlated with the amino acid content and the photosynthetic CO_2 assimilation rate (Figure 6.2). Accordingly, other work also showed a positive correlation of both NR activity and amino acids with some genes involved in photosynthesis and carbohydrate metabolism

(Vicente *et al.*, 2018). These findings suggest a tight regulation of NR activity for adjusting amino acid biosynthesis to the supply of C skeletons provided by photosynthesis. The slight increase in nitrate content (Table 6.3) in the leaves of high-yielding genotypes might be linked to a limitation of nitrate reduction (Bloom *et al.*, 2010; Igarashi *et al.*, 2021), which was accompanied by a decreasing trend in leaf PEPCase activity when compared to low-yielding ones (Table 6.4). This result points to a possible limitation in leaf PEPCase, which operates together with malate dehydrogenase to produce malate required as counter-anion to replace nitrate for maintenance of pH balance and prevent alkalinization during nitrate assimilation (Martinoia and Rentsch, 1994; Stitt *et al.*, 2002). In line with this suggestion, we observed a positive correlation between PEPCase and PK with amino acids highlighting the important role these enzymes could play in regulating glycolysis to promote the C flux into organic acids and subsequent amino acid biosynthesis. Our data resemble a previous work with nitrate deficient wild-type tobacco plants showing a marked decrease in leaf PEPCase activity and transcripts for the gene encoding such protein accompanied by a decrease of malate, other organic acids and 2-oxoglutarate (Scheible *et al.*, 1997a).

Interestingly, the pattern of changes in Fru1,6bisPase, G6PDH, PK, IDH and GS activities resembled that previously described for PEPCase activity (Table 6.4) when compared high- and low-yielding genotypes. The most likely explanation of our findings is that, in high-yielding genotypes, there was an inhibition of carbon flux from glycolysis to organic acid synthesis to provide 2-oxoglutarate required as acceptor for ammonium in the GS-GOGAT pathway, and other carbon precursors which enter the amino acid biosynthesis pathways. The opposite trend observed for the GDH activity (Table 6.4), involved mainly in the recycling of ammonium during protein breakdown and senescence, may point out the predominance of protein catabolism for providing amino acids to support plant metabolism and growth under the studied environmental conditions, contributing to a reduction in leaf organic N-compounds, as shown in other studies (Bloom *et al.*, 2002; Pérez *et al.*, 2005; Vicente *et al.*, 2019). Similarly, a repression of genes involved in glycolysis, oxidative pentose phosphate and TCA cycle, together with an upregulation of the gene encoding the GDH, mainly at a low N supply, has been found in durum wheat grown under elevated CO_2 in field temperature-gradient chambers (Vicente *et al.*, 2015b) and hydroponically in controlled environment chambers (Vicente *et al.*, 2016). A decline in the activity and the level of transcripts of some of these enzymes was found in nitrate deficient wild-type tobacco plants (Scheible *et al.*, 1997a), and the transcriptional response also resembled that of durum wheat to nitrogen starvation (Curci *et al.*, 2017). Conversely, it may be inferred that the stimulation of the flux into the organic acid synthesis triggered in the low-yielding genotypes may ensure the provision of C skeletons, energy and reducing equivalents for nitrate reduction and further amino acid biosynthesis, concurrent with the improvement in N status.

These results are in agreement with the upregulation of genes linked to glycolysis and TCA cycle reported in other studies (Li *et al.*, 2008; Watanabe *et al.*, 2014) and the repression of the gene encoding for GDH (Vicente *et al.*, 2017). Therefore, our results provide evidence that changes induced by elevated CO_2 in the expression of genes involved in the C and N metabolism pathways also resulted in changes in the activities of the encoded enzymes.

Intriguingly, although the accumulation of starch in the flag leaf of the most productive wheat genotypes was greater than in the least productive ones, those changes were not ascribed to similar changes in the activity of the AGPase, the key enzyme for starch biosynthesis (Table 6.4). In tobacco, (Scheible *et al.*, 1997a) showed that starch synthesis is regulated by nitrate in two ways, including the repression of the gene encoding for the regulatory subunit of AGPase or through the stimulation of flux to organic acid synthesis, which may lead to a decrease in 3-phosphoglycerate and result in allosteric inhibition of AGPase and subsequent starch synthesis.

Overall, these results suggest that there was a differential reprogramming of primary metabolism among wheat genotypes for improving adaptation to combined elevated CO_2 and temperature.

6.2.4. Correlation network provides valuable information about C-N metabolism regulation in the wheat flag leaf under elevated CO_2 and temperature at ear emergence

Network analysis of physiological and biochemical parameters in the flag leaves of spring wheat genotypes provides relevant information about the complex regulatory adaptive responses to the environment (Vicente *et al.*, 2018). It is worth nothing that the activities of six representative enzymes from central C and N metabolism, including PEPCase, G6PDH, Fru1,6bisPase, PK, IDH and GS were positively correlated with each other (Figure 6.2), indicating an effective and coordinated regulation of C and N assimilation pathway. In agreement with our observation, (Mitchell-Olds and Pedersen, 1998) found positive correlations between five enzyme activities of central C-metabolism (Fru1,6bisPase, G6PDH, phosphoglucose isomerase, phosphoglucomutase and glucose-6-phosphatase) in an Arabidopsis RIL population. Coordinated changes of C-N enzyme activities have also been reported in a study including 24 genetically diverse Arabidopsis accessions, strengthening the view that natural variation can generate coordinated changes of enzyme activities (Cross *et al.*, 2006). The correlation with the highest Spearman coefficient was found between PEPCase and PK, which have related functions mainly involved in the production of C skeletons for the amino acid

synthesis, and other biosynthetic pathways, in accordance with the positive correlation found between them and amino acids as outlined above. It is also of interest the positive correlation found between the amino acids and NR activity with the leaf N percentage, as well as between both traits with NBI (Figure 6.2), suggesting that an improved N status is accompanied by a higher amino acid content and NR activity. Moreover, the amino acid content was positively correlated with transpiration underlying the relevance of nutrient mass flow and transpiration, in particular N, which is assimilated into amino acids (Cramer *et al.*, 2009). Likewise, the transpiration was negatively correlated with *WUE*, which indicates that decreased transpiration might increase *WUE*. Plants optimise *WUE* by adjusting the photosynthetic rate relative to that of transpiration (Chaves and Oliveira, 2004) through tight stomatal control of water loss.

In addition, we observed negative correlations between NR activity and amino acid content with ORAC, and between NR and flavonoids, whereas nitrate was positively correlated with ORAC (Figure 6.2). These findings may indicate that impaired N metabolism is accompanied by a shift away from N-compounds to C-rich secondary metabolites, including polyphenols, flavonoids, etc., as a mechanism to divert excess carbon from central metabolism. A high accumulation of secondary metabolites has been observed in plants exposed to elevated CO_2 (Ghasemzadeh *et al.*, 2010). Similarly, previous works at transcriptional level provide evidence that the alteration of primary metabolism induced by elevated CO_2 may lead to marked changes for secondary metabolism (Ainsworth *et al.*, 2006; Vicente *et al.*, 2019), as well as under low levels of nitrate (Fritz *et al.*, 2006).

Intriguingly, the positive correlation found between ascorbate and GDH activity may indicate that, together with its role in amino acid catabolism, GDH may likely function as a shunt to divert C skeletons from N metabolism to C metabolism and the TCA cycle (Miflin and Habash, 2002; Lea and Miflin, 2003). Likewise, ascorbate was negatively correlated with ICH, PEPCase and PK, whereas starch was not only negatively correlated with those enzymes, but also with G6PDH and amino acids. A negative correlation was also found between fructan content with amino acids, and with PEPCase and G6PDH activities. These results may reflect that the down-regulation of glycolysis could be seen as a mechanism to adjust the partitioning of C between its use for N assimilation and its storage or export as sucrose, preventing N depletion when C-fixation is enhanced under elevated CO_2. In this context, we also found a negative correlation of Fru1,6bisPase, involved in sucrose synthesis (Herzog *et al.*, 1984), with nitrate, as well as a negative association of nitrate with G6PDH (Figure 6.2). This illustrates that the C and N metabolism control each other with both positive and negative signals to achieve plant homeostasis.

Our study provides evidence for the importance of measuring enzyme activities, which integrates changes in transcription, posttranscription, posttranslational and protein turnover (Gibon *et al.*, 2004) to complement transcript and metabolite analyses (Vicente *et al.*, 2018, 2019) for understanding genotypes performance under future environmental conditions.

6.2.5. The associations between traits at ear emergence and physiological maturity reveal that photosynthesis is not associated with grain yield but is slightly correlated with the grain number

In the present study, we have not only explored the variability among genotypes in a range of photosynthetic and chlorophyll fluorescence parameters, as well as other physiological traits, antioxidants, metabolites and enzyme activities of primary metabolism at ear emergence, but also their associations with grain yield and quality at physiological maturity under combined elevated atmospheric CO_2 and temperature.

In this regard, hierarchical clustering analysis (Figure 6.4) displayed the tendency of traits of the same class (grain nutritional quality, biomass, yield-related traits) to cluster together. In fact, we observed a cluster including grain nutritional quality traits and HI at maturity as well as plant area and N and water percentages at ear emergence showing positive correlations with most of the leaf photosynthetic traits, enzyme activities, amino acids and N and water percentages at ear emergence. This suggests that improved photosynthetic rates and water and N status at ear emergence is translated into an increase in grain protein and nutrient concentrations, and thereby better nutritional quality of grains at maturity. Moreover, the second cluster representing plant biomass at both developmental stages as well as plant C/N ratio at ear emergence and the grain total antioxidant capacity and content of starch, K, Na, S and B at maturity displayed negative correlations with plant N and water percentages at ear emergence together with the photosynthetic parameters, enzyme activities and amino acid content. Although positive correlations of those traits mainly with leaf starch, fructan, nitrate and ascorbate content were also observed (Figure 6.4). These results support the idea that a down-regulation of photosynthetic capacity and impair leaf N assimilation could be involved in the decline of organic N-compounds and the increase of storage carbohydrates and C-rich compounds for maintaining enhanced growth and biomass accumulation not only at ear emergence, but also at physiological maturity. These changes are accompanied by a higher grain starch content and some

mineral nutrients, as well as total antioxidant capacity. It is worth mentioning that the impoverishment in grain protein and other important nutrients in the most productive genotypes is compensated by the enrichment of other mineral nutrients and bioactive compounds with beneficial effects on human health, as reported recently by Marcos-Barbero *et al.* (2021a). Likewise, the third cluster grouped tiller number, C percentage and plant fresh weight at ear emergence together with grain and ear numbers, GNE, and grain Ca concentration at maturity (Figure 6.4). This cluster displayed a correlation pattern similar to the previous one as shown by the negative associations with enzyme activities, proteins, Chl, among other traits, but, at variance with that cluster, exhibited a slight positive correlation with photosynthetic parameters (Figure 6.4). These findings highlight that optimising carbon source-sink relationship might play a crucial role in the regulation of plant growth and yield response to CO_2 enrichment, in agreement with other published works (Ainsworth and Long, 2004; Aranjuelo *et al.*, 2011). Indeed, an increase in the photosynthesis rate at elevated CO_2 results in higher carbohydrates production, which are available for development of new sink organs such as tillers and seeds. The developmental plasticity of these organs determines the final growth response to elevated CO_2 (Gamage *et al.*, 2018). Although tillering capacity is influenced by both genotype and prevailing environmental conditions (Dreccer *et al.*, 2013), it is recognized as an important factor in yield response to elevated CO_2, and higher temperatures (Fitzgerald *et al.*, 2016), in line with our observations in the present work and previous one (Marcos-Barbero *et al.*, 2021b).

It is well known that photosynthesis is the primary determinant of plant productivity (Faralli and Lawson, 2020), and any improvement in photosynthetic efficiency has the potential to enhance grain crop yields (Zhu *et al.*, 2010). Consistent with this, Ainsworth and Long (2004) demonstrated the link between photosynthesis and yield in response to CO_2 enrichment. Previous studies on wheat exploring natural variation in photosynthesis have provided evidence of a positive relationship between grain yield and photosynthesis (Blum, 1990; Fischer *et al.*, 1998; Reynolds *et al.*, 2000; Carmo-Silva *et al.*, 2017), but no significant relationship has also been found in the study by Driever *et al.* (2014) similar to the present work. The lack of correlation is not surprising because many factors can contribute to variations in both photosynthesis rate and yield (Jiang *et al.*, 2003), including the growth conditions (Xue *et al.*, 2002) and developmental stage (Reynolds *et al.*, 2000). Nevertheless, photosynthesis was slightly correlated with the grain number in our study (Figure 6.4) in line with the significant relationship between both traits reported by Fischer *et al.* (1998). The correlation of photosynthesis with a particular yield component rather than overall grain yield can be related to the fact that the different yield-related traits are determined at specific phenological stages (Faralli and Lawson, 2020). Recently, Sinclair (2019) pointed to that past crop yield increases are not associated with increased photosynthesis, suggesting that yield increases are closely dependent on nitrogen

accumulation as an essential component of seeds. Furthermore, the photosynthesis from flag leaves is not the only source of photoassimilates during grain filling, while other factors such as the reserves stored in stems on ear photosynthesis should be considered specially under limited conditions (Sanchez-Bragado *et al.*, 2020; Araus *et al.*, 2021). Thus, the inconsistency in such association emphasizes the complexity of the relationship between photosynthesis, plant growth and yield, which require further investigation considering water and nitrogen availability under the conditions anticipated by global climate change.

Our study provides evidence of a differential reprogramming of primary metabolism among high- and low-yielding wheat genotypes for improving adaptation to combined elevated CO_2 and temperature. The least productive genotype displayed improved photosynthetic rates and water and N status accompanied by a lower accumulation of carbohydrates and up-regulation of the activity of enzymes from central C and N metabolism, indicating a stimulation of the C flux from glycolysis into the organic acid synthesis to ensure the provision of C skeletons, energy and reducing equivalents for nitrate reduction and further amino acid biosynthesis. The improved N status at ear emergence is translated into an increase in grain protein and nutrient concentrations, and thereby better nutritional quality of grains at maturity. While the opposite behaviour was found in the high-yielding genotypes, suggesting that the decreased N content may constrain the benefits of the studied environmental conditions on grain yield and affect their nutritional value for human health. In addition, leaf starch could be considered as a positive marker, based on its correlation with biomass and grain yield at maturity, for selection of high-yielding wheat genotypes under combined elevated CO_2 and temperature predicted by the end of this century.

CHAPTER 7

Conclusions

First. This study demonstrates that the exploration of genetic diversity is a powerful approach, not only for the selection of genotypes that are better adapted to future global warming, but also for the identification of those genotypes with improved grain nutritional quality.

Second. The CIMMYT genotypes performed better than Gazul genotype under combined elevated CO_2 and high temperature, providing evidence for the success of the CIMMYT breeding programs under warmer temperatures and the plants' plasticity to respond to the concurrence of several environmental factors.

Third. The dissection of yield-related traits in the present study discloses that the bread wheat genotypes employed diverse strategies to achieve the final grain yield under the studied environmental conditions, most probably derived from the contrasting breeding programs used to improve grain yield throughout the 20^{th} century.

Fourth. The increased grain yield was driven by an increase in grain numbers and ears per plant, rather than in grain weight. Thus, those genotypes that can preferentially increase grain and ear numbers per plant will attain better grain yield responses under combined elevated CO_2 and high temperature.

Fifth. Phenology, in particular earliness of heading, did not appear to be the only cause of variability in grain yield and consequently other features should be considered. Tillering capacity, and hence the increased number of fertile tillers, will be an important factor in yield response functioning as sinks for the allocation of excess carbohydrates produced under the studied environmental conditions.

Sixth. An improved grain protein nutritional quality can be achieved at the cost of a lower yield, which is accompanied by a lower concentration of some mineral nutrients and total antioxidant capacity in the grain, particularly in Gazul.

Seventh. A high-yielding genotype with slightly lower total grain protein concentration, which is compensated by the enrichment of some mineral nutrients and bioactive compounds with beneficial effects on human health, could be selected for its promising nutritional characteristics.

Eighth. Enhanced transpiration and water and nitrogen status in Gazul led to improved photoassimilate translocation and antioxidant capacity accompanied by a lower carbohydrate accumulation and up-regulation of the carbon and nitrogen enzyme activities promoting the carbon flux from glycolysis into organic acids and subsequent amino acid biosynthesis. The improved

nitrogen status at ear emergence was translated into an increase in grain protein and nutrient concentrations, and thereby better nutritional quality of grains at maturity.

Ninth. High-yielding genotypes were more prone to nitrogen depletion and exhibited an upward trend in glutamate dehydrogenase activity pointing to the predominance of protein catabolism to provide nitrogen compounds to support further growth. In addition, decreased nitrogen content may constrain the benefits of the combined elevated CO_2 and high temperature on grain yield and affect their nutritional value for human health.

Tenth. This study provides new insights into the differential reprogramming of primary carbon and nitrogen metabolism among high-and low-yielding wheat genotypes under future climate conditions, and reveals that flag leaf starch content could be considered as a positive marker for selection of high-yielding genotypes under global warming.

Eleventh. Further research is needed to investigate whether the high-yielding genotypes identified in the present study will be able to maintain their yield advantage, regardless of nutrient availability or drought stress, combined with high temperature and elevated CO_2, opening new opportunities for the selection of widely adapted climate resilient wheat genotypes.

CHAPTER 8

Summary

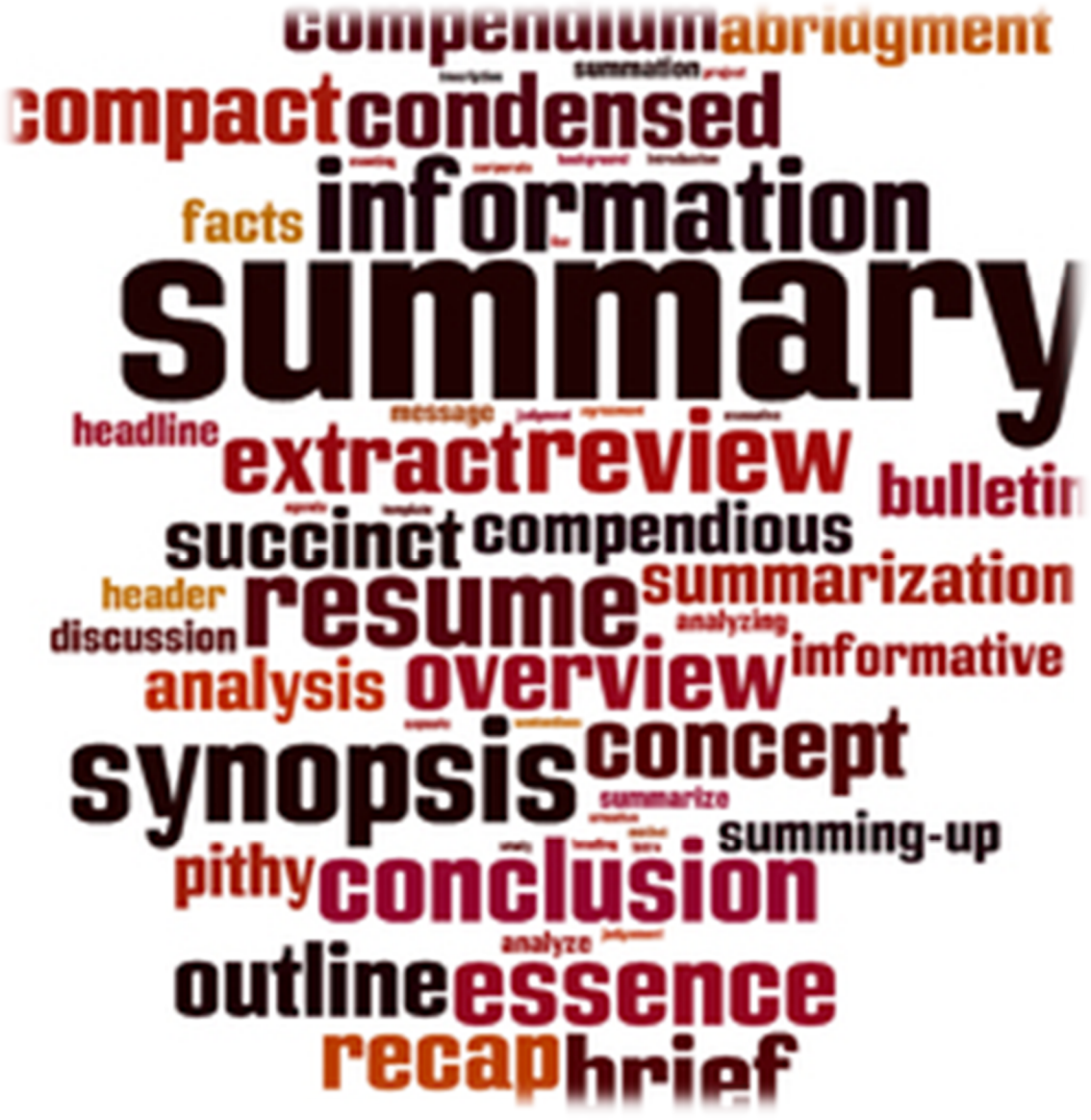

TITLE: Study of the wheat genotypic variability for the improvement of grain yield and quality and its dependence on leaf carbon-nitrogen metabolism under elevated CO_2 and high temperature

Estudio de la variabilidad genotípica del trigo para la mejora del rendimiento y la calidad del grano y su dependencia del metabolismo foliar del carbono y nitrógeno bajo CO_2 elevado y temperatura alta

ÍNDICE REDUCIDO

8.1. Introducción

El rendimiento de los cultivos es particularmente vulnerable a las alteraciones ambientales y las previsiones de cambio climático global auguran una elevación de la temperatura de la superficie terrestre en asociación con un aumento notable de la concentración atmosférica de CO_2 para finales de siglo (IPCC, 2021a). El crecimiento y la producción de las plantas dependen de la asimilación fotosintética del carbono y de la asimilación de nutrientes inorgánicos, de los que el nitrógeno es cuantitativamente el más importante, y de los programas de desarrollo que influyen en la eficiencia de la conversión del carbono en biomasa (Sulpice *et al.*, 2013). El CO_2 elevado puede tener un impacto positivo en la productividad de los cultivos agrícolas, incluido el trigo, al estimular la fotosíntesis porque aumenta el sustrato para la reacción de carboxilación catalizada por la Ribulosa-1,5-bisfosfato carboxilasa/oxigenasa (Rubisco) y disminuye la oxigenación, lo cual contribuye a aumentar el crecimiento y la producción de biomasa de las plantas (Long *et al.*, 2004). La estimulación del crecimiento es el resultado no sólo del aumento de la fotosíntesis sino también de la mejora en la eficiencia en el uso del agua debido a un descenso de la conductancia estomática por el

cierre de estomas. Sin embargo, el aumento inicial de la fotosíntesis disminuye a medida que progresa el tiempo de exposición al CO_2 elevado (Martínez-Carrasco *et al.*, 2005; Pérez *et al.*, 2005; Gutiérrez *et al.*, 2009a; Aranjuelo *et al.*, 2011; Vicente *et al.*, 2019). Esta pérdida de capacidad fotosintética se conoce como fenómeno de aclimatación de la fotosíntesis al crecimiento prolongado en CO_2 elevado (Stitt and Krapp, 1999; Long *et al.*, 2004) y se acompaña de un descenso de actividad y proteína Rubisco, un aumento del contenido de carbohidratos y una menor concentración de nitrógeno en la planta (Pérez *et al.*, 2005; Aranjuelo *et al.*, 2011; Vicente *et al.*, 2015a, 2019). La aclimatación al CO_2 elevado se ha relacionado con una represión de los genes que codifican las subunidades grande y pequeña (*rbcS* and *rbcL*) de la Rubisco mediada por la acumulación de carbohidratos foliares (Nie *et al.*, 1995; Moore *et al.*, 1999; Rolland *et al.*, 2006) (Nie *et al.*, 1995; Moore *et al.*, 1999; Rolland *et al.*, 2006) junto a otros genes fotosintéticos entre los que se incluyen la subunidad β de la ATPasa cloroplástica o la glutamil-tRNA reductasa (Vicente *et al.*, 2015a). Aunque en nuestros experimentos con trigo cultivado en el campo en cámaras de gradiente de temperatura el descenso de Rubisco se ha relacionado con una pérdida de nitrógeno foliar (Pérez *et al.*, 2005; Gutiérrez del Pozo, 2010; Aranjuelo *et al.*, 2011) (Pérez et al 2005, Gutiérrez 2010, Aranjuelo et al 2011). Asimismo, una aceleración de la senescencia foliar (Zhu *et al.*, 2009) o bien una limitación en la disponibilidad de nitrógeno (Stitt and Krapp, 1999) o en la capacidad de sumidero (Long *et al.*, 2004; Aranjuelo *et al.*, 2011) se han propuesto como posibles factores para explicar el fenómeno de aclimatación de la fotosíntesis. En línea con esta última observación, se ha propuesto que los factores genéticos o ambientales que limitan el desarrollo de la fuerza del sumidero hacen que las plantas sean más susceptibles a una mayor aclimatación de la fotosíntesis y se atenúe la estimulación de la fotosíntesis por el CO_2 elevado (Long *et al.*, 2004; Ainsworth and Rogers, 2007). Por tanto, la relación fuente-sumidero parece desempeñar un papel importante en la regulación de la respuesta de las plantas al crecimiento prolongado en condiciones de CO_2 elevado (Ainsworth and Long, 2004; Tausz-Posch *et al.*, 2013a). Así, se ha observado una mayor respuesta al CO_2 elevado en variedades de trigo ancestrales que en variedades modernas que parece relacionarse con una mayor capacidad de ahijamiento de las primeras. Dado que el aumento en el desarrollo de tallos hijos facilitaría que funcionasen como sumideros para la adscripción del excedente de carbohidratos originado en condiciones de CO_2 elevado (Ziska *et al.*, 2004; Ziska, 2008).

Muchos estudios han mostrado que el crecimiento prolongado en una atmósfera enriquecida en CO_2 conduce a una pérdida del contenido de nitrógeno de la planta (Stitt and Krapp, 1999; Long *et al.*, 2004; del Pozo *et al.*, 2007; Morcuende *et al.*, 2011; Vicente *et al.*, 2015a). Por ello, la aclimatación de la fotosíntesis se asocia con el estado nitrogenado de la planta ((Bloom *et al.*, 2010) y se ha mostrado que fue más acusada en plantas deficientes en nitrógeno (Stitt and Krapp, 1999;

Vicente *et al.*, 2015b), aun cuando con un bajo aporte de fertilizante nitrogenado, suministrado en proporción directa al crecimiento del trigo cultivado hidropónicamente, la aclimatación no tuvo lugar (Vicente *et al.*, 2017). A nivel transcripcional, la pérdida de compuestos nitrogenados que experimentan las plantas que crecen en CO_2 elevado se asoció con una represión de genes involucrados en la fotosíntesis y la asimilación de nitrógeno que fue más acusada en plantas deficientes en nitrógeno (Vicente *et al.*, 2015b). Se desconoce el mecanismo por el que el CO_2 alto conduce a una pérdida de proteínas y compuestos nitrogenados y son varias las hipótesis propuestas, entre ellas la dilución del nitrógeno por acumulación de carbohidratos no estructurales(Stitt and Krapp, 1999; Gifford *et al.*, 2000), un descenso asociado a un desarrollo o crecimiento más rápido de la planta (Bernacchi *et al.*, 2007), una restricción en la absorción de nitrógeno como consecuencia del descenso de transpiración (del Pozo *et al.*, 2007; Taub and Wang, 2008), redistribución de nitrógeno en la planta (Nakano *et al.*, 1997) o la limitación de la asimilación de nitrógeno en proteínas (Bloom *et al.*, 2002, 2010; Vicente *et al.*, 2016). Esta última propuesta se relaciona parcialmente con la inhibición de la fotorrespiración y la dependencia de la asimilación de nitrógeno de dicho proceso (Bloom, 2015a). Recientemente, se han mostrado evidencias de que alteración del metabolismo primario de la planta inducida por el CO_2 promueve el metabolismo secundario como mecanismo para desviar el exceso de carbono del metabolismo central de la planta (Vicente *et al.*, 2019). La pérdida de nitrógeno que experimentan las plantas que crecen en una atmósfera enriquecida en CO_2 se ha propuesto como una de las causas por las que la productividad de los cultivos sea menor de la esperada (Long *et al.*, 2006a). En definitiva, la reducción del estado nitrogenado de la planta conlleva a una alteración del balance C-N que refleja la estrecha coordinación de ambos metabolismos para el mantenimiento del crecimiento y desarrollo de las plantas en respuesta al ambiente (Stitt and Krapp, 1999; Morcuende *et al.*, 2011; Vicente *et al.*, 2018). Dicha alteración puede, a su vez, repercutir en la calidad nutricional del grano de trigo como muestra el descenso en el contenido proteico del grano observado en diferentes estudios (Högy and Fangmeier, 2008; Högy *et al.*, 2009b).

Las previsiones de cambio climático global auguran que el aumento de los niveles atmosféricos de CO_2 irá acompañado de una elevación de la temperatura de la superficie terrestre. El aumento simultáneo de ambos factores ambientales tendrá un impacto directo o indirecto en el crecimiento y productividad de los cultivos, así como en la calidad del grano y deberían ser evaluados conjuntamente. Las temperaturas elevadas reducen la fotosíntesis porque disminuye la especificidad de la Rubisco para el CO_2 y aumenta la fotorrespiración. Además, la Rubisco activasa es sensible a temperaturas moderadamente elevadas que inestabilizan la proteína, lo cual conduce a una limitación de la Rubisco y la fotosíntesi (Salvucci and Crafts-Brandner, 2004). Además, las temperaturas elevadas aceleran el desarrollo del cultivo y acortan la duración del período de llenado de grano, así

como de la biosíntesis y deposición de almidón en el mismo, lo cual conduce a una reducción de la productividad agrícola (Asseng *et al.*, 2015) y una alteración en la composición nutricional y calidad de los cultivos (Nuttall *et al.*, 2017). Esto sugiere que los potenciales beneficios del CO_2 pueden disminuir rápidamente con temperaturas más cálidas.

La demanda de productos agrícolas a nivel mundial aumentará significativamente durante las próximas décadas debido al crecimiento de la población, a los cambios en sus hábitos alimenticios y a la proliferación de usos de los cultivos agroalimentarios con fines bioenergéticos (Parry and Hawkesford, 2010). Trigo, maíz y arroz son los tres alimentos básicos principales de la población mundial. De estos cereales, el trigo es el cultivo más importante a escala global y el cambio climático amenaza con reducir la producción del trigo en muchas regiones del mundo, incluida la Mediterránea. La tasa de aumento de los rendimientos lograda con la mejora genética convencional es demasiado baja para igualar la demanda creciente de alimento, por lo que hay una necesidad urgente de incorporar nuevas metodologías que identifiquen atributos deseables para aumentar el rendimiento a través de la mejora.

El sector agroalimentario es uno de los más vulnerables al impacto del cambio climático y la necesidad de aumentar la cantidad y calidad de los cultivos constituye uno de los grandes retos que deberá de afrontar el sector en las próximas décadas. **Este trabajo de Tesis Doctoral aborda estos desafíos y utiliza el trigo por ser uno de los cultivos más importantes a nivel mundial**. Además, el trigo proporciona un 20 % de las calorías y un 22% de las proteínas en la dieta humana. El grano es una fuente importante de carbohidratos, proteínas, aminoácidos, lípidos, minerales, fibra del grano, entre otros, y determinan el valor nutricional y las características de calidad en función del uso final al que se destine (Shewry, 2009). El contenido de proteínas del grano se considera un factor crucial para la calidad del grano y también un factor económico importante, dado que la fracción de proteínas del gluten confiere las propiedades viscoelásticas que permiten que la masa sea procesada para pan, pasta u otros productos alimentarios (ver introducción de esta Tesis Doctoral).

El trigo destaca por ser uno de los cultivos más extendidos en la región mediterránea, una de las más vulnerables al cambio climático. Como se ha indicado previamente, el aumento de la concentración de CO_2 atmosférica irá acompañado de un aumento de la temperatura de la superficie terrestre. Ambos factores ambientales regulan los procesos fisiológicos y fenológicos de las plantas, por lo que tendrán un impacto potencial en la productividad del trigo y la calidad del grano y deberá evaluarse conjuntamente. Por tanto, la mejora del rendimiento y su sostenibilidad en un momento de extrema variabilidad climática es urgente para satisfacer la demanda de alimentos de la creciente población mundial. Para hacer frente a estas limitaciones, se requerirán variedades de cultivos mejor

adaptadas a las nuevas condiciones ambientales para garantizar la seguridad alimentaria y la exploración de la variación natural en la respuesta del trigo a las condiciones climáticas futuras puede ser una herramienta adecuada. El Centro Internacional de Mejoramiento de Maíz y Trigo (CIMMYT) dispone de una gran población de genotipos de trigo en pruebas en ambientes cálidos, a través de su programa de colaboraciones internacionales (la colección 8TH HTWSN). En este estudio se pretende inspeccionar dicha población.

8.2. Objetivos

La hipótesis de trabajo se basa en que la investigación de la variación natural de la tolerancia a la combinación de CO_2 elevado y temperatura alta en un gran número de genotipos de trigo con variabilidad en su respuesta a temperaturas más cálidas permitirá identificar aquellos con productividad contrastante. Estos genotipos constituirán una herramienta de utilidad para la caracterización de los cambios en los parámetros fisiológicos y el estado metabólico y antioxidante que confieren adaptación a las condiciones anticipadas por el calentamiento global.

Con este propósito, **el objetivo principal de esta Tesis Doctoral** fue investigar los mecanismos de adaptación del crecimiento y la producción de trigo a la combinación de CO_2 elevado y temperatura alta, estudiando la relación de la biomasa con los metabolitos y actividades enzimáticas del metabolismo primario del carbono y del nitrógeno, y el estatus antioxidante de la colección del CIMMYT, así como su repercusión en la calidad nutricional del grano.

Para lograr este objetivo general, se propusieron los siguientes **objetivos específicos**:

1) Evaluar la variación natural existente en el rendimiento del trigo en respuesta a la combinación de CO_2 elevado y temperatura alta.

Para alcanzar este objetivo, un amplio grupo de 60 genotipos de trigo se cultivaron en cámaras de ambiente controlado para obtener un control total de los parámetros climáticos. El estudio incluyó 59 genotipos de la colección del CIMMYT previamente seleccionados por su alto rendimiento en temperaturas más cálidas, junto con el genotipo Gazul con alta adaptabilidad al clima mediterráneo de la región de Salamanca (España).

2) Investigar la variación en el rendimiento y la calidad nutricional del grano en varios genotipos de trigo con diferente productividad cultivados bajo CO_2 elevado y temperatura alta.

Con este propósito, se usaron 10 genotipos seleccionados entre los 60 previamente evaluados en la respuesta del rendimiento en las mismas condiciones ambientales.

3) Caracterizar los mecanismos fisiológicos y bioquímicos involucrados en la variación en el rendimiento entre los 10 genotipos de trigo que previamente mostraron diferencias en el rendimiento y la calidad nutricional del grano bajo condiciones de CO_2 elevado y temperatura alta.

Con este objetivo, se evaluó la variabilidad genotípica en un rango de parámetros fisiológicos de la hoja, el status antioxidante, metabolitos y actividades de enzimas del metabolismo primario, así como sus asociaciones con el rendimiento y los caracteres de calidad del grano.

Esta actividad de investigación se alinea con los Desafíos de la sociedad, en particular el Desafío 2: **Seguridad**, **calidad de los alimentos**; productividad y sostenibilidad de la actividad agrícola.

8.3. Metodología

Aun cuando son muchos los estudios que han investigado la magnitud del impacto del cambio climático en la fisiología y la productividad de las plantas, en su mayoría se han realizado con un único genotipo y sin considerar el efecto combinado del CO_2 elevado y la temperatura alta. Para la simulación del ambiente futuro según previsiones de cambio climático para finales de siglo, en los dos experimentos realizados en esta tesis doctoral se emplearon cámaras de crecimiento de ambientes controlado disponibles en el Servicio de Fitrotrón (IRNASA-CSIC). Así, las plantas se cultivaron desde la siembra hasta la madurez del cultivo en una atmósfera enriquecida en CO_2 (700 µmol mol^{-1}), que se alcanzó insuflando CO_2 puro, con un fotoperiodo de 16 horas de luz y 8 horas de oscuridad, con una intensidad luminosa de unos 400 µmol m^{-2} s^{-1} y una humedad relativa de 40 %/ 60% día/noche (Vicente *et al.*, 2015b, 2016). La temperatura en el interior de las cámaras se elevó en 4 ºC las temperaturas actuales simulando las oscilaciones diarias y estacionales típicas en ambientes naturales en la región de Salamanca, en base a las temperaturas promedio recogidas durante 10 años en la finca experimental de Muñovela del IRNASA-CSIC(Vicente *et al.*, 2015b). Para las fluctuaciones diarias de temperatura se establecieron cuatro secciones correspondientes a la noche y las partes inicial, central y final del fotoperiodo como se describe en (Marcos-Barbero *et al.*, 2021b). Además, estas temperaturas se incrementaron en tres niveles para reproducir las oscilaciones estacionales a lo largo del desarrollo del trigo, correspondientes a las fases vegetativas, emergencia de la espiga y llenado del grano de trigo. Los diferentes genotipos de trigo se cultivaron en macetas de 5 L provistas de una mezcla de turba y perlita en proporción (4:1). Se aplicó fertilizante a razón de 4 g of KNO_3 and 4 g of KH_2PO_4 por maceta mientras que la turba proporcionó el resto de nutrientes (Córdoba *et al.*, 2015; Marcos-Barbero *et al.*, 2021a, 2021b). Se sembraron 7 semillas por maceta y después de la emergencia de las plántulas se procedió al aclarado hasta dejar 5 plantas por maceta. El

riego se realizó tres veces por semana hasta capacidad de campo y las macetas se rotaron en el interior de las cámaras para evitar el efecto borde.

En el primer experimento se cultivaron los sesenta genotipos de trigo en las condiciones ambientales descritas previamente y en la madurez del cultivo se recogió el material vegetal para la estimación de la biomasa y los componentes del rendimiento.

En el segundo experimento, se cultivaron 10 genotipos con diferente productividad (9 de la colección 8TH HTWSN y la variedad Gazul). En la emergencia de la espiga, se recogieron muestras de la hoja bandera el trigo por inmersión inmediata en nitrógeno líquido para la realización de los diferentes análisis bioquímicos planteados en este trabajo de investigación, así como muestras para el análisis del crecimiento de las plantas. Además, en la madurez se recogieron muestras para la estimación del rendimiento y la evaluación de los parámetros de calidad del grano de trigo.

Los resultados más relevantes de este trabajo de investigación se describen en varios de los capítulos de esta Tesis Doctoral, y algunos de ellos ya han sido publicados en revistas científicas internacional les del primer cuartil (Marcos-Barbero *et al.*, 2021a, 2021b).

A continuación, se detallan **las conclusiones de este trabajo de Tesis Doctoral**:

8.4. Conclusiones

Primera. Este estudio demuestra que la exploración de la diversidad genética es una herramienta apropiada, no sólo para la selección de genotipos con mejor capacidad de adaptación al futuro calentamiento global, sino también para la identificación de aquellos genotipos con mejor calidad nutricional del grano.

Segunda. Los genotipos del CIMMYT respondieron mejor que el genotipo Gazul en condiciones de CO_2 y temperatura elevados, lo que demuestra el éxito de los programas de mejora del CIMMYT en temperaturas más cálidas y la plasticidad de las plantas para responder a la concurrencia de varios factores ambientales.

Tercera. La disección de los caracteres relacionados con el rendimiento en el presente estudio revela que los genotipos de trigo emplearon diversas estrategias para lograr el rendimiento final de grano en las condiciones ambientales estudiadas, muy probablemente derivadas de los diferentes

programas de mejora vegetal utilizados para incrementar el rendimiento de grano a lo largo del siglo XX.

Cuarta. El mayor rendimiento de grano se asoció con un aumento en el número de granos y espigas por planta, más que con el peso por grano. Por tanto, aquellos genotipos que pueden aumentar preferentemente el número de granos y espigas por planta conseguirán un mayor rendimiento de grano en condiciones de CO_2 y temperatura elevados.

Quinta. La fenología, en particular la precocidad de espigado, no parece ser la única causa de la variabilidad en el rendimiento de grano y, por ello, deberían de considerarse otras características. La capacidad de ahijamiento, y por tanto un aumento en el número de tallos productivos, será un factor importante en la respuesta del rendimiento al funcionar como sumideros para la adscripción del exceso de carbohidratos producidos en las condiciones ambientales estudiadas.

Sexta. Una mejora en el contenido de proteína y calidad nutricional del grano puede conseguirse a costa de un menor rendimiento, que se acompaña de una menor concentración de algunos nutrientes minerales y capacidad antioxidante total en el grano, particularmente en Gazul.

Séptima. Un genotipo de alto rendimiento con una concentración de proteínas en el grano ligeramente menor, que se compensa con un enriquecimiento en algunos nutrientes minerales y compuesto bioactivos con efectos beneficiosos para la salud humana, podría seleccionarse por sus prometedoras características nutricionales.

Octava. El aumento de la transpiración y del estado hídrico y nitrogenado en Gazul condujo a una mejora en la translocación de fotoasimilados y la capacidad antioxidante que se acompañó de una menor acumulación de carbohidratos y un aumento de la actividad de enzimas del metabolismo del carbono y nitrógeno que promueve el flujo del carbono desde la glicolisis a la síntesis a la síntesis de ácidos orgánicos y posterior biosíntesis de aminoácidos. La mejora del estado nitrogenado en la emergencia de la espiga se tradujo en un aumento en la concentración de proteínas y nutrientes en el grano y, por ende, en una mejor calidad nutricional de los granos en la madurez.

Novena. Los genotipos de alto rendimiento fueron más proclives a una reducción de nitrógeno y mostraron un aumento en la actividad glutamato deshidrogenasa, lo cual indica un predominio del catabolismo de proteínas para proporcionar compuestos nitrogenados para el mantenimiento del crecimiento. Además, el descenso del contenido de nitrógeno puede limitar los beneficios de la combinación del CO2 elevado y la temperatura alta en el rendimiento de grano y afectar su valor nutricional para la salud humana.

Décima. Este estudio proporciona nuevos conocimientos sobre la reprogramación diferencial del metabolismo primario del carbono y el nitrógeno entre genotipos de trigo de alto y bajo rendimiento en condiciones climáticas futuras, y revela que el contenido de almidón de la hoja bandera podría considerarse un marcador positivo para la selección de genotipos de alto rendimiento frente al calentamiento global.

Décimo primera. Será necesario investigar si los genotipos de alto rendimiento identificados en este estudio podrán mantener su mejora en el rendimiento, con independencia de la disponibilidad nutricional e hídrica, en combinación con la temperatura alta y el CO_2 elevado, lo cual abre nuevas oportunidades para la selección de genotipos de trigo ampliamente adaptados resilientes al clima.

CHAPTER 9

Supplementary material

Introduction

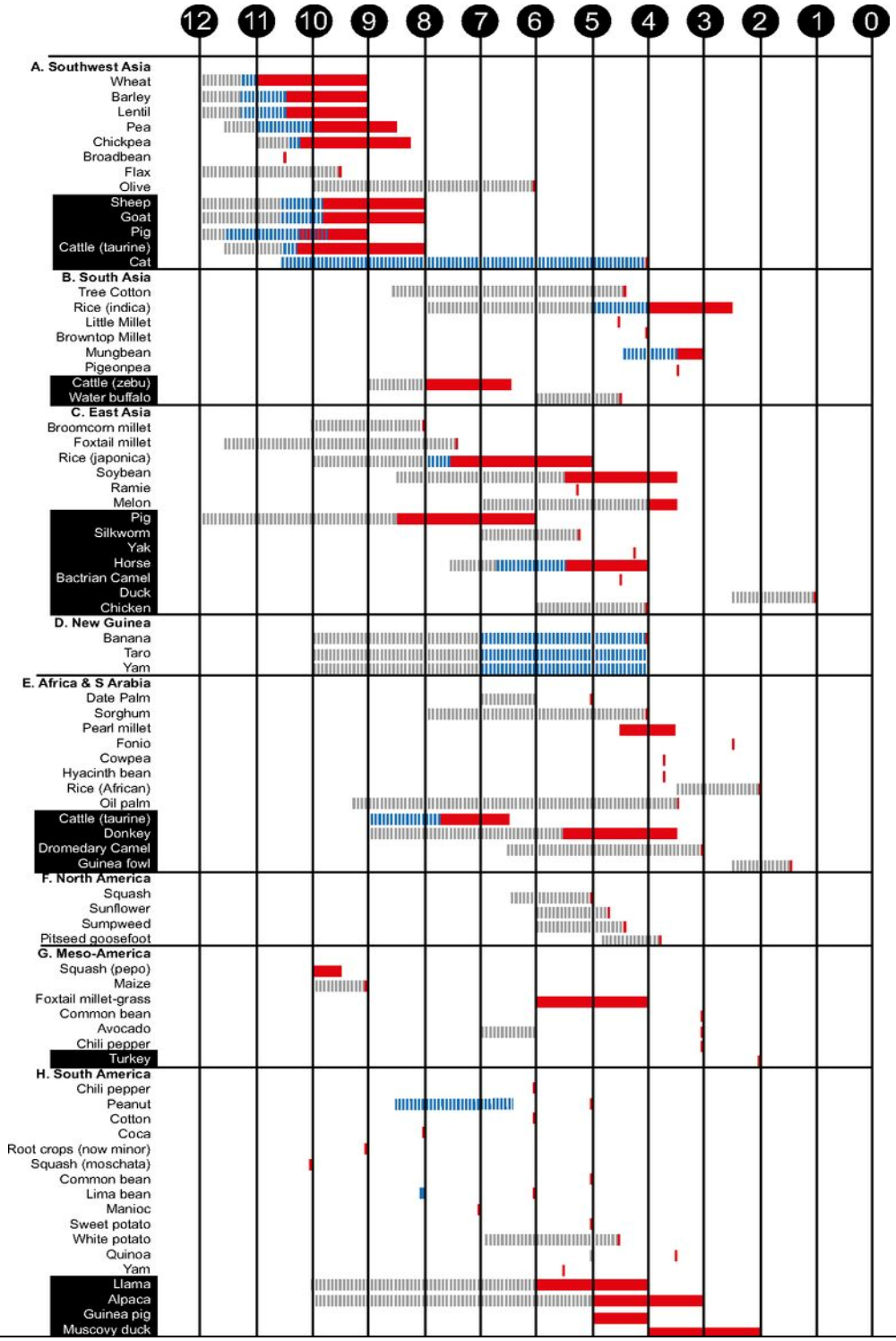

Figure S1.1. A chronological chart listing the regions where, and the time frames over which, key plants and animals were domesticated.

Numbers in black circles represent thousands of years before present. Dashed lines represent pre-domestication exploitation (grey) and management during domestication (blue) of plants and animals. Red bars indicate appearance of morphological modifications in domesticated species. Letters A–H correspond to those found in Figure 1.1. Retrieved from (Larson *et al.*, 2014).

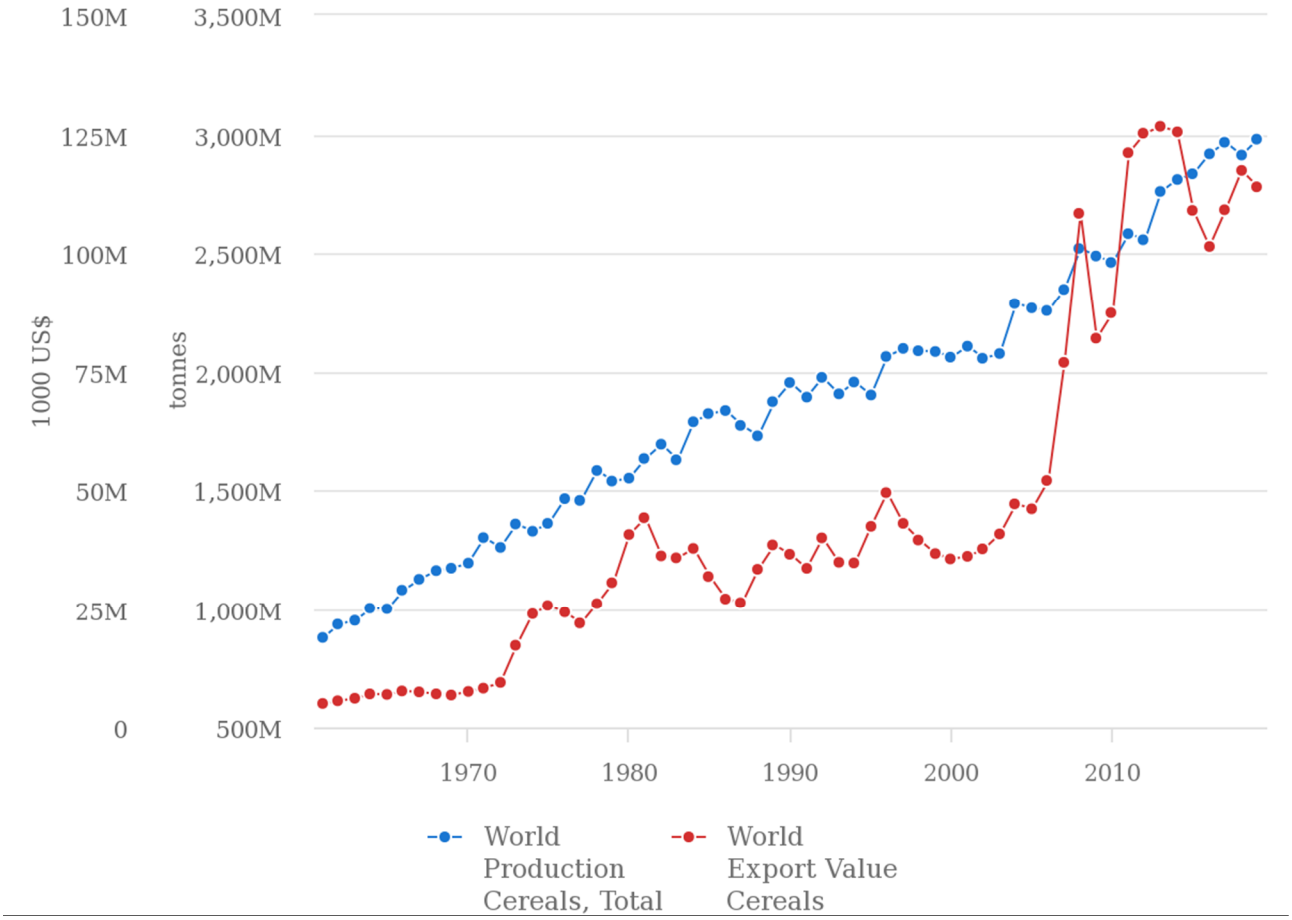

Figure S1.2. Trends in global cereal production (blue) and export value (red).

Retrieved from (FAO, 2021)

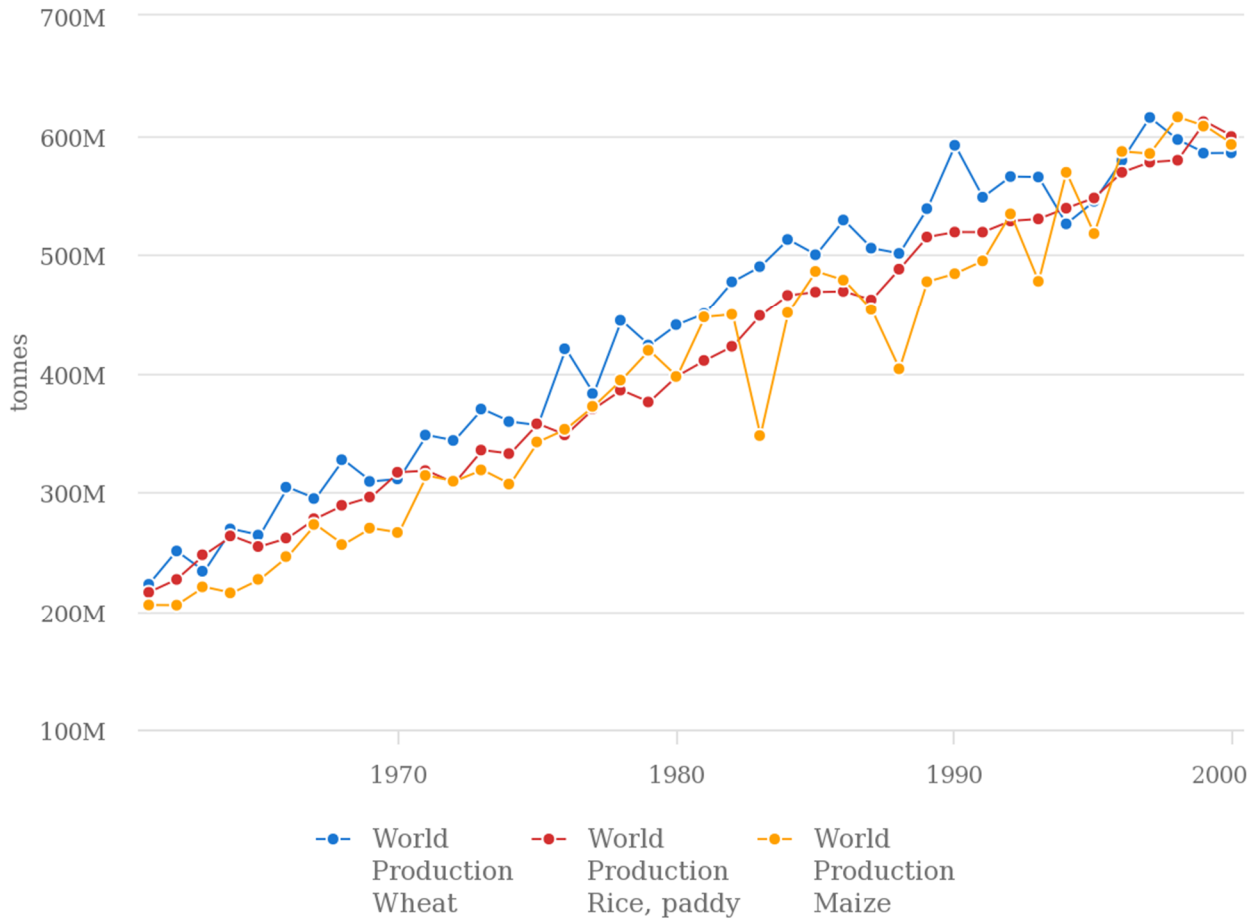

Figure S1.3. Trends in global production of wheat(blue), rice (red) and maize (yellow).

Retrieved from (FAO, 2021)

Materials and methods

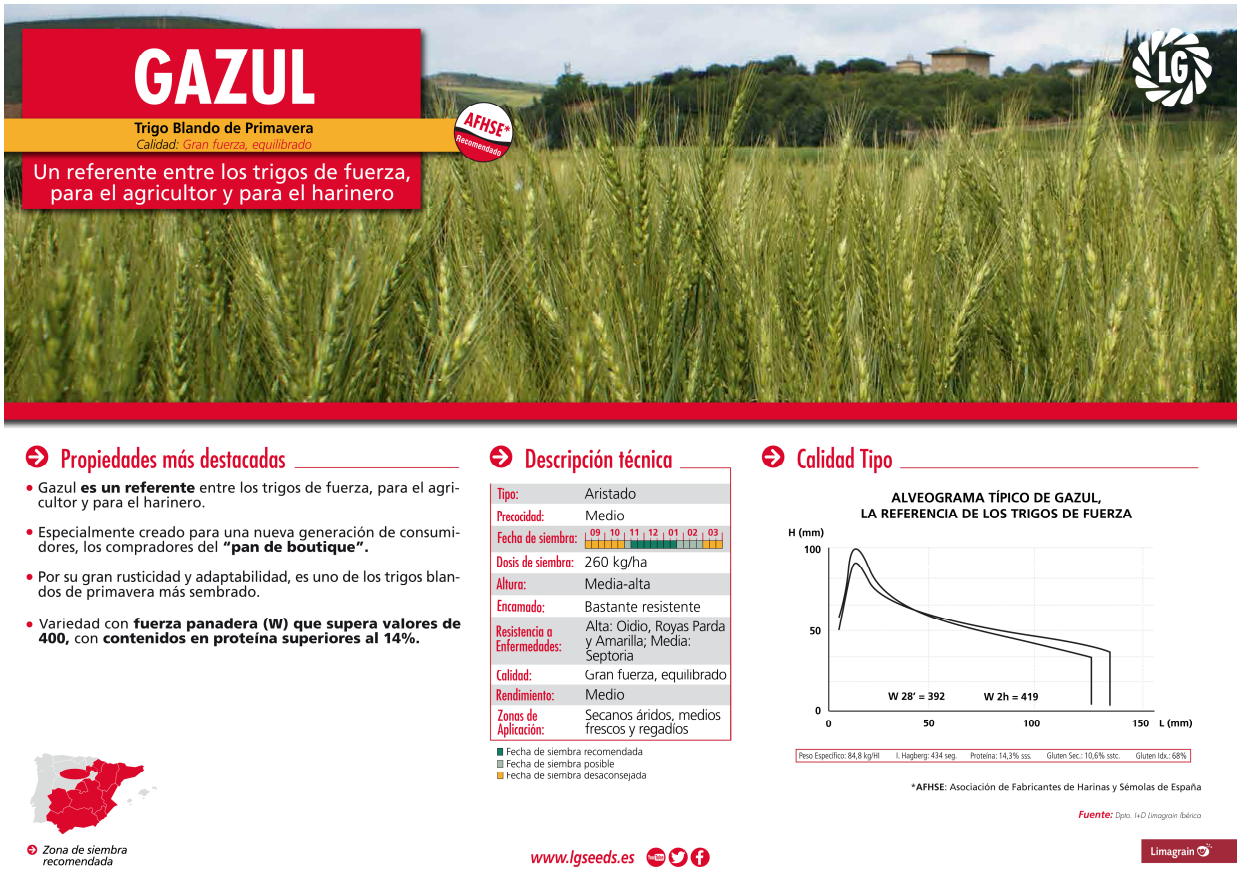

Figure S3.1. Gazul variety technical datasheet.

Retrieved from (https://www.lgseeds.es/media/GAZUL.pdf).

Table S3.1. Glutamine Synthetase continuous assay.

Assay Mix (50 µL/well)	1 Plate (110 Well)			2 Plates (220 Well)		
	V_o	V_{Sat}	Total	V_o	V_{Sat}	Total
• ***A01 Assay buffer 5x (20 µL/well)***	**1100 µl**	**1100 µl**	**2200 µl**	**2200 µl**	**2200 µl**	**4400 µl**
▪ *$MgCl_2$ 0.1M*						
▪ *Hepes/KOH 0.5M pH 7.5*						
▪ *$NaVO_3$ 2mM (phosphatase inhibitor)*						
▪ *5',5' Diadenosinpentaphosphate 0.4 mM (Myokinase-Inhibitor)*						
▪ *NH_4Cl 20mM*						
▪ *EDTA10 mM*						
▪ *Triton x100 0.25%*						
• ***Glycerol 100% W/V (10 µL/well)***	**550 µL**	**550 µL**	**1100 µl**	**1100 µl**	**1100 µl**	**2200 µl**
• ***PEP 20mM (5 µL/well)***	**275 µL**	**275 µL**	**550 µL**	**550 µL**	**550 µL**	**1100 µl**
• ***ATP 100mM (5 µL/well)***	**275 µL**	**275 µL**	**550 µL**	**550 µL**	**550 µL**	**1100 µl**
• ***H_2O (6 µL/well)***	**330 µl**	**330 µl**	**660 µl**	**660 µl**	**660 µl**	**1320 µl**
• ***NADH 60mM in 60mM NaOH (1 µL/well)***	**55 µl**	**55 µl**	**110 µl**	**110 µl**	**110 µl**	**220 µl**
• ***Pyruvate kinase 50 u/mL in 200mM Hepes/KOH pH 7.5, 10 mM $MgCl_2$ (2 µL/well)****	**110 µl**	**110 µl**	**220 µl**	**220 µl**	**220 µl**	**440 µl**
• ***Lactate DH 60 u/mL in 200mM Hepes/KOH pH 7.5, 10 mM $MgCl_2$ (1 µL/well)****	**55 µl**	**55 µl**	**110 µl**	**110 µl**	**110 µl**	**220 µl**
• ***H_2O (45 µL/well)***	**2475 µl**	----------	**2475 µl**	**4950 µl**	----------	**4950 µl**
• ***L-Glutamate 100 mM (45 µL/well)***	----------	**2475 µl**	**2475 µl**	----------	**4950 µl**	**4950 µl**
TOTAL	**5225 µl**	**5225 µl**	**10450 µl**	**10450 µl**	**10450 µl**	**20900 µl**

Table S3.2. Glucose−6−Phosphate Dehydrogenase continuous assay.

Assay Mix (95 µL/well)	1 Plate (110 Well)			2 Plates (220 Well)		
	V_o	V_{Sat}	Total	V_o	V_{Sat}	Total
• ***A15 Assay buffer 5x (20 µL/well)***	**1100 µl**	**1100 µl**	**2200 µl**	**2200 µl**	**2200 µl**	**4400 µl**
▪ *Tricine/KOH 0.5M pH 8.5*						
▪ *$MgCl_2$ 0.05M*						
▪ *Triton x100 0.25%*						
• ***H_2O (22.5 µL/well)***	**1237,5 µl**	**1237,5 µl**	**2475 µl**	**2475 µl**	**2475 µl**	**4950 µl**
• ***$NADP^+$ 20m (2.5 µL/well)***	**137,5 µl**	**137,5 µl**	**275 µl**	**275 µl**	**275 µl**	**550 µl**
• ***H_2O (50 µL/well)***	**2750 µl**	----------	**2750 µl**	**5500 µl**	----------	**5500 µl**
• ***G6P 50 mM (50 µL/well)***	----------	**2750 µl**	**2750 µl**	----------	**5500 µl**	**5500 µl**
TOTAL	**5225 µl**	**5225 µl**	**10450 µl**	**10450 µl**	**10450 µl**	**20900 µl**

Table S3.3. Phosphoenolpyruvate Carboxylase continuous assay.

Assay Mix (95 µL/well)	1 Plate (110 Well)			2 Plates (220 Well)		
	V_o	V_{Sat}	Total	V_o	V_{Sat}	Total
• ***A13 Assay buffer 5x (20 µL/well)***	**1100 µl**	**1100 µl**	**2200 µl**	**2200 µl**	**2200 µl**	**4400 µl**
• *$MgCl_2$ 100 mM*						
▪ *Tricine/KOH 0.5M pH8*						
▪ *$NaHCO_3$ 50 mM*						
▪ *Triton x100 0.25%*						
• ***H_2O (54 µL/well)***	**2970 µl**	**2970 µl**	**5940 µl**	**5940 µl**	**5940 µl**	**11880 µl**
• ***Malate DH 100 u/mL in 200mM Tricine/KOH pH 8.0, 10 mM $MgCl_2$ (10 µL/well)****	**550 µl**	**550 µl**	**1100 µl**	**1100 µl**	**1100 µl**	**2200 µl**
• ***PEP 20 mM (10 µL/well)***	----------	**550 µl**	**550 µl**	----------	**1100 µl**	**1100 µl**
• ***H_2O (10 µL/well)***	**550 µl**	----------	**550 µl**	**1100 µl**	----------	**1100 µl**
• ***NADH 60 mM in 60 mM NaOH (1 µL/well)***	**55 µl**	**55 µl**	**110 µl**	**110 µl**	**110 µl**	**220 µl**
TOTAL	**5225 µl**	**5225 µl**	**10450 µl**	**10450 µl**	**10450 µl**	**20900 µl**

Table S3.4. ADP-Glucose Pyrophosphorylase discontinuous assay.

Assay Mix (18 µL/well)	1 Plate (110 Well)			2 Plates (220 Well)		
	V_o	V_{Sat}	Total	V_o	V_{Sat}	Total
• ***B02 Assay buffer 5x (4 µL/well)***	**220 µl**	**220 µl**	**440 µl**	**440 µl**	**440 µl**	**880 µl**
▪ *Hepes/KOH 0.25M pH 7.5*						
▪ *NaF 7.5mM*						
▪ *$MgCl_2$ 25mM*						
▪ *3-Phosphoglycerate 5mM*						
▪ *Triton X 100 0.25%*						
• ***H_2O (9.4 µL/well)***	**517 µl**	**517 µl**	**1034 µl**	**1034 µl**	**1034 µl**	**2068 µl**
• ***H_2O (0.4 µL/well)***	**22 µl**	----------	**22 µl**	**44 µl**	----------	**44 µl**
• ***ADP-Glucose 100 mM (0.4 µL/well)***	----------	**22 µl**	**22 µl**	----------	**44 µl**	**44 µl**
• ***PPi 20 mM (2 µL/well)***	**110 µl**	**110 µl**	**220 µl**	**220 µl**	**220 µl**	**440 µL**
• ***DAPP 2 mM (2 µL/well)***	**110 µl**	**110 µl**	**220 µl**	**220 µl**	**220 µl**	**440 µL**
• ***Glycerokinase (E. Coli) 200 u/mL in 200mM Tricine/ KOH pH 8.0, 10 mM $MgCl_2$ (0.2 µL/well)****	**11 µl**	**11 µl**	**22 µl**	**22 µl**	**22 µl**	**44 µL**
TOTAL	**990 µl**	**990 µl**	**1980 µl**	**1980 µl**	**1980 µl**	**3960 µl**
Add Extract (2 µL/well), mix and incubate at 25ºC 20min						
Add HCl 0.5M in 100mM Tricine/KOH pH 9 (20 µL/well)						
Mix, spin down, incubate at 95ºC for 10 min, cool and spin down						
Add NaOH 0.5M (20 µL/well)						
Determination Mix (50 µL/well)	**1 Plate (125 Well)**			**2 Plates (250 Well)**		
	V_o	V_{Sat}	Total	V_o	V_{Sat}	Total
• ***H_2O (37.8 µL/well)***	2362.5 µl	2362.5µl	**4725 µl**	4725 µl	4725 µl	**9450 µl**
• ***Tricine/KOH 1M pH 8 (10 µL/well)***	625 µl	625 µl	**1250 µl**	1250 µl	1250 µl	**2500 µl**
• ***$MgCl_2$ 1M (0.2 µL/well)***	12.5 µl	12.5 µl	**25 µl**	25 µl	25 µl	**50 µl**
• ***Glycerol 3-Phosphate DH 200 u/mL in 200mM Tricine/KOH pH 8.0, 10 mM $MgCl_2$ (0.5 µL/well)****	31.25 µl	31.25 µl	**62.5 µl**	62.5 µl	62.5 µl	**125 µl**
• ***GPOX 500 u/mL in 200mM Tricine/KOH pH 8.0, 10 mM $MgCl_2$ (0.5 µL/well)****	31.25 µl	31.25 µl	**62.5 µl**	62.5 µl	62.5 µl	**125 µl**
• ***NADH 66mM in NaOH 60mM (1 µL/well)***	62.5 µl	62.5 µl	**125 µl**	125 µl	125 µl	**250 µl**
TOTAL	3125 µl	3125 µl	**6250 µl**	6250 µl	6250 µl	**12500 µl**

Table S3.5. Pyruvate Kinase discontinuous assay.

Assay Mix (18 µL/well)	1 Plate (110 Well)			2 Plates (220 Well)		
	V_o	V_{Sat}	Total	V_o	V_{Sat}	Total
• ***B04 Assay buffer 5x (4 µL/well)***	**220 µl**	**220 µl**	**440 µl**	**440 µl**	**440 µl**	**880 µl**
▪ *Tricine/KOH 0.5M pH 8*						
▪ *KCl 0.5mM*						
▪ *$MgCl_2$ 50mM*						
▪ *EDTA 2mM*						
▪ *Triton X 100 0.25%*						
• ***H_2O (10.6 µL/well)***	**583 µl**	**583 µl**	**1166 µl**	**1166 µl**	**1166 µl**	**2332 µl**
• ***H_2O (2 µL/well)***	**110 µl**	----------	**110 µl**	**220 µl**	----------	**220 µl**
• ***PEP (Phosphoenolpyruvate) 50mM (2 µL/well)***	----------	**110 µl**	**110 µl**	----------	**220 µl**	**220 µl**
• ***ADP 20mM (1 µL/well)***	**55 µl**	**55 µl**	**110 µl**	**110 µl**	**110 µl**	**220 µL**
• ***AMP 100 mM (0.2 µL/well)***	**11 µl**	**11 µl**	**22 µl**	**22 µl**	**22 µl**	**44 µL**
• ***Glycerokinase (E. Coli) 200 u/mL in 200mM Tricine/ KOH pH 8.0, 10 mM $MgCl_2$ (0.2 µL/well)****	**11 µl**	**11 µl**	**22 µl**	**22 µl**	**22 µl**	**44 µL**
TOTAL	**990 µl**	**990 µl**	**1980 µl**	**1980 µl**	**1980 µl**	**3960 µl**
Add Extract (2 µL/well), mix and incubate at 25ºC 20min						
Add HCl 0.5M in 100mM Tricine/KOH pH 9 (20 µL/well)						
Mix, spin down, incubate at 95ºC for 10 min, cool and spin down						
Add NaOH 0.5M (20 µL/well)						
Determination Mix (50 µL/well)	**1 Plate (125 Well)**			**2 Plates (250 Well)**		
	V_o	V_{Sat}	Total	V_o	V_{Sat}	Total
• ***H_2O (37.8 µL/well)***	2362.5 µl	2362.5µl	**4725 µl**	4725 µl	4725 µl	**9450 µl**
• ***Tricine/KOH 1M pH 8 (10 µL/well)***	625 µl	625 µl	**1250 µl**	1250 µl	1250 µl	**2500 µl**
• ***$MgCl_2$ 1M (0.2 µL/well)***	12.5 µl	12.5 µl	**25 µl**	25 µl	25 µl	**50 µl**
• ***Glycerol 3-Phosphate DH 200 u/mL in 200mM Tricine/KOH pH 8.0, 10 mM $MgCl_2$ (0.5 µL/well)****	31.25 µl	31.25 µl	**62.5 µl**	62.5 µl	62.5 µl	**125 µl**
• ***GPOX 500 u/mL in 200mM Tricine/KOH pH 8.0, 10 mM $MgCl_2$ (0.5 µL/well)****	31.25 µl	31.25 µl	**62.5 µl**	62.5 µl	62.5 µl	**125 µl**
• ***NADH 66mM in NaOH 60mM (1 µL/well)***	62.5 µl	62.5 µl	**125 µl**	125 µl	125 µl	**250 µl**
TOTAL	3125 µl	3125 µl	**6250 µl**	6250 µl	6250 µl	**12500 µl**

Table S3.6. Cytosolic Fructose-1,6-Bisphosphatese discontinuous assay.

Assay Mix (18 µL/well)	1 Plate (110 Well)			2 Plates (220 Well)		
	V_o	V_{Sat}	Total	V_o	V_{Sat}	Total
• ***C01 Assay buffer 5x (4 µL/well)***	**220 µl**	**220 µl**	**440 µl**	**440 µl**	**440 µl**	**880 µl**
▪ *Hepes/KOH 0.25M pH 7*						
▪ *$MgCl_2$ 10mM*						
▪ *Triton X 100 0.25%*						
• ***H_2O (11 µL/well)***	**605 µl**	**605 µl**	**1210 µl**	**1210 µl**	**1210 µl**	**2420 µl**
• ***H_2O (2 µL/well)***	**110 µl**	----------	**110 µl**	**220 µl**	----------	**220 µl**
• ***Fru1,6BP 200 µM (2 µL/well)***	----------	**110 µl**	**110 µl**	----------	**220 µl**	**220 µl**
• ***$NADP^+$ 20 mM (0.4 µL/well)***	**22 µl**	**22 µl**	**44 µl**	**44 µl**	**44 µl**	**88 µL**
• ***G6PDH grade II 50 u/mL in 200mM Tricine/ KOH pH 8.0, 10 mM $MgCl_2$ (0.4 µL/well)****	**22 µl**	**22 µl**	**44 µl**	**44 µl**	**44 µl**	**88 µL**
• ***PGI 100 u/mL in 200 mM Tricine/ KOH pH 8.0, 10 mM $MgCl_2$ (0.2 µL/well)****	**11 µl**	**11 µl**	**22 µl**	**22 µl**	**22 µl**	**44 µl**
TOTAL	**990 µl**	**990 µl**	**1980 µl**	**1980 µl**	**1980 µl**	**3960 µl**
Add Extract (2 µL/well), mix and incubate at 25ºC 20min						
Add NaOH 0.5M (20 µL/well)						
Mix, spin down, incubate at 95ºC for 10 min, cool and spin down						
Add HCl 0.5M in 100mM Tricine/KOH pH 9 (20 µL/well)						
Determination Mix (50 µL/well)	**1 Plate (125 Well)**			**2 Plates (250 Well)**		
	V_o	V_{Sat}	Total	V_o	V_{Sat}	Total
• ***H_2O (18.5 µL/well)***	**1156.25 µl**	**1156.25 µl**	**2312.5 µl**	**2312.5 µl**	**2312.5 µl**	**4625 µl**
• ***Tricine/KOH 1M pH 9 (10 µL/well)***	**625 µl**	**625 µl**	**1250 µl**	**1250 µl**	**1250 µl**	**2500 µl**
• ***EDTA 200mM (4 µL/well)***	**250 µl**	**250 µl**	**500 µl**	**500 µl**	**500 µl**	**1000 µl**
• ***G6P 250mM (2 µL/well)***	**125 µl**	**125 µl**	**250 µl**	**250 µl**	**250 µl**	**500 µl**
• ***G6PDH grade I 500 u/mL in 200mM Tricine/ KOH pH 9.0, 10 mM $MgCl_2$ (0.5 µL/well)****	**31.25 µl**	**31.25 µl**	**62.5 µl**	**62.5 µl**	**62.5 µl**	**125 µl**
• ***MTT 10mM (10 µL/well) *****	**625 µl**	**625 µl**	**1250 µl**	**1250 µl**	**1250 µl**	**2500 µl**
• ***PES 4mM (5 µL/well) *****	**312.5 µl**	**312.5 µl**	**625 µl**	**625 µl**	**625 µl**	**1250 µl**
TOTAL	**3125 µl**	**3125 µl**	**6250 µl**	**6250 µl**	**6250 µl**	**12500 µl**

Table S3.7. NADP-dependent Isocitrate Dehydrogenase discontinuous assay..

Assay Mix (18 µL/well)	1 Plate (110 Well)			2 Plates (220 Well)		
	V_o	V_{Sat}	Total	V_o	V_{Sat}	Total
• ***C04 Assay buffer 5x (4 µL/well)***	**220 µl**	**220 µl**	**440 µl**	**440 µl**	**440 µl**	**880 µl**
▪ *Tricine/KOH 0.5M pH 8.5*						
▪ *$MgCl_2$ 40mM*						
▪ *Triton X 100 0.25%*						
• ***H_2O (7 µL/well)***	**385 µl**	**385 µl**	**770 µl**	**770 µl**	**770 µl**	**1540 µl**
• ***H_2O (2 µL/well)***	**110 µl**	----------	**110 µl**	**220 µl**	----------	**220 µl**
• ***Isocitrate 20 mM (2 µL/well)***	----------	**110 µl**	**110 µl**	----------	**220 µl**	**220 µl**
• ***$NADP^+$ 20 mM (5µL/well)***	**275 µl**	**275 µl**	**550 µl**	**550 µl**	**550 µl**	**1100 µL**
TOTAL	**990 µl**	**990 µl**	**1980 µl**	**1980 µl**	**1980 µl**	**3960 µl**
Add Extract (2 µL/well), mix and incubate at 25ºC 20min						
Add NaOH 0.5M (20 µL/well)						
Mix, spin down, incubate at 95ºC for 10 min, cool and spin down						
Add HCl 0.5M in 100mM Tricine/KOH pH 9 (20 µL/well)						
Determination Mix (50 µL/well)	**1 Plate (125 Well)**			**2 Plates (250 Well)**		
	V_o	V_{Sat}	Total	V_o	V_{Sat}	Total
• ***H_2O (18.5 µL/well)***	1156.25 µl	1156.25 µl	**2312.5 µl**	2312.5 µl	2312.5 µl	**4625 µl**
• ***Tricine/KOH 1M pH 9 (10 µL/well)***	625 µl	625 µl	**1250 µl**	1250 µl	1250 µl	**2500 µl**
• ***EDTA 200mM (4 µL/well)***	250 µl	250 µl	**500 µl**	500 µl	500 µl	**1000 µl**
• ***G6P 250mM (2 µL/well)***	125 µl	125 µl	**250 µl**	250 µl	250 µl	**500 µl**
• ***G6PDH grade I 500 u/mL in 200mM Tricine/ KOH pH 9.0, 10 mM $MgCl_2$ (0.5 µL/well)****	31.25 µl	31.25 µl	**62.5 µl**	62.5 µl	62.5 µl	**125 µl**
• ***MTT 10mM (10 µL/well) *****	625 µl	625 µl	**1250 µl**	1250 µl	1250 µl	**2500 µl**
• ***PES 4mM (5 µL/well) *****	312.5 µl	312.5 µl	**625 µl**	625 µl	625 µl	**1250 µl**
TOTAL	3125 µl	3125 µl	**6250 µl**	6250 µl	6250 µl	**12500 µl**

Table S3.8. Glutamate Dehydrogenase discontinuous assay.

Assay Mix (18 µL/well)	1 Plate (110 Well)			2 Plates (220 Well)		
	V_o	V_{Sat}	Total	V_o	V_{Sat}	Total
• ***D02 Assay buffer 5x (4 µL/well)***	**220 µl**	**220 µl**	**440 µl**	**440 µl**	**440 µl**	**880 µl**
▪ *Tricine/KOH 0.5M pH 8*						
▪ *$CaCl_2$ 5mM*						
▪ *NH_4 Acetate 3.2M*						
▪ *Triton X 100 0.25%*						
• ***H_2O (11.6 µL/well)***	**638 µl**	**638 µl**	**1276 µl**	**1276 µl**	**1276 µl**	**2552 µl**
• ***H_2O (2 µL/well)***	**110 µl**	----------	**110 µl**	**220 µl**	----------	**220 µl**
• ***2-oxoglutarate 150mM (2 µL/well)***	----------	**110 µl**	**110 µl**	----------	**220 µl**	**220 µl**
• ***NADH 5 mM in 5mM NaOH (0.4 µL/well)***	**22 µl**	**22 µl**	**44 µl**	**44 µl**	**44 µl**	**88 µl**
TOTAL	**990 µl**	**990 µl**	**1980 µl**	**1980 µl**	**1980 µl**	**3960 µl**
Add Extract (2 µL/well), mix and incubate at 25ºC 20min						
Add HCl 0.5M in 100mM Tricine/KOH pH 9 (20 µL/well)						
Mix, spin down, incubate at 90ºC for 10 min, cool and spin down						
Add NaOH 0.5M (20 µL/well)						
Determination Mix (50 µL/well)	**1 Plate (125 Well)**			**2 Plates (250 Well)**		
	V_o	V_{Sat}	Total	V_{Sat}	V_o	Total
• ***H_2O (18 µL/well)***	1125 µl	1125 µl	**2250 µl**	2250 µl	2250 µl	**4500 µl**
• ***Tricine/KOH 1M pH 9 (10 µL/well)***	625 µl	625 µl	**1250 µl**	1250 µl	1250 µl	**2500 µl**
• ***EDTA 200mM (4 µL/well)***	250 µl	250 µl	**500 µl**	500 µl	500 µl	**1000 µl**
• ***Ethanol 50% (2 µL/well)***	125 µl	125 µl	**250 µl**	250 µl	250 µl	**500 µl**
• ***Alcohol Dehydrogenase 2000 u/mL in 200mM Tricine/ KOH pH 9.0, 10 mM $MgCl_2$ (1 µL/well)****	62.5 µl	62.5 µl	**125 µl**	125 µl	125 µl	**250 µl**
• ***MTT 10mM (10 µL/well) *****	625 µl	625 µl	**1250 µl**	1250 µl	1250 µl	**2500 µl**
• ***PES 4mM (5 µL/well) *****	312.5 µl	312.5 µl	**625 µl**	625 µl	625 µl	**1250 µl**
TOTAL	2750 µl	2750 µl	**6250 µl**	6250 µl	6250 µl	**12500 µl**

Experiment I. Study I

Table S4.1. MANOVA of genotype factor for the grain yield and their related traits in the response of 60 wheat genotypes grown under combined elevated atmospheric CO_2 and temperature at maturity.

Traits	df1	df2	Statistic	*p*-value	Effect size
Grain yield [I]	59	180	3.55	**$4.08x10^{-11}$**	0.54
Aboveground [I]	59	180	3.70	**$8.82x10^{-12}$**	0.55
Stalk [I]	59	180	3.27	**$6.67x10^{-10}$**	0.52
Chaff [I]	59	180	4.92	**$8.18x10^{-17}$**	0.62
Height [I]	59	180	8.74	**$6.38x10^{-30}$**	0.74
Grain number [I]	59	180	7.26	**$2.85x10^{-25}$**	0.70
Ear number [I]	59	180	4.86	**$1.37x10^{-16}$**	0.61
Grain weight [I]	59	180	8.20	**$2.85x10^{-28}$**	0.73
GYE [I]	59	180	4.24	**$4.72x10^{-14}$**	0.58
GNE [I]	59	180	8.23	**$2.32x10^{-28}$**	0.58
HI [I]	59	180	3.00	**$5.22x10^{-6}$**	0.50

df: degrees of freedom; *GNE*: grain number ear^{-1}; *GYE*: grain yield ear^{-1}; *HI*: harvest index.

Calculation of the effect size was performed using one-way ANOVA function ([I]). Values in bold represent significance ($p < 0.05$).

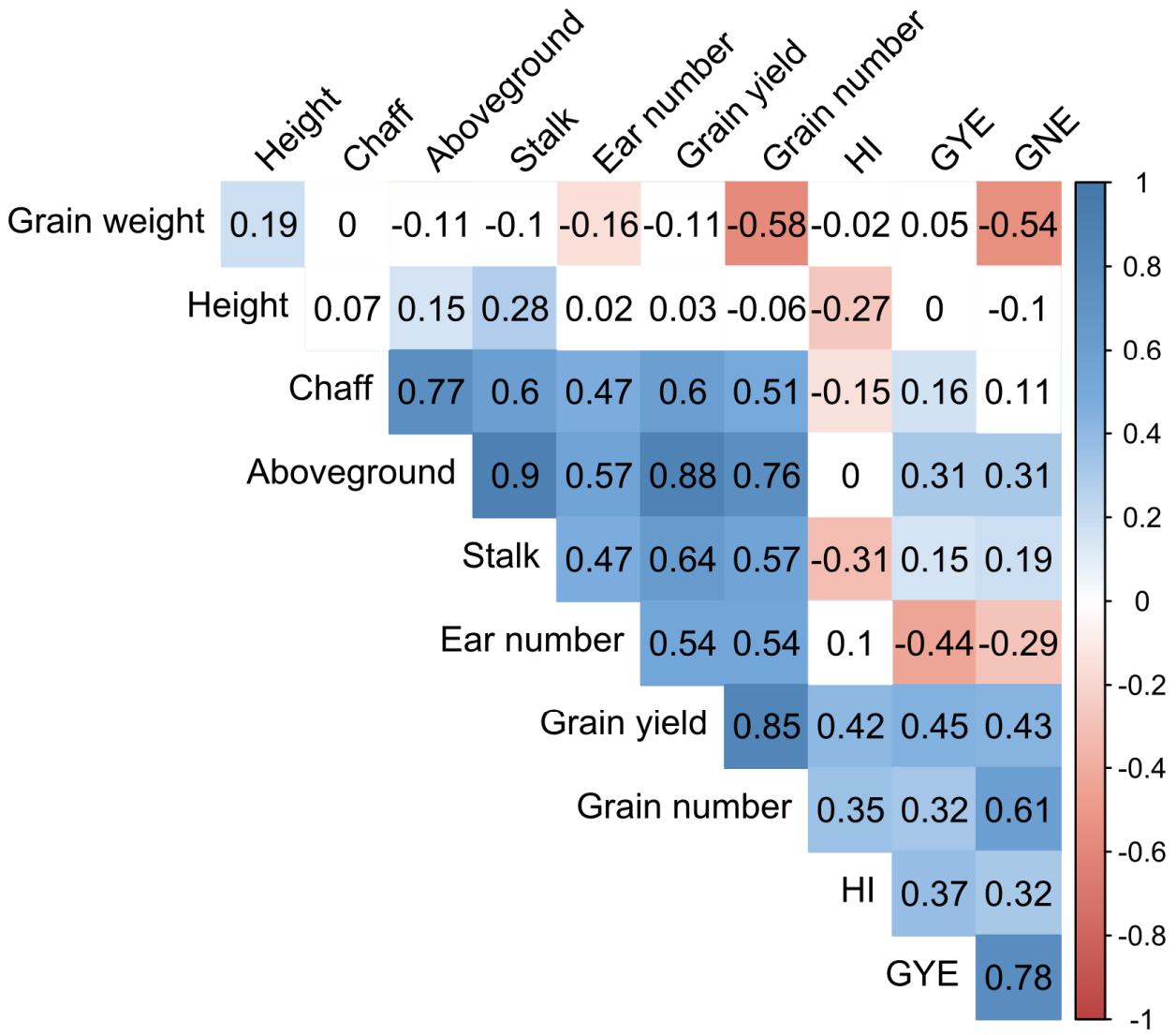

Figure S4.1. Correlogram for wheat production and grain yield components in the response of 60 wheat genotypes grown under elevated CO_2 and high temperature at maturity.

GNE: grain number ear^{-1}; *GYE*: grain yield ear^{-1}; *HI*: harvest index.

Data (r_s) was generated from Spearman correlation analysis. Statistically significant correlations ($p < 0.05$) were coloured.

Table S4.2. One-way ANOVA of cluster factor for the grain yield and their related traits in the response of 60 wheat genotypes grown under combined elevated atmospheric CO_2 and temperature at maturity.

Traits	df1	df2	Statistic	*p*-value	Effect size
Grain yield [II]	2	237	55.67	**$1.50x10^{-20}$**	0.32
Aboveground [II]	2	237	58.98	**$1.60x10^{-21}$**	0.33
Stalk [II]	2	237	34.52	**$7.00x10^{-14}$**	0.23
Chaff [II]	2	237	36.02	**$2.20x10^{-14}$**	0.23
Height [V]	2	237	79.57	**$0.00x10^{0}$**	0.4
Grain number [II]	2	237	101.74	**$1.30x10^{-32}$**	0.46
Ear number [V]	2	237	35.02	**$0.00x10^{0}$**	0.22
Grain weight [II]	2	237	42.96	**$1.20x10^{-16}$**	0.27
GYE [II]	2	237	26.44	**$4.30x10^{-11}$**	0.18
GNE [VI]	2	237	103.87	**$2.80x10^{-23}$**	0.46
HI [VI]	2	237	15.52	**$4.30x10^{-4}$**	0.11

df: degrees of freedom; *GNE*: grain number ear^{-1}; *GYE*: grain yield ear^{-1}; *HI*: harvest index.

([II]) One-way ANOVA with correction for unbalanced data. ([V]) One-way K-W ANOVA. ([VI]) Robust One-way ANOVA for medians. Values in bold represent significance ($p < 0.05$).

Table S4.3. Average days from sowing to ear emergence, anthesis and maturity developmental stages in the response of 60 wheat genotypes grown under elevated CO_2 and high temperature at maturity.

Genotype	Ear emergence	Anthesis	Maturity	Genotype	Ear emergence	Anthesis	Maturity
150	58	60	95	**114**	62	63	93
74	65	66	99	**97**	62	63	94
23	68	69	102	**113**	66	67	97
8	65	66	97	**25**	60	62	96
76	64	65	99	**18**	59	61	93
15	60	63	97	**70**	66	67	102
73	61	63	95	**63**	60	61	94
21	64	66	101	**105**	63	65	98
9	65	66	97	**88**	65	66	99
118	57	60	92	**93**	60	61	94
81	63	65	97	**35**	57	60	95
77	65	66	99	**4**	60	62	96
115	57	60	92	**26**	59	61	95
87	65	66	99	**48**	59	62	96
29	60	62	99	**99**	65	65	96
46	63	64	95	**53**	57	59	94
119	63	65	96	**59**	61	63	97
6	60	62	97	**83**	66	67	102
110	64	65	98	**10**	63	64	98
71	62	64	96	**65**	61	63	94
16	64	65	99	**42**	61	63	95
22	63	65	98	**107**	61	63	96
13	63	64	95	**11**	60	62	96
92	66	67	102	**58**	65	66	100
117	62	64	93	**5**	58	60	93
79	61	63	96	**43**	61	62	98
33	59	61	96	**94**	63	65	97
69	64	65	98	**95**	58	60	93
31	57	61	95	**61**	62	64	95
19	66	66	100	**41**	59	61	96

GNE: grain number ear^{-1}; *GYE*: grain yield ear^{-1}; *HI*: harvest index.

Data (r_s) was generated from Spearman correlation analysis and order according to increased grain yield. Values in bold represent significance ($p < 0.05$).

Minimum Maximum

Table S4.5. Correlation coefficient matrix for average wheat production and grain yield components with days from sowing to ear emergence, anthesis and maturity developmental stages in the response of 60 wheat genotypes grown under elevated CO_2 and high temperature.

Traits	Ear emergence	Anthesis	Maturity
Aboveground	-0.25	**-0.29**	**-0.33**
Stalk	-0.12	-0.16	**-0.31**
Chaff	**-0.37**	**-0.42**	**-0.40**
Grain yield	-0.24	-0.28	-0.22
Grain number	-0.09	-0.13	-0.10
Ear number	**-0.30**	**-0.30**	**-0.35**
Grain weight	-0.08	-0.03	-0.03
GYE	0.11	0.07	0.18
GNE	0.14	0.09	0.19
HI	-0.04	-0.01	0.23
Height	0.21	0.21	-0.13

GNE: grain number ear-1; GYE: grain yield ear-1; HI: harvest index.

Data (r_s) was generated from Spearman correlation analysis. Values in bold represent significance ($p < 0.05$).

Experiment II. Study II

Table S5.1. One-way ANOVA of genotype factor for wheat production, grain yield, non-mineral and mineral quality components in the response of ten wheat genotypes grown under combined elevated atmospheric CO_2 and temperature at maturity.

Traits	df1	df2	Statistic	*p*-value	Effect size
Aboveground [I]	9	40.00	3.20	**$5.22x10^{-3}$**	0.42
Stalk [I]	9	40.00	2.18	**$4.41x10^{-2}$**	0.33
Chaff [IIIa]	9	16.24	3.96	**$8.00x10^{-3}$**	0.00
Grain yield [I]	9	40.00	4.20	**$7.06x10^{-4}$**	0.49
Grain number [IIIa]	9	16.23	4.03	**$7.00x10^{-3}$**	0.00
Ear number [IIIa]	9	16.19	1.67	$1.76x10^{-1}$	0.09
Grain weight [IIIa]	9	16.18	4.61	**$4.00x10^{-3}$**	0.00
GYE [I]	9	40.00	3.96	**$1.14x10^{-3}$**	0.47
GNE [I]	9	40.00	6.80	**$7.37x10^{-6}$**	0.61
HI [IIIa]	9	15.82	6.19	**$8.64x10^{-4}$**	0.00
Starch [I]	9	40.00	2.04	$6.02x10^{-2}$	0.31
TP [IIIa]	9	15.96	3.57	**$1.30x10^{-2}$**	0.01
TAC [I]	9	40.00	3.82	**$1.49x10^{-3}$**	0.46
TPhC [I]	9	40.00	2.75	**$1.33x10^{-2}$**	0.38
B [IIIa]	9	16.19	2.54	**$4.90x10^{-2}$**	0.03
Ca [I]	9	40.00	6.16	**$2.11x10^{-5}$**	0.58
Cu [I]	9	40.00	3.40	**$3.47x10^{-3}$**	0.43
Fe [I]	9	40.00	1.59	$1.52x10^{-1}$	0.26
K [I]	9	40.00	9.27	**$2.01x10^{-7}$**	0.68
Mg [I]	9	40.00	3.86	**$1.39x10^{-3}$**	0.46
Na [IIIa]	9	15.83	4.20	**$6.00x10^{-3}$**	0.00
P [I]	9	40.00	2.20	**$4.24x10^{-2}$**	0.33
S [I]	9	40.00	4.47	**$4.29x10^{-4}$**	0.50
Zn [I]	9	40.00	2.25	**$3.82x10^{-2}$**	0.34

A: net CO_2 assimilation rate; *Chl*: chlorophyll; *Ci*: leaf internal CO_2 concentration; *df*: degrees of freedom; *E*: transpiration; *ETR*: electron transport rate; *Flav*: flavonoids; *Ft*: chlorophyll fluorescence steady-state; *gs*: stomatal conductance; *NBI*: nitrogen-balance index; Φ_{PSII}: quantum yield of PSII electron transport; *Temp*: foliar temperature.

([I]) One-way ANOVA. ([IIIa]) One-way ANOVA with heteroscedasticity correction using *welch_anova_test* Values in bold represent significance ($p < 0.05$).

Table S5.2. Eigenvalues and explained variance for the dimensions of the CB.

Dimension	Eigenvalue	Explained variance	Cumulative
1	3.98	32.45	32.45
2	3.18	20.73	53.18
3	2.80	16.07	69.26
4	2.36	11.39	80.65
5	1.74	6.22	86.87
6	1.67	5.75	92.62
7	1.38	3.89	96.51
8	1.09	2.45	98.96
9	0.71	1.04	100.00

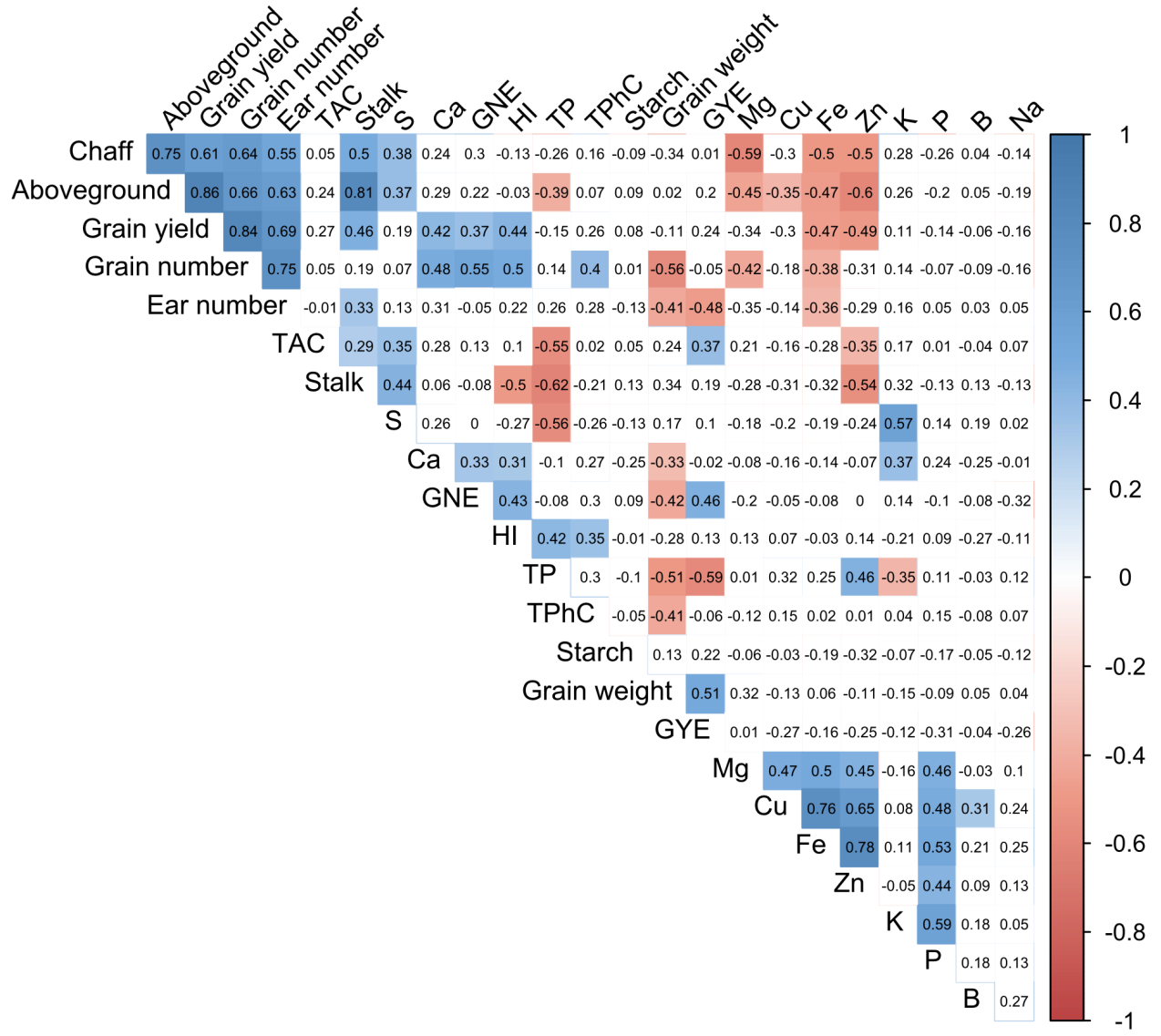

Figure S5.1. Correlogram for wheat production, grain yield, non-mineral and mineral quality components in the response of ten wheat genotypes grown under combined elevated atmospheric CO_2 and temperature at maturity.

GNE: grain number ear^{-1}; *GYE*: grain yield ear^{-1}; *HI*: harvest index; *TAC*: total antioxidant capacity; *TP*: total protein; *TPhC*: Total phenolic compounds.

Data (r_s) was generated from Spearman correlation analysis. Statistically significant correlations ($p < 0.05$) were coloured.

Table S5.3. One-way ANOVA of genotype factor for grain and plant non-mineral nutrient contents in the response of ten wheat genotypes grown under combined elevated atmospheric CO_2 and temperature at maturity.

Mineral and non-mineral nutrient content per grain

Traits	df1	df2	Statistic	*p*-value	Effect size
Starch [I]	9	40.00	3.91	**1.26x10^{-3}**	0.47
TP [IIIa]	9	15.85	33.87	**1.08x10^{-8}**	0.01
TAC [IIIa]	9	15.88	8.95	**9.90x10^{-5}**	0.00
TPhC [IIIa]	9	16.25	7.66	**2.27x10^{-4}**	0.00
B [I]	9	40.00	1.45	1.99x10^{-1}	0.25
Ca [I]	9	40.00	5.14	**1.24x10^{-4}**	0.54
Cu [I]	9	40.00	3.73	**1.79x10^{-3}**	0.46
Fe [I]	9	40.00	2.71	1.46x10^{-1}	0.38
K [IIIa]	9	16.20	3.23	**1.90x10^{-2}**	0.01
Mg [I]	9	40.00	3.99	**1.06x10^{-3}**	0.47
Na [IIIa]	9	15.90	4.44	**5.00x10^{-3}**	0.00
P [IIIa]	9	16.22	4.38	**5.00x10^{-3}**	0.00
S [IIIa]	9	16.13	3.42	**1.50x10^{-2}**	0.01
Zn [I]	9	40.00	5.15	**1.22x10^{-4}**	0.54

Mineral and non-mineral nutrient content per plant

Traits	df1	df2	Statistic	*p*-value	Effect size
Starch [IIIa]	9	16.20	7.36	**2.91x10^{-4}**	0.00
TP [IIIa]	9	16.19	1.16	3.81x10^{-1}	0.17
TAC [I]	9	40.00	5.14	**1.22x10^{-4}**	0.54
TPhC [I]	9	40.00	4.31	**5.71x10^{-4}**	0.49
B [I]	9	40.00	1.53	1.70x10^{-1}	0.26
Ca [IIIa]	9	16.20	7.78	**2.10x10^{-4}**	0.00
Cu [I]	9	40.00	4.75	**2.50x10^{-4}**	0.52
Fe [I]	9	16.16	2.29	7.00x10^{-2}	0.04
K [I]	9	40.00	11.45	**1.29x10^{-8}**	0.72
Mg [I]	9	16.03	7.16	**3.58x10^{-4}**	0.00
Na [IIIa]	9	15.96	3.35	**1.70x10^{-2}**	0.01
P [I]	9	40.00	7.28	**3.48x10^{-6}**	0.62
S [I]	9	40.00	5.99	**2.82x10^{-5}**	0.57
Zn [I]	9	40.00	3.15	**5.77x10^{-3}**	0.42

TAC: total antioxidant capacity; *TP*: total protein; *TPhC*: Total phenolic compounds.

([I]) One-way ANOVA. ([IIIa]) One-way ANOVA with heteroscedasticity correction using *welch_anova_test*. Values in bold represent significance ($p < 0.05$).

Table S5.4. One-way ANOVA of grain non-mineral and mineral nutrient contents in the response of ten wheat genotypes grown under combined elevated atmospheric CO_2 and temperature at maturity.

Genotype	Starch (µmol grain^{-1})			TP (mg grain^{-1})			TAC (µmol eq Trolox grain^{-1})			TPhC (µmol eq Galic Ac. grain^{-1})			B (µg grain^{-1})			Ca (µg grain^{-1})			Cu (µg grain^{-1})		
	Mean	**SD**		**Mean**	**SD**		**Mean**	**SD**		**Mean**	**SD**		**Mean**	**SD**		**Mean**	**SD**		**Mean**	**SD**	
8	141.65	± 20.41	**ab**	3.70	± 0.32	**abc**	0.05	± 0.01	**ab**	0.24	± 0.02	**ab**	0.09	± 0.03	**a**	10.97	± 0.72	**a**	0.27	± 0.02	**ab**
23	132.99	± 12.23	**ab**	3.50	± 0.12	**a**	0.05	± 0.00	**a**	0.26	± 0.01	**a**	0.07	± 0.02	**a**	12.87	± 1.21	**abc**	0.26	± 0.04	**ab**
41	114.67	± 19.98	**a**	2.68	± 0.05	**b**	0.05	± 0.01	**ab**	0.21	± 0.01	**b**	0.05	± 0.02	**a**	13.09	± 0.84	**abc**	0.22	± 0.02	**ab**
43	140.15	± 5.62	**ab**	2.97	± 0.08	**c**	0.05	± 0.01	**ab**	0.24	± 0.02	**ab**	0.05	± 0.02	**a**	12.72	± 1.26	**abc**	0.22	± 0.03	**a**
61	123.28	± 11.84	**ab**	2.89	± 0.20	**bc**	0.04	± 0.01	**ab**	0.21	± 0.02	**b**	0.07	± 0.02	**a**	12.18	± 0.93	**ab**	0.22	± 0.03	**ab**
74	151.21	± 8.70	**b**	3.57	± 0.15	**a**	0.05	± 0.01	**ab**	0.23	± 0.01	**ab**	0.07	± 0.03	**a**	13.31	± 1.19	**abc**	0.28	± 0.03	**b**
76	133.94	± 7.96	**ab**	3.29	± 0.21	**abc**	0.05	± 0.01	**ab**	0.24	± 0.01	**ab**	0.05	± 0.01	**a**	13.77	± 2.29	**bc**	0.21	± 0.02	**a**
94	123.87	± 16.37	**ab**	3.03	± 0.34	**abc**	0.05	± 0.01	**ab**	0.22	± 0.02	**ab**	0.05	± 0.02	**a**	12.80	± 1.27	**abc**	0.23	± 0.04	**ab**
95	152.20	± 16.75	**b**	3.08	± 0.21	**abc**	0.06	± 0.00	**a**	0.26	± 0.03	**ab**	0.05	± 0.01	**a**	15.02	± 0.58	**c**	0.24	± 0.03	**ab**
150	125.13	± 12.59	**ab**	3.28	± 0.17	**ac**	0.04	± 0.00	**b**	0.21	± 0.01	**b**	0.06	± 0.04	**a**	10.98	± 0.74	**a**	0.23	± 0.02	**ab**
Average	133.91	± 13.25		3.20	± 0.19		0.05	± 0.01		0.23	± 0.02		0.06	± 0.02		12.77	± 1.10		0.24	± 0.03	
***p*-value**	**1.26x10^{-3}**			**1.08x10^{-8}**			**9.90x10^{-5}**			**2.27x10^{-4}**			1.99x10^{-1}			**1.24x10^{-4}**			**1.79x10^{-3}**		

Genotype	Fe (µg grain^{-1})			K (µg grain^{-1})			Mg (µg grain^{-1})			Na (µg grain^{-1})			P (µg grain^{-1})			S (µg grain^{-1})			Zn (µg grain^{-1})		
	Mean	**SD**		**Mean**	**SD**		**Mean**	**SD**		**Mean**	**SD**		**Mean**	**SD**		**Mean**	**SD**		**Mean**	**SD**	
8	0.89	± 0.12	**ab**	135.25	± 16.54	**a**	51.76	± 6.20	**abc**	0.58	± 0.28	**ab**	215.43	± 17.17	**ab**	1.39	± 1.36	**a**	1.39	± 0.13	**abc**
23	0.88	± 0.11	**ab**	138.44	± 8.14	**a**	53.71	± 4.88	**ab**	0.50	± 0.24	**ab**	217.58	± 12.69	**ab**	1.71	± 0.68	**a**	1.53	± 0.14	**ab**
41	0.72	± 0.06	**a**	139.14	± 17.40	**a**	43.63	± 7.84	**ac**	0.48	± 0.30	**ab**	190.36	± 23.92	**ab**	3.54	± 1.51	**a**	1.18	± 0.08	**c**
43	0.70	± 0.13	**a**	140.87	± 21.40	**a**	46.25	± 7.05	**abc**	0.14	± 0.06	**a**	204.94	± 26.44	**ab**	3.01	± 1.31	**a**	1.21	± 0.16	**c**
61	0.69	± 0.14	**a**	138.45	± 22.44	**a**	40.53	± 4.82	**c**	0.49	± 0.39	**ab**	191.73	± 24.55	**ab**	2.78	± 0.99	**a**	1.20	± 0.18	**c**
74	1.04	± 0.34	**b**	150.27	± 10.28	**a**	56.19	± 4.78	**b**	0.32	± 0.05	**b**	232.12	± 16.46	**a**	3.20	± 0.92	**a**	1.66	± 0.23	**a**
76	0.78	± 0.08	**ab**	148.80	± 7.08	**a**	47.74	± 6.00	**abc**	0.72	± 0.48	**ab**	214.81	± 9.64	**ab**	3.07	± 0.36	**a**	1.32	± 0.14	**bc**
94	0.76	± 0.08	**ab**	121.81	± 13.78	**a**	46.51	± 5.76	**abc**	0.44	± 0.19	**ab**	189.14	± 15.02	**ab**	2.41	± 0.57	**a**	1.35	± 0.15	**bc**
95	0.80	± 0.10	**ab**	153.14	± 9.37	**a**	50.81	± 4.11	**abc**	0.41	± 0.26	**ab**	223.59	± 14.84	**ab**	3.71	± 0.60	**a**	1.38	± 0.08	**abc**
150	0.76	± 0.12	**ab**	126.51	± 10.50	**a**	42.50	± 4.17	**ac**	0.23	± 0.08	**ab**	182.95	± 13.55	**b**	2.33	± 0.56	**a**	1.35	± 0.14	**abc**
Average	0.80	± 0.13		139.27	± 13.69		47.96	± 5.56		0.43	± 0.23		206.27	± 17.43		2.72	± 0.89		1.36	± 0.14	
***p*-value**	1.46x10^{-1}			**1.90x10^{-2}**			**1.06x10^{-3}**			**5.00x10^{-3}**			**5.00x10^{-3}**			**1.50x10^{-2}**			**1.22x10^{-4}**		

TAC: total antioxidant capacity; *TP*: total protein; *TPhC*: total phenolic compounds.

Values represent measures of central tendency (*Mean*: mean) and dispersion (*SD*: standard deviation) of five replicates (n=5) for each genotype or all genotypes and replicates (*Average*; N=50). The calculation of statistical significances (p-value) for each trait is based on one-way ANOVA applying corrections for ANOVA assumptions. Values in bold represent significance ($p < 0.05$). Within columns, numbers followed by the same letter indicate non-statistically significant differences at $p < 0.05$ as determined by post-hoc tests.

Traits

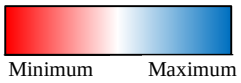

Table S5.5. One-way ANOVA of plant non-mineral and mineral nutrient contents in the response of ten wheat genotypes grown under combined elevated atmospheric CO_2 and temperature at maturity.

Genotype	Starch (µmol plant^{-1})		TP (mg plant^{-1})		TAC (µmol eq Trolox plant^{-1})		TPhC (µmol eq Galic Ac. plant^{-1})		B (µg plant^{-1})		Ca (µg plant^{-1})		Cu (µg plant^{-1})	
	Mean	**SD**	**Mean**	**SD**	**Mean**	**SD**	**Mean**	**SD**	**Mean**	**SD**	**Mean**	**SD**	**Mean**	**SD**
8	29318.50	± 5927.51 **abc**	772.20	± 159.02 **a**	9.80	± 2.72 **bc**	50.57	± 8.65 **abc**	17.25	± 4.31 **a**	2285.94	± 442.30 **ab**	55.98	± 7.18 **abc**
23	30381.51	± 4151.67 **abc**	802.25	± 113.74 **a**	12.65	± 2.33 **ab**	60.81	± 10.97 **abc**	15.32	± 3.57 **a**	2976.23	± 645.75 **abc**	59.32	± 6.88 **ab**
41	34406.62	± 2332.87 **abc**	828.55	± 173.33 **a**	14.37	± 2.54 **a**	64.57	± 11.71 **ab**	15.65	± 5.45 **a**	4002.65	± 614.49 **abc**	67.70	± 10.82 **a**
43	39424.74	± 2454.80 **a**	836.75	± 70.96 **a**	14.71	± 2.80 **a**	67.71	± 6.93 **b**	12.85	± 3.50 **a**	3575.09	± 362.67 **c**	61.12	± 5.42 **ab**
61	35043.01	± 2167.23 **ab**	828.51	± 122.38 **a**	12.43	± 1.97 **ab**	60.07	± 5.06 **abc**	19.96	± 4.71 **a**	3478.51	± 368.50 **ac**	63.16	± 7.21 **ab**
74	30587.65	± 5719.54 **abc**	723.87	± 138.85 **a**	11.05	± 2.91 **abc**	45.90	± 8.72 **c**	13.77	± 8.13 **a**	2694.76	± 516.89 **abc**	55.98	± 5.77 **abc**
76	27333.42	± 3848.16 **bc**	680.17	± 158.90 **a**	10.74	± 1.74 **abc**	50.11	± 10.82 **ac**	10.56	± 2.99 **a**	2834.92	± 767.08 **abc**	44.02	± 9.15 **c**
94	29613.29	± 4179.90 **abc**	735.09	± 154.97 **a**	11.83	± 1.06 **abc**	52.24	± 5.16 **abc**	11.32	± 2.54 **a**	3063.95	± 356.62 **abc**	54.14	± 2.41 **abc**
95	35131.05	± 6110.72 **abc**	709.29	± 88.71 **a**	13.48	± 0.89 **ab**	59.52	± 6.98 **abc**	12.73	± 3.33 **a**	3447.33	± 252.38 **ac**	55.95	± 7.50 **abc**
150	27402.41	± 2362.03 **c**	720.35	± 68.08 **a**	7.68	± 0.74 **c**	46.34	± 3.95 **c**	13.64	± 8.52 **a**	2412.85	± 245.39 **b**	49.34	± 2.28 **bc**
Average	31864.22	± 3925.44	763.70	± 124.89	11.87	± 1.97	55.78	± 7.90	14.31	± 4.71	3077.22	± 457.21	56.67	± 6.46
***p*-value**	**2.91x10^{-4}**		3.81x10^{-1}		**1.22x10^{-4}**		**5.71x10^{-4}**		1.70x10^{-1}		**2.10x10^{-4}**		**2.50x10^{-4}**	

Genotype	Fe (µg plant^{-1})		K (µg plant^{-1})		Mg (µg plant^{-1})		Na (µg plant^{-1})		P (µg plant^{-1})		S (µg plant^{-1})		Zn (µg plant^{-1})	
	Mean	**SD**	**Mean**	**SD**	**Mean**	**SD**	**Mean**	**SD**	**Mean**	**SD**	**Mean**	**SD**	**Mean**	**SD**
8	182.15	± 9.32 **a**	27741.60	± 2889.98 **a**	10670.17	± 1590.98 **ab**	116.17	± 52.19 **a**	44424.25	± 5551.27 **bc**	251.78	± 213.33 **b**	285.78	± 27.82 **ab**
23	200.49	± 12.99 **a**	31632.09	± 3623.82 **a**	12213.84	± 976.25 **a**	115.14	± 49.19 **a**	49690.85	± 5418.76 **abc**	379.36	± 107.55 **ab**	348.52	± 34.19 **a**
41	218.38	± 30.51 **a**	42148.88	± 4941.11 **b**	13081.57	± 971.56 **a**	152.08	± 113.63 **a**	57560.79	± 5451.60 **a**	1030.45	± 306.22 **c**	360.70	± 56.53 **a**
43	193.71	± 23.10 **a**	39379.06	± 3761.11 **b**	12965.48	± 1693.85 **ab**	39.42	± 14.29 **a**	57396.44	± 4981.54 **a**	829.80	± 310.09 **acd**	337.57	± 27.63 **ab**
61	194.55	± 16.31 **a**	39152.51	± 3497.31 **b**	11506.53	± 846.12 **ab**	129.32	± 88.50 **a**	54383.18	± 4092.67 **ab**	771.47	± 193.90 **acd**	339.04	± 34.04 **ab**
74	211.68	± 91.88 **a**	30169.80	± 3852.21 **a**	11259.32	± 1339.14 **ab**	64.77	± 14.34 **a**	46580.49	± 5780.98 **bc**	655.76	± 280.13 **abcd**	331.51	± 37.88 **ab**
76	159.64	± 24.83 **a**	30391.81	± 4414.16 **a**	9755.57	± 1904.94 **ab**	152.19	± 126.32 **a**	44005.25	± 7467.12 **bc**	641.14	± 182.04 **bcd**	270.71	± 52.05 **b**
94	182.24	± 16.29 **a**	29011.76	± 2017.17 **a**	11053.08	± 396.29 **a**	105.58	± 45.57 **a**	45144.47	± 2569.71 **bc**	566.56	± 66.50 **abd**	321.84	± 37.05 **ab**
95	182.41	± 14.13 **a**	35139.84	± 2851.25 **ab**	11653.92	± 1043.20 **ab**	98.72	± 73.64 **a**	51279.06	± 3922.19 **ab**	859.28	± 189.07 **cd**	315.97	± 15.92 **ab**
150	166.32	± 17.68 **a**	27718.09	± 2157.27 **a**	9294.07	± 586.99 **b**	50.55	± 14.75 **a**	40062.47	± 2274.15 **c**	516.75	± 143.49 **abd**	296.10	± 17.72 **ab**
Average	189.16	± 25.70	33248.54	± 3400.54	11345.36	± 1134.93	102.39	± 59.24	49052.73	± 4751.00	650.24	± 199.23	320.77	± 34.08
***p*-value**	7.00x10^{-2}		**1.29x10^{-8}**		**3.58x10^{-4}**		**1.70x10^{-2}**		**3.48x10^{-6}**		**2.82x10^{-5}**		**5.77x10^{-3}**	

TAC: total antioxidant capacity; *TP*: total protein; *TPhC*: total phenolic compounds.

Values represent measures of central tendency (*Mean*: mean) and dispersion (*SD*: standard deviation) of five replicates (n=5) for each genotype or all genotypes and replicates (*Average*; N=50). The calculation of statistical significances (p-value) for each trait is based on one-way ANOVA applying corrections for ANOVA assumptions. Values in bold represent significance ($p < 0.05$). Within columns, numbers followed by the same letter indicate non-statistically significant differences at $p < 0.05$ as determined by post-hoc tests.

Traits

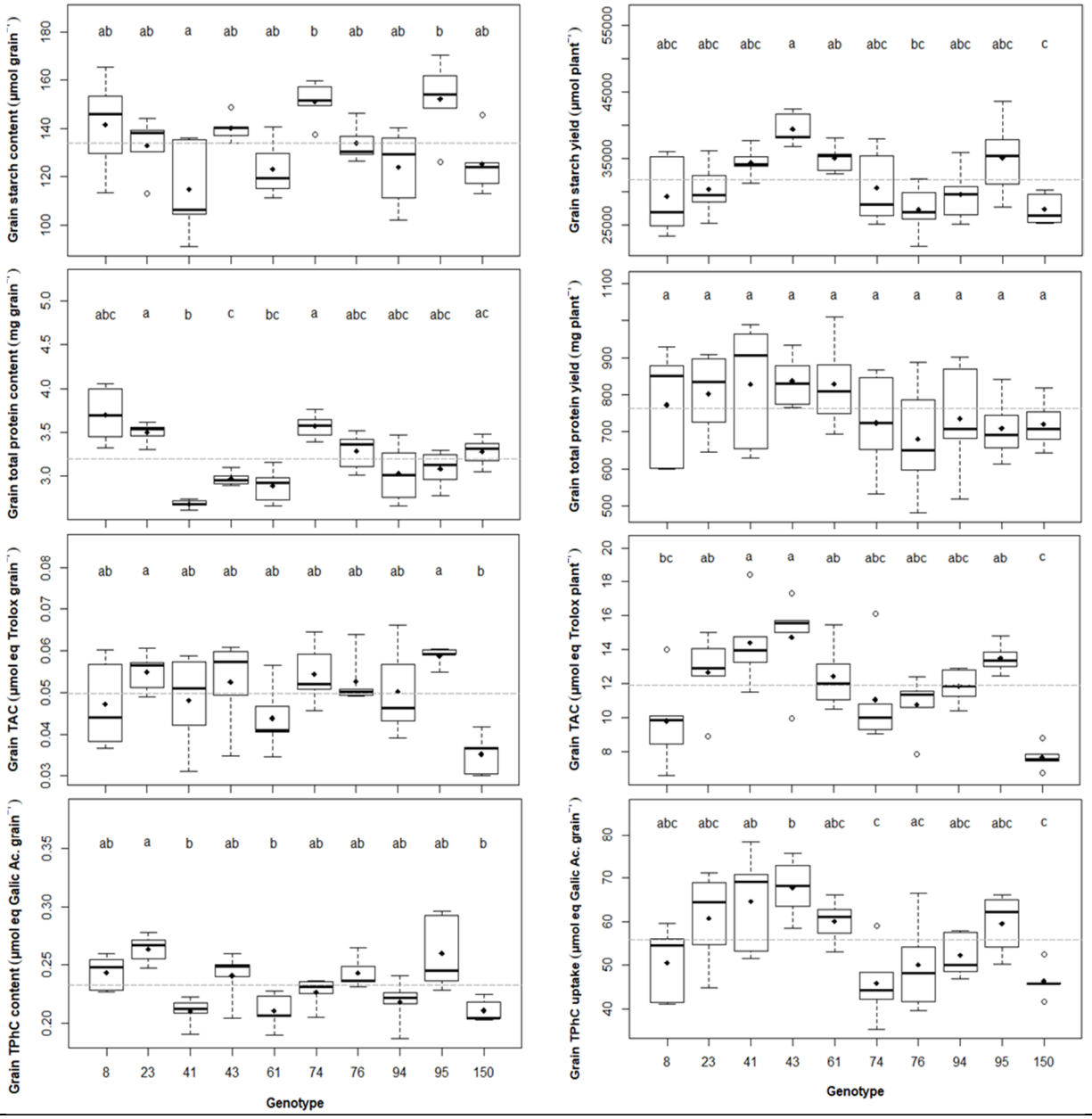

Figure S5.2. One-way ANOVA of wheat grain and plant non-mineral nutrient contents in the response of ten wheat genotypes grown under combined elevated atmospheric CO_2 and temperature at ear maturity.

TAC: total antioxidant capacity; *TP*: total protein; *TPhC*: Total phenolic compounds.

Black dots represent the mean of the five replicates (n=5) per genotype. The grey dotted line represents the mean among all the genotypes and replicates (N=50). Among columns, numbers followed by the same letter are not significantly different at $p < 0.05$ for post-hoc tests.

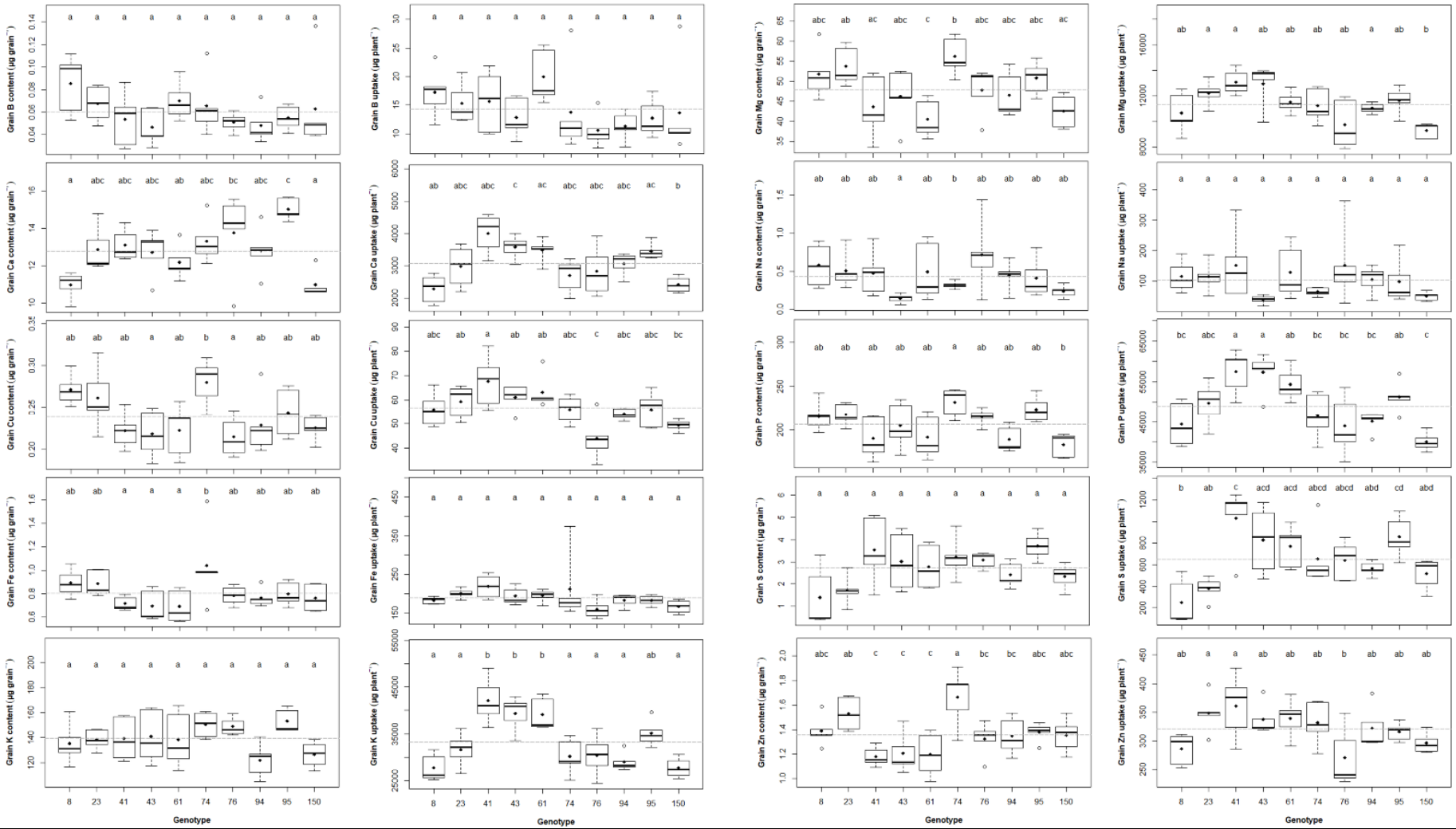

Figure S5.3. One-way ANOVA of wheat grain and plant non-mineral nutrient contents in the response of ten wheat genotypes grown under combined elevated atmospheric CO_2 and temperature at maturity.

Black dots represent the mean of the five replicates (n=5) per genotype. The grey dotted line represents the mean among all the genotypes and replicates (N=50). Among columns, numbers followed by the same letter are not significantly different at $p < 0.05$ for post-hoc tests.

Experiment II. Study III

Table S6.1. One-way ANOVA of genotype factor for leaf and plant parameters at ear emergence growth stage in the response of ten wheat genotypes grown under combined elevated atmospheric CO_2 and temperature.

Leaf	Trait	df1	df2	Statistic	*p*-value	Effect size	Trait	df1	df2	Statistic	*p*-value	Effect size
	FW [V]	9	40	20.88	**1.32x10^{-2}**	0.78	**PEPcase** [IV]	9	40	6.01	**9.45x10^{-3}**	0.82
	DW [V]	9	40	23.88	**4.49x10^{-3}**	0.80	**PK** [I]	9	40	2.64	**1.69x10^{-2}**	0.37
	LDMC [IV]	9	40	6.99	**6.23x10^{-3}**	0.46	**GSH** [IV]	9	40	4.98	**1.66x10^{-2}**	0.59
	H % [V]	9	40	10.57	3.06x10^{-1}	0.63	**NR** [V]	9	40	10.93	2.80x10^{-1}	0.64
	Area [V]	9	40	24.95	**3.03x10^{-3}**	0.81	**Asa** [IV]	9	40	3.58	**4.24x10^{-2}**	0.57
	LMA [IV]	9	40	11.78	**1.14x10^{-3}**	0.57	**Frap** [IV]	9	40	11.26	**1.15x10^{-3}**	0.90
	Gluc [IV]	9	40	69.98	**1.35x10^{-6}**	0.59	**TPhC** [IV]	9	40	1.89	1.92x10^{-1}	0.93
	Fru [IV]	9	40	128.85	**1.90x10^{-7}**	1.17	**ORAC** [IV]	9	40	6.86	**6.32x10^{-3}**	0.72
	Suc [IV]	9	40	72.56	**1.88x10^{-6}**	1.08	**Chl** [V]	9	40	26.80	**1.51x10^{-3}**	0.82
	Fruct [IV]	9	40	280.71	**1.67x10^{-8}**	0.76	**Flav** [IV]	9	40	8.74	**2.72x10^{-3}**	0.64
	Starch [IV]	9	40	1.36	3.47x10^{-1}	0.62	**NBI** [IV]	9	40	21.24	**1.11x10^{-4}**	0.76
	Protein [V]	9	40	12.21	2.02x10^{-1}	0.89	***Vcx*** [V]	9	40	4.78	8.53x10^{-1}	0.41
	Nitrate [IV]	9	40	17.31	**3.06x10^{-4}**	0.67	***Jx*** [IV]	9	40	0.51	8.29x10^{-1}	0.21
	Aa [I]	9	40	0.40	9.27x10^{-1}	0.78	***Rd*** [V]	9	40	11.05	2.72x10^{-1}	0.64
	C % [I]	9	40	3.18	**5.46x10^{-3}**	0.08	***TPU*** [IV]	9	40	0.47	8.59x10^{-1}	0.44
	N % [IV]	9	40	2.09	1.56x10^{-1}	0.42	***CRbcx*** [IV]	9	40	1.23	3.92x10^{-1}	0.55
	C/N [IV]	9	40	2.42	1.13x10^{-1}	0.60	***ARbcx*** [I]	9	40	1.14	3.58x10^{-1}	0.20
	AGPase [V]	9	40	16.53	5.67x10^{-2}	0.62	***C_i*** [I]	9	40	0.92	5.16x10^{-1}	0.17
	Fru16bP [IV]	9	40	2.13	1.49x10^{-1}	0.74	***g_s*** [IV]	9	40	3.84	**3.64x10^{-2}**	0.57
	G6PDH [IV]	9	40	1.72	2.32x10^{-1}	0.70	***A*** [IV]	9	40	1.11	4.51x10^{-1}	0.44
	GDH [IV]	9	40	2.80	8.08x10^{-2}	0.65	***E*** [IV]	9	40	0.19	9.89x10^{-1}	0.54
	GS [IV]	9	40	2.99	7.53x10^{-2}	0.56	***WUE*** [IV]	9	40	0.29	9.58x10^{-1}	0.20
	IDH [IV]	9	40	4.74	**1.97x10^{-2}**	0.82	***ΦPSII*** [IV]	9	40	3.85	**3.52x10^{-2}**	0.49

Plant	Trait	df1	df2	Statistic		Effect size	Trait	df1	df2	Statistic	*p*-value	Effect size
	FW [I]	9	40	3.62	**2.22x10^{-3}**	0.45	**PMA** [V]	9	40	8.05	5.30x10^{-1}	0.56
	DW [IV]	9	40	4.42	**2.00x10^{-2}**	0.88	**Stem number** [I]	9	40	5.27	**9.69x10^{-5}**	0.54
	PDMC [IV]	9	40	4.42	2.40x10^{-1}	0.88	**C %** [IV]	9	40	4.63	**2.00x10^{-2}**	0.90
	H % [V]	9	40	8.56	4.80x10^{-1}	0.58	**N %** [V]	9	40	9.37	4.00x10^{-1}	0.60
	Area [I]	9	40	2.18	**4.44x10^{-2}**	0.33	**C/N** [V]	9	40	10.31	3.30x10^{-1}	0.63

A: net CO_2 assimilation rate; *Aa*: amino acids; *AGPase*: ADP-glucose pyrophosphorylase; *ARbcx*: maximum value of photosynthesis limited by Rubisco activity; *Asa*: ascorbic acid; *Chl*: chlorophyll; C_i: leaf internal CO_2 concentration; *C/N*: carbon-nitrogen ratio; *C %*: percentage of carbon; *CRbcx*: CO_2 intercellular concentration at maximum photosynthesis limited by Rubisco activity; *df*: degrees of freedom; *DW*: dry weight; *E*: transpiration; *Flav*: flavonoids; *FRAP*: ferric ion reducing antioxidant power; *Fru*: fructose; *Fru1,6bisP*: fructose-1,6-bisphosphatase; *Fruct*: fructans; *FW*: fresh weight; *G6PDH*: glucose-6-phosphate dehydrogenase; *GDH*: glutamate dehydrogenase; *Gluc*: glucose; *GS*: glutamine synthetase; g_s: stomatal conductance; *GSH*: glutathione; *H %*: percentage of humidity; *IDH*: isocitrate dehydrogenase; *Jx*: maximum rate of electron transport; *LDMC*: leaf dry matter content; *LMA*: leaf dry mass per area; *NBI*: nitrogen-balance index; *N %*: percentage of nitrogen; *NR*: nitrate reductase; *ORAC*: oxygen radical absorbance capacity; *PDMC*: plant dry matter content; *PEPCase*: phosphoenolpyruvate carboxylase; Φ_{PSII}: quantum yield of PSII electron transport; *PK*: pyruvate kinase; *PMA*: plant mass per area; *Rd*: respiration rate; *Suc*: sucrose; *TPhC*: total phenolic compounds; *TPU*: maximum rate of triose phosphate use; *Vcx*: maximum carboxylation rate of Rubisco; *WUE*: water-use efficiency.

([I]) One-way ANOVA. ([IV]) 20% trimmed mean one-way ANOVA. ([V]) Robust Kruskal-Wallis ANOVA.

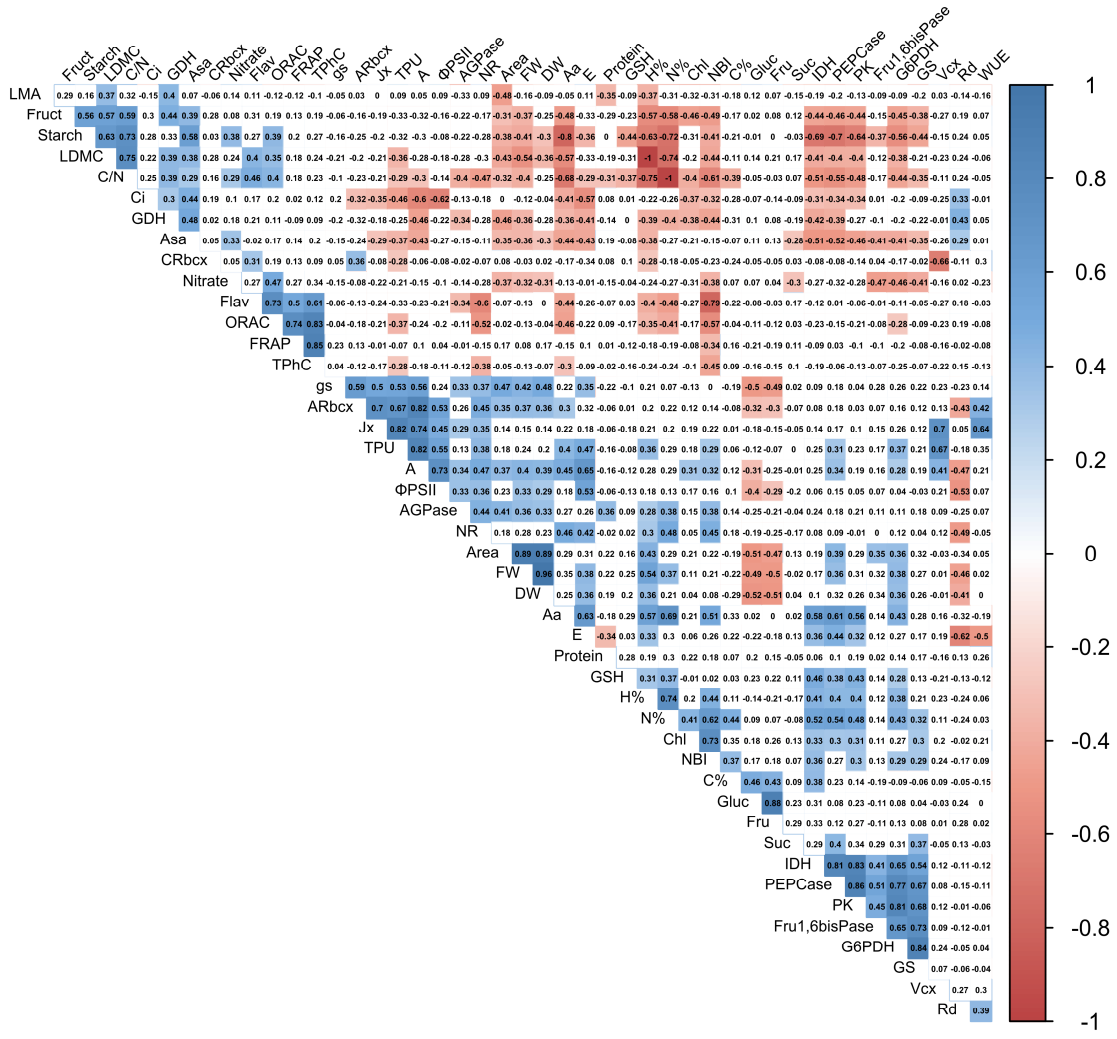

Figure S6.1. Correlogram for the biomass, morphology, C and N metabolites, enzyme activities, chlorophyll spectral indices, antioxidants, C-N percentages related traits evaluated in the flag leaves of ten wheat genotypes grown under elevated CO_2 and high temperature at ear emergence.

A: photosynthetic CO_2 assimilation rate ; *Aa*: amino acids; *AGPase*: ADP-glucose pyrophosphorylase; *ARbcx*: maximum value of photosynthesis limited by Rubisco activity; *Asa*: ascorbic acid; *Chl*: chlorophyll; C_i: intercellular CO_2 concentration; *C/N*: carbon-nitrogen ratio; *C %*: carbon percentage; *CRbcx*: intercellular CO_2 concentration at maximum photosynthesis limited by Rubisco activity; *DW*: dry weight; *E*: transpiration; *Flav*: flavonoids; *FRAP*: ferric ion reducing antioxidant power; *Fru*: fructose; *Fru1,6bisPase*: cytosolic fructose-1,6-bisphosphatase; *Fruct*: fructans; *FW*: fresh weight; *G6PDH*: glucose-6-phosphate dehydrogenase; *GDH*: glutamate dehydrogenase; *Gluc*: glucose; *GS*: glutamine synthetase; g_s: stomatal conductance; *GSH*: glutathione; *H %*: water percentage; *IDH*: NADP-dependent isocitrate dehydrogenase; *Jx*: maximum rate of electron transport; *LDMC*: leaf dry matter content; *LMA*: leaf dry mass per area; *NBI*: nitrogen balance index; *N %*: nitrogen percentage; *NR*: nitrate reductase; *ORAC*: oxygen radical absorbance capacity; *PEPCase*: phosphoenolpyruvate carboxylase; Φ_{PSII}: quantum yield of PSII electron transport; *PK*: pyruvate kinase; *Rd*: day respiration; *Suc*: sucrose; *TPhC*: total phenolic compounds; *TPU*: maximum rate of triose phosphate use; *Vcx*: maximum carboxylation rate of Rubisco; *WUE*: water-use efficiency.

Data (r_s) was generated from Spearman correlation analysis. Statistically significant correlations ($p < 0.05$) were coloured.

Table S6.2. Plant biomass (FW, DW, PDMC and H %) and green area (Area and PMA) related traits, as well as tiller number in the response of ten wheat genotypes grown under elevated CO_2 and high temperature.

Genotype	FW (g plant^{-1})			DW (g plant^{-1})			PDMC			H %			Area (cm^2 plant^{-1})		
	Mean	SD		Trim	MAD		Trim	MAD		Med	MAD		Mean	SD	
8	50.46	± 6.90	**a**	12.55	± 0.63	**a**	0.26	± 0.00	**a**	72.68	± 0.07	**a**	794.48	± 188.06	**a**
23	52.90	± 9.51	**a**	12.38	± 0.82	**a**	0.24	± 0.04	**a**	75.24	± 3.94	**a**	829.61	± 141.68	**a**
41	57.75	± 3.93	**ab**	14.44	± 1.91	**a**	0.25	± 0.03	**a**	74.94	± 2.90	**a**	988.03	± 108.91	**a**
43	56.62	± 5.44	**ab**	13.98	± 0.85	**a**	0.26	± 0.01	**a**	73.94	± 1.24	**a**	863.82	± 129.41	**a**
61	67.04	± 4.92	**b**	18.15	± 1.86	**a**	0.27	± 0.02	**a**	72.49	± 1.54	**a**	1049.52	± 93.03	**a**
74	55.61	± 6.28	**ab**	13.91	± 1.27	**a**	0.27	± 0.02	**a**	73.89	± 1.82	**a**	912.89	± 119.21	**a**
76	57.76	± 5.09	**ab**	14.78	± 1.97	**a**	0.25	± 0.02	**a**	73.46	± 2.88	**a**	912.08	± 94.11	**a**
94	48.45	± 1.99	**a**	12.21	± 2.45	**a**	0.25	± 0.05	**a**	74.28	± 4.56	**a**	861.08	± 82.04	**a**
95	59.70	± 5.20	**ab**	15.19	± 0.34	**a**	0.26	± 0.01	**a**	73.55	± 0.65	**a**	959.60	± 95.29	**a**
150	56.40	± 7.96	**ab**	13.30	± 0.58	**a**	0.23	± 0.02	**a**	77.24	± 1.63	**a**	829.73	± 125.50	**a**
Average	56.27	± 7.37		14.04	± 2.02		0.25	± 0.02		74.11	± 2.30		900.08	± 133.89	
***p*-value**	**2.22x10^{-3}**			**2.00x10^{-2}**			2.40x10^{-1}			4.80x10^{-1}			**4.44x10^{-2}**		

Genotype	PMA (mg plant DW cm^{-2})			Stem number			C %			N %			C/N		
	Med	MAD		Mean	SD		Trim	MAD		Med	MAD		Med	MAD	
8	0.018	± 0.002	**a**	5.45	± 0.93	**a**	44.52	± 0.07	**a**	1.02	± 0.14	**a**	43.36	± 7.06	**a**
23	0.015	± 0.002	**a**	5.20	± 0.69	**a**	43.79	± 0.18	**a**	1.04	± 0.09	**a**	42.17	± 0.49	**a**
41	0.015	± 0.003	**a**	7.15	± 0.60	**b**	44.39	± 0.13	**a**	0.93	± 0.21	**a**	47.96	± 12.81	**a**
43	0.018	± 0.000	**a**	5.35	± 0.65	**a**	44.21	± 0.29	**a**	0.92	± 0.07	**a**	47.96	± 3.41	**a**
61	0.018	± 0.001	**a**	6.85	± 0.55	**bc**	44.40	± 0.19	**a**	0.84	± 0.02	**a**	52.55	± 1.17	**a**
74	0.016	± 0.001	**a**	6.35	± 0.58	**abc**	44.21	± 0.11	**a**	0.97	± 0.09	**a**	45.54	± 3.80	**a**
76	0.016	± 0.001	**a**	6.25	± 0.68	**abc**	44.31	± 0.17	**a**	0.99	± 0.07	**a**	44.33	± 3.67	**a**
94	0.015	± 0.003	**a**	5.65	± 0.22	**ac**	44.20	± 0.08	**a**	1.12	± 0.30	**a**	39.38	± 12.52	**a**
95	0.017	± 0.001	**a**	6.00	± 0.64	**abc**	44.63	± 0.20	**a**	1.05	± 0.09	**a**	42.19	± 2.67	**a**
150	0.015	± 0.001	**a**	5.45	± 0.74	**a**	44.40	± 0.07	**a**	1.19	± 0.18	**a**	37.15	± 4.73	**a**
Average	0.016	± 0.002		5.97	± 0.87		44.32	± 0.27		1.02	± 0.15		43.04	± 7.54	
***p*-value**	5.30x10^{-1}			**9.69x10^{-5}**			**2.00x10^{-2}**			4.00x10^{-1}			3.30x10^{-1}		

C/N: carbon-nitrogen ratio; *C %*: carbon percentage; *DW*: dry weight; *FW*: fresh weight; *H %*: water percentage; *N %*: nitrogen percentage; *PDMC*: plant dry matter content; *PMA*: plant dry mass per area.

Values represent measures of central tendency (*Me*: median; *Mean*: mean; *Trim*: 20% trimmed mean) and dispersion (*MAD*: median absolute deviation; *SD*: standard deviation) of five replicates (n=5) for each genotype or all genotypes and replicates (*Average*; N=50). The calculation of statistical significances (p-value) for each trait is based on one-way ANOVA applying corrections for ANOVA assumptions. Values in bold represent significance ($p < 0.05$). Within columns, numbers followed by the same letter indicate non-statistically significant differences at $p < 0.05$ as determined by post-hoc tests

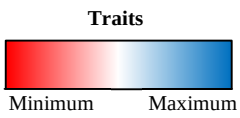

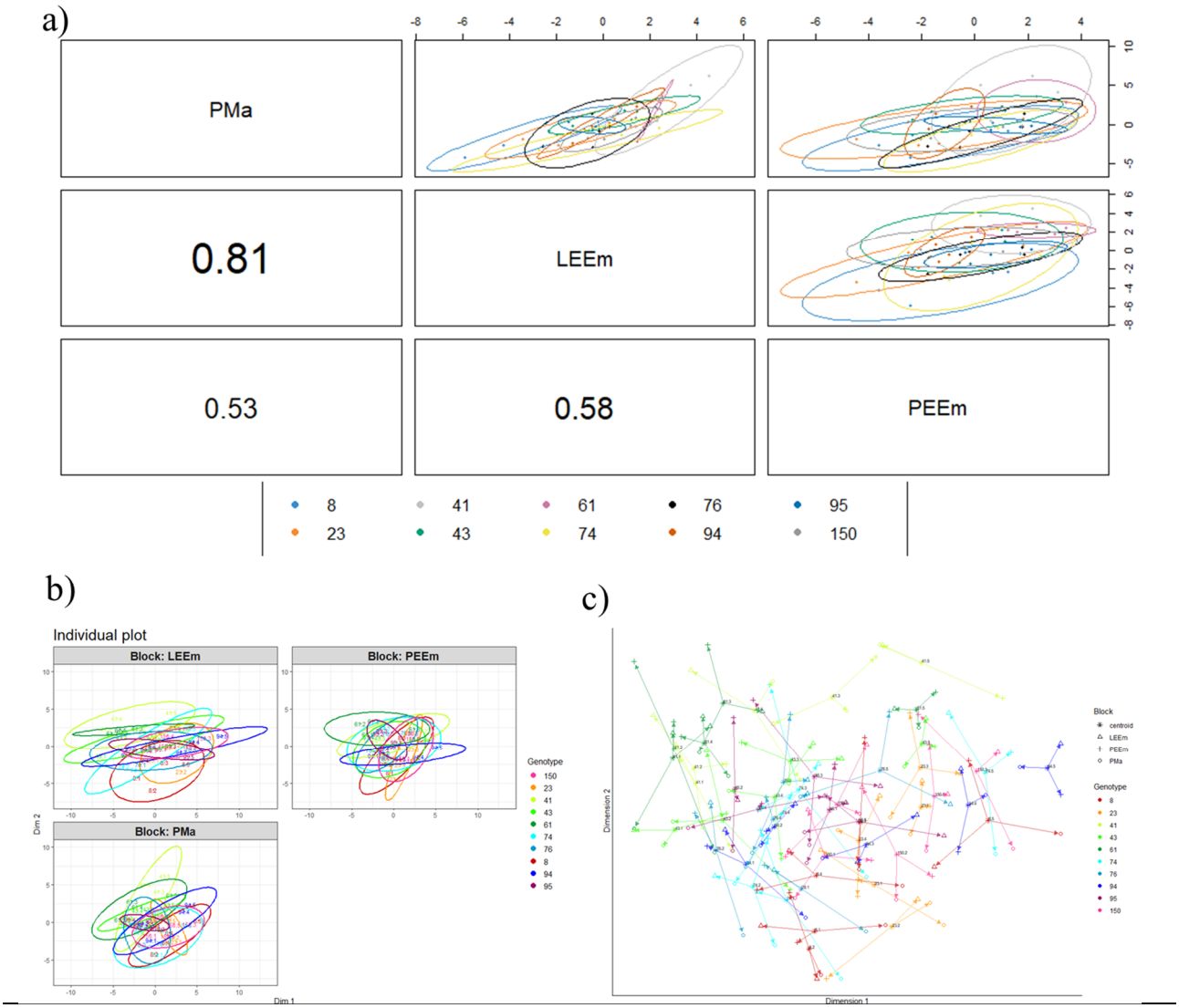

Figure S6.2. DIABLO plots based on DIABLO analysis of three datasets from flag leaf and plant traits measured at ear emergence growth stage and grain yield and quality components at maturity in the response of ten wheat genotypes grown under elevated CO_2 and high temperature.

Three datasets containing values of plant grain yield-quality components at maturity (*PMa*) and leaf and plant traits at ear emergence growth stage (*LEEm* and *PEEm*) were employed to perform DIABLO analysis.

(a) *PlotDIABLO* shows the correlations among the first two components for each dataset and the components of the outcome. The lower triangular panel indicates the Pearson's correlation coefficient, the upper triangular panel the scatter plot. (b) The *individual plot* projects each sample into a plot for each dataset. *Ellipses* around each genotype were added. Tips of arrows in the *arrow plot* (c) indicates the localisation of each sample from each dataset superposed in a common space. Centroids between all datasets for a given sample are shown as *asterisks*.

Table S6.3. Correlations of the flag leaf and plant traits measured at ear emergence growth stage and grain yield and quality components at maturity in the response of ten wheat genotypes grown under elevated CO_2 and high temperature with the first two dimensions of the DIABLO analysis.

Dim. 1				Dim. 2			
Trait	**Corr.**	**Trait**	**Corr.**	**Trait**	**Corr.**	**Trait**	**Corr.**
N %	0.93	**GNE**	-0.01	**Area**	0.94	**TAC**	0.03
N %	0.83	**Tiller number**	-0.03	**Grain number**	0.94	**Na**	0.03
TP	0.80	**Na**	-0.03	**FW**	0.92	**Cu**	0.00
H %	0.78	**Gluc**	-0.04	**Tiller number**	0.89	**Asa**	-0.02
H %	0.76	**Fru**	-0.04	**Ear number**	0.76	**GDH**	-0.03
Aa	0.73	**C %**	-0.05	**Ca**	0.72	**Fruct**	-0.04
Zn	0.72	**Ca**	-0.07	**Grain yield**	0.65	**Zn**	-0.05
PEPCase	0.69	**B**	-0.12	**DW**	0.64	**Stalk**	-0.06
IDH	0.69	**Starch**	-0.15	**HI**	0.57	**N %**	-0.06
G6PDH	0.67	**FW**	-0.16	**GNE**	0.56	**Starch**	-0.08
NBI	0.64	**FRAP**	-0.16	**TPhC**	0.53	**TPhC**	-0.08
FW	0.63	**Grain number**	-0.18	**NR**	0.52	***CRbcx***	-0.10
PK	0.63	***CRbcx***	-0.19	**Chaff**	0.49	C_i	-0.10
GS	0.62	**Ear number**	-0.23	**C %**	0.48	**Fru1,6bisPase**	-0.13
Area	0.58	**GYE**	-0.32	g_s	0.46	**NBI**	-0.13
A	0.54	**Grain weight**	-0.33	Φ_{PSII}	0.45	**LDMC**	-0.17
AGPase	0.52	***Rd***	-0.34	***A***	0.41	**C/N**	-0.17
DW	0.52	**TPhC**	-0.34	**Aboveground**	0.41	***WUE***	-0.18
Fru1,6bisPase	0.49	**LMA**	-0.35	**K**	0.39	**GYE**	-0.18
TPU	0.49	**TAC**	-0.41	***E***	0.37	**PEPCase**	-0.19
NR	0.48	C_i	-0.41	**FW**	0.32	**ORAC**	-0.20
Cu	0.46	**K**	-0.44	***ARbcx***	0.32	**Fe**	-0.20
Chl	0.45	**Nitrate**	-0.45	**DW**	0.32	**B**	-0.20
Fe	0.42	**ORAC**	-0.48	**TP**	0.29	**Flav**	-0.22
HI	0.41	**Grain yield**	-0.51	**H %**	0.28	**C %**	-0.24
Jx	0.39	**Flav**	-0.52	**LMA**	0.28	**PDMC**	-0.24
E	0.38	**GDH**	-0.53	**AGPase**	0.26	**G6PDH**	-0.25
ARbcx	0.37	**Asa**	-0.55	**TPU**	0.24	**GS**	-0.27
Mg	0.36	**S**	-0.63	**N %**	0.24	**GSH**	-0.27
GSH	0.36	**Chaff**	-0.63	**Area**	0.20	**PDMA**	-0.32
Φ_{PSII}	0.30	**Fruct**	-0.64	**P**	0.20	**Mg**	-0.33
g_s	0.30	**DW**	-0.72	**Aa**	0.18	**Protein**	-0.34
TPhC	0.25	**LDMC**	-0.76	**Nitrate**	0.18	**IDH**	-0.36
Vcx	0.24	**Starch**	-0.80	**H %**	0.17	**Chl**	-0.46
C %	0.22	**Aboveground**	-0.82	***Jx***	0.17	**PK**	-0.48
P	0.21	**C/N**	-0.84	**Starch**	0.17	**Suc**	-0.51
Protein	0.20	**PDMA**	-0.86	**S**	0.11	***Rd***	-0.57
Area	0.14	**Stalk**	-0.87	**C/N**	0.09	**Gluc**	-0.71
WUE	0.03	**PDMC**	-0.92	***Vcx***	0.08	**Fru**	-0.75
Suc	0.03	**C/N**	-0.95	**FRAP**	0.05	**Grain weight**	-0.80

A: photosynthetic CO_2 assimilation rate ; *Aa*: amino acids; *AGPase*: ADP-glucose pyrophosphorylase; *ARbcx*: maximum value of photosynthesis limited by Rubisco activity; *Asa*: ascorbic acid; *Chl*: chlorophyll; C_i: intercellular CO_2 concentration; *C/N*: carbon-nitrogen ratio; *C %*: carbon percentage; *CRbcx*: intercellular CO_2 concentration at maximum photosynthesis limited by Rubisco activity; *DW*: dry weight; *E*: transpiration; *Flav*: flavonoids; *FRAP*: ferric ion reducing antioxidant power; *Fru*: fructose; *Fru1,6bisPase*: cytosolic fructose-1,6-bisphosphatase; *Fruct*: fructans; *FW*: fresh weight; *G6PDH*: glucose-6-phosphate dehydrogenase; *GDH*: glutamate dehydrogenase; *Gluc*: glucose; *GNE*: grain number ear^{-1}; *GS*: glutamine synthetase; g_s: stomatal conductance; *GSH*: glutathione; *GYE*: grain yield ear^{-1}: *H %*: water percentage; *IDH*: NADP-dependent isocitrate dehydrogenase; *Jx*: maximum rate of electron transport; *LDMC*: leaf dry matter content; *LMA*: leaf dry mass per area; *NBI*: nitrogen balance index; *N %*: nitrogen percentage; *NR*: nitrate reductase; *ORAC*: oxygen radical absorbance capacity; *PDMC*: plant dry matter content; *PEPCase*: phosphoenolpyruvate carboxylase; Φ_{PSII}: quantum yield of PSII electron transport; *PK*: pyruvate kinase; *PMA*: plant mass per area; *Rd*: respiration rate; *Suc*: sucrose; *TAC*: total antioxidant capacity; *TP*: total protein; *TPhC*: total phenolic compounds; *TPU*: maximum rate of triose phosphate use; *Vcx*: maximum carboxylation rate of Rubisco; *WUE*: water-use efficiency.

Three datasets containing values of plant grain yield-quality components at maturity (*PMa*) and leaf and plant traits at ear emergence growth stage (*LEEm* and *PEEm*) were employed to perform DIABLO analysis. Different colour backgrounds were employed to identify the dataset belonging to each trait (PMa:orange; LEEm: green; PEEm: grey).

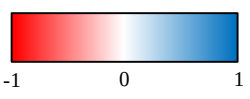

CHAPTER 10

Bibliography

Abbo, S., Pinhasi van-Oss, R., Gopher, A., Saranga, Y., Ofner, I. and Peleg, Z. (2014) 'Plant domestication versus crop evolution: A conceptual framework for cereals and grain legumes', *Trends in Plant Science*, 19(6), pp. 351–360. doi:10.1016/j.tplants.2013.12.002.

AbdElgawad, H., Farfan-Vignolo, E.R., Vos, D. de and Asard, H. (2015) 'Elevated CO_2 mitigates drought and temperature-induced oxidative stress differently in grasses and legumes', *Plant Science*, 231(2015), pp. 1–10. doi:10.1016/j.plantsci.2014.11.001.

Acreche, M.M. and Slafer, G.A. (2006) 'Grain weight response to increases in number of grains in wheat in a Mediterranean area', *Field Crops Research*, 98(1), pp. 52–59. doi:10.1016/j.fcr.2005.12.005.

Agencia Estatal Boletín Oficial del Estado (2010) 'Real Decreto 1615/2010, de 7 de diciembre, por el que se aprueba la norma de calidad del trigo', *Boletín Oficial del Estado*, pp. 102674–102680.

Ahmad, H.I., Ahmad, M.J., Jabbir, F., Ahmar, S., Ahmad, N., Elokil, A.A. and Chen, J. (2020) 'The Domestication Makeup: Evolution, Survival, and Challenges', *Frontiers in Ecology and Evolution*, 8(May), pp. 1–17. doi:10.3389/fevo.2020.00103.

Ainsworth, E.A. and Gillespie, K.M. (2007) 'Estimation of total phenolic content and other oxidation substrates in plant tissues using Folin–Ciocalteu reagent', *Nature Protocols*, 2(4), pp. 875–877. doi:10.1038/nprot.2007.102.

Ainsworth, E.A. and Long, S.P. (2004) 'What have we learned from 15 years of free-air CO_2 enrichment (FACE)? A meta-analytic review of the responses of photosynthesis, canopy properties and plant production to rising CO_2', *New Phytologist*, 165(2), pp. 351–372. doi:10.1111/j.1469-8137.2004.01224.x.

Ainsworth, E.A. and Long, S.P. (2021) '30 years of free-air carbon dioxide enrichment (FACE): What have we learned about future crop productivity and its potential for adaptation?', *Global Change Biology*, 27(1), pp. 27–49. doi:10.1111/gcb.15375.

Ainsworth, E.A. and Rogers, A. (2007) 'The response of photosynthesis and stomatal conductance to rising [CO_2]: Mechanisms and environmental interactions', *Plant, Cell and Environment*, 30(3), pp. 258–270. doi:10.1111/j.1365-3040.2007.01641.x.

Ainsworth, E.A., Rogers, A., Nelson, R. and Long, S.P. (2004) 'Testing the "source-sink" hypothesis of down-regulation of photosynthesis in elevated [CO_2] in the field with single gene substitutions in Glycine max', *Agricultural and Forest Meteorology*, 122(1–2), pp. 85–94. doi:10.1016/j.agrformet.2003.09.002.

Ainsworth, E.A., Rogers, A., Vodkin, L.O., Walter, A. and Schurr, U. (2006) 'The effects of elevated CO_2 concentration on soybean gene expression. An analysis of growing and mature leaves', *Plant Physiology*, 142(1), pp. 135–147. doi:10.1104/pp.106.086256.

Al-Ghussain, L. (2019) 'Global warming: review on driving forces and mitigation', *Environmental Progress and Sustainable Energy*, 38(1), pp. 13–21. doi:10.1002/ep.13041.

Almanza-Pinzón, M.I., Khairallah, M., Fox, P.N. and Warburton, M.L. (2003) 'Comparison of molecular markers and coefficients of parentage for the analysis of genetic diversity among spring bread wheat accessions', *Euphytica*, 130(1), pp. 77–86. doi:10.1023/A:1022310014075.

Anagnostou, E., John, E.H., Edgar, K.M., Foster, G.L., Ridgwell, A., Inglis, G.N., Pancost, R.D., Lunt, D.J. and Pearson, P.N. (2016) 'Changing atmospheric CO_2 concentration was the primary driver of early Cenozoic climate', *Nature*, 533(7603), pp. 380–384. doi:10.1038/nature17423.

Anderson, W.K. and Garlinge, J.R. (2000) 'The Wheat Book', *Department of Primary*

Industries and Regional Development, Western Australia, Perth. Bulletin 4443. [Preprint].

Andersson, I. and Backlund, A. (2008) 'Structure and function of Rubisco', *Plant Physiology and Biochemistry*, 46(3), pp. 275–291. doi:10.1016/j.plaphy.2008.01.001.

Aoki, N., Whitfeld, P., Hoeren, F., Scofield, G., Newell, K., Patrick, J. *et al.* (2002) 'Three sucrose transporter genes are expressed in the developing grain of hexaploid wheat', *Plant Molecular Biology*, 50(3), pp. 453–462. doi:10.1023/A:1019846832163.

Aranjuelo, I., Cabrera-Bosquet, L., Morcuende, R., Avice, J.C., Nogués, S., Araus, J.L., Martínez-Carrasco, R. and Pérez, P. (2011) 'Does ear C sink strength contribute to overcoming photosynthetic acclimation of wheat plants exposed to elevated CO 2?', *Journal of Experimental Botany*, 62(11), pp. 3957–3969. doi:10.1093/jxb/err095.

Aranjuelo, I., Erice, G., Nogués, S., Morales, F., Irigoyen, J.J. and Sánchez-Díaz, M. (2008) 'The mechanism(s) involved in the photoprotection of PSII at elevated CO_2 in nodulated alfalfa plants', *Environmental and Experimental Botany*, 64(3), pp. 295–306. doi:10.1016/j.envexpbot.2008.01.002.

Araus, J.L., Sanchez-Bragado, R. and Vicente, R. (2021) 'Improving crop yield and resilience through optimization of photosynthesis: panacea or pipe dream?', *Journal of Experimental Botany*, 72(11), pp. 3936–3955. doi:10.1093/jxb/erab097.

Araus, J.L., Slafer, G.A., Royo, C. and Serret, M.D. (2008) 'Breeding for yield potential and stress adaptation in cereals', *Critical Reviews in Plant Sciences*, 27(6), pp. 377–412. doi:10.1080/07352680802467736.

Arzani, A. and Ashraf, M. (2017) 'Cultivated ancient wheats (*Triticum* spp.): A potential source of health-beneficial food Products', *Comprehensive Reviews in Food Science and Food Safety*, 16(3), pp. 477–488. doi:10.1111/1541-4337.12262.

Asif, M., Yilmaz, O. and Ozturk, L. (2017) 'Elevated carbon dioxide ameliorates the effect of Zn deficiency and terminal drought on wheat grain yield but compromises nutritional quality', *Plant and Soil*, 411(1–2), pp. 57–67. doi:10.1007/s11104-016-2996-9.

Asseng, S., Ewert, F., Martre, P., Rötter, R.P., Lobell, D.B., Cammarano, D. *et al.* (2015) 'Rising temperatures reduce global wheat production', *Nature Climate Change*, 5(2), pp. 143–147. doi:10.1038/nclimate2470.

Atkin, O.K., Millar, A.H., Gardeström, P. and Day, D.A. (2000) 'Photosynthesis, carbohydrate metabolism and respiration in leaves of higher plants', in Leegood, R.C., Sharkey, T.D. and von Caemmerer, S. (eds) *Physiology*. Dordrecht: Springer Netherlands (Advances in Photosynthesis and Respiration), pp. 153–175. doi:10.1007/0-306-48137-5_7.

Austin, R.B., Ford, M.A., Morgan, C.L., Brancourt-Hulmel, M., Doussinault, G., Lecomte, C. *et al.* (1989) 'Physiological processes associated with wheat yield progress in the UK', *Crop Science*, 10(1), pp. 457–472. doi:10.1071/AR9890457.

Avigad, G. and Dey, P.M. (1997) 'Carbohydrate metabolism: Storage carbohydrates', in *Plant Biochemistry*. Elsevier, pp. 143–204. doi:10.1016/B978-012214674-9/50005-9.

Bánki, O., Roskov, Y., Döring, M., Ower, G., Vandepitte, L., Hobern, D. *et al.* (2021) 'Catalogue of life checklist'. Leiden, Netherlands: Catalogue of Life. doi:10.48580/d4t44.

Barnabás, B., Jäger, K. and Fehér, A. (2008) 'The effect of drought and heat stress on reproductive processes in cereals', *Plant, Cell and Environment*, 31(1), pp. 11–38. doi:10.1111/j.1365-3040.2007.01727.x.

Barneix, A.J. (2007) 'Physiology and biochemistry of source-regulated protein accumulation in

the wheat grain', *Journal of Plant Physiology*, 164(5), pp. 581–590. doi:10.1016/j.jplph.2006.03.009.

Baxter, A., Mittler, R. and Suzuki, N. (2014) 'ROS as key players in plant stress signalling', *Journal of Experimental Botany*, 65(5), pp. 1229–1240. doi:10.1093/jxb/ert375.

Ben-Shachar, M., Lüdecke, D. and Makowski, D. (2020) 'effectsize: Estimation of Effect Size Indices and Standardized Parameters', *Journal of Open Source Software*, 5(56), p. 2815. doi::10.21105/joss.01412.

Bénard, C. and Gibon, Y. (2016) 'Measurement of enzyme activities and optimization of continuous and discontinuous assays', *Current Protocols in Plant Biology*, 1(2), pp. 247–262. doi:10.1002/cppb.20003.

Bencze, S., Makádi, M., Aranyos, T.J., Földi, M., Hertelendy, P., Mikó, P., Bosi, S., Negri, L. and Drexler, D. (2020) 'Re-introduction of ancient wheat cultivars into organic agriculture-Emmer and Einkorn cultivation experiences under marginal conditions', *Sustainability (Switzerland)*, 12(4). doi:10.3390/su12041584.

Bender, D.A. (2003) 'Tricarboxylic acid cycle', in *Encyclopedia of Food Sciences and Nutrition*. Elsevier, pp. 5851–5856. doi:10.1016/B0-12-227055-X/01363-8.

Benzie, I.F.F. and Strain, J.J. (1996) 'The ferric reducing ability of plasma (FRAP) as a measure of "antioxidant power": The FRAP assay', *Analytical Biochemistry*, 239(1), pp. 70–76. doi:10.1006/abio.1996.0292.

Berardy, A., Lynch, H. and Wharton, C. (2019) *Food systems: Description and trends, Environmental Nutrition: Connecting Health and Nutrition with Environmentally Sustainable Diets*. Elsevier Inc. doi:10.1016/B978-0-12-811660-9.00002-3.

Bergkamp, B., Impa, S.M., Asebedo, A.R., Fritz, A.K. and Jagadish, S.V.K. (2018) 'Prominent winter wheat varieties response to post-flowering heat stress under controlled chambers and field based heat tents', *Field Crops Research*, 222, pp. 143–152. doi:10.1016/j.fcr.2018.03.009.

Bernacchi, C.J., Kimball, B.A., Quarles, D.R., Long, S.P. and Ort, D.R. (2007) 'Decreases in stomatal conductance of soybean under open-air elevation of [CO_2] are closely coupled with decreases in ecosystem evapotranspiration', *Plant Physiology*, 143(1), pp. 134–144. doi:10.1104/pp.106.089557.

Berry, J. and Bjorkman, O. (1980) 'Photosynthetic response and adaptation to temperature in higher plants', *Annual Review of Plant Physiology*, 31(1), pp. 491–543. doi:10.1146/annurev.pp.31.060180.002423.

Bhandari, H., Bhanu, A.N., Srivastava, K., Singh, M., Shreya and Hemantaranjan, A. (2017) 'Assessment of genetic diversity in crop plants - an overview', *Advances in Plants & Agriculture Research*, 7(3), pp. 279–286. doi:10.15406/apar.2017.07.00255.

Bhattacharya, A. (2019) 'Nitrogen-use efficiency under changing climatic conditions', in *Changing Climate and Resource Use Efficiency in Plants*. Elsevier, pp. 181–240. doi:10.1016/B978-0-12-816209-5.00004-0.

Bielecka, M., Watanabe, M., Morcuende, R., Scheible, W.R., Hawkesford, M.J., Hesse, H. and Hoefgen, R. (2015) 'Transcriptome and Metabolome analysis of plant sulfate starvation and resupply provides novel information on transcriptional regulation of metabolism associated with sulfur, nitrogen and phosphorus nutritional responses in *Arabidopsis*', *Frontiers in Plant Science*, 5(JAN), pp. 1–18. doi:10.3389/fpls.2014.00805.

Bloom, A.J. (2015a) 'Photorespiration and nitrate assimilation: A major intersection between plant carbon and nitrogen', *Photosynthesis Research*, 123(2), pp. 117–128. doi:10.1007/s11120-014-

0056-y.

Bloom, A.J. (2015b) 'The increasing importance of distinguishing among plant nitrogen sources', *Current Opinion in Plant Biology*, 25(2), pp. 10–16. doi:10.1016/j.pbi.2015.03.002.

Bloom, A.J., Burger, M., Asensio, J.S.R. and Cousins, A.B. (2010) 'Carbon dioxide enrichment inhibits nitrate assimilation in wheat and *Arabidopsis*', *Science*, 328(5980), pp. 899–903. doi:10.1126/science.1186440.

Bloom, A.J., Burger, M., Kimball, B.A. and Pinter, P.J. (2014) 'Nitrate assimilation is inhibited by elevated CO_2 in field-grown wheat', *Nature Climate Change*, 4(6), pp. 477–480. doi:10.1038/nclimate2183.

Bloom, A.J., Smart, D.R., Nguyen, D.T. and Searles, P.S. (2002) 'Nitrogen assimilation and growth of wheat under elevated carbon dioxide', *Proceedings of the National Academy of Sciences of the United States of America*, 99(3), pp. 1730–1735. doi:10.1073/pnas.022627299.

Blum, A. (1990) 'Variation among wheat cultivars in the response of leaf gas exchange to light', *The Journal of Agricultural Science*, 115(3), pp. 305–311. doi:10.1017/S0021859600075717.

Bongaarts, J. (2009) 'Human population growth and the demographic transition', *Philosophical Transactions of the Royal Society B: Biological Sciences*, 364(1532), pp. 2985–2990. doi:10.1098/rstb.2009.0137.

Boukid, F., Folloni, S., Sforza, S., Vittadini, E. and Prandi, B. (2018) 'Current trends in ancient grains-based foodstuffs: Insights into nutritional aspects and technological applications', *Comprehensive Reviews in Food Science and Food Safety*, 17(1), pp. 123–136. doi:10.1111/1541-4337.12315.

Bourgault, M., Brand, J., Tausz-Posch, S., Armstrong, R.D., O'Leary, G.L., Fitzgerald, G.J. and Tausz, M. (2017) 'Yield, growth and grain nitrogen response to elevated CO_2 in six lentil (*Lens culinaris*) cultivars grown under Free Air CO_2 Enrichment (FACE) in a semi-arid environment', *European Journal of Agronomy*, 87(February), pp. 50–58. doi:10.1016/j.eja.2017.05.003.

Bourgault, M., Dreccer, M.F., James, A.T. and Chapman, S.C. (2013) 'Genotypic variability in the response to elevated CO_2 of wheat lines differing in adaptive traits', *Functional Plant Biology*, 40(2), pp. 172–184. doi:10.1071/FP12193.

Bradford, M.M. (1976) 'A rapid and sensitive method for the quantitation of microgram quantities of protein utilizing the principle of protein-dye binding', *Analytical Biochemistry*, 72(1–2), pp. 248–254. doi:10.1016/0003-2697(76)90527-3.

Brestic, M., Zivcak, M., Hauptvogel, P., Misheva, S., Kocheva, K., Yang, X., Li, X. and Allakhverdiev, S.I. (2018) 'Wheat plant selection for high yields entailed improvement of leaf anatomical and biochemical traits including tolerance to non-optimal temperature conditions', *Photosynthesis Research*, 136(2), pp. 245–255. doi:10.1007/s11120-018-0486-z.

Brinton, J. and Uauy, C. (2019) 'A reductionist approach to dissecting grain weight and yield in wheat', *Journal of Integrative Plant Biology*, 61(3), pp. 337–358. doi:10.1111/jipb.12741.

Broberg, M., Högy, P. and Pleijel, H. (2017) 'CO_2-induced changes in wheat grain composition: Meta-analysis and response functions', *Agronomy*, 7(2), p. 32. doi:10.3390/agronomy7020032.

Brouns, F., Hemery, Y., Price, R. and Anson, N.M. (2012) 'Wheat Aleurone: Separation, Composition, Health Aspects, and Potential Food Use', *Critical Reviews in Food Science and Nutrition*, 52(6), pp. 553–568. doi:10.1080/10408398.2011.589540.

Brown, T.A., Jones, M.K., Powell, W. and Allaby, R.G. (2009) 'The complex origins of domesticated crops in the Fertile Crescent', *Trends in Ecology & Evolution*, 24(2), pp. 103–109.

doi:10.1016/j.tree.2008.09.008.

Brydges, C.R. (2019) 'Effect Size Guidelines, Sample Size Calculations, and Statistical Power in Gerontology', *Innovation in Aging*, 3(4), pp. 1–8. doi:10.1093/geroni/igz036.

Buchanan, E.M., Gillenwaters, A., Scofield, J.E. and Valentine, K.D. (2019) 'MOTE: Measure of the Effect: Package to assist in effect size calculations and their confidence intervals'. Available at: http://github.com/doomlab/MOTE.

Cai, C., Yin, X., He, S., Jiang, W., Si, C., Struik, P.C. *et al.* (2016) 'Responses of wheat and rice to factorial combinations of ambient and elevated CO_2 and temperature in FACE experiments', *Global Change Biology*, 22(2), pp. 856–874. doi:10.1111/gcb.13065.

Calderini, D.F., Savin, R., Abeledo, L.G., Reynolds, M.P. and Slafer, G.A. (2001) 'The importance of the period immediately preceding anthesis for grain weight determination in wheat', *Euphytica*, 119(1–2), pp. 199–204. doi:10.1023/A:1017597923568.

Calderini, D.F., Torres-León, S. and Slafer, G.A. (1995) 'Consequences of wheat breeding on nitrogen and phosphorus yield, grain nitrogen and phosphorus concentration and associated traits', *Annals of Botany*, pp. 315–322. doi:10.1006/anbo.1995.1101.

Campbell, N., Urry, L., Cain, M., Wasserman, S., Minorsky, P. and Orr, R. (2020) *Biology 12th Edition, Pearson Education*.

Canevara, M.G., Romani, M., Corbellini, M., Perenzin, M. and Borghi, B. (1994) 'Evolutionary trends in morphological, physiological, agronomical and qualitative traits of Triticum aestivum L. cultivars bred in Italy since 1900', *European Journal of Agronomy*, 3(3), pp. 175–185. doi:10.1016/S1161-0301(14)80081-6.

Carlisle, E., Myers, S., Raboy, V. and Bloom, A. (2012) 'The effects of inorganic nitrogen form and CO_2 concentration on wheat yield and nutrient accumulation and distribution', *Frontiers in Plant Science*, 3(SEP), pp. 1–13. doi:10.3389/fpls.2012.00195.

Carmo-Silva, E., Andralojc, P.J., Scales, J.C., Driever, S.M., Mead, A., Lawson, T., Raines, C.A. and Parry, M.A.J. (2017) 'Phenotyping of field-grown wheat in the UK highlights contribution of light response of photosynthesis and flag leaf longevity to grain yield', *Journal of Experimental Botany*, 68(13), pp. 3473–3486. doi:10.1093/jxb/erx169.

Castro-Rodríguez, V., Cañas, R.A., De La Torre, F.N., Pascual, M.B., Avila, C. and Cánovas, F.M. (2017) 'Molecular fundamentals of nitrogen uptake and transport in trees', *Journal of Experimental Botany*, 68(10), pp. 2489–2500. doi:10.1093/jxb/erx037.

Cawse, P.A. (1967) 'The determination of nitrate in soil solutions by ultraviolet spectrophotometry', *The Analyst*, 92(1094), pp. 311–315. doi:10.1039/AN9679200311.

Cerovic, Z.G., Ounis, A., Cartelat, A., Latouche, G., Goulas, Y., Meyer, S. and Moya, I. (2002) 'The use of chlorophyll fluorescence excitation spectra for the non-destructive in situ assessment of UV-absorbing compounds in leaves', *Plant, Cell and Environment*, 25(12), pp. 1663–1676. doi:10.1046/j.1365-3040.2002.00942.x.

Chatzav, M., Peleg, Z., Ozturk, L., Yazici, A., Fahima, T., Cakmak, I. and Saranga, Y. (2010) 'Genetic diversity for grain nutrients in wild emmer wheat: Potential for wheat improvement', *Annals of Botany*, 105(7), pp. 1211–1220. doi:10.1093/aob/mcq024.

Chavan, S.G., Duursma, R.A., Tausz, M. and Ghannoum, O. (2019) 'Elevated CO_2 alleviates the negative impact of heat stress on wheat physiology but not on grain yield', *Journal of Experimental Botany*, 70(21), pp. 6447–6459. doi:10.1093/jxb/erz386.

Chaves, M.M. and Oliveira, M.M. (2004) 'Mechanisms underlying plant resilience to water

deficits: Prospects for water-saving agriculture', *Journal of Experimental Botany*, 55(407), pp. 2365–2384. doi:10.1093/jxb/erh269.

Chhetri, N. and Chaudhary, P. (2011) 'Green Revolution: Pathways to food security in an era of climate variability and change?', *Journal of Disaster Research*, 6(5), pp. 486–497. doi:10.20965/jdr.2011.p0486.

Chibbar, R.N., Jaiswal, S., Gangola, M. and Båga, M. (2015) 'Carbohydrate metabolism', *Encyclopedia of Food Grains: Second Edition*, 2–4, pp. 161–173. doi:10.1016/B978-0-12-394437-5.00089-9.

Christ, R.A. and Körner, C. (1995) 'Responses of shoot and root gas exchange, leaf blade expansion and biomass production to pulses of elevated CO_2 in hydroponic wheat', *Journal of Experimental Botany*, 46(11), pp. 1661–1667. doi:10.1093/jxb/46.11.1661.

Ciardini, V., Contessa, G.M., Falsaperla, R., Gómez-Amo, J.L., Meloni, D., Monteleone, F. *et al.* (2016) 'Global and Mediterranean climate change: a short summary.', *Annali dell'Istituto superiore di sanita*, 52(3), pp. 325–337. doi:10.4415/ANN_16_03_04.

Cimini, S., Locato, V., Vergauwen, R., Paradiso, A., Cecchini, C., Vandenpoel, L. *et al.* (2015) 'Fructan biosynthesis and degradation as part of plant metabolism controlling sugar fluxes during durum wheat kernel maturation', *Frontiers in Plant Science*, 6(February), pp. 1–10. doi:10.3389/fpls.2015.00089.

Cole, C. V., Duxbury, J., Freney, J., Heinemeyer, O., Minami, K., Mosier, A. *et al.* (1997) 'Global estimates of potential mitigation of greenhouse gas emissions by agriculture', *Nutrient Cycling in Agroecosystems*, 49(1–3), pp. 221–228. doi:10.1023/a:1009731711346.

Conroy, J. and Hocking, P. (1993) 'Nitrogen nutrition of C3 plants at elevated atmospheric CO_2 concentrations', *Physiologia Plantarum*, 89(3), pp. 570–576. doi:10.1111/j.1399-3054.1993.tb05215.x.

Córdoba, J., Molina-Cano, J.L., Martínez-Carrasco, R., Morcuende, R. and Pérez, P. (2016) 'Functional and transcriptional characterization of a barley mutant with impaired photosynthesis', *Plant Science*, 244, pp. 19–30. doi:10.1016/j.plantsci.2015.12.006.

Córdoba, J., Molina-Cano, J.L., Pérez, P., Morcuende, R., Moralejo, M., Savé, R. and Martínez-Carrasco, R. (2015) 'Photosynthesis-dependent/independent control of stomatal responses to CO_2 in mutant barley with surplus electron transport capacity and reduced SLAH3 anion channel transcript', *Plant Science*, 239, pp. 15–25. doi:10.1016/j.plantsci.2015.07.011.

Córdoba, J., Pérez, P., Morcuende, R., Molina-Cano, J.-L. and Martinez-Carrasco, R. (2017) 'Acclimation to elevated CO_2 is improved by low Rubisco and carbohydrate content, and enhanced Rubisco transcripts in the G132 barley mutant', *Environmental and Experimental Botany*, 137, pp. 36–48. doi:10.1016/j.envexpbot.2017.02.005.

Cossani, C.M. and Reynolds, M.P. (2012) 'Physiological traits for improving heat tolerance in wheat', *Plant Physiology*, 160(4), pp. 1710–1718. doi:10.1104/pp.112.207753.

Cowling, W.A. (2007) 'Genetic diversity in Australian canola and implications for crop breeding for changing future environments', *Field Crops Research*, 104(1–3), pp. 103–111. doi:10.1016/j.fcr.2006.12.014.

Cramer, M.D., Hawkins, H.-J. and Verboom, G.A. (2009) 'The importance of nutritional regulation of plant water flux', *Oecologia*, 161(1), pp. 15–24. doi:10.1007/s00442-009-1364-3.

Cross, J.M., Von Korff, M., Altmann, T., Bartzetko, L., Sulpice, R., Gibon, Y., Palacios, N. and Stitt, M. (2006) 'Variation of enzyme activities and metabolite levels in 24 arabidopsis

accessions growing in carbon-limited conditions', *Plant Physiology*, 142(4), pp. 1574–1588. doi:10.1104/pp.106.086629.

Curci, P.L., Aiese Cigliano, R., Zuluaga, D.L., Janni, M., Sanseverino, W. and Sonnante, G. (2017) 'Transcriptomic response of durum wheat to nitrogen starvation', *Scientific Reports*, 7(1), p. 1176. doi:10.1038/s41598-017-01377-0.

Dai, Z., Plessis, A., Vincent, J., Duchateau, N., Besson, A., Dardevet, M. *et al.* (2015) 'Transcriptional and metabolic alternations rebalance wheat grain storage protein accumulation under variable nitrogen and sulfur supply', *Plant Journal*, 83(2), pp. 326–343. doi:10.1111/tpj.12881.

Daly, A.J., Baetens, J.M. and De Baets, B. (2018) 'Ecological diversity: Measuring the unmeasurable', *Mathematics*, 6(7). doi:10.3390/math6070119.

Davies, W.P. (2003) 'An historical perspective from the Green Revolution to the Gene Revolution', *Nutrition Reviews*, 61(suppl_6), pp. S124–S134. doi:10.1301/nr.2003.jun.s124-s134.

Davis, P.H., Mill, R.R. and Tan, K. (1985) 'Flora of Turkey and the East Aegean Islands. Volume 9', in. Edinburgh University Press.

Dechorgnat, J., Nguyen, C.T., Armengaud, P., Jossier, M., Diatloff, E., Filleur, S. and Daniel-Vedele, F. (2011) 'From the soil to the seeds: The long journey of nitrate in plants', *Journal of Experimental Botany*, 62(4), pp. 1349–1359. doi:10.1093/jxb/erq409.

DePoy, E. and Gitlin, L.N. (2016) 'Statistical analysis for experimental-type designs', in *Introduction to Research*. Elsevier, pp. 282–310. doi:10.1016/B978-0-323-26171-5.00020-3.

Distelfeld, A., Cakmak, I., Peleg, Z., Ozturk, L., Yazici, A.M., Budak, H., Saranga, Y. and Fahima, T. (2007) 'Multiple QTL-effects of wheat Gpc-B1 locus on grain protein and micronutrient concentrations', *Physiologia Plantarum*, 129(3), pp. 635–643. doi:10.1111/j.1399-3054.2006.00841.x.

Djanaguiraman, M., Narayanan, S., Erdayani, E. and Prasad, P.V.V. (2020) 'Effects of high temperature stress during anthesis and grain filling periods on photosynthesis, lipids and grain yield in wheat', *BMC Plant Biology*, 20(1), pp. 1–12. doi:10.1186/s12870-020-02479-0.

Doebley, J.F., Gaut, B.S. and Smith, B.D. (2006) 'The molecular genetics of crop domestication', *Cell*, 127(7), pp. 1309–1321. doi:10.1016/j.cell.2006.12.006.

Donmez, E., Sears, R.G., Shroyer, J.P. and Paulsen, G.M. (2001) 'Genetic gain in yield attributes of winter wheat in the Great Plains', *Crop Science*, 41(5), pp. 1412–1419. doi:10.2135/cropsci2001.4151412x.

Dreccer, M.F., Chapman, S.C., Rattey, A.R., Neal, J., Song, Y., Christopher, J. (Jack) T. and Reynolds, M. (2013) 'Developmental and growth controls of tillering and water-soluble carbohydrate accumulation in contrasting wheat (Triticum aestivum L.) genotypes: can we dissect them?', *Journal of Experimental Botany*, 64(1), pp. 143–160. doi:10.1093/jxb/ers317.

Driever, S.M., Lawson, T., Andralojc, P.J., Raines, C.A. and Parry, M.A.J. (2014) 'Natural variation in photosynthetic capacity, growth, and yield in 64 field-grown wheat genotypes', *Journal of Experimental Botany*, 65(17), pp. 4959–4973. doi:10.1093/jxb/eru253.

Duggan, B.L., Richards, R.A., van Herwaarden, A.F. and Fettell, N.A. (2005) 'Agronomic evaluation of a tiller inhibition gene (tin) in wheat. I. Effect on yield, yield components, and grain protein', *Australian Journal of Agricultural Research*, 56(2), p. 169. doi:10.1071/AR04152.

Dyer, G.A., López-Feldman, A., Yúnez-Naude, A. and Taylor, J.E. (2014) 'Genetic erosion in maize's center of origin', *Proceedings of the National Academy of Sciences of the United States of America*, 111(39), pp. 14094–14099. doi:10.1073/pnas.1407033111.

Ebeling, M.E. (1968) 'The Dumas method for nitrogen in feeds', *Journal of AOAC INTERNATIONAL*, 51(4), pp. 766–770. doi:10.1093/jaoac/51.4.766.

Ellis, P.D. (2010) *The Essential Guide to Effect Sizes: Statistical Power, Meta-Analysis, and the Interpretation of Research Results*. Cambridge: Cambridge University Press. doi:10.1017/CBO9780511761676.

Elmqvist, T., Folke, C., Nyström, M., Peterson, G., Bengtsson, J., Walker, B. and Norberg, J. (2003) 'Response diversity, ecosystem change, and resilience', *Frontiers in Ecology and the Environment*, 1(9), pp. 488–494. doi:10.1890/1540-9295(2003)001[0488:RDECAR]2.0.CO;2.

Erbs, M., Manderscheid, R., Jansen, G., Seddig, S., Pacholski, A. and Weigel, H.J. (2010) 'Effects of free-air CO_2 enrichment and nitrogen supply on grain quality parameters and elemental composition of wheat and barley grown in a crop rotation', *Agriculture, Ecosystems and Environment*, 136(1–2), pp. 59–68. doi:10.1016/j.agee.2009.11.009.

Ercoli, L., Lulli, L., Arduini, I., Mariotti, M. and Masoni, A. (2011) 'Durum wheat grain yield and quality as affected by S rate under Mediterranean conditions', *European Journal of Agronomy*, 35(2), pp. 63–70. doi:10.1016/j.eja.2011.03.007.

Erice, G., Sanz-Sáez, Á., González-Torralba, J., Méndez-Espinoza, A.M., Urretavizcaya, I., Nieto, M.T. *et al.* (2019) 'Impact of elevated CO_2 and drought on yield and quality traits of a historical (Blanqueta) and a modern (Sula) durum wheat', *Journal of Cereal Science*, 87(October 2018), pp. 194–201. doi:10.1016/j.jcs.2019.03.012.

Evans, J.R. and Poorter, H. (2001) 'Photosynthetic acclimation of plants to growth irradiance: the relative importance of specific leaf area and nitrogen partitioning in maximizing carbon gain', *Plant, Cell & Environment*, 24(8), pp. 755–767. doi:10.1046/j.1365-3040.2001.00724.x.

Evenson, R.E. and Gollin, D. (2003) 'Assessing the impact of the Green Revolution, 1960 to 2000', *Science*, 300(5620), pp. 758–762. doi:10.1126/science.1078710.

Fan, M.S., Zhao, F.J., Fairweather-Tait, S.J., Poulton, P.R., Dunham, S.J. and McGrath, S.P. (2008) 'Evidence of decreasing mineral density in wheat grain over the last 160 years', *Journal of Trace Elements in Medicine and Biology*, 22(4), pp. 315–324. doi:10.1016/j.jtemb.2008.07.002.

Fangmeier, A., De Temmerman, L., Mortensen, L., Kemp, K., Burke, J., Mitchell, R., Van Oijen, M. and Weigel, H.J. (1999) 'Effects on nutrients and on grain quality in spring wheat crops grown under elevated CO_2 concentrations and stress conditions in the European, multiple-site experiment "ESPACE-wheat"', *European Journal of Agronomy*, 10(3–4), pp. 215–229. doi:10.1016/S1161-0301(99)00012-X.

FAO (2014) *The future of food and agriculture – Trends and challenges*. Rome: FAO. Available at: www.fao.org.

FAO (2021) *FAOSTAT*. Available at: http://www.fao.org/faostat/en/#data (Accessed: 13 September 2021).

FAO, IFAD, UNICEF, WFP and WHO (2018) *The state of food security and nutrition in the world 2018. Building climate resilience for food security and nutrition*. Rome. Available at: https://www.wfp.org/publications/2018-state-food-security-and-nutrition-world-sofi-report.

FAO, IFAD, UNICEF, WFP and WHO (2019) *The State of Food Security and Nutrition in the World 2019. Safeguarding against economic slowdowns and downturns*. Rome. Available at: http://www.fao.org/state-of-food-security-nutrition.

FAO, IFAD, UNICEF, WFP and WHO (2021) *The state of food security and nutrition in the world 2021*. Rome,: FAO, IFAD, UNICEF, WFP and WHO. doi:10.4060/cb4474en.

Faralli, M. and Lawson, T. (2020) 'Natural genetic variation in photosynthesis: an untapped resource to increase crop yield potential?', *Plant Journal*, 101(3), pp. 518–528. doi:10.1111/tpj.14568.

Farooq, M., Bramley, H., Palta, J.A. and Siddique, K.H.M. (2011) 'Heat stress in wheat during reproductive and grain-filling phases', *Critical Reviews in Plant Sciences*, 30(6), pp. 491–507. doi:10.1080/07352689.2011.615687.

Farquhar, G.D., Caemmerer, S. and Berry, J.A. (1980) 'A biochemical model of photosynthetic CO_2 assimilation in leaves of C3 species', *Planta*, 149(1), pp. 78-90–90. Available at: http://dx.doi.org/10.1007/BF00386231.

Feekes, W. (1941) 'De tarwe en haar milieu [Wheat and its environment].', in *Verslagen van de Technische Tarwe Commissie.*, pp. 523–888.

Feng, Z., Rütting, T., Pleijel, H., Wallin, G., Reich, P.B., Kammann, C.I. *et al.* (2015) 'Constraints to nitrogen acquisition of terrestrial plants under elevated CO_2', *Global Change Biology*, 21(8), pp. 3152–3168. doi:10.1111/gcb.12938.

Fernandez-Orozco, R., Li, L., Harflett, C., Shewry, P.R. and Ward, J.L. (2010) 'Effects of environment and genotype on phenolic acids in wheat in the HEALTHGRAIN diversity screen', *Journal of Agricultural and Food Chemistry*, 58(17), pp. 9341–9352. doi:10.1021/jf102017s.

Fernando, N., Panozzo, J., Tausz, M., Norton, R., Fitzgerald, G. and Seneweera, S. (2012) 'Rising atmospheric CO_2 concentration affects mineral nutrient and protein concentration of wheat grain', *Food Chemistry*, 133(4), pp. 1307–1311. doi:10.1016/j.foodchem.2012.01.105.

Fernando, N., Panozzo, J., Tausz, M., Norton, R.M., Neumann, N., Fitzgerald, G.J. and Seneweera, S. (2014) 'Elevated CO_2 alters grain quality of two bread wheat cultivars grown under different environmental conditions', *Agriculture, Ecosystems and Environment*, 185, pp. 24–33. doi:10.1016/j.agee.2013.11.023.

Fischer, R.A. (1985) 'Number of kernels in wheat crops and the influence of solar radiation and temperature', *The Journal of Agricultural Science*, 105(2), pp. 447–461. doi:10.1017/S0021859600056495.

Fischer, R.A. (2011) 'Wheat physiology: a review of recent developments', *Crop and Pasture Science*, 62(2), p. 95. doi:10.1071/CP10344.

Fischer, R.A., Rees, D., Sayre, K.D., Lu, Z. -M., Condon, A.G. and Saavedra, A.L. (1998) 'Wheat yield progress associated with higher stomatal conductance and photosynthetic rate, and cooler canopies', *Crop Science*, 38(6), pp. 1467–1475. doi:10.2135/cropsci1998.0011183X003800060011x.

Fitzgerald, G.J., Tausz, M., O'Leary, G., Mollah, M.R., Tausz-Posch, S., Seneweera, S. *et al.* (2016) 'Elevated atmospheric [CO_2] can dramatically increase wheat yields in semi-arid environments and buffer against heat waves', *Global Change Biology*, 22(6), pp. 2269–2284. doi:10.1111/gcb.13263.

Fleischman, D. (2012) 'Photosynthesis', in *Cell Physiology Source Book*. Fourth Edi. Elsevier, pp. 909–924. doi:10.1016/B978-0-12-387738-3.00051-2.

Forman, H.J., Zhang, H. and Rinna, A. (2009) 'Glutathione: Overview of its protective roles, measurement, and biosynthesis', *Molecular Aspects of Medicine*, 30(1–2), pp. 1–12. doi:10.1016/j.mam.2008.08.006.

Foulkes, M.J., Slafer, G.A., Davies, W.J., Berry, P.M., Sylvester-Bradley, R., Martre, P., Calderini, D.F., Griffiths, S. and Reynolds, M.P. (2011) 'Raising yield potential of wheat. III.

Optimizing partitioning to grain while maintaining lodging resistance', *Journal of Experimental Botany*, 62(2), pp. 469–486. doi:10.1093/jxb/erq300.

Foyer, C.H. and Noctor, G. (2005) 'Redox homeostasis and antioxidant signaling: A metabolic interface between stress perception and physiological responses', *The Plant Cell*, 17(7), pp. 1866–1875. doi:10.1105/tpc.105.033589.

Foyer, C.H. and Noctor, G. (2011) 'Ascorbate and glutathione: The heart of the redox hub', *Plant Physiology*, 155(1), pp. 2–18. doi:10.1104/pp.110.167569.

Foyer, C.H. and Noctor, G. (2016) 'Stress-triggered redox signalling: What's in pROSpect?', *Plant Cell and Environment*, 39(5), pp. 951–964. doi:10.1111/pce.12621.

Franco-Robles, E. and López, M.G. (2015) 'Implication of fructans in health: Immunomodulatory and antioxidant mechanisms', *The Scientific World Journal*, 2015, pp. 1–15. doi:10.1155/2015/289267.

Fritz, C., Palacios-Rojas, N., Feil, R. and Stitt, M. (2006) 'Regulation of secondary metabolism by the carbon-nitrogen status in tobacco: Nitrate inhibits large sectors of phenylpropanoid metabolism', *Plant Journal*, 46(4), pp. 533–548. doi:10.1111/j.1365-313X.2006.02715.x.

Fu, Y.-B. (2006) 'Impact of plant breeding on genetic diversity of agricultural crops: searching for molecular evidence', *Plant Genetic Resources*, 4(1), pp. 71–78. doi:10.1079/pgr2006116.

Fu, Y.B. (2015) 'Understanding crop genetic diversity under modern plant breeding', *Theoretical and Applied Genetics*, 128(11), pp. 2131–2142. doi:10.1007/s00122-015-2585-y.

Fu, Y.B. and Somers, D.J. (2009) 'Genome-wide reduction of genetic diversity in wheat breeding', *Crop Science*, 49(1), pp. 161–168. doi:10.2135/cropsci2008.03.0125.

Gamage, D., Thompson, M., Sutherland, M., Hirotsu, N., Makino, A. and Seneweera, S. (2018) 'New insights into the cellular mechanisms of plant growth at elevated atmospheric carbon dioxide concentrations', *Plant Cell and Environment*, 41(6), pp. 1233–1246. doi:10.1111/pce.13206.

Gámez, A.L., Vicente, R., Sanchez-Bragado, R., Jauregui, I., Morcuende, R., Goicoechea, N. and Aranjuelo, I. (2020) 'Differential flag leaf and ear photosynthetic performance under elevated (CO_2) conditions during grain filling period in Durum Wheat', *Frontiers in Plant Science*, 11. doi:10.3389/fpls.2020.587958.

García-Pérez, A. (2005) 'Métodos avanzados de estadística aplicada. Métodos robustos y de remuestreo', p. 256. Available at: http://e-spacio.uned.es/fez/view/bibliuned:editorial-Educacionpermanente-0186080EP03A01 (Accessed: 17 June 2020).

García, G.A., Dreccer, M.F., Miralles, D.J. and Serrago, R.A. (2015) 'High night temperatures during grain number determination reduce wheat and barley grain yield: A field study', *Global Change Biology*, 21(11), pp. 4153–4164. doi:10.1111/gcb.13009.

Garvin, D.F., Welch, R.M. and Finley, J.W. (2006) 'Historical shifts in the seed mineral micronutrient concentration of US hard red winter wheat germplasm', *Journal of the Science of Food and Agriculture*, 86(13), pp. 2213–2220. doi:10.1002/jsfa.2601.

Geiger, M., Haake, V., Ludewig, F., Sonnewald, U. and Stitt, M. (1999) 'The nitrate and ammonium nitrate supply have a major influence on the response of photosynthesis, carbon metabolism, nitrogen metabolism and growth to elevated carbon dioxide in tobacco', *Plant, Cell & Environment*, 22(10), pp. 1177–1199. doi:10.1046/j.1365-3040.1999.00466.x.

Geiger, M., Walch-Liu, P., Engels, C., Harnecker, J., Schulze, E.-D., Ludewig, F., Sonnewald, U., Scheible, W.-R. and Stitt, M. (1998) 'Enhanced carbon dioxide leads to a modified diurnal rhythm of nitrate reductase activity in older plants, and a large stimulation of nitrate reductase

activity and higher levels of amino acids in young tobacco plants', *Plant, Cell and Environment*, 21(3), pp. 253–268. doi:10.1046/j.1365-3040.1998.00277.x.

Ghasemzadeh, A., Jaafar, H.Z.E. and Rahmat, A. (2010) 'Elevated carbon dioxide increases contents of flavonoids and phenolic compounds, and antioxidant activities in Malaysian young ginger (*Zingiber officinale Roscoe*.) Varieties', *Molecules*, 15(11), pp. 7907–7922. doi:10.3390/molecules15117907.

Gibon, Y., Blaesing, O.E., Hannemann, J., Carillo, P., Höhne, M., Hendriks, J.H.M. *et al.* (2004) 'A robot-based platform to measure multiple enzyme activities in *Arabidopsis* using a set of cycling assays: Comparison of changes of enzyme activities and transcript levels during diurnal cycles and in prolonged darkness', *Plant Cell*, 16(12), pp. 3304–3325. doi:10.1105/tpc.104.025973.

Gifford, R.M., Barrett, D.J. and Lutze, J.L. (2000) 'The effects of elevated [CO_2] on the C:N and C:P mass ratios of plant tissues', *Plant and Soil*, 224(1), pp. 1–14. doi:10.1023/A:1004790612630.

Gillespie, K.M., Chae, J.M. and Ainsworth, E.A. (2007) 'Rapid measurement of total antioxidant capacity in plants', *Nature Protocols*, 2(4), pp. 867–870. doi:10.1038/nprot.2007.100.

Glémin, S. and Bataillon, T. (2009) 'A comparative view of the evolution of grasses under domestication: Tansley review', *New Phytologist*, 183(2), pp. 273–290. doi:10.1111/j.1469-8137.2009.02884.x.

Gödecke, T., Stein, A.J. and Qaim, M. (2018) 'The global burden of chronic and hidden hunger: Trends and determinants', *Global Food Security*, 17(March), pp. 21–29. doi:10.1016/j.gfs.2018.03.004.

Gomez-Becerra, H.F., Yazici, A., Ozturk, L., Budak, H., Peleg, Z., Morgounov, A., Fahima, T., Saranga, Y. and Cakmak, I. (2010) 'Genetic variation and environmental stability of grain mineral nutrient concentrations in Triticum dicoccoides under five environments', *Euphytica*, 171(1), pp. 39–52. doi:10.1007/s10681-009-9987-3.

Gómez, M.I., Barrett, C.B., Raney, T., Pinstrup-Andersen, P., Meerman, J., Croppenstedt, A., Carisma, B. and Thompson, B. (2013) 'Post-green revolution food systems and the triple burden of malnutrition', *Food Policy*, 42, pp. 129–138. doi:10.1016/j.foodpol.2013.06.009.

Goncharov, N.P. (2011) 'Genus Triticum L. taxonomy: The present and the future', *Plant Systematics and Evolution*, 295(1), pp. 1–11. doi:10.1007/s00606-011-0480-9.

González, F.G., Slafer, G.A. and Miralles, D.J. (2005) 'Floret development and survival in wheat plants exposed to contrasting photoperiod and radiation environments during stem elongation', *Functional Plant Biology*, 32(3), pp. 189–197. doi:10.1071/FP04104.

González, I., Cao, K.A.L., Davis, M.J. and Déjean, S. (2012) 'Visualising associations between paired "omics" data sets', *BioData Mining*, 5(1), pp. 1–23. doi:10.1186/1756-0381-5-19.

Goulas, Y., Cerovic, Z.G., Cartelat, A. and Moya, I. (2004) 'Dualex: A new instrument for field measurements of epidermal ultraviolet absorbance by chlorophyll fluorescence', *Applied Optics*, 43(23), pp. 4488–4496. doi:10.1364/AO.43.004488.

Gourdji, S.M., Mathews, K.L., Reynolds, M., Crossa, J. and Lobell, D.B. (2013) 'An assessment of wheat yield sensitivity and breeding gains in hot environments', *Proceedings of the Royal Society B: Biological Sciences*, 280(1752). doi:10.1098/rspb.2012.2190.

Gray, S.B. and Brady, S.M. (2016) 'Plant developmental responses to climate change', *Developmental Biology*, 419(1), pp. 64–77. doi:10.1016/j.ydbio.2016.07.023.

Griffith, O.W. (1980) 'Determination of glutathione and glutathione disulfide using glutathione-

reductase and 2-vinylpyridine', *Analytical Biochemistry*, 106(1), pp. 207–212. doi:10.1016/0003-2697(80)90139-6.

Gross, M. (2013) 'The paradoxical evolution of agriculture', *Current Biology*, 23(16), pp. R667–R670. doi:10.1016/j.cub.2013.08.001.

Gu, L., Pallardy, S.G., Tu, K., Law, B.E. and Wullschleger, S.D. (2010) 'Reliable estimation of biochemical parameters from C3 leaf photosynthesis-intercellular carbon dioxide response curves', *Plant, Cell & Environment*, 33(11), pp. 1852–1874. doi:10.1111/j.1365-3040.2010.02192.x.

Guarda, G., Padovan, S. and Delogu, G. (2004) 'Grain yield, nitrogen-use efficiency and baking quality of old and modern Italian bread-wheat cultivars grown at different nitrogen levels', *European Journal of Agronomy*, 21(2), pp. 181–192. doi:10.1016/j.eja.2003.08.001.

Guo, T., Xuan, H., Yang, Y., Wang, L., Wei, L., Wang, Y. and Kang, G. (2014) 'Transcription analysis of genes encoding the wheat root transporter NRT1 and NRT2 families during nitrogen starvation', *Journal of Plant Growth Regulation*, 33(4), pp. 837–848. doi:10.1007/s00344-014-9435-z.

Gutiérrez, D., Gutiérrez, E., Pérez, P., Morcuende, R., Verdejo, A.L. and Martinez-Carrasco, R. (2009a) 'Acclimation to future atmospheric CO_2 levels increases photochemical efficiency and mitigates photochemistry inhibition by warm temperatures in wheat under field chambers', *Physiologia Plantarum*, 137(1), pp. 86–100. doi:10.1111/j.1399-3054.2009.01256.x.

Gutiérrez del Pozo, D. (2010) *Aclimatación de la fotosíntesis en el dosel vegetal de trigo al aumento del CO_2 atmosférico. Función del nitrógeno y las citoquinas en cultivos en cámaras de campo con clima mediterráneo.* Universidad de Salamanca. Facultad de Biología.

Gutiérrez, E., Gutiérrez, D., Morcuende, R., Verdejo, A.L., Kostadinova, S., Martinez-Carrasco, R. and Pérez, P. (2009b) 'Changes in leaf morphology and composition with future increases in CO_2 and temperature revisited: Wheat in field chambers', *Journal of Plant Growth Regulation*, 28(4), pp. 349–357. doi:10.1007/s00344-009-9102-y.

Haas, M., Schreiber, M. and Mascher, M. (2019) 'Domestication and crop evolution of wheat and barley: Genes, genomics, and future directions', *Journal of Integrative Plant Biology*, 61(3), pp. 204–225. doi:10.1111/jipb.12737.

Habash, D., Paul, M., Parry, M.J., Keys, A. and Lawlor, D. (1995) 'Increased capacity for photosynthesis in wheat grown at elevated CO_2: the relationship between electron transport and carbon metabolism', *Planta*, 197(3). doi:10.1007/BF00196670.

Hall, R.G. and Nleya, T. (2019) 'Winter and spring wheat growth stages', *South Dakota Board of Regents*, pp. 23–34. Available at: www.iGrow.org.

Hammer, K. (1984) 'The domestication syndrome', *Die Kulturpflanze*, 32(1), pp. 11–34. doi:10.1007/BF02098682.

Hammer, K., Knüpffer, H., Xhuveli, L. and Perrino, P. (1996) 'Estimating genetic erosion in landraces - Two case studies', *Genetic Resources and Crop Evolution*, 43(4), pp. 329–336. doi:10.1007/BF00132952.

Hammer, K. and Laghetti, G. (2005) 'Genetic erosion - Examples from Italy', *Genetic Resources and Crop Evolution*, 52(5), pp. 629–634. doi:10.1007/s10722-005-7902-x.

Hare, P.E. (1977) 'Subnanomole-range amino acid analysis', *Methods in Enzymology*, 47(C), pp. 3–18. doi:10.1016/0076-6879(77)47003-4.

Harper, K.N. and Armelagos, G.J. (2013) 'Genomics, the origins of agriculture, and our changing microbe-scape: Time to revisit some old tales and tell some new ones', *American Journal*

of Physical Anthropology, 152, pp. 135–152. doi:10.1002/ajpa.22396.

Hatfield, J.L., Boote, K.J., Kimball, B.A., Ziska, L.H., Izaurralde, R.C., Ort, D., Thomson, A.M. and Wolfe, D. (2011) 'Climate impacts on agriculture: Implications for crop production', *Agronomy Journal*, 103(2), pp. 351–370. doi:10.2134/agronj2010.0303.

Haun, J.R. (1973) 'Visual quantification of wheat development', *Agronomy Journal*, 65(1), pp. 116–119. doi:10.2134/agronj1973.00021962006500010035x.

Hawkesford, M.J., Araus, J.L., Park, R., Calderini, D., Miralles, D., Shen, T., Zhang, J. and Parry, M.A.J. (2013) 'Prospects of doubling global wheat yields', *Food and Energy Security*, 2(1), pp. 34–48. doi:10.1002/fes3.15.

Haworth, M., Marino, G. and Centritto, M. (2018) 'An introductory guide to gas exchange analysis of photosynthesis and its application to plant phenotyping and precision irrigation to enhance water use efficiency', *Journal of Water and Climate Change*, 9(4), pp. 786–808. doi:10.2166/wcc.2018.152.

Hendriks, J.H.M., Kolbe, A., Gibon, Y., Stitt, M. and Geigenberger, P. (2003) 'ADP-Glucose Pyrophosphorylase is activated by posttranslational redox-modification in response to light and to sugars in leaves of *Arabidopsis* and other plant species', *Plant Physiology*, 133(2), pp. 838–849. doi:10.1104/pp.103.024513.

Hernández, L., Afonso, D., Rodríguez, E.M. and Díaz, C. (2011) 'Phenolic compounds in wheat grain cultivars', *Plant Foods for Human Nutrition*, 66(4), pp. 408–415. doi:10.1007/s11130-011-0261-1.

Herzog, B., Stitt, M. and Heldt, H.W. (1984) 'Control of photosynthetic sucrose synthesis by fructose 2,6-bisphosphate', *Plant Physiology*, 75, pp. 561–565. doi:10.1104/pp.79.3.599.

Heslop-Harrison, J.S. and Schwarzacher, T. (2012) *Genetics and genomics of crop domestication*. First Edit, *Plant Biotechnology and Agriculture*. First Edit. Elsevier Inc. doi:10.1016/B978-0-12-381466-1.00001-8.

Hesse, H., Nikiforova, V., Gakière, B. and Hoefgen, R. (2004) 'Molecular analysis and control of cysteine biosynthesis: Integration of nitrogen and sulphur metabolism', *Journal of Experimental Botany*, 55(401), pp. 1283–1292. doi:10.1093/jxb/erh136.

Hoad, S.P., Russell, G., Lucas, M.E. and Bingham, I.J. (2001) 'The management of wheat, barley, and oat root systems', *Advances in Agronomy*, 74, pp. 193–246.

Hodkinson, T.R. (2018) 'Evolution and taxonomy of the grasses (*Poaceae*): A model family for the study of species-rich groups', in *Annual Plant Reviews online*. Wiley, pp. 255–294. doi:10.1002/9781119312994.apr0622.

Hofius, D. and Börnke, F.A.J. (2007) 'Photosynthesis, carbohydrate metabolism and source-sink relations', in *Potato Biology and Biotechnology: Advances and Perspectives*. Elsevier, pp. 257–285. doi:10.1016/B978-044451018-1/50055-5.

Högy, P., Brunnbauer, M., Koehler, P., Schwadorf, K., Breuer, J., Franzaring, J., Zhunusbayeva, D. and Fangmeier, A. (2013) 'Grain quality characteristics of spring wheat (*Triticum aestivum*) as affected by free-air CO_2 enrichment', *Environmental and Experimental Botany*, 88, pp. 11–18. doi:10.1016/j.envexpbot.2011.12.007.

Högy, P. and Fangmeier, A. (2008) 'Effects of elevated atmospheric CO_2 on grain quality of wheat', *Journal of Cereal Science*, 48(3), pp. 580–591. doi:10.1016/j.jcs.2008.01.006.

Högy, P., Keck, M., Niehaus, K., Franzaring, J. and Fangmeier, A. (2010) 'Effects of atmospheric CO_2 enrichment on biomass, yield and low molecular weight metabolites in wheat grain',

Journal of Cereal Science, 52(2), pp. 215–220. doi:10.1016/j.jcs.2010.05.009.

Högy, P., Kottmann, L., Schmid, I. and Fangmeier, A. (2019) 'Heat, wheat and CO_2: The relevance of timing and the mode of temperature stress on biomass and yield', *Journal of Agronomy and Crop Science*, 205(6), pp. 608–615. doi:10.1111/jac.12345.

Högy, P., Wieser, H., Köhler, P., Schwadorf, K., Breuer, J., Erbs, M., Weber, S. and Fangmeier, A. (2009a) 'Does elevated atmospheric CO_2 allow for sufficient wheat grain quality in the future?', *Journal of Applied Botany and Food Quality*, 82(2), pp. 114–121.

Högy, P., Wieser, H., Köhler, P., Schwadorf, K., Breuer, J., Franzaring, J., Muntifering, R. and Fangmeier, A. (2009b) 'Effects of elevated CO_2 on grain yield and quality of wheat: Results from a 3-year free-air CO_2 enrichment experiment', *Plant Biology*, 11(SUPPL.1), pp. 60–69. doi:10.1111/j.1438-8677.2009.00230.x.

Hu, S., Dilcher, D.L., Jarzen, D.M. and Taylor, D.W. (2008) 'Early steps of angiosperm-pollinator coevolution', *Proceedings of the National Academy of Sciences of the United States of America*, 105(1), pp. 240–245. doi:10.1073/pnas.0707989105.

Huang, X.Q., Wolf, M., Ganal, M.W., Orford, S., Koebner, R.M.D. and Röder, M.S. (2007) 'Did modern plant breeding lead to genetic erosion in European winter wheat varieties?', *Crop Science*, 47(1), pp. 343–349. doi:10.2135/cropsci2006.04.0261.

Hyles, J., Bloomfield, M.T., Hunt, J.R., Trethowan, R.M. and Trevaskis, B. (2020) 'Phenology and related traits for wheat adaptation', *Heredity*, 125(6), pp. 417–430. doi:10.1038/s41437-020-0320-1.

Hymus, G.J., Baker, N.R. and Long, S.P. (2001) 'Growth in elevated CO_2 can both increase and decrease photochemistry and photoinhibition of photosynthesis in a predictable manner. Dactylis glomerata grown in two levels of nitrogen nutrition', *Plant Physiology*, 127(3), pp. 1204–1211. doi:10.1104/pp.010248.

Igarashi, M., Yi, Y. and Yano, K. (2021) 'Revisiting why plants become N deficient under elevated CO_2: Importance to meet n demand regardless of the fed-form', *Frontiers in Plant Science*, 12. doi:10.3389/fpls.2021.726186.

Inda, L.A., Segarra-Moragues, J.G., Müller, J., Peterson, P.M. and Catalán, P. (2008) 'Dated historical biogeography of the temperate Loliinae (Poaceae, Pooideae) grasses in the northern and southern hemispheres', *Molecular Phylogenetics and Evolution*, 46(3), pp. 932–957. doi:10.1016/j.ympev.2007.11.022.

Initiatives, D. (2021) *2021 Global nutrition report: The state of global nutrition*. Bristol, UK: Development Initiatives. Available at: https://globalnutritionreport.org/reports/2021-global-nutrition-report/foreword/.

IPCC (2018) *Global Warming of 1.5°C. An IPCC special report on the impacts of global warming of 1.5°C above pre-industrial levels and related global greenhouse gas emission pathways, in the context of strengthening the global response to the threat of climate change, IPCC*. Available at: https://www.ipcc.ch/site/assets/uploads/sites/2/2019/06/SR15_Full_Report_High_Res.pdf.

IPCC (2021a) *Climate change 2021: The physical science basis. Summary for policymakers.*

IPCC (2021b) *Climate change 2021: The physical science basis*. Available at: https://www.ipcc.ch/report/ar6/wg1/.

Jauregui, I., Aparicio-Tejo, P.M., Avila, C., Cañas, R., Sakalauskiene, S. and Aranjuelo, I. (2016) 'Root-shoot interactions explain the reduction of leaf mineral content in *Arabidopsis* plants grown under elevated [CO_2] conditions', *Physiologia Plantarum*, 158(1), pp. 65–79.

doi:10.1111/ppl.12417.

Jensen, R.G. (2000) 'Activation of Rubisco regulates photosynthesis at high temperature and CO_2', *Proceedings of the National Academy of Sciences*, 97(24), pp. 12937–12938. doi:10.1073/pnas.97.24.12937.

Jiang, G.M., Sun, J.Z., Liu, H.Q., Qu, C.M., Wang, K.J., Guo, R.J., Bai, K.Z., Gao, L.M. and Kuang, T.Y. (2003) 'Changes in the rate of photosynthesis accompanying the yield increase in wheat cultivars released in the past 50 years', *Journal of Plant Research*, 116(5), pp. 347–354. doi:10.1007/s10265-003-0115-5.

Johnson, J.W., R. Dewey Lee and Barnett, R.D. (2017) *Southern small grains. Resource management handbook*. Edited by G.D. Buntin and Barry M. Cunfer. Univerwsity of Georgia College of Agricultural and Environmental Science Cooperative Extension.

Johnson, M.P. (2016) 'Photosynthesis', *Essays in Biochemistry*, 60(3), pp. 255–273. doi:10.1042/EBC20160016.

Jones, M.G.K., Outlaw, W.H. and Lowry, O.H. (1977) 'Enzymic assay of 10^{-7} to 10^{-14} moles of sucrose in plant tissues', *Plant Physiology*, 60(3), pp. 379–383. doi:10.1104/pp.60.3.379.

Jones, R., Ougham, H., Thomas, H. and Waaland, S. (2013) *The molecular life of plants*. The Atrium, Southern Gate, Chichester, West Sussex, PO19 8SQ, UK: John Wiley & Sons, Ltd.

Kaminski, A., Austin, R.B., Ford, M.A. and Morgan, C.L. (1990) 'Flag leaf anatomy of Triticum and Aegilops species in relation to photosynthetic rate', *Annals of Botany*, 66(3), pp. 359–365. doi:10.1093/oxfordjournals.aob.a088035.

Kassambara, A. (2019) *Practical Statistics in R II - Comparing Groups: Numerical Variables, DataNovia*. Datanovia. Available at: https://www.datanovia.com/en/product/practical-statistics-in-r-for-comparing-groups-numerical-variables/.

Kassambara, A. (2021) 'rstatix: Pipe-friendly framework for basic statistical tests'. Available at: https://cran.r-project.org/package=rstatix.

Kaur, B., Kaur, G. and Asthir, B. (2017) 'Biochemical aspects of nitrogen use efficiency: An overview', *Journal of Plant Nutrition*, 40(4), pp. 506–523. doi:10.1080/01904167.2016.1240196.

Kellogg, E. a (2001) 'Evolutionary history of the grasses', *Plant Physiology*, 125(3), pp. 1198–1205. doi:10.1104/pp.125.3.1198.

Kellogg, E.A. (2015) *Flowering plants. Monocots: Poaceae, The families and genera of vascular plants*. Edited by K. Kubitzki. Springer International Publishing. doi:10.1007/978-3-319-15332-2.

Khan, A., Ahmad, M., Ahmed, M. and Iftikhar Hussain, M. (2021) 'Rising atmospheric temperature impact on wheat and thermotolerance strategies', *Plants*, 10(1), pp. 1–24. doi:10.3390/plants10010043.

Khoury, C.K., Brush, S., Costich, D.E., Curry, H.A., Haan, S., Engels, J.M.M. *et al.* (2022) 'Crop genetic erosion: understanding and responding to loss of crop diversity', *New Phytologist*, 233(1), pp. 84–118. doi:10.1111/nph.17733.

Khush, G.S. (1999) 'Green revolution: Preparing for the 21st century', *Genome*, 42(4), pp. 646–655. doi:10.1139/g99-044.

Khush, G.S. (2001) 'Green revolution: The way forward', *Nature Reviews Genetics*, 2(10), pp. 815–822. doi:10.1038/35093585.

Kimber, G. and Feldman, M. (1987) 'Wild wheat. An introduction.', *Wild wheat. An*

introduction. [Preprint], (No. 353).

Kobza, J. and Edwards, G.E. (1987) 'Influences of leaf temperature on photosynthetic carbon metabolism in wheat', *Plant Physiology*, 83(1), pp. 69–74. doi:10.1104/pp.83.1.69.

Korres, N.E., Norsworthy, J.K., Tehranchian, P., Gitsopoulos, T.K., Loka, D.A., Oosterhuis, D.M. *et al.* (2016) 'Cultivars to face climate change effects on crops and weeds: a review', *Agronomy for Sustainable Development*, 36(1), pp. 1–22. doi:10.1007/s13593-016-0350-5.

Kotrlik, J., Williams, H. and Jabor, K. (2011) 'Reporting and Interpreting Effect Size in Quantitative Agricultural Education Research', *Journal of Agricultural Education*, 52(1), pp. 132–142. doi:10.5032/jae.2011.01132.

Kramer, P.J. and Boyer, J.S. (1995) 'Stomata and gas exchange', in *Water Relations of Plants and Soils*. Elsevier, pp. 257–282. doi:10.1016/B978-012425060-4/50008-5.

Krapp, A. (2015) 'Plant nitrogen assimilation and its regulation: a complex puzzle with missing pieces', *Current Opinion in Plant Biology*, 25, pp. 115–122. doi:10.1016/j.pbi.2015.05.010.

Lancien, M., Gadal, P. and Hodges, M. (2000) 'Enzyme Redundancy and the Importance of 2-Oxoglutarate in Higher Plant Ammonium Assimilation', *Plant Physiology*, 123(3), pp. 817–824. doi:10.1104/pp.123.3.817.

Larsen, C.S. (2006) 'The agricultural revolution as environmental catastrophe: Implications for health and lifestyle in the Holocene', *Quaternary International*, 150(1), pp. 12–20. doi:10.1016/j.quaint.2006.01.004.

Larson, G., Piperno, D.R., Allaby, R.G., Purugganan, M.D., Andersson, L., Arroyo-Kalin, M. *et al.* (2014) 'Current perspectives and the future of domestication studies', *Proceedings of the National Academy of Sciences of the United States of America*, 111(17), pp. 6139–6146. doi:10.1073/pnas.1323964111.

Lawson, T. and Blatt, M.R. (2014) 'Stomatal size, speed, and responsiveness impact on photosynthesis and water use efficiency', *Plant Physiology*, 164(4), pp. 1556–1570. doi:10.1104/pp.114.237107.

Lê, S., Josse, J. and Husson, F. (2008) 'FactoMineR: An R package for multivariate analysis', *Journal of Statistical Software*, 25(1), pp. 1–18. doi:10.18637/jss.v025.i01.

Lea, P.J. and Miflin, B.J. (2003) 'Glutamate synthase and the synthesis of glutamate in plants', *Plant Physiology and Biochemistry*, 41(6–7), pp. 555–564. doi:10.1016/S0981-9428(03)00060-3.

Leakey, A.D.B., Ainsworth, E.A., Bernacchi, C.J., Rogers, A., Long, S.P. and Ort, D.R. (2009) 'Elevated CO_2 effects on plant carbon, nitrogen, and water relations: Six important lessons from FACE', *Journal of Experimental Botany*, 60(10), pp. 2859–2876. doi:10.1093/jxb/erp096.

Leegood, R.C. (2013) 'Photosynthesis', in *Encyclopedia of Biological Chemistry*. Elsevier, pp. 492–496. doi:10.1016/B978-0-12-378630-2.00049-9.

Lemoine, R. (2000) 'Sucrose transporters in plants: Update on function and structure', *Biochimica et Biophysica Acta - Biomembranes*, 1465(1–2), pp. 246–262. doi:10.1016/S0005-2736(00)00142-5.

Lennard, C. (2005) 'Fingerprint techniques', in *Encyclopedia of Analytical Science*. Elsevier, pp. 414–423. doi:10.1016/B0-12-369397-7/00200-4.

Leváková, L. and Lacko-Bartošová, M. (2017) 'Phenolic acids and antioxidant activity of wheat species: A review', *Agriculture*, 63(3), pp. 92–101. doi:10.1515/agri-2017-0009.

Li, L., Shewry, P.R. and Ward, J.L. (2008) 'Phenolic acids in wheat varieties in the healthgrain

diversity screen', *Journal of Agricultural and Food Chemistry*, 56(21), pp. 9732–9739. doi:10.1021/jf801069s.

Li, T., Liao, K., Xu, X., Gao, Y., Wang, Z., Zhu, X., Jia, B. and Xuan, Y. (2017) '*Wheat ammonium transporter* (AMT) Gene Family: Diversity and possible role in host–pathogen interaction with stem rust', *Frontiers in Plant Science*, 8(September), pp. 1–13. doi:10.3389/fpls.2017.01637.

Link, P.K. (2009) '"Icehouse" (Cold) Climates', in *Encyclopedia of Paleoclimatology and Ancient Environments*. Dordrecht: Springer Netherlands, pp. 463–471. doi:10.1007/978-1-4020-4411-3_112.

Lizana, X.C. and Calderini, D.F. (2013) 'Yield and grain quality of wheat in response to increased temperatures at key periods for grain number and grain weight determination: Considerations for the climatic change scenarios of Chile', *Journal of Agricultural Science*, 151(2), pp. 209–221. doi:10.1017/S0021859612000639.

Lobell, D.B. and Field, C.B. (2007) 'Global scale climate–crop yield relationships and the impacts of recent warming', *Environmental Research Letters*, 2(1), p. 014002. doi:10.1088/1748-9326/2/1/014002.

Long, S.P., Ainsworth, E.A., Leakey, A.D.B., Nösberger, J. and Ort, D.R. (2006a) 'Food for thought: Lower-than-expected crop yield stimulation with rising CO_2 concentrations', *Science*, 312(5782), pp. 1918–1921. doi:10.1126/science.1114722.

Long, S.P., Ainsworth, E.A., Rogers, A. and Ort, D.R. (2004) 'Rising atmospheric carbon dioxide: Plants FACE the future', *Annual Review of Plant Biology*, 55, pp. 591–628. doi:10.1146/annurev.arplant.55.031903.141610.

Long, S.P., Zhu, X.G., Naidu, S.L. and Ort, D.R. (2006b) 'Can improvement in photosynthesis increase crop yields?', *Plant, Cell and Environment*, 29(3), pp. 315–330. doi:10.1111/j.1365-3040.2005.01493.x.

Lopes, M.S., Reynolds, M.P., Manes, Y., Singh, R.P., Crossa, J. and Braun, H.J. (2012) 'Genetic yield gains and changes in associated traits of CIMMYT spring bread wheat in a "Historic" set representing 30 years of breeding', *Crop Science*, 52(3), pp. 1123–1131. doi:10.2135/cropsci2011.09.0467.

Lopez, F.B. and Barclay, G.F. (2017) 'Plant anatomy and physiology', in *Pharmacognosy*. Elsevier, pp. 45–60. doi:10.1016/B978-0-12-802104-0.00004-4.

Löve, Á. (1984) 'Conspectus of the Triticeae', *Feddes Repertorium*, 95(7–8). doi:10.1002/fedr.4910950702.

Lüthi, D., Le Floch, M., Bereiter, B., Blunier, T., Barnola, J.M., Siegenthaler, U. *et al.* (2008) 'High-resolution carbon dioxide concentration record 650,000-800,000 years before present', *Nature*, 453(7193), pp. 379–382. doi:10.1038/nature06949.

Ma, W., Yu, Z., She, M., Zhao, Y. and Islam, S. (2019) 'Wheat gluten protein and its impacts on wheat processing quality', *Frontiers of Agricultural Science and Engineering*, 6(3), p. 279. doi:10.15302/J-FASE-2019267.

Macabuhay, A., Houshmandfar, A., Nuttall, J., Fitzgerald, G.J., Tausz, M. and Tausz-Posch, S. (2018) 'Can elevated CO_2 buffer the effects of heat waves on wheat in a dryland cropping system?', *Environmental and Experimental Botany*, 155(June), pp. 578–588. doi:10.1016/j.envexpbot.2018.07.029.

Magurran, A.E. (2005) 'Biological diversity', *Current Biology*, 15(4), pp. R116–R118. doi:10.1016/j.cub.2005.02.006.

Mair, P., Schoenbrodt, F. and Wilcox, R. (2016) 'WRS2: Wilcox robust estimation and testing'. Available at: https://cran.r-project.org/package=WRS2.

Mair, P. and Wilcox, R. (2020) 'Robust Statistical Methods Using WRS2', *Behavior Research Methods*, 52(2), pp. 464–488. doi:10.3758/s13428-019-01246-w.

Mair, P., Wilcox, R. and Patil, I. (2021) 'Robust Statistical Methods Using WRS2 (vignette)', p. 41. Available at: https://cran.r-project.org/web/packages/WRS2/vignettes/WRS2.pdf.

Makino, A. and Tadahiko, M. (1999) 'Photosynthesis and plant growth at elevated levels of CO_2', *Plant and Cell Physiology*, 40(10), pp. 999–1006. doi:10.1093/oxfordjournals.pcp.a029493.

Mangiafico, S. (2020) 'rcompanion: Functions to Support Extension Education Program Evaluation'. Available at: https://cran.r-project.org/package=rcompanion.

Marcos-Barbero, E.L., Pérez, P., Martínez-Carrasco, R., Arellano, J.B. and Morcuende, R. (2021a) 'Genotypic variability on grain yield and grain nutritional quality characteristics of wheat grown under elevated CO_2 and high temperature', *Plants*, 10(6), p. 1043. doi:10.3390/plants10061043.

Marcos-Barbero, E.L., Pérez, P., Martínez-Carrasco, R., Arellano, J.B. and Morcuende, R. (2021b) 'Screening for higher grain yield and biomass among sixty bread wheat genotypes grown under elevated CO_2 and high-temperature conditions', *Plants*, 10(8), p. 1596. doi:10.3390/plants10081596.

Martínez-Carrasco, R., Pérez, P. and Morcuende, R. (2005) 'Interactive effects of elevated CO_2, temperature and nitrogen on photosynthesis of wheat grown under temperature gradient tunnels', *Environmental and Experimental Botany*, 54(1), pp. 49–59. doi:10.1016/j.envexpbot.2004.05.004.

Martinoia, E. and Rentsch, D. (1994) 'Malate compartmentation-responses to a complex metabolism', *Annual Review of Plant Physiology and Plant Molecular Biology*, 45(1), pp. 447–467. doi:10.1146/annurev.pp.45.060194.002311.

Masclaux-Daubresse, C., Daniel-Vedele, F., Dechorgnat, J., Chardon, F., Gaufichon, L. and Suzuki, A. (2010) 'Nitrogen uptake, assimilation and remobilization in plants: Challenges for sustainable and productive agriculture', *Annals of Botany*, 105(7), pp. 1141–1157. doi:10.1093/aob/mcq028.

Mastrangelo, A.M. and Cattivelli, L. (2021) 'What makes bread and durum wheat different?', *Trends in Plant Science*, 26(7), pp. 677–684. doi:10.1016/j.tplants.2021.01.004.

Matimati, I., Verboom, G.A. and Cramer, M.D. (2014) 'Nitrogen regulation of transpiration controls mass-flow acquisition of nutrients', *Journal of Experimental Botany*, 65(1), pp. 159–168. doi:10.1093/jxb/ert367.

McCaldin, D.J. (1960) 'The chemistry of ninhydrin', *Chemical Reviews*, 60(1), pp. 39–51. doi:10.1021/cr60203a004.

McCleary, B. V., Murphy, A., Mugford, D.C., Andersen, R., Ashton, J., Blakeney, T. *et al.* (2000) 'Measurement of total fructan in foods by enzymatic/spectrophotometric method: Collaborative study', *Journal of AOAC International*, 83(2), pp. 356–364. doi:10.1093/jaoac/83.2.356.

McKee, I.F., Farage, P.K. and Long, S.P. (1995) 'The interactive effects of elevated CO_2 and O_2 concentration on photosynthesis in spring wheat', *Photosynthesis Research*, 45(2), pp. 111–119. doi:10.1007/BF00032582.

McMaster, G.S. (1997) 'Phenology, Development, and Growth of the Wheat (Triticum Aestivum

L.) Shoot Apex: A Review', in *Advances in Agronomy*, pp. 63–118. doi:10.1016/S0065-2113(08)60053-X.

Mellado-Ortega, E., Zabalgogeazcoa, I., Vázquez de Aldana, B.R. and Arellano, J.B. (2017) 'Solutions to decrease a systematic error related to AAPH addition in the fluorescence-based ORAC assay', *Analytical Biochemistry*, 519, pp. 27–29. doi:10.1016/j.ab.2016.12.009.

Méndez, A.M., Castillo, D., del Pozo, A., Matus, I. and Morcuende, R. (2011) 'Differences in stem soluble carbohydrate contents among recombinant chromosome substitution lines (RCSLs) of barley under drought in a mediterranean-type environment', *Agronomy Research*, 9(SPPL. ISS. 2), pp. 433–438.

Meyer, R.S. and Purugganan, M.D. (2013) 'Evolution of crop species: genetics of domestication and diversification', *Nature Reviews Genetics*, 14(12), pp. 840–852. doi:10.1038/nrg3605.

Miflin, B.J. and Habash, D.Z. (2002) 'The role of glutamine synthetase and glutamate dehydrogenase in nitrogen assimilation and possibilities for improvement in the nitrogen utilization of crops', *Journal of Experimental Botany*, 53(370), pp. 979–987. doi:10.1093/jexbot/53.370.979.

Miller, R. and Horneck, D. (1997) 'Determination of total nitrogen in plant tissue', in *Handbook of Reference Methods for Plant Analysis*. CRC Press. doi:10.1201/9781420049398.CH9.

Mills, B.J.W., Krause, A.J., Scotese, C.R., Hill, D.J., Shields, G.A. and Lenton, T.M. (2019) 'Modelling the long-term carbon cycle, atmospheric CO_2, and Earth surface temperature from late Neoproterozoic to present day', *Gondwana Research*, 67(January 2019), pp. 172–186. doi:10.1016/j.gr.2018.12.001.

Miralles, D.J., Katz, S.D., Colloca, A. and Slafer, G.A. (1998) 'Floret development in near isogenic wheat lines differing in plant height', *Field Crops Research*, 59(1), pp. 21–30. doi:10.1016/S0378-4290(98)00103-8.

Miralles, D.J. and Slafer, G.A. (1995) 'Individual grain weight responses to genetic reduction in culm length in wheat as affected by source-sink manipulations', *Field Crops Research*, 43(2–3), pp. 55–66. doi:10.1016/0378-4290(95)00041-N.

Misran, A. and Jaafar, A.H. (2019) 'Protein', in *Postharvest Physiology and Biochemistry of Fruits and Vegetables*. Elsevier, pp. 315–334. doi:10.1016/B978-0-12-813278-4.00015-4.

Mitchell-Olds, T. and Pedersen, D. (1998) 'The molecular basis of quantitative genetic variation in central and secondary metabolism in *Arabidopsis*', *Genetics*, 149(2), pp. 739–747. doi:10.1093/genetics/149.2.739.

Mittler, R., Finka, A. and Goloubinoff, P. (2012) 'How do plants feel the heat?', *Trends in Biochemical Sciences*, 37(3), pp. 118–125. doi:10.1016/j.tibs.2011.11.007.

Molino, I.M.M. Del, Rojo, B., Martinez-Carrasco, R. and Pérez, P. (1988) 'Amino acid composition of wheat grain. 1: Changes during development', *Journal of the Science of Food and Agriculture*, 42(1), pp. 29–37. doi:10.1002/jsfa.2740420105.

Møller, I.M. (2001) 'Plant mitochondria and oxidative stress: Electron transport, NADPH turnover, and metabolism of reactive oxygen species', *Annual Review of Plant Biology*, 52, pp. 561–591. doi:10.1146/annurev.arplant.52.1.561.

Mondal, S., Dutta, S., Crespo-Herrera, L., Huerta-Espino, J., Braun, H.J. and Singh, R.P. (2020) 'Fifty years of semi-dwarf spring wheat breeding at CIMMYT: Grain yield progress in optimum, drought and heat stress environments', *Field Crops Research*, 250(February), p. 107757. doi:10.1016/j.fcr.2020.107757.

Moore, B.D., Cheng, S.H., Sims, D. and Seemann, J.R. (1999) 'The biochemical and molecular

basis for photosynthetic acclimation to elevated atmospheric CO_2', *Plant, Cell and Environment*, 22(6), pp. 567–582. doi:10.1046/j.1365-3040.1999.00432.x.

Morcuende, R., Kostadinova, S., Pérez, P., Martín Del Molino, I.M. and Martínez-Carrasco, R. (2004a) 'Nitrate is a negative signal for fructan synthesis, and the fructosyltransferase-inducing trehalose inhibits nitrogen and carbon assimilation in excised barley leaves', *New Phytologist*, 161(3), pp. 749–759. doi:10.1046/j.1469-8137.2004.00990.x.

Morcuende, R., Kostadinova, S., Pérez, P. and Martínez-Carrasco, R. (2005) 'Fructan synthesis is inhibited by phosphate in warm-grown, but not in cold-treated, excised barley leaves', *New Phytologist*, 168(3), pp. 567–574. doi:10.1111/j.1469-8137.2005.01534.x.

Morcuende, R., Kostadinova, S., Pérez Pérez, P., Martín del Molino, I. and Martínez-Carrasco, R. (2004b) 'Nitrate is a negative signal for fructan synthesis and the fructosyltransferaseinducing trehalose inhibits nitrogen and carbon assimilation in excised barley leaves.', *New Phytologist*, 161, pp. 749–759. doi:10.1111/j.1469-8137.2003.00990.x.

Morcuende, R., Krapp, A., Hurry, V. and Stitt, M. (1998) 'Sucrose-feeding leads to increased rates of nitrate assimilation, increased rates of α-oxoglutarate synthesis, and increased synthesis of a wide spectrum of amino acids in tobacco leaves', *Planta*, 206(3), pp. 394–409. doi:10.1007/s004250050415.

Morcuende, R., Pérez, P., Martínez-Carrasco, R. and Gutiérrez, E. (2011) 'Nitrogen modulates the diurnal regulation of nitrate reductase in wheat plants - projections towards climate change', *Agronomy Research*, 9(SPPL. ISS. 2), pp. 443–450.

Morgounov, A., Gómez-Becerra, H.F., Abugalieva, A., Dzhunusova, M., Yessimbekova, M., Muminjanov, H., Zelenskiy, Y., Ozturk, L. and Cakmak, I. (2007) 'Iron and zinc grain density in common wheat grown in Central Asia', *Euphytica*, 155(1–2), pp. 193–203. doi:10.1007/s10681-006-9321-2.

Morgounov, A., Zykin, V., Belan, I., Roseeva, L., Zelenskiy, Y., Gomez-Becerra, H.F., Budak, H. and Bekes, F. (2010) 'Genetic gains for grain yield in high latitude spring wheat grown in Western Siberia in 1900-2008', *Field Crops Research*, 117(1), pp. 101–112. doi:10.1016/j.fcr.2010.02.001.

Mpofu, A., Sapirstein, H.D. and Beta, T. (2006) 'Genotype and environmental variation in phenolic content, phenolic acid composition, and antioxidant activity of hard spring wheat', *Journal of Agricultural and Food Chemistry*, 54(4), pp. 1265–1270. doi:10.1021/jf052683d.

Mueller, U.G. and Gerardo, N. (2002) 'Fungus-farming insects: Multiple origins and diverse evolutionary histories', *Proceedings of the National Academy of Sciences of the United States of America*, 99(24), pp. 15247–15249. doi:10.1073/pnas.242594799.

Mueller, U.G., Gerardo, N.M., Aanen, D.K., Six, D.L. and Schultz, T.R. (2005) 'The evolution of agriculture in insects', *Annual Review of Ecology, Evolution, and Systematics*, 36, pp. 563–595. doi:10.1146/annurev.ecolsys.36.102003.152626.

Munné-Bosch, S., Queval, G. and Foyer, C.H. (2012) 'The impact of global change factors on redox signaling underpinning stress tolerance', *Plant Physiology*, 161(1), pp. 5–19. doi:10.1104/pp.112.205690.

Murphy, K.M., Reeves, P.G. and Jones, S.S. (2008) 'Relationship between yield and mineral nutrient concentrations in historical and modern spring wheat cultivars', *Euphytica*, 163(3), pp. 381–390. doi:10.1007/s10681-008-9681-x.

Myers, S.S., Zanobetti, A., Kloog, I., Huybers, P., Leakey, A.D.B., Bloom, A.J. *et al.* (2014) 'Increasing CO_2 threatens human nutrition', *Nature*, 510(7503), pp. 139–142.

doi:10.1038/nature13179.

N'Danikou, S. and Tchokponhoue, D.A. (2019) 'Plant Domestication for Enhanced Food Security', in Leal Filho, W., Azul, A.M., Brandli, L., Özuyar, P.G. and Wall, T. (eds) *Zero Hunger. Encyclopedia of the UN Sustainable Development Goals.* Cham: Springer International Publishing (Encyclopedia of the UN Sustainable Development Goals), pp. 1–11. doi:10.1007/978-3-319-69626-3_96-1.

Nacry, P., Bouguyon, E. and Gojon, A. (2013) 'Nitrogen acquisition by roots: Physiological and developmental mechanisms ensuring plant adaptation to a fluctuating resource', *Plant and Soil*, 370(1–2), pp. 1–29. doi:10.1007/s11104-013-1645-9.

Nakandalage, N. and Seneweera, S. (2018) 'Micronutrients use efficiency of crop-plants under changing climate', in *Plant Micronutrient Use Efficiency*. Elsevier, pp. 209–224. doi:10.1016/B978-0-12-812104-7.00015-0.

Nakano, H., Makino, A. and Mae, T. (1997) 'The effect of elevated partial pressures of CO_2 on the relationship between photosynthetic capacity and N content in rice leaves', *Plant Physiology*, 115(1), pp. 191–198. doi:10.1104/pp.115.1.191.

Nelson, C.J. and Moore, K.J. (2020) 'Grass Morphology', in *Forages*. Wiley, pp. 23–49. doi:10.1002/9781119436669.ch2.

Nelson, D.L. and Cox, M.M. (2013) *Lehninger's principles of biochemistry*. sixth edit, *Journal of Chemical Information and Modeling*. sixth edit. New York, NY: W. H. Freeman and Company.

Newton, A.C., Johnson, S.N. and Gregory, P.J. (2011) 'Implications of climate change for diseases, crop yields and food security', *Euphytica*, 179(1), pp. 3–18. doi:10.1007/s10681-011-0359-4.

Nie, G., Hendrix, D.L., Webber, A.N., Kimball, B.A. and Long, S.P. (1995) 'Increased accumulation of carbohydrates and decreased photosynthetic gene transcript levels in wheat grown at an elevated CO_2 concentration in the field', *Plant Physiology*, 108(3), pp. 975–983. doi:10.1104/pp.108.3.975.

NOAA-ESRL (2022) *Trends in Atmospheric Carbon Dioxide*. Available at: https://www.esrl.noaa.gov/gmd/ccgg/trends/index.html.

Noctor, G., Mhamdi, A., Chaouch, S., Han, Y., Neukermans, J., Marquez-Garcia, B., Queval, G. and Foyer, C.H. (2012) 'Glutathione in plants: An integrated overview', *Plant, Cell and Environment*, 35(2), pp. 454–484. doi:10.1111/j.1365-3040.2011.02400.x.

Nunes-Nesi, A., Fernie, A.R. and Stitt, M. (2010) 'Metabolic and signaling aspects underpinning the regulation of plant carbon nitrogen interactions', *Molecular Plant*, 3(6), pp. 973–996. doi:10.1093/mp/ssq049.

Nurseries (2021). Available at: http://wheatatlas.org/nurseries/iwin (Accessed: 15 October 2021).

Nuttall, J.G., O'Leary, G.J., Panozzo, J.F., Walker, C.K., Barlow, K.M. and Fitzgerald, G.J. (2017) 'Models of grain quality in wheat—A review', *Field Crops Research*, 202, pp. 136–145. doi:10.1016/j.fcr.2015.12.011.

O'Leary, B.M. and Plaxton, W.C. (2016) 'Plant Respiration', in *eLS*. Wiley, pp. 1–11. doi:10.1002/9780470015902.a0001301.pub3.

Occhipinti, A. (2013) 'Plant coevolution: evidences and new challenges', *Journal of Plant Interactions*, 8(3), pp. 188–196. doi:10.1080/17429145.2013.816881.

Olson, R., Gavin-Smith, B., Ferraboschi, C. and Kraemer, K. (2021) 'Food fortification: The

advantages, disadvantages and lessons from sight and life programs', *Nutrients*, 13(4). doi:10.3390/nu13041118.

Onipe, O.O., Jideani, A.I.O. and Beswa, D. (2015) 'Composition and functionality of wheat bran and its application in some cereal food products', *International Journal of Food Science and Technology*, pp. 2509–2518. doi:10.1111/ijfs.12935.

Osborne, T.B. (1907) *The proteins of the wheat kernel*. Washington D.C.: Carnegie Institution of Washington.

Oury, F.X., Leenhardt, F., Rémésy, C., Chanliaud, E., Duperrier, B., Balfourier, F. and Charmet, G. (2006) 'Genetic variability and stability of grain magnesium, zinc and iron concentrations in bread wheat', *European Journal of Agronomy*, 25(2), pp. 177–185. doi:10.1016/j.eja.2006.04.011.

Ozkan, H., Brandolini, A., Torun, A., AltIntas, S., Eker, S., Kilian, B., Braun, H.J., Salamini, F. and Cakmak, I. (2007) 'Natural Variation And Identification Of Microelements Content In Seeds Of Einkorn Wheat (Triticum Monococcum)', in Buck, H.T., Nisi, J.E. and Salomón, N. (eds) *Wheat Production in Stressed Environments. Developments in Plant Breeding, vol 12*. Springer Dordrecht, pp. 455–462. doi:10.1007/1-4020-5497-1_55.

Padhan, B.K., Sathee, L., Meena, H.S., Adavi, S.B., Jha, S.K. and Chinnusamy, V. (2020) 'CO_2 Elevation Accelerates Phenology and Alters Carbon/Nitrogen Metabolism vis-à-vis ROS Abundance in Bread Wheat', *Frontiers in Plant Science*, 11(July), pp. 1–18. doi:10.3389/fpls.2020.01061.

Pan, C., Ahammed, G.J., Li, X. and Shi, K. (2018) 'Elevated CO_2 photosynthesis under high temperature by attenuating the functional limitations to energy fluxes, electron transport and redox homeostasis in tomato leaves', *Frontiers in Plant Science*, 871(November), pp. 1–11. doi:10.3389/fpls.2018.01739.

Pandey, A., Khan, M.K., Hakki, E.E., Thomas, G., Hamurcu, M., Gezgin, S., Gizlenci, O. and Akkaya, M.S. (2016) 'Assessment of genetic variability for grain nutrients from diverse regions: potential for wheat improvement', *SpringerPlus*, 5(1). doi:10.1186/s40064-016-3586-2.

Panozzo, J.F., Walker, C.K., Partington, D.L., Neumann, N.C., Tausz, M., Seneweera, S. and Fitzgerald, G.J. (2014) 'Elevated carbon dioxide changes grain protein concentration and composition and compromises baking quality. A FACE study', *Journal of Cereal Science*, 60(3), pp. 461–470. doi:10.1016/j.jcs.2014.08.011.

Parr, C.S., Wilson, N., Leary, P., Schulz, K., Lans, K., Walley, L. *et al.* (2014) 'The encyclopedia of life v2: Providing global access to knowledge about life on earth', *Biodiversity Data Journal*, 2(1), p. 28. doi:10.3897/BDJ.2.e1079.

Parry, M.A.J. and Hawkesford, M.J. (2010) 'Food security: Increasing yield and improving resource use efficiency', *Proceedings of the Nutrition Society*, 69(4), pp. 592–600. doi:10.1017/S0029665110003836.

Parry, M.A.J., Keys, A.J., Madgwick, P.J., Carmo-Silva, A.E. and Andralojc, P.J. (2008) 'Rubisco regulation: A role for inhibitors', *Journal of Experimental Botany*, 59(7), pp. 1569–1580. doi:10.1093/jxb/ern084.

Patil, I. (2021) 'Visualizations with statistical details: The "ggstatsplot" approach', *PsyArxiv* [Preprint]. doi:10.31234/osf.io/p7mku.

Peleg, Z., Cakmak, I., Ozturk, L., Yazici, A., Jun, Y., Budak, H., Korol, A.B., Fahima, T. and Saranga, Y. (2009) 'Quantitative trait loci conferring grain mineral nutrient concentrations in durum wheat × wild emmer wheat RIL population', *Theoretical and Applied Genetics*, 119(2), pp. 353–369.

doi:10.1007/s00122-009-1044-z.

Peng, J.H., Sun, D. and Nevo, E. (2011) 'Domestication evolution, genetics and genomics in wheat', *Molecular Breeding*, 28(3), pp. 281–301. doi:10.1007/s11032-011-9608-4.

Peretó, J. (2011) 'Oxygenic Photosynthesis', in *Encyclopedia of Astrobiology*. Berlin, Heidelberg: Springer Berlin Heidelberg, pp. 1209–1209. doi:10.1007/978-3-642-11274-4_1721.

Pérez, P., Alonso, A., Zita, G., Morcuende, R. and Martínez-Carrasco, R. (2011) 'Down-regulation of Rubisco activity under combined increases of CO_2 and temperature minimized by changes in Rubisco kcat in wheat', *Plant Growth Regulation*, 65(3), pp. 439–447. doi:10.1007/s10725-011-9613-y.

Pérez, P., Morcuende, R., Martín del Molino, I., Sánchez de la Puente, L. and Martínez-Carrasco, R. (2001) 'Contrasting responses of photosynthesis and carbon metabolism to low temperatures in tall fescue and clovers', *Physiologia Plantarum*, 112(4), pp. 478–486. doi:10.1034/j.1399-3054.2001.1120404.x.

Pérez, P., Morcuende, R., Martín del Molino, I. and Martínez-Carrasco, R. (2005) 'Diurnal changes of Rubisco in response to elevated CO_2, temperature and nitrogen in wheat grown under temperature gradient tunnels', *Environmental and Experimental Botany*, 53(1), pp. 13–27. doi:10.1016/j.envexpbot.2004.02.008.

Peshev, D., Vergauwen, R., Moglia, A., Hideg, É. and Van Den Ende, W. (2013) 'Towards understanding vacuolar antioxidant mechanisms: A role for fructans?', *Journal of Experimental Botany*, 64(4), pp. 1025–1038. doi:10.1093/jxb/ers377.

Philipp, N., Weichert, H., Bohra, U., Weschke, W., Schulthess, A.W. and Weber, H. (2018) 'Grain number and grain yield distribution along the spike remain stable despite breeding for high yield in winter wheat', *PLoS ONE*, 13(10). doi:10.1371/journal.pone.0205452.

Pimentel, D. (1996) 'Green revolution agriculture and chemical hazards', *Science of The Total Environment*, 188, pp. S86–S98. doi:10.1016/s0048-9697(96)90512-4.

Pingali, P.L. (2012) 'Green Revolution: Impacts, limits, and the path ahead', *Proceedings of the National Academy of Sciences*, 109(31), pp. 12302–12308. doi:10.1073/pnas.0912953109.

Plaxton, W.C. (1996) 'The organization and regulation of plant glycolysis', *Annual Review of Plant Physiology and Plant Molecular Biology*, 47(1), pp. 185–214. doi:10.1146/annurev.arplant.47.1.185.

Pleijel, H. and Högy, P. (2015) 'CO_2 dose-response functions for wheat grain, protein and mineral yield based on FACE and open-top chamber experiments', *Environmental Pollution*, 198, pp. 70–77. doi:10.1016/j.envpol.2014.12.030.

Pleijel, H. and Uddling, J. (2012) 'Yield vs. Quality trade-offs for wheat in response to carbon dioxide and ozone', *Global Change Biology*, 18(2), pp. 596–605. doi:10.1111/j.1365-2486.2011.2489.x.

Pohlert, T. (2020) 'PMCMRplus: Calculate Pairwise Multiple Comparisons of Mean Rank Sums Extended'. Available at: https://cran.r-project.org/package=PMCMRplus.

Porter, A.S., Evans-Fitz.Gerald, C., McElwain, J.C., Yiotis, C. and Elliott-Kingston, C. (2015) 'How well do you know your growth chambers? Testing for chamber effect using plant traits', *Plant Methods*, 11(1), pp. 1–10. doi:10.1186/s13007-015-0088-0.

del Pozo, A., Matus, I., Serret, M.D. and Araus, J.L. (2014) 'Agronomic and physiological traits associated with breeding advances of wheat under high-productive Mediterranean conditions. The case of Chile', *Environmental and Experimental Botany*, 103, pp. 180–189.

doi:10.1016/j.envexpbot.2013.09.016.

del Pozo, A., Pérez, P., Gutiérrez, D., Alonso, A., Morcuende, R. and Martínez-Carrasco, R. (2007) 'Gas exchange acclimation to elevated CO2 in upper-sunlit and lower-shaded canopy leaves in relation to nitrogen acquisition and partitioning in wheat grown in field chambers', *Environmental and Experimental Botany*, 59(3), pp. 371–380. doi:10.1016/j.envexpbot.2006.04.009.

Prasad, P.V.V. and Djanaguiraman, M. (2014) 'Response of floret fertility and individual grain weight of wheat to high temperature stress: Sensitive stages and thresholds for temperature and duration', *Functional Plant Biology*, 41(12), pp. 1261–1269. doi:10.1071/FP14061.

Purugganan, M.D. (2019) 'Evolutionary Insights into the Nature of Plant Domestication', *Current Biology*, 29(14), pp. R705–R714. doi:10.1016/j.cub.2019.05.053.

Purugganan, M.D. and Fuller, D.Q. (2009) 'The nature of selection during plant domestication', *Nature*, 457(7231), pp. 843–848. doi:10.1038/nature07895.

Purvis, A. and Hector, A. (2000) 'Getting the measure of biodiversity', *Nature*, 405(6783), pp. 212–219. doi:10.1038/35012221.

R Core Team (2021) 'R: A language and environment for statistical computing'. Vienna, Austria. Available at: https://www.r-project.org/.

Raghavendra, A.S. (2003) 'Photosynthesis and partitioning | C_3 Plants', in *Encyclopedia of Applied Plant Sciences*. Elsevier, pp. 673–680. doi:10.1016/B0-12-227050-9/00094-6.

Rasmusson, D.C. and Phillips, R.L. (1997) 'Plant breeding progress and genetic diversity from de novo variation and elevated epistasis', *Crop Science*, 37(2), pp. 303–310. doi:10.2135/cropsci1997.0011183X003700020001x.

Rauf, S., da Silva, J., Khan, A. and Naveed, A. (2010) 'Consequences of Plant Breeding on Genetic Diversity', *International Journal of Plant Breeding*, 4(1), pp. 1–21.

Razzaq, A., Kaur, P., Akhter, N., Wani, S.H. and Saleem, F. (2021) 'Next-generation breeding strategies for climate-ready crops', *Frontiers in Plant Science*, 12(July), pp. 1–27. doi:10.3389/fpls.2021.620420.

Reif, J.C., Zhang, P., Dreisigacker, S., Warburton, M.L., van Ginkel, M., Hoisington, D., Bohn, M. and Melchinger, A.E. (2005) 'Wheat genetic diversity trends during domestication and breeding', *Theoretical and Applied Genetics*, 110(5), pp. 859–864. doi:10.1007/s00122-004-1881-8.

Rentsch, D., Schmidt, S. and Tegeder, M. (2007) 'Transporters for uptake and allocation of organic nitrogen compounds in plants', *FEBS Letters*, 581(12), pp. 2281–2289. doi:10.1016/j.febslet.2007.04.013.

Revelle, W. (2020) 'psych: Procedures for psychological, psychometric, and personality research'. Evanston, Illinois. Available at: https://cran.r-project.org/package=psych.

Reynolds, M., Foulkes, M.J., Slafer, G.A., Berry, P., Parry, M.A.J., Snape, J.W. and Angus, W.J. (2009) 'Raising yield potential in wheat', *Journal of Experimental Botany*, 60(7), pp. 1899–1918. doi:10.1093/jxb/erp016.

Reynolds, M.P., Delgado B., M.I., Gutiérrez-Rodríguez, M. and Larqué-Saavedra, A. (2000) 'Photosynthesis of wheat in a warm, irrigated environment I: Genetic diversity and crop productivity', *Field Crops Research*, 66(1), pp. 37–50. doi:10.1016/S0378-4290(99)00077-5.

Rezaei, E.E., Siebert, S., Hüging, H. and Ewert, F. (2018) 'Climate change effect on wheat phenology depends on cultivar change', *Scientific Reports*, 8(1), pp. 1–10. doi:10.1038/s41598-018-23101-2.

Roderick, M.L., Berry, S.L., Noble, I.R. and Farquhar, G.D. (1999) 'A theoretical approach to linking the composition and morphology with the function of leaves', *Functional Ecology*, 13(5), pp. 683–695. doi:10.1046/j.1365-2435.1999.00368.x.

Roehm, K. (2001) 'Electron Carriers: Proteins and Cofactors in Oxidative Phosphorylation', in *eLS*. Wiley, pp. 1–8. doi:10.1038/npg.els.0001373.

Rogers, D. and McGuire, P. (2015) 'Genetic erosion: context is key', in Ahuja, M.R. and Jain, S.M. (eds) *Genetic Diversity and Erosion in Plants: Indicators and Prevention*. Cham: Springer International Publishing, pp. 1–24. doi:10.1007/978-3-319-25637-5_1.

Rohart, F., Gautier, B., Singh, A. and Lê Cao, K.A. (2017) 'mixOmics: An R package for 'omics feature selection and multiple data integration', *PLoS Computational Biology*, 13(11), pp. 1–19. doi:10.1371/journal.pcbi.1005752.

Rolland, F., Baena-Gonzalez, E. and Sheen, J. (2006) 'Sugar sensing and signaling in plants: Conserved and novel mechanisms', *Annual Review of Plant Biology*, 57(1), pp. 675–709. doi:10.1146/annurev.arplant.57.032905.105441.

Royo, C. and Briceño-Felix, G.A. (2011) 'Spanish wheat pool', in Bojean, A.P., Angus, W.J. and Ginkel, M. van (eds) *The World Wheat Book. A History of Wheat Breeding*. New York: NY: Lavoisier, pp. 121–154. Available at: https://www.researchgate.net/publication/284483131.

Royo, C., Martos, V., Ramdani, A., Villegas, D., Rharrabti, Y. and García Del Moral, L.F. (2008) 'Changes in yield and carbon isotope discrimination of Italian and Spanish durum wheat during the 20th century', *Agronomy Journal*, 100(2), pp. 352–360. doi:10.2134/agronj2007.0060.

Ruggiero, M.A., Gordon, D.P., Orrell, T.M., Bailly, N., Bourgoin, T., Brusca, R.C., Cavalier-Smith, T., Guiry, M.D. and Kirk, P.M. (2015) 'A Higher Level Classification of All Living Organisms', *PLOS ONE*. Edited by E. V. Thuesen, 10(4), p. e0119248. doi:10.1371/journal.pone.0119248.

Ruiz-Vera, U.M., De Souza, A.P., Long, S.P. and Ort, D.R. (2017) 'The role of sink strength and nitrogen availability in the down-regulation of photosynthetic capacity in field-grown Nicotiana tabacum L. at elevated CO_2 concentration', *Frontiers in Plant Science*, 8(June), pp. 1–12. doi:10.3389/fpls.2017.00998.

S.R. Simmons, E.A. Oelke and Anderson, P.M. (1985) *Growth and development guide for spring wheat*. Minnesota: University of Minnesota, Minnesota Extension Service Folder AG-FO-2547. Available at: https://conservancy.umn.edu/bitstream/handle/11299/165834/Growth and Development Guide for Spring Wheat.pdf?sequence=1&isAllowed=y.

Sabella, E., Aprile, A., Negro, C., Nicolì, F., Nutricati, E., Vergine, M., Luvisi, A. and De Bellis, L. (2020) 'Impact of climate change on durum wheat yield', *Agronomy*, 10(6). doi:10.3390/agronomy10060793.

Sadras, V.O. and Slafer, G.A. (2012) 'Environmental modulation of yield components in cereals: Heritabilities reveal a hierarchy of phenotypic plasticities', *Field Crops Research*, 127, pp. 215–224. doi:10.1016/j.fcr.2011.11.014.

Sage, R.F., Way, D.A. and Kubien, D.S. (2008) 'Rubisco, Rubisco activase, and global climate change', *Journal of Experimental Botany*, 59(7), pp. 1581–1595. doi:10.1093/jxb/ern053.

Salvucci, M.E. and Crafts-Brandner, S.J. (2004) 'Inhibition of photosynthesis by heat stress: The activation state of Rubisco as a limiting factor in photosynthesis', *Physiologia Plantarum*, 120(2), pp. 179–186. doi:10.1111/j.0031-9317.2004.0173.x.

Sanchez-Bragado, R., Vicente, R., Molero, G., Serret, M.D., Maydup, M.L. and Araus, J.L.

(2020) ‘New avenues for increasing yield and stability in C3 cereals: exploring ear photosynthesis’, *Current Opinion in Plant Biology*, 56, pp. 223–234. doi:10.1016/j.pbi.2020.01.001.

Sanchez-Garcia, M., Royo, C., Aparicio, N., Martín-Sánchez, J.A. and Álvaro, F. (2013) ‘Genetic improvement of bread wheat yield and associated traits in Spain during the 20th century’, *Journal of Agricultural Science*, 151(1), pp. 105–118. doi:10.1017/S0021859612000330.

Sánchez De La Puente, L., Pérez Pérez, P., Martínez-Carrasco, R., Morcuende Morcuende, R. and Martín Del Molino, I.M. (2000) ‘Action of elevated C02 and high temperatures on the mineral chemical composition of two varieties of wheat’, *Agrochimica*, 44(5–6), pp. 221–230.

Saunders, J., Smith, T. and Stroud, M. (2019) ‘Malnutrition and undernutrition’, *Medicine (United Kingdom)*, 47(3), pp. 152–158. doi:10.1016/j.mpmed.2018.12.012.

Sayre, K.D., Rajaram, S. and Fischer, R.A. (1997) ‘Yield potential progress in short bread wheats in northwest Mexico’, *Crop Science*, 37(1), pp. 36–42. doi:10.2135/cropsci1997.0011183X003700010006x.

Scarascia-mugnozza, G., Angelis, P., Matteucci, G. and Valentini, R. (1996) ‘Long-term exposure to elevated [CO2] in a natural Quercus ilex L. community: net photosynthesis and photochemical efficiency of PSII at different levels of water stress’, *Plant, Cell and Environment*, 19(6), pp. 643–654. doi:10.1111/j.1365-3040.1996.tb00399.x.

Scheible, W.-R., Morcuende, R., Czechowski, T., Fritz, C., Osuna, D., Palacios-Rojas, N. *et al.* (2004) ‘Genome-wide reprogramming of primary and secondary metabolism, protein synthesis, cellular growth processes, and the regulatory infrastructure of *Arabidopsis* in response to nitrogen’, *Plant Physiology*, 136(1), pp. 2483–2499. doi:10.1104/pp.104.047019.

Scheible, W.R., González-Fontes, A., Lauerer, M., Müller-Röber, B., Caboche, M. and Stitt, M. (1997a) ‘Nitrate acts as a signal to induce organic acid metabolism and repress starch metabolism in tobacco’, *Plant Cell*, 9(5), pp. 783–798. doi:10.1105/tpc.9.5.783.

Scheible, W.R., González-Fontes, A., Morcuende, R., Lauerer, M., Geiger, M., Glaab, J., Gojon, A., Schulze, E.D. and Stitt, M. (1997b) ‘Tobacco mutants with a decreased number of functional *nia* genes compensate by modifying the diurnal regulation of transcription, post-translational modification and turnover of nitrate reductase’, *Planta*, 203(3), pp. 304–319. doi:10.1007/s004250050196.

Seneweera, S., Makino, A., Hirotsu, N., Norton, R. and Suzuki, Y. (2011) ‘New insight into photosynthetic acclimation to elevated CO_2: The role of leaf nitrogen and Ribulose-1,5-bisphosphate carboxylase/oxygenase content in rice leaves’, *Environmental and Experimental Botany*, 71(2), pp. 128–136. doi:10.1016/j.envexpbot.2010.11.002.

Shannon, P. (2003) ‘Cytoscape: A Software Environment for Integrated Models of Biomolecular Interaction Networks’, *Genome Research*, 13(11), pp. 2498–2504. doi:10.1101/gr.1239303.

Sharkey, T.D., Bernacchi, C.J., Farquhar, G.D. and Singsaas, E.L. (2007) ‘Fitting photosynthetic carbon dioxide response curves for C3 leaves’, *Plant, Cell & Environment*, 30(9), pp. 1035–1040. doi:10.1111/j.1365-3040.2007.01710.x.

Shearman, V.J., Sylvester-Bradley, R., Scott, R.K. and Foulkes, M.J. (2005) ‘Physiological processes associated with wheat yield progress in the UK’, *Crop Science*, 45(1), pp. 175–185. doi:10.2135/cropsci2005.0175.

Shewry, P.R. (2009) ‘Wheat’, *Journal of Experimental Botany*, 60(6), pp. 1537–1553. doi:10.1093/jxb/erp058.

Shewry, P.R. and Hey, S.J. (2015) ‘The contribution of wheat to human diet and health’, *Food*

and Energy Security, 4(3), pp. 178–202. doi:10.1002/FES3.64.

Shi, R., Li, H., Tong, Y., Jing, R., Zhang, F. and Zou, C. (2008) 'Identification of quantitative trait locus of zinc and phosphorus density in wheat (Triticum aestivum L.) grain', *Plant and Soil*, 306(1–2), pp. 95–104. doi:10.1007/s11104-007-9483-2.

Signorell, A. and mult. al. (2020) 'DescTools: Tools for descriptive statistics R'. Available at: https://cran.r-project.org/package=DescTools.

Sinclair, T.R. (2019) '"The biological yield and harvest index of cereals as agronomic and plant breeding criteria" by C.M. Donald and J. Hamblin, Advances in Agronomy (1976) 28:361-405', *Crop Science*, 59(3), pp. 850–852. doi:10.2135/cropsci2018.10.0645.

Singh, A., Shannon, C.P., Gautier, B., Rohart, F., Vacher, M., Tebbutt, S.J. and Cao, K.A.L. (2019) 'DIABLO: An integrative approach for identifying key molecular drivers from multi-omics assays', *Bioinformatics*, 35(17), pp. 3055–3062. doi:10.1093/bioinformatics/bty1054.

Slafer, G.A. (2003) 'Genetic basis of yield as viewed from a crop physiologist's perspective', *Annals of Applied Biology*, 142(2), pp. 117–128. doi:10.1111/j.1744-7348.2003.tb00237.x.

Slafer, G.A. (2007) 'Physiology of determination of major wheat yield components', in *Wheat Production in Stressed Environments*. Dordrecht: Springer Netherlands, pp. 557–565. doi:10.1007/1-4020-5497-1_68.

Slafer, G.A. and Andrade, F.H. (1991) 'Changes in physiological attributes of the dry matter economy of bread wheat (Triticum aestivum) through genetic improvement of grain yield potential at different regions of the world - A review', *Euphytica*, 58(1), pp. 37–49. doi:10.1007/BF00035338.

Slafer, G.A., Kantolic, A.G., Appendino, M.L., Tranquilli, G., Miralles, D.J. and Savin, R. (2015) 'Genetic and environmental effects on crop development determining adaptation and yield', in *Crop Physiology*. Second Edi. Elsevier, pp. 285–319. doi:10.1016/B978-0-12-417104-6.00012-1.

Slafer, G.A., Savin, R., Pinochet, D. and Calderini, D.F. (2021) 'Wheat', in *Crop Physiology Case Histories for Major Crops*. Elsevier, pp. 98–163. doi:10.1016/B978-0-12-819194-1.00003-7.

Van Slagern MW (1994) *Wild wheats: a monograph of Aegilops L. and Amblyopyrum, Wageningen Agricultural University Papers.*

Smirnoff, N., Conklin, P.L. and Loewus, F. a (2001) 'Biosynthesis of ascorbic acid in plants: Contents', *Annual Review of Plant Physiology*, 52, pp. 437–467.

Smith, M.R. and Myers, S.S. (2018) 'Impact of anthropogenic CO_2 emissions on global human nutrition', *Nature Climate Change*, 8(9), pp. 834–839. doi:10.1038/s41558-018-0253-3.

Smýkal, P., Nelson, M.N., Berger, J.D. and Von Wettberg, E.J.B. (2018) 'The impact of genetic changes during crop domestication', *Agronomy*, 8(7), pp. 1–22. doi:10.3390/agronomy8070119.

Soreng, R.J., Peterson, P.M., Romaschenko, K., Davidse, G., Teisher, J.K., Clark, L.G., Barberá, P., Gillespie, L.J. and Zuloaga, F.O. (2017) 'A worldwide phylogenetic classification of the Poaceae (Gramineae) II: An update and a comparison of two 2015 classifications', *Journal of Systematics and Evolution*, 55(4), pp. 259–290. doi:10.1111/jse.12262.

Soreng, R.J., Peterson, P.M., Romaschenko, K., Davidse, G., Zuloaga, F.O., Judziewicz, E.J., Filgueiras, T.S., Davis, J.I. and Morrone, O. (2015) 'A worldwide phylogenetic classification of the Poaceae (Gramineae)', *Journal of Systematics and Evolution*, 53(2), pp. 117–137. doi:10.1111/jse.12150.

de Sousa, T., Ribeiro, M., Sabença, C. and Igrejas, G. (2021) 'The 10,000-year success story of wheat!', *Foods*, 10(9). doi:10.3390/foods10092124.

Staehelin, L.A. (2003) 'Chloroplast structure: From chlorophyll granules to supra-molecular architecture of thylakoid membranes', *Photosynthesis Research*, 76(1–3), pp. 185–196. doi:10.1023/A:1024994525586.

Stangoulis, J.C.R., Huynh, B.L., Welch, R.M., Choi, E.Y. and Graham, R.D. (2007) 'Quantitative trait loci for phytate in rice grain and their relationship with grain micronutrient content', *Euphytica*, 154(3), pp. 289–294. doi:10.1007/s10681-006-9211-7.

Stapper, M. (2007) 'Crop Monitoring and Zadoks Growth Stages for Wheat', p. 17. Available at: http://www.biologicagfood.com.au/wp-content/uploads/STAPPER-Crop-Monitoring-v21.pdf.

Statista (2019) *Statista - The statistics portal for market data, market research and market studies*. Available at: https://www.statista.com/ (Accessed: 11 October 2021).

Stein, O. and Granot, D. (2019) 'An overview of sucrose synthases in plants', *Frontiers in Plant Science*, 10(February), pp. 1–14. doi:10.3389/fpls.2019.00095.

Steuer, R., Nesi, A.N., Fernie, A.R., Gross, T., Blasius, B. and Selbig, J. (2007) 'From structure to dynamics of metabolic pathways: Application to the plant mitochondrial TCA cycle', *Bioinformatics*, 23(11), pp. 1378–1385. doi:10.1093/bioinformatics/btm065.

Sthapit, S.R., Marlowe, K., Covarrubias, D.C., Ruff, T.M., Eagle, J.D., McGinty, E.M. *et al.* (2020) 'Genetic diversity in historical and modern wheat varieties of the U.S. Pacific Northwest', *Crop Science*, 60(6), pp. 3175–3190. doi:10.1002/csc2.20299.

Stitt, M. (2002) 'Steps towards an integrated view of nitrogen metabolism', *Journal of Experimental Botany*, 53(370), pp. 959–970. doi:10.1093/jexbot/53.370.959.

Stitt, M. and Krapp, A. (1999) 'The interaction between elevated carbon dioxide and nitrogen nutrition: The physiological and molecular background', *Plant, Cell and Environment*, 22(6), pp. 583–621. doi:10.1046/j.1365-3040.1999.00386.x.

Stitt, M., Lilley, R.M., Gerhardt, R. and Heldt, H.W. (1989) 'Metabolite levels in specific cells and subcellular compartments of plant leaves', in *Methods in Enzymology*, pp. 518–552. doi:10.1016/0076-6879(89)74035-0.

Stitt, M., Lunn, J. and Usadel, B. (2010) '*Arabidopsis* and primary photosynthetic metabolism - More than the icing on the cake', *Plant Journal*, 61(6), pp. 1067–1091. doi:10.1111/j.1365-313X.2010.04142.x.

Stitt, M., Müller, C., Matt, P., Gibon, Y., Carillo, P., Morcuende, R., Scheible, W.R. and Krapp, A. (2002) 'Steps towards an integrated view of nitrogen metabolism', *Journal of Experimental Botany*, 53(370), pp. 959–970. doi:10.1093/jexbot/53.370.959.

Sullivan, G.M. and Feinn, R. (2012) ' Using Effect Size—or Why the P Value Is Not Enough ', *Journal of Graduate Medical Education*, 4(3), pp. 279–282. doi:10.4300/jgme-d-12-00156.1.

Sulpice, R., Nikoloski, Z., Tschoep, H., Antonio, C., Kleessen, S., Larhlimi, A. *et al.* (2013) 'Impact of the carbon and nitrogen supply on relationships and connectivity between metabolism and biomass in a broad panel of *Arabidopsis* accessions', *Plant Physiology*, 162(1), pp. 347–363. doi:10.1104/pp.112.210104.

Suzuki, Y. and Makino, A. (2013) 'Translational downregulation of RBCL is operative in the coordinated expression of Rubisco genes in senescent leaves in rice', *Journal of Experimental Botany*, 64(4), pp. 1145–1152. doi:10.1093/jxb/ers398.

Svara, A., Tarkowski, Ł.P., van Rensburg, H.C.J., Deleye, E., Vaerten, J., De Storme, N., Keulemans, W. and Van den Ende, W. (2020) 'Sweet immunity: The effect of exogenous fructans on the susceptibility of apple (malus × domestica borkh.) to venturia inaequalis', *International*

Journal of Molecular Sciences, 21(16), pp. 1–16. doi:10.3390/ijms21165885.

Sweetlove, L.J., Beard, K.F.M., Nunes-Nesi, A., Fernie, A.R. and Ratcliffe, R.G. (2010) 'Not just a circle: flux modes in the plant TCA cycle', *Trends in Plant Science*, 15(8), pp. 462–470. doi:10.1016/j.tplants.2010.05.006.

Tadesse, W., Amri, A., Ogbonnaya, F.C., Sanchez-Garcia, M., Sohail, Q. and Baum, M. (2016) 'Wheat', in *Genetic and Genomic Resources for Grain Cereals Improvement*. Elsevier, pp. 81–124. doi:10.1016/B978-0-12-802000-5.00002-2.

Taiz, L., Zeiger, E., Møller, I.M. (Ian M. and Murphy, A.S. (2015) *Plant physiology and development*. Sinauer Associates, Incorporated. Available at: http://www.forskningsdatabasen.dk/da/catalog/2262296489 (Accessed: 18 September 2017).

Tarkowski, Ł., Van de Poel, B., Höfte, M. and Van den Ende, W. (2019) 'Sweet immunity: Inulin boosts resistance of lettuce (*Lactuca sativa*) against grey mold (*Botrytis cinerea*) in an ethylene-dependent manner', *International Journal of Molecular Sciences*, 20(5), p. 1052. doi:10.3390/ijms20051052.

Tashiro, T. and Wardlaw, I. (1990) 'The Response to High Temperature Shock and Humidity Changes Prior to and During the Early Stages of Grain Development in Wheat', *Functional Plant Biology*, 17(5), p. 551. doi:10.1071/pp9900551.

Taub, D.R. and Wang, X. (2008) 'Why are Nitrogen Concentrations in Plant Tissues Lower under Elevated CO_2? A Critical Examination of the Hypotheses', *Journal of Integrative Plant Biology*, 50(11), pp. 1365–1374. doi:10.1111/j.1744-7909.2008.00754.x.

Tausz-Posch, S., Borowiak, K., Dempsey, R.W., Norton, R.M., Seneweera, S., Fitzgerald, G.J. and Tausz, M. (2013a) 'The effect of elevated CO_2 on photochemistry and antioxidative defence capacity in wheat depends on environmental growing conditions – A FACE study', *Environmental and Experimental Botany*, 88, pp. 81–92. doi:10.1016/j.envexpbot.2011.12.002.

Tausz-Posch, S., Dempsey, R.W., Seneweera, S., Norton, R.M., Fitzgerald, G. and Tausz, M. (2015) 'Does a freely tillering wheat cultivar benefit more from elevated CO_2 than a restricted tillering cultivar in a water-limited environment?', *European Journal of Agronomy*, 64, pp. 21–28. doi:10.1016/j.eja.2014.12.009.

Tausz-Posch, S., Norton, R.M., Seneweera, S., Fitzgerald, G.J. and Tausz, M. (2013b) 'Will intra-specific differences in transpiration efficiency in wheat be maintained in a high CO_2 world? A FACE study', *Physiologia Plantarum*, 148(2), pp. 232–245. doi:10.1111/j.1399-3054.2012.01701.x.

Tausz-Posch, S., Seneweera, S., Norton, R.M., Fitzgerald, G.J. and Tausz, M. (2012) 'Can a wheat cultivar with high transpiration efficiency maintain its yield advantage over a near-isogenic cultivar under elevated CO_2?', *Field Crops Research*, 133, pp. 160–166. doi:10.1016/j.fcr.2012.04.007.

Tausz-Posch, S., Tausz, M. and Bourgault, M. (2020) 'Elevated [CO_2] effects on crops: Advances in understanding acclimation, nitrogen dynamics and interactions with drought and other organisms', *Plant Biology*, 22(S1), pp. 38–51. doi:10.1111/plb.12994.

Tausz, M., Tausz-Posch, S., Norton, R.M., Fitzgerald, G.J., Nicolas, M.E. and Seneweera, S. (2013) 'Understanding crop physiology to select breeding targets and improve crop management under increasing atmospheric CO_2 concentrations', *Environmental and Experimental Botany*, 88, pp. 71–80. doi:10.1016/j.envexpbot.2011.12.005.

Team R Development Core (2018) 'A language and environment for statistical computing', *R Foundation for Statistical Computing*. Vienna, Austria, p. https://www.R-project.org. Available at: http://www.r-project.org.

Tetlow, I.J. and Emes, M.J. (2017) 'Starch biosynthesis in the developing endosperms of grasses and cereals', *Agronomy*, 7(4). doi:10.3390/agronomy7040081.

Thierry, A. and Larbi, R. (2018) 'Storage proteins accumulation and aggregation in developing wheat grains', *Global Wheat Production* [Preprint]. doi:10.5772/intechopen.75182.

Thudi, M., Chitikineni, A., Liu, X., He, W., Roorkiwal, M., Yang, W. *et al.* (2016) 'Recent breeding programs enhanced genetic diversity in both desi and kabuli varieties of chickpea (*Cicer arietinum* L.)', *Scientific Reports*, 6(May), pp. 1–10. doi:10.1038/srep38636.

Torralbo, F., Vicente, R., Morcuende, R., González-Murua, C. and Aranjuelo, I. (2019) 'C and N metabolism in barley leaves and peduncles modulates responsiveness to changing CO_2', *Journal of Experimental Botany*, 70(2), pp. 599–611. doi:10.1093/jxb/ery380.

Trethowan, R.M., Reynolds, M.P., Ortiz-Monasterio, J.I. and Ortiz, R. (2007) 'The genetic basis of the green revolution in wheat production', in *Plant Breeding Reviews*. Hoboken, NJ, USA: John Wiley & Sons, Inc., pp. 39–58. doi:10.1002/9780470168028.ch2.

Uauy, C., Distelfeld, A., Fahima, T., Blechl, A. and Dubcovsky, J. (2006) 'A NAC Gene Regulating Senescence Improves Grain Protein, Zinc, and Iron Content in Wheat', *Science*, 314(5803), pp. 1298–1301. doi:10.1126/science.1133649.

United Nations (2019) *World population prospects 2019: Highlights.* Available at: https://population.un.org/wpp/.

United Nations (2021) *World population clock: 7.9 Billion people (2021)*, *Worldometer*. Available at: https://www.worldometers.info/world-population/ (Accessed: 18 January 2022).

Valladares, F. and Pearcy, R.W. (1997) 'Interactions between water stress, sun-shade acclimation, heat tolerance and photoinhibition in the sclerophyll Heteromeles arbutifolia', *Plant, Cell and Environment*, 20(1), pp. 25–36. doi:10.1046/j.1365-3040.1997.d01-8.x.

Vicente-Villardon, J.L. (2019) 'MultBiplotR: MULTivariate analysis using BIPLOTs'. Available at: https://cran.r-project.org/package=MultBiplotR.

Vicente, R., Bolger, A.M., Martínez-Carrasco, R., Pérez, P., Gutiérrez, E., Usadel, B. and Morcuende, R. (2019) '*De Novo* transcriptome analysis of durum wheat flag leaves provides new insights into the regulatory response to elevated CO_2 and high temperature', *Frontiers in Plant Science*, 10(December), pp. 1–18. doi:10.3389/fpls.2019.01605.

Vicente, R., Martínez-Carrasco, R., Pérez, P. and Morcuende, R. (2018) 'New insights into the impacts of elevated CO_2, nitrogen, and temperature levels on the regulation of C and N metabolism in durum wheat using network analysis', *New Biotechnology*, 40(September 2016), pp. 192–199. doi:10.1016/j.nbt.2017.08.003.

Vicente, R., Morcuende, R. and Babiano, J. (2011) 'Differences in Rubisco and chlorophyll content among tissues and growth stages in two tomato (*Lycopersicon esculentum* Mill.) varieties', *Agronomy Research*, 9(SPPL. ISS. 2), pp. 501–507.

Vicente, R., Pérez, P., Martínez-Carrasco, R., Feil, R., Lunn, J.E., Watanabe, M. *et al.* (2016) 'Metabolic and transcriptional analysis of durum wheat responses to elevated CO_2 at low and high nitrate supply', *Plant and Cell Physiology*, 57(10), pp. 2133–2146. doi:10.1093/pcp/pcw131.

Vicente, R., Pérez, P., Martínez-Carrasco, R., Gutiérrez, E. and Morcuende, R. (2015a) 'Nitrate supply and plant development influence nitrogen uptake and allocation under elevated CO_2 in durum wheat grown hydroponically', *Acta Physiologiae Plantarum*, 37(6), p. 114. doi:10.1007/s11738-015-1867-y.

Vicente, R., Pérez, P., Martínez-Carrasco, R. and Morcuende, R. (2017) 'Improved responses

to elevated CO_2 in durum wheat at a low nitrate supply associated with the upregulation of photosynthetic genes and the activation of nitrate assimilation', *Plant Science*, 260, pp. 119–128. doi:10.1016/j.plantsci.2017.04.009.

Vicente, R., Pérez, P., Martínez-Carrasco, R., Usadel, B., Kostadinova, S. and Morcuende, R. (2015b) 'Quantitative RT–PCR platform to measure transcript levels of C and N metabolism-related genes in durum wheat: Transcript profiles in elevated [CO_2] and high temperature at different levels of N supply', *Plant and Cell Physiology*, 56(8), pp. 1556–1573. doi:10.1093/pcp/pcv079.

Vreugdenhil, D., Aarts, M.G.M., Koornneef, M., Nelissen, H. and Ernst, W.H.O. (2004) 'Natural variation and QTL analysis for cationic mineral content in seeds of *Arabidopsis thaliana*', *Plant, Cell and Environment*, 27(7), pp. 828–839. doi:10.1111/j.1365-3040.2004.01189.x.

Waddington, S.R., Ransom, J.K., Osmanzai, M. and Saunders, D.A. (1986) ' Improvement in the Yield Potential of Bread Wheat Adapted to Northwest Mexico 1 ', *Crop Science*, 26(4), pp. 698–703. doi:10.2135/cropsci1986.0011183x002600040012x.

Wang, L., Feng, Z. and Schjoerring, J.K. (2013) 'Effects of elevated atmospheric CO_2 on physiology and yield of wheat (*Triticum aestivum* L.): A meta-analytic test of current hypotheses', *Agriculture, Ecosystems and Environment*, 178(2013), pp. 57–63. doi:10.1016/j.agee.2013.06.013.

Wang, X. and Liu, F. (2021) 'Effects of elevated CO_2 and heat on wheat grain quality', *Plants*, 10(5), p. 1027. doi:10.3390/plants10051027.

Watanabe, C.K., Sato, S., Yanagisawa, S., Uesono, Y., Terashima, I. and Noguchi, K. (2014) 'Effects of elevated CO_2 on levels of primary metabolites and transcripts of genes encoding respiratory enzymes and their diurnal patterns in Arabidopsis thaliana: possible relationships with respiratory rates', *Plant and Cell Physiology*, 55(2), pp. 341–357. doi:10.1093/pcp/pct185.

Wei, T. and Simko, V. (2021) 'R package "corrplot": Visualization of a correlation matrix'. Available at: https://github.com/taiyun/corrplot.

Weichert, H., Högy, P., Mora-Ramirez, I., Fuchs, J., Eggert, K., Koehler, P., Weschke, W., Fangmeier, A. and Weber, H. (2017) 'Grain yield and quality responses of wheat expressing a barley sucrose transporter to combined climate change factors', *Journal of Experimental Botany*, 68(20), pp. 5511–5525. doi:10.1093/jxb/erx366.

Weide, A. and Weide, A. (2015) 'On the identification of domesticated emmer wheat, *Triticum turgidum* subsp. *dicoccum* (*Poaceae*), in the Aceramic Neolithic of the Fertile Crescent', *On the Identification of Domesticated Emmer Wheat, Triticum turgidum subsp. dicoccum (Poaceae), in the Aceramic Neolithic of the Fertile Crescent*, 38(1), pp. 381–424. doi:10.11588/ai.2015.1.26205.

Wheat production, 2018 (2020). Available at: https://ourworldindata.org/grapher/wheat-production (Accessed: 27 September 2021).

White, A.C., Rogers, A., Rees, M. and Osborne, C.P. (2016) 'How can we make plants grow faster? A source-sink perspective on growth rate', *Journal of Experimental Botany*, 67(1), pp. 31–45. doi:10.1093/jxb/erv447.

White, J. (2008) *Procrop wheat growth and development*. Edited by J. White and J. Edwards. NSW Department of Primary Industries. Available at: https://www.dpi.nsw.gov.au/__data/assets/pdf_file/0008/516185/Procrop-wheat-growth-and-development.pdf.

Whitney, H.M. and Glover, B.J. (2013) 'Coevolution: Plant–Insect', in *eLS*. Wiley, pp. 1–8. doi:10.1002/9780470015902.a0001762.pub2.

Wickham, H. (2016) *ggplot2: Elegant graphics for data analysis*. Springer-Verlag New York.

Available at: https://ggplot2.tidyverse.org.

Wieser, H., Koehler, P. and Scherf, K.A. (2020) 'The two faces of wheat', *Frontiers in Nutrition*, 7(October). doi:10.3389/fnut.2020.517313.

Wieser, H., Manderscheid, R., Erbs, M. and Weigel, H.J. (2008) 'Effects of elevated atmospheric CO_2 concentrations on the quantitative protein composition of wheat grain', *Journal of Agricultural and Food Chemistry*, 56(15), pp. 6531–6535. doi:10.1021/jf8008603.

Wilson, M.H. and Lovell, S.T. (2016) 'Agroforestry-The next step in sustainable and resilient agriculture', *Sustainability (Switzerland)*, 8(6), pp. 1–15. doi:10.3390/su8060574.

Wollenweber, B., Porter, J.R. and Schellberg, J. (2003) 'Lack of Interaction between Extreme High-Temperature Events at Vegetative and Reproductive Growth Stages in Wheat', *Journal of Agronomy and Crop Science*, 189(3), pp. 142–150. doi:10.1046/j.1439-037X.2003.00025.x.

Worldometers (2021) 'Worldometer - real time world statistics'. Available at: https://www.worldometers.info/ (Accessed: 2 January 2022).

van de Wouw, M., van Hintum, T., Kik, C., van Treuren, R. and Visser, B. (2010a) 'Genetic diversity trends in twentieth century crop cultivars: A meta analysis', *Theoretical and Applied Genetics*, 120(6), pp. 1241–1252. doi:10.1007/s00122-009-1252-6.

van de Wouw, M., Kik, C., van Hintum, T., van Treuren, R. and Visser, B. (2010b) 'Genetic erosion in crops: concept, research results and challenges', *Plant Genetic Resources*, 8(1), pp. 1–15. doi:10.1017/S1479262109990062.

Xiao, Y.G., Qian, Z.G., Wu, K., Liu, J.J., Xia, X.C., Ji, W.Q. and He, Z.H. (2012) 'Genetic Gains in Grain Yield and Physiological Traits of Winter Wheat in Shandong Province, China, from 1969 to 2006', *Crop Science*, 52(1), pp. 44–56. doi:10.2135/cropsci2011.05.0246.

Xu, Z., Jiang, Y., Jia, B. and Zhou, G. (2016) 'Elevated-CO_2 response of stomata and its dependence on environmental factors', *Frontiers in Plant Science*, 7(MAY2016), pp. 1–15. doi:10.3389/fpls.2016.00657.

Xue, Q., Soundararajan, M., Weiss, A., Arkebauer, T.J. and Stephen Baenziger, P. (2002) 'Genotypic variation of gas exchange parameters and carbon isotope discrimination in winter wheat', *Journal of Plant Physiology*, 159(8), pp. 891–898. doi:10.1078/0176-1617-00780.

Yahia, E.M., Carrillo-López, A. and Bello-Perez, L.A. (2019) 'Carbohydrates', in *Postharvest Physiology and Biochemistry of Fruits and Vegetables*. Elsevier, pp. 175–205. doi:10.1016/B978-0-12-813278-4.00009-9.

Yang, J. and Zhang, J. (2006) 'Grain filling of cereals under soil drying', *New Phytologist*, 169(2), pp. 223–236. doi:10.1111/j.1469-8137.2005.01597.x.

Yin, L.-P., Li, P., Wen, B., Taylor, D. and Berry, J.O. (2007) 'Characterization and expression of a high-affinity nitrate system transporter gene (TaNRT2.1) from wheat roots, and its evolutionary relationship to other NTR2 genes', *Plant Science*, 172(3), pp. 621–631. doi:10.1016/j.plantsci.2006.11.014.

You, J. and Chan, Z. (2015) 'ROS regulation during abiotic stress responses in crop plants', *Frontiers in Plant Science*, 6(DEC), pp. 1–15. doi:10.3389/fpls.2015.01092.

Zadoks, J.C., Chang, T.T. and Konzak, C.F. (1974) 'A decimal code for the growth stages of cereals', *Weed Research*, 14(6), pp. 415–421. doi:10.1111/j.1365-3180.1974.tb01084.x.

Zaharieva, M., Ayana, N.G., Hakimi, A. Al, Misra, S.C. and Monneveux, P. (2010) 'Cultivated emmer wheat (Triticum dicoccon Schrank), an old crop with promising future: a review', *Genetic*

Resources and Crop Evolution, 57(6), pp. 937–962. doi:10.1007/s10722-010-9572-6.

Zeder, M.A. (2008) 'Domestication and early agriculture in the Mediterranean Basin: Origins, diffusion, and impact', *Proceedings of the National Academy of Sciences*, 105(33), pp. 11597–11604. doi:10.1073/pnas.0801317105.

Zhang, X., Shi, Z., Jiang, D., Högy, P. and Fangmeier, A. (2019a) 'Independent and combined effects of elevated CO_2 and post-anthesis heat stress on protein quantity and quality in spring wheat grains', *Food Chemistry*, 277(May 2018), pp. 524–530. doi:10.1016/j.foodchem.2018.11.010.

Zhang, X., Shi, Z., Jiang, D., Högy, P. and Fangmeier, A. (2019b) 'Independent and combined effects of elevated CO_2 and post-anthesis heat stress on protein quantity and quality in spring wheat grains', *Food Chemistry*, 277(November 2018), pp. 524–530. doi:10.1016/j.foodchem.2018.11.010.

Zhao, H.L., Chang, T.G., Xiao, Y. and Zhu, X.G. (2021) 'Potential metabolic mechanisms for inhibited chloroplast nitrogen assimilation under high CO_2', *Plant Physiology*, 187(3), pp. 1812–1833. doi:10.1093/plphys/kiab345.

Zheng, T.C., Zhang, X.K., Yin, G.H., Wang, L.N., Han, Y.L., Chen, L. *et al.* (2011) 'Genetic gains in grain yield, net photosynthesis and stomatal conductance achieved in Henan Province of China between 1981 and 2008', *Field Crops Research*, 122(3), pp. 225–233. doi:10.1016/j.fcr.2011.03.015.

Zheng, X.-T., Yu, Z.-C., Tang, J.-W., Cai, M.-L., Chen, Y.-L., Yang, C.-W., Chow, W.S. and Peng, C.-L. (2021) 'The major photoprotective role of anthocyanins in leaves of *Arabidopsis thaliana* under long-term high light treatment: antioxidant or light attenuator?', *Photosynthesis Research*, 149(1–2), pp. 25–40. doi:10.1007/s11120-020-00761-8.

Zhu, C., Zhu, J., Zeng, Q., Liu, G., Xie, Z., Tang, H., Cao, J. and Zhao, X. (2009) 'Elevated CO_2 accelerates flag leaf senescence in wheat due to ear photosynthesis which causes greater ear nitrogen sink capacity and ear carbon sink limitation', *Functional Plant Biology*, 36(4), pp. 291–299. doi:10.1071/FP08269.

Zhu, X.-G., Long, S.P. and Ort, D.R. (2010) 'Improving photosynthetic efficiency for greater yield', *Annual Review of Plant Biology*, 61(1), pp. 235–261. doi:10.1146/annurev-arplant-042809-112206.

Žilić, S. (2016) 'Phenolic Compounds of Wheat. Their Content, Antioxidant Capacity and Bioaccessibility', *MOJ Food Processing & Technology*, 2(3), pp. 85–89. doi:10.15406/mojfpt.2016.02.00037.

Zinta, G., Abdelgawad, H., Domagalska, M.A., Vergauwen, L., Knapen, D., Nijs, I., Janssens, I.A., Beemster, G.T.S. and Asard, H. (2014) 'Physiological, biochemical, and genome-wide transcriptional analysis reveals that elevated CO_2 mitigates the impact of combined heat wave and drought stress in *Arabidopsis thaliana* at multiple organizational levels', *Global Change Biology*, 20(12), pp. 3670–3685. doi:10.1111/gcb.12626.

Zinta, G., AbdElgawad, H., Peshev, D., Weedon, J.T., Van den Ende, W., Nijs, I., Janssens, I.A., Beemster, G.T.S. and Asard, H. (2018) 'Dynamics of metabolic responses to periods of combined heat and drought in *Arabidopsis thaliana* under ambient and elevated atmospheric CO_2', *Journal of Experimental Botany*, 69(8), pp. 2159–2170. doi:10.1093/jxb/ery055.

Ziska, L.H. (2008) 'Three-year field evaluation of early and late 20th century spring wheat cultivars to projected increases in atmospheric carbon dioxide', *Field Crops Research*, 108(1), pp. 54–59. doi:10.1016/j.fcr.2008.03.006.

Ziska, L.H., Morris, C.F. and Goins, E.W. (2004) 'Quantitative and qualitative evaluation of selected wheat varieties released since 1903 to increasing atmospheric carbon dioxide: Can yield

sensitivity to carbon dioxide be a factor in wheat performance?', *Global Change Biology*, 10(10), pp. 1810–1819. doi:10.1111/j.1365-2486.2004.00840.x.

Zörb, C., Ludewig, U. and Hawkesford, M.J. (2018) 'Perspective on Wheat Yield and Quality with Reduced Nitrogen Supply', *Trends in Plant Science*, 23(11), pp. 1029–1037. doi:10.1016/j.tplants.2018.08.012.

Zunjarrao, S.S., Tellis, M.B., Joshi, S.N. and Joshi, R.S. (2020) 'Plant-Insect Interaction: The Saga of Molecular Coevolution', in *Reference Series in Phytochemistry*, pp. 19–45. doi:10.1007/978-3-319-96397-6_42.